Characterization of cytochrome P450-mediated pyrethroid resistance in *Anopheles funestus* with special reference to transfluthrin

'Thesis submitted in accordance with the requirements of the Liverpool School of Tropical Medicine for the degree of Doctor in Philosophy by *Melanie Nolden*.'

January 2023

“*Das Leben ist nicht immer nur Pommes und Disko*“

Christian Steiffen

Abstract

Vector control tools that target malaria transmitting mosquitoes of the *Anopheles* genus are responsible for averting 80 % of malaria cases between 2000 and 2015. However, 88 % of all WHO-recommended products for vector control products rely on pyrethroids. Pyrethroids are a class of synthetic insecticides that act on the voltage gated sodium channel. Frequent application has led to a selection of alleles conferring pyrethroid resistance. In the major malaria mosquito *Anopheles funestus,* pyrethroid resistance is driven by metabolic resistance associated with upregulated P450-monooxygenases (P450s), in particular CYP6P9a and CYP6P9b. The polyfluorinated pyrethroid transfluthrin has been shown to control the highly pyrethroid-resistant laboratory *An. funestus* FUMOZ-R strain. This volatile molecule is increasingly used in materials for vector control such as eave ribbons, chairs, or sandals. However, to date transfluthrin metabolism by P450s has not been elucidated. Synergists that inhibit P450s can also restore pyrethroid-susceptibility. Piperonylbutoxide (PBO) is the only synergist used in vector control, however there is recent evidence that mosquitoes develop resistance towards PBO.

The toxicology of common pyrethroids and transfluthrin towards pyrethroid resistant *An. funestus* FUMOZ-R and a susceptible FANG strain were evaluated using glazed-tile contact bioassays. Bioassays to examine synergistic effects of PBO and azole fungicides were conducted to evaluate the involvement of P450s in pyrethroids metabolism in *An. funestus* FUMOZ-R and to assess the feasibility of using azoles as an alternative to PBO in vector control products. Baculovirus recombinant expression of CYP6P9a and CYP6P9b in insect cells in the presence and absence of cytochrome b5 was used to examine the role of this redox partner in pyrethroid metabolism. Finally, incubation of CYP6P9a and CYP6P9b with deltamethrin, permethrin and transfluthrin with subsequent UPLC-MS/MS analysis were conducted to examine the breakdown of these compounds.

We have shown that cytochrome b5 is not necessary in deltamethrin metabolism using recombinant baculovirus/high-5 cell expression, however it can enhance the metabolism of fluorescent model substrates. Site directed mutagenesis of valine to isoleucine residue at position 310 of CYP6P9b, which is part of the substrate recognition site (SRS) 4 and 9.8 Å distanced from the Heme revealed enhanced metabolism towards fluorescent model

substrates and towards permethrin. This mutation is present in permethrin resistant populations in Benin, confirming a potential resistance marker for permethrin resistance. Furthermore, we have revealed in-vivo the synergism of the azole fungicides 1-ABT and triflumizole in combination with different pyrethroids towards resistant *An. funestus* and shown the nanomolar inhibition of triflumizole, prochloraz and ketoconazole towards recombinant CYP6P9a and CYP6P9b. Finally, we have shown that transfluthrin is protected from P450 oxidation due to the fluorination of common sites of attack on the benzyl ring and the lack of the phenoxybenzylether. The cleavage of the phenoxybenzylether as well as hydroxylation of 4'-para- position is a preferred route of metabolism of the P450 enzymes CYP6P9a and CYP6P9b conferring high level of deltamethrin and permethrin resistance.

This work emphasizes the resistant breaking potential of transfluthrin and suggests the further evaluation of azole fungicides in vector control products to extend the lifetime of pyrethroids.

Acknowledgements

A massive thank you to Dr. Ralf Nauen and Dr. Mark Paine, who are amazing supervisors and great scientists. I certainly would not be here without them! I am very thankful for Ralfs tremendous support and motivation and the passion he puts in his everyday work. Thanks a lot, Mark for being so patient and flexible supervising this thesis mainly virtually and all the good given advice.

I am very thankful for the support of the "Envu Germany" Team, which not only funded the whole project, but also have been always there for me – professionally and personally. Thanks, Sebastian Horstmann, Kai-Uwe Brüggen, Arunas Damijonaitis, Claudia Radecki and Uwe Pluschkell. All the thousand mosquitoes which have been killed by me were provided and reared by Jörg Egger and Frederik Kaeding, who always do their best in rearing strong and happy mosquitoes and never leaving a last-minute-request open.

Thanks to the IVCC, who partly funded this project and in particular Sarah Rees, who has been a mentor to me along the four years. Thanks a lot for our great and inspiring discussions.

A huge amount of gratitude to everyone in Ralfs lab, especially Bettina Lueke for introducing me into the world of biochemistry and for always having a solution ready. A big thank you to Julian Haas, who has been sometimes my only contact in the Covid-months, thanks for the fun and all the scientific discussions we have had. Also, a big thank you to Debora Boaventura, Viola Müller and Laura Franz who have made the PhD experience enjoyable, thanks for the great time we have had and all your support!

The analytical department, especially Johannes Glaubitz, Birgit Nebelsiek and Udo König. Thanks for the work you have done, this project would not have worked without you.

I am very grateful for the immense (mental) support I receive from my friends during this whole project.

Thanks a lot to my mum, dad and brother, who are the anchor in my life since 32 years. Who never put any pressure on me and let me grow to the person I became. Thanks for all the love and trust you have in me, you are the best family someone can wish for, and I am tremendously thankful that you are mine.

Finally, I want to thank the amazing human being David-Vincent, for his happiness and positiveness, his massive trust, love, and pride. Thanks for your patience, your believe in me and for always being there for me. The past four years would have been much harder (probably impossible) without you being on my side.

Contents

Abbrevations

1-ABT	1-Aminobenzotriazole
AChE	Acetylcholine Esterase
ATSB	Attractive targeted sugar baits
BOMFC	7-benzyloxymethoxy-4-trifluoromethylcoumarin
BFC	7-benzyloxy-4-trifluoromethylcoumarin
BSA	bovine serum albumin
Bti	Bacillus thuringiensis israelensis
CDC	Center for disease control and prevention
CE	Carboxylesterases
CPR	Cytochrome P450 reductase
CRISPR	Clustered regularly interspaced short palindromic repeats
CYB5	Cytochrome b5
DDT	Dichlorodiphenyltrichloroethane
DEET	Diethyltoluamid
DMSO	Dimethyl sulfoxide
DNA	Deoxyribonucleic acid
DTT	Dithiotreitol
EFC	7-ethoxy-4-trifluoromethylcoumarin
EC50	Effective concentration 50
e.g.	Exempli gratia
FeII	Ferrous iron
FeIII	Ferric iron
GST	Glutathione-S-transferase
GSH	Glutathione
HPLC	High pressure liquid chromatography
IC50	Inhibition concentration 50
i.e.	Id est
IRAC	Insecticide resistance action committee
IRS	Indoor residual spray
IVCC	Innovative vector control consortium
ITN	Insecticidal treated bednet
K^+	Potassium ion
K_m	Michaelis-Menten constant
KDR	Knock down resistance
LC50	Lethal concentration 50
LD	Lethal dose
LLIN	Long lasting impregnated bednet
LSTM	Liverpool School of tropical medicine
M	Molar
Mg^{2+}	Magnesium ion
MoA	Mode of action
MoI	Multiplicity of infection
mRNA	Messenger RNA
MS	Mass spectrometry

Na^+	Sodium ion
NADPH	β-Nicotinamide adenine dinucleotide 2’-phosphate
P450	P450 monooxygenases
PDB	Protein database
PBO	Piperonylbutoxide
PCR	Polymerase chain reaction
RNA	Ribonucleic acid
RNAi	RNA interference
RR	Resistance ratio
RT qPCR	Realtime quantitative polymerase chain reaction
Sf9	Spodoptera frugiperda 9 cell line
SNP	Single nucleotide polymorphism
SR	Synergistic ratio
SRS	Substrate recognition site
TF	Transfluthrin
UPLC	Ultra-performance liquid chromatography
V_{max}	Rate of reaction when the enzyme is fully saturated with substrate
VSGC	Voltage gated sodium channel
WHO	World Health Organization

1. Chapter 1. Introduction and literature review

Vector-borne diseases (VBD) account for 17 % of all infectious diseases causing more than 700 000 deaths annually (WHO, 2020). Malaria is the VBD that is responsible for most deaths worldwide, it is caused by parasites of the *Plasmodium* genus which is transmitted by *Anopheline* mosquitoes. During the 1980s and 90s the burden of malaria increased resulting in >1 million deaths globally in 2000 (WHO, 2005), most likely due to resistance to antimalarial drugs.

Chemical vector control interventions have been implemented since the early 1930s using indoor residual sprays, which included the active ingredient (a.i.) pyrethrum and kerosene and later DDT (M. Coetzee et al., 2013a). Insecticide treated bednets (ITN) were introduced in 1980s (Robert, 2020), however, their use was sporadic and uncoordinated. The launch of the Roll Back Malaria (RBM) initiative in 1998, the publication of the millennium development goals and Presidents Malaria Initiative (PMI) in 2000 attracted the Bill & Melinda Gates foundation and other funders and initiated coordinated efforts for vector control that involved ramping up ITN distribution and IRS (WHO, 2005). This was hugely successful, preventing an estimated 663 million malaria cases from 2000 until 2015 (Bhatt et al., 2015). In 2015, globally 212 million cases and 429 000 deaths were reported (WHO, 2016). However, since then cases stagnated and started to rise again. Thus, has resulted in an estimated 241 million cases and 619 000 deaths worldwide in 2021, of which 593 000 occur in Africa (WHO, 2022a). The reasons are unclear, but insecticide resistance is likely to be a major factor due to the limited number of insecticides available (Hemingway et al., 2016; WHO, 2021).

Chemical vector control relies heavily on four insecticidal classes: pyrethroids, carbamates, organophosphates, and organochlorines. New classes have recently been introduced, such as the pyrrole chlorfenapyr (in combination with the pyrethroid alpha-cypermethrin), the neonicotinoid clothianidin (alone and in combination with the pyrethroid deltamethrin) and the butenolide flupyradifurone (combined with a pyrethroid transfluthrin) (Figure 1.2.1).
Understanding the mechanism of resistance is essential to aid design of a.i's and develop mitigating strategies. Insecticide resistance in all its facets, is a major threat to the global goal to eradicate malaria in 2040.

1.1. Epidemiology of Malaria transmitted by *Anopheles funestus*

Human malaria is a major burden to countries in Africa, where 96 % of worldwide Malaria cases occurred in 2020 (WHO, 2021). The disease is caused by unicellular parasites from the *Plasmodium* genus, which have different life stages in humans and mosquitoes that are necessary for the reproduction of the parasites. The parasite is transmitted during a blood meal of a female *Anopheles* mosquito (Figure 1.1). The mosquito cycle (sporogonic cycle) takes 9-16 days, until sporozoites can be released (Phillips et al., 2017).

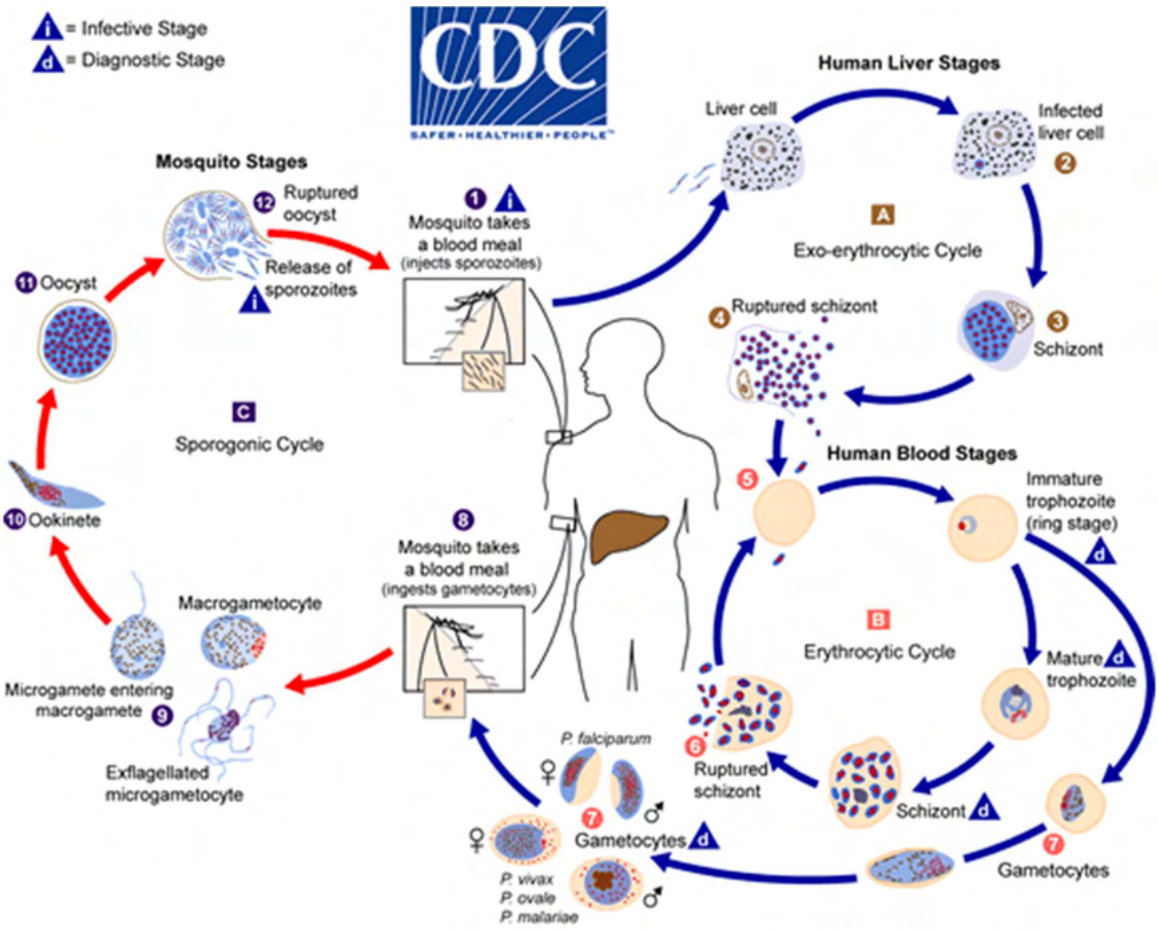

Figure 1.1 Plasmodium cycle.

During a blood meal, sporozoites are injected into the human blood cycle and transferred to the liver, where they infect liver-cells and form a schizont. They are released into the blood cycle and infect red-blood cells and form male and female gametocytes, which are uptaken when a mosquito is obtaining a blood meal. Another cycle in the human bloodstream includes trophozoites in red blood cells which are developing to schizonts which are ruptures and releasing merozoites, which are causing malaria symptoms in humans. Within the mosquito, a zygote is formed, becoming an ookinete, which is invading the mosquito's midgut wall and developing to an oocyst, which is releasing sporozoites in the mosquito's salivary glands. Source: www.cdc.gov/malaria/about/biology/index.html

Six different Plasmodium species can cause human malaria: *P. falciparum*, *P. vivax*, *P. ovale curtisi*, *P. ovale wallikeri*, *P. malariae* and *P. knowlesi,* of which, *P. falciparum* is responsible for most of the severe malaria cases in the African subcontintent (WHO, 2021).

Approximately 40 *Anopheles* species are competent vectors of *Plasmodium* spp (Sinka et al., 2011, 2010a, 2010b) In Sub-Saharan Africa (SSA) mosquitoes belonging to the *Anopheles gambiae* s.l. complex and Funestus subgroup are the major vectors of malaria (Sinka et al., 2010a). Within the *An. gambiae* s.l. complex, *An.gambiae* Giles, *An. colluzzi* Coetzee & Wilkerson (Coetzee et al., 2013b) and *An. arabiensis* Patton have emerged as the main vectors of the eight species belonging to *An.gambiae* s.l. (Gillies and Coetzee, 1987). The Funestus subgroup is comprised of *An. funestus* Giles, *An. parensis*, *An. vaneedeni*, *An. aruni* and *An. confuses*, of which only *An. funestus* Giles is an important vector of human malaria (Coetzee and Koekemoer, 2013; Sinka et al., 2010a). The Asian malaria vector *An. stephensi* has recently been associated with increasing malaria transmission in Africa, which has led the World Health Organization (WHO) and the global vector community to enhance vector surveillance in SSA (WHO, 2021). Unlike other African malaria vectors, *An. stephensi* has adapted to urban habitats, which is a major threat to the current strategies of malaria control in SSA (Sinka et al., 2020; WHO, 2021).

An. funestus is found in sub-Saharan rural Africa (Sinka et al., 2016) and reported as a mostly indoor biting (endophagic), indoor resting (endophilic) mosquito. *An. funestus* mosquitoes obtain their blood meals from human hosts (anthropophagic), most commonly between midnight and early morning (Antonio-Nkondjio et al., 2002; Awolola et al., 2005; Dia et al., 2013; Ojuka et al., 2015; Oyewole et al., 2007; Sherrard-Smith et al., 2019; Temu et al., 2007). After obtaining a blood meal, female *An. funestus* females lay their eggs in semi-permanent or permanent water bodies or paddy fields containing vegetation in rural areas (Dia et al., 2013). Despite their major role in malaria transmission, research on *An. funestus* has lagged behind that of *An. gambiae* due to the difficulties in laboratory rearing (Coetzee and Koekemoer, 2013)

1.2. Vector control

Along with medical treatment and chemoprophylaxis, the control of mosquitoes has been an important factor in the fight against diseases such as malaria, dengue fever and yellow fever, either by reducing mosquito populations or by interrupting transmission by preventing mosquito-human contact. Alternative methods such as the treatment of different materials with insecticides (Kaindoa et al., 2021), attractive targeted sugar baits (ATSB) and genetically modified (GM) mosquitoes are deployed or under current development (Fraser et al., 2021; Zheng et al., 2019). To sustainably fight mosquito-vectors, integrated vector management approaches are needed. These include frequent surveillance of mosquito-vectors, community engagement and integration of socio-economic aspects, education of the population, surveillance of breeding sites or breeding site management and chemical vector control targeting adults and developing stages.

1.2.1. Insecticides in vector control and their mode of action

Insecticides for vector control applications are used against indoor biting adult mosquitoes using ITNs and IRS, and outdoors using space-spraying-applications or larvicides. Larvicides, which target the juvenile stages of *Anopheles* mosquitoes, play a minor role in vector control programmes (WHO, 2006). Chemical and microbial larvicides commonly work by inhibiting larval growth (Table 1.2.1).

The use of chemicals for vector control started with DDT in the early 1940s (Figure 1.2.1). Despite emerging environmental safety concerns towards DDT in the 1970s (Soderlund et al., 2017) it is still being used in vector control applications (WHO, 2021). Even though novel insecticides have been developed for the agriculture market, alternative insecticides for vector control applications are lacking as commercial interest in the vector control market is low, highlighted by the fact that DDT is still used. Over the last few decades, the market has been dominated by four classes of insecticides: organochlorines, organophosphates, carbamates and pyrethroids, which share only two modes of action (Figure 1.2.1) (Nauen, 2007). It is only recently, driven by increased funding and the establishment of the product-development-partnership (PDP) Innovative Vector Control Consortium (IVCC) in 2005, that insecticides with new modes of action have been introduced into the vector control market. Since then, the pyrrole chlorfenapyr, an uncoupler of the respiration system, has been

introduced in combination with alpha-cypermethrin in ITNs (Interceptor G2) (Tungu et al., 2021). Clothianidin, a neonicotinoid, is being used for IRS applications alone or in combination with deltamethrin (Animut and Horstmann, 2022; Fongnikin et al., 2020), and the juvenile hormone mimic pyriproxyfen is being used in combination with alpha-cypermethrin in ITNs (Ngufor et al., 2020). Most recently, the butenolide flupyradifurone in combination with transfluthrin were introduced as a novel space spray against outdoor active mosquitoes (Bayer, 2022).

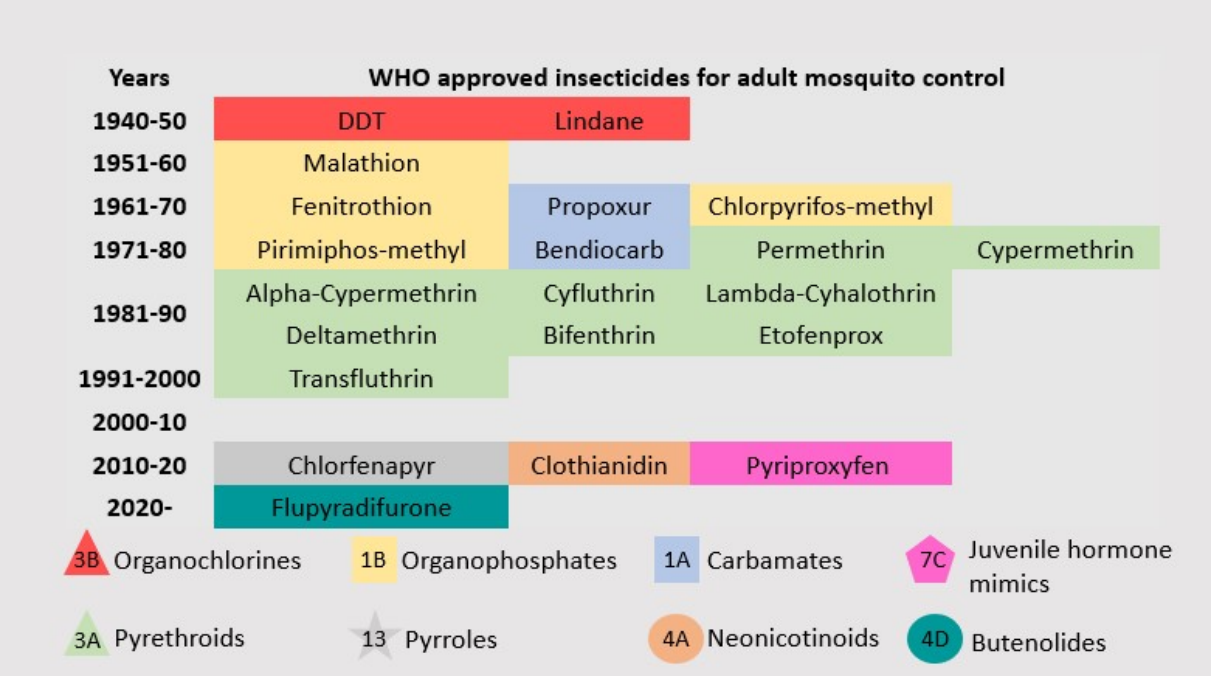

Figure 1.2.1 History of insecticides approved by the WHO for the control of adult mosquitoes, adapted from Nauen, 2007. Different shapes indicate mode of action including the current IRAC classification: triangle: voltage gated sodium channel, square: acetylcholinesterase (AChE) inhibitors, asterisk: Uncouplers of oxidative phosphorylation via disruption of the proton gradient, circle: nicotinic acetylcholine receptor (nAChR) competitive modulators, pentagon: juvenile hormone mimics

Table 1.2.1 Larvicides and their mode of action based on the current Insecticide Resistance Action Committee (IRAC) classification scheme

Target site (Mode of Action)	Chemical class	IRAC class	Insecticide
Acetylcholinesterase	Organophosphate	1A	Chlorpyrifos, Fenthion, Pirimiphos-methyl, Temephos
Juvenile hormone (JH) mimic	JH analogues	7A	Methoprene
	Pyriproxyfen	7C	Pyriproxyfen
Chitin biosynthesis	Benzoylureas	15	Diflubenzuron, Novaluron
Microbial disruptors of insect midgut membranes	Biopesticide	11A	*Bacillus thuringiensis israelensis*

1.2.2. Common pyrethroids and transfluthrin

Until 2017, pyrethroids were the only class recommended for use in ITNs by the WHO. In 2013 two thirds of IRS formulations contained pyrethroids, today 78 % of certified IRS formulations contain pyrethroids (Hemingway et al., 2016; WHO, 2022b) and 82 % of all certified space sprays (WHO, 2022b). New insecticides have been approved for the use in bed nets, however, all are combined with a pyrethroid (Figure 1.2.1) (WHO, 2022a). Since the 1980s, the percentage of pyrethroids in global insecticidal market sales (inclusive of agriculture) has remained between15-20 % (Sparks and Lorsbach, 2017) with a market value of ~$2.6 billion in sales in 2017 (Sparks et al., 2019).

Pyrethroids bind to the voltage gated sodium channel (VGSC), which causes a prolonged opening of the VGSC with an enhanced influx of sodium-ions (Soderlund, 2020). The VGSC comprises a pore-forming alpha subunit that consists of four homologous domains (I-IV). Each domain has six transmembrane segments (S1-S6) (Figure 1.4.1) (O'Reilly et al., 2006). As insecticide binding sites domain II and domain III were identified (O'Reilly et al., 2006; Usherwood et al., 2007; Vais et al., 2003). Synthetic pyrethroids are based on pyrethrins, naturally occurring compounds originating from plants of the chrysanthemum genus and first discovered in 1967 (Elliott et al., 1967). In the 1970s and 1980s many structurally different pyrethroids were developed and introduced into the vector control market (Khambay and Jewess, 2010) (Figure 1.2.1). Pyrethroids are classified as IRAC group 3 and are divided into type I, lacking the alpha-cyano substituent (e.g., permethrin or transfluthrin) and type II pyrethroids, such as deltamethrin or alpha-cypermethrin (Soderlund, 2020). Pyrethroids are widely used in vector control applications due to the following characteristics: firstly, pyrethroids are fast acting, which

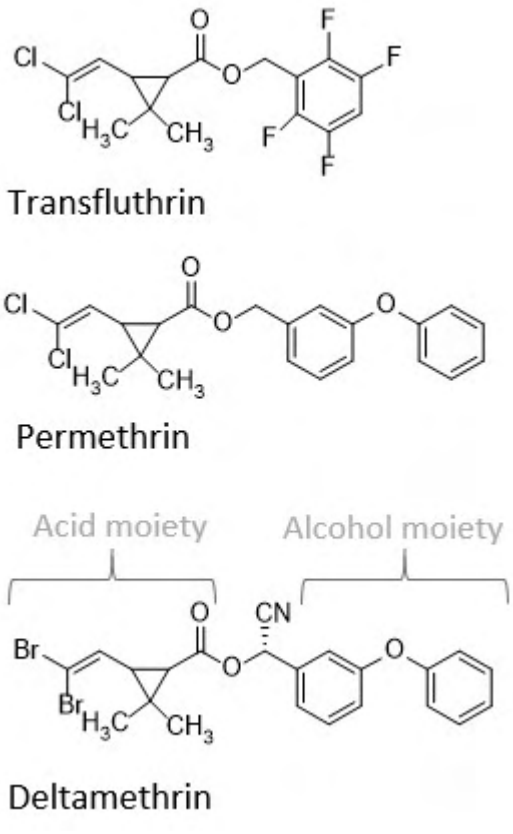

Figure 1.2.2 Chemical structure of transfluthrin, permethrin and deltamethrin

makes them good insecticides towards mosquitoes, which are often in contact for only a few seconds with the insecticides (Parker et al., 2015; Spitzen et al., 2014). Secondly, pyrethroids have high contact-efficacy, important in vector control products such as ITNs where the major uptake route is via tarsae. Thirdly, they are highly toxic towards insects (deltamethrin LC_{50} 0.02 mg kg^{-1} applied to *Musca domestica*) with low toxicity towards mammals (deltamethrin LC_{50} approximately 100 mg kg^{-1} applied orally to rats) (Davies et al., 2007; Khambay and Jewess, 2010; Pulman, 2011).

Synthetic pyrethroids contain an acid- and alcohol moiety (Figure 1.2.2) (Silvério et al., 2009) and can have multiple enantiomeric structures, i.e. R/S configuration and cis/trans isomers (Casida et al., 1983; Khambay and Jewess, 2010; Soderlund and Casida, 1977). Deltamethrin and permethrin are the most commonly used pyrethroids in vector control applications. 19 % of current approved IRS, 27 % of space sprays and 41 % of ITN use permethrin or deltamethrin alone or in combination with other insecticides (WHO, 2022b). Both pyrethroids contain a phenoxybenzyl-moiety, whereas the acid moiety in permethrin is substituted with chlorine and in deltamethrin with bromine (Figure 1.2.1). Deltamethrin is used in its cis-deltamethrin configuration, whereas permethrin is most commonly a racemate with certain cis- and trans-proportions (Soderlund and Casida, 1977).

The polyfluorinated volatile pyrethroid transfluthrin (2,3,5,6-tetrafluorobenzyl(1R,3S)-3-(2,2-dichlorovinyl)-2,2-dimethylcyclo-propanecarboxylate; syn. Benfluthrin) was invented in 1996 and is suggested to be less affected by xenobiotic metabolism than common pyrethroids, such as permethrin and deltamethrin (Horstmann and Sonneck, 2016). Horstmann and Sonneck (2016) postulated that transfluthrin is protected by fluorination of the sites exposed to P450 oxidation on the benzene-ring structure. In their study they included the non-fluorinated derivative of transfluthrin and found lower toxicity towards the pyrethroid-resistant *An. funestus* FUMOZ-R strain and higher synergism in comparison to transfluthrin with the synergist piperonylbutoxide (PBO). However, bio efficacy comparisons to a susceptible *An. funestus* FANG strain were lacking. A series of transfluthrin derivatives have been produced in Bayer with different patterns of fluorination. These have been used to evaluate their toxicity towards the pyrethroid resistant FUMOZ-R strain and the susceptible *An. funestus*

FANG strain and tested their binding affinity at the VGSC to elucidate their toxicity at the target.

In comparison to permethrin, transfluthrin is used in an enantiomerically pure form. Due to its volatility transfluthrin exhibits spatial repellent activity against mosquitoes and is used in several complementary vector control applications, such as mosquito coils, eave ribbons or sandals (Bibbs et al., 2018; Kline and Urban, 2018; Masalu et al., 2020; Ogoma et al., 2014, 2012b; Swai et al., 2019).

1.2.3. Insecticidal bednets

Insecticide treated bednets (ITN) target endophilic and endophagic adult mosquitoes and offer protection as a barrier to protect a sleeping person and through the insecticidal activity (Pryce et al., 2018). Bednets can reduce the number of mosquitoes through their insecticidal effect and provide both personal and community protection (Hawley et al., 2003). In recent decades a scale up of bednet distribution has occured. In 2020, 229 million ITNs were delivered to malaria endemic countries (WHO, 2021), resulting in 65 % of households in SSA having at least one ITN, whereas in 2000 only 5 % of households owned an ITN (WHO, 2021). In the year 2000 pyrethroid resistance in malaria vectors was rarely detected now it is endemic across Africa (Ranson and Lissenden, 2016; Riveron et al., 2018; WHO, 2018). Currently three different types of bednets are distributed. These include pyrethroid-only nets that accounted for 75.4 % of all nets distributed in 2020, two types of “next-generation-nets” that contain the P450-inhibitor piperonylbutoxide (PBO) or a second active ingredient (a.i.), such as chlorfenapyr or pyriproxyfen. Both, pyrethroid/PBO nets and pyrethroid/2nd a.i. nets have been proven to control pyrethroid-resistant *Anopheles*-mosquitoes in high pyrethroid-resistant areas (N’Guessan et al., 2010; Ngufor et al., 2020; Tungu et al., 2021).

1.2.4. Synergism in vector control

Synergist is defined as a compound used in combination with insecticides which enhance the killing effect of the insecticide and do not exhibit toxicity to the target if applied alone. There are different modes of insecticide synergism. Most of them including the inhibition of enzymes involved in the metabolism of the target insecticide. PBO inhibits mainly P450 monooxygenases (Casida, 1970; Feyereisen, 2015; Hodgson and Levi, 1999) and has been

shown to synergise pyrethroids in *An. funestus* (Brooke et al., 2001) and in *Ae. aegypti* (Cataldo et al., 2020). On top of the inhibition of P450s, it was demonstrated to inhibit resistance related esterases in *Helicoverpa armigera* and in *Aphid gossypii* and *Myzus persicae* (Gunning et al., 1998).

In general, the use of synergists in laboratory or field assays provides evidence of the involvement of enzymes in the detoxification process of a certain insecticide and including PBO in bednets for malaria control is used to overcome pyrethroid-resistance issues.

There is evidence that PBO-nets effectively control pyrethroid resistant *Anopheles* mosquitoes under field conditions in rural SSA (Corbel et al., 2010; Hien et al., 2021; Matowo et al., 2022; Menze et al., 2020; Toe et al., 2018). However, there is only one randomized control trial (RCT) available that has investigated effects on malaria transmission. It was found that PBO-nets can offer protection against malaria transmission where pyrethroid-resistant malaria vectors are prevalent (Gleave et al., 2018; Protopopoff et al., 2018). In 2017, the WHO recommended the use of PBO-nets in areas with intermediate level of pyrethroid resistance in *Anopheles*-vectors (WHO, 2017).

It is noteworthy, that some pro-insecticides such as chlorfenapyr or organophosphates are transformed via P450s to their active and toxicological relevant forms, hence the application of P450 inhibitors combined with pyrethroids to enhance their efficacy can have the reverse effect of decreasing the efficacy of pro-insecticides.

To date PBO is the only synergist used in agriculture and vector control applications (WHO, 2022b). A recent study has shown PBO nets to have reduced efficacy in high-pyrethroid resistance areas (Riveron et al., 2019), flagging an over-reliance on a single synergistic compound for vector control. Expanding the chemical range of synergists that target P450s is needed to protect the long-term use of pyrethroids, and other insecticides exposed to metabolic resistance. Synergistic effects of other compounds have been studied in honey bees, with neonicotinoids and pyrethroids combined with fungicides *in vivo* (Iwasa et al., 2004; Pilling and Jepson, 1993) and *in vitro* (Haas et al., 2021; Haas and Nauen, 2021). Against recombinant *An. gambiae* CYP6Z2, azole fungicides such as ketoconazole show inhibition in

the micromolar range (McLaughlin et al., 2008). Azole-fungicides are known to inhibit the 14-demethylase (CYP51), a fungal P450-enzyme involved in the ergosterol biosynthesis (Nakata et al., 1991; Ortiz De Montellano, 2018). This thesis aims to explore the potential of azole fungicides to synergise pyrethroids in bioassays towards highly pyrethroid resistant *An. funestus* mosquitoes and evaluate their inhibition potential towards recombinantly expressed *An. funestus* P450s. Considering the urgent need of new insecticides for the vector control market, synergists might help to fill this gap and assist to overcome insecticide resistance challenges.

1.2.5. Indoor residual sprays (IRS)

Indoor residual sprays (IRS) are applied on the walls of houses to target endophilic and endophagic adult mosquitoes and to repel mosquitoes from entering the house. Until the introduction of the neonicotinoid clothianidin into the vector control market in 2017 IRS relied on two modes of actions: pyrethroids and DDT targeting the VGSC and carbamates and organophosphates targeting the acetylcholinesterase (AChE).

For the successful implementation of IRS applications trained technicians are needed to apply the IRS, while expensive spraying-equipment and complex infrastructure and operational management of resources are needed. Hence, in comparison to the distribution of bednets, IRS application are expensive and resource heavy. IRS alone and in addition to bednets has been shown to reduce vector abundance (Sinka et al., 2016) and malaria infections (Katureebe et al., 2016; Kleinschmidt et al., 2009; Pluess et al., 2010; Pryce et al., 2022; Sherrard-Smith et al., 2018). However, the evidence-base and the success of this intervention mainly rely on the local setting e.g., vector abundance, malaria prevalence and resistance status of mosquitoes.

1.2.6. Space spraying

Space spraying is mainly an outdoor application conducted manually with hand carried space sprayers or applied using trucks or airplanes. It can be applied as thermal fogs or cold aerosols and targets adult exophilic and exophagic mosquitoes, therefore predominantly used against *Aedes* sp. It is often used in the early stages of arboviral outbreaks to reduce infection

numbers, although the effectiveness of space spraying interventions is still unclear due to limited evidence (Bowman et al., 2016).

Indoor space-spraying is also recommended in areas not accessible with vehicles. Eighty-two percent of all space sprays contain pyrethroids alone or in combination with PBO, neonicotinoids or a butanolide (WHO, 2022b). Space spraying can be an efficient tool to quickly react to urgent outbreaks of vector-borne diseases, however, they are costly and should be considered based on environmental consequences (WHO, 2006). Most malaria interventions are conducted indoors, however outdoor applications can reduce "residual malaria" in settings where malaria is also transmitted by outdoor-active *Anopheles* mosquitoes (WHO, 2006). There is evidence that indoor interventions may lead to a shift from exophilic to exophagic *Anopheles* species (Killeen and Moore, 2012; Sinka et al., 2016).

1.2.7. Larvicides

Larvicides are applied to breeding sites of mosquito vectors to target the developing stages of mosquitoes. Chemicals or microbial treatment using *Bacillus thuringiensis* spp. (*Bti*) can be used that offer a broader range of mode of actions (Table 1.1). For malaria control larvicides are recommended as a complimentary intervention with bednets and IRS in areas where breeding sites are accessible (WHO, 2006). Bti larviciding has been shown to reduce female malaria vector abundance in rural Burkina Faso by 70 % if all breeding sites were treated (Dambach et al., 2019).

1.2.8. Other vector control interventions

For indoor active mosquitoes such as *An. funestus* improved housing that prevents mosquito entry has been shown to reduce malaria transmission (Kua and Lee, 2021; McCann et al., 2021). Another method, larval source management with the aim to remove breeding sites is also proven to reduce malaria transmission (McCann et al., 2021).

There are also a variety of insecticide treated materials that protect humans by killing adult mosquitoes by contact or through a repellent effect. These include chairs (Masalu et al., 2020), insecticide treated clothes (Banks et al., 2014), hammocks (Sochantha et al., 2010) or topically applied insecticides to livestock (Ruiz-Castillo et al., 2022). Livestock can also be

treated with endectocide, such as ivermectin or fipronil to target zoophagic *Anopheles* vectors (Ruiz-Castillo et al., 2022).

Eave ribbons, treated with transfluthrin that produce a barrier for mosquitoes to enter houses, have been shown to prevent mosquito bites (Kaindoa et al., 2021; Mwanga et al., 2019). All these approaches are either new to the market or under development and are considered as complementary tools against mosquitoes. Furthermore, evidence to which extent they reduce risk of malaria transmission needs to be evaluated.

Repellent approaches may also be considered that includes using volatile insecticides or non-insecticidal substances in mosquito coils or emanators (Ogoma et al., 2012a), or topical repellents, such as DEET or picaridin, which applied to the skin that offer short-term protection against mosquito bites (Goodyer and Schofield, 2018; Grant et al., 2020).

The mass release of genetically modified (GM) mosquitoes, in particular *Aedes*-mosquitoes are under current development. Mosquitoes are radiation- or chemo-sterilized (sterile insect technique SIT) (Oliva et al., 2021), which leads to reduced reproduction and a decrease of the populations, which has been tested under field conditions (Zheng et al., 2019). *Wolbachia* induced cytoplasmic incompatibility (IIT) also leads to reduced reproduction and supressed population (Zabalou et al., 2004).

A promising vector control tool is the use of attractive targeted sugar baits (ATSB), which consists of a sugar-lure that attracts male and female mosquitoes, and an insecticidal component. A major benefit of this approach is that it selectively targets mosquitoes, thus minimises off-target species effects (Fiorenzano et al., 2017). ATSBs can be applied as sprays to plants or in the form of a membrane -pouch placed inside or outside houses. In contrast to other vector control interventions that rely on cuticular uptake, ATSBs are ingested, this offering a greater range of insecticidal compounds. ATSBs are complementary interventions which might help in the fight against residual malaria. In a field study in Florida ATSB was shown to reduce abundance of several mosquitoes, including *Anopheles crucians* by 62 % (Qualls et al., 2014). A two-year field study in Mali also demonstrated a reduction in female *Anopheles* density by 19.8 % to 57.4 % depending on the season and catching method (Qualls et al., 2014; Traore et al., 2020). In a further study in Mali, it was shown that ATSB control *Anopheles* mosquitoes quickly enough, so they cannot develop the infective *Plasmodium* life

stage and therefore, malaria transmission is reduced by 30 % based on predictive modelling (Fraser et al., 2021).

1.3. Pyrethroid/Xenobiotic metabolism in mosquitoes and insects with special focus on P450 monooxygenases

Metabolism of xenobiotics is a three phased process that involves: oxidation, reduction, or hydrolysis of the parent compound, generally by P450s and non-specific carboxylesterases (CE) to produce a more solvent compound (phase I), followed by excretion or conjugation to glucuronic acid, sugars, amino acids or glutathione (Phase II) and excretion (Phase III) by ABC transporters (Amezian et al., 2021).

The most commonly used pyrethroids in vector control applications are permethrin, deltamethrin and alpha cypermethrin that contain a 3-(2,2-dihalovinyl)-2,2-dimethylcyclopropanecarboxylic acid- moiety and (alpha-cyano-) 3-phenoxybenzyl moiety, respectively (Figure 1.2). The phenoxybenzyl-moiety is primarily hydroxylated at the 4'para-position, however, hydroxylation of 2- and 6' position has been reported for permethrin in mice and rats and 2' and 5' position for cyper- and deltamethrin, respectively in mammals (Casida and Ruzo, 1980; Shono et al., 1979). It has also been shown that the hydroxylation pattern of cis- and trans permethrin differ in mammals and houseflies (Shono et al., 1979), hence in this thesis we investigated the different toxicological profiles of cis and trans permethrin towards susceptible and resistant An. funestus mosquitoes and also evaluated their metabolism by recombinantly expressed CYP6P9a and CYP6P9b.

In insects, oxidation of the 4'para position on the phenoxybenzyl ring is one of the primary targets of P450 metabolism of pyrethroids such as permethrin and deltamethrin (Kasai et al., 2014; Stevenson et al., 2011; Zimmer et al., 2014).

Oxidation of the geminal dimethyl group, ester- and ether cleavage, as well as cascaded metabolism of the metabolites can also occur (Stevenson et al., 2011). Stevenson et al. (2011) found that 4'OH deltamethrin is further oxidised to cyano-(3-hydroxyphenyl) methyl deltamethrate by *An.gambiae* CYP6M2 following ether cleavage. Apart from CYP6M2 and deltamethrin, there have been surprisingly few studies that have characterised the products pyrethroid metabolism by mosquito P450s, or if 4'OH metabolites are commonly further metabolised, e.g., the type I pyrethroid permethrin or other structurally different pyrethroids.

This has been addressed in this thesis through the analysis of pyrethroid metabolism by CYP6P9a and b.

Given the increasing use of transfluthrin as a volatile insecticide, it is important to establish whether this molecule is susceptible to P450 metabolism. Transfluthrin is hydrolysed in rat studies, suggesting it could be susceptible to mosquito P450 metabolism (Yoshida, 2013, 2012). Although most potential sites of metabolism on the phenoxybenzyl ring are protected by fluorine groups, it lacks a fluorine at the 4' para position (Figure 1.1.1.1), thus potentially vulnerable to P450 metabolism.

1.3.1. Cytochrome P450 monooxygenases

P450 monooxygenases (P450s) are a diverse superfamily of mostly membrane-bound enzymes involved in the oxidation of a broad range of endogenous and exogenous substrates that play an important role in xenobiotic metabolism in most organisms (Ortiz De Montellano, 2005). P450 enzymes are divided into two classes, type I and type II. Type I involve bacterial and mitochondrial P450s which have NAD(P)H-ferredoxin reductase and ferredoxin partners and type II P450s, which are eukaryotic, bound to the endoplasmic reticulum and receive electrons from NADPH cytochrome P450 reductase (CPR) and include microsomal P450s (Paine et al., 2005). P450s are heme-thiolate proteins with a heme molecule bound to the thiolate group of a conserved cysteine residue, acting as monooxygenases by inserting a molecule of oxygen into their substrates (Dermauw et al., 2020). P450s in insects and mosquitoes have mainly evolved by gene duplication and subsequent diversification. However, neofunctionalization and death i.e. pseudogenization or deletion also play a role in P450-evolution (Dermauw et al., 2020; Feyereisen, 2011).

CYP genes are classified in CYP clans (Nelson, 1998). Arthropods have six CYP clans. The majority of the CYPs belong to the CYP2, CYP3, CYP4 and mitochondria clans. Most recently CYP16 and CYP20 clans have been identified, in which a minority of arthropodal CYPs are represented, i.e. 0.2 % of P450 sequences are presented in the CYP16 clan in a study which compared 40 arthropod sequences and 0.7 % in clan 20 (Dermauw et al., 2020). In insects the CYP16 clan is only present in the *Archaaeognatha* and *Zygentoma* species and the CYP20 clan is found in *Archaeognatha*, *Zygentoma*, *Odonata* and *Ephemeroptera* (Dermauw et al., 2020). The CYP3 clan comprises the CYP6 and the CYP9 families, which are often associated with an

enhanced insecticide metabolism in insects and mosquitoes (Feyereisen, 2019; Nauen et al., 2021; Vontas et al., 2020). The total number of CYP genes in an organism is defined as the CYPome (excluding pseudogenes). The arbovirus vector *Ae. aegypti* has 160 CYP genes (Strode et al., 2008), the malaria mosquitoes *An. gambiae* and *An. funestus* have 105 CYP genes (Ranson et al., 2002; Ghurye et al., 2019). In comparison to other insects, the CYPome of mosquitoes are large, for example the honey bee *Apis mellifera* has 46 CYP genes and *D. melanogaster* has 88 CYP genes (Feyereisen, 2019). The human CYPome consists of 57 CYP genes and 46 pseudogenes (Poulos, 2003).

Eukaryote P450s can be located in both mitochondrial membranes and the endoplasmic reticulum. In bacteria P450s are also found in soluble forms. P450s are generally isolated in the microsomal fraction of cell homogenates follow ultracentrifugation of 100 000 g. Microsomes are a very crude mixture of ER membranes and other cellular material.

Microsomal preparations are a useful tool to investigate P450-activity in organisms. Single P450s are difficult to functionally characterise as they are membrane bound and require cytochrome P450 reductase (CPR) to function. However, they have been functionally expressed in *E.coli*, yeast with CPR co-expression, or baculovirus system with a final expression in insect cells by co expression with CPR. This provides the means to characterise enzyme-substrate interactions, with numerous insect P450s shown to metabolise insecticides. In order to establish phenotypic effects, transgenic over expression or gene knockouts can be used, but are difficult in mosquitoes. However, transgenic expression in *D. melanogaster* is relatively easy and successfully used (Vontas et al., 2020).

The expression of P450s in *E.coli* is a time- and cost efficient method of recombinant expression in comparison to baculovirus and yeast expression and most importantly, *E. coli* lacks endogenous P450 activity (Nauen et al., 2021). However, one drawback of *E. coli* expression is that this system does not offer post translational modifications, which is arguable as P450s are not generally post-translationally modified (Nauen et al., 2021). Most recombinantly expressed P450s from mosquitoes are expressed in *E. coli* membranes, and from the malaria mosquito *An. funestus* to date no P450 was expressed using baculovirus expression system (chapter 3, table 1) As this study focused primarily on P450s from *An.*

funestus we were interested to determine if expression in baculovirus could be successfully conducted and if differences in e.g., pyrethroid metabolism can be observed.

Camphor hydrolysing P450 from *Pseudomonas putida* (P450cam) is a soluble P450 (i.e. no membrane anchor) which was easily produced and purified, hence it was the first P450 to be crystallized and the secondary/ tertiary structure mapped into substrate recognition sites (SRS) (Poulos et al., 1987). In 1993 for the first-time high quantities of bovine P450C17 in *E. coli* were produced, which paved the way for the production of eukaryotic P450s (Barnes et al., 1991; Sagara et al., 1993). The first mammalian crystalized structure was rabbit CYP2C5 in 2000 (Williams et al., 2000). However, the most important advance was the crystallisation of human CYP3A4, which is the most important human drug metabolising enzyme since it metabolises ~ 50 % of all drugs (Williams et al., 2002) and accounts for 29 % of the total P450 content in humans (Paine et al., 2006). Since it has a promiscuous active site, it is the best template for producing structural models of pyrethroid metabolising P450s, which tend to have a broad substrate range.

P450s generally consist of 13 helices, which are named in alphabetical order (A-L). They contain five conserved regions or "P450 motifs" that structurally define a P450s s. The first or C-Helix motif WxxxR, the second motif GxE/DTT/S, the third motif ExLR, the fourth or PERF motif PxxFxPE/DRF and the fifth motif PFxxGxRxCxG/A, which contains the conserved cysteine residue which forms the heme is thiolate bond. However, not all motifs need to be present in a certain P450 enzyme. The last motif with the highly conserved cysteine is part of the so called heme binding loop which is also considered as the P450 signature sequence. Microsomal P450s also have in common a lipophilic membrane anchor at the N-terminal of the enzyme which is responsible for the for the binding to the endoplasmic reticulums. Helix F, helix G and the F/G loop form the access channel for substrates to the active heme site of the P450s (Feyereisen, 2019; Poulos, 2003).

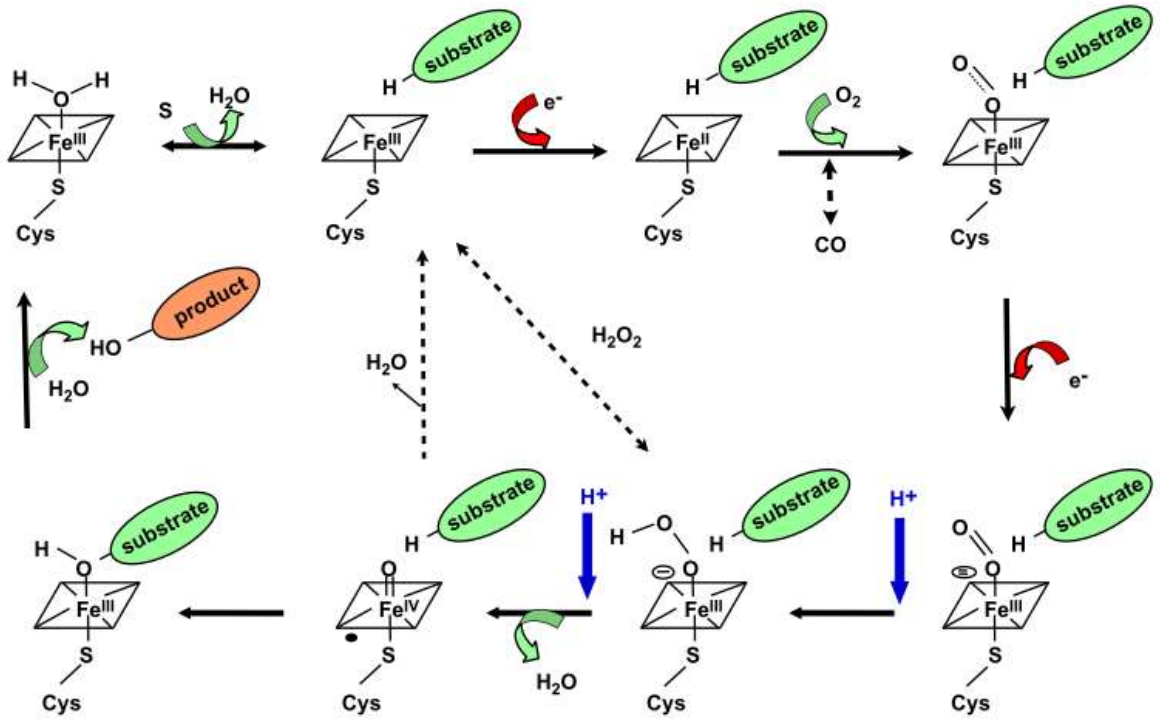

Figure 1.3.1 Catalytic cycle of P450 enzymes in monooxygenase reactions, adapted from Feyereisen, R. 2019

In general, the reaction conducted by P450s can be described as:

$RH + O_2 + 2e^- + 2H^+ \rightarrow R\text{-}OH + H_2O$ (Poulos, 2003).

A water molecule is bound to the Fe-molecule. In this state, iron is present in its ferric (Fe^{III}) form. Substrate binding removes the H_2O molecule bound to Fe^{III} and lowers the redox potential (~100 mV), enabling the transfer of an electron from NADPH via CPR, in the case of microsomal P450's. This reduces the iron to its ferrous (Fe^{II}) form, which binds O_2. Following the transfer of a second electron to the P450-substrate-O_2 complex by CPR or presumably cytochrome b5, the iron is oxidized to its ferric form to form a peroxide-anion. One molecule of oxygen is reduced to H_2O and the other forms a reactive Fe^{IV}=O product, which abstracts the hydrogen-atom from the substrate-RH complex, leading to a substrate-R radical abstracts the OH-functional group leading to a substrate-OH product, which is released (Figure 1.3.2) (Feyereisen, 2019; Ortiz De Montellano, 2005). P450 enzymes can also bind CO to form a stable P450-CO complex that produces an absorbance peak at 450 nm. This state can be photometrically determined to confirm P450 activity and to determine the quantity of contained P450 enzymes (Guengerich et al., 2009).

Substrates entering the active site of P450s are recognized by the so-called substrate recognition sites (SRS) SRS1- SRS6, based on (Gotoh, 1992). A numerous studies of insect P450s characterized residue changes within SRS as being key determinants towards xenobiotic metabolism and substrate septicity. In *Anopheles gambiae* CYP6Z1 and CYP6Z2 differences in SRS 1, SRS 2 and SRS 4 contributing to the fact that CYP6Z1 is capable of metabolizing DDT, whereas CYP6Z2 is not (Chiu et al., 2008). In a broad study with different CYP6ER1-variants from brown plant hopper *Nilaparvata lugens* a serine at position 318 in SRS 4 contributed to faster imidacloprid metabolism (Zimmer et al., 2018). Based on 3D modelling, it was shown that xanthotoxin binds differently into the active site of CYP6B1 from *P. polyxenes* and CYP6B3 based on six different residues in all six SRS. Xanthotoxin metabolism was decreased in CYP6B3, but furanochromones metabolism was increased, again highlighting the importance of the residues in the SRS (Schuler and Berenbaum, 2013; Wen et al., 2006). In the cotton bollworm *Helicoverpa armigera* CYP6AE subfamily sharing high sequence identities and single residues of SRS 1 and SRS 6 were identified likely being responsible for differences in metabolic activities towards xenobiotics, but also a substitution in SRS4 of valine to isoleucine is present in the variants with higher metabolic activity (Shi et al., 2020). In human CYP2A1 and CYP2A2 substitutions in SRS 4 leading to higher hydroxylation rates and residues 318 and 319 in CYP1A2 mutants changed catalytic parameters towards ethoxy-coumarin O-de-alkylation (Hanioka et al., 1992; Hiroya et al., 1994). In *An. funestus* two duplicated P450s are commonly associated with pyrethroid resistance: CYP6P9a and CYP6P9b. Both consist of 509 amino acid residues and share 94.3 % sequence identity, differing in 29 residues. Six of these are located on SRS's associated with substrate binding and metabolism, of which only one differs in SRS4: residue 310. CY6P9a contains an isoleucine and CYP6P9b a valine in this position, which is located close the heme centre where it could potentially influence substrate binding. Interestingly, this matches a polymorphism in a wild pyrethroid resistant *An. funestus* population from Benin, although the effect on pyrethroid metabolism has yet to be investigated (Ibrahim et al., 2015).

Although there has been increasing interest towards insect P450s and their xenobiotic-metabolism in crop pests, pollinators, and insect vectors within the last decades, to date no insect P450 was crystalized, hence 3D-analysis of P450 protein structure relies on homology

models retrieved from mammal P450 structures such as rabbit CYP2C5 (Williams et al., 2000) or human CYP3A4.

1.3.2. Cytochrome P450 reductase

Cytochrome P450 reductase is a dual flavin reductase containing FAD, FMN and NADPH binding domains, and located in the ER (Murataliev and Feyereisen, 1999). The major function of CPR is to act as a transformer to accept two electrons from NADPH and transfer a single electron to P450 via a series of electron transfer reactions from FAD to FMN and into the P450 active site (Gutierrez et al., 2003; Murataliev et al., 2004). CPR is generally encoded by a single gene in most organisms including insects (Feyereisen, 2019). The FMN and FAD domain architecture in CPR is highly conserved, thus CPRs can generally interact with P450s across species (Feyereisen, 2019).

In mammals CPR has been shown to be involved in several essential functions, such as the biosynthesis of retinoic acid, sterols, prostaglandins, and steroids which are dependent on P450 catalysis (Paine et al., 2005). Most notably, CPR is the redox partner for heme-oxygenase and P450 monooxygenases (Porter, 2012). Furthermore, it has a role in heme-detoxification and potentially reproduction in mosquitoes (Spencer et al., 2018). *Anopheline* CPR was first characterised in 2011 using *E.coli* expression system (Lian et al., 2011). In some cases, CPR silencing approaches with RNAi, antibodies, or gene-knockout, offering evidence about the function and involvement of the CPR in the respective P450 substrate metabolism pathway or a certain function. For example, recombinant expression of P450s with a RNAi-silenced CPR is decreasing its metabolic activity, as seen in *L.migratoria* towards ethoxcoumarin metabolism (Jiao et al., 2020). RNAi knockout of CPR in *Tetranychus urticae* increased susceptibility to acaricides, abamectin, bifenthrin and fenpyroximate (Adesanya et al., 2020) and RNAi treatment of CPR in resistant *Cimex lectularius* increased suscebtibilty towards deltamethrin (Zhu et al., 2012). Knockout of CPR in *An. gambiae* increased toxicity of permethrin (Lycett et al., 2006), indicating the vital role of CPR in P450 metabolism and suggesting the CPR as a potential target to restore susceptibility in metabolic resistant *An. gambiae* populations. Houseflies treated with antibodies to inhibit CPR function can lead to an inhibition of P450 reactions, such as O-de-alkylation (Feyereisen and Vincent, 1984).

Removal of the germline of CPR in embryos of mice was lethal, highlighting its essential role (Shen et al., 2002).

CPR is crucial for P450 metabolism to transfer electrons from NADPH to the P450-substrate complex, thus inclusion in recombinant P450 expression systems is required. In most recombinant expression systems for mosquitoes *An. gambiae* or *M. domestica* CPR is used, even for recombinant P450 proteins from *An. funestus* (Chapter 3, table 1). However, there are some studies indicating higher metabolic activity if the species-respective CPR is used (Nauen et al., 2021). For a functioning in-vitro system a correct ratio of P450:CPR is necessary. Naturally the ratio in insect microsomes of all P450 to CPR is about 6-18 to 1 (Feyereisen, 2019). This thesis for the first time is recombinantly expressing *An. funestus* CYP6P9a and CYP6P9b using baculovirus expression with co-expression of *An. gambiae* CPR and *An. funestus* CPR and comparing the metabolic activity of P450 model substrates for both CPR. Furthermore, considering the high upregulation of CYP6P9a and CYP6P9b, we were interested in the expression level of the respective CPR.

The first 3D structure was rat CPR crystalized in 1997 (Wang et al., 1997) and the first insect CPR sequence was characterized in 1993 from *M. domestica* (Koener et al., 1993). The CPR from *M. domestica* comprises 671 amino acids and shares 75 % identity with *An. gambiae* CPR (Nikou et al., 2003) and 76 % identity with CPR from *An. funestus* (Matambo et al., 2010), both consist of 679 amino acids.

1.3.3. Cytochrome b_5

The role and impact of the second redox partner of microsomal P450s, cytochrome b5 (CYB5) has mainly been investigated in recombinantly expressed mammal P450 enzymes. Early studies have shown that addition of CYB5 enhanced the activity of the major human drug metabolising P450, CYP3A4 (Schenkman and Jansson, 1999). Since then, it has been shown to have varying ability to enhance P450 activity. The role of CYB5 is not clear. It may be either involved in the transfer of the second electron to P450-substrate complex, as suggested by Guzov et al. (Guzov et al., 1996) as its' reduction potential to transfer the first electron is too positive, or by allosteric interactions (Murataliev et al., 2008; Schenkman and Jansson, 2003). The germline deletion of CYB5 in mice did not lead to a lethal phenotype, hence its role might be substituted by other enzymes (Finn et al., 2011). Hepatic deletion of microsomal CYB5 in mice led to reduced metabolism of several drugs, such as midazolam, metoprolol and

tolbutamide whereas chlorzoxazone-metabolism remained unchanged (Finn et al., 2008). The knockout of CYB5 in mice resulted in a higher expression of some P450s, but the actual in-vitro and in-vivo metabolism was reduced (Henderson et al., 2014). In a crossing study of CYB5- knockout mouse with a mouse carrying the human CYP3A4 and CYP2D6 it was shown that CYB5-deletion decreased metabolic clearance of bufuralol and debrisoquine by 40-60 % (Henderson et al., 2015). A CRISPR/Cas9 knockout of CYB5 in a human hepatic cell line decreased activity of CYP2C8 dependent amidaquine N-deethylation (Heintze et al., 2021).

In insects CYB5 contribution to P450 metabolism was firstly studied in the housefly *M. domestica*, where CYB5 inhibition with anti-CYB5 antiserum in microsomal preparations led to reduced coumarin O-dealkylation but resorufin metabolism was unaffected (Zhang and Scott, 1994). In the pyrethroid resistant *M. domestica* LPR strain, the formation of 4'OH cypermethrin was inhibited if CYB5 was repressed with antibodies (Zhang and Scott, 1996). If CYB5 was co expressed with CYP6FD1 and CPR from *L. migratoria*, ethoxycoumarin metabolism was enhanced (Jiao et al., 2020). These examples reflect the divergent role of CYB5 in oxidative xenobiotic metabolism. Many mosquito P450s have been expressed, mostly using *E.coli* expression system (Vontas et al., 2020) and although CYB5 sequences from *An gambiae* (Nikou et al., 2003) and *An. funestus* (Matambo et al., 2010) are already described, the contribution of CYB5 towards xenobiotic metabolism has only been studied with CYP6M2 from *An. gambiae* (Stevenson et al., 2011), not in *An. funestus*.

The primary structure of human CYB5 comprises 134 amino acids and shares 44.5 % similarity with *An. funestus* CYB5 (128 amino acids). To investigate the influence of CYB5 towards recombinantly expressed P450, it can either be co expressed with P450 and CPR or added exogenously to the reaction. The majority of studies using *An. gambiae* P450s co-expressed with *An. gambiae* CPR in *E. coli* have resulted in augmented insecticide metabolism with *An. gambiae* CYB5 (Chapter 3, table 1). There have been fewer mosquito P450s expressed using baculovirus systems. These include CYP6Z1, CYP6Z2 from *An. gambiae* (Chiu et al., 2008), CYP6AA3 (Boonsuepsakul et al., 2008) and CYP6P7 (Duangkaew et al., 2011) from *An. minimus*, of which only CYP6Z1and CYP6Z2 were co expressed with *M. domestica* CPR and *D. melanogaster* CYB5. For *An. gambiae* CYP6M2 expressed in *E.coli* an enhanced deltamethrin metabolism was shown if CYB5 was added to the reaction (Stevenson et al., 2011). This thesis

aims to determine if CYB5 is upregulated in highly pyrethroid resistant *An. funestus* FUMOZ-R mosquitoes and to what extent addition of CYB5 can help to enhance deltamethrin metabolism of *An. funestus* CYP6P9a and CYP6P9b expressed using baculovirus-expression.

1.4. Pyrethroid resistance in *An. funestus*

Insecticide resistance is the ability of insects to survive exposure to a standard dose of insecticide based on physiological or behavioural adaptions (WHO, 2018). The invention of DDT, carbamates and organophosphates from the 1940s to the 1960s and their intensive use has led to exponentially increasing resistance in crop pests and disease vectors (Sparks et al., 2019; Sparks and Nauen, 2015). Frequent and continuous use of an insecticide over a long period leads to a natural selection of pre-adapted mosquitoes carrying resistance genes, which can survive and pass them to their offspring (IRAC, 2016). In mosquitoes, resistance has been reported towards the four major insecticidal classes DDT, organophosphates, carbamates and pyrethroids, (Hancock et al., 2020; Hemingway et al., 2016; Moyes et al., 2017; WHO, 2018). Resistance has already been reported for new insecticides in the vector control market, such as clothianidin (Fouet et al., 2020), which may have been primed by their previous agricultural use. The relationship between the use of insecticides in agriculture and the evolution of insecticide resistance in mosquitoes is unclear and an important consideration in the use of vector control products (Nkya et al., 2014).

The WHO considers insecticide resistance in mosquitoes in three different ways; the evidence of phenotypical resistance, the underlying mechanism of resistance and the impact on vector control interventions or epidemiological evidence of resistance. Phenotypical resistance in field-mosquitoes is commonly measured according to WHO standard protocols. These include using either a WHO susceptibility assay with defined discriminating doses, in which 24 h mortality is assessed, or the CDC bottle assay with diagnostic doses is used and incapacitation of mosquitoes evaluated post exposure (WHO, 2022c, 2018).

Cross resistance is the phenomenon that occurs if an insect is resistant to more than one insecticide based on the same resistance-mechanism (IRAC, 2021). This case is reported for example for DDT and pyrethroids (Davies et al., 2008) or carbamates and organophosphates (Ahoua Alou et al., 2010), which share the same mode of action (WHO, 2018). Another reason

for cross resistance occurs if the insecticides are processed by the same enzyme e.g., CYP6M2 (Lees et al., 2020; Yunta et al., 2019, 2016).

Most vector control applications use pyrethroids (see 1.2.1), and their escalating use in a wide range of different vector control applications has led to the selection of alleles conferring pyrethroid resistance. Pyrethroid-resistance is a major threat to current vector control programmes impacting the efficacy of vector control products such as bed nets or IRS (Hemingway and Ranson, 2000; Kleinschmidt et al., 2018; Moyes et al., 2017; Ranson et al., 2011; Ranson and Lissenden, 2016). Between 2010 and 2016, 61 of 76 malaria endemic countries have reported insecticide resistance towards at least one insecticidal class, and in Africa 78.2 % of tested sites have reported resistance towards pyrethroids (WHO, 2018). In the past few years two major resistance mechanism against pyrethroids have emerged in mosquitoes: target site resistance with an altered VGSC (Clarkson et al., 2021; Silva et al., 2014), which leads to inefficient binding of pyrethroids and metabolic resistance (WHO, 2018). Metabolic resistance leads to enhanced metabolism of pyrethroids mainly driven by P450 enzymes, of which CYP6P3 and CYP6M2 (Adolfi et al., 2019; Müller et al., 2008; Stevenson et al., 2011) from *An. gambiae* and CYP6P9a and CYP6P9b from *An. funestus* (Riveron et al., 2014a, 2013; Weedall et al., 2019; Yunta et al., 2019) (ortholog to CYP6P3 from *An. gambiae*) are prominent examples.

1.4.1. Target site resistance at the voltage gated sodium channel (VGSC)

The intensive use of DDT from 1940 and pyrethroids in the 1970s against crop pests and disease vectors caused the emergence of the knockdown resistance (kdr) phenotype across insects (Davies et al., 2008). It was first assigned as kdr in a DDT resistant *M.domestica* strain (Milani, 1954). The molecular mechanism was described 1996 in *M.domestica* (Williamson et al., 1996) and *Bl. germanica* (Miyazaki et al., 1996): a TTG to TTC point mutation converting leucine to phenylalanine at position 1014 (*M.domestica* nomenclature, position 995 in *An. gambiae*) in the centre of the second domain in the S6 transmembrane segment of the VGSC causes a perturbation of ion transfer within the VGSC (Figure 1.3.1) (Davies et al., 2007). The kdr mutation results in a 10-20-fold decrease in efficacy of DDT and pyrethroids and is the most widespread resistance mechanism reported in insects (Hemingway and Ranson, 2000). A second mutation M918Tproduces a super-kdr phenotype with greatly increased resistance

(1000-fold) (Vais et al., 2001). Other amino acid mutations leading to pyrethroid resistance in *Anopheles* mosquitoes (Silva et al., 2014) include V1016G (Brengues et al., 2003), S989P (Srisawat et al., 2010), F1534C (Yanola et al., 2011) or N1575Y (Jones et al., 2012), I1527T and M490I (Clarkson et al., 2021) in *Aedes* and *Anopheles* mosquitoes, respectively (Silva and Scott, 2020) (Figure 1.3.1).

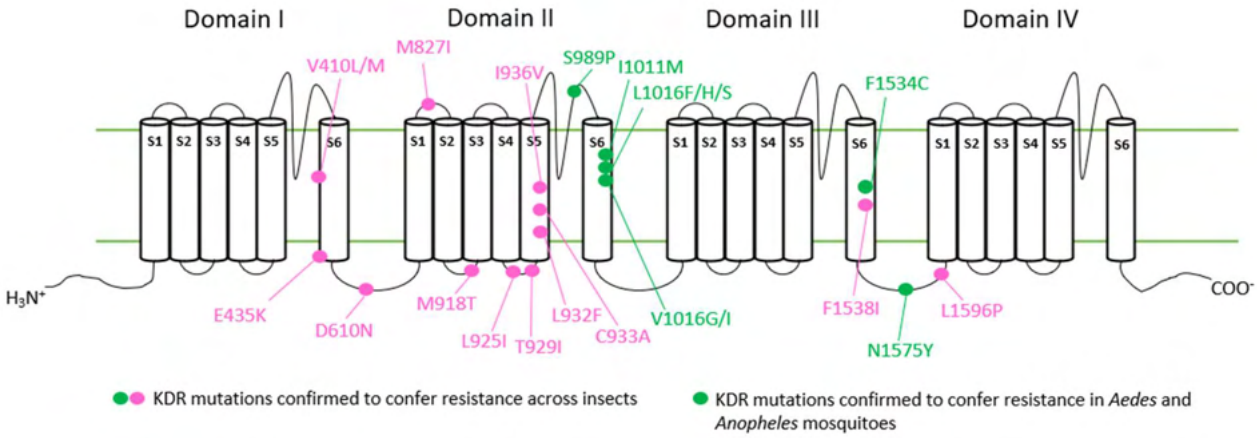

Figure 1.4.1 Schematic structure of the VGSC. Dots are indicating major KDR mutations which confer pyrethroid resistance. Green dots are major KDR found in *Anopheles* and *Aedes* mosquitoes. Nomenclature is based on *M. domestica* VGSC (Accession number: X96668.1). Modified based on Silva and Scott (2020) and Davies et al. (2007).

As yet, kdr mutations have not been reported in *An. funestus,* possibly due to restricted gene flow and high-level fitness costs (Irving and Wondji, 2017), although polymorphisms have been found in VGSC with no association towards pyrethroid resistance in *An. funestus* (I877L, V881L, A1007S, F1021C) (Irving and Wondji, 2017).

1.4.2. Metabolic resistance

Different mechanisms can lead to enhanced metabolic activity towards pyrethroids, with most associated with enhanced metabolic activity by P450s (see 1.3.2.1).

Table 1.4.2 Metabolic resistance mechanisms towards the four major class of insecticides. Green circles indicate a role in the resistance mechanism. The bigger the green circle, the bigger the influence of the respective enzymes class. Modified based on WHO (2018b).

Metabolic mechanism of resistance

	Esterases	P450s	GST
Pyrethroids	●	●	
DDT		●	●
Carbamates	●	●	
Organophosphates	●	●	

1.4.2.1. Upregulation of P450-monooxygenases

P450 mediated resistance is one of the major causes of metabolic pyrethroid resistance, mostly caused by the constitutive overexpression of one or more P450 enzymes. Other causes of enhanced pyrethroid metabolism include gene duplication or non-synonymous polymorphism in a CYP or the respective promoter (Sun et al., 2021). Historically, in mosquitoes the assessment of upregulated detoxifying enzymes started with the development of the first microarray chip in 2005 (David et al., 2005). Since then, many studies used microarrays to assess gene upregulation in mosquitoes (Müller et al., 2008; Saavedra-Rodriguez et al., 2014; Vontas et al., 2005). Nowadays the overexpression or upregulation of P450 enzymes is usually evaluated by transcriptomic analysis or RT qPCR approaches (Boaventura et al., 2021; Ibrahim et al., 2018; Ingham et al., 2018; Matowo et al., 2022; Simma et al., 2019; Wondji et al., 2022). However, the upregulation in a pyrethroid-resistant insect or mosquito strain does not necessarily indicate their capability to metabolize pyrethroids. Functional evidence for insecticide metabolism is usually assessed by recombinant expression or the incorporation of resistance candidate genes in transgenic insects (Nauen et al., 2021; Vontas et al., 2020). Several P450s associated with pyrethroid resistance in *An. funestus* have been shown to metabolize pyrethroids following *E.coli* expression: CYP6M7 metabolises permethrin, bifenthrin, λ cyhalotrin, etofenprox and deltamethrin (Riveron et al., 2014a), CYP6Z1 is capable of metabolizing pyrethroids, carbamates and resorufins (Ibrahim et al., 2016), CYP6AA1 and CYP9J11 were shown to deplete pyrethroids, carbamates, DDT and organophosphates (Ibrahim et al., 2018; Riveron et al., 2017) and CYP6P9a and CYP6P9b were

shown to metabolize permethrin, bifenthrin, λ cyhalotrin, etofenprox (CYP6P9a) and deltamethrin (Riveron et al., 2014a, 2013).

1.4.2.2. Esterases

Non-specific carboxylesterases (CE) are hydrolases for a range of endogenous and exogenous compounds such as xenobiotics or pheromones. In insects they play an important role in the detoxification of pyrethroids, carbamates or organophosphates that contain an ester, amide or phosphate bond or by sequestration (Table 1.3.2) (Karunaratne et al., 2018; Montella et al., 2012). In *Ae. aegypti* several upregulated esterases are associated with temephos-resistance (Grigoraki et al., 2016; Poupardin et al., 2014). In *An. gambiae*, COEAE8O is upregulated in pyrethroid-resistant *An.gambiae* VK7 from Burkina Faso and an M'BE strain from Cote d'Ivoire (Ingham et al., 2018). Microarray analysis has revealed the upregulation of one esterase gene in a DDT resistant *An. funestus* strain (Riveron et al., 2014b).

1.4.2.3. Gluthathione-S-transferases (GST)

GSTs are involved in the detoxification of endogenous and exogenous compounds by primarily conjugating their substrates with the thiol group of reduced glutathione (GSH), resulting in polar and excretable compounds (see 1.3.1). Their involvement in insecticide-resistance is associated with all major classes of insecticides (Enayati et al., 2005; Hemingway and Ranson, 2000), but as some GSTs dechlorinate DDT (Clark and Shamaan, 1984) their upregulation can lead to metabolic breakdown of DDT leading to-resistance in mosquitoes, reviewed in Enayati et al. (2005). For this step no GSH is needed. In microarray assays, GSTs are also found upregulated in a Nigerian field population of pyrethroid-resistant *Anopheline* mosquitoes (Awolola et al., 2009). In *An. funestus* within the GSTe2 gene a SNP L119F was shown to confer resistance towards DDT by being more efficient in metabolizing DDT than the GSTe2 wildtype. This SNP is found in *An. funestus* populations from Nigeria, Benin and Burkina Faso (Djouaka et al., 2016; Menze et al., 2016; Tchigossou et al., 2020). Furthermore, the upregulation of GSTe2 is leading to a DDT and permethrin resistant phenotype (Riveron et al., 2014b) and is found upregulated in *An. funestus* populations from Nigeria, Burkina Faso and Benin (Tchigossou et al., 2020). No association between the L119F allele and blood feeding behaviour of female *An. funestus* was observed (Nouage et al., 2020). Recombinantly expressed GSTe2 was shown to metabolize permethrin and transgenic *D. melanogaster*

carrying GSTe2 were shown to be resistant towards DDT and permethrin (Riveron et al., 2014b). Transgenic *An. gambiae* mosquitoes carrying the GSTe2 gene reported resistance towards DDT and the organophosphate fenitrothion, but not malathion (Adolfi et al., 2019). More recently, it was found that the GSTe2 gene might be associated with the parasite rate of *An. funestus* mosquitoes, however, evidence for supporting this claim is not very strong (Nouage et al., 2020).

1.4.2.4. Other pyrethroid resistance mechanisms

Other resistance mechanism in mosquitoes include cuticular resistance and reduced insecticide uptake, which is either through a thickened cuticle or a reduction in permeability (Balabanidou et al., 2018; Ranson et al., 2011). Insecticides incorporated into IRS or bednets are taken up by the adult mosquito mostly via the tarsae, hence cuticular resistance can have a big impact towards the efficacy of these interventions. In *An. gambiae*, cuticular proteins CPCLG3 and CPCLG4 have been found upregulated and associated with a thicker cuticle, which can impede insecticide uptake (Awolola et al., 2009; Vannini et al., 2014; Yahouédo et al., 2017). CYP4G16 and CYP4G17 are probably involved in the final step of the cuticular hydrocarbon synthesis (Balabanidou et al., 2016), and CPAP3-E and CPlCX1, are found upregulated following exposure to permethrin, deltamethrin and DDT (Yahouédo et al., 2017). In *An. funestus,* a thicker cuticle was also associated with permethrin resistance (Wood et al., 2010).

Another resistance mechanism is behavioural resistance, which results in the avoidance of vector control applications. Often this phenomenon describes malaria vectors that “avoiding” indoor interventions such as IRS and bednets through a shift to biting outdoors or earlier in the evening (Gatton et al., 2013; Ranson et al., 2011). Behavioural resistance is challenging to analyse as a lot of factors such as human and mosquito behaviour, environmental conditions and also other aspects such as temperature sensitivity of the plasmodium parasite can influence malaria transmission and biting times (Suh et al., 2020). It is noteworthy, that based on natural species composition and behaviour, only 79 % of malaria transmission occurs when people are under a bednet (Sherrard-Smith et al., 2019). However, since 2000 the proportion of mosquito bites on people sleeping beneath a bednet has decreased nearly 10 % (Lindsay et al., 2021; Sherrard-Smith et al., 2019), with much of the outdoor transmission due to

changes in human behaviour. In Papua New Guinea, malaria transmission increased after three years of bednet distribution due to a shift to earlier biting (Thomsen et al., 2017). In Tanzania biting rates of *Anopheline* mosquitoes also shifted to earlier and outdoor biting after bednet distribution from 1997 to 2009 based on a species shift within *An. gambiae* complex to *An. arabiensis* and a change in feeding behaviour of *An. funestus* (Russell et al., 2011; Thomsen et al., 2017). A recent study in Burkina Faso observed biting behaviour after two years of bednet distribution, concluding that outdoor and early biting behaviour based on species shift is slowly increasing (Sanou et al., 2021). Despite high coverage with ITN and frequent IRS applications, residual Malaria transmission in Zanzibar is present, which is likely due to outdoor biting and resting *An. arabiensis* (Musiba et al., 2022).

1.4.3. Impact of pyrethroid resistance towards the success of vector control

During the scale up of insecticidal vector control interventions in the last few decades the reported insecticide resistance frequencies have increased globally in *Anopheline* and *Aedes* vectors (Bhatt et al., 2015; Hancock et al., 2020; Liu, 2015; Moyes et al., 2020, 2017; Ranson et al., 2008; WHO, 2018). To what extent is insecticide resistance reducing the success of vector control interventions? The answer remains controversial as the direct association between insecticide resistant mosquitoes and the outcome of vector control interventions and diseases prevalence is challenging to assess. Other factors such as climate conditions, vector abundance, natural seasonal variations amongst other things can confound the evaluation of insecticide resistance and its implication on disease transmission (Paine and Brooke, 2016). Furthermore, historical, stringent and evidence-based data is missing. Some examples from the past indicate a link between insecticide resistance and the failure of vector control interventions (Paine and Brooke, 2016), such as the malaria outbreak that occurred in Pakistan in the 1970s, which was likely due to mosquito-resistance to DDT. As a response, vector control applications switched from DDT to malathion IRS and lowered malaria cases dramatically. This is partially explained with DDT resistance of the vector *An. stephensi*. A second example was the dramatic increase in malaria incidences from 1996-2000 in South Africa and Mozambique, which was likely due to failure of pyrethroid IRS due to the resurgence of pyrethroid-resistant *An. funestus* (Hargreaves et al., 2000). Further reintroduction of DDT for IRS applications led to a decline in malaria cases (M. Coetzee et al., 2013; Paine and Brooke, 2016). Hence, the direct causal association between chemical vector

control interventions and insecticide resistance is challenging to study. Nevertheless, insecticide resistance to all major insecticidal classes is increasing and alternative chemistries that can overcome insecticide resistance mechanism are lacking.

In areas of high pyrethroid-resistance, pyrethroid nets still offer protection against malaria transmission to net users (Bradley et al., 2017; Glunt et al., 2017; Kleinschmidt et al., 2018; Ochomo et al., 2017) since they offer other advantages, such as barrier-protection, repellent-activity and community protection. Furthermore, despite pyrethroid resistance, ITNs produce higher mosquito mortality than control nets containing no insecticide (Strode et al., 2014). However, field studies have shown that pyrethroid-resistance in mosquitoes is reducing the efficacy of pyrethroid-vector control interventions (Pang et al., 2015; Protopopoff et al., 2018), while models predict that malaria incidences are likely to increase during a lifetime of a bednet even in low pyrethroid- resistant areas, (Churcher et al., 2016).

A comprehensive study has monitored malaria cases and positive (plasmodium) rates alongside bednet distribution over a 5-year time frame in a highly pyrethroid-resistant area in Uganda. Results showed that a switch from pyrethroid bednets to bendiocarb-IRS lowered malaria cases and plasmodium rates dramatically, indicating that pyrethroid-bednets in this setting were no longer offering protection of malaria infection (Katureebe et al., 2016).

1.5. Aim and objectives

There is a lot of work that has identified genes associated with pyrethroid resistance in *An. funestus*. However, while P450s that metabolise pyrethroids have been discovered, there is a gap in understanding the molecular mechanisms of pyrethroid breakdown. Given the rapid evolution of metabolic resistance there is a drive to develop resistance breaking strategies that include inhibiting P450 activity with synergists or developing pyrethroids resistant to metabolism, e.g., fluorinated pyrethroids. However, their interactions with mosquito P450s are poorly understood. The aims are therefore to understand how pyrethroids are metabolised, in particular fluorinated pyrethroids and to identify synergists with potential to extend the lifetime of pyrethroids. The specific research objectives were to:

1. Elucidate the toxicological profile of the pyrethroid resistant *An. funestus* FUMOZ-R towards different pyrethroids, transfluthrin and transfluthrin derivatives to find putative oxidations sites and to evaluate azole fungicides as possible synergists for future vector control applications.
2. Investigate the role of cytochrome b5 towards metabolism of pyrethroids and coumarin model substrates in recombinantly expressed CYP6P9a and CYP6P9b from *An. funestus* using baculovirus expression system.
3. Clarify sequential permethrin and deltamethrin metabolism of recombinantly expressed CYP6P9a and CYP6P9b from *An. funestus* and characterise the impact of residue 310 of recombinantly expressed CYP6P9-variants towards pyrethroid metabolism. Furthermore, the inhibitory potential of azole-fungicides is biochemically assessed towards CYP6P9 variants.
4. Elucidate transfluthrin metabolism by recombinantly expressed CYP6P9a and CYP6P9b.

1.6. References

Adesanya, A.W., Cardenas, A., Lavine, M.D., Walsh, D.B., Lavine, L.C., Zhu, F., 2020. RNA interference of NADPH-cytochrome P450 reductase increases susceptibilities to multiple acaricides in *Tetranychus urticae*. Pestic Biochem Physiol 165, 104550. https://doi.org/10.1016/j.pestbp.2020.02.016

Adolfi, A., Poulton, B., Anthousi, A., Macilwee, S., Ranson, H., Lycett, G.J., 2019. Functional genetic validation of key genes conferring insecticide resistance in the major African malaria vector, *Anopheles gambiae*. Proc Natl Acad Sci U S A 116, 25764–25772. https://doi.org/10.1073/pnas.1914633116

Ahoua Alou, L.P., Koffi, A.A., Adja, M.A., Tia, E., Kouassi, P.K., Koné, M., Chandre, F., 2010. Distribution of ace-1Rand resistance to carbamates and organophosphates in *Anopheles gambiae* s.s. populations from Côte d'Ivoire. Malar J. https://doi.org/10.1186/1475-2875-9-167

Amezian, D., Nauen, R., Le Goff, G., 2021. Transcriptional regulation of xenobiotic detoxification genes in insects - An overview. Pestic Biochem Physiol. https://doi.org/10.1016/j.pestbp.2021.104822

Animut, A., Horstmann, S., 2022. Residual efficacy of Fludora Fusion against *Anopheles arabiensis* in simple huts in Ethiopia. PLoS One 17, e0263840. https://doi.org/10.1371/journal.pone.0263840

Antonio-Nkondjio, C., Awono-Ambene, P., Toto, J.-C., Meunier, J.-Y., Zebaze-Kemleu, S., Nyambam, R., Wondji, C.S., Tchuinkam, T., Fontenille, D., 2002. High Malaria Transmission Intensity in a Village Close to Yaounde, the Capital City of Cameroon. J Med Entomol. https://doi.org/10.1603/0022-2585-39.2.350

Awolola, T.S., Oduola, O.A., Strode, C., Koekemoer, L.L., Brooke, B., Ranson, H., 2009. Evidence of multiple pyrethroid resistance mechanisms in the malaria vector *Anopheles gambiae* sensu stricto from Nigeria. Trans R Soc Trop Med Hyg. https://doi.org/10.1016/j.trstmh.2008.08.021

Awolola, T.S., Oyewole, I.O., Koekemoer, L.L., Coetzee, M., 2005. Identification of three members of the *Anopheles funestus* (Diptera: Culicidae) group and their role in malaria transmission in two ecological zones in Nigeria. Trans R Soc Trop Med Hyg 99, 525–531. https://doi.org/10.1016/j.trstmh.2004.12.003

Balabanidou, V., Grigoraki, L., Vontas, J., 2018. Insect cuticle: a critical determinant of insecticide resistance. Curr Opin Insect Sci 27, 68–74. https://doi.org/10.1016/j.cois.2018.03.001

Balabanidou, V., Kampouraki, A., Maclean, M., Blomquist, G.J., Tittiger, C., Juárez, M.P., Mijailovsky, S.J., Chalepakis, G., Anthousi, A., Lynd, A., Antoine, S., Hemingway, J., Ranson, H., Lycett, G.J., Vontas, J., 2016. Cytochrome P450 associated with insecticide resistance catalyzes cuticular hydrocarbon production in *Anopheles gambiae*. Proc Natl Acad Sci U S A 113, 9268–9273. https://doi.org/10.1073/pnas.1608295113

Banks, S.D., Murray, N., Wilder-Smith, A., Logan, J.G., 2014. Insecticide-treated clothes for the control of vector-borne diseases: A review on effectiveness and safety. Med Vet Entomol 28, 14–25. https://doi.org/10.1111/mve.12068

Bayer, 2022. Bayer Vector Control Environmental Science [WWW Document]. Bayer. URL https://www.vectorcontrol.bayer.com/product-portfolio/products/fludora-comax

Bhatt, S., Weiss, D.J., Cameron, E., Bisanzio, D., Mappin, B., Dalrymple, U., Battle, K.E., Moyes, C.L., Henry, A., Eckhoff, P.A., Wenger, E.A., Briët, O., Penny, M.A., Smith, T.A., Bennett, A., Yukich, J., Eisele, T.P., Griffin, J.T., Fergus, C.A., Lynch, M., Lindgren, F., Cohen, J.M., Murray, C.L.J., Smith, D.L., Hay, S.I., Cibulskis, R.E., Gething, P.W., 2015. The effect of malaria control on *Plasmodium falciparum* in Africa between 2000 and 2015. Nature 526, 207–211. https://doi.org/10.1038/nature15535

Bibbs, C.S., Tsikolia, M., Bloomquist, J.R., Bernier, U.R., Xue, R. De, Kaufman, P.E., 2018. Vapor toxicity of five volatile pyrethroids against *Aedes aegypti*, *Aedes albopictus*, *Culex quinquefasciatus*, and *Anopheles quadrimaculatus* (Diptera: Culicidae). Pest Manag Sci 74, 2699–2706. https://doi.org/10.1002/ps.5088

Boaventura, D., Buer, B., Hamaekers, N., Maiwald, F., Nauen, R., 2021. Toxicological and molecular profiling of insecticide resistance in a Brazilian strain of fall armyworm resistant to Bt Cry1 proteins. Pest Manag Sci 77, 3713–3726. https://doi.org/10.1002/ps.6061

Boonsuepsakul, S., Luepromchai, E., Rongnoparut, P., 2008. Characterization of *Anopheles minimus* CYP6AA3 expressed in a recombinant baculovirus system. Arch Insect Biochem Physiol 69, 13–21. https://doi.org/10.1002/arch.20248

Bowman, L.R., Donegan, S., McCall, P.J., 2016. Is Dengue Vector Control Deficient in Effectiveness or Evidence?: Systematic Review and Meta-analysis. PLoS Negl Trop Dis 10, 1–24. https://doi.org/10.1371/journal.pntd.0004551

Bradley, J., Ogouyèmi-Hounto, A., Cornélie, S., Fassinou, J., De Tove, Y.S.S., Adéothy, A.A., Tokponnon, F.T., Makoutode, P., Adechoubou, A., Legba, T., Houansou, T., Kinde-Gazard, D., Akogbeto, M.C., Massougbodji, A., Knox, T.B., Donnelly, M., Kleinschmidt, I., 2017. Insecticide-treated nets provide protection against malaria to children in an area of insecticide resistance in Southern Benin. Malar J 16, 1–5. https://doi.org/10.1186/s12936-017-1873-1

Brengues, C., Hawkesy, N.J., Chandre, F., McCarroll, L., Duchon, S., Guillet, P., Manguin, S., Morgan, J.C., Hemingway, J., 2003. Pyrethroid and DDT crossresistance in *Aedes aegypti* is correlated with novel mutations in the voltage-gated sodium channel. Med Vet Entomol 17, 87–94.

Brooke, B.D., Kloke, G., Hunt, R.H., Koekemoer, L.L., Tem, E.A., Taylor, M.E., Small, G., Hemingway, J., Coetzee, M., 2001. Bioassay and biochemical analyses of insecticide resistance in southern African *Anopheles funestus* (Diptera: Culicidae). Bull Entomol Res 91, 265–272. https://doi.org/10.1079/ber2001108

Casida, J.E., 1970. Mixed-Function Oxidase Involvement in the Biochemistry of Insecticide Synergists. J Agric Food Chem 18, 753–772. https://doi.org/10.1021/jf60171a013

Casida, J.E., Gammon, D.W., Glickman, A.H., Lawrence, L.J., 1983. Mechanism of Selective Action of Pyrethroid. Annual Review Pharmacology Toxicology 413–438.

Casida, J.E., Ruzo, L.O., 1980. Metabolic chemistry of pyrethroid insecticides. Pestic Sci 11, 257–269. https://doi.org/10.1002/ps.2780110219

Cataldo, N.P., Lea, C.S., Kelley, T., Richards, S.L., 2020. Assessment of Resistance to Organophosphates and Pyrethroids in *Aedes aegypti* (Diptera: Culicidae): Do Synergists Affect Mortality? J Med Entomol 1–5. https://doi.org/10.1093/jme/tjaa101

Chiu, T.L., Wen, Z., Rupasinghe, S.G., Schuler, M.A., 2008. Comparative molecular modelling of *Anopheles gambiae* CYP6Z1, a mosquito P450 capable of metabolizing DDT. Proc Natl Acad Sci U S A 105, 8855–8860. https://doi.org/10.1073/pnas.0709249105

Churcher, T.S., Lissenden, N., Griffin, J.T., Worrall, E., Ranson, H., 2016. The impact of pyrethroid resistance on the efficacy and effectiveness of bednets for malaria control in Africa. Elife. https://doi.org/10.7554/eLife.16090

Clark, A.G., Shamaan, N.A., 1984. Evidence that DDT-dehydrochlorinase from the house fly is a glutathione S-transferase. Pestic Biochem Physiol 22, 249–261. https://doi.org/10.1016/0048-3575(84)90018-X

Clarkson, C.S., Miles, A., Harding, N.J., O'Reilly, A.O., Weetman, D., Kwiatkowski, D., Donnelly, M.J., 2021. The genetic architecture of target-site resistance to pyrethroid insecticides in the African malaria vectors *Anopheles gambiae* and *Anopheles coluzzii*. Mol Ecol 30, 5303–5317. https://doi.org/10.1111/mec.15845

Coetzee, M., Hunt, R.H., Wilkerson, R., Torre, A. Della, Coulibaly, M.B., Besansky, N.J., 2013a. *Anopheles coluzzii* and *Anopheles amharicus*, new members of the *Anopheles gambiae* complex. Zootaxa. https://doi.org/10.11646/zootaxa.3619.3.2

Coetzee, M., Koekemoer, L.L., 2013b. Molecular systematics and insecticide resistance in the major African malaria vector *Anopheles funestus*. Annu Rev Entomol 58, 393–412. https://doi.org/10.1146/annurev-ento-120811-153628

Coetzee, M., Kruger, P., Hunt, R.H., Durrheim, D.N., Urbach, J., Hansford, C.F., 2013. Malaria in South Africa: 110 years of learning to control the disease. South African Medical Journal 103, 770–778. https://doi.org/10.7196/SAMJ.7446

Corbel, V., Chabi, J., Dabiré, R.K., Etang, J., Nwane, P., Pigeon, O., Akogbeto, M., Hougard, J.M., 2010. Field efficacy of a new mosaic long-lasting mosquito net (PermaNet® 3.0) against pyrethroid-resistant malaria vectors: A multi centre study in Western and Central Africa. Malar J. https://doi.org/10.1186/1475-2875-9-113

Dambach, P., Baernighausen, T., Traoré, I., Ouedraogo, S., Sié, A., Sauerborn, R., Becker, N., Louis, V.R., 2019. Reduction of malaria vector mosquitoes in a large-scale intervention trial in rural Burkina Faso using Bti based larval source management. Malar J 18, 311. https://doi.org/10.1186/s12936-019-2951-3

David, J.-P., Strode, C., Vontas, J., Nikou, D., Vaughan, A., Pignatelli, P.M., Louis, C., Hemingway, J., Ranson, H., 2005. The *Anopheles gambiae* detoxification chip: A highly specific microarray to study metabolic-based insecticide resistance in malaria vectors. Proceedings of the National Academy of Science 102.

Davies, T.G.E., Field, L.M., Usherwood, P.N.R., Williamson, M.S., 2007. DDT, pyrethrins, pyrethroids and insect sodium channels. IUBMB Life 59, 151–162. https://doi.org/10.1080/15216540701352042

Davies, T.G.E., O'Reilly, A.O., Field, L.M., Wallace, B.A., Williamson, M.S., 2008. Knockdown resistance to DDT and pyrethroids: From target-site mutations to molecular modelling. Pest Manag Sci. https://doi.org/10.1002/ps.1617

Dia, I., Moussa Wamdaogo Guelbeogo, Ayala, D., 2013. Advances and Perspectives in the Study of the Malaria Mosquito *Anopheles funestus*, in: *Anopheles* Mosquitoes - New Insights into Malaria Vectors. pp. 197–220.

Djouaka, R., Riveron, J.M., Yessoufou, A., Tchigossou, G., Akoton, R., Irving, H., Djegbe, I., Moutairou, K., Adeoti, R., Tamò, M., Manyong, V., Wondji, C.S., 2016. Multiple insecticide resistance in an infected population of the malaria vector *Anopheles funestus* in Benin. Parasit Vectors 9, 453. https://doi.org/10.1186/s13071-016-1723-y

Duangkaew, P., Pethuan, S., Kaewpa, D., Boonsuepsakul, S., Sarapusit, S., Rongnoparut, P., 2011. Characterization of mosquito CYP6P7 and CYP6AA3: Differences in substrate preference and kinetic properties. Arch Insect Biochem Physiol 76, 236–248. https://doi.org/10.1002/arch.20413

Elliott, M., Farnham, A.W., Janes, N.F., Needham, P.H., Pearson, B.C., 1967. 5-Benzyl-3-furylmethyl Chrysanthemate: a New Potent Insecticide. Nature 213, 493–494.

Enayati, A.A., Ranson, H., Hemingway, J., 2005. Insect glutathione transferases and insecticide resistance. Insect Mol Biol 14, 3–8. https://doi.org/10.1111/j.1365-2583.2004.00529.x

Feyereisen, R., 2019. Insect CYP Genes and P450 Enzymes, Reference Module in Life Sciences. https://doi.org/10.1016/b978-0-12-809633-8.04040-1

Feyereisen, R., 2015. Insect P450 inhibitors and insecticides: Challenges and opportunities. Pest Manag Sci 71, 793–800. https://doi.org/10.1002/ps.3895

Feyereisen, R., Vincent, D.R., 1984. Characterization of antibodies to house fly NADPH-cytochrome P-450 reductase. Insect Biochem 14, 163–168. https://doi.org/10.1016/0020-1790(84)90025-8

Finn, R.D., McLaughlin, L.A., Hughes, C., Song, C., Henderson, C.J., Wolf, R.R., 2011. Cytochrome b5 null mouse: a new model for studying inherited skin disorders and the role of unsaturated fatty acids in normal homeostasis. Transgenic Res 20, 491–502. https://doi.org/10.1007/s11248-010-9426-1

Finn, R.D., McLaughlin, L.A., Ronseaux, S., Rosewell, I., Houston, J.B., Henderson, C.J., Wolf, C.R., 2008. Defining the in vivo role for cytochrome b5 in cytochrome P450 function through the conditional hepatic deletion of microsomal cytochrome b5. Journal of Biological Chemistry 283, 31385–31393. https://doi.org/10.1074/jbc.M803496200

Fiorenzano, J.M., Koehler, P.G., Xue, R. de, 2017. Attractive toxic sugar bait (ATSB) for control of mosquitoes and its impact on non-target organisms: A review. Int J Environ Res Public Health 14. https://doi.org/10.3390/ijerph14040398

Fongnikin, A., Houeto, N., Agbevo, A., Odjo, A., Syme, T., N'Guessan, R., Ngufor, C., 2020. Efficacy of Fludora® Fusion (a mixture of deltamethrin and clothianidin) for indoor residual spraying against pyrethroid-resistant malaria vectors: Laboratory and experimental hut evaluation. Parasit Vectors 13, 466. https://doi.org/10.1186/s13071-020-04341-6

Fouet, C., Ashu, A.F., Ambadiang, M.M., Tchapga, W.T., Wondji, C.S., Kamdem, C., 2020. Resistance of *Anopheles gambiae* to the new insecticide clothianidin associated with unrestricted use of agricultural neonicotinoids in Yaounde, Cameroon. bioRxiv 2020.08.06.239509. https://doi.org/10.1101/2020.08.06.239509

Fraser, K.J., Mwandigha, L., Traore, S.F., Traore, M.M., Doumbia, S., Junnila, A., Revay, E., Beier, J.C., Marshall, J.M., Ghani, A.C., Müller, G., 2021. Estimating the potential impact of Attractive Targeted Sugar Baits (ATSBs) as a new vector control tool for *Plasmodium falciparum* malaria. Malar J 20. https://doi.org/10.1186/s12936-021-03684-4

Gatton, M.L., Chitnis, N., Churcher, T., Donnelly, M.J., Ghani, A.C., Godfray, H.C.J., Gould, F., Hastings, I., Marshall, J., Ranson, H., Rowland, M., Shaman, J., Lindsay, S.W., 2013. The importance of mosquito behavioural adaptations to malaria control in Africa. Evolution (N Y). https://doi.org/10.1111/evo.12063

Gillies, M.T., Coetzee, M., 1987. A supplement to the *Anophelinae* of Africa South of the Sahara. South African Institute for Medical Research.

Gleave, K., Lissenden, N., Richardson, M., Ranson, H., 2018. Piperonyl butoxide (PBO) combined with pyrethroids in long-lasting insecticidal nets (LLINs) to prevent malaria in Africa. Cochrane Database of Systematic Reviews. https://doi.org/10.1002/14651858.CD012776

Glunt, K.D., Coetzee, M., Huijben, S., Koffi, A.A., Lynch, P.A., N'Guessan, R., Oumbouke, W.A., Sternberg, E.D., Thomas, M.B., 2017. Empirical and theoretical investigation into the potential impacts of insecticide resistance on the effectiveness of insecticide-treated bed nets. Evol Appl 11, 431–441. https://doi.org/10.1111/eva.12574

Goodyer, L., Schofield, S., 2018. Mosquito repellents for the traveller: Does picaridin provide longer protection than DEET? J Travel Med 25, S10–S15. https://doi.org/10.1093/jtm/tay005

Gotoh, O., 1992. Substrate recognition sites in cytochrome P450 family 2 (CYP2) proteins inferred from comparative analyses of amino acid and coding nucleotide sequences. Journal of Biological Chemistry 267, 83–90. https://doi.org/10.1016/s0021-9258(18)48462-1

Grant, G.G., Estrera, R.R., Pathak, N., Hall, C.D., Tsikolia, M., Linthicum, K.J., Bernier, U.R., Hall, A.C., 2020. Interactions of DEET and Novel Repellents With Mosquito Odorant Receptors. J Med Entomol 57, 1032–1040. https://doi.org/10.1093/jme/tjaa010

Grigoraki, L., Balabanidou, V., Meristoudis, C., Miridakis, A., Ranson, H., Swevers, L., Vontas, J., 2016. Functional and immunohistochemical characterization of CCEae3a, a carboxylesterase associated with temephos resistance in the major arbovirus vectors *Aedes aegypti* and *Ae. albopictus*. Insect Biochem Mol Biol. https://doi.org/10.1016/j.ibmb.2016.05.007

Gunning, R. V., Moores, G.D., Devonshire, A.L., 1998. Inhibition of Resistance-related Esterases by Piperonyl Butoxide in Helicoverpa armigera (Lepidoptera: Noctuidae) and *Aphis gossypii* (Hemiptera: Aphididae) 215–226.

Gutierrez, A., Grunau, A., Paine, M., Munro, A.W., Wolf, C.R., Roberts, G.C.K., Scrutton, N.S., 2003. Enzyme Mechanism – A Structural Perspective Electron transfer in human cytochrome P450 reductase Cytochrome P450 reductase (CPR) and its component domains 497–501.

Guzov, V.M., Houston, H.L., Murataliev, M.B., Walker, F.A., Feyereisen, R., 1996. Molecular cloning, overexpression in *Escherichia coli*, structural and functional characterization of house fly cytochrome b5. Journal of Biological Chemistry 271, 26637–26645. https://doi.org/10.1074/jbc.271.43.26637

Haas, J., Glaubitz, J., Koenig, U., Nauen, R., 2021. A mechanism-based approach unveils metabolic routes potentially mediating chlorantraniliprole synergism in honey bees, *Apis mellifera* L., by azole fungicides. Pest Manag Sci. https://doi.org/10.1002/ps.6706

Haas, J., Nauen, R., 2021. Pesticide risk assessment at the molecular level using honey bee cytochrome P450 enzymes: A complementary approach. Environ Int 147, 106372. https://doi.org/10.1016/j.envint.2020.106372

Hancock, P.A., Hendriks, C.J.M., Tangena, J.-A., Gibson, H., Hemingway, J., Coleman, M., Gething, P.W., Cameron, E., Bhatt, S., Moyes, C.L., 2020. Mapping trends in insecticide resistance phenotypes in African malaria vectors. PLoS Biol 18, e3000633. https://doi.org/10.1371/journal.pbio.3000633

Hargreaves, K., Koekemoer, L.L., Brooke, B.D., Hunt, R.H., Mthembu, J., Coetzee, M., 2000. *Anopheles funestus* resistant to pyrethroid insecticides in South Africa. Med Vet Entomol 14, 181–189. https://doi.org/10.1046/j.1365-2915.2000.00234.x

Hawley, W.A., Phillips-Howard, P.A., Ter Kuile, F.O., Nahlen, B.L., Alaii, J.A., Gimnig, J.E., Kolczak, M.S., Terlouw, D.J., Kariuki, S.K., Shi, Y.P., Kachur, S.P., Hightower, A.W., Vulule, J.M., Ombok, M., Nahlen, B.L., Giminig, J.E., Kariuki, S.K., Kolczak, M.S., Hightower, A.W., 2003. Community-wide effects of permethrin-treated bed nets on child mortality and malaria morbidity in western Kenya. American Journal of Tropical Medicine and Hygiene 68, 121–127. https://doi.org/10.4269/ajtmh.2003.68.10

Heintze, T., Klein, K., Hofmann, U., Zanger, U.M., 2021. Differential effects on human cytochromes P450 by CRISPR/Cas9-induced genetic knockout of cytochrome P450 reductase and cytochrome b5 in HepaRG cells. Sci Rep 11, 1–14. https://doi.org/10.1038/s41598-020-79952-1

Hemingway, J., Ranson, H., 2000. Insecticide Resistance in Insect Vectors of Human Diseases. Annu Rev Entomol 45, 371–391.

Hemingway, J., Ranson, H., Magill, A., Kolaczinski, J., Fornadel, C., Gimnig, J., Coetzee, M., Simard, F., Roch, D.K., Hinzoumbe, C.K., Pickett, J., Schellenberg, D., Gething, P., Hoppé, M., Hamon, N., 2016. Averting a malaria disaster: Will insecticide resistance derail malaria control? The Lancet 387, 1785–1788. https://doi.org/10.1016/S0140-6736(15)00417-1

Henderson, C.J., McLaughlin, L.A., Finn, R.D., Ronseaux, S., Kapelyukh, Y., Wolf, C.R., 2014. A role for cytochrome b5 in the in vivo disposition of anticancer and cytochrome P450 probe drugs in mice. Drug Metabolism and Disposition 42, 70–77. https://doi.org/10.1124/dmd.113.055277

Henderson, C.J., McLaughlin, L.A., Scheer, N., Stanley, L.A., Wolf, C.R., 2015. Cytochrome b5 is a major determinant of human cytochrome P450 CYP2D6 and CYP3A4 activity in vivo. Mol Pharmacol 87, 733–739. https://doi.org/10.1124/mol.114.097394

Hien, A.S., Soma, D.D., Maiga, S., Coulibaly, D., Diabaté, A., Belemvire, A., Diouf, M.B., Jacob, D., Koné, A., Dotson, E., Awolola, T.S., Oxborough, R.M., Dabiré, R.K., 2021. Evidence supporting deployment of next generation insecticide treated nets in Burkina Faso: bioassays with either chlorfenapyr or piperonyl butoxide increase mortality of pyrethroid-resistant *Anopheles gambiae*. Malar J 20, 1–12. https://doi.org/10.1186/s12936-021-03936-3

Hodgson, E., Levi, P.E., 1999. Interactions of Piperonyl Butoxide with Cytochrome P450. Piperonyl Butoxide. https://doi.org/10.1016/b978-012286975-4/50005-x

Horstmann, S., Sonneck, R., 2016. Contact Bioassays with Phenoxybenzyl and Tetrafluorobenzyl Pyrethroids against Target-Site and Metabolic Resistant Mosquitoes. PLoS One 11, e0149738. https://doi.org/10.1371/journal.pone.0149738

Ibrahim, S.S., Amvongo-Adjia, N., Wondji, M.J., Irving, H., Riveron, J.M., Wondji, C.S., 2018. Pyrethroid resistance in the major malaria vector *Anopheles funestus* is exacerbated by overexpression and overactivity of the P450 CYP6AA1 across Africa. Genes (Basel) 9, 1–17. https://doi.org/10.3390/genes9030140

Ibrahim, S.S., Ndula, M., Riveron, J.M., Irving, H., Wondji, C.S., 2016. The P450 CYP6Z1 confers carbamate/pyrethroid cross-resistance in a major African malaria vector beside a novel carbamate-insensitive N485I acetylcholinesterase-1 mutation. Mol Ecol 25, 3436–3452. https://doi.org/10.1111/mec.13673

Ibrahim, S.S., Riveron, J.M., Bibby, J., Irving, H., Yunta, C., Paine, M.J.I., Wondji, C.S., 2015. Allelic Variation of Cytochrome P450s Drives Resistance to Bednet Insecticides in a Major Malaria Vector. PLoS Genet 11, e1005618. https://doi.org/10.1371/journal.pgen.1005618

Ingham, V.A., Wagstaff, S., Ranson, H., 2018. Transcriptomic meta-signatures identified in *Anopheles gambiae* populations reveal previously undetected insecticide resistance mechanisms. Nat Commun 9. https://doi.org/10.1038/s41467-018-07615-x

IRAC, 2021. Insecticide Resistance Training Basic Module: Crop Protection.

Irving, H., Wondji, C.S., 2017. Investigating knockdown resistance (kdr) mechanism against pyrethroids/DDT in the malaria vector *Anopheles funestus* across Africa. BMC Genet 18, 76. https://doi.org/10.1186/s12863-017-0539-x

Iwasa, T., Motoyama, N., Ambrose, J.T., Roe, R.M., 2004. Mechanism for the differential toxicity of neonicotinoid insecticides in the honey bee, *Apis mellifera*. Crop Protection 23, 371–378. https://doi.org/10.1016/j.cropro.2003.08.018

Jiao, L., Xue-yao, Z., Hai-hua, W., Wen, M., Wen-ya, Z., ZHU, K.-Y., En-bo, M., ZHANG Jian-zhen, 2020. Characteristics and roles of cytochrome b5 in cytochrome P450- mediated oxidative reactions in *Locusta migratoria* LIU. J Integr Agric 19, 1512–1521. https://doi.org/10.1016/S2095-3119(19)62827-3

Jones, C.M., Liyanapathirana, M., Agossa, F.R., Weetman, D., Ranson, H., Donnelly, M.J., Wilding, C.S., 2012. Footprints of positive selection associated with a mutation (N1575Y) in the voltage-gated sodium channel of *Anopheles gambiae*. Proc Natl Acad Sci U S A 109, 6614–6619. https://doi.org/10.1073/pnas.1201475109

Kaindoa, E.W., Mmbando, A.S., Shirima, R., Hape, E.E., Okumu, F.O., 2021. Insecticide - treated eave ribbons for malaria vector control in low - income communities. Malar J 1–12. https://doi.org/10.1186/s12936-021-03945-2

Karunaratne, P., De Silva, P., Weeraratne, T., Surendran, N., 2018. Insecticide resistance in mosquitoes: Development, mechanisms and monitoring. Ceylon Journal of Science 47, 299. https://doi.org/10.4038/cjs.v47i4.7547

Kasai, S., Komagata, O., Itokawa, K., Shono, T., Ng, L.C., Kobayashi, M., Tomita, T., 2014. Mechanisms of Pyrethroid Resistance in the Dengue Mosquito Vector, *Aedes aegypti*: Target Site

Insensitivity, Penetration, and Metabolism. PLoS Negl Trop Dis 8, e2948. https://doi.org/10.1371/journal.pntd.0002948

Katureebe, A., Zinszer, K., Arinaitwe, E., Rek, J., Kakande, E., Charland, K., Kigozi, R., Kilama, M., Nankabirwa, J., Yeka, A., Mawejje, H., Mpimbaza, A., Katamba, H., Donnelly, M.J., Rosenthal, P.J., Drakeley, C., Lindsay, S.W., Staedke, S.G., Smith, D.L., Greenhouse, B., Kamya, M.R., Dorsey, G., 2016. Measures of Malaria Burden after Long-Lasting Insecticidal Net Distribution and Indoor Residual Spraying at Three Sites in Uganda: A Prospective Observational Study. PLoS Med 13, 1–22. https://doi.org/10.1371/journal.pmed.1002167

Khambay, B.P.S., Jewess, P.J., 2010. Pyrethroids, in: Gilbert, L.I., Gill, S.S. (Eds.), Insect Control. Elsevier, pp. 1–29.

Killeen, G.F., Moore, S.J., 2012. Target product profiles for protecting against outdoor malaria transmission. Malar J 11, 1–6.

Kleinschmidt, I., Bradley, J., Knox, T.B., Mnzava, A.P., Kafy, H.T., Mbogo, C., Ismail, B.A., Bigoga, J.D., Adechoubou, A., Raghavendra, K., Cook, J., Malik, E.M., Nkuni, Z.J., Macdonald, M., Bayoh, N., Ochomo, E., Fondjo, E., Awono-Ambene, H.P., Etang, J., Akogbeto, M., Bhatt, R.M., Chourasia, M.K., Swain, D.K., Kinyari, T., Subramaniam, K., Massougbodji, A., Okê-Sopoh, M., Ogouyemi-Hounto, A., Kouambeng, C., Abdin, M.S., West, P., Elmardi, K., Cornelie, S., Corbel, V., Valecha, N., Mathenge, E., Kamau, L., Lines, J., Donnelly, M.J., 2018. Implications of insecticide resistance for malaria vector control with long-lasting insecticidal nets: a WHO-coordinated, prospective, international, observational cohort study. Lancet Infect Dis 18, 640–649. https://doi.org/10.1016/S1473-3099(18)30172-5

Kleinschmidt, I., Schwabe, C., Shiva, M., Segura, J.L., Sima, V., Mabunda, S.J.A., Coleman, M., 2009. Combining Indoor Residual Spraying and Insecticide-Treated Net Interventions. American Journal of Tropical Medicine and Hygiene 81, 519–524.

Kline, D.L., Urban, J., 2018. Potential for utilization of spatial repellents in mosquito control interventions. ACS Symposium Series 1289, 237–248. https://doi.org/10.1021/bk-2018-1289.ch013

Koener, J.F., Cariño, F.A., Feyereisen, R., 1993. The cDNA and deduced protein sequence of house fly NADPH-cytochrome P450 reductase. Insect Biochem Mol Biol 23, 439–447. https://doi.org/10.1016/0965-1748(93)90051-S

Kua, K.P., Lee, S.W.H., 2021. Randomized trials of housing interventions to prevent malaria and *Aedes*-transmitted diseases: A systematic review and meta-analysis. PLoS One 16, 1–23. https://doi.org/10.1371/journal.pone.0244284

Lees, R.S., Ismail, H.M., Logan, R.A.E., Malone, D., Davies, R., Anthousi, A., Adolfi, A., Lycett, G.J., Paine, M.J.I., 2020. New insecticide screening platforms indicate that Mitochondrial Complex I inhibitors are susceptible to cross-resistance by mosquito P450s that metabolise pyrethroids. Sci Rep 10, 1–10. https://doi.org/10.1038/s41598-020-73267-x

Lian, L.Y., Widdowson, P., McLaughlin, L.A., Paine, M.J.I., 2011. Biochemical comparison of *Anopheles gambiae* and human NADPH P450 reductases reveals different 2'-5'-ADP and FMN binding traits. PLoS One 6. https://doi.org/10.1371/journal.pone.0020574

Lindsay, S.W., Thomas, M.B., Kleinschmidt, I., 2021. Threats to the effectiveness of insecticide-treated bednets for malaria control: thinking beyond insecticide resistance. Lancet Glob Health 9, e1325–e1331. https://doi.org/10.1016/S2214-109X(21)00216-3

Liu, N., 2015. Insecticide resistance in mosquitoes: Impact, mechanisms, and research directions. Annu Rev Entomol 60, 537–559. https://doi.org/10.1146/annurev-ento-010814-020828

Lycett, G.J., McLaughlin, L.A., Ranson, H., Hemingway, J., Kafatos, F.C., Loukeris, T.G., Paine, M.J.I., 2006. *Anopheles gambiae* P450 reductase is highly expressed in oenocytes and in vivo knockdown increases permethrin susceptibility. Insect Mol Biol 15, 321–327. https://doi.org/10.1111/j.1365-2583.2006.00647.

Masalu, J.P., Finda, M., Killeen, G.F., Ngowo, H.S., Pinda, P.G., Okumu, F.O., 2020. Creating mosquito-free outdoor spaces using transfluthrin-treated chairs and ribbons. Malar J 19, 109. https://doi.org/10.1186/s12936-020-03180-1

Matambo, T.S., Paine, M.J., Coetzee, M., Koekemoer, L.L., 2010. Sequence characterization of cytochrome P450 CYP6P9 in pyrethroid resistant and susceptible *Anopheles funestus* (Diptera: Culicidae). Genet Mol Res 9, 554–564. https://doi.org/10.4238/vol9-1gmr719

Matowo, J., Weetman, D., Pignatelli, P., Wright, A., Charlwood, J.D., Kaaya, R., Shirima, B., Moshi, O., Lukole, E., Mosha, J., Manjurano, A., Mosha, F., Rowland, M., Protopopoff, N., 2022. Expression of pyrethroid metabolizing P450 enzymes characterizes highly resistant *Anopheles* vector species targeted by successful deployment of PBO-treated bednets in Tanzania. PLoS One 17, e0249440. https://doi.org/10.1371/journal.pone.0249440

McCann, R.S., Kabaghe, A.N., Moraga, P., Gowelo, S., Mburu, M.M., Tizifa, T., Chipeta, M.G., Nkhono, W., di Pasquale, A., Maire, N., Manda-Taylor, L., Mzilahowa, T., van den Berg, H., Diggle, P.J., Terlouw, D.J., Takken, W., van Vugt, M., Phiri, K.S., 2021. The effect of community-driven larval source management and house improvement on malaria transmission when added to the standard malaria control strategies in Malawi: a cluster-randomized controlled trial. Malar J 20, 1–16. https://doi.org/10.1186/s12936-021-03769-0

McLaughlin, L.A., Niazi, U., Bibby, J., David, J.P., Vontas, J., Hemingway, J., Ranson, H., Sutcliffe, M.J., Paine, M.J.I., 2008. Characterization of inhibitors and substrates of *Anopheles gambiae* CYP6Z2. Insect Mol Biol 17, 125–135. https://doi.org/10.1111/j.1365-2583.2007.00788.x

Menze, B.D., Kouamo, M.F., Wondji, M.J., Tchapga, W., Tchoupo, M., Kusimo, M.O., Mouhamadou, C.S., Riveron, J.M., Wondji, C.S., 2020. An experimental hut evaluation of PBO-based and pyrethroid-only nets against the malaria vector *Anopheles funestus* reveals a loss of bed nets efficacy associated with GSTe2 metabolic resistance. Genes (Basel) 11. https://doi.org/10.3390/genes11020143

Menze, B.D., Riveron, J.M., Ibrahim, S.S., Irving, H., Antonio-Nkondjio, C., Awono-Ambene, P.H., Wondji, C.S., 2016. Multiple insecticide resistance in the malaria vector *Anopheles funestus* from Northern Cameroon is mediated by metabolic resistance alongside potential target site insensitivity mutations. PLoS One 11, 1–14. https://doi.org/10.1371/journal.pone.0163261

Miyazaki, M., Ohyama, K., Dunlap, D.Y., Matsumura, F., 1996. Cloning and sequencing of the para-type sodium channel gene from susceptible and kdr-resistant German cockroaches (*Blattella germanica*) and house fly (*Musca domestica*). Molecular and General Genetics 252, 61–68. https://doi.org/10.1007/s004389670007

Montella, I.R., Schama, R., Valle, D., 2012. The classification of esterases: An important gene family involved in insecticide resistance - A review. Mem Inst Oswaldo Cruz 107, 437–449. https://doi.org/10.1590/S0074-02762012000400001

Moyes, C.L., Athinya, D.K., Seethaler, T., Battle, K.E., Sinka, M., Hadi, M.P., Hemingway, J., Coleman, M., Hancock, P.A., 2020. Evaluating insecticide resistance across African districts to aid malaria control decisions. Proceedings of the National Academy of Sciences 117, 202006781. https://doi.org/10.1073/pnas.2006781117

Moyes, C.L., Vontas, J., Martins, A.J., Ng, L.C., Koou, S.Y., Dusfour, I., Raghavendra, K., Pinto, J., Corbel, V., David, J.P., Weetman, D., 2017. Contemporary status of insecticide resistance in the major *Aedes* vectors of arboviruses infecting humans. PLoS Negl Trop Dis. https://doi.org/10.1371/journal.pntd.0005625

Müller, P., Warr, E., Stevenson, B.J., Pignatelli, P.M., Morgan, J.C., Steven, A., Yawson, A.E., Mitchell, S.N., Ranson, H., Hemingway, J., Paine, M.J.I., Donnelly, M.J., 2008. Field-caught permethrin-resistant *Anopheles gambiae* overexpress CYP6P3, a P450 that metabolises pyrethroids. PLoS Genet 4. https://doi.org/10.1371/journal.pgen.1000286

Murataliev, M.B., Feyereisen, R., 1999. Mechanism of cytochrome P450 reductase from the house fly: Evidence for an FMN semiquinone as electron donor. FEBS Lett. https://doi.org/10.1016/S0014-5793(99)00723-1

Murataliev, M.B., Feyereisen, R., Walker, F.A., 2004. Electron transfer by diflavin reductases. Biochem Biophys Acta Proteins Proteom 1698, 1–26. https://doi.org/10.1016/j.bbapap.2003.10.003

Murataliev, M.B., Guzov, V.M., Walker, F.A., Feyereisen, R., 2008. P450 reductase and cytochrome b5 interactions with cytochrome P450: Effects on house fly CYP6A1 catalysis. Insect Biochem Mol Biol 38, 1008–1015. https://doi.org/10.1016/j.ibmb.2008.08.007

Musiba, R.M., Tarimo, B.B., Monroe, A., Msaky, D., Ngowo, H., Mihayo, K., Limwagu, A., Chilla, G.T., Shubis, G.K., Ibrahim, A., Greer, G., Mcha, J.H., Haji, K.A., Abbas, F.B., Ali, A., Okumu, F.O., Kiware, S.S., 2022. Outdoor biting and pyrethroid resistance as potential drivers of persistent malaria transmission in Zanzibar. Malar J 21, 1–14. https://doi.org/10.1186/s12936-022-04200

Mwanga, E.P., Mmbando, A.S., Mrosso, P.C., Stica, C., Mapua, S.A., Finda, M.F., Kifungo, K., Kafwenji, A., Monroe, A.C., Ogoma, S.B., Ngowo, H.S., Okumu, F.O., 2019. Eave ribbons treated with transfluthrin can protect both users and non - users against malaria vectors. Malar J 1–14. https://doi.org/10.1186/s12936-019-2958-9

Nakata, A., Hashimoto, S., Ikura, K., Katsuura, K., 1991. Development of a New Fungicide, Triflumizole. J Pestic Sci 16, 301–313.

Nauen, R., 2007. Insecticide resistance in disease vectors of public health importance. Pest Manag Sci 63, 628–633. https://doi.org/10.1002/ps.1406

Nauen, R., Zimmer, C., Vontas, J., 2021. Heterologous expression of insect P450 enzymes that metabolize xenobiotics. Curr Opin Insect Sci 43, 78–84. https://doi.org/10.1016/j.cois.2020.10.011

Nelson, D.R., 1998. Metazoan cytochrome P450 evolution. Comparative Biochemistry and Physiology - C Pharmacology Toxicology and Endocrinology 121, 15–22. https://doi.org/10.1016/S0742-8413(98)10027-0

N'Guessan, R., Asidi, A., Boko, P., Odjo, A., Akogbeto, M., Pigeon, O., Rowland, M., 2010. An experimental hut evaluation of PermaNet®3.0, a deltamethrin-piperonyl butoxide combination net, against pyrethroid-resistant *Anopheles gambiae* and *Culex quinquefasciatus* mosquitoes in southern Benin. Trans R Soc Trop Med Hyg. https://doi.org/10.1016/j.trstmh.2010.08.008

Ngufor, C., Agbevo, A., Fagbohoun, J., Fongnikin, A., Rowland, M., 2020. Efficacy of Royal Guard, a new alpha-cypermethrin and pyriproxyfen treated mosquito net, against pyrethroid-resistant malaria vectors. Sci Rep 10, 1–15. https://doi.org/10.1038/s41598-020-69109-5

Nikou, D., Ranson, H., Hemingway, J., 2003. An adult-specific CYP6 P450 gene is overexpressed in a pyrethroid- resistant strain of the malaria vector, Anopheles gambiae. Gene. https://doi.org/10.1016/S0378-1119(03)00763-7

Nkya, T.E., Poupardin, R., Laporte, F., Akhouayri, I., Mosha, F., Magesa, S., Kisinza, W., David, J.P., 2014. Impact of agriculture on the selection of insecticide resistance in the malaria vector *Anopheles gambiae*: A multigenerational study in controlled conditions. Parasit Vectors. https://doi.org/10.1186/s13071-014-0480-z

Nouage, L., Elanga-Ndille, E., Binyang, A., Tchouakui, M., Atsatse, T., Ndo, C., Kekeunou, S., Wondji, C., 2020. Influence of GST- and P450-based metabolic resistance to pyrethroids on blood feeding in the major African malaria vector *Anopheles funestus* 1–17. https://doi.org/10.1101/2020.03.16.993535

Ochomo, E., Chahilu, M., Cook, J., Kinyari, T., Bayoh, N.M., West, P., Kamau, L., Osangale, A., Ombok, M., Njagi, K., Mathenge, E., Muthami, L., Subramaniam, K., Knox, T., Mnavaza, A., Donnelly, M.J., Kleinschmidt, I., Mbogo, C., 2017. Insecticide-treated nets and protection against Insecticide-Resistant malaria vectors in Western Kenya. Emerg Infect Dis 23, 758–764. https://doi.org/10.3201/eid2305.161315

Ogoma, S.B., Moore, S.J., Maia, M.F., 2012a. A systematic review of mosquito coils and passive emanators: Defining recommendations for spatial repellency testing methodologies. Parasit Vectors 5, 1. https://doi.org/10.1186/1756-3305-5-287

Ogoma, S.B., Ngonyani, H., Simfukwe, E.T., Mseka, A., Moore, J., Killeen, G.F., 2012b. Spatial repellency of transfluthrin-treated hessian strips against laboratory-reared *Anopheles arabiensis* mosquitoes in a semi-field tunnel cage. Parasit Vectors 5, 54. https://doi.org/10.1186/1756-3305-5-54

Ogoma, S.B., Ngonyani, H., Simfukwe, E.T., Mseka, A., Moore, J., Maia, M.F., Moore, S.J., Lorenz, L.M., 2014. The mode of action of spatial repellents and their impact on vectorial capacity of *Anopheles gambiae* sensu stricto. PLoS One 9, e110433. https://doi.org/10.1371/journal.pone.0110433

Ojuka, P., Boum, Y., Denoeud-Ndam, L., Nabasumba, C., Muller, Y., Okia, M., Mwanga-Amumpaire, J., De Beaudrap, P., Protopopoff, N., Etard, J.F., 2015. Early biting and insecticide resistance in the malaria vector *Anopheles* might compromise the effectiveness of vector control intervention in Southwestern Uganda. Malar J. https://doi.org/10.1186/s12936-015-0653-z

Oliva, C., Benedict, M., Collins, M., Baldet, T., Bellini, R., Bossin, H., Bouyer, J., Corbel, V., Facchinelli, L., Fouque, F., Geier, M., Michaelakis, A., Roiz, D., Simard, F., Tur, C., Gouagna, L.-C., 2021. Sterile Insect Technique (SIT) against *Aedes* Species Designing, Implementing and Evaluating Pilot Field Trials. Insects 12, 191.

O'Reilly, A.O., Khambay, B.P.S., Williamson, M.S., Field, L.M., Wallace, B.A., Davies, T.G.E., 2006. Modelling insecticide-binding sites in the voltage-gated sodium channel. Biochemical Journal 396, 255–263. https://doi.org/10.1042/BJ20051925

Ortiz De Montellano, P.R., 2018. 1-Aminobenzotriazole: A Mechanism-Based Cytochrome P450 Inhibitor and Probe of Cytochrome P450 Biology. Medical Chemistry 8. https://doi.org/10.4172/2161-0444.1000495

Ortiz De Montellano, P.R., 2005. Cytochrome P450 Structure, Mechanism, and Biochemistry, Third. ed. Kluwer Academic, New York, Boston, Dordrecht, London, Moscow.

Oyewole, I.O., Awolola, T.S., Ibidapo, C.A., Oduola, A.O., Okwa, O.O., Obansa, J.A., 2007. Behaviour and population dynamics of the major anopheline vectors in a malaria endemic area in southern Nigeria. J Vector Borne Dis 44, 56–64.

Paine, M.J.I., Brooke, B., 2016. Insecticide Resistance and Its Impact on Vector Control, in: Horowitz, A.R., Ishaaya, I. (Eds.), Advances in Insect Control and Resistance Management. Springer International Publishing Switzerland, pp. 286–312. https://doi.org/DOI 10.1007/978-3-319-31800-4_15 287

Paine, M.J.I., Scrutton, N.S., Munro, A.W., Gutierrez, A., Gordon C.K. Roberts, Wolf, C.R., 2005. Electron Transfer Partners of Cytochrome P450, in: Cytochrome P450 Structure, Mechanism and Biochemistry. pp. 115–148.

Pang, S.C., Chiang, L.P., Tan, C.H., Vythilingam, I., Lam-Phua, S.G., Ng, L.C., 2015. Low efficacy of delthamethrin-treated net against singapore aedes aegypti is associated with kdr-type resistance. Trop Biomed 32, 140–150.

Parker, J.E.A., Angarita-Jaimes, N., Abe, M., Towers, C.E., Towers, D., McCall, P.J., 2015. Infrared video tracking of *Anopheles gambiae* at insecticide-treated bed nets reveals rapid decisive impact after brief localised net contact. Sci Rep 5, 1–14. https://doi.org/10.1038/srep13392

Phillips, M.A., Burrows, J.N., Manyando, C., Van Huijsduijnen, R.H., Van Voorhis, W.C., Wells, T.N.C., 2017. Malaria. Nat Rev Dis Primers 3. https://doi.org/10.1038/nrdp.2017.50

Pilling, E.D., Jepson, P.C., 1993. Synergism between EBI fungicides and a pyrethroid insecticide in the honeybee (*Apis mellifera*). Pestic Sci 39, 293–297. https://doi.org/10.1002/ps.2780390407

Pluess, B., Tanser, F., Lengeler, C., Sharp, B., 2010. Indoor residual spraying for preventing malaria. Cochrane Database of Systematic Reviews 2010. https://doi.org/10.1002/14651858.CD006657.pub2

Porter, T.D., 2012. New insights into the role of cytochrome P450 reductase (POR) in microsomal redox biology. Acta Pharm Sin B 2, 102–106. https://doi.org/10.1016/j.apsb.2012.02.002

Poulos, T.L., 2003. Cytochrome P450 flexibility. Proc Natl Acad Sci U S A 100, 13121–13122. https://doi.org/10.1073/pnas.2336095100

Poulos, T.L., Finzel, B.C., Howard, A.J., 1987. High-resolution crystal structure of cytochrome P450cam. J Mol Biol 195, 687–700. https://doi.org/10.1016/0022-2836(87)90190-2

Poupardin, R., Srisukontarat, W., Yunta, C., Ranson, H., 2014. Identification of Carboxylesterase Genes Implicated in Temephos Resistance in the Dengue Vector *Aedes aegypti*. PLoS Negl Trop Dis 8. https://doi.org/10.1371/journal.pntd.0002743

Protopopoff, N., Mosha, J.F., Lukole, E., Charlwood, J.D., Wright, A., Mwalimu, C.D., Manjurano, A., Mosha, F.W., Kisinza, W., Kleinschmidt, I., Rowland, M., 2018. Effectiveness of a long-lasting piperonyl butoxide-treated insecticidal net and indoor residual spray interventions, separately and together, against malaria transmitted by pyrethroid-resistant mosquitoes: a cluster, randomised controlled, two-by-two fact. The Lancet 391, 1577–1588. https://doi.org/10.1016/S0140-6736(18)30427-6

Pryce, J., Medley, N., Choi, L., Pryce, J., Medley, N., Choi, L., 2022. Indoor residual spraying for preventing malaria in communities using insecticide-treated nets (Review). https://doi.org/10.1002/14651858.CD012688.pub3.www.cochranelibrary.com

Pryce, J., Richardson, M., Lengeler, C., 2018. Insecticide-treated nets for preventing malaria. Cochrane Database of Systematic Reviews. https://doi.org/10.1002/14651858.CD000363.pub3

Pulman, D.A., 2011. Deltamethrin: The cream of the crop. J Agric Food Chem 59, 2770–2772. https://doi.org/10.1021/jf102256s

Qualls, W.A., Müller, G.C., Revay, E.E., Allan, S.A., Arheart, K.L., Beier, J.C., Smith, M.L., Scott, J.M., Kravchenko, V.D., Hausmann, A., Yefremova, Z.A., Xue, R. de, 2014. Evaluation of attractive toxic sugar bait (ATSB)-Barrier for control of vector and nuisance mosquitoes and its effect on non-target organisms in sub-tropical environments in Florida. Acta Trop 131, 104–110. https://doi.org/10.1016/j.actatropica.2013.12.004

Ranson, H., Burhani, J., Lumjuan, N., Black IV, W.C., 2008. Insecticide resistance in dengue vectors. Tropika 307–316.

Ranson, H., Lissenden, N., 2016. Insecticide Resistance in African *Anopheles* Mosquitoes: A Worsening Situation that Needs Urgent Action to Maintain Malaria Control. Trends Parasitol. https://doi.org/10.1016/j.pt.2015.11.010

Ranson, H., N'Guessan, R., Lines, J., Moiroux, N., Nkuni, Z., Corbel, V., 2011. Pyrethroid resistance in African anopheline mosquitoes: What are the implications for malaria control? Trends Parasitol 27, 91–98. https://doi.org/10.1016/j.pt.2010.08.004

Riveron, J.M., Huijben, S., Tchapga, W., Tchouakui, M., Wondji, M.J., Tchoupo, M., Irving, H., Cuamba, N., Maquina, M., Paaijmans, K., Wondji, C.S., 2019. Escalation of Pyrethroid Resistance in the Malaria Vector *Anopheles funestus* Induces a Loss of Efficacy of Piperonyl Butoxide–Based Insecticide-Treated Nets in Mozambique. J Infect Dis 220, 467–475. https://doi.org/10.1093/infdis/jiz139

Riveron, J.M., Ibrahim, S.S., Chanda, E., Mzilahowa, T., Cuamba, N., Irving, H., Barnes, K.G., Ndula, M., Wondji, C.S., 2014a. The highly polymorphic CYP6M7 cytochrome P450 gene partners with the directionally selected CYP6P9a and CYP6P9b genes to expand the pyrethroid resistance front in the malaria vector *Anopheles funestus* in Africa. BMC Genomics 15, 817. https://doi.org/10.1186/1471-2164-15-817

Riveron, J.M., Ibrahim, S.S., Mulamba, C., Djouaka, R., Irving, H., Wondji, M.J., Ishak, I.H., Wondji, C.S., 2017. Genome-wide transcription and functional analyses reveal heterogeneous molecular mechanisms driving pyrethroids resistance in the major malaria vector *Anopheles funestus* across Africa. G3: Genes, Genomes, Genetics 7, 1819–1832. https://doi.org/10.1534/g3.117.040147

Riveron, J.M., Irving, H., Ndula, M., Barnes, K.G., Ibrahim, S.S., Paine, M.J.I., Wondji, C.S., 2013. Directionally selected cytochrome P450 alleles are driving the spread of pyrethroid resistance in the major malaria vector *Anopheles funestus*. Proceedings of the National Academy of Sciences 110, 252–257. https://doi.org/10.1073/pnas.1216705110

Riveron, J.M., Tchouakui, M., Mugenzi, L., Menze, B.D., Chiang, M.-C., Wondji, C.S., 2018. Insecticide Resistance in Malaria Vectors: An Update at a Global Scale, in: Manguin, S. (Ed.), Towards Malaria Elimination, A Leap Forward. Intechopen, pp. 149–175. https://doi.org/http://dx.doi.org/10.5772/intechopen.78375

Riveron, J.M., Yunta, C., Ibrahim, S.S., Djouaka, R., Irving, H., Menze, B.D., Ismail, H.M., Hemingway, J., Ranson, H., Albert, A., Wondji, C.S., 2014b. A single mutation in the GSTe2 gene allows tracking of metabolically based insecticide resistance in a major malaria vector. Genome Biol 15, 1–20. https://doi.org/10.1186/gb-2014-15-2-r27

Robert, V., 2020. Brief history of insecticide-treated bed nets in the fight against Malaria: A testimony on the crucial 1980's decade. Bulletin de la Societe de Pathologie Exotique 113, 88–103. https://doi.org/10.3166/BSPE-2020-0128

Ruiz-Castillo, P., Rist, C., Rabinovich, R., Chaccour, C., 2022. Insecticide-treated livestock: a potential One Health approach to malaria control in Africa. Trends Parasitol 38, 112–123. https://doi.org/10.1016/j.pt.2021.09.006

Russell, T.L., Govella, N.J., Azizi, S., Drakeley, C.J., Kachur, S.P., Killeen, G.F., 2011. Increased proportions of outdoor feeding among residual malaria vector populations following increased use of insecticide-treated nets in rural Tanzania. Malar J 10, 1–10. https://doi.org/10.1186/1475-2875-10-80

Saavedra-Rodriguez, K., Strode, C., Flores, A.E., Garcia-Luna, S., Reyes-Solis, G., Ranson, H., Hemingway, J., Black IV, W.C., 2014. Differential transcription profiles in *Aedes aegypti* detoxification genes after temephos selection. Insect Mol Biol 23, 199–215. https://doi.org/10.1111/imb.12073

Sanou, A., Nelli, L., Guelbéogo, W.M., Cissé, F., Tapsoba, M., Ouédraogo, P., Sagnon, N., Ranson, H., Matthiopoulos, J., Ferguson, H.M., 2021. Insecticide resistance and behavioural adaptation as a response to long-lasting insecticidal net deployment in malaria vectors in the Cascades region of Burkina Faso. Sci Rep 11, 1–14. https://doi.org/10.1038/s41598-021-96759-w

Schenkman, J.B., Jansson, I., 2003. The many roles of cytochrome b5. Pharmacol Ther 97, 139–152. https://doi.org/10.1016/S0163-7258(02)00327-3

Schenkman, J.B., Jansson, I., 1999. Interactions between cytochrome P450 and cytochrome b5. Drug Metab Rev 31, 351–364. https://doi.org/10.1081/DMR-100101923

Shen, A.L., O'Leary, K.A., Kasper, C.B., 2002. Association of multiple developmental defects and embryonic lethality with loss of microsomal NADPH-cytochrome P450 oxidoreductase. Journal of Biological Chemistry 277, 6536–6541. https://doi.org/10.1074/jbc.M111408200

Sherrard-Smith, E., Griffin, J.T., Winskill, P., Corbel, V., Pennetier, C., Djénontin, A., Moore, S., Richardson, J.H., Müller, P., Edi, C., Protopopoff, N., Oxborough, R., Agossa, F., N'Guessan, R., Rowland, M., Churcher, T.S., 2018. Systematic review of indoor residual spray efficacy and effectiveness against *Plasmodium falciparum* in Africa. Nat Commun. https://doi.org/10.1038/s41467-018-07357-w

Sherrard-Smith, E., Skarp, J.E., Beale, A.D., Fornadel, C., Norris, L.C., Moore, S.J., Mihreteab, S., Charlwood, J.D., Bhatt, S., Winskill, P., Griffin, J.T., Churcher, T.S., 2019. Mosquito feeding behavior and how it influences residual malaria transmission across Africa. Proceedings of the National Academy of Sciences 116, 15086–15095. https://doi.org/10.1073/pnas.1820646116

Shono, T., Ohsawa, K., Casida, J.E., 1979. Metabolism of trans-and cis-Permethrin, trans-and cis-Cypermethrin, and Decamethrin by Microsomal Enzymes. J Agric Food Chem 27, 316–325. https://doi.org/10.1021/jf60222a059

Silva, A.P.B., Santos, J.M.M., Martins, A.J., 2014. Mutations in the voltage-gated sodium channel gene of anophelines and their association with resistance to pyrethroids - A review. Parasit Vectors 7. https://doi.org/10.1186/1756-3305-7-450

Silva, J.J., Scott, J.G., 2020. Conservation of the voltage-sensitive sodium channel protein within the Insecta. Insect Mol Biol 29, 9–18. https://doi.org/10.1111/imb.12605

Silvério, F.O., de Alvarenga, E.S., Moreno, S.C., Picanço, M.C., 2009. Synthesis and insecticidal activity of new pyrethroids. Pest Manag Sci 65, 900–905. https://doi.org/10.1002/ps.1771

Simma, E.A., Dermauw, W., Balabanidou, V., Snoeck, S., Bryon, A., Clark, R.M., Yewhalaw, D., Vontas, J., Duchateau, L., Van Leeuwen, T., 2019. Genome-wide gene expression profiling reveals that cuticle alterations and P450 detoxification are associated with deltamethrin and DDT resistance in *Anopheles arabiensis* populations from Ethiopia. Pest Manag Sci 75, 1808–1818. https://doi.org/10.1002/ps.5374

Sinka, M.E., Bangs, M.J., Manguin, S., Coetzee, M., Mbogo, C.M., Hemingway, J., Patil, A.P., Temperley, W.H., Gething, P.W., Kabaria, C.W., Okara, R.M., Boeckel, T. Van, Godfray, H.C.J., Harbach, R.E., Hay, S.I., 2010a. The dominant *Anopheles* vectors of human malaria in Africa, Europe and the Middle East: occurrence data, distribution maps and bionomic précis. Parasit Vectors 3, 117.

Sinka, M.E., Golding, N., Massey, N.C., Wiebe, A., Huang, Z., Hay, S.I., Moyes, C.L., 2016. Modelling the relative abundance of the primary African vectors of malaria before and after the implementation of indoor, insecticide-based vector control. Malar J 15, 142. https://doi.org/10.1186/s12936-016-1187-8

Sinka, M.E., Pironon, S., Massey, N.C., Longbottom, J., Hemingway, J., Moyes, C.L., Willis, K.J., 2020. A new malaria vector in Africa: Predicting the expansion range of *Anopheles stephensi* and identifying the urban populations at risk. Proc Natl Acad Sci U S A 117, 24900–24908. https://doi.org/10.1073/pnas.2003976117

Sinka, M.E., Rubio-Palis, Y., Manguin, S., Patil, A.P., Temperley, W.H., Gething, P.W., Van Boeckel, T., Kabaria, C.W., Harbach, R.E., Hay, S.I., 2011. The dominant *Anopheles* vectors of human malaria in the Asia-Pacific region: occurrence data, distribution maps and bionomic précis. Parasit Vectors 4. https://doi.org/10.1186/1756-3305-4-210

Sinka, M.E., Rubio-Palis, Y., Manguin, S., Patil, A.P., Temperley, W.H., Gething, P.W., Van Boeckel, T., Kabaria, C.W., Harbach, R.E., Hay, S.I., 2010b. The dominant *Anopheles* vectors of human malaria in the Americas: Occurrence data, distribution maps and bionomic précis. Parasit Vectors 4, 1–26. https://doi.org/10.1186/1756-3305-4-210

Sochantha, T., van Bortel, W., Savonnaroth, S., Marcotty, T., Speybroeck, N., Coosemans, M., 2010. Personal protection by long-lasting insecticidal hammocks against the bites of forest malaria vectors. Tropical Medicine and International Health 15, 336–341. https://doi.org/10.1111/j.1365-3156.2009.02457.x

Soderlund, D.M., 2020. Neurotoxicology of pyrethroid insecticides, in: Neurotoxicity of Pesticides. Elsevier Inc., pp. 113–165. https://doi.org/10.1016/bs.ant.2019.11.002

Soderlund, D.M., Casida, J.E., 1977. Effects of pyrethroid structure on rates of hydrolysis and oxidation by mouse liver microsomal enzymes. Pestic Biochem Physiol 7, 391–401. https://doi.org/10.1016/0048-3575(77)90043-8

Soderlund, D.M., York, N., States, U., 2017. Targeting Voltage-Gated Sodium Channels for Insect Control : Past , Present , and Future.

Sparks, T.C., Lorsbach, B.A., 2017. Agrochemical Discovery - Building the Next Generation of Insect Control Agents 1–17.

Sparks, T.C., Nauen, R., 2015. IRAC: Mode of action classification and insecticide resistance management. Pestic Biochem Physiol 121, 122–128. https://doi.org/10.1016/j.pestbp.2014.11.014

Sparks, T.C., Wessels, F.J., Lorsbach, B.A., Nugent, B.M., Watson, G.B., 2019. The new age of insecticide discovery-the crop protection industry and the impact of natural products. Pestic Biochem Physiol 161, 12–22. https://doi.org/10.1016/j.pestbp.2019.09.002

Spencer, C.S., Yunta, C., de Lima, G.P.G., Hemmings, K., Lian, L.Y., Lycett, G., Paine, M.J.I., 2018. Characterisation of *Anopheles gambiae* heme oxygenase and metalloporphyrin feeding suggests a potential role in reproduction. Insect Biochem Mol Biol 98, 25–33. https://doi.org/10.1016/j.ibmb.2018.04.010

Spitzen, J., Ponzio, C., Koenraadt, C.J.M., Jamet, H.V.P., Takken, W., 2014. Absence of Close-Range Excitorepellent Effects in Malaria Mosquitoes Exposed to Deltamethrin-Treated Bed Nets 90, 1124–1132. https://doi.org/10.4269/ajtmh.13-0755

Srisawat, R., Komalamisra, N., Eshita, Y., Zheng, M., Ono, K., Itoh, T.Q., Matsumoto, A., Petmitr, S., Rongsriyam, Y., 2010. Point mutations in domain II of the voltage-gated sodium channel gene in deltamethrin-resistant aedes aegypti (diptera: culicidae). Appl Entomol Zool 45, 275–282. https://doi.org/10.1303/aez.2010.275

Stevenson, B.J., Bibby, J., Pignatelli, P., Muangnoicharoen, S., O'Neill, P.M., Lian, L.Y., Müller, P., Nikou, D., Steven, A., Hemingway, J., Sutcliffe, M.J., Paine, M.J.I., 2011. Cytochrome P450 6M2 from the malaria vector Anopheles gambiae metabolizes pyrethroids: Sequential metabolism of deltamethrin revealed. Insect Biochem Mol Biol 41, 492–502. https://doi.org/10.1016/j.ibmb.2011.02.003

Strode, C., Donegan, S., Garner, P., Enayati, A.A., Hemingway, J., 2014. The Impact of Pyrethroid Resistance on the Efficacy of Insecticide-Treated Bed Nets against African Anopheline

Mosquitoes: Systematic Review and Meta-Analysis. PLoS Med 11. https://doi.org/10.1371/journal.pmed.1001619

Suh, E., Grossman, M.K., Waite, J.L., Dennington, N.L., Sherrard-Smith, E., Churcher, T.S., Thomas, M.B., 2020. The influence of feeding behaviour and temperature on the capacity of mosquitoes to transmit malaria. Nat Ecol Evol 7, 940–951. https://doi.org/10.1038/s41559-020-1182-x

Sun, H., Mertz, R.W., Smith, L.B., Scott, J.G., 2021. Transcriptomic and proteomic analysis of pyrethroid resistance in the CKR strain of *Aedes aegypti*. PLoS Negl Trop Dis 15, e0009871. https://doi.org/10.1371/journal.pntd.0009871

Swai, J.K., Mmbando, A.S., Ngowo, H.S., Odufuwa, O.G., Finda, M.F., Mponzi, W., Nyoni, A.P., Kazimbaya, D., Limwagu, A.J., Njalambaha, R.M., Abbasi, S., Moore, S.J., Schellenberg, J., Lorenz, L.M., Okumu, F.O., 2019. Protecting migratory farmers in rural Tanzania using eave ribbons treated with the spatial mosquito repellent, transfluthrin. Malar J 1–13. https://doi.org/10.1186/s12936-019-3048-8

Tchigossou, G.M., Atoyebi, S.M., Akoton, R., Tossou, E., Innocent, D., Riveron, J., Irving, H., Yessoufou, A., Wondji, C., Djouaka, R., 2020. Investigation of DDT resistance mechanisms in *Anopheles funestus* populations from northern and southern Benin reveals a key role of the GSTe2 gene. Malar J 1–12. https://doi.org/10.1186/s12936-020-03503-2

Temu, E.A., Minjas, J.N., Tuno, N., Kawada, H., Takagi, M., 2007. Identification of four members of the *Anopheles funestus (*Diptera: Culicidae) group and their role in *Plasmodium falciparum* transmission in Bagamoyo coastal Tanzania. Acta Trop 102, 119–125. https://doi.org/10.1016/j.actatropica.2007.04.009

Thomsen, E.K., Koimbu, G., Pulford, J., Jamea-Maiasa, S., Ura, Y., Keven, J.B., Siba, P.M., Mueller, I., Hetzel, M.W., Reimer, L.J., 2017. Mosquito behavior change after distribution of bednets results in decreased protection against malaria exposure. Journal of Infectious Diseases 215, 790–797. https://doi.org/10.1093/infdis/jiw615

Toe, K.H., Mueller, P., Badolo, A., Traore, A., N'Falé, S., Dabire, R.K., Ranson, H., 2018. Do bednets including piperonyl butoxide offer additional protection against populations of *Anopheles gambiae* s.l. that are highly resistant to pyrethroids? An experimental hut evaluation in Burkina Faso.

Traore, M.M., Junnila, A., Traore, S.F., Doumbia, S., Revay, E.E., Kravchenko, V.D., Schlein, Y., Arheart, K.L., Gergely, P., Xue, R. de, Hausmann, A., Beck, R., Prozorov, A., Diarra, R.A., Kone, A.S., Majambere, S., Bradley, J., Vontas, J., Beier, J.C., Müller, G.C., 2020. Large-scale field trial of attractive toxic sugar baits (ATSB) for the control of malaria vector mosquitoes in Mali, West Africa. Malar J 19, 1–16. https://doi.org/10.1186/s12936-020-3132-0

Tungu, P.K., Michael, E., Sudi, W., Kisinza, W.W., Rowland, M., 2021. Efficacy of interceptor ® G2 , a long - lasting insecticide mixture net treated with chlorfenapyr and alpha - cypermethrin against *Anopheles funestus* : experimental hut trials in north - eastern Tanzania. Malar J 20. https://doi.org/10.1186/s12936-021-03716-z

Usherwood, P.N.R., Davies, T.G.E., Mellor, I.R., O'Reilly, A.O., Peng, F., Vais, H., Khambay, B.P.S., Field, L.M., Williamson, M.S., 2007. Mutations in DIIS5 and the DIIS4-S5 linker of *Drosophila melanogaster* sodium channel define binding domains for pyrethroids and DDT. FEBS Lett 581, 5485–5492. https://doi.org/10.1016/j.febslet.2007.10.057

Vais, H., Atkinson, S., Pluteanu, F., Goodson, S.J., Devonshire, A.L., Williamson, M.S., Usherwood, P.N.R., 2003. Mutations of the para sodium channel of *Drosophila melanogaster* identify putative binding sites for pyrethroids. Mol Pharmacol 64, 914–922. https://doi.org/10.1124/mol.64.4.914

Vais, H., Williamson, M.S., Devonshire, A.L., Usherwood, P.N.R., 2001. The molecular interactions of pyrethroid insecticides with insect and mammalian sodium channels. Pest Manag Sci 57, 877–888. https://doi.org/10.1002/ps.392

Vannini, L., Reed, T.W., Willis, J.H., 2014. Temporal and spatial expression of cuticular proteins of *Anopheles gambiae* implicated in insecticide resistance or differentiation of M/S incipient species. Parasit Vectors 7, 1–11. https://doi.org/10.1186/1756-3305-7-24

Vontas, J., Blass, C., Koutsos, A.C., David, J.P., Kafatos, F.C., Louis, C., Hemingway, J., Christophides, G.K., Ranson, H., 2005. Gene expression in insecticide resistant and susceptible *Anopheles gambiae* strains constitutively or after insecticide exposure. Insect Mol Biol. https://doi.org/10.1111/j.1365-2583.2005.00582.x

Vontas, J., Katsavou, E., Mavridis, K., 2020. Cytochrome P450-based metabolic insecticide resistance in *Anopheles* and *Aedes* mosquito vectors: Muddying the waters. Pestic Biochem Physiol 170, 104666. https://doi.org/10.1016/j.pestbp.2020.104666

Wang, M., Roberts, D.L., Paschke, R., Shea, T.M., Masters, B.S.S., Kim, J.J.P., 1997. Three-dimensional structure of NADPH-cytochrome P450 reductase: Prototype for FMN- and FAD-containing enzymes. Proc Natl Acad Sci U S A 94, 8411–8416. https://doi.org/10.1073/pnas.94.16.8411

Weedall, G.D., Mugenzi, L.M.J., Menze, B.D., Tchouakui, M., Ibrahim, S.S., Amvongo-Adjia, N., Irving, H., Wondji, M.J., Tchoupo, M., Djouaka, R., Riveron, J.M., Wondji, C.S., 2019. A cytochrome P450 allele confers pyrethroid resistance on a major African malaria vector, reducing insecticide-treated bednet efficacy. Sci Transl Med 11, eaat7386. https://doi.org/10.1126/scitranslmed.aat7386

WHO, 2022a. World Malaria Report 2022.

WHO, 2022b. Prequalified Vector Control Products.

WHO, 2022c. Determining discriminating concentrations of insecticides for monitoring resistance in mosquitoes: report of a multi-centre laboratory study and WHO expert consultations.

WHO, 2021. World Malaria Report, World Malaria Report 2021.

WHO, 2020. Vector-borne diseases, Vector-borne diseases. URL https://www.who.int/news-room/fact-sheets/detail/vector-borne-diseases

WHO, 2018. Global report on insecticide resistance in malaria vectors: 2010-2016.

WHO, 2017. Conditions for deployment of mosquito nets treated with a pyrethroid and piperonyl butoxide. Global Malaria Programme, World Health Organization 2017, 1–4.

WHO, 2016. World Malaria Report 2016.

WHO, 2006. Pesticide and their Application for the control of vectors and pests of Public Health importance. World Health Organization 6. https://doi.org/10.1371/journal.pone.0170079

WHO, 2005. World Malaria Report. World Health Organization 316. https://doi.org/10.1007/SpringerReference_83401

Williams, P.A., Cosme, J., Sridhar, V., Johnson, E.F., McRee, D.E., 2000. Mammalian microsomal cytochrome P450 monooxygenase: Structural adaptations for membrane binding and functional diversity. Mol Cell 5, 121–131. https://doi.org/10.1016/S1097-2765(00)80408-6

Williamson, M.S., Martinez-Torres, D., Hick, C.A., Devonshire, A.L., 1996. Identification of mutations in the housefly para-type sodium channel gene associated with knockdown resistance (kdr) to pyrethroid insecticides. Molecular and General Genetics. https://doi.org/10.1007/BF02173204

Wondji, C.S., Hearn, J., Irving, H., Wondji, M.J., Weedall, G., 2022. RNAseq-based gene expression profiling of the *Anopheles funestus* pyrethroid-resistant strain FUMOZ highlights the predominant role of the duplicated CYP6P9a/b cytochrome P450s. G3: Genes, Genomes, Genetics 12. https://doi.org/10.1093/G3JOURNAL/JKAB352

Wood, O.R., Hanrahan, S., Coetzee, M., Koekemoer, L.L., Brooke, B.D., 2010. Cuticle thickening associated with pyrethroid resistance in the major malaria vector *Anopheles funestus*. Parasit Vectors 3, 67. https://doi.org/10.1186/1756-3305-3-67

Yahouédo, G.A., Chandre, F., Rossignol, M., Ginibre, C., Balabanidou, V., Mendez, N.G.A., Pigeon, O., Vontas, J., Cornelie, S., 2017. Contributions of cuticle permeability and enzyme detoxification to pyrethroid resistance in the major malaria vector *Anopheles gambiae*. Sci Rep 7, 1–10. https://doi.org/10.1038/s41598-017-11357-z

Yanola, J., Somboon, P., Walton, C., Nachaiwieng, W., Somwang, P., Prapanthadara, L. aied, 2011. High-throughput assays for detection of the F1534C mutation in the voltage-gated sodium channel gene in permethrin-resistant *Aedes aegypti* and the distribution of this mutation throughout Thailand. Tropical Medicine and International Health 16, 501–509. https://doi.org/10.1111/j.1365-3156.2011.02725.x

Yoshida, T., 2013. Analytical method for urinary metabolites of the fluorine-containing pyrethroids metofluthrin, profluthrin and transfluthrin by gas chromatography / mass spectrometry. Journal of Chromatography B 913–914, 77–83. https://doi.org/10.1016/j.jchromb.2012.11.025

Yoshida, T., 2012. Identification of urinary metabolites in rats administered the fluorine-containing pyrethroids metofluthrin, profluthrin, and transfluthrin 94, 1789–1804. https://doi.org/10.1080/02772248.2012.729838

Yunta, C., Grisales, N., Nász, S., Hemmings, K., Pignatelli, P., Voice, M., Ranson, H., Paine, M.J.I., 2016. Pyriproxyfen is metabolized by P450s associated with pyrethroid resistance in *An. gambiae*. Insect Biochem Mol Biol 78, 50–57. https://doi.org/10.1016/j.ibmb.2016.09.001

Yunta, C., Hemmings, K., Stevenson, B., Koekemoer, L.L., Matambo, T., Pignatelli, P., Voice, M., Nász, S., Paine, M.J.I., 2019. Cross-resistance profiles of malaria mosquito P450s associated with pyrethroid resistance against WHO insecticides. Pestic Biochem Physiol 161, 61–67. https://doi.org/10.1016/j.pestbp.2019.06.007

Zabalou, S., Riegler, M., Theodorakopoulou, M., Stauffer, C., Savakis, C., Bourtzis, K., 2004. Wolbachia-induced cytoplasmic incompatibility as a means for insect pest population control. Proc Natl Acad Sci U S A 101, 15042–15045. https://doi.org/10.1073/pnas.0403853101

Zhang, M., Scott, J.G., 1996. Cytochrome b5 is essential for cytochrome P450 6D1-mediated cypermethrin resistance in LPR house flies. Pestic Biochem Physiol 55, 150–156. https://doi.org/10.1006/pest.1996.0044

Zhang, M., Scott, J.G., 1994. Cytochrome b5 involvement in cytochrome P450 monooxygenase activities in house fly microsomes. Arch Insect Biochem Physiol 27, 205–216. https://doi.org/10.1002/arch.940270306

Zheng, X., Zhang, D., Li, Y., Yang, C., Wu, Y., Liang, X., Liang, Y., Pan, X., Hu, L., Sun, Q., Wang, X., Wei, Y., Zhu, J., Qian, W., Yan, Z., Parker, A.G., Gilles, J.R.L., Bourtzis, K., Bouyer, J., Tang, M., Zheng, B., Yu, J., Liu, J., Zhuang, J., Hu, Zhigang, Zhang, M., Gong, J.T., Hong, X.Y., Zhang, Z., Lin, L., Liu, Q., Hu, Zhiyong, Wu, Z., Baton, L.A., Hoffmann, A.A., Xi, Z., 2019. Incompatible and sterile insect techniques combined eliminate mosquitoes. Nature 572, 56–61. https://doi.org/10.1038/s41586-019-1407-9

Zhou, G., Li, Y., Jeang, B., Wang, X., Cummings, R.F., Zhong, D., Yan, G., 2022. Emerging Mosquito Resistance to Piperonyl Butoxide-Synergized Pyrethroid Insecticide and Its Mechanism. J Med Entomol 1–10. https://doi.org/https://doi.org/10.1093/jme/tjab231

Zhu, F., Sams, S., Moural, T., Haynes, K.F., Potter, M.F., Palli, S.R., 2012. RNA interference of NADPH-cytochrome P450 reductase results in reduced insecticide resistance in the bed bug, cimex lectularius. PLoS One 7. https://doi.org/10.1371/journal.pone.0031037

Zimmer, C.T., Bass, C., Williamson, M.S., Kaussmann, M., Wölfel, K., Gutbrod, O., Nauen, R., 2014. Molecular and functional characterization of CYP6BQ23, a cytochrome P450 conferring resistance to pyrethroids in European populations of pollen beetle, *Meligethes aeneus*. Insect Biochem Mol Biol 45, 18–29. https://doi.org/10.1016/j.ibmb.2013.11.008

2. Chapter 2. - Towards understanding transfluthrin efficacy in a pyrethroid-resistant strain of the malaria vector *Anopheles funestus* with special reference to cytochrome P450-mediated detoxification

Melanie Nolden [a,b], Andreas Brockmann [a,c], Ulrich Ebbinghaus-Kintscher [a], Kai-Uwe Brueggen [a], Sebastian Horstmann [a], Mark J.I. Paine [b], Ralf Nauen [a,*]

[a] *Bayer AG, Crop Science Division, Alfred Nobel Str. 50, D-40789 Monheim am Rhein, Germany*

[b] *Department of Vector Biology, Liverpool School of Tropical Medicine, Pembroke Place, Liverpool L3 5QA, United Kingdom*

[c] *Rheinische Friedrich-Wilhelms-Universität Bonn, D-53113 Bonn, Germany*

* Corresponding author. Bayer AG, Crop Science Division, Alfred Nobel Str. 50, D-40789 Monheim am Rhein, Germany

E-mail address: ralf.nauen@bayer.com

Abstract

Malaria vector control interventions rely heavily on the application of insecticides against anopheline mosquitoes, in particular the fast acting pyrethroids that target insect voltage-gated sodium channels (VGSC). Frequent applications of pyrethroids has resulted in resistance development in the major malaria vectors including *Anopheles funestus*, where resistance is primarily metabolic and driven by the overexpression of microsomal cytochrome P450 monooxygenases (P450s). Here we examined the pattern of cross-resistance of the pyrethroid-resistant *An. funestus* strain FUMOZ-R towards transfluthrin and multi-halogenated benzyl derivatives, permethrin, cypermethrin and deltamethrin in comparison to the susceptible reference strain FANG. Transfluthrin and two multi-fluorinated derivatives exhibited micromolar potency - comparable to permethrin - to functionally expressed dipteran VGSC in a cell-based cation influx assay. The activity of transfluthrin and its derivatives on VGSC was strongly correlated with their contact efficacy against strain FUMOZ-

R, although no such correlation was obtained for the other pyrethroids due to their rapid detoxification by the resistant strain. The low resistance levels for transfluthrin and derivatives in strain FUMOZ-R were only weakly synergized by known P450 inhibitors such as piperonyl butoxide (PBO), triflumizole and 1-aminobenzotriazole (1-ABT). In contrast, deltamethrin toxicity in FUMOZ-R was synergized > 100-fold by all three P450 inhibitors. The biochemical profiling of a range of fluorescent resorufin and coumarin compounds against FANG and FUMOZ-R microsomes identified 7-benzyloxymethoxy-4-trifluoromethylcoumarin (BOMFC) as a highly sensitive probe substrate for P450 activity. BOMFC was used to develop a fluorescence-based high-throughput screening assay to measure the P450 inhibitory action of potential synergists. Azole fungicides prochloraz and triflumizole were identified as extremely potent nanomolar inhibitors of microsomal P450s, strongly synergizing deltamethrin toxicity in *An. funestus*. Overall, the present study contributed to the understanding of transfluthrin efficacy at the molecular and organismal level and identified azole compounds with potential to synergize pyrethroid efficacy in malaria vectors.
Keywords: *Anopheles*; Pyrethroid resistance; P450; Synergists; Azole fungicides; Sodium channel; Deltamethrin; FUMOZ-R; Malaria

2.1. Introduction

The annual infection of humans with malaria remains high with an estimated 219 million cases and 435,000 deaths worldwide in 2017 (WHO, 2018a), the majority (~80%) occurring in sub-Saharan Africa. In Africa malaria is primarily transmitted by sibling species from the Gambiae complex such as *Anopheles gambiae* and *An. arabiensis*, and *An. funestus* (Diptera: Culicidae) from the Funestus subgroup (Sinka et al., 2010; Wiebe et al., 2017). *Anopheles funestus* is one of the major malaria vectors in sub-Saharan-Africa (Temu et al., 2007; Sinka et al., 2010), but its predicted geographical occurrence differs from *An. gambiae* (Wiebe at al., 2017).

Vector control interventions targeting anopheline mosquitoes mainly rely on long-lasting insecticidal nets (LLINs) or indoor residual sprays (IRS) (Bhatt et al., 2015; Sinka et al., 2016), using longstanding chemical classes of insecticides addressing a few modes of action (Nauen, 2007; Hoppé et al., 2016). For over 50 years adult mosquito control has relied on four different chemical classes of insecticides, i.e. DDT, organophosphates, carbamates and pyrethroids, addressing two modes of action. This contrasts with a much larger arsenal of insecticides

targeting a much wider range of modes of action that are available for the control of agricultural pest species (Hemingway et al., 2006; Nauen, 2006; Sparks and Nauen, 2015). It is only very recently that the neonicotinoid clothianidin was introduced, an agricultural pesticide with a new mode of action for vector control uses either alone or in combination with a pyrethroid (Fuseini et al., 2019; Fongnikin et al., 2020).

The success of pyrethroids as insecticides such as deltamethrin (Pulman, 2011) is mainly based on their broad activity against a diverse range of pests and their fast knock-down action (Soderlund, 2020) resulting from the modulation of voltage-gated sodium channels (VGSC) in the insects' central nervous system (Field et al., 2017; Scott, 2019). Pyrethroids are broadly divided into two classes designated as type-I and type-II pyrethroids (Soderlund, 2020), based on the respective absence and presence of an α-cyano substituent that increases VGSC potency that determines the evoked physiological responses (Casida et al., 1983; Laufer et al., 1984; Soderlund and Bloomquist, 1989). Pyrethroids as insecticide sprays for vector control were introduced in the early 1970's (permethrin) and remained the cornerstone for vector control through the introduction of pyrethroid treated bednets 20 years ago, an intervention amongst others contributing to a significant decline in clinical cases of malaria between 2000 and 2015 (Bhatt et al., 2015). However, the spatially expanded exposure of anopheline mosquitoes to pyrethroids in impregnated bed nets (ITNs) and LLINs, resulted in an increasing selection of alleles conferring resistance (Coleman et al., 2017; Moyes et al., 2020; WHO, 2018b). Therefore, the efficacy of these control measures is increasingly compromised by the development and spread of pyrethroid resistance alleles in anopheline mosquitoes, including *An. funestus* (Hemingway et al., 2016; Coleman et al., 2017; Hemingway, 2019).

Two major mechanisms have been described to confer pyrethroid resistance in anopheline mosquitoes (Hemingway et al., 2004; Coleman et al., 2017); metabolic resistance, in particular detoxification mediated by elevated levels of microsomal cytochrome P450 monooxygenases (P450s) (Vontas et al., 2020) known to be involved in oxidative metabolism of xenobiotics (Feyereisen, 1999), and target-site mutations resulting in decreased affinity of pyrethroids to their site of binding in VGSC due to amino acid substitutions, also called knock-down resistance (kdr) (Davies et al., 2007; Scott, 2019; Smith et al., 2019). Other mechanisms such

as changes in cuticular hydrocarbons - resulting in decreased penetration of pyrethroids - are factors shown to contribute to resistance (Balabanidou et al., 2018).

Pyrethroid resistance in *An. funestus* was first described in South Africa (Hargreaves et al., 2000) and shown to be synergized by piperonyl butoxide (PBO), an inhibitor of P450 enzymes (Brooke et al., 2001). Bednets co-impregnated with PBO and pyrethroids were only recently endorsed to mitigate the effects of P450 associated resistance (Gleave et al., 2018; Moyes et al., 2020). Interestingly, despite high levels of pyrethroid resistance in *An. funestus* VGSC mutations known to confer kdr have not yet been described (Irving and Wondji, 2017), whilst kdr has become essentially fixed in populations of *An. gambiae* (Coetzee and Koekemoer, 2013). Upregulated levels of P450s linked to pyrethroid resistance in *An. funestus* have been reported in many field studies in Africa (Cuamba et al., 2010; Morgan et al., 2010; Irving et al., 2012; Djouaka et al., 2016; Sangba et al., 2016; Tchigossou et al., 2018). The genetically duplicated and highly overexpressed P450 alleles CYP6P9a and CYP6P9b are key determinants of pyrethroid-resistance in *An. funestus* (Wondji et al., 2009; Riveron et al., 2013), that have been shown to compromise the efficacy of pyrethroid-treated bednets (Weedall et al., 2019). Many laboratory studies were conducted with the field-collected *An. funestus* colony FUMOZ, especially strain FUMOZ-R, a laboratory-selected reference strain expressing high levels of P450-mediated pyrethroid resistance and lacking kdr (Coetzee and Koekemoer, 2013). It was also shown that cuticle thickening in *An. funestus* (FUMOZ) could apparently affect pyrethroid penetration and thus contributing as an adjunct to the primary mechanism of resistance based on P450 overexpression (Wood et al., 2010).

Not all pyrethroids are similarly affected by P450-mediated resistance in *An. funestus* as recently demonstrated for the multi-halogenated benzyl pyrethroid transfluthrin (Horstmann and Sonneck, 2016). Transfluthrin (2,3,5,6-tetrafluorobenzyl(1R,3S)-3-(2,2-dichlorovinyl)-2,2-dimethylcyclo-propanecarboxylate; syn. benfluthrin) is an enantiomerically pure and volatile pyrethroid exhibiting spatial repellent activity against mosquitoes (Ogoma et al., 2012, 2014; Bibbs et al., 2018). It is under scrutiny as a complementary outdoor-protection tool to current vector control interventions (Kline and Urban, 2018; Masalu et al., 2020).

Here, we have examined the cross-resistance pattern of transfluthrin and halogenated benzyl derivatives against a susceptible strain (FANG) and the FUMOZ-R pyrethroid-resistant strain of *An. funestus*. We have also measured the interactions of pyrethroids with recombinantly expressed dipteran VGSC and explored the role of microsomal P450s in transfluthrin metabolism and resistance by synergist studies *in vivo* and *in vitro*. Overall, this has provided new insights on the efficacy and resistance-breaking properties of transfluthrin in pyrethroid-resistant *An. funestus* that will aid the development of new malaria control products.

2.2. Materials and methods

2.2.1. Mosquito strains

Anopheles funestus FUMOZ-R strain was obtained in 2011 from the National Institute for Communicable Diseases - Vector Control Reference Unit (VCRU) (Johannesburg, South Africa) and maintained at Bayer AG (Monheim, Germany) without insecticide selection pressure. It was originally collected in 2000 in South Mozambique and is highly resistant to pyrethroids (Brooke et al., 2001; Hunt et al., 2005), driven by the overexpression of cytochrome P450 monooxygenases (P450s) (Amenya et al., 2008). The insecticide susceptible *An. funestus* FANG strain was obtained in 2019 from the Liverpool Insecticide Testing Establishment (LITE) at the Liverpool School of Tropical Medicine (LSTM). The strain was originally received from the National Institute for Communicable Diseases (NICD) in South Africa and collected in Angola. Both strains were kept at 27.5 ± 0.5 °C, 65 ± 5% relative humidity and a photoperiod of 12/12 L:D with one-hour dusk/dawn. Adults were kept in rearing cages (46 cm × 33 cm × 20 cm) and five days after hatching the first blood meal (bovine blood, obtained from Elocin Lab, Oberhausen, Germany) was provided according to standard protocols (Das et al., 2007; Human Disease Vectors (HDV) group of the Insect Pest Control Laboratory, 2017).

2.2.2. Chemicals

Transfluthrin (CAS: 118712-89-3), deltamethrin (CAS: 52918-63-5), permethrin (CAS: 52645-53-1), 1-aminobenzotriazole (1-ABT) (CAS: 1614-12-6), triflumizole (CAS: 68694-11-1) and piperonyl butoxide (PBO) (CAS: 51-03-6) were obtained from Sigma-Aldrich/Merck (Darmstadt, Germany) of the highest purity available. Cypermethrin, and the transfluthrin derivatives TF-0, TF-1, TF-3 and TF-5 (Fig. 1) were of analytical grade and obtained internally from Bayer (Leverkusen, Germany). TF-5 is also known as fenfluthrin (Behrenz and Elbert,

1985). Transfluthrin is an enantiomerically pure compound (> 98% 1R-trans; < 1.0% 1S-trans). A similar enantiomeric purity is expected for the transfluthrin derivatives, which were synthesized starting from reactions of optically active 1R-trans-permethric acid chloride with the respective halogenated benzyl alcohol as described elsewhere (Naumann, 1990).

β-Nicotinamide adenine dinucleotide 2'-phosphate (NADPH) reduced tetrasodium salt hydrate (CAS: 2646-71-1 anhydrous, purity ≥ 93%), 7-ethoxycoumarin (EC; CAS: 31005-02-4, purity > 99%), 7-methoxy-4-trifluoromethylcoumarin (MFC; CAS: 575-04-2, purity ≥ 99%), 7-Ethoxy-4-trifluoromethylcoumarin (EFC; CAS: 115453-82-2, purity ≥ 98%) 7-benzyloxy-4-trifluoromethylcoumarin (BFC; CAS: 220001-53-6, purity ≥ 99%), 7- hydroxy-coumarin (HC; CAS: 93-35-6, purity 99%) 7-hydroxy-4-trifluoromethylcoumarin (HFC; CAS: 575-03-1, purity 98%), 7-methoxyresorufin (MR; CAS: 5725-89-3, purity ≥ 98 %), 7-ethoxyresorufin (ER; CAS: 5725-91-7, purity ≥ 95 %), 7-benzoxyresorufin (BR; CAS: 87687-02-3), 7-n-pentoxyresorufin (PR; CAS: 87687-03-4) and resorufin sodium salt (CAS: 34994-50-8) were purchased from Sigma-Aldrich/Merck (Darmstadt, Germany). 7-Benzyloxymethoxy resorufin (BOMR; CAS: 87687-02-3; Vivid™ P2951) was purchased from Invitrogen, Thermo Fisher Scientific, Waltham, USA). 7-benzyloxymethoxy-4-trifluoromethylcoumarin (BOMFC; CAS: 277309-33-8; purity 95%) was synthesized by Enamine (Riga, Latvia). All chemicals were of analytical grade unless otherwise stated.

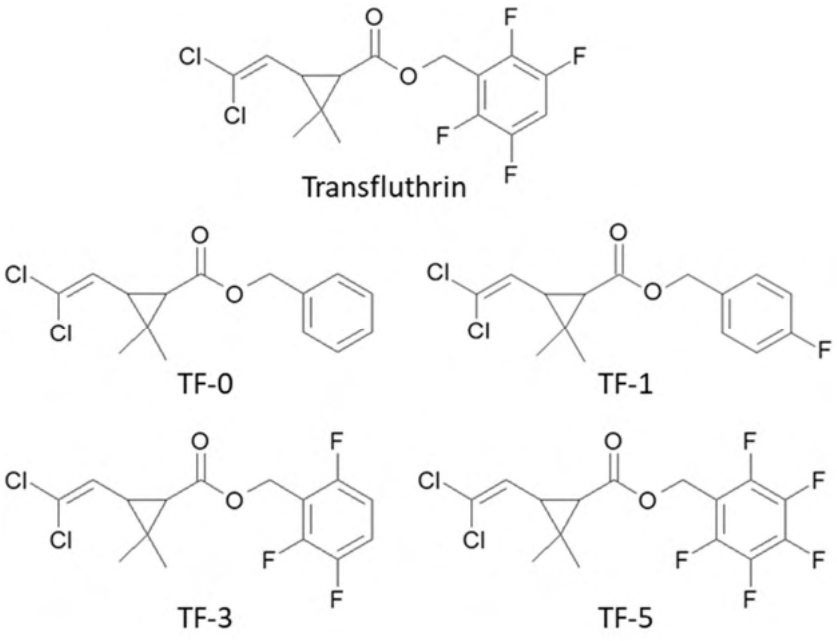

Figure 1. Chemical structures of transfluthrin and its derivatives used in this study

2.2.3. Glazed tile bioassay

To generate dose-response curves of pyrethroids, *An. funestus* FANG and FUMOZ-R mosquitoes were exposed to a range of different concentrations in a glazed tile assay as recently described by Horstmann and Sonneck (2016). Briefly: three to five days-old mosquitoes were anesthetized by placing them for one minute at -20 °C and afterwards on a cooling plate at 2 °C. Ten females were placed in a Petri dish (diameter: 5 cm; height: 1 cm, including 12 ventilation holes) covered with a paper card. Insecticides were dissolved in acetone with a starting concentration of 2000 ppm (equal to 100 mg/m^2) and diluted in 1:5 steps to 0.0256 ppm/0.00512 ppm (0.00128/0.000256 mg/m^2). Using an Eppendorf pipette 1,125 µl of each concentration was applied onto a glazed tile (15 cm × 15 cm, ceramic, Vitra, Germany). After the evaporation of acetone and mosquito recovery from anaesthetation (1 h), mosquitoes were exposed in two replicates (n = 10) for 30 min to each insecticide concentration and afterwards transferred back to the untreated paper card and kept in Petri dishes overnight. A 10% dextrose solution was provided overnight as a food source. Mortality was scored 24 hours post-exposure. Acetone alone served as a control. Control mortality between 5–20 % was corrected using Abbotts formula (Abbott, 1925), and bioassays exceeding 20% control mortality were considered invalid. All bioassays were replicated at least five times with two replicates (n = 10) unless otherwise stated.

2.2.4. Synergist bioassays

Final synergist concentrations of PBO, 1-ABT and triflumizole were chosen based on pre-assays assessing the toxicity of each P450 inhibitor by exposing adults of both strains for 30 minutes to a range of concentrations (10,000, 7,500, 5,000, 4,000, 2,000, 1,000, 500 and 250 ppm in acetone) in a glazed tile assay as described above. After 24 hours, the mortality was evaluated. For the final bioassays the following concentrations were chosen: 2,000 ppm (100 mg/m^2) of triflumizole and PBO, and 5,000 ppm (250 mg/m^2) of 1-ABT for strain FUMOZ-R; 500 ppm (25 mg/m^2) of triflumizole and PBO, and 1,000 ppm (50 mg/m^2) of 1-ABT for strain FANG. Final synergist concentrations were applied onto glazed tiles as described above. Ten female adults were exposed for 30 min to each synergist and immediately afterwards transferred to pyrethroid treated glazed tiles as described above. As a control group, mosquitoes which were not exposed to the synergist and completely untreated mosquitoes were included. Mortality figures were corrected according to Abbott (1925), and tests

exceeding 20% control mortality were considered invalid. All synergist bioassays were replicated at least twice.

2.2.5. UPLC-MS/MS analysis

As the synergists were applied *via* tarsal contact, ultra-performance liquid chromatography and mass spectrometry (UPLC/MS) was used to confirm their uptake by exemplarily analyzing exposed FUMOZ-R mosquito adults. PBO (2,000 ppm), triflumizole (2,000 ppm) and 1-ABT (5,000 ppm) were dissolved in acetone and applied onto a glazed tile as described above. After acetone evaporation (1 h) ten female FUMOZ-R adults were exposed for 30 min to each synergist in replicates (n = 2). After exposure, mosquitoes were placed onto a cooling plate (2 °C) to separate legs and mosquito bodies. Legs and body fractions of ten mosquitoes were pooled (n = 20) in a 1.5 ml reaction tube, washed five times in 1100 µl acetonitrile/water (80/20) and subsequently grinded using a micro-pestle in 1100 µl acetonitrile/water (80/20). The samples were centrifuged at 12,000× g for 10 min at room temperature (Centrifuge 5418R, Eppendorf, Hamburg, Germany) and the supernatant was transferred into a glass vial for subsequent UPLC-MS/MS analysis with slight modifications according to a previously published protocol (Manjon et al., 2018). Briefly, for the chromatography on an Agilent 1290 Infinity II, a Waters Acquity HSS T3 column (2.1 × 50 mm, 1.8 mm) with 0.025% formic acid in acetonitrile and 0.02% formic acid in water as the eluent in gradient mode was employed. After positive electrospray ionization, ion transitions were recorded on a Sciex API6500 Triple Quad. PBO, triflumizole and 1-ABT were measured in positive ion mode (ion transitions: PBO 356 > 177, triflumizole 346 > 278, 1-ABT 135 > 90.9). The peak integrals were calibrated externally against a standard calibration curve. The linear range for the quantification of PBO, triflumizole, and 1-ABT was 0.25–75 ng/ml, 0.25–100 ng/ml, and 0.5–1,000 ng/ml, respectively. Samples were diluted prior to measurement if needed. Recovery rates of mosquitoes exposed to the chosen synergist concentrations and acetone only were normally close to 100%.

2.2.6. Voltage-gated sodium channel measurements

The intrinsic potential of transfluthrin, its derivatives and common pyrethroids were measured in a HEK293 cell line expressing para-type voltage-gated sodium channels of *Musca domestica* (GenBank: AAB47604.1) using a Fluorescent Imaging Plate Reader, FLIPR Tetra

(Molecular Devices, San Jose, CA, USA) fluorescence-based membrane potential assay (Molecular Devices, #R8034). Cells were plated at a density of 40,000 cells/well two days prior to the assay on black poly-D-lysine coated µClear 384-welll plates (Greiner Bio-One, Essen, Germany), incubated overnight at 37 °C (5% CO_2) and subsequently stored 24 hours at 26 °C. The FLIPR voltage membrane potential sensitive (MPs) dye assay was conducted with slight modifications according to Tay et al. (2019). Cell medium was removed, and cells were incubated for one hour with 20 µl per well Tyrode buffer (Sigma T2397) containing 0.01% brilliant black (CAS: 2519-30-4) and 0.75 mg/ml MPs dye in the dark. Common pyrethroids and transfluthrin derivatives were pre-diluted in DMSO and further diluted to a final assay concentration of 50–0.0032 µM (deltamethrin: 50–0.0000256 µM; cypermethrin 10–0.00064 µM) in Tyrode buffer containing 0.03% Pluronic™ F-68 (Thermo Fisher Scientific, Waltham, USA) (final DMSO concentration: 0.5%). Five µl of each concentration was added to each well and replicated four times and immediately measured every five seconds using the FLIPR high throughput cellular screening system at an emission wavelength of 565–625 nm while excited at 510–545 nm. Maximal response-over-baseline of each kinetic was subjected to further analysis using GraphPad Prism 8.4 (GraphPad Software, San Diego, USA). The assay was repeated three times on different days.

2.2.7. Isolation of microsomes and cytochrome P450 activity assays

Thirty to fifty adult mosquitoes (FUMOZ-R or FANG) were homogenized in an Eppendorf tube (2 ml) with a micro pestle in 500 µl homogenization-buffer (0.1 M K_2HPO_4, 1 mM DTT, 1 mM EDTA, 200 mM saccharose, pH 7.6) on ice and afterwards centrifuged at 5,000× *g* at 4 °C for 5 min. The supernatant was centrifuged again for 20 min at 15,000× *g* and 4°C. The resulting supernatant was centrifuged for one hour at 100,000× *g* and 4 °C (Beckman Coulter, Germany; Optima MAX-XP Benchtop Ultracentrifuge, rotor: MLA 130) and the microsomal pellet was resuspended in 250 µl 0.1 M buffer (0.1 M K_2HPO_4, 1 mM DTT, 0.1 mM EDTA, 5% glycerol, pH 7.6). The protein amount was determined according to Bradford (1976) and adjusted to 0.2 mg protein/ml.

The activity of microsomal monooxygenases was measured using a fluorescent probe assay with different model substrates at 20 ± 1°C. Depending on the substrate, the final assay concentrations of fluorescence probes were 100 µM (PC), 50 µM (BFC, EC, EFC, MFC), 10 µM

(BOMFC) and 4 µM (BOMR, BR, ER, MR, PR) adapted from Zimmer et al. (2014) and Manjon et al. (2018) . Substrate stock solutions were prepared in DMSO at 100 mM (PC), 50 mM (BOMFC, BFC, EC, EFC, MFC), 2 mM (BOMR) and 1 mM (BR, ER, MR), and then diluted to the respective concentration with 0.1 M potassium-phosphate buffer (pH 7.6). Twenty-five µl of diluted substrate solution plus 25 µl of diluted enzymes were incubated for one hour with and without 250 µM NADPH in a black 384-well plate (Greiner bio-one, F-bottom, PS). The reaction was replicated four times and stopped by adding 50 µl of red-ox mix (25% DMSO, 50 mM Tris-HCl buffer (pH 10), 5 mM glutathione oxidized, and 0.2 U glutathione reductase). Fluorescence was evaluated using a microplate reader (Tecan, Spark) at the respective excitation and emission wavelengths as described by Zaworra and Nauen (2019). As a positive control, rat liver microsomes (20 mg protein/ml; Sigma-Aldrich) were tested. The resulting reaction products, i.e. HC, HFC and resorufin were used to generate standard curves to calculate the amount of the respective product in pmol per mg/min (Ullrich and Weber, 1972; Manjon et al., 2018).

2.2.8. Michaelis-Menten kinetics of BOMFC O-dearylation by mosquito microsomes

Substrate concentration dependent microsomal monooxygenase kinetics was evaluated using eleven different BOMFC concentrations (stock 100 mM in DMSO) between 200 µM and 0.195 µM diluted in 0.1 M potassium-phosphate buffer (pH 7.6) containing 0.01% zwittergent 3-10 (CAS 15163-36-7, Sigma-Aldrich) and 1 mM NADPH at 20 ± 1 °C. Mosquito microsomal membranes were diluted in buffer (0.1 M K_2HPO_4, 0.1 mM EDTA, 1 mM DTT, 5% glycerol pH 7.6), 0.05% bovine serum albumin (BSA), 0.01% zwittergent 3-10) to 0.16 mg/ml corresponding to 4 µg protein per 25 µl enzyme solution. Twenty-five µl enzyme solution and 25 µl substrate solution were incubated for one hour in a black 384-well plate and the reaction was stopped as described above. Each reaction was replicated four times and the fluorescent product HFC was measured at 405 nm while excited at 510 nm. Substrate saturation kinetics were analyzed using GraphPad Prism 8.4 (Michaelis-Menten model).

2.2.8.1. Microsomal P450 inhibition kinetics

For the determination of IC50-values of different azole compounds and PBO on mosquito (FUMOZ-R) microsomal P450s the probe substrate BOMFC was used at a single concentration around the apparent Km value, i.e. 5 µM (Supplementary Figure S1), following the general protocol recently described by Haas and Nauen (2021) with minor modifications. The chosen

assay conditions were optimized for linearity with time and protein content of 7-hydroxy-4-(trifluoromethyl) coumarin (HC) fluorescent product formation. Microsomes of strain FUMOZ-R were incubated to eleven different concentrations of each inhibitor. Therefore, inhibitors were dissolved in 1:3.3 steps in DMSO at a final concentration of 0.5%, except for epoxiconazole (2%) and uniconazole (1%) to prevent precipitation at the highest concentration. Stock solutions were diluted with 0.1 M potassium-phosphate buffer (pH 7.6) containing 0.01% zwittergent 3-10 (final concentration range between 0.000596 µM and 1,000 µM). Microsomal preparation was diluted in buffer (0.1 M K_2HPO_4, 0.1 mM EDTA, 1 mM DTT, 5% glycerol, pH 7.6) containing 0.01% zwittergent and 0.05% BSA) to 0.16 mg/ml protein corresponding to 4 µg protein/well. Inhibitors and diluted microsomal preparations were applied to a 384-well microplate (384 wells, Greiner bio-one, F-bottom, PS) and incubated for ten minutes at 20 ± 1°C. Subsequently, 25 µl BOMFC/NADPH (final concentration 5 µM/125 µM) solution was added to each well and after 60 min the reaction was stopped as described above. Each reaction was repeated four times. Final assay evaluation was conducted in a microplate reader (Tecan Spark; Excitation: 405 nm; Emission: 510 nm) and reaction mix containing no inhibitor served as full enzyme activity control (100% activity). The controls lacking NADPH and BOMFC were subtracted from each data point. A standard curve was generated using HC to calculate the reaction velocity in pmol HC formed/min × mg protein^{-1}. Data were analysed and IC_{50}-values calculated using a four-parameter non-linear regression fitting routine in GraphPad Prism 8.4.

2.2.9. RNA extraction and cDNA preparation

RNA was extracted from ten adult female mosquitoes of each strain using TRIzol™ reaction kit following manufacturer's instructions. Afterwards RNA was purified using RNAeasy MINI Kit (Qiagen, Hilden, Germany) following manufacturer's instructions, including a DNAse-digest (RNase-free DNAse Set, 79254, Qiagen, Hilden, Germany) (modifications: Trizol incubation: 10 min, the column containing RNA sample was eluated twice to enhance RNA yields). The RNA concentrations were photometrically determined using 260/280 nm and 230/260 nm ratios (NanoQuant Infinite 200, Tecan, Switzerland). All samples were adjusted to 20 ng/µl.

Afterwards the RNA quality was checked using QIAxcel capillary electrophoresis technology following manufacturer instructions (QIAxcel Advanced, RNA Handbook, Qiagen, Hilden, Germany). RNA cartridge (QIAxcel RNA QC Kit v2.0, ID: 929104) and method CL-RNA were used. QX RNA Size Marker 200–6000 nt (Qiagen ID: 929580) and QX RNA alignment marker (Qiagen ID: 929510) served as size marker and alignment marker, respectively. Once the RNA quality was confirmed, 0.3 µg of total RNA in 20 µl reaction volume was used for reverse transcription using IScript cDNA synthesis Kit (Bio-Rad, Hercules, USA) following manufacturer's instructions.

2.2.10. RT-qPCR

RT-qPCR measuring expression levels of CYP6P9a and CYP6P9b was done according to the method recently described by Boaventura et al. (2020) using SsoAdvanced Universal SYBR Green Supermix (Bio-Rad, Hercules, USA) with a total volume of 10 µl using CFX384™ Real-Time system (Bio-Rad, Hercules, USA). Samples were run in triplicate and a non-template control was included as the negative control. Two µl of cDNA with 5 ng/µl and each primer with 200 nM final concentrations were used. The PCR program was as follows: 95 °C for 30 s; 95 °C for 15 s; 55.5 °C for 15 s plate read; steps two and three were repeated 39 times followed by a melting curve from 65 °C to 95 °C in 0.5 °C steps for 5 s. Ribosomal protein S7 (RPS 7) and Actin 5c (Act) served as reference genes in this study. Primer efficiency for each target- and reference gene was determined in advance with serial 1:5 cDNA dilution and revealed: CYP6P9a: 109.8%, CYP6P9b: 102.8%, Actin 5c: 105.9% and RPS 7: 104.3%. Stability of the reference genes was checked with Bio-Rad CFX Maestro 1.0 v 4.0 software (Bio-Rad, 2017, Hercules, USA) (Vandesompele et al., 2002) and were used for normalization. In this study three to four biological replicates of each strain (FANG and FUMOZ-R) with three technical replicates were measured. Primers and GenBank accession numbers are given in the supplementary information (Supplementary Table S1).

2.2.11. Statistical analysis

Probit analysis of mosquito bioassay data was performed to calculate LC_{50} values and its 95% confidence intervals using SPSS version 25 (heterogeneity factor 0.5). EC_{50}-values for voltage-gated sodium channel binding of the different pyrethroids were calculated using GraphPad Prism 8.4 (Nonlinear regression, four parameters, variable slope, constraints: bottom: 0, top:

100). Pearson's correlations between mosquito bioassay data and EC_{50}-values were analyzed using GraphPad Prism 8.4. A one-way-ANOVA was performed to analyze data for significant differences between data obtained for strains FANG and FUMOZ-R in the biochemical assays. Gene expression analysis was carried out employing Bio-Rad CFX Maestro 1.0 v 4.0 software (Bio-Rad, 2017, Hercules, USA) followed by subsequent unpaired t-tests in qbase (Biogazelle) to compare for significant differences in gene expression levels.

2.3. Results

2.3.1. Efficacy of different pyrethroids in glazed tile bioassays

Full dose-response glazed tile bioassays produced a small difference in transfluthrin contact toxicity between *An. funestus* strains FANG and FUMOZ-R, resulting in a resistance ratio (RR) of 2.5 (Table 1). In contrast, FUMOZ-R exhibited high RRs of 223 and 78 against deltamethrin and cypermethrin, respectively. Permethrin and the transfluthrin derivatives TF-0 and TF-1 were the weakest pyrethroids against both strains, with highest LC_{50}-values, as opposed to transfluthrin and its multifluorinated benzyl derivatives TF-3 and TF-5 (Table 1). TF-5 (fenfluthrin) exhibited high contact activity similar to transfluthrin against both strains with a low RR for FUMOZ-R of 1.88, indicating a lack of cross-resistance with deltamethrin and cypermethrin. Based on LC_{50}-values the following efficacy ranking was obtained for the transfluthrin derivatives in glazed tile bioassays with strains FANG and FUMOZ-R: TF = TF-5 > TF-3 >> TF-0 = TF-1 and TF = TF-5 > TF-3 > TF-1 > TF-0, respectively. Those transfluthrin derivatives with a para-fluorinated benzyl ring, TF-1 and TF-5, showed the lowest RRs (< 2) in strain FUMOZ-R, followed by transfluthrin (2.51), TF-0 (3.77) and TF-3 (5.77).

Table 1. Log-dose probit-mortality data (24h) for different pyrethroids against female adults of *Anopheles funestus* strains FANG and FUMOZ-R in glazed tile bioassays after contact exposure (30 min).

Compound	*An. funestus* FANG (susceptible)					*An. funestus* FUMOZ-R (resistant)					RR[b]
	LC_{50} (mg/m²)	95 % CI[a]	Slope	±SE	n	LC_{50} (mg/m²)	95 % CI	Slope	±SE	n	
Transfluthrin (TF)	0.023	(0.0155-0.0324)	1.47	0.168	420	0.0576	(0.0191-0.112)	1.6	0.218	360	2.51
TF-0	1.19	(0.565-1.79)	2.90	0.932	140	4.47	(2.89-6.01)	3.17	0.655	360	3.77
TF-1	1.42	(1.02-1.85)	2.97	0.453	560	1.41	(1.15-1.83)	4.79	0.772	350	0.99
TF-3	0.0494	(0.0350-0.0664)	1.96	0.256	420	0.285	(0.225-0.354)	3.32	0.495	360	5.77
TF-5	0.0237	(0.0132-0.0394)	2.03	0.243	420	0.0446	(0.0299-0.0592)	2.08	0.316	560	1.88
Permethrin	0.543	(0.409-0.702)	2.28	0.294	420	4.21	(2.79-5.88)	1.99	0.278	360	7.76
Cypermethrin	0.0968	(0.0686-0.126)	2.74	0.479	420	7.54	(5.24-10.4)	1.86	0.204	540	77.9
Deltamethrin	0.0206	(0.0153-0.0273)	1.38	0.119	420	4.61	(2.73-7.5)	1.07	0.102	540	223

[a] 95% confidence interval (CI); [b] Resistance ratio (RR) = LC_{50} FUMOZ-R divided by LC_{50} FANG

2.3.2. Sensitivity of recombinantly expressed VGSC to pyrethroids

Pyrethroid activity to *M. domestica* VGSCs heterologously expressed in HEK293 cells was measured by sensing membrane potential changes using fluorescence imaging upon pyrethroid application (Fig. 2). The addition of deltamethrin to HEK293-VGSC cells increased the fluorescence signal in a concentration-dependent manner with an EC_{50}-value of 5.29 nM (95% CI: 4.43–6.30), suggesting high intrinsic VGSC activation (Supplementary Table S3). Cypermethrin and permethrin were significantly less effective and showed EC_{50}-values of 38.9 nM (95% CI: 34.2–44.3) and 721 nM (95% CI: 591–882), respectively (Fig. 2A; Supplementary Table S3). The most potent compound from the transfluthrin series was TF-5 exhibiting an EC_{50}-value similar to permethrin (736 nM (95% CI: 650–834)), followed by transfluthrin, TF-3, TF-1 and TF-0 (Fig. 2B, Supplementary Table S3). The EC_{50}-values of transfluthrin derivatives obtained *in vitro* were strongly correlated with their observed *in vivo* potential in glazed tile bioassays against adult mosquitoes of both strain FANG (Fig. 2C) and FUMOZ-R (Fig. 2D). Such a correlation was also observed for deltamethrin, cypermethrin and permethrin, but only in the pyrethroid susceptible strain FANG (Fig. 2C). In contrast no such correlation was obtained for the resistant strain FUMOZ-R (Fig. 2D). Interestingly transfluthrin and TF-5, despite being more than 100-fold less active on VGSC, exhibited a similar *in vivo* efficacy based on LC_{50}-values in glazed tile bioassays as deltamethrin against strain FANG (Fig. 2C), suggesting additional factors involved in acute contact toxicity than potency on VGSC.

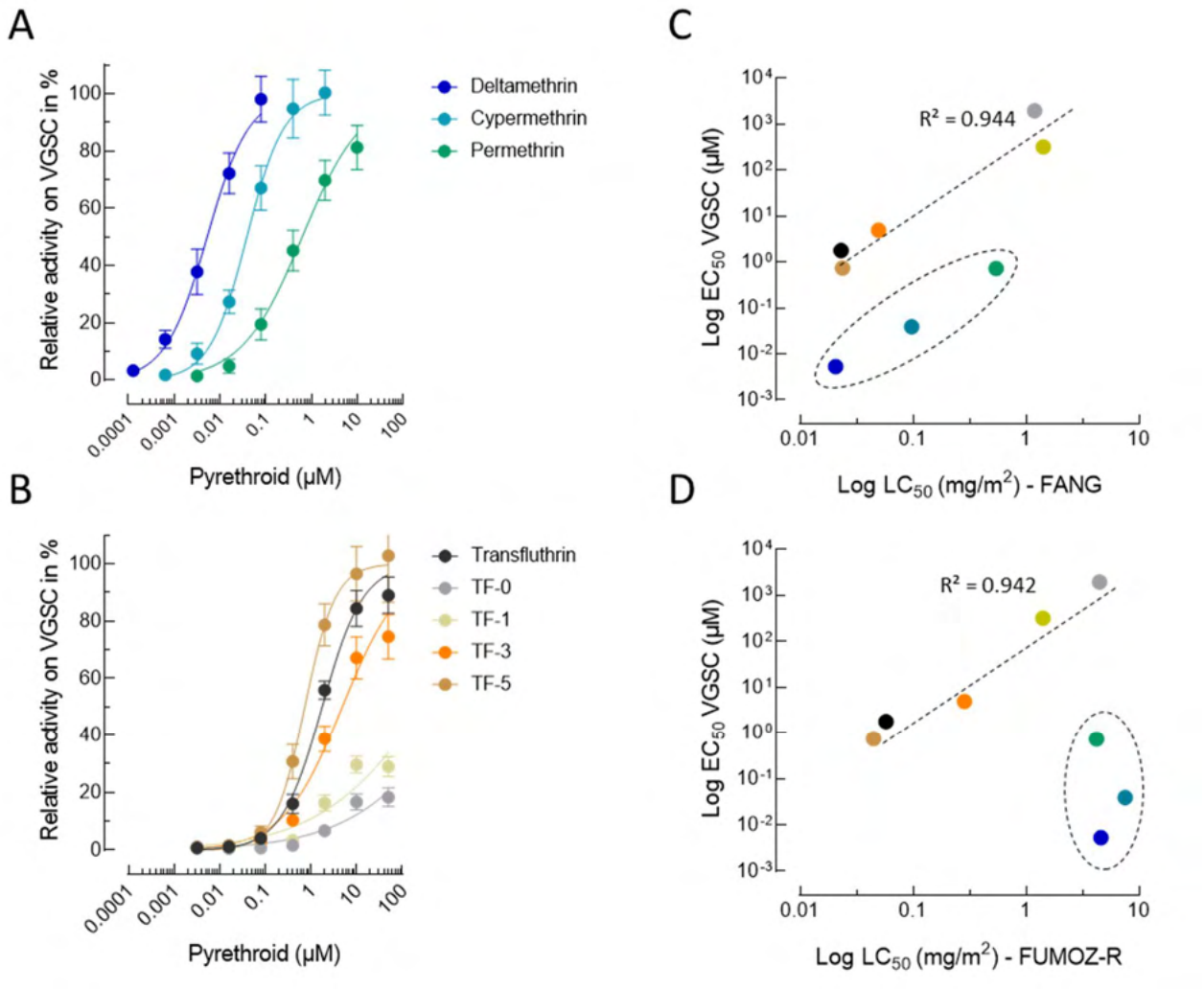

Figure 2. Concentration response curves for common pyrethroids (A) and transfluthrin derivatives (B) measured on functionally expressed house fly voltage-gated sodium channels (VGSC) using a fluorescence-based membrane potential cation influx assay. Data are mean values ± SD (n=12). (C, D) Pearson correlation analysis between *in vitro* VGSC EC_{50}-values and *in vivo* LC_{50}-values obtained from glazed tile bioassays against female adults of *An. funestus* strains FANG (C) and FUMOZ-R (D). Data points circled with a dashed line represent deltamethrin, cypermethrin and permethrin.

2.3.3. Synergism of pyrethroid efficacy by different P450 inhibitors

Synergists were first tested for their solo contact toxicity in glazed tile assays to select concentrations not affecting adult survival. At the highest 1-ABT concentration tested (750 mg/m^2), mortality in both strains was < 10 %. In contrast PBO and triflumizole were toxic against both strains, but at high concentrations. PBO and triflumizole were more active against the susceptible FANG strain with an LC_{50}-value of 325 mg/m^2 (95% CI: 199–707) and 136 mg/m^2 (95% CI: 40.5–188) respectively. Whereas both synergists were less toxic to the resistant strain FUMOZ-R as demonstrated by LC_{50}-values of > 1,000 mg/m^2 and 392 mg/m^2

(95% CI: 293–508) for PBO and triflumizole respectively. Sublethal concentrations of all synergists applied to glazed tiles were readily taken up after 30 min contact by FUMOZ-R adults as shown by UPLC/MS analysis of legs and body extracts, confirming their internalization (Fig. 3). All synergists were highly effective in strain FUMOZ-R in combination with deltamethrin (Fig. 4). This included both the azole compounds triflumizole and 1-ABT not previously tested for their synergistic potential in *An. funestus*. The synergistic ratios for deltamethrin in strain FUMOZ-R were > 100-fold, whereas permethrin, transfluthrin and derivatives were significantly lower (Fig. 4, Supplementary Table S4). There was minimal synergism of transfluthrin and derivative toxicity in the pyrethroid susceptible strain FANG, whereas moderate synergism was detected for the other pyrethroids - depending on the synergist applied (Supplementary Table S4). The synergistic ratios obtained for the transfluthrin derivatives tested against FUMOZ-R revealed weak or no synergism for TF-1 and TF-5 (Fig. 4), which are fluorinated at the para position of the benzyl ring (Fig. 1). A summary of all bioassay data including 64 calculated LC_{50}-values, resistance factors and synergistic ratios is provided in Supplementary Table S3.

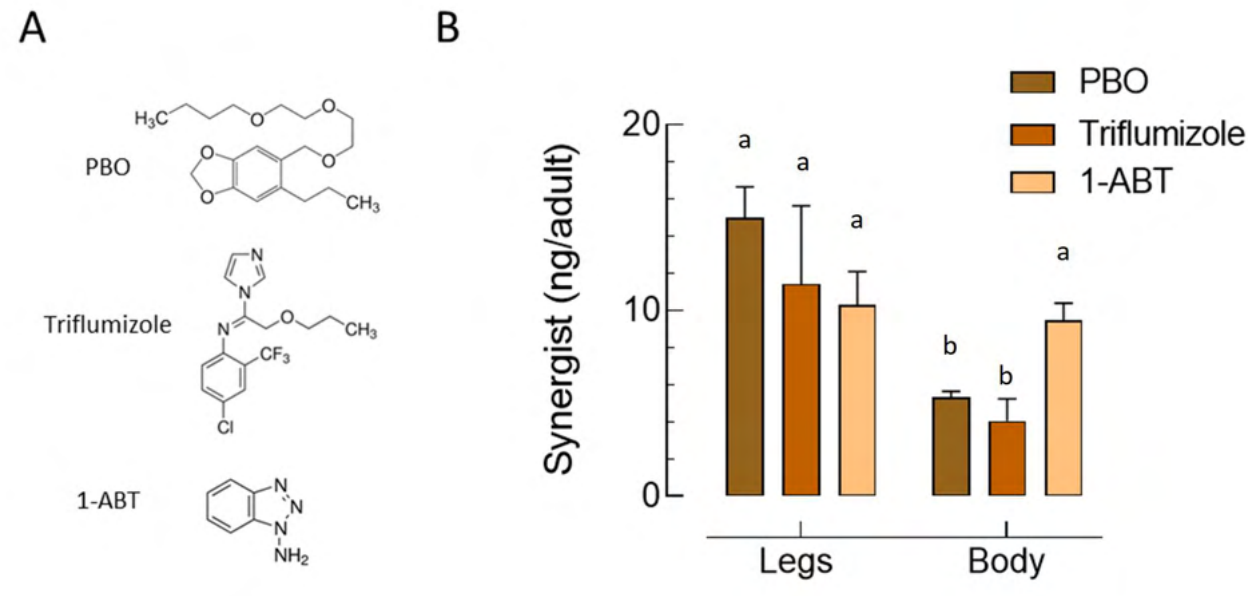

Figure 3. Tarsal uptake of different synergists by adult females of *An. funestus* strain FUMOZ-R by contact exposure for 30 min on glazed tiles. (A) Three different synergists were tested *in vivo*: piperonyl butoxide (PBO; 100mg/m²), triflumizole (100 mg/m²) and 1-aminobenzotriazole (1-ABT; 250 mg/m²). (B) Amount of synergist internalized and detected in mosquito legs and bodies analyzed by UPLC/MS. Different letters denote a significant difference (One-way ANOVA; post hoc Tukey comparison, $P < 0.05$). Data are mean values ± SD (n=20).

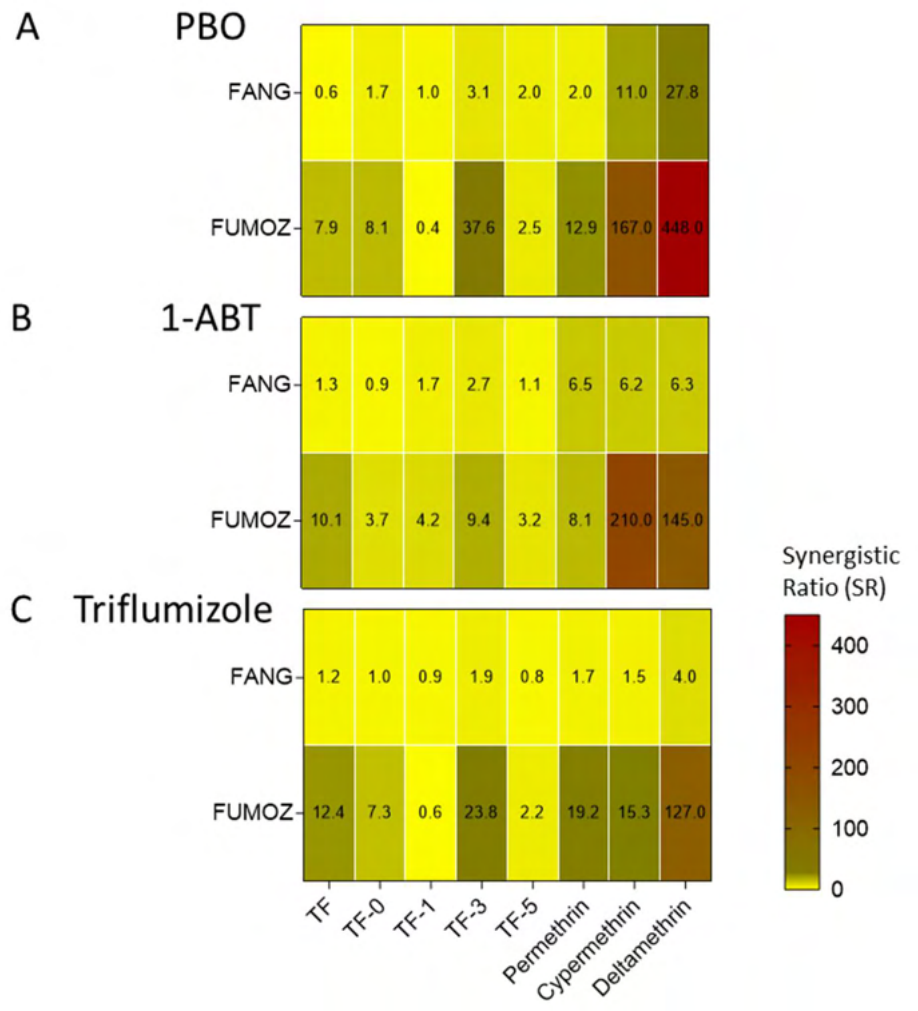

Figure 4. Heat maps displaying the synergistic ratio obtained in glazed tile bioassays for different pyrethroid insecticides in *An. funestus* strain FANG (susceptible) and FUMOZ-R (resistant) upon contact exposure to (A) piperonyl butoxide (PBO), (B) 1-amino-benzotriazole (1-ABT) and (C) triflumizole, directly prior to insecticide application. Synergistic ratios (SR) were calculated by dividing the LC_{50} of the insecticide by the LC_{50} of the insecticide + synergist (Table S3).

2.3.4. Activity and inhibition of *An. funestus* microsomal cytochrome P450 monooxygenases

Microsomal membranes of *An. funestus* strain FUMOZ-R were isolated and tested for their capacity to metabolize a range of different coumarin and resorufin fluorescent probe substrates. The substrate profile obtained for FUMOZ-R microsomes revealed a clear preference for coumarins over resorufins. It is noteworthy that the O-debenzylation of bulkier substrates such as BFC, BOMFC and BOMR was the preferred reaction catalyzed by *An. funestus* microsomal P450s, followed by the O-dealkylation of smaller substrates such as EFC and MFC (Fig. 5). Those substrates showing the highest activity with FUMOZ-R microsomes

were also tested with FANG microsomes. As expected, probe activity was consistently lower when compared to FUMOZ-R, consistent with higher P450 activity in the pyrethroid-resistant strain. The most active probe substrate was BOMFC. O-debenzylation by both FANG and FUMOZ-R microsomes followed Michaelis-Menten kinetics with apparent Km- and Vmax-values of 5.76 µM (95% CI: 3.31–9.67) and 21.5 pmol HFC/min/mg protein (95% CI: 18.9–24.4), and 4.41 µM (95% CI: 3.64–5.33) 114 pmol HFC/min/mg protein (95% CI: 109–119), respectively (Supplementary Figure S1). The significantly higher microsomal BOMFC probe activity of FUMOZ-R compared to FANG was correlated with the overexpression of the well-known P450 variants CYP6P9a and CYP6P9b, as shown by RT-qPCR (Fig. 6).

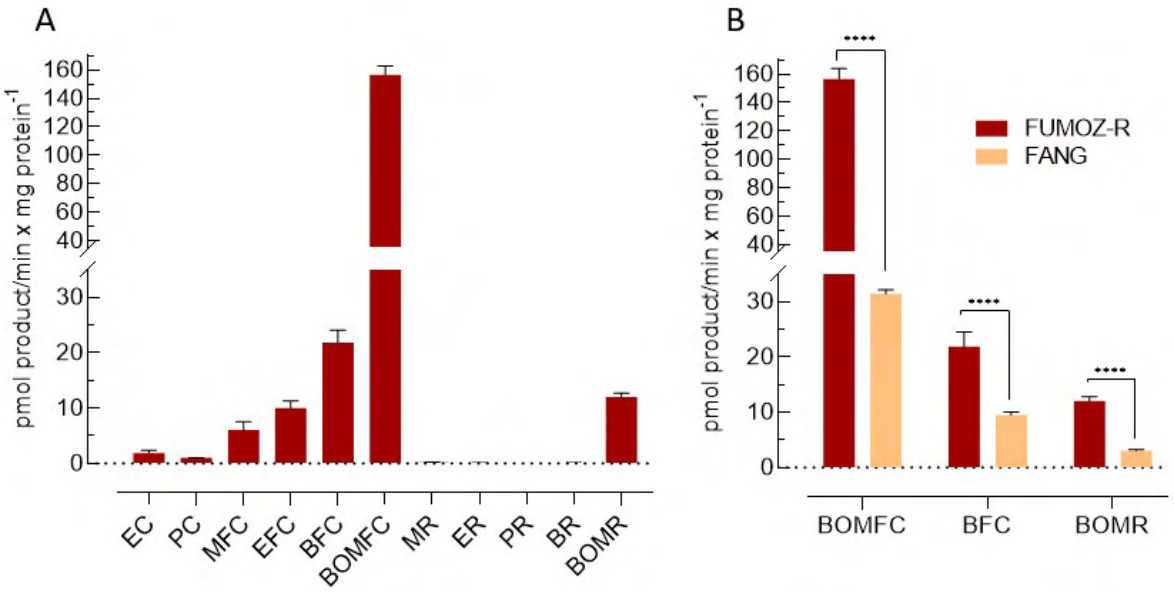

Figure 5. Metabolism of different cytochrome P450 coumarin and resorufin model substrates by microsomal preparations of *A. funestus,* (A) strain FUMOZ-R and (B) strain FANG in comparison to FUMOZ-R with those substrates displaying highest cytochrome P450 activity. Data are mean values ± SD (n=4). Significant differences are denoted by ****p≤0.0001. Substrate abbrevations: EC: 7-ethoxycoumarin, PC: 7-pentoxycoumarin, MFC: 7-methoxy-4-trifluoromethylcoumarin, EFC: 7-ethoxy-4-trifluoromethylcoumarin, BFC: 7-benzyloxy-4-trifluoromethylcoumarin, BOMFC: 7-benzyloxymethoxy-4-trifluoromethylcoumarin, MR: 7-methoxyresorufin, ER: 7-ethoxyresorufin, PR: 7-n-pentoxyresorufin, BR: 7-benzyloxyresorufin ether, BOMR: 7-benzyloxymethoxyresorufin.

Using the highly active probe substrate BOMFC we developed a fluorescence-based high-throughput 384-well plate assay allowing us to assess compounds for their potential to inhibit P450 activity in microsomal preparations of *An. funestus* strain FUMOZ-R. PBO is a potent nanomolar P450 inhibitor that is commonly used in products to inhibit P450-based metabolism, whereas azole fungicides are known to act synergistically in combination with certain neonicotinoids and pyrethroids, particularly in honey bees (Iwasa et al., 2004). The

azole fungicides prochloraz (IC_{50} = 5.92 nM), triflumizole (IC_{50} = 46.8 nM), uniconazole (IC_{50} = 107 nM) were stronger inhibitors than PBO (IC_{50} = 260 nM), whereas ketoconazole (IC_{50} = 260 nM) was similar (Table 2). Interestingly, 1-ABT, a widely known P450 inhibitor, showed a rather weak inhibitory potential (IC_{50} = 119 µM), although its synergistic potential *in vivo* in combination with pyrethroids such as deltamethrin against strain FUMOZ-R was comparable to triflumizole and PBO (Supplementary Table S4).

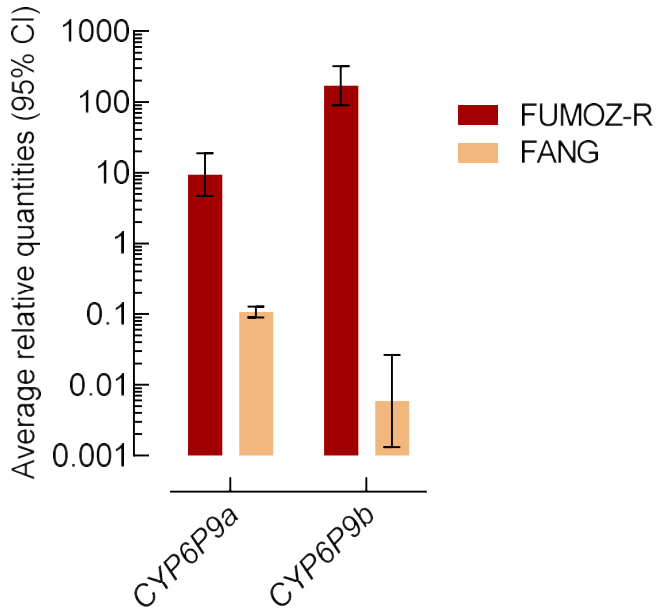

Figure 6. Expression level (log scale) of *CYP6P9A* and *CYP6P9B* in *A. funestus* strains FUMOZ-R and FANG measured by qPCR. The expression level was normalized to *RPS7* and *Act* (5c) reference genes. Data are mean values ± 95% CI (n=4 FUMOZ-R and n=3 for FANG).

Table 2. Inhibition of cytochrome P450 activity in microsomal preparations of *Anopheles funestus* FUMOZ-R by different azole fungicides using BOMFC as a substrate. The calculated IC_{50}-values are based on the inhibition of total microsomal monooxygenase activity. Data are mean values (n=4).

Compound	IC_{50} (µM)	95 % CI[a]
PBO	0.26	0.221-0.306
1-ABT	119	102-140
Triflumizole	0.0468	0.0416-0.0526
Prochloraz	0.00592	0.00527-0.00664
Uniconazole	0.107	0.0878-0.131
Propiconazole	0.35	0.313-0.39
Epoxiconazole	6.93	5.55-8.71
Triadimefon	1.09	0.967-1.23
Triadimenol	12.3	10.6-14.4
Tebuconazole	0.492	0.444-0.545
Ketoconazole	0.26	0.223-0.302

2.4. Discussion

Based on the lack of synergism with PBO, transfluthrin has been previously described to be less affected than phenoxybenzyl-substituted pyrethroids (e.g. deltamethrin) by P450-mediated metabolic resistance in the *An. funestus* laboratory strain FUMOZ-R (Horstmann and Sonneck, 2016), which has elevated levels of P450 activity driven by CYP6P9a and CYP6P9b (Hunt et al., 2005; Amenya et al., 2008; Coetzee and Koekemoer, 2013; Riveron et al., 2013). This study has confirmed that a very low level of cross-resistance exists between transfluthrin (RR = 2.57), and common pyrethroids such as deltamethrin (RR = 223) and cypermethrin (RR = 77.9) in FUMOZ-R compared to the susceptible strain FANG. The low resistance ratios also extended to other transfluthrin derivatives with varied levels of benzyl fluorination. The surprisingly low level of permethrin resistance in FUMOZ-R is comparable to a RR of 11.49 recently reported by Williams et al. (2019) in tarsal contact (glass plate) bioassays, but in comparison to the insecticide susceptible *An. gambiae* strain Kisumu.

Oxidation of the 4'-position on the phenoxybenzyl ring is one of the primary targets of P450 mediated metabolism of pyrethroids (Shono et al., 1979; Stevenson et al., 2011; Kasai et al., 2014; Zimmer et al., 2014), while other routes of metabolism include the gem dimethyl hydroxylation and an ester- or ether-cleavage (Casida et al., 1983; Weerasinghe et al., 2001; Stevenson et al., 2011). The most active compounds against the resistant FUMOZ-R strain were transfluthrin and TF-5 (fenfluthrin), followed by TF-3, where fluorination of the transfluthrin benzyl ring is expected to offer protection against P450 attack (Horstmann and Sonneck, 2016). However, this does not explain the low resistance ratio for the non-fluorinated TF-0 (RR = 3.77), where other factors may be contributing to reduced P450 metabolism. The most likely explanation is the lack of the 3-phenoxybenzyl moiety, which has been shown to be less susceptible to P450 metabolism in other pyrethroid-resistant insects such cotton bollworm (Tan and McCaffery, 2007) and does not correlate with pyrethroid resistance in house flies (Khan et al., 2017). Furthermore, P450 metabolism of transfluthrin in rats is *via* hydrolysis rather than benzyl ring hydroxylation (Yoshida, 2013, 2012). The RR for permethrin was also 10 to 30-fold lower than for cypermethrin and deltamethrin, respectively. Taken together, this suggests a strong preference for the presence of a 3-phenoxybenzyl moiety and an alpha-cyano group in pyrethroid metabolism by *An. funestus* FUMOZ-R, possibly driven by the extensive use of deltamethrin-treated LLINs for malaria control in Africa that may have applied selective pressure on P450s with an active-site preference for deltamethrin and structurally related pyrethroids.

Pyrethroid resistance in *An. funestus* is strongly linked to the overexpression of CYP6P9a and CYP6P9b that can metabolize deltamethrin and permethrin (Riveron et al., 2014, 2013; Yunta et al., 2019). However, depending on the geographical origin of *An. funestus*, other P450s such as CYP6M7 were also shown to be highly overexpressed and involved in pyrethroid resistance (Riveron et al., 2014). Both CYP6P9a and CYP6P9b were highly expressed in the resistant FUMOZ-R strain relative to the susceptible FANG strain and the lack of cross-resistance with deltamethrin or cypermethrin suggests a limited role in transfluthrin metabolism, however we did not test the expression level of CYP6M7. Transfluthrin has a 2,3,5,6-tetrafluorobenzyl substitution pattern that leaves the benzyl para-position (4'-position) free for P450 attack. In comparing the synergist ratios of the P450 inhibitors PBO, 1-ABT and triflumizole (Fig. 4) where a high ratio is indicative of P450 metabolism, it was striking

that a single fluorination of the 4'-position in TF-1 was equally effective at blocking P450 metabolism as the fully fluorinated TF-5, as evidenced by very low synergist ratios. Whereas transfluthrin, TF-3 and TF-0 produced higher synergist ratios indicative of greater P450 metabolism possibly depending on the halogenation pattern, thus confirming to some extent previous mosquito studies on the importance of the 4'-position for oxidative attack (Horstmann and Sonneck, 2016).

The acute contact toxicity of permethrin against FANG was significantly lower compared to deltamethrin and cypermethrin. Interestingly, transfluthrin, TF-3 and TF-5 were also up-to 25-fold more active than permethrin in glazed tile bioassays against strain FANG, although their intrinsic activity on recombinantly expressed house fly VGSC *in vitro* was not different. Since we had no access to a mosquito VGSC, we employed a surrogate from *M. domestica*, a phylogenetically related dipteran species. Dipteran VGSC proteins show a high level of conservation (Silva and Scott, 2020) and a comparison of important amino acid residues described for pyrethroid binding and known to confer different levels of target-site resistance revealed 100% identity between *An. funestus* (GenBank KY499806.1) and *M. domestica* (GenBank X96668.1) VGSC (O'Reilly et al., 2006; Field et al., 2017). Therefore, the agonistic potency on house fly VGSC obtained here should be a good estimate of intrinsic pyrethroid potency in mosquitoes as well. This assumption is supported by earlier results showing a Kd of 4.7 nM for deltamethrin on *Drosophila* wildtype VGSC functionally expressed in *Xenopus* oocytes (Vais et al., 2003), a value strikingly similar to the EC_{50} of 5.3 nM we measured (Supplementary Table S2), albeit in a different assay system. Electrophysiological recordings on expressed *Drosophila* para VGSC also revealed weaker activity of permethrin (Warmke et al., 1997), and another study with fenfluthrin (TF-5) on wildtype *Drosophila* VGSC reported a similar action to that for permethrin at low micromolar concentrations (Usherwood et al., 2007), correlating with our finding on house fly VGSC. The discrepancy in VGSC potency between deltamethrin and transfluthrin (and some of its derivatives) did not correlate with their almost identical contact toxicity in glazed tile bioassays and merits further research.

Fluorescent substrates are frequently used to measure P450 activity and could be applied to monitor changes in P450 activity associated with insecticide resistance. The biochemical profiling of resorufins and coumarins against P450-containing microsomes from *An. funestus*

FUMOZ-R showed a strong preference for BOMFC, BFC and BOMR, all bulky substrates substituted with a benzyloxy-group. These were rapidly O-debenzylated to provide a robust and reliable fluorescence read-out through conversion to umbelliferone. A similar substrate preference has been described for CYP6BQ9 and CYP6BQ23 that are also associated with pyrethroid resistance in *Tribolium castaneum* and *Meligethes aeneus*, respectively (Zhu et al., 2010; Zimmer et al., 2014). Resorufin ether substrates have been used with mixed success, being suitable as substrate probes for *An. gambiae* CYP6M2, CYP6Z2 and CYP6P3, but unreactive against pyrethroid metabolising *Aedes aegypti* P450s. However, BOMR to the best of our knowledge was not included in previous studies with malaria vectors, though alternative resorufin substrates were described in combination with CYP6P9-variants (Ibrahim et al., 2015, 2016). In comparison with resorufin, the coumarin based substrates produced much stronger fluorescence signals (Fig. 5). BOMFC produced the highest fluorescence activity suggesting that this probe substrate could be applied to biochemically profile P450 activity in mosquito populations. This is supported by the fact that microsomal membrane preparations of strain FUMOZ-R were significantly more active with BOMFC than those of strain FANG. Considering the upregulation of CYP6P9a and CYP6P9b in strain FUMOZ-R tested here, it is likely that these P450s are contributing to BOMFC O-debenzylation and hydroxycoumarin formation, although we cannot exclude a potential role of other P450s.

We have used BOMFC to develop a biochemical microplate (384 wells) assay to screen the inhibitory potential of a range of azole compounds with *An. funestus* microsomal P450s. The assay is largely based on a recently described mechanistic bee pollinator risk assessment approach to assess pesticide synergism issues in honeybees (Haas and Nauen, 2021). Synergistic effects of azole fungicides in combination with pyrethroids and neonicotinoids, respectively, have been described in honeybees at the phenotypic level (Pilling and Jepson, 1993; Iwasa et al., 2004), but were only recently deciphered at the molecular level (Haas and Nauen, 2021). Here, we identified prochloraz and triflumizole as extremely potent nanomolar inhibitors of microsomal P450s of *An. funestus*, and at least for triflumizole we could confirm its synergistic potential in combination with 3-phenoxybenzyl pyrethroids against FUMOZ-R *in vivo*. Quite surprising was the rather low inhibitory potential of the triazole 1-ABT, a well-known pan-specific P450 inhibitor (Ortiz De Montellano, 2018). Despite its weak inhibition of FUMOZ-R microsomal P450s *in vitro* it was highly active in glazed tile bioassays, e.g. in

combination with cypermethrin. However, future work is needed to further investigate the basis of the contrasting results. It would also be interesting to assess the efficacy of triflumizole and other azole compounds against functionally expressed *An. funestus* P450s such as CYP6P9a and CYP6P9b. McLaughlin et al. (2008) tested several drugs for their inhibitory action on the O-debenzylation of benzyloxy-resorufin by *An. gambiae* CYP6Z2, including clotrimazole and ketoconazole, but IC_{50} values were in the micromolar range and no *in vivo* synergist trials were conducted. Here we demonstrated that azole compounds such as triflumizole could serve as an alternative to PBO, known for its synergistic potential against pyrethroid-resistant mosquitoes. Our results would be a good starting point to foster additional studies on the potential of azoles as synergists to overcome P450-mediated pyrethroid resistance in anopheline mosquitoes.

2.5. Conclusions

The progress in malaria reduction since the turn of millennium has largely stagnated since 2015 with mosquito resistance to pyrethroids that are commonly used in vector control tools such as IRS and ITNs being a threat to the goal of eradicating malaria by 2040 (https://zeroby40.com/). For sustainable vector control interventions, it is therefore important to implement resistance management strategies that are based on the most active molecules available from chemical classes with the same mode of action. Such molecules may not necessarily break but could substantially delay resistance. The pyrethroids most often used in vector control possess the common structural motif of a phenoxybenzyl alcohol coupled with a cyclopropane ring with cross-resistance trends detectable across pyrethroid-resistant populations of *An. funestus, An. gambiae, An. arabiensis* and *An. coluzzii* (Moyes et al., 2021). It has been suggested that pyrethroid cross-resistance might be mitigated by employing structurally diverse pyrethroids such as bifenthrin (Moyes et al., 2021) and transfluthrin (Horstmann and Sonneck, 2016). Here, we provide further evidence that multifluorinated benzyl pyrethroids offer potential resistance breaking properties against P450-driven pyrethroid resistance in *An. funestus* that require further verification in resistant field populations. Since pyrethroid resistance in *An. funestus* field strains is largely driven by P450-mediated detoxification, we think that the findings presented here on transfluthrin and pyrethroid synergism are highly relevant for applied field conditions. Furthermore, we have expanded the vector control research toolbox by the introduction of a sensitive fluorescent

probe substrate BOMFC for the biochemical monitoring of P450-mediated resistance, and the identification of azoles such as triflumizole as new compounds with potential to synergize pyrethroid toxicity in *An. funestus* FUMOZ-R.

2.6. References

Abbott, W.S., 1925. A method of computing the effectiveness of an insecticide. J. Econ. Entomol. 18, 265–267.

Amenya, D.A., Naguran, R., Lo, T.-C.M., Ranson, H., Spillings, B.L., Wood, O.R., et al., 2008. Over expression of a cytochrome P450 (CYP6P9) in a major African malaria vector. Insect Mol. Biol. 17, 19–25.

Balabanidou, V., Grigoraki, L., Vontas, J., 2018. Insect cuticle: a critical determinant of insecticide resistance. Curr. Opin. Insect Sci. 27, 68–74.

Bhatt, S., Weiss, D.J., Cameron, E., Bisanzio, D., Mappin, B., Dalrymple, U., et al., 2015. The effect of malaria control on *Plasmodium falciparum* in Africa between 2000 and 2015. Nature 526, 207–211.

Bibbs, C.S., Tsikolia, M., Bloomquist, J.R., Bernier, U.R., Xue, R. De, Kaufman, P.E., 2018. Vapor toxicity of five volatile pyrethroids against *Aedes aegypti*, *Aedes albopictus*, *Culex quinquefasciatus*, and *Anopheles quadrimaculatus* (Diptera: Culicidae). Pest Manag. Sci. 74, 2699–2706.

Boaventura, D., Ulrich, J., Lueke, B., Bolzan, A., Okuma, D., Gutbrod, O., et al., 2020. Molecular characterization of Cry1F resistance in fall armyworm, *Spodoptera frugiperda* from Brazil. Insect Biochem. Mol. Biol. 116, 103280.

Bradford, M.M., 1976. A rapid and sensitive method for the quantitation microgram quantities of protein utilizing the principle of protein-dye binding. Anal. Biochem. 72, 248–254.

Brooke, B.D., Kloke, G., Hunt, R.H., Koekemoer, L.L., Tem, E.A., Taylor, M.E., et al., 2001. Bioassay and biochemical analyses of insecticide resistance in southern African *Anopheles funestus* (Diptera: Culicidae). Bull. Entomol. Res. 91, 265–272.

Casida, J.E., Gammon, D.W., Glickman, A.H., Lawrence, L.J., 1983. Mechanism of selective action of pyrethroid. Annu. Rev. Pharmacol. Toxicol. 413–438.

Coetzee, M., Koekemoer, L.L., 2013. Molecular systematics and insecticide resistance in the major African malaria vector *Anopheles funestus*. Annu. Rev. Entomol. 58, 393–412.

Coleman, M., Hemingway, J., Gleave, K.A., Wiebe, A., Gething, P.W., Moyes, C.L., 2017. Developing global maps of insecticide resistance risk to improve vector control. Malar. J. 16, 86.

Cuamba, N., Morgan, J.C., Irving, H., Steven, A., Wondji, C.S., 2010. High level of pyrethroid resistance in an *Anopheles funestus* population of the Chokwe district in Mozambique. PLoS One 5, e11010.

Das, S., Garver, L., Dimopoulos, G., 2007. Protocol for mosquito rearing (*A. gambiae*), J. Vis. Exp. 5, 221.

Davies, T.G.E., Field, L.M., Usherwood, P.N.R., Williamson, M.S., 2007. A comparative study of voltage-gated sodium channels in the Insecta: Implications for pyrethroid resistance in Anophelinae and other Neopteran species. Insect Mol. Biol. 16, 361–375.

Djouaka, R., Riveron, J.M., Yessoufou, A., Tchigossou, G., Akoton, R., Irving, H., et al., 2016. Multiple insecticide resistance in an infected population of the malaria vector *Anopheles funestus* in Benin. Parasit. Vectors 9, 453.

Feyereisen, R., 1999. Insect P450 enzymes. Annu. Rev. Entomol. 44, 507–533.

Field, L.M., Emyr Davies, T.G., O'Reilly, A.O., Williamson, M.S., Wallace, B.A., 2017. Voltage-gated sodium channels as targets for pyrethroid insecticides. Eur. Biophys. J. 46, 675–679.

Fongnikin, A., Houeto, N., Agbevo, A., Odjo, A., Syme, T., N'Guessan, R., Ngufor, C., 2020. Efficacy of Fludora® Fusion (a mixture of deltamethrin and clothianidin) for indoor residual spraying against pyrethroid-resistant malaria vectors: Laboratory and experimental hut evaluation. Parasit. Vectors 13, 466.

Fuseini, G., Phiri, W.P., von Fricken, M.E., Smith, J., Garcia, G.A., 2019. Evaluation of the residual effectiveness of FludoraTM fusion WP-SB, a combination of clothianidin and deltamethrin, for the control of pyrethroid-resistant malaria vectors on Bioko Island, Equatorial Guinea. Acta Trop. 196, 42–47.

Gleave, K., Lissenden, N., Richardson, M., Ranson, H., 2018. Piperonyl butoxide (PBO) combined with pyrethroids in long-lasting insecticidal nets (LLINs) to prevent malaria in Africa. Cochrane Database Syst. Rev., doi.org//10.1002/14651858.CD012776.pub2

Haas, J., Nauen, R., 2021. Pesticide risk assessment at the molecular level using honey bee cytochrome P450 enzymes: A complementary approach. Environ. Int. 147, 106372.

Hargreaves, K., Koekemoer, L.L., Brooke, B.D., Hunt, R.H., Mthembu, J., Coetzee, M., 2000. *Anopheles funestus* resistant to pyrethroid insecticides in South Africa. Med. Vet. Entomol. 14, 181–189.

Hemingway, J., 2019. Malaria parasite tackled in mosquitoes. Nature 567, 185–186.

Hemingway, J., Beaty, B.J., Rowland, M., Scott, T.W., Sharp, B.L., 2006. The Innovative Vector Control Consortium: improved control of mosquito-borne diseases. Trends Parasitol. 22, 308–312.

Hemingway, J., Hawkes, N.J., McCarroll, L., Ranson, H., 2004. The molecular basis of insecticide resistance in mosquitoes. Insect Biochem. Mol. Biol. 34, 653–665.

Hemingway, J., Ranson, H., Magill, A., Kolaczinski, J., Fornadel, C., Gimnig, J., et al., 2016. Averting a malaria disaster: Will insecticide resistance derail malaria control? Lancet 387, 1785–1788.

Hoppé, M., Hueter, O.F., Bywater, A., Wege, P., Maienfisch, P., 2016. Evaluation of commercial agrochemicals as new tools for malaria vector control. Chimia (Aarau). 70, 721–729.

Horstmann, S., Sonneck, R., 2016. Contact bioassays with phenoxybenzyl and tetrafluorobenzyl pyrethroids against target-site and metabolic resistant mosquitoes. PLoS One 11, e0149738.

Human Disease Vectors (HDV) group of the Insect Pest Control Laboratory, 2017. Guidelines for standardised mass rearing of *Anopheles* mosquitoes.

Hunt, R.H., Brooke, B.D., Pillay, C., Koekemoer, L.L., Coetzee, M., 2005. Laboratory selection for and characteristics of pyrethroid resistance in the malaria vector *Anopheles funestus*. Med. Vet. Entomol. 19, 271–275.

Ibrahim, S.S., Ndula, M., Riveron, J.M., Irving, H., Wondji, C.S., 2016. The P450 CYP6Z1 confers carbamate/pyrethroid cross-resistance in a major African malaria vector beside a novel carbamate-insensitive N485I acetylcholinesterase-1 mutation. Mol. Ecol. 25, 3436–3452.

Ibrahim, S.S., Riveron, J.M., Bibby, J., Irving, H., Yunta, C., Paine, M.J.I., Wondji, C.S., 2015. Allelic variation of cytochrome P450s drives resistance to bednet insecticides in a major malaria vector. PLoS Genet. 11, e1005618.

Irving, H., Riveron, J.M., Ibrahim, S.S., Lobo, N.F., Wondji, C.S., 2012. Positional cloning of rp2 QTL associates the P450 genes CYP6Z1, CYP6Z3 and CYP6M7 with pyrethroid resistance in the malaria vector *Anopheles funestus*. Heredity (Edinb). 109, 383–392.

Irving, H., Wondji, C.S., 2017. Investigating knockdown resistance (kdr) mechanism against pyrethroids/DDT in the malaria vector *Anopheles funestus* across Africa. BMC Genetics 18, 76.

Iwasa, T., Motoyama, N., Ambrose, J.T., Roe, R.M., 2004. Mechanism for the differential toxicity of neonicotinoid insecticides in the honey bee, *Apis mellifera*. Crop Prot. 23, 371–378.

Kasai, S., Komagata, O., Itokawa, K., Shono, T., Ng, L.C., Kobayashi, M., Tomita, T., 2014. Mechanisms of pyrethroid resistance in the dengue mosquito vector, *Aedes aegypti*: Target site insensitivity, penetration, and metabolism. PLoS Negl. Trop. Dis. 8, e2948.

Khan, H.A.A., Akram, W., Fatima, A., 2017. Resistance to pyrethroid insecticides in house flies, *Musca domestica* L. (Diptera: Muscidae) collected from urban areas in Punjab, Pakistan. Parasitol. Res. 116, 3381–3385.

Kline, D.L., Urban, J., 2018. Potential for utilization of spatial repellents in mosquito control interventions. ACS Symp. Ser. 1289, 237–248.

Laufer, J., Rochet, M., Pelhate, M., Elliotti, M., Janes, N.F., Sattelle, D.B., 1984. Pyrehtroids insecticides: Actions of deltamethrin and related compounds on insect axonal sodium channels. J. Insect Physiol. 30, 341–349.

Manjon, C., Troczka, B.J., Zaworra, M., Beadle, K., Randall, E., Hertlein, G., et al., 2018. Unravelling the molecular determinants of bee sensitivity to neonicotinoid insecticides. Curr. Biol. 28, 1137–1143.

Masalu, J.P., Finda, M., Killeen, G.F., Ngowo, H.S., Pinda, P.G., Okumu, F.O., 2020. Creating mosquito-free outdoor spaces using transfluthrin-treated chairs and ribbons. Malar. J. 19, 109.

McLaughlin, L.A., Niazi, U., Bibby, J., David, J.P., Vontas, J., Hemingway, J., et al., 2008. Characterization of inhibitors and substrates of *Anopheles gambiae* CYP6Z2. Insect Mol. Biol. 17, 125–135.

Morgan, J.C., Irving, H., Okedi, L.M., Steven, A., Wondji, C.S., 2010. Pyrethroid resistance in an *Anopheles funestus* population from uganda. PLoS One 5, e11872.

Moyes, C.L., Athinya, D.K., Seethaler, T., Battle, K.E., Sinka, M., Hadi, M.P., et al., 2020. Evaluating insecticide resistance across African districts to aid malaria control decisions. Proc. Natl. Acad. Sci. 117, 202006781.

Moyes, C.L., Lees, R.S., Yunta, C., Walker, K.J., Hemmings, K., Oladepo, F., et al., 2021. Assessing cross-resistance within the pyrethroids in terms of their interactions with key cytochrome P450 enzymes and resistance in vector populations. Parasit. Vectors 14, 115.

Nauen, R., 2007. Insecticide resistance in disease vectors of public health importance. Pest Manag. Sci. 63, 628–633.

Nauen, R., 2006. Insecticide mode of action: return of the ryanodine receptor. Pest Manag. Sci. 62, 690–692.

Naumann, K. (Ed.), 1990. Synthetic pyrethroid insecticides: Formation of the pyrethroid-ester-linkage, chemistry and patents. In: Chemistry of Plant Protection, Vol. 5. Springer Verlag, Weinheim. pp. 129–173.

O'Reilly, A.O., Khambay, B.P.S., Williamson, M.S., Field, L.M., Wallace, B.A., Davies, T.G.E., 2006. Modelling insecticide-binding sites in the voltage-gated sodium channel. Biochem. J. 396, 255–263.

Ogoma, S.B., Ngonyani, H., Simfukwe, E.T., Mseka, A., Moore, J., Killeen, G.F., 2012. Spatial repellency of transfluthrin-treated hessian strips against laboratory-reared *Anopheles arabiensis* mosquitoes in a semi-field tunnel cage. Parasit. Vectors 5, 54.

Ogoma, S.B., Ngonyani, H., Simfukwe, E.T., Mseka, A., Moore, J., Maia, M.F., et al., 2014. The mode of action of spatial repellents and their impact on vectorial capacity of *Anopheles gambiae sensu stricto*. PLoS One 9, e110433.

Ortiz De Montellano, P.R., 2018. 1-Aminobenzotriazole: A mechanism-based cytochrome P450 inhibitor and probe of cytochrome P450 biology. Med. Chem. 8(3), 038.

Pilling, E.D., Jepson, P.C., 1993. Synergism between EBI fungicides and a pyrethroid insecticide in the honeybee (*Apis mellifera*). Pestic. Sci. 39, 293–297.

Pulman, D.A., 2011. Deltamethrin: The cream of the crop. J. Agric. Food Chem. 59, 2770–2772.

Riveron, J.M., Ibrahim, S.S., Chanda, E., Mzilahowa, T., Cuamba, N., Irving, H., et al., 2014. The highly polymorphic CYP6M7 cytochrome P450 gene partners with the directionally selected CYP6P9a and CYP6P9b genes to expand the pyrethroid

resistance front in the malaria vector *Anopheles funestus* in Africa. BMC Genomics 15, 817.

Riveron, J.M., Irving, H., Ndula, M., Barnes, K.G., Ibrahim, S.S., Paine, M.J.I., Wondji, C.S., 2013. Directionally selected cytochrome P450 alleles are driving the spread of pyrethroid resistance in the major malaria vector *Anopheles funestus*. Proc. Natl. Acad. Sci. 110, 252–257.

Sangba, M.L.O., Deketramete, T., Wango, S.P., Kazanji, M., Akogbeto, M., Ndiath, M.O., 2016. Insecticide resistance status of the *Anopheles funestus* population in Central African Republic: A challenge in the war. Parasit. Vectors 9, 230.

Scott, J.G., 2019. Life and death at the voltage-sensitive sodium channel: Evolution in response to insecticide use. Annu. Rev. Entomol. 64, 243–257.

Shono, T., Ohsawa, K., Casida, J.E., 1979. Metabolism of trans-and cis-permethrin, trans-and cis-cypermethrin, and decamethrin by microsomal enzymes. J. Agric. Food Chem. 27, 316–325.

Silva, J.J., Scott, J.G., 2020. Conservation of the voltage-sensitive sodium channel protein within the Insecta. Insect Mol. Biol. 29, 9–18.

Sinka, M.E., Bangs, M.J., Manguin, S., Coetzee, M., Mbogo, C.M., Hemingway, J., et al., 2010. The dominant *Anopheles* vectors of human malaria in Africa, Europe and the Middle East: occurrence data, distribution maps and bionomic précis. Parasit. Vectors 3, 117.

Sinka, M.E., Golding, N., Massey, N.C., Wiebe, A., Huang, Z., Hay, S.I., Moyes, C.L., 2016. Modelling the relative abundance of the primary African vectors of malaria before and after the implementation of indoor, insecticide-based vector control. Malar. J. 15, 142.

Smith, L.B., Sears, C., Sun, H., Mertz, R.W., Kasai, S., Scott, J.G., 2019. CYP-mediated resistance and cross-resistance to pyrethroids and organophosphates in *Aedes aegypti* in the presence and absence of kdr. Pestic. Biochem. Physiol. 160, 119–126.

Soderlund, D.M., 2020. Neurotoxicology of pyrethroid insecticides. In: Neurotoxicity of Pesticides. Elsevier Inc., Amsterdam, pp. 113–165.

Soderlund, D.M., Bloomquist, J.R., 1989. Neurotoxic actions of pyrethroid insecticides. Annu. Rev. Entomol. 34, 77–96.

Sparks, T.C., Nauen, R., 2015. IRAC: Mode of action classification and insecticide resistance management. Pestic. Biochem. Physiol. 121, 122–128.

Stevenson, B.J., Bibby, J., Pignatelli, P., Muangnoicharoen, S., O'Neill, P.M., Lian, L.Y., et al., 2011. Cytochrome P450 6M2 from the malaria vector *Anopheles gambiae* metabolizes pyrethroids: Sequential metabolism of deltamethrin revealed. Insect Biochem. Mol. Biol. 41, 492–502.

Tan, J., McCaffery, A.R., 2007. Efficacy of various pyrethroid structures against a highly metabolically resistant isogenic strain of *Helicoverpa armigera* (Lepidoptera: Noctuidae) from China). Pest Manag. Sci. 63, 960–968.

Tay, B., Stewart, T.A., Davis, F.M., Deuis, J.R., Vetter, I., 2019. Development of a high-throughput fluorescent no-wash sodium influx assay. PLoS One 14(3), e0213751.

Tchigossou, G., Djouaka, R., Akoton, R., Riveron, J.M., Irving, H., Atoyebi, S., et al., 2018. Molecular basis of permethrin and DDT resistance in an *Anopheles funestus* population from Benin. Parasit. Vectors 11, 602.

Temu, E.A., Minjas, J.N., Tuno, N., Kawada, H., Takagi, M., 2007. Identification of four members of the *Anopheles funestus* (Diptera: Culicidae) group and their role in *Plasmodium falciparum* transmission in Bagamoyo coastal Tanzania. Acta Trop. 102, 119–125.

Ullrich, V., Weber, P., 1972. The O-dealkylation of 7-ethoxycoumarin by liver microsomes. Hoppe. Seylers. Z. Physiol. Chem. 353, 1171–1177.

Usherwood, P.N.R., Davies, T.G.E., Mellor, I.R., O'Reilly, A.O., Peng, F., Vais, H., et al., 2007. Mutations in DIIS5 and the DIIS4-S5 linker of *Drosophila melanogaster* sodium channel define binding domains for pyrethroids and DDT. FEBS Lett. 581, 5485–5492.

Vais, H., Atkinson, S., Pluteanu, F., Goodson, S.J., Devonshire, A.L., Williamson, M.S., Usherwood, P.N.R., 2003. Mutations of the para sodium channel of *Drosophila melanogaster* identify putative binding sites for pyrethroids. Mol. Pharmacol. 64, 914–922.

Vandesompele, J., Preter, K. De, Pattyn, F., Poppe, B., Van Roy, N., De Paepe, A., Speleman, F., 2002. Accurate normalization of real-time quantitative RT-PCR data by geometric averaging of multiple internal control genes. Genome Biol. 3, 7.

Vontas, J., Katsavou, E., Mavridis, K., 2020. Cytochrome P450-based metabolic insecticide resistance in *Anopheles* and *Aedes* mosquito vectors: Muddying the waters. Pestic. Biochem. Physiol. 170, 104666.

Warmke, J.W., Reenan, R.A.G., Wang, P., Qian, S., Arena, J.P., Wang, J., et al., 1997. Functional expression of *Drosophila* para sodium channels modulation by the membrane protein tipE and toxin pharmacology. J. Gen. Physiol. 110, 119–133.

Weedall, G.D., Mugenzi, L.M.J., Menze, B.D., Tchouakui, M., Ibrahim, S.S., Amvongo-Adjia, N., et al., 2019. A cytochrome P450 allele confers pyrethroid resistance on a major African malaria vector, reducing insecticide-treated bednet efficacy. Sci. Transl. Med. 11, eaat7386.

Weerasinghe, I.S., Kasai, S., Shono, T., 2001. Correlation of pyrethroid structure and resistance level in *Culex quinquefasciatus* Say from Saudi Arabia. J. Pestic. Sci. 26, 158-161.

WHO, 2018a. World Malaria Report 2018. World Health Organization, Geneva. https://www.who.int.

WHO, 2018b. Global report on insecticide resistance in malaria vectors: 2010–2016. World Health Organization, Geneva. https://www.who.int.

Wiebe, A., Longbottom, J., Gleave, K., Shearer, F.M., Sinka, M.E., Massey, N.C., et al., 2017. Geographical distributions of African malaria vector sibling species and evidence for insecticide resistance. Malar. J. 16, 85.

Williams, J., Flood, L., Praulins, G., Ingham, V.A., Morgan, J., Lees, R.S., Ranson, H., 2019. Characterisation of *Anopheles* strains used for laboratory screening of new vector control products. Parasit. Vectors 12, 522.

Wondji, C.S., Irving, H., Morgan, J., Lobo, N.F., Collins, F.H., Hunt, R.H., et al., 2009. Two duplicated P450 genes are associated with pyrethroid resistance in *Anopheles funestus*, a major malaria vector. Genome Res. 19, 452–459.

Wood, O.R., Hanrahan, S., Coetzee, M., Koekemoer, L.L., Brooke, B.D., 2010. Cuticle thickening associated with pyrethroid resistance in the major malaria vector *Anopheles funestus*. Parasit. Vectors 3, 67.

Yoshida, T., 2013. Analytical method for urinary metabolites of the fluorine-containing pyrethroids metofluthrin , profluthrin and transfluthrin by gas chromatography / mass spectrometry. J. Chromatogr. B 913–914, 77–83.

Yoshida, T., 2012. Identification of urinary metabolites in rats administered the fluorine-containing pyrethroids metofluthrin, profluthrin, and transfluthrin 94, 1789–1804.

Yunta, C., Hemmings, K., Stevenson, B., Koekemoer, L.L., Matambo, T., Pignatelli, P., et al., 2019. Cross-resistance profiles of malaria mosquito P450s associated with pyrethroid resistance against WHO insecticides. Pestic. Biochem. Physiol. 161, 61–67.

Zaworra, M., Nauen, R., 2019. New approaches to old problems: Removal of phospholipase A2 results in highly active microsomal membranes from the honey bee, *Apis mellifera*. Pestic. Biochem. Physiol. 161, 68–76.

Zhu, F., Parthasarathy, R., Bai, H., Woithe, K., Kaussmann, M., Nauen, R., et al., 2010. A brain-specific cytochrome P450 responsible for the majority of deltamethrin resistance in the QTC279 strain of Tribolium castaneum. Proc. Natl. Acad. Sci. U.S.A. 107, 8557–8562.

Zimmer, C.T., Bass, C., Williamson, M.S., Kaussmann, M., Wölfel, K., Gutbrod, O., Nauen, R., 2014. Molecular and functional characterization of CYP6BQ23, a cytochrome P450 conferring resistance to pyrethroids in European populations of pollen beetle, *Meligethes aeneus*. Insect Biochem. Mol. Biol. 45, 18–29.

2.7. Supplements (chapter 2)

Table S1. LC_{50}-values (ppm) of PBO and triflumizole after 30 minutes contact exposure. No mortality for1-1-ABT up to a tested concentration of 15 000 ppm was observed. Data are mean values, n=2.

Species	**Strain**	**Inhibitor**	**LC_{50} (ppm)**	**95 % CI**	
An. funestus	FUMOZ-R	PBO	26665	-	
An. funestus	FUMOZ-R	Triflumizole	7834	5852-	10155
An. funestus	FANG	PBO	6499	3970-	14047
An. funestus	FANG	Triflumizole	2714	810-	3761

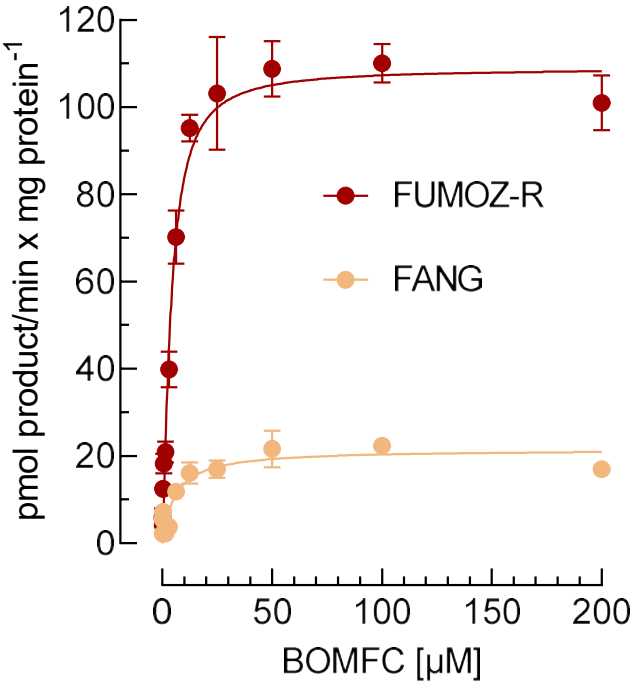

Figure S1. Steady-state kinetics of BOMFC O-dearylation leading to 7-hydroxy-4-(trifluoromethyl)coumarin (HC) by cytochrome P450s of microsomal preparations of *A. funestus* strain FANG und FUMOZ-R. Data points are mean values ± SD (n = 3). The calculated K_m- and V_{max}-values for BOMFC are apparent values based on general microsomal monooxygenase activity.

Table S2: Primer sequences and GenBank numbers for target and reference genes used in qPCR

Gene name	Forward 5' to 3'	Reverse 5' to 3'	Amplicon (bp)
Ribosomal Protein S7	GTGTTCGGTTCCAAGGTGAT	TCCGAGTTCATTTCCAGCTC	111
Actin 5c	TTAAACCCAAAAGCCAATCG	ACCGGATGCATACAGTGACA	98
CYP6P9A	AACTTGCGGCACAGGCATTC	TCTCCTCGATTGCTTGGTTG	144
CYP6P9B	CGATCCACTATCAGGACATC	AAGTGCCACATCCCATAGTG	130

Gene name	Vector Base code	GenBank Acc.	UniProt
Ribosomal Protein S7	AFUN007153	EF450776.1	A0A182RLN5
Actin 5c	AFUN006819-RA	not available	A0A182RKQ1
CYP6P9A	AFUN015792	KR866022.1	A0A0S1S5U9
CYP6P9B	AFUN015889	KR866046.1	A0A096XPX9

Table S3. EC_{50}-values (µM) of common pyrethroids and transfluthrin derivatives measured on functionally expressed house fly voltage-gated sodium channels (VGSC) using a cell-based membrane potential cation influx assay. Data were taken from figures 2A and 2B.

	EC_{50} (µM)	95 % CI	-LogEC_{50} (M)	95 % CI
Deltamethrin	0.00529	0.00443 - 0.0063	8.28	8.20 - 8.35
Cypermethrin	0.0389	0.0342 - 0.0443	7.41	7.35 - 7.47
Permethrin	0.721	0.591 - 0.882	6.14	6.05 – 6.27
Transfluthrin	1.77	1.62 - 1.94	5.75	5.71 – 5.79
TF-0	1920*	1109 - 3748	2.72	2.43 – 2.95
TF-1	315*	207 - 525	3.50	3.28 – 3.68
TF-3	4.89	4.23 - 5.66	5.31	5.25 – 5.37
TF-5	0.736	0.65 - 0.834	6.13	6.08 - 6.19

* Extrapolated value

Table S4. LC_{50}-values (mg/m²) of different pyrethroids against *An. funestus* strains FANG and FUMOZ-R in glazed tile contact bioassays. Synergists were applied prior to insecticide exposure.

	A. funestus FANG						*A. funestus* FUMOZ-R							
	LC_{50}	Synergistic Ratio (FANG)	95 % CI	Slope ± SE		n	LC_{50}	95 % CI	Slope ± SE		n	Resistance Ratio	Synergistic Ratio (FUMOZ-R)
TF	0.023		0.0155 -0.0324	1.47	0.168	420	0.0576	0.0191 -0.112	1.6	0.218	360	2.51	-
+ PBO	0.0389	0.591	0.0201 -0.0699	4.10	1.48	140	0.00733	0.00389 -0.0148	4.07	1.51	120	0.319	7.86
+ 1-ABT	0.0184	1.25	0.00502 -0.0337	2.38	0.676	140	0.0057	0.000468 -0.00867	3.51	1.62	120	0.248	10.1
+ Triflumizole	0.0187	1.23	0.00999 -0.0279	2.28	0.499	280	0.00465	0.0000688 -0.0167	1.55	0.395	120	0.203	12.4
TF-0	1.19		0.565 -1.79	2.90	0.932	140	4.47	2.89 -6.01	3.17	0.655	360	3.77	-
+ PBO	0.691	1.72	0.223 -1.65	1.59	0.304	140	0.553	0.281 -0.805	3.52	1.13	120	0.47	8.07
+ 1-ABT	1.33	0.895	0.849 -2.05	2.66	0.565	140	1.21	0.601 -3.025	3.63	0.917	120	1.02	3.69
+ Triflumizole	1.16	1.026	0.761 -1.78	3.24	0.823	140	0.609	0.316 -0.944	2.79	0.798	120	0.51	7.34
TF-1	1.42		1.02 -1.85	2.97	0.453	560	1.41	1.15 -1.83	4.78	0.772	350	0.99	-
+ PBO	1.4	1.01	0.872 2.19	3.12	0.813	140	3.77	2.4 -5.93	2.60	0.576	140	2.65	0.376
+ 1-ABT	0.843	1.68	0.434 -1.44	3.43	1.16	140	0.34	0.0645 -0.579	1.72	0.434	420	0.403	4.16
+ Triflumizole	1.62	0.877	1.03 -2.54	3.04	0.688	140	2.42	0.537 -5.42	2.80	0.758	140	1.70	0.584
TF-3	0.0494		0.0350 -0.0664	1.96	0.256	420	0.285	0.225 -0.354	3.32	0.495	360	5.77	-
+ PBO	0.0158	3.13	0.00652 -0.0314	1.41	0.285	140	0.00759	0.00212 -0.0142	1.93	0.513	120	0.154	37.6
+ 1-ABT	0.0183	2.7	0.00795 -0.0257	4.53	1.43	140	0.0304	0.0187 -0.0483	3.70	1.11	120	0.617	9.36
+ Triflumizole	0.0263	1.87	0.0132 -0.0419	2.52	0.688	140	0.012	0.00408 -0.0214	2.94	0.788	120	0.243	23.8
TF-5	0.0237		0.0132 -0.0394	2.03	0.243	420	0.0446	0.0299 -0.0592	2.08	0.316	560	1.88	-
+ PBO	0.012	1.98	0.00686 -0.0258	4.24	1.40	140	0.018	0.00558 -0.0338	2.23	0.574	140	0.758	2.48
+ 1-ABT	0.0224	1.06	0.00174 -0.0468	2.05	0.695	140	0.0141	0.00515 -0.0241	2.36	0.687	140	0.593	3.17
+ Triflumizole	0.0283	0.837	0.0143 -0.0481	1.91	0.414	140	0.0203	0.00372 -0.0384	2.28	0.706	140	0.856	2.20
Permethrin	0.543		0.409 -0.702	2.28	0.294	420	4.21	2.79 -5.88	1.99	0.278	360	7.76	-
+ PBO	0.273	1.99	0.197 -0.471	5.18	1.43	140	0.327	0.128 -0.516	4.13	1.2	120	0.602	12.9
+ 1-ABT	0.0834	6.51	0.0478 -0.14	1.80	0.331	140	0.523	0.147 -0.935	2.48	0.693	120	0.962	8.06
+ Triflumizole	0.329	1.65	0.0884 -0.505	2.69	1.03	140	0.22	0.102 -0.422	2.46	0.496	120	0.404	19.2
Cypermethrin	0.0968		0.0686 -0.126	2.74	0.479	420	7.54	5.24 -10.4	1.86	0.204	540	77.9	-
+ PBO	0.00882	11	0.00277 -0.0178	1.8	0.459	140	0.0451	0.0140 -0.0880	1.73	0.4	140	0.466	167
+ 1-ABT	0.0157	6.17	0.00408 -0.0327	1.34	0.323	140	0.0358	0.0057 -0.146	1.34	0.243	140	0.37	210
+ Triflumizole	0.065	1.49	0.0312 -0.121	1.95	0.371	140	0.493	0.168 -0.95	1.23	0.171	400	5.1	15.3
Deltamethrin	0.0206		0.0153 -0.0273	1.38	0.119	560	4.61	2.73 -7.5	1.07	0.102	540	223	-
+ PBO	0.00074	27.8	0.000224 -0.0016	1.23	0.356	280	0.0103	0.0037 -0.0231	1.88	0.341	140	0.499	448
+ 1-ABT	0.00327	6.29	0.00090 -0.0105	0.741	0.242	140	0.0318	0.00515 -0.0822	1.43	0.337	140	1.54	145
+ Triflumizole	0.00518	3.98	0.00142 -0.0126	1.40	0.263	140	0.0364	0.0239 -0.053	1.34	0.137	460	1.77	127

3. Chapter 3. Biochemical profiling of functionally expressed CYP6P9 variants of the malaria vector *Anopheles funestus* with special reference to cytochrome b_5 and its role in pyrethroid and coumarin substrate metabolism

Melanie Nolden [a, b], Mark J.I. Paine [b], Ralf Nauen [a, *]

[a] *Bayer AG, Crop Science Division, Alfred Nobel Str. 50, D-40789 Monheim am Rhein, Germany*

[b] *Department of Vector Biology, Liverpool School of Tropical Medicine, Pembroke Place, Liverpool L3 5QA, United Kingdom*

*** Corresponding author**

Email: ralf.nauen@bayer.com

Phone: +49-2173-384441

ORCID: 0000-0002-7525-8589

ABSTRACT

Cytochrome P450 monooxygenases (P450s) are well studied enzymes catalyzing the oxidative metabolism of xenobiotics in insects including mosquitoes. Their duplication and upregulation in agricultural and public health pests such as anopheline mosquitoes often leads to an enhanced metabolism of insecticides which confers resistance. In the laboratory strain *Anopheles funestus* FUMOZ-R the duplicated P450s CYP6P9a and CYP6P9b are highly upregulated and proven to confer pyrethroid resistance. Microsomal P450 activity is regulated by NADPH cytochrome P450 oxidoreductase (CPR) required for electron transfer, whereas the modulatory role of cytochrome b_5 (CYB5) on insect P450 activity is less clear. In previous studies CYP6P9a and CYP6P9b were recombinantly expressed in tandem with *An. gambiae* CPR using *E. coli*-expression systems and CYB5 added to the reaction mix to enhance activity. However, the precise role of CYB5 on substrate turn-over when combined with CYP6P9a and CYP6P9b remains poorly investigated, thus one objective of our study was to address this knowledge gap. In contrast to the *CYP6P9* variants, the expression levels of both *CYB5* and *CPR* were not upregulated in the pyrethroid resistant FUMOZ-R strain when compared to the susceptible FANG strain, suggesting no immediate regulatory role of these genes in pyrethroid resistance in FUMOZ-R. Here, for the first time we recombinantly expressed *CYP6P9a* and *CYP6P9b* from *An. funestus* in a baculovirus expression system using High-5 insect cells. Co-expression of each enzyme with CPR from either *An. gambiae* or *An. funestus* did not reveal noteworthy differences in catalytic capacity. Whereas the co-expression of *An. funestus* CYB5 – tested at different multiplicity of infection (MOI) ratios – resulted in a significantly higher metabolization of coumarin substrates as measured by fluorescence assays. This was confirmed by Michaelis-Menten kinetics using the most active substrate, 7-benzyloxymethoxy-4-trifluoromethylcoumarin (BOMFC). We observed a similar increase in coumarin substrate turnover by adding human CYB5 to the reaction mix. Finally, we compared by UPLC-MS/MS analysis the depletion rate of deltamethrin and the formation of 4'OH-deltamethrin by recombinantly expressed CYP6P9a and CYP6P9b with and without CYB5 and detected no difference in the extent of deltamethrin metabolism. Our results suggest that co-expression (or addition) of CYB5 with CYP6P9 variants, recombinantly

expressed in insect cells, can significantly enhance their metabolic capacity to oxidize coumarins, but not deltamethrin.

Keywords: Cytochrome P450, cytochrome b5, *Anopheles funestus*, CYP6P9, resistance, pyrethroid

3.1. Introduction

Cytochrome P450 monooxygenases (P450s, encoded by *CYP* genes) are a diverse superfamily of membrane-bound heme-thiolate enzymes described across all kingdoms of life (Nelson, 2018), and involved in the oxidation of a vast range of endogenous and exogenous substrates (Coon, 2005; Esteves et al., 2021; Feyereisen, 2012; Schuler, 2011). P450s play a key role in the metabolism of xenobiotics (Lu et al., 2021; Nauen et al., 2022), including insecticides in many pests of agricultural and public health importance including mosquito vectors of human diseases (Feyereisen, 2012; Vontas et al., 2020). The control of *Anopheline* malaria vectors over the last decades has heavily relied on pyrethroids such as deltamethrin, cypermethrin and permethrin, incorporated in insecticide treated bed nets (ITN) and applied as indoor residual sprays (IRS) (WHO, 2018). This chemical class of insecticides acts on voltage-gated sodium channels in the central nervous system and induces a quick knock-down of pest insects upon contact exposure (Soderlund, 2020). Due to frequent applications and continuous selection pressure, mosquitoes have developed resistance to pyrethroids that is often linked to the upregulation of P450 isoforms, which facilitate pyrethroid metabolism in resistant phenotypes (Hemingway and Ranson, 2000). In *Anopheles funestus* s.s., one of the major malaria transmitting mosquitoes in Sub-Saharan-Africa (Coetzee and Koekemoer, 2013), a number of P450s have been associated with pyrethroid resistance, including CYP6P9a, CYP6P9b, CYP6M7, CYP6AA1, CYP9J11, CYP6Z1 and, very recently, CYP325A (Ibrahim et al., 2016a, 2018; Riveron et al., 2013, 2014, 2017; Wamba et al., 2021). Indeed, *CYP6P9a* and *CYP6P9b* are highly upregulated in *An. funestus* and have been functionally shown to play a key role in the oxidative metabolism of pyrethroids (Cuamba et al., 2010; Ibrahim et al., 2015; Riveron et al., 2013; Weedall et al., 2019). This upregulation was first demonstrated in one of the global laboratory reference strains, FUMOZ-R (Wondji et al., 2009), originally collected in 2000 in Mozambique (Brooke et al., 2001), and since then maintained in the laboratory under pyrethroid selection pressure (Hunt et al., 2005).

Functional validation of the importance of upregulated P450 isoforms in conferring insecticide resistance in both agricultural pests and mosquitoes is usually provided by their recombinant expression and subsequent analysis of insecticide depletion and metabolite formation *in vitro*, or alternatively, by the ectopic expression of candidate genes in model insects such as *Drosophila melanogaster* (Nauen et al., 2022). The most important systems employed for the functional expression of insect P450s are based on *Escherichia coli* and insect cell lines utilizing a baculovirus expression system (reviewed in (Nauen et al., 2021). Interestingly the majority of mosquito P450s involved in insecticide resistance, including *An. funestus* CYP6P9a and CYP6P9b, have been expressed using *E. coli* along with *Anopheles gambiae* cytochrome P450 reductase (CPR) (Table 1). CPR is an essential membrane-bound flavoprotein, located in close vicinity to P450s, and the principal redox-partner of microsomal P450s required for electron transfer utilizing NADPH as a co-factor (Gutierrez et al., 2003). In mammals, CPR has been shown to have many more essential functions, e.g., in steroid hormone synthesis, cholesterol homeostasis, heme catabolism and cholesterol biosynthesis (Porter, 2012). Its essential role is reflected by the fact that the germline deletion of CPR in mice was embryonic lethal (Shen et al., 2002). However, such studies are lacking in insects, but silencing of CPR by RNAi in *An. gambiae* showed enhanced sensitivity to permethrin (Lycett et al., 2006), while pest invertebrates resistant to insecticides resulted in increased insecticide sensitivity compared to susceptible individuals, indicating that lower expression of CPR negatively affected P450-mediated metabolism (Moural et al., 2020; Shi et al., 2015; Zhu et al., 2012).

The coupling of insect microsomal P450s and CPR in heterologous expression systems is essential for catalytic activity, whereas the role of another potential electron donor, cytochrome b_5 (CYB5), which is of particular importance in mammals (Schenkman and Jansson, 2003), remains nebulous in insects. Drug metabolism by several mammalian microsomal P450 isoforms was shown to be maximized by CYB5, either catalytically or allosterically, because its deletion resulted in a marked decrease in activity of several hepatic P450s (Finn et al., 2008; McLaughlin et al., 2010). CYB5 was also shown to significantly modulate the activity of some major human P450s such as CYP3A4 and CYP2D6 (Henderson et al., 2015). Therefore, CYB5 is considered to stimulate hepatic drug metabolism in combination with several P450 isoforms, rather than being an auxiliary player (Porter, 2012). However, despite its functional role, germline deletion of CYB5 in mice was not lethal, possibly

indicating that other redox-proteins may substitute for its function (Finn et al., 2011). Its modulating role on insect P450 activity was first demonstrated using house fly microsomal preparations, where its inhibition resulted in decreased O-dealkylation of two coumarin substrates, while the metabolism of resorufins remained unaffected (Zhang and Scott, 1994). Another study confirmed its role as a modulator of house fly P450 activity by enhancing heptachlor epoxidation in a reconstituted system with CPR and CYP6A1 (Guzov et al., 1996). A more recent study revealed that CYB5 significantly increased the O-deethylation of 7-ethoxycoumarin by CYP6FD1 from *Locusta migratoria* (Liu et al., 2020). Although CYB5 was cloned and sequenced from two major anopheline mosquitoes, *An. gambiae* and *An. funestus*, many years ago (Matambo et al., 2010; Nikou et al., 2003), functional studies investigating its role in combination with CPR and pyrethroid-metabolizing P450s such as CYP6P9a and CYP6P9b are lacking.

To evaluate the role of CYB5 on the activity of recombinantly expressed insect P450s, it can either be co-expressed with the respective CPR and P450 of interest or added to the reaction mix, as done in most studies with heterologously expressed mosquito P450s utilizing an *E. coli* expression system (Table 1). *Aedes aegypti* CYP9M6 and CYP6BB2 were one of the few mosquito P450s heterologously expressed in Sf9 cells using the baculovirus system, but without CYB5 (Kasai et al., 2014). To the best of our knowledge only four *Anopheline* P450 isoforms, i.e. CYP6AA3 and CYP6P7 from *An. minimus* and CYP6Z1 and CYP6Z2 from *An. gambiae,* were yet expressed using a baculovirus expression system (Boonsuepsakul et al., 2008; Duangkaew et al., 2011). Whereas CYP6AA3 and CYP6P7 were co-expressed with *An. minimus* CPR (without CYB5), *An. gambiae* CYP6Z1 and CYP6Z2 were co-expressed with *M. domestica* CPR and *D. melanogaster* CYB5 (Chiu et al., 2008). None of the pyrethroid-metabolizing *An. funestus* P450s have yet been expressed in insect cells using a baculovirus expression system. Interestingly, most, if not all, of the functional insecticide metabolization assays with recombinantly expressed *An. funestus* P450s, particularly CYP6P9a and CYP6P9b, relied on the co-expression of CPR from *An. gambiae* and the addition of *An. gambiae* CYB5 (Table 1, and references cited there-in).

The role of CYB5 on substrate turn-over when combined with CYP6P9a and CYP6P9b has not been fully investigated, so the objective of our study was to address this knowledge gap. In this study, we expressed for the first time *An. funestus* CYP6P9a and CYP6P9b in High-5 cells utilizing a baculovirus expression system. We compared the impact of co-expressed *An.*

gambiae CPR and *An. funestus* CPR in a fluorescent probe assay on CYP6P9-mediated substrate conversion. Furthermore, we either co-expressed or added *An. funestus* CYB5 to reaction mixes with recombinantly expressed CYP6P9a and CYP6P9b (and CPR) and tested different MOIs (multiplicity of infection rates). Finally, we conducted metabolism studies with and without co-expressed CYB5 to evaluate its impact on deltamethrin metabolism catalyzed by CYP6P9a and CYP6P9b.

Table 1. Selected examples of addition/co-expression of cytochrome b5 (CYB5) in heterologously expressed mosquito CYP genes

Insect	*CYP*	Expression system	CPR* origin	CYB5 origin	CYB5 addition	Reference
Ae. aegypti	*CYP6Z8*	Yeast	*Ae. aegypti*	*Ae. aegypti*	Ratio 80 pmol:50 pmol (b5:P450) added to reaction mix	(Chandor-Proust et al., 2013)
Ae. aegypti	*CYP6CB1*	*E. coli*	*An. gambiae*	*An. gambiae*	Ratio 0.8:0.1 µM (b5:P450) added to reaction mix	(Stevenson et al., 2012)
Ae. aegypti	*CYP9J19*	*E. coli*	*An. gambiae*	*An. gambiae*	Ratio 0.8:0.1 µM (b5:P450) added to reaction mix	Ibid.
Ae. aegypti	*CYP9J24*	*E. coli*	*An. gambiae*	*An. gambiae*	Ratio 0.8:0.1 µM (b5:P450) added to reaction mix	Ibid.
Ae. aegypti	*CYP9J26*	*E. coli*	*An. gambiae*	*An. gambiae*	Ratio 0.8:0.1 µM (b5:P450) added to reaction mix	Ibid.
Ae. aegypti	*CYP9J28*	*E. coli*	*An. gambiae*	*An. gambiae*	Ratio 0.8:0.1 µM (b5:P450) added to reaction mix	Ibid.
Ae. aegypti	*CYP9J32*	*E. coli*	*An. gambiae*	*An. gambiae*	Ratio 0.8:0.1 µM (b5:P450) added to reaction mix	Ibid.
Ae. aegypti	*CYP9M6*	bac-to-bac, Sf9	*Ae. aegypti*	*Ae. aegypti*	Not indicated	(Kasai et al., 2014)
Ae. aegypti	*CYP6BB2*	bac-to-bac, Sf9	*Ae. aegypti*	*Ae. aegypti*	Not indicated	Ibid.
An. arabiensis	*CYP6P4*	*E. coli*	*An. gambiae*	*An. gambiae*	Not indicated	(Ibrahim et al., 2016b)
An. funestus	*CYP6P9a/b*	*E. coli*	*An. gambiae*	*An. gambiae*	Ratio 0.8 µM:45 pmol (b5:P450) added to reaction mix	(Riveron et al., 2014)
An. funestus	*CYP6M7*	*E. coli*	*An. gambiae*	*An. gambiae*	Ratio 0.8 µM:45 pmol (b5:P450) added to reaction mix	Ibid.
An. funestus	*CYP6Z1*	*E. coli*	*An. gambiae*	*An. gambiae*	Not indicated	(Ibrahim et al., 2016a)
An. funestus	*CYP6AA1*	*E. coli*	*An. gambiae*	*An. gambiae*	Not indicated	(Ibrahim et al., 2018)
An. funestus	*CYP9J11*	*E. coli*	*An. gambiae*	*An. gambiae*	Ratio 0.8 µM:45 pmol (b5:P450) added to reaction mix	(Riveron et al., 2017)
An. gambiae	*CYP6M2*	*E. coli*	*An. gambiae*	*An. gambiae*	Ratio 0.8 µM:0.1 µM (b5:P450) added to reaction mix	(Stevenson et al., 2011)
An. gambiae	*CYP6P3*	*E. coli*	*An. gambiae*	-	Without *CYB5*	(Müller et al., 2008)
An. gambiae	*CYP6Z2*	*E. coli*	*An. gambiae*	-	Without *CYB5*	(Mclaughlin et al., 2008)
An. gambiae	*CYP6Z1/2*	bac-to-bac, Sf9	*M. domestica*	*D. melanogaster*	co-expression, MOI 2:2:0.1	(Chiu et al., 2008)
An. gambiae	*CYP9J5*	*E. coli*	*An. gambiae*	*An. gambiae*	Ratio 10:1 (b5:P450) added to reaction mix	(Yunta et al., 2016) (2019)
An. gambiae	*CYP6P4*	*E. coli*	*An. gambiae*	*An. gambiae*	Ratio 10:1 (b5:P450) added to reaction mix	Ibid.
An. gambiae	*CYP6P2*	*E. coli*	*An. gambiae*	*An. gambiae*	Ratio 10:1 (b5:P450) added to reaction mix	Ibid.
An. gambiae	*CYP6P5*	*E. coli*	*An. gambiae*	*An. gambiae*	Ratio 10:1 (b5:P450) added to reaction mix	Ibid.
An. minimus	*CYP6AA3*	bac-to-bac, Sf9	*An. minimus*	-	Without *CYB5*	(Boonsuepsakul et al., 2008)
An. minimus	*CYP6P7*	bac-to-bac, Sf9	*An. minimus*	-	Without *CYB5*	(Duangkaew et al., 2011)

3.2. Material and methods

3.2.1. Chemicals

Deltamethrin (CAS: 52918-63-5), β-Nicotinamide adenine dinucleotide 2'-phosphate (NADPH) reduced tetrasodium salt hydrate (CAS: 2646-71-1 anhydrous, purity ≥93 %), 7-ethoxycoumarin (EC; CAS: 31005-02-4, >99 %), 7-methoxy-4-trifluoromethylcoumarin (MFC; CAS: 575-04-2, ≥99 %), 7-Ethoxy-4-trifluoromethylcoumarin (EFC; CAS: 115453-82-2, ≥98 %) 7-benzyloxy-4-trifluoromethylcoumarin (BFC; CAS: 220001-53-6, ≥ 99 %), 7- hydroxy-coumarin (HC; CAS: 93-35-6, 99 %) 7-hydroxy-4-trifluoromethylcoumarin (HFC; CAS: 575-03-1, 98) were purchased from Sigma Aldrich/Merck (Darmstadt, Germany). 7-benzyloxymethoxy-4-trifluoromethylcoumarin (BOMFC; CAS: 277309-33-8; purity 95 %) was synthesized by Enamine Ltd. (Riga, Latvia). 7-pentoxycoumarin and 4'OH-deltamethrin (CAS: 66855-89-8) were internally synthetized (Leverkusen, Germany). Human CYB5 was purchased from Sigma (St. Louis, MO, USA; product no. C1427). All other chemicals and solvents were of analytical grade unless otherwise stated.

3.1.1. Insects

Anopheles funestus strains FANG and FUMOZ-R are known reference strains susceptible and resistant to pyrethroids (Amenya et al., 2008), respectively. Both strains were kept at 27.5 ± 0.5 °C, 65 ± 5 % relative humidity and a photoperiod of 12/12 L:D with one-hour dusk/dawn period, under laboratory conditions as described elsewhere (Nolden et al., 2021). The LC_{50}-values for deltamethrin against adults of strain FANG and FUMOZ-R maintained in our laboratory were 0.021 (CL95%: 0.015-0.027) and 4.61 (CL95%: 2.73-7.50) mg/m² in glazed tile bioassays, respectively, resulting in a resistance ratio of >200-fold (Nolden et al., 2021).

3.1.2. mRNA extraction and RT-qPCR

RNA was extracted from ten 3-5 days old adult females of strain FANG and FUMOZ-R TRIzol™ reaction kit following manufacturer's instructions. Afterwards RNA was purified using RNAeasy MINI Kit (Qiagen, Hilden, Germany) following manufacturer's instructions, including a DNAse-digest (RNase-free DNAse Set, 79254, Qiagen, Hilden, Germany) (modifications: Trizol incubation: 10 min, the column containing RNA sample was eluated twice to enhance RNA yields). RNA quantity was determined photometrically by measuring 260/280 nm and 230/260 nm ratios (NanoQuant Infinite 200, Tecan, Switzerland). All samples were adjusted to 20 ng/µL and RNA quality was checked using QIAxcel capillary electrophoresis as recently

described (Nolden et al., 2021). For cDNA synthesis 0.3 µg of total RNA in 20 µL reaction volume was used employing IScript cDNA synthesis Kit (Bio-Rad, Hercules, USA).

Expression levels of the potential P450 redox partners CYB5 and CPR were measured by RT-qPCR following the method described earlier (Boaventura et al., 2020) using SsoAdvanced Universal SYBR Green Supermix (Bio-Rad, Hercules, USA) with a total volume of 10 µL using Real-Time CFX384™system (Bio-Rad, Hercules, USA). Samples were run in triplicate and a non-template control was included as negative control. Two µL of cDNA with 5 ng μL^{-1} of each primer with 200 nM final concentrations were used following the PCR program recently described (Nolden et al., 2021). Two reference genes were employed for normalization, *ribosomal protein S7* (*RPS 7*) and *actin 5c* (*Act*). Primer efficiencies were as follows: CYB5 99.5 % and CPR 100 %. The experiment was replicated (biological replicates) at least three times. Primer sequences and GenBank accession numbers of all relevant genes are given in Table S1.

3.1.3. Recombinant expression of CYP genes and their redox partners in insect cells

Gene sequences of *An. funestus CYP6P9a*, *CYP6P9b*, CPR (*AfCPR*), *CYB5*, and *An. gambiae* CPR (*AgCPR*) were retrieved from GenBank (Table S1). The respective expression plasmids were created using GeneArt server (Thermo Fisher), and PFastBac1 with BamHI and HindIII restriction sites was chosen. The sequences were codon optimized for final expression in High-Five cells (*Trichoplusia ni*). A PFastBac1 vector containing no insert served as a control. For the recombinant expression of P450 genes and their respective redox partners we followed the baculovirus expression protocol previously published (Manjon et al., 2018). In brief: MaxEfficiencyDH10 (Invitrogen, Waltham, MA, USA) competent *E. coli* cells containing a baculovirus shuttle vector (bacmid) were transformed according to manufacturer's instructions. The final bacmid was extracted using Large construct Kit (Qiagen, Hilden, Germany) following standard protocols. Subsequently Sf9 cells (Gibco™, kept in Sf-900-SFM (1X) cell culture medium, containing 25 µg/ml gentamycin) were virus transfected and the virus titer was determined according to Rapid Titer Kit (Takara Bio, San Jose, CA, USA).

High five cells were kept at 27 °C and 120 rpm in Express five medium (SFM (1X), Gibco™, Thermo Fisher, Waltham, MA, USA) containing 18 mM GlutaMAX (100X, Gibco™) and 10 µg mL^{-1} gentamycin (Gibco™). Preliminary experiments revealed highest CYP6P9a and CYP6P9b activity with a multiplicity of infection (MOI) of 1:0.5 for CYP6P9a/b:CPR (Figure S2). To obtain the best working MOI for CYB5 co-expression we tested the following MOIs

(CYP6P9a/b:CPR:CYB5): 1:0.5:0.1; 1:0.5:0.2; 1:0.5:0.5. Cells were diluted to a concentration of $1.5x10^6$ cells mL^{-1} and incubated with 0.5 % fetal bovine serum (FBS; Sigma Aldrich), 0.2 mM delta-aminolevulinic acid (d-ALA; Sigma Aldrich), 0.2 mM Fe III citrate (Sigma Aldrich) and the respective amount of virus for 52 hours at 27 °C and 120 rpm. After harvesting, cells were resuspended in homogenization buffer (0.1 M K_2HPO_4, 1 mM DTT, 1mM EDTA, 200 mM saccharose, pH 7.6). FastPrep device (MP Biomedicals, Irvine, CA, USA) was used for grinding the cells following a 10 min centrifugation step at 4 °C and 700 g. The resulting supernatant was centrifuged for one hour at 100,000 g and 4 °C. The resulting microsomal pellet was resuspended with a Dounce tissue grinder in buffer (0.1 M K_2HPO_4, 0.1 mM EDTA, 1 mM DTT, 5 % Glycerol, pH 7.6) and protein amount was determined according to Bradford (Bradford, 1976). The functional expression of P450s was validated by their capacity to metabolize coumarin substrates and deltamethrin, and their concentrations were calculated based on CO difference spectra as described elsewhere (Omura and Sato, 1964).

3.1.4. Fluorescent probe bioassays

The enzymatic activity and substrate profile of each functionally expressed CYP6P9 co-expressed with CPR (± CYB5) at different MOIs was measured in 384-well plates with six different coumarin substrates using the same fluorescent probe assay as recently described (Haas and Nauen, 2021; Nolden et al., 2021). *An. funestus* CYB5 was either co-expressed with the different CYP6P9 variants, or commercial human CYB5 was added to the reaction mix at a concentration of 0.8 µM. This concentration was based on other studies utilizing *An. gambiae* CYB5 (Table 1). Each assay was replicated four times. Michaelis Menten kinetics of BOMFC O-debenzylation by CYP6P9a and CYP6P9b with and without *An. funestus* CYB5 in order to check the impact of CYB5 on substrate conversion followed the same protocol as mentioned above. All incubations were done under conditions linear with respect to time and protein concentration.

3.1.5. UPLC-MS/MS measurement of deltamethrin metabolism

UPLC-MS/MS analysis was carried out with slight modifications as previously described (Manjon et al., 2018). Briefly, for the chromatography on an Agilent 1290 Infinity II, a Waters Acquity HSS T3 column (2.1 x 50 mm, 1.8 mm) with 2 mM ammonium-acetate in methanol and 2mM ammonium-acetate in water as the eluent in gradient mode was employed. After positive electrospray ionization, ion transitions were recorded on a Sciex API6500 Triple Quad.

Deltamethrin and 4'OH deltamethrin were measured in positive ion mode (ion transitions: deltamethrin 523.000 > 281.000, 4'OH deltamethrin 539.000 > 281.000). The peak integrals were calibrated externally against a standard calibration curve. The linear ranges for the quantification of deltamethrin and 4'OH deltamethrin were 0.5 - 100 ng/mL and 0.1 - 200 ng/mL, respectively. Samples were diluted prior to measurement if needed. The experiment was replicated thrice.

3.1.6. Data analysis

Gene expression analysis was done by employing Bio-Rad CFX Maestro 1.0 v 4.0 software (Bio-Rad, 2017, Hercules, USA) followed by subsequent unpaired t-tests in qbase (Biogazelle, Zwijnaarde, Belgium) to compare for significant differences in gene expression levels. Michaelis Menten kinetics were analyzed by nonlinear regression using Graph Pad Prism 9.0 (GraphPad Software Inc., CA, USA). CYB5 sequence alignments were conducted using the Geneious Alignment tool in Geneious software v. 10.2.3 (Biomatters Ltd., New Zealand).

3.2. Results

3.2.1. Expression levels of CPR and CYB5

As described previously LC_{50}-values for deltamethrin against adults of *An. funestus* strain FANG and FUMOZ-R maintained in our laboratory were 0.021 (CL95%: 0.015-0.027) and 4.61 (CL95%: 2.73-7.50) mg/m² in glazed tile bioassays, respectively, resulting in a resistance ratio of >200-fold (Nolden et al., 2021). Deltamethrin resistance in strain FUMOZ-R is correlated with the upregulation of *CYP6P9a* and *CYP6P9b* in comparison to strain FANG (Figure 1a). In contrast to the *CYP6P9* variants, the expression levels of both *CYB5* and *CPR* as measured by RT-qPCR were not upregulated in female adults of the pyrethroid resistant FUMOZ-R strain

Figure 1. RT-qPCR analysis of gene expression in female adults. Expression level of (A) *CYP6P9a* and *CYP6P9b*, and (B) cytochrome b5 (CYB5) and cytochrome P450-reductase (CPR) of *An. funestus* strains FUMOZ-R and FANG measured by RT-qPCR. The expression levels were normalized to *RPS7* and *Act* (5c) reference genes. Data are mean values ± 95% CI (n=4). The expression data shown in (A) were taken from Nolden et al. (2021).

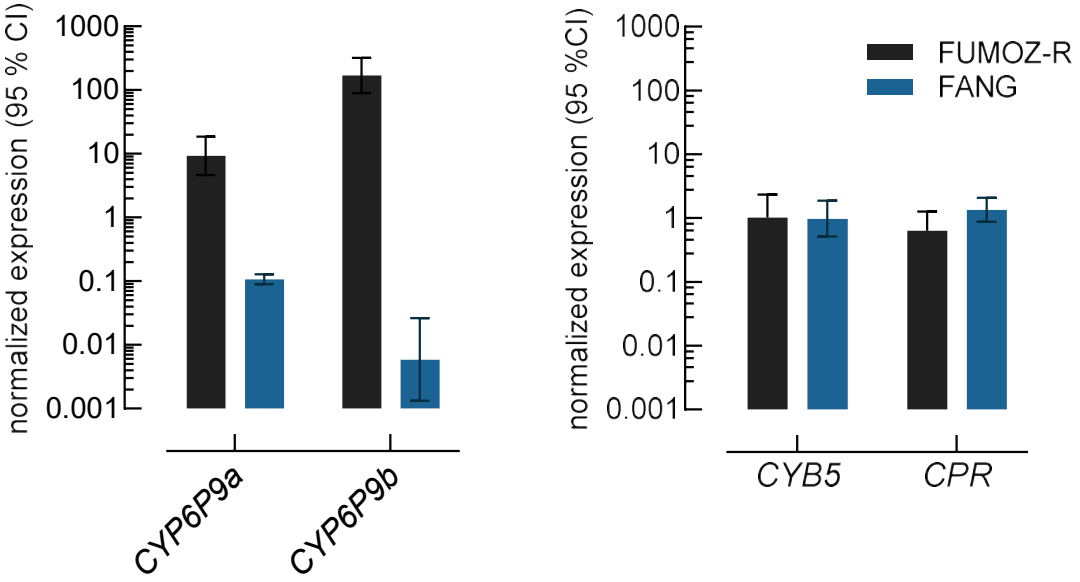

when compared to the susceptible FANG strain, suggesting no immediate regulatory role of these P450 redox partners in pyrethroid resistance in FUMOZ-R (Figure 1b).

3.2.2. Functional expression and coumarin substrate profiling of *An. funestus* CYP6P9 variants in concert with CPR and CYB5 in insect cells

The heterologous baculovirus-mediated expression of CYP6P9a and CYP6P9b in High-5 cells co-infected with *An. gambiae* CPR (AgCPR) at different multiplicity of infection (MOI) ratios, revealed highest fluorescent probe substrate metabolization capacity in the presence of NADPH at a P450:CPR ratio of 1:0.5 across six different alkylated and benzylated coumarins (Table S2). No basal metabolizing activity against any of the six coumarin probe substrates was detected when microsomal membranes resulting from mock virus infections were incubated with NADPH (data not shown), suggesting that the observed substrate profile is based on the expression of the respective *An. funestus* CYP6P9 variant. This confirmed functional expression in High-5 cells despite weak CO difference spectra (Figure S2). The O-debenzylation of 7-benzyloxymethoxy-4-(trifluoromethyl)-coumarin (BOMFC) resulting in 7-hydroxy-4-(trifluoromethyl)coumarin (HC) revealed the highest enzyme activity with both P450s at all tested P450:CPR MOIs (Figure 3A-C), followed by the O-debenzylation of 7-

benzyloxy-4-trifluoromethylcoumarin (BFC). Less preferred substrates were the alkylated coumarin derivatives tested such as 7-methoxy-4-trifluoromethylcoumarin (MFC). However, we observed a slight, but significant difference between CYP6P9a and CYP6P9b in their ability to metabolize BFC and EFC, with CYP6P9b showing higher activity. The overall results and trends in coumarin substrate preference did not change when CYP6P9a and CYP6P9b were co-expressed with *An. funestus* CPR (AfCPR) instead of AgCPR at a MOI of 1:0.5 (Figure 2A and Figure S3D). Based on these results we decided to conduct all other experiments with recombinantly expressed CYP6P9a and CYP6P9b in concert with AfCPR.

Next, we tested the impact of the co-expression of *An. funestus* CYB5 (AfCYB5) on coumarin substrate metabolism at different MOIs in combination with CYP6P9 variants and AfCPR. The highest enzyme activity was obtained from microsomal preparations of High-5 cells infected at a MOI of 1:0.5:0.1 (P450:CPR:CYB5) (Figure 2B). Increasing the level of co-expressed AfCYB5 resulted in a significantly lower enzyme activity with all tested coumarin substrates (Figure 2B). The overall coumarin substrate profile of both CYP6P9 variants did not change when co-expressed with AfCYB5. However, at a MOI of 1:0.5:0.1 (P450:CPR:CYB5) the activity of both CYP6P9 isoforms was significantly higher with the preferred probe substrates BOMFC, BFC, and EFC when compared to CYP6P9 expressions without AfCYB5. Finally, we checked if the addition of a mammalian CYB5, commercial human CYB5, results in a similar increase in activity. We demonstrated that human CYB5 added to the reaction mix at 0.8 µM increased the activity of CYP6P9a and CYP6P9b co-expressed with AfCPR (MOI 1:0.5) without changing the substrate profile (Figure 2C), confirming its ability to substitute *An. funestus* or *An. gambiae* CYB5. The metabolic activity of both CYP6P9 variants towards preferred coumarin substrates is not influenced by the choice of the CPR source (AgCPR vs. AfCPR), but the addition of CYB5 increased their activity up to ~ 6-fold depending on the coumarin substrate (e.g., BFC, Table S2).

Figure 2. Coumarin substrate profiling of recombinantly expressed CYP6P9a and CYP6P9b co-expressed with *An. funestus* CPR with and without CYB5. (A) Coumarin substrate metabolism by recombinantly expressed CYP6P9a and CYP6P9b co-expressed with *An. funestus* cytochrome P450-reductase (Af CPR) at MOI 1:0.5, (B) co-expressed with *An. funestus* CYB5 at different MOI ratios stated as P450:CPR:CYB5, and (C) supplemented with exogenous 0.8 µM human CYB5 (exCYB5) while expressed at MOI 1:0.5 (P450:CPR). Data are mean values ± SD (n=4). Abbreviations: BFC, 7-benzyloxy-4-trifluoromethyl coumarin; MFC, 7-methoxy-4-trifluoromethyl coumarin; EFC, 7-ethoxy-4-rifluoromethyl coumarin; BOMFC, 7-benzyloxymethoxy-4-trifluoromethyl coumarin; PC, 7-n-pentoxy coumarin; EC, 7-ethoxy coumarin.

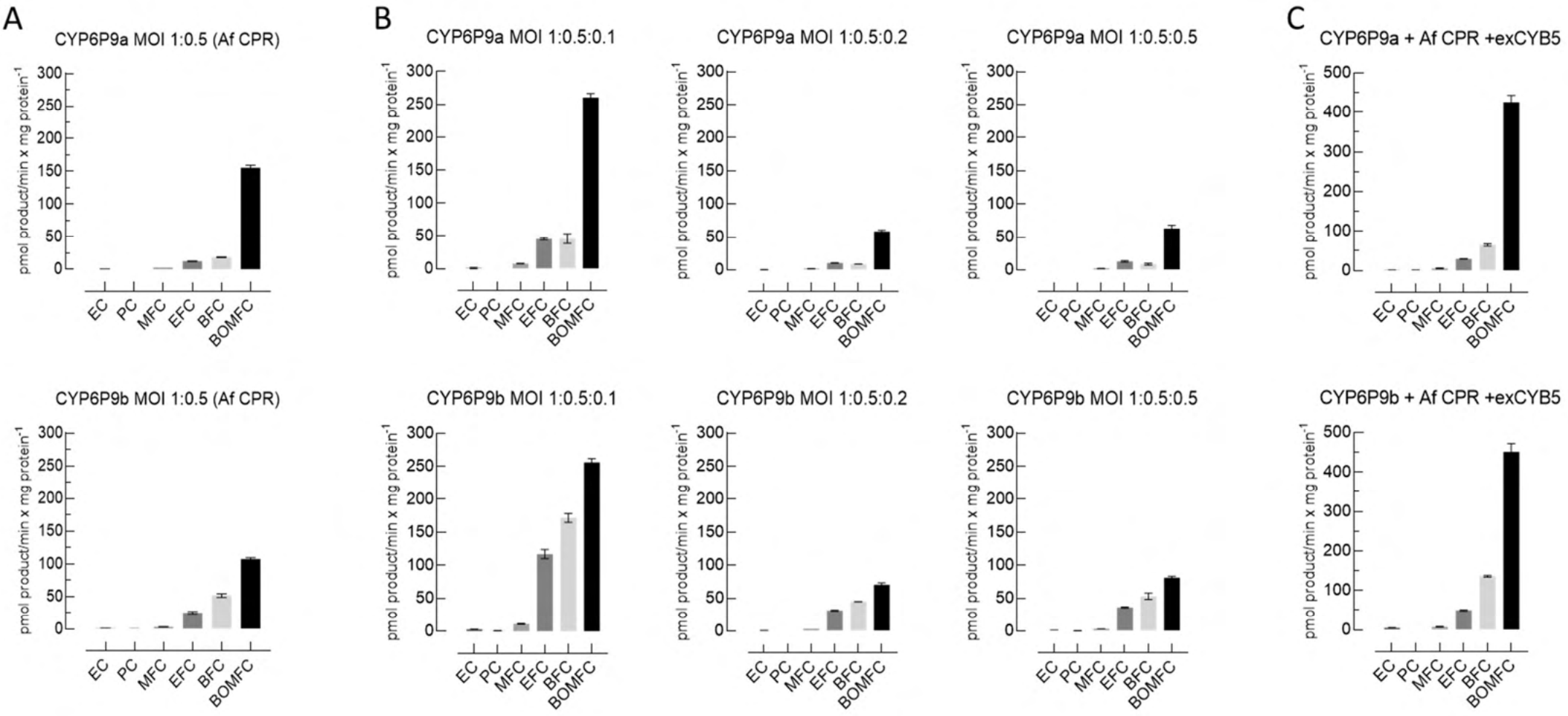

3.2.3. Michaelis Menten kinetics of the O-debenzylation of BOMFC by CYP6P9 variants

Based on the probe substrate activity profiling presented above we have chosen the coumarin substrate BOMFC for a more detailed steady-state kinetic analysis with recombinantly expressed CYP6P9a and CYP6P9b with and without the co-expression of *An. funestus* CYB5. The rate of the O-debenzylation of BOMFC by recombinantly expressed CYP6P9a and CYP6P9b was time dependent and followed Michaelis-Menten kinetics in response to BOMFC concentration (Figure 3), resulting in a K_m-value of 4.07 µM (CI95%: 3.44-4.80) and 2.13 µM (CI95%: 1.62-2.79), and a catalytic activity K_{cat} of 1.59 ± 0.034 min^{-1} and 1.10 ± 0.034 min^{-1}, respectively. The co-expression of CYB5 did not significantly change the K_m-value obtained for BOMFC; CYP6P9a: 4.89 µM (CI95%: 4.10-5.83), and CYP6P9b: 3.25 µM (CI95%: 2.61-4.05). Whereas K_{cat} increased significantly at 2.83 ± 0.067 min^{-1} and 2.29 ± 0.064 min^{-1} in the presence of CYB5 for CYP6P9a and CYP6P9b, respectively. Thus, suggesting a supportive role of CYB5 in CYP6P9 driven BOMFC metabolism, and overall, a slightly lower catalytic capacity of CYP6P9a compared to CYP6P9b.

Figure 3. Steady-state enzyme kinetics of product formation. Michaelis-Menten kinetics of BOMFC O-debenzylation leading to 7-hydroxy-4-(trifluoromethyl)coumarin (HC) by recombinantly expressed CYP6P9a and CYP6P9b (co-expressed with AfCPR, MOI 1:0.5) with and without co-expression of cytochrome b5 (CYB5; MOI 1:0.5:0.1). Data are mean values ± SD (n=4). K_m- and V_{max}-values (and 95% confidence intervals) were calculated by nonlinear regression analysis using GraphPad Prism 9.0.

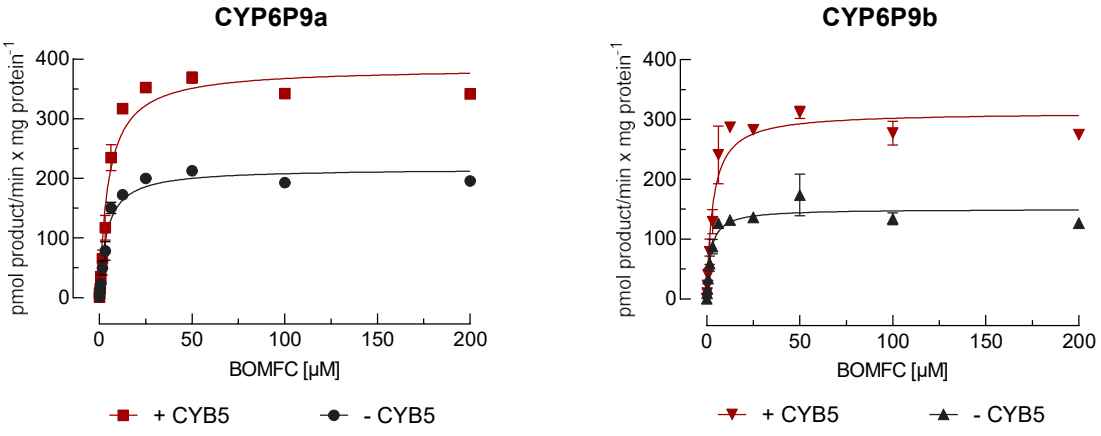

3.2.4. Deltamethrin metabolism by CYP6P9 variants with and without CYB5

UPLC-MS/MS analysis of microsomal preparations of High-5 cells expressing CYP6P9a and CYP6P9b, respectively, in concert with *An. funestus* CPR at a MOI of 1:0.5 revealed a time-dependent depletion of deltamethrin in the presence of NADPH (Figure 4A and 4B). The co-expression of *An. funestus* CYB5 did not change the metabolic efficiency of both enzymes. Furthermore, we confirmed the formation of 4'OH deltamethrin by both enzymes (Figure 4C and 4D), suggesting that the deltamethrin depletion is largely based on its metabolism rather than sequestration. The co-expression of CYB5 had no impact on the extent of hydroxylated deltamethrin formation. However, we noticed a stochiometric inconsistency between deltamethrin depletion and 4´OH deltamethrin formation, possibly suggesting the presence of other undetected metabolites.

Figure 4. Kinetics of deltamethrin metabolism by baculovirus-expressed *An. funestus* CYP6P9 variants. Deltamethrin depletion and formation of the respective 4'OH metabolite in the presence of NADPH by recombinantly expressed *An. funestus* CYP6P9a (A,C) and CYP6P9b (B,D) co-expressed with (open circles) and without (closed circles) *An. funestus* cytochrome b5 (CYB5). Data are mean values ± SD (n=3).

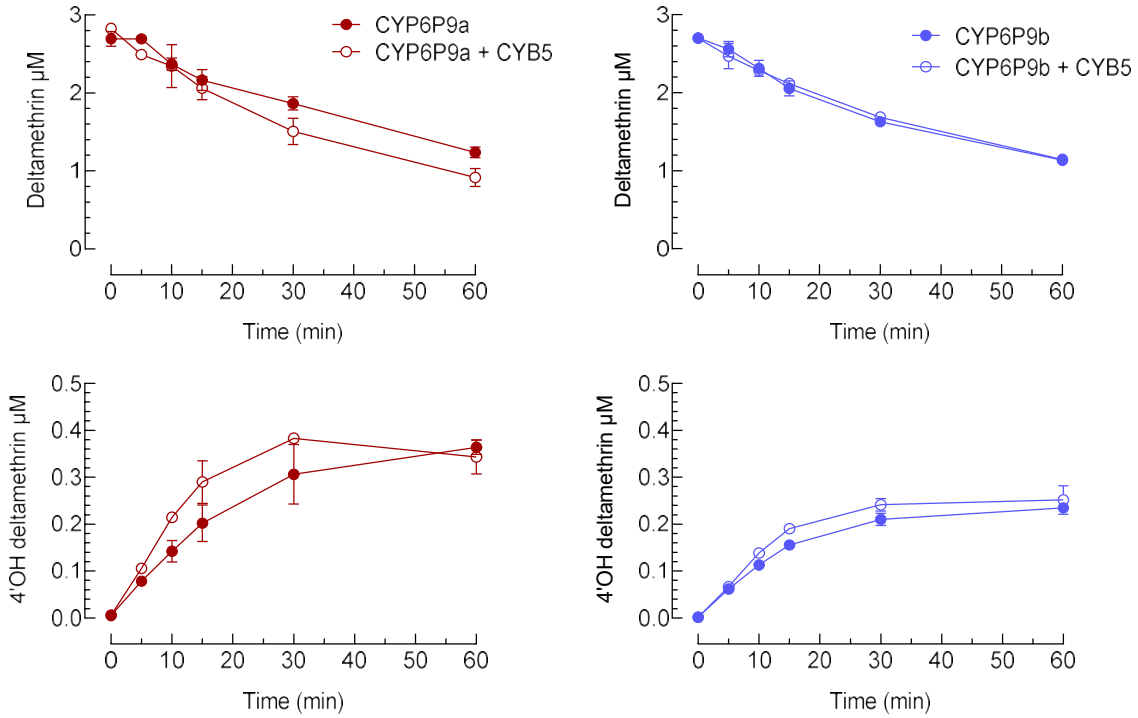

3.3. Discussion

Metabolic resistance towards pyrethroids in anopheline mosquitoes such as *An. funestus* is largely driven by upregulated P450s of which a number have been recombinantly expressed, most of them in bacterial expression systems using competent *E. coli* cells (Nauen et al., 2021; Vontas et al., 2020). Among upregulated P450s mediating pyrethroid resistance in *An. funestus,* CYP6P9a and CYP6P9b, were most prominent and shown to metabolize different pyrethroids when functionally expressed in *E. coli* (Riveron et al., 2013; Weedall et al., 2019). Here we successfully expressed both P450 genes in combination with either AfCPR or AgCPR at different MOI ratios in High-5 cells employing a baculovirus expression system. Microsomal insect cell preparations revealed highest CYP6P9a/b activities with the fluorescent probe substrate BOMFC at a MOI ratio of 1:0.5 (P450:CPR), resembling findings with other insect P450s utilizing similar expression conditions (Bass et al., 2013; Manjon et al., 2018; Zimmer et al., 2018). Many functional studies conducted with recombinantly expressed *An. funestus* P450s showed that their co-expression with *An. gambiae* CPR as a surrogate for the homologous *An. funestus* CPR worked well (Table 1). Our study demonstrated and confirmed that the overall enzymatic activity of the duplicated CYP6P9 isoforms did not differ if co-expressed with either *An. gambiae* CPR or *An. funestus* CPR. Indeed, CPR incompatibilities as observed for *Tetranychus urticae* CYP392A11 and CYP392A16 ectopically expressed in phylogenetically distant *Drosophila melanogaster*, are rather unlikely in closely related species (Riga et al., 2020).

The baculovirus system recruiting High-5 cells for P450 expression is thought to offer some advantages over *E. coli* such as insect-specific posttranslational modifications of the expressed P450s, though meaningful comparative studies with insect P450s are lacking. Comparative studies utilizing prokaryotic and eukaryotic expression systems were especially conducted with human P450 isoforms (Hiratsuka, 2012), and revealed for example significantly different catalytic efficiencies in benzo[a]pyrene detoxification by functionally expressed human CYP1A1, possibly linked to differences in lipid membrane composition (Stiborová et al., 2017). Although optimized *E. coli* expression systems often resulted in higher P450 yields as demonstrated for human CYP3A4 and CYP17A1 (Schroer et al., 2010), it was shown that they have limitations in contrast to insect and mammalian cells (Kumondai et al., 2020). On the other hand, *E. coli* preparations do not express basal P450 activity as they lack

endogenous P450s possibly interfering with those P450s recombinantly expressed (Nauen et al., 2021), which facilitates the screening of compounds for metabolic liabilities including insecticides (Lees et al., 2020; Yunta et al., 2019). Future studies with insect P450s are necessary to shed light on possible differences in P450 catalytic efficiency towards various substrates between prokaryotic and eukaryotic expression systems.

We recently confirmed high expression levels of the duplicated *CYP6P9* genes in the laboratory reference strain FUMOZ-R(Nolden et al., 2021), whereas *CPR*, the principal redox partner of microsomal P450s, is not overexpressed when compared to the susceptible strain FANG. Another potential redox partner, *CYB5*, often added or co-expressed along with mosquito P450s such as CYP6P9a and CYP6P9b (Table 1), is also not overexpressed in strain FUMOZ-R compared to FANG. In contrast to our findings, Nikou et al. (2003) found a 2.3-fold upregulation of *CYB5* expression in the pyrethroid resistant *An. gambiae* RSP strain in comparison to the susceptible Kisumu strain. This was also demonstrated in a cypermethrin resistant strain of *Plutella xylostella* showing elevated *CPR* and *CYB5* expression levels (Chen and Zhang, 2015). It would be interesting to evaluate *CPR* and *CYB5* expression levels in pyrethroid resistant field-collected populations of *An. funestus* to rule out possible effects related to the fact that FUMOZ-R has been kept without selection pressure under laboratory conditions for many years. However, our qPCR data do not suggest an obvious role of CYB5 in the amplification of CYP6P9-mediated pyrethroid resistance in *An. funestus* strain FUMOZ-R. This is supported by experimental data showing no difference in deltamethrin depletion measured by UPLC-MS/MS when recombinantly expressed CYP6P9a and CYP6P9b were co-expressed with and without *An. funestus* CYB5. Interestingly, pyrethroid-mimetic activity-based probes were far less active in labelling P450s in CYB5 deficient mouse microsomes, indicating potential species and/or enzyme differences in CYB5 effects (Ismail et al., 2013). In contrast we were able to demonstrate that *An. funestus* CYB5 co-expressed at a MOI ratio of 1:0.5:0.1 (P450:CPR:CYB5) significantly increased the catalytic capacity of both CYP6P9a and CYP6P9b to O-debenzylate BOMFC and BFC, the preferred coumarin substrates as recently shown with microsomal preparations of female adults of FUMOZ-R (Nolden et al., 2021). Thus, suggesting that at least for some of the coumarin substrates CYB5 possibly improved the electron transfer through CPR, but didn´t change the coumarin substrate profile. However, the coumarin profiling results obtained in this study also indicated that both CYP6P9

isoforms contributed greatly to the microsomal P450 activity of the pyrethroid resistant FUMOZ-R recently described (Nolden et al., 2021), and that CYB5 is not necessary to resemble *in vivo* microsomal activity. Other tested MOI ratios using higher amounts of CYB5 resulted in lower enzyme activity, possibly linked to lower overall expression yields of the respective CYP genes as for example shown for human CYP1A2, CYP2C9 and CYP3A4 in other heterologous expression systems (Kumondai et al., 2020). Studies with recombinantly expressed human CYP2B4 revealed that depending on the P450:CYB5 ratio its catalytic efficiency was impaired, because CPR and CYB5 are competing for the same binding site at the enzyme (Zhang et al., 2008). These findings are in line with our results of different MOI ratios tested: A ratio of 1:0.5:0.1 (CYP:CPR:CYB5) revealed highest coumarin substrate activity, whereas a ratio of 1:0.5:0.2 drastically reduced P450 activity.

CYP6M2 from *An. gambiae* was shown to better metabolize deltamethrin and permethrin if 0.8 µM *An. gambiae* CYB5 was supplemented to the reaction (Stevenson et al., 2011), whereas in our study with *An. funestus* CYP6P9 variants the co-expression of CYB5 did not enhance deltamethrin metabolism, suggesting a minor, if any role for CYB5 in facilitating deltamethrin metabolism. Future studies with CYP6P9a/b are necessary to clarify if this is also true for other pyrethroids than deltamethrin. High-5 cell microsomal membranes are highly likely to contain endogenous CYB5 possibly sufficient to support P450 mediated deltamethrin hydroxylation as an additional redox partner. Knock-out of the endogenous *CYB5* in High-5 cells by genome editing would help to address this point. Such an endogenous CYB5 supply is absent in *E. coli* expression systems, possibly explaining why supplementation with exogenous *An. gambiae* CYB5 may have a larger impact, e.g., on recombinantly expressed CYP6M2 (Stevenson et al., 2011).

Quite a few studies demonstrated elevated microsomal levels of CYB5 linked to a resistant phenotype in insects. In a multiple resistant house fly strain microsomal P450 and CYB5 levels were found upregulated in some tissues (Zhang et al., 1998). Similar results were obtained with microsomal fractions of a carbamate and pyrethroid resistant *Blattella germanica* strain (Valles and Yu, 1996). In the cypermethrin resistant house fly LPR strain CYP6D1 and CYB5 were found to be upregulated, and inhibition of CYB5 with a specific antibody prevented the formation of 4'OH-cypermethrin (Liu and Scott, 1996; Zhang and Scott, 1996). In a previous study the same authors reported that specific CYB5 inhibition in house fly microsomes did not

affect methoxyresorufin-O-demethylase and ethoxyresorufin-O-deethylase activity, but ethoxycoumarin-O-deethylase activity. Another study demonstrated an enhanced metabolism of heptachlor and aldrin if CYP6A2 from *D. melanogaster* was supplemented with CYB5 (Dunkov et al., 1997). This was also observed with recombinantly expressed house fly CYP6A1 and it was shown that even apo-CYB5 (devoid of heme) enhanced the metabolic activity against heptachlor and steroid-substrates, and it was concluded that CYB5 mainly enhanced metabolism by CYP6A1 in two ways, by delivering the second electron to CYP6A1 and by allosteric interactions (Murataliev et al., 2008). Similar interactions were also described between a number of recombinantly expressed human P450s and apo-CYB5 (Yamazaki et al., 2002). For recombinantly expressed CYP6FD1 from *L. migratoria* it was shown that silencing of the respective CYB5 gene, did not alter metabolism towards deltamethrin, chlorpyrifos, imidacloprid and carbaryl, but the co-expression of recombinant CYP6FD1 with CYB5 enhanced the metabolism of 7-ethoxycoumarin (Liu et al., 2020).

The examples above and our data obtained with CYP6P9 variants suggest that the involvement of CYB5 in xenobiotic P450-mediated metabolism depends on P450 and substrate-specificity, as reviewed earlier (Schenkman and Jansson, 2003). Our results suggest that co-expression (or addition) of CYB5 with CYP6P9 variants, recombinantly expressed in insect cells, can significantly enhance their metabolic capacity to degrade coumarins, but not deltamethrin.

Acknowledgements

We greatly acknowledge the help of Johannes Glaubitz and Birgit Nebelsiek with the UPC-MS/MS analysis.

Declaration of competing interests

RN is employed by Bayer AG, a manufacturer of pesticides. MN is a PhD student affiliated with the LSTM and funded by the Innovative Vector Control Consortium (IVCC) and Bayer AG.

3.4. References

Amenya, D.A., Naguran, R., Lo, T.-C.M., Ranson, H., Spillings, B.L., Wood, O.R., Brooke, B.D., Coetzee, M., Koekemoer, L.L., 2008. Over expression of a Cytochrome P450 (CYP6P9) in a Major African Malaria Vector, *Anopheles Funestus*, Resistant to Pyrethroids. Insect Mol. Biol. 17, 19–25. https://doi.org/10.1111/j.1365-2583.2008.00776.x

Bass, C., Zimmer, C.T., Riveron, J.M., Wilding, C.S., Wondji, C.S., Kaussmann, M., Field, L.M., Williamson, M.S., Nauen, R., 2013. Gene amplification and microsatellite polymorphism underlie a recent insect host shift. Proc. Natl. Acad. Sci. 110, 19460–19465. https://doi.org/10.1073/pnas.1314122110

Boaventura, D., Martin, M., Pozzebon, A., Mota-Sanchez, D., Nauen, R., 2020. Monitoring of Target-Site Mutations Conferring Insecticide Resistance in *Spodoptera frugiperda*. Insects 11, 545. https://doi.org/10.3390/insects11080545

Boonsuepsakul, S., Luepromchai, E., Rongnoparut, P., 2008. Characterization of *Anopheles minimus* CYP6AA3 expressed in a recombinant baculovirus system. Arch. Insect Biochem. Physiol. 69, 13–21. https://doi.org/10.1002/arch.20248

Bradford, M.M., 1976. A rapid and sensitive method for the quantitation of microgram quantities of protein utilizing the principle of protein-dye binding. Anal. Biochem. 72, 248–254. https://doi.org/10.1016/0003-2697(76)90527-3

Brooke, B.D., Kloke, G., Hunt, R.H., Koekemoer, L.L., Tem, E.A., Taylor, M.E., Small, G., Hemingway, J., Coetzee, M., 2001. Bioassay and biochemical analyses of insecticide resistance in southern African *Anopheles funestus* (Diptera: Culicidae). Bull. Entomol. Res. 91, 265–272. https://doi.org/10.1079/ber2001108

Chandor-Proust, A., Bibby, J., Régent-Kloeckner, M., Roux, J., Guittard-Crilat, E., Poupardin, R., Riaz, M.A., Paine, M., Dauphin-Villemant, C., Reynaud, S., David, J.-P., 2013. The central role of mosquito cytochrome P450 CYP6Zs in insecticide detoxification revealed by functional expression and structural modelling. Biochem. J. 455, 75–85. https://doi.org/10.1042/BJ20130577

Chen, X., Zhang, Y., 2015. Identification and characterization of NADPH-dependent cytochrome P450 reductase gene and cytochrome b5 gene from *Plutella xylostella*: Possible involvement in resistance to beta-cypermethrin. Gene 558, 208–214. https://doi.org/10.1016/j.gene.2014.12.053

Chiu, T.-L., Wen, Z., Rupasinghe, S.G., Schuler, M.A., 2008. Comparative molecular modeling of *Anopheles gambiae* CYP6Z1, a mosquito P450 capable of metabolizing DDT. Proc. Natl. Acad. Sci. 105, 8855–8860. https://doi.org/10.1073/pnas.0709249105

Coetzee, M., Koekemoer, L.L., 2013. Molecular Systematics and Insecticide Resistance in the Major African Malaria Vector *Anopheles funestus*. Annu. Rev. Entomol. 58, 393–412. https://doi.org/10.1146/annurev-ento-120811-153628

Coon, M.J., 2005. CYTOCHROME P450: Nature's Most Versatile Biological Catalyst. Annu. Rev. Pharmacol. Toxicol. 45, 1–25. https://doi.org/10.1146/annurev.pharmtox.45.120403.100030

Cuamba, N., Morgan, J.C., Irving, H., Steven, A., Wondji, C.S., 2010. High Level of Pyrethroid Resistance in an *Anopheles funestus* Population of the Chokwe District in Mozambique. PLOS ONE 5, e11010. https://doi.org/10.1371/journal.pone.0011010

Duangkaew, P., Pethuan, S., Kaewpa, D., Boonsuepsakul, S., Sarapusit, S., Rongnoparut, P., 2011. Characterization of mosquito CYP6P7 and CYP6AA3: Differences in substrate preference and kinetic properties. Arch. Insect Biochem. Physiol. 76, 236–248. https://doi.org/10.1002/arch.20413

Dunkov, B.C., Guzov, V.M., Mocelin, G., Shotkoski, F., Brun, A., Amichot, M., Ffrench-Constant, R.H., Feyereisen, R., 1997. The *Drosophila* Cytochrome P450 Gene Cyp6a2: Structure, Localization, Heterologous Expression, and Induction by Phenobarbital. DNA Cell Biol. 16, 1345–1356. https://doi.org/10.1089/dna.1997.16.1345

Esteves, F., Rueff, J., Kranendonk, M., 2021. The Central Role of Cytochrome P450 in Xenobiotic Metabolism—A Brief Review on a Fascinating Enzyme Family. J. Xenobiotics 11, 94–114. https://doi.org/10.3390/jox11030007

Feyereisen, R., 2012. 8 - Insect CYP Genes and P450 Enzymes, in: Gilbert, L.I. (Ed.), Insect Molecular Biology and Biochemistry. Academic Press, San Diego, pp. 236–316. https://doi.org/10.1016/B978-0-12-384747-8.10008-X

Finn, R.D., McLaughlin, L.A., Hughes, C., Song, C., Henderson, C.J., Roland Wolf, C., 2011. Cytochrome b5 null mouse: a new model for studying inherited skin disorders and the role of unsaturated fatty acids in normal homeostasis. Transgenic Res. 20, 491–502. https://doi.org/10.1007/s11248-010-9426-1

Finn, R.D., McLaughlin, L.A., Ronseaux, S., Rosewell, I., Houston, J.B., Henderson, C.J., Wolf, C.R., 2008. Defining the in Vivo Role for Cytochrome b5 in Cytochrome P450 Function through the Conditional Hepatic Deletion of Microsomal Cytochrome b5. J. Biol. Chem. 283, 31385–31393. https://doi.org/10.1074/jbc.M803496200

Gutierrez, A., Grunau, A., Paine, M., Munro, A.W., Wolf, C.R., Roberts, G.C.K., Scrutton, N.S., 2003. Electron transfer in human cytochrome P450 reductase. Biochem. Soc. Trans. 31, 497–501. https://doi.org/10.1042/bst0310497

Guzov, V.M., Houston, H.L., Murataliev, M.B., Walker, F.A., Feyereisen, R., 1996. Molecular Cloning, Overexpression in *Escherichia coli*, Structural and Functional Characterization of House Fly Cytochrome b5. J. Biol. Chem. 271, 26637–26645. https://doi.org/10.1074/jbc.271.43.26637

Haas, J., Nauen, R., 2021. Pesticide risk assessment at the molecular level using honey bee cytochrome P450 enzymes: A complementary approach. Environ. Int. 147, 106372. https://doi.org/10.1016/j.envint.2020.106372

Hemingway, J., Ranson, H., 2000. Inseciticide Resistance in Insect Vectors of Human Diseases. Annu. Rev. Entomol. 45, 371–391.

Henderson, C.J., McLaughlin, L.A., Scheer, N., Stanley, L.A., Wolf, C.R., 2015. Cytochrome b5 Is a Major Determinant of Human Cytochrome P450 CYP2D6 and CYP3A4 Activity In Vivo. Mol. Pharmacol. 87, 733–739. https://doi.org/10.1124/mol.114.097394

Hiratsuka, M., 2012. *In Vitro* Assessment of the Allelic Variants of Cytochrome P450. Drug Metab. Pharmacokinet. 27, 68–84. https://doi.org/10.2133/dmpk.DMPK-11-RV-090

Hunt, R.H., Brooke, B.D., Pillay, C., Koekemoer, L.L., Coetzee, M., 2005. Laboratory selection for and characteristics of pyrethroid resistance in the malaria vector *Anopheles funestus*. Med. Vet. Entomol. 19, 271–275. https://doi.org/10.1111/j.1365-2915.2005.00574.x

Ibrahim, S.S., Amvongo-Adjia, N., Wondji, M.J., Irving, H., Riveron, J.M., Wondji, C.S., 2018. Pyrethroid resistance in the major malaria vector *Anopheles funestus* is exacerbated by overexpression and overactivity of the P450 CYP6AA1 across Africa. Genes 9, 1–17. https://doi.org/10.3390/genes9030140

Ibrahim, S.S., Ndula, M., Riveron, J.M., Irving, H., Wondji, C.S., 2016a. The P450 CYP6Z1 confers carbamate/pyrethroid cross-resistance in a major African malaria vector beside a novel carbamate-insensitive N485I acetylcholinesterase-1 mutation. Mol. Ecol. 25, 3436–3452. https://doi.org/10.1111/mec.13673

Ibrahim, S.S., Riveron, J.M., Bibby, J., Irving, H., Yunta, C., Paine, M.J.I., Wondji, C.S., 2015. Allelic Variation of Cytochrome P450s Drives Resistance to Bednet Insecticides in a Major Malaria Vector. PLOS Genet. 11, e1005618. https://doi.org/10.1371/journal.pgen.1005618

Ibrahim, S.S., Riveron, J.M., Stott, R., Irving, H., Wondji, C.S., 2016b. The cytochrome P450 CYP6P4 is responsible for the high pyrethroid resistance in knockdown resistance-free *Anopheles arabiensis*. Insect Biochem. Mol. Biol. 68, 23–32. https://doi.org/10.1016/j.ibmb.2015.10.015

Ismail, H.M., O'Neill, P.M., Hong, D.W., Finn, R.D., Henderson, C.J., Wright, A.T., Cravatt, B.F., Hemingway, J., Paine, M.J.I., 2013. Pyrethroid activity-based probes for profiling cytochrome P450 activities associated with insecticide interactions. Proc. Natl. Acad. Sci. 110, 19766–19771. https://doi.org/10.1073/pnas.1320185110

Kasai, S., Komagata, O., Itokawa, K., Shono, T., Ng, L.C., Kobayashi, M., Tomita, T., 2014. Mechanisms of Pyrethroid Resistance in the Dengue Mosquito Vector, Aedes aegypti: Target Site Insensitivity, Penetration, and Metabolism. PLoS Negl. Trop. Dis. 8, e2948. https://doi.org/10.1371/journal.pntd.0002948

Kumondai, M., Hishinuma, E., Gutiérrez Rico, E.M., Ito, A., Nakanishi, Y., Saigusa, D., Hirasawa, N., Hiratsuka, M., 2020. Heterologous expression of high-activity cytochrome P450 in mammalian cells. Sci. Rep. 10, 14193. https://doi.org/10.1038/s41598-020-71035-5

Lees, R.S., Ismail, H.M., Logan, R.A.E., Malone, D., Davies, R., Anthousi, A., Adolfi, A., Lycett, G.J., Paine, M.J.I., 2020. New insecticide screening platforms indicate that Mitochondrial

Complex I inhibitors are susceptible to cross-resistance by mosquito P450s that metabolise pyrethroids. Sci. Rep. 10, 16232. https://doi.org/10.1038/s41598-020-73267-x

Liu, J., Zhang, X., Wu, H., Ma, W., Zhu, W., Zhu, K.-Y., Ma, E., Zhang, J., 2020. Characteristics and roles of cytochrome b5 in cytochrome P450-mediated oxidative reactions in *Locusta migratoria*. J. Integr. Agric. 19, 1512–1521. https://doi.org/10.1016/S2095-3119(19)62827-3

Liu, N., Scott, J.G., 1996. Genetic analysis of factors controlling high-level expression of cytochrome P450, CYP6D1, cytochrome b5, P450 reductase, and monooxygenase activities in LPR house flies, *Musca domestica*. Biochem. Genet. 34, 133–148. https://doi.org/10.1007/BF02396246

Lu, K., Song, Y., Zeng, R., 2021. The role of cytochrome P450-mediated detoxification in insect adaptation to xenobiotics. Curr. Opin. Insect Sci. 43, 103–107. https://doi.org/10.1016/j.cois.2020.11.004

Lycett, G.J., McLaughlin, L.A., Ranson, H., Hemingway, J., Kafatos, F.C., Loukeris, T.G., Paine, M.J.I., 2006. *Anopheles gambiae* P450 reductase is highly expressed in oenocytes and in vivo knockdown increases permethrin susceptibility. Insect Mol. Biol. 15, 321–327. https://doi.org/10.1111/j.1365-2583.2006.00647.x

Manjon, C., Troczka, B.J., Zaworra, M., Beadle, K., Randall, E., Hertlein, G., Singh, K.S., Zimmer, C.T., Homem, R.A., Lueke, B., Reid, R., Kor, L., Kohler, M., Benting, J., Williamson, M.S., Davies, T.G.E., Field, L.M., Bass, C., Nauen, R., 2018. Unravelling the Molecular Determinants of Bee Sensitivity to Neonicotinoid Insecticides. Curr. Biol. 28, 1137-1143.e5. https://doi.org/10.1016/j.cub.2018.02.045

Matambo, T.S., Paine, M.J.I., Coetzee, M., Koekemoer, L.L., 2010. Sequence characterization of cytochrome P450 CYP6P9 in pyrethroid resistant and susceptible *Anopheles funestus* (Diptera: Culicidae). Genet. Mol. Res. 9, 554–564. https://doi.org/10.4238/vol9-1gmr719

Mclaughlin, L.A., Niazi, U., Bibby, J., David, J.-P., Vontas, J., Hemingway, J., Ranson, H., Sutcliffe, M.J., Paine, M.J.I., 2008. Characterization of inhibitors and substrates of *Anopheles gambiae* CYP6Z2. Insect Mol. Biol. 17, 125–135. https://doi.org/10.1111/j.1365-2583.2007.00788.x

McLaughlin, L.A., Ronseaux, S., Finn, R.D., Henderson, C.J., Roland Wolf, C., 2010. Deletion of Microsomal Cytochrome b_5 Profoundly Affects Hepatic and Extrahepatic Drug Metabolism. Mol. Pharmacol. 78, 269–278. https://doi.org/10.1124/mol.110.064246

Moural, T.W., Ban, L., Hernandez, J.A., Wu, M., Zhao, C., Palli, S.R., Alyokhin, A., Zhu, F., 2020. Silencing NADPH-Cytochrome P450 reductase affects imidacloprid susceptibility, fecundity, and embryonic development in *Leptinotarsa decemlineata*. https://doi.org/10.1101/2020.09.29.318634

Müller, P., Warr, E., Stevenson, B.J., Pignatelli, P.M., Morgan, J.C., Steven, A., Yawson, A.E., Mitchell, S.N., Ranson, H., Hemingway, J., Paine, M.J.I., Donnelly, M.J., 2008. Field-Caught Permethrin-Resistant *Anopheles gambiae* Overexpress CYP6P3, a P450 That Metabolises Pyrethroids. PLOS Genet. 4, e1000286. https://doi.org/10.1371/journal.pgen.1000286

Murataliev, M.B., Guzov, V.M., Walker, F.A., Feyereisen, R., 2008. P450 reductase and cytochrome b5 interactions with cytochrome P450: Effects on house fly CYP6A1 catalysis. Insect Biochem. Mol. Biol. 38, 1008–1015. https://doi.org/10.1016/j.ibmb.2008.08.007

Nauen, R., Bass, C., Feyereisen, R., Vontas, J., 2022. The Role of Cytochrome P450s in Insect Toxicology and Resistance. Annu. Rev. Entomol. 67, null. https://doi.org/10.1146/annurev-ento-070621-061328

Nauen, R., Zimmer, C.T., Vontas, J., 2021. Heterologous expression of insect P450 enzymes that metabolize xenobiotics. Curr. Opin. Insect Sci. 43, 78–84. https://doi.org/10.1016/j.cois.2020.10.011

Nikou, D., Ranson, H., Hemingway, J., 2003. An adult-specific CYP6 P450 gene is overexpressed in a pyrethroid-resistant strain of the malaria vector, *Anopheles gambiae*. Gene 318, 91–102. https://doi.org/10.1016/S0378-1119(03)00763-7

Nolden, M., Brockmann, A., Ebbinghaus-Kintscher, U., Brueggen, K.-U., Horstmann, S., Paine, M.J.I., Nauen, R., 2021. Towards understanding transfluthrin efficacy in a pyrethroid-resistant strain of the malaria vector *Anopheles funestus* with special reference to cytochrome P450-mediated detoxification. Curr. Res. Parasitol. Vector-Borne Dis. 1, 100041. https://doi.org/10.1016/j.crpvbd.2021.100041

Omura, T., Sato, R., 1964. The Carbon Monoxide-binding Pigment of Liver Microsomes: I. EVIDENCE FOR ITS HEMOPROTEIN NATURE. J. Biol. Chem. 239, 2370–2378. https://doi.org/10.1016/S0021-9258(20)82244-3

Porter, T.D., 2012. New insights into the role of cytochrome P450 reductase (POR) in microsomal redox biology. Acta Pharm. Sin. B, Drug Metabolism and Transport 2, 102–106. https://doi.org/10.1016/j.apsb.2012.02.002

Riga, M., Ilias, A., Vontas, J., Douris, V., 2020. Co-Expression of a Homologous Cytochrome P450 Reductase Is Required for In Vivo Validation of the *Tetranychus urticae* CYP392A16-Based Abamectin Resistance in Drosophila. Insects 11, 829. https://doi.org/10.3390/insects11120829

Riveron, J.M., Ibrahim, S.S., Chanda, E., Mzilahowa, T., Cuamba, N., Irving, H., Barnes, K.G., Ndula, M., Wondji, C.S., 2014. The highly polymorphic CYP6M7 cytochrome P450 gene partners with the directionally selected CYP6P9a and CYP6P9b genes to expand the pyrethroid resistance front in the malaria vector *Anopheles funestus* in Africa. BMC Genomics 15, 817. https://doi.org/10.1186/1471-2164-15-817

Riveron, J.M., Ibrahim, S.S., Mulamba, C., Djouaka, R., Irving, H., Wondji, M.J., Ishak, I.H., Wondji, C.S., 2017. Genome-wide transcription and functional analyses reveal heterogeneous molecular mechanisms driving pyrethroids resistance in the major malaria vector *Anopheles funestus* across Africa. G3 Genes Genomes Genet. 7, 1819–1832. https://doi.org/10.1534/g3.117.040147

Riveron, J.M., Irving, H., Ndula, M., Barnes, K.G., Ibrahim, S.S., Paine, M.J.I., Wondji, C.S., 2013. Directionally selected cytochrome P450 alleles are driving the spread of pyrethroid

resistance in the major malaria vector *Anopheles funestus.* Proc. Natl. Acad. Sci. 110, 252–257. https://doi.org/10.1073/pnas.1216705110

Schenkman, J.B., Jansson, I., 2003. The many roles of cytochrome b5. Pharmacol. Ther. 97, 139–152. https://doi.org/10.1016/S0163-7258(02)00327-3

Schroer, K., Kittelmann, M., Lütz, S., 2010. Recombinant human cytochrome P450 monooxygenases for drug metabolite synthesis. Biotechnol. Bioeng. 106, 699–706. https://doi.org/10.1002/bit.22775

Schuler, M.A., 2011. P450s in plant–insect interactions. Biochim. Biophys. Acta BBA - Proteins Proteomics, Cytochrome P450: Structure, biodiversity and potential for application 1814, 36–45. https://doi.org/10.1016/j.bbapap.2010.09.012

Shen, A.L., O'Leary, K.A., Kasper, C.B., 2002. Association of Multiple Developmental Defects and Embryonic Lethality with Loss of Microsomal NADPH-Cytochrome P450 Oxidoreductase. J. Biol. Chem. 277, 6536–6541. https://doi.org/10.1074/jbc.M111408200

Shi, L., Zhang, J., Shen, G., Xu, Z., Wei, P., Zhang, Y., Xu, Q., He, L., 2015. Silencing NADPH-cytochrome P450 reductase results in reduced acaricide resistance in *Tetranychus cinnabarinus* (Boisduval). Sci. Rep. 5, 15581. https://doi.org/10.1038/srep15581

Soderlund, D.M., 2020. Neurotoxicology of pyrethroid insecticides, in: Advances in Neurotoxicology. Elsevier, pp. 113–165. https://doi.org/10.1016/bs.ant.2019.11.002

Stevenson, B.J., Bibby, J., Pignatelli, P., Muangnoicharoen, S., O'Neill, P.M., Lian, L.-Y., Müller, P., Nikou, D., Steven, A., Hemingway, J., Sutcliffe, M.J., Paine, M.J.I., 2011. Cytochrome P450 6M2 from the malaria vector *Anopheles gambiae* metabolizes pyrethroids: Sequential metabolism of deltamethrin revealed. Insect Biochem. Mol. Biol., Special Issue: Toxicology and Resistance 41, 492–502. https://doi.org/10.1016/j.ibmb.2011.02.003

Stevenson, B.J., Pignatelli, P., Nikou, D., Paine, M.J.I., 2012. Pinpointing P450s Associated with Pyrethroid Metabolism in the Dengue Vector, *Aedes aegypti*: Developing New Tools to Combat Insecticide Resistance. PLoS Negl. Trop. Dis. 6, e1595. https://doi.org/10.1371/journal.pntd.0001595

Stiborová, M., Indra, R., Moserová, M., Bořek-Dohalská, L., Hodek, P., Frei, E., Kopka, K., Schmeiser, H.H., Arlt, V.M., 2017. Comparison of human cytochrome P450 1A1-catalysed oxidation of benzo[a]pyrene in prokaryotic and eukaryotic expression systems. Monatshefte Für Chem. - Chem. Mon. 148, 1959–1969. https://doi.org/10.1007/s00706-017-2002-0

Valles, S.M., Yu, S.J., 1996. Detection and Biochemical Characterization of Insecticide Resistance in the German Cockroach (Dictyoptera: Blattellidae). J. Econ. Entomol. 89, 21–26. https://doi.org/10.1093/jee/89.1.21

Vontas, J., Katsavou, E., Mavridis, K., 2020. Cytochrome P450-based metabolic insecticide resistance in Anopheles and Aedes mosquito vectors: Muddying the waters. Pestic. Biochem. Physiol. 170, 104666. https://doi.org/10.1016/j.pestbp.2020.104666

Wamba, A.N.R., Ibrahim, S.S., Kusimo, M.O., Muhammad, A., Mugenzi, L.M.J., Irving, H., Wondji, M.J., Hearn, J., Bigoga, J.D., Wondji, C.S., 2021. The cytochrome P450 CYP325A is a major driver of pyrethroid resistance in the major malaria vector *Anopheles funestus* in Central Africa. Insect Biochem. Mol. Biol. 138, 103647. https://doi.org/10.1016/j.ibmb.2021.103647

Weedall, G.D., Mugenzi, L.M.J., Menze, B.D., Tchouakui, M., Ibrahim, S.S., Amvongo-Adjia, N., Irving, H., Wondji, M.J., Tchoupo, M., Djouaka, R., Riveron, J.M., Wondji, C.S., 2019. A cytochrome P450 allele confers pyrethroid resistance on a major African malaria vector, reducing insecticide-treated bednet efficacy. Sci. Transl. Med. 11, eaat7386. https://doi.org/10.1126/scitranslmed.aat7386

WHO, 2018. Global report on insecticide resistance in malaria vectors: 2010-2016.

Wondji, C.S., Irving, H., Morgan, J., Lobo, N.F., Collins, F.H., Hunt, R.H., Coetzee, M., Hemingway, J., Ranson, H., 2009. Two duplicated P450 genes are associated with pyrethroid resistance in *Anopheles funestus*, a major malaria vector. Genome Res. 19, 452–459. https://doi.org/10.1101/gr.087916.108

Yamazaki, H., Nakamura, M., Komatsu, T., Ohyama, K., Hatanaka, N., Asahi, S., Shimada, N., Guengerich, F.P., Shimada, T., Nakajima, M., Yokoi, T., 2002. Roles of NADPH-P450 Reductase and Apo- and Holo-Cytochrome b5 on Xenobiotic Oxidations Catalyzed by 12 Recombinant Human Cytochrome P450s Expressed in Membranes of *Escherichia coli*. Protein Expr. Purif. 24, 329–337. https://doi.org/10.1006/prep.2001.1578

Yunta, C., Grisales, N., Nász, S., Hemmings, K., Pignatelli, P., Voice, M., Ranson, H., Paine, M.J.I., 2016. Pyriproxyfen is metabolized by P450s associated with pyrethroid resistance in *An. gambiae*. Insect Biochem. Mol. Biol. 78, 50–57. https://doi.org/10.1016/j.ibmb.2016.09.001

Yunta, C., Hemmings, K., Stevenson, B., Koekemoer, L.L., Matambo, T., Pignatelli, P., Voice, M., Nász, S., Paine, M.J.I., 2019. Cross-resistance profiles of malaria mosquito P450s associated with pyrethroid resistance against WHO insecticides. Pestic. Biochem. Physiol., Special issue: 2018 INSTAR Summit 161, 61–67. https://doi.org/10.1016/j.pestbp.2019.06.007

Zhang, H., Hamdane, D., Im, S.-C., Waskell, L., 2008. Cytochrome b5 Inhibits Electron Transfer from NADPH-Cytochrome P450 Reductase to Ferric Cytochrome P450 2B4. J. Biol. Chem. 283, 5217–5225. https://doi.org/10.1074/jbc.M709094200

Zhang, L., Kasai, S., Shono, T., 1998. In vitro metabolism of pyriproxyfen by microsomes from susceptible and resistant housefly larvae. Arch. Insect Biochem. Physiol. 37, 215–224. https://doi.org/10.1002/(SICI)1520-6327(1998)37:3<215::AID-ARCH4>3.0.CO;2-R

Zhang, M., Scott, J.G., 1996. Cytochrome b5Is Essential for Cytochrome P450 6D1-Mediated Cypermethrin Resistance in LPR House Flies. Pestic. Biochem. Physiol. 55, 150–156. https://doi.org/10.1006/pest.1996.0044

Zhang, M., Scott, J.G., 1994. Cytochrome b5 involvement in cytochrome P450 monooxygenase activities in house fly microsomes. Arch. Insect Biochem. Physiol. 27, 205–216. https://doi.org/10.1002/arch.940270306

Zhu, F., Sams, S., Moural, T., Haynes, K.F., Potter, M.F., Palli, S.R., 2012. RNA Interference of NADPH-Cytochrome P450 Reductase Results in Reduced Insecticide Resistance in the Bed Bug, *Cimex lectularius*. PLOS ONE 7, e31037. https://doi.org/10.1371/journal.pone.0031037

Zimmer, C.T., Garrood, W.T., Singh, K.S., Randall, E., Lueke, B., Gutbrod, O., Matthiesen, S., Kohler, M., Nauen, R., Davies, T.G.E., Bass, C., 2018. Neofunctionalization of Duplicated P450 Genes Drives the Evolution of Insecticide Resistance in the Brown Planthopper. Curr. Biol. 28, 268-274.e5. https://doi.org/10.1016/j.cub.2017.11.060

3.5. Supplements (chapter 3)

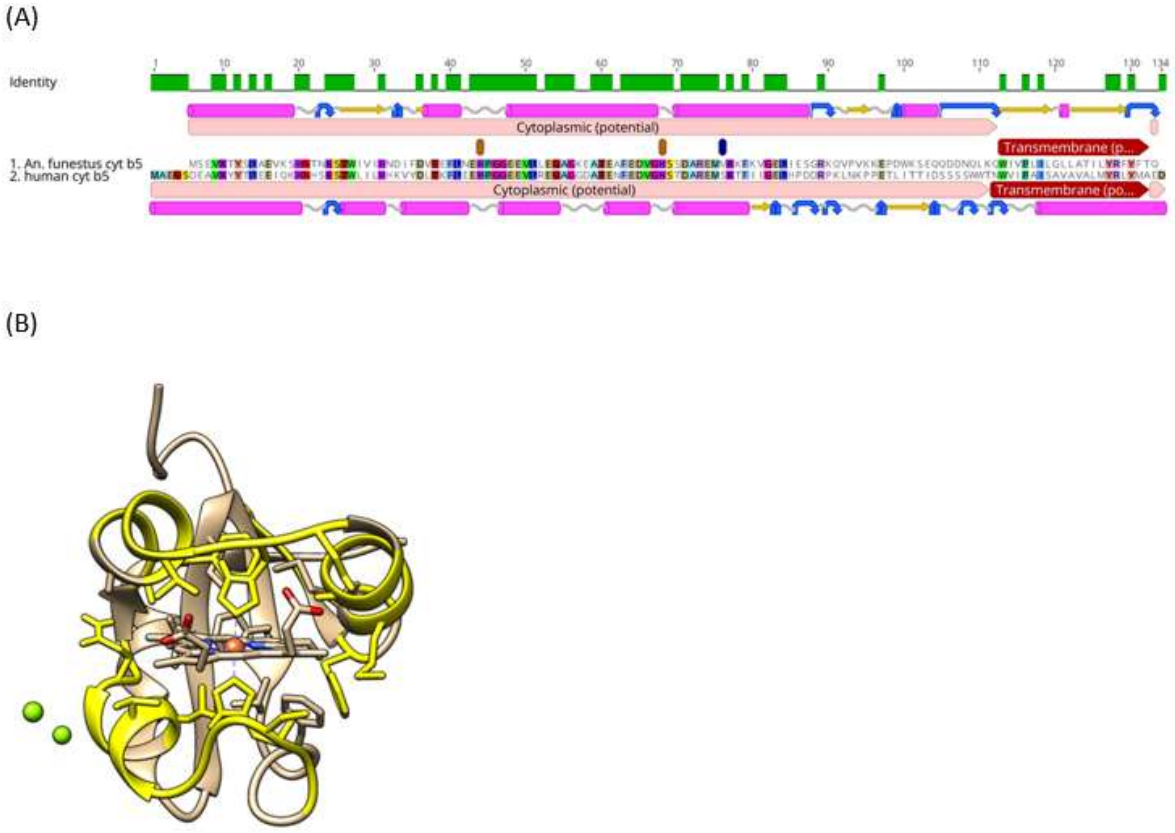

Figure S1. (A) Amino acid sequence alignment of *An. funestus* (EF 035450.1) and human cytochrome b5 (NP 683725.1) showing 44.5 % identity. Brown dots mark heme-ligand residues histidine 39 and histidine 63, and the blue spot indicates residue 71, which is typically serine in mammals. (B) Homology model of *An. funestus* CYB5 based on house fly CYB5 (PDB 2IBJ). Sequence identities between human cytochrome b5 and *An. funestus* cytochrome b5 are highlighted in yellow. Modelling was performed using UCSF Chimera 1.15.

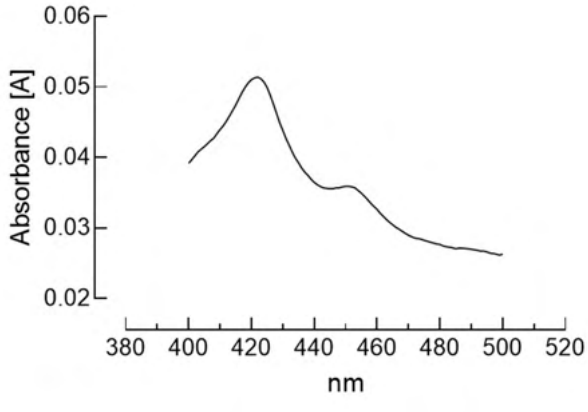

Figure S2. Example of a CO difference spectrum of microsomal membranes containing CYP6P9a recombinantly expressed in High-5 cells. The respective preparation depleted deltamethrin by >50% within 60min as shown in figure 4 of the main text, suggesting the presence of functional enzyme as indicated by the shoulder at 450nm.

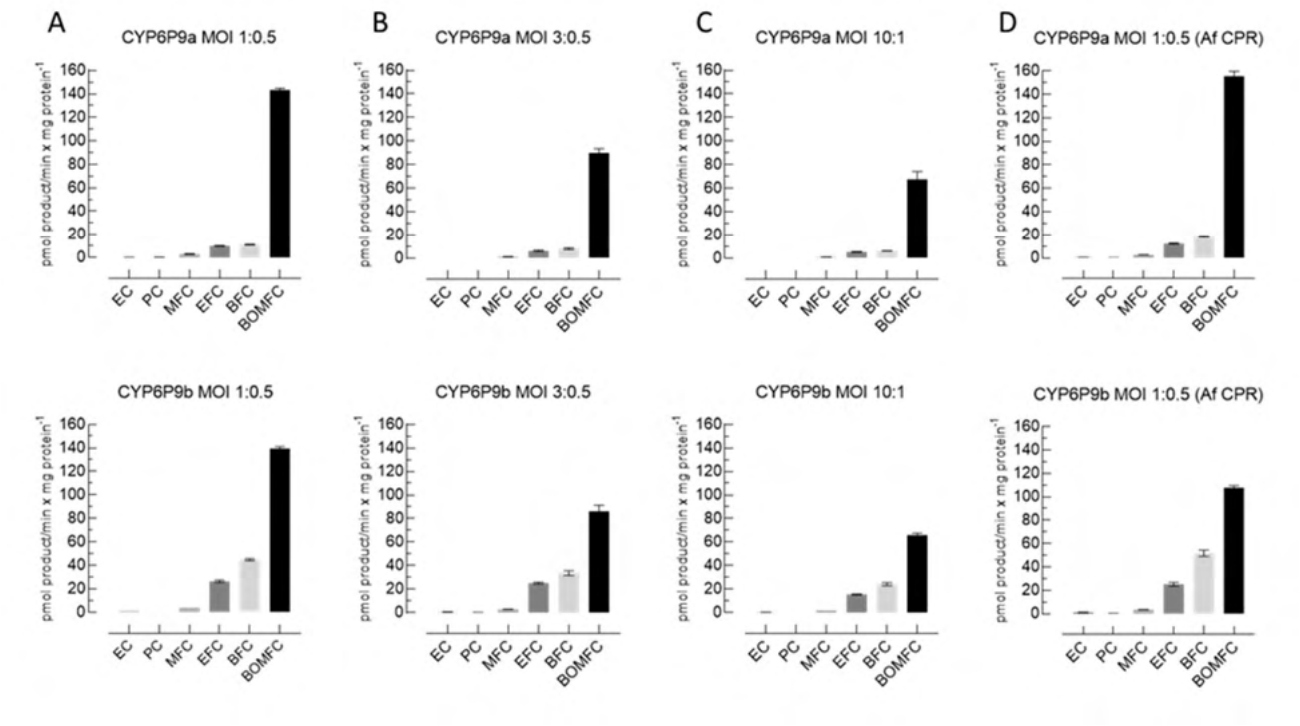

Figure S3. Coumarin substrate profiling utilizing different MOI (multiplicity of infection) ratios for CYP6P9a and CYP6P9b co-expressed with (A-C) *An. gambiae* CPR, and (D) *An. funestus* CPR. The MOI ratio is stated as P450:CPR. The resulting fluorescent products were 7-hydroxy-coumarin (EC, PC) or 7-hydroxy-4-(trifluoromethyl)coumarin (MFC, EFC, BFC, BOMFC). Data are mean values ± SD (n=4).

Table S1. Primer sequences and GenBank (Vector Base ID) numbers for target and reference genes used throughout the study.

Gene name	Forward 5' to 3'	Reverse 5' to 3'	Amplicon (bp)	Vector Base #	Gen Bank Acc #
Ribosomal Protein S7	GTGTTCGGTTCCAAGGTGAT	TCCGAGTTCATTTCCAGCTC	111	AFUN007153	EF450776.1
Actin 5c	TTAAACCCAAAAGCCAATCG	ACCGGATGCATACAGTGACA	98	AFUN006819-RA	
b5	AACTGATCGAATCCGGACGC	ACCGATAGAGGATGGTTGCG	138		EF035450.1
Af CPR	AGTTCCTGCGGTTCATCTCG	ACGTGATCGATCGGTGGATG	133		EF152578.1
For recombinant expression only					
CYP6P9a				AFUN015792	KR866022.1
CYP6P9b				AFUN015889	KR866046.1
Ag CPR					AY183375.1

Table S2. Fold-change of metabolic conversion of different 4-trifluoromethyl-coumarin substrates by recombinantly expressed *An. funestus* CYP6P9a and CYP6P9b co-expressed with *An. funestus* cytochrome P450 reductase (Af CPR) supplemented with *An. funestus* cytochrome b5 (co-expressed CYB5) or 0.8 µM human cytochrome b5 (exogenous CYB5) in comparison to recombinantly expressed CYP6P9a and CYP6P9b co-expressed with P450-reductase of *An. gambiae* (Ag CPR). Abbreviations: MFC, 7-methoxy-4-trifluoromethylcoumarin; EFC, 7-Ethoxy-4-trifluoromethylcoumarin; BFC, 7-benzyloxy-4-trifluoromethylcoumarin; BOMFC, 7-benzyloxymethoxy-4-trifluoromethylcoumarin.

CYP6P9a +	BOMFC			MFC			EFC			BFC		
	Mean	CI95[a] (LL-UL)		Mean	CI95 (LL-UL)		Mean	CI95 (LL-UL)		Mean	CI95 (LL-UL)	
Ag CPR	**1**			**1**			**1**			**1**		
Af CPR	**1.08**	1.04	1.13	**0.928**	0.860	1	**1.25**	1.17	1.33	**1.69**	1.61	1.77
Af CPR (co-expressed CYB5)	**1.82**	1.75	1.88	**2.83**	2.66	3	**4.64**	4.38	4.91	**4.22**	3.16	5.28
Af CPR (exogenous CYB5)	**2.97**	2.79	3.16	**1.92**	1.54	2.29	**3.01**	2.88	3.15	**5.91**	5.52	6.31

CYP6P9b +	BOMFC			MFC			EFC			BFC		
	Mean	CI95 (LL-UL)		Mean	CI95 (LL-UL)		Mean	CI95 (LL-UL)		Mean	CI95 (LL-UL)	
Ag CPR	**1**			**1**			**1**			**1**		
Af CPR	**0.772**	0.750	0.794	**0.923**	0.840	1.01	**0.955**	0.859	1.05	**1.15**	1.06	1.24
Af CPR (co-expressed CYB5)	**1.84**	1.77	1.90	**2.89**	2.72	3.07	**4.43**	4.02	4.84	**3.83**	3.60	4.06
Af CPR (exogenous CYB5)	**3.24**	3	3.47	**1.91**	1.63	2.19	**1.87**	1.79	1.95	**3.04**	2.97	3.11

[a] CI95 (LL-UL): Confidence Interval 95% (lower limit – upper limit)

4. Chapter 4. Sequential phase I metabolism of pyrethroids by duplicated CYP6P9 variants results in the loss of the terminal benzene moiety and determines resistance in the malaria mosquito *Anopheles funestus*

Melanie Nolden [a, b], Mark J.I. Paine [b,*], Ralf Nauen [a,*]

[a] *Bayer AG, Crop Science Division, Alfred Nobel Str. 50, D-40789 Monheim am Rhein, Germany*

[b] *Department of Vector Biology, Liverpool School of Tropical Medicine, Pembroke Place, Liverpool L3 5QA, United Kingdom*

[*] Corresponding authors

Ralf Nauen, ralf.nauen@bayer.com

Mark Paine, Mark.Paine@lstmed.ac.uk

Abstract

Pyrethroid resistance in *Anopheles funestus* is threatening the eradication of malaria. One of the major drivers of pyrethroid resistance in *An. funestus* are cytochrome P450 monooxygenases CYP6P9a and CYP6P9b, which are found upregulated in resistant *An. funestus* populations from Sub-Saharan Africa and are known to metabolise pyrethroids. Here, we have functionally expressed CYP6P9a and CYP6P9b variants and investigated their interactions with azole-fungicides and pyrethroids. Some azole fungicides such as prochloraz inhibited CYP6P9a and CYP6P9b at nanomolar concentrations, whereas pyrethroids were weak inhibitors (> 100 µM). Amino acid sequence comparisons suggested that a valine to isoleucine substitution at position 310 in the active site cavity of CYP6P9a and CYP6P9b, respectively, might affect substrate binding and metabolism. We therefore swapped the residues by site directed mutagenesis to produce CYP6P9a^{I310V} and CYP6P9b^{V310I}. CYP6P9b^{V310I} produced stronger metabolic activity towards coumarin substrates and pyrethroids, particularly permethrin. 'This V310I difference between paralogs is also observed as a polymorphism identified in a pyrethroid resistant field population of *An. funestus* in Benin. Additionally, we found the first metabolite of permethrin and deltamethrin after hydroxylation, 4'OH permethrin and 4'OH deltamethrin, were also suitable substrates for CYP6P9-variants, and were depleted by both enzymes to a higher extent than as their respective parent compounds (approximately 20 % more active). Further, we found that both metabolites were toxic against *An. funestus* FANG (pyrethroid susceptible) but not towards FUMOZ-R (pyrethroid resistant) mosquitoes, the latter suggesting detoxification by overexpressed CYP6P9a and CYP6P9b. We confirmed by mass-spectrometric analysis that CYP6P9a and CYP6P9b are capable of cleaving phenoxybenzyl-ethers in type I pyrethroid permethrin and type II pyrethroid deltamethrin and that both enzymes preferentially metabolise trans-permethrin. This provides new insight into the metabolism of pyrethroids and a greater understanding of the molecular mechanisms of pyrethroid resistance in *An. funestus*.

Keywords: Cytochrome P450, vector control, pyrethroid, insecticide, resistance, Anopheles

4.1. Introduction

In 2020 Malaria caused 627 000 deaths globally, with the large majority (602 000 deaths) occurring in Africa (WHO, 2021). The use of interventions such as insecticide treated bednets (ITN) and indoor residual sprays (IRS) to control indoor biting mosquitoes was estimated to have been responsible for ~80% of the reduction in Malaria cases from 2000 to 2019 (Bhatt et al., 2015; WHO, 2020). Until recently pyrethroids were the only insecticidal class used in ITN thus driving the rapid spread of pyrethroid resistance in *Anopheles* populations across the African continent (WHO, 2018). Pyrethroid resistance is mainly conferred by an altered target, the voltage gated sodium channel (VGSC), and/or upregulated P450 enzymes, which are responsible for phase I xenobiotic metabolism and clearance (David et al., 2013; Martinez-Torres et al., 1998; Nauen et al., 2022; Ranson et al., 2011)

Pyrethroids are synthetic insecticides derived from the natural compound pyrethrin. They are designated as type I and type II pyrethroids based on the respective absence or presence of an *alpha*-cyano group, which enhances the toxicity of the insecticide (Soderlund, 2020). Permethrin and deltamethrin, type I and II pyrethroids respectively, are amongst the most widely used insecticides for vector control applications. Structurally similar, they share a phenoxybenzyl moiety and a cyclopropane ring. It is widely accepted that the 4'para position of the phenoxybenzyl structure is the preferred site of oxidation by insect P450s (Ruzo et al., 1978; Stevenson et al., 2011; Nolden et al., 2022; Zimmer et al., 2014), along with other routes of metabolism including hydroxylation of the gem-dimethyl site or ester-cleavage (Casida et al., 1983; Shono et al., 1979). Furthermore, analysis of deltamethrin metabolism by *Anopheles gambiae* CYP6M2 has revealed that sequential breakdown of the 4'-hydroxy deltamethrin primary metabolite can occur (Stevenson et al, 2011) as well as ether-cleavage of the diphenyl moiety. To date CYP6M2 is the only insect P450 enzyme in which this has been shown (Feyereisen, 2019). Permethrin is composed of four different isomers (R-cis, S-cis, R-trans and S-trans) although their individual interactions with P450 enzymes are not clear. Structurally different pyrethroids, such as etofenprox (non-ester-pyrethroid), bifenthrin or transfluthrin are also used as insecticides, where fluorination of P450 sites of oxidation can limit metabolism and reduce cross-resistance (Moyes et al., 2021; Zimmer and Nauen, 2011).

Anopheles funestus s.s. is a major vector for the transmission of malaria in Africa. Unlike *An. gambiae* and many other anopheline malaria vectors, knock down resistance (*kdr*) mutations to the voltage gated sodium channel are uncommon (Irving and Wondji, 2017). Instead,

pyrethroid resistance is driven primarily by metabolic mechanisms that are predominantly associated with the upregulation of P450 enzymes (Amenya et al., 2008; Ibrahim et al., 2018, 2016; Riveron et al., 2014, 2013). These include CYP6P9a and CYP6P9b, which are the result of a gene duplication event and often highly expressed in pyrethroid resistant field populations of *An. funestus* as well as the laboratory reference strain FUMOZ-R (Nolden et al., 2021; Wondji et al., 2022) . Since inhibition of P450 activity can revert metabolic resistant mosquitoes to a susceptible phenotype (Brooke et al., 2001), the inclusion of piperonyl butoxide (PBO), a strong P450 inhibitor, is being used in the latest generation of pyrethroid treated bednets to combat pyrethroid resistance (Gleave et al., 2018; Protopopoff et al., 2018). We have recently shown that BOMFC is a highly active fluorescent probe substrate for recombinant CYP6P9a and CYP6P9b (Nolden et al., 2022), and demonstrated that azole fungicides are also efficient inhibitors of P450 activity in microsomal preparations of *An. funestus,* recommending further characterization of their interactions with individual P450s associated with pyrethroid resistance (Nolden et al., 2021).

CYP6P9a and CYP6P9b can metabolise pyrethroids (Riveron et al., 2014, 2013; Yunta et al., 2019), although detailed biochemical characterisation of their interactions with pyrethroid substrates and products of metabolism are lacking. The two P450s are highly similar sharing 94% amino acid sequence identity (Figure S1a). While this suggests a similar substrate profile, even single amino acid changes can have a profound effect on substrate binding, altering substrate specificity and metabolism (Paine et al., 2003). We were therefore interested in comparing the interactions of CYP6P9a and CYP6P9b with pyrethroid insecticides and azole inhibitors and to identify amino acid residues in the active sites of the enzymes that might differentiate substrate binding and metabolism. As a starting point we focussed on I-helix amino acid residue 310, which is close (~10 Å) to the reactive heme iron centre and different between CYP6P9a and CYP6P9b. It is present as an isoleucine residue in CYP6P9a and valine in CYP6P9b (Figure S1b).

In this study, we have compared the enzymatic activity of the recombinantly expressed gene duplicates, *CYP6P9a* and *CYP6P9b* against various substrates. We have also used mass-spectrometry to identify the products of deltamethrin, racemic permethrin (and its *cis*- and *trans*-diastereomers) metabolism by CYP6P9a and CYP6P9b and the mechanism of substrate breakdown. We have carried out site-directed mutagenesis to create two mutants CYP6P9a^{I310V} and CYP6P9b^{V310I} to compare their metabolic activity with CYP6P9a and CYP6P9b

towards permethrin, deltamethrin and fluorescent probe substrates to examine the role of amino acid 310 in CYP6P9a/b substrate metabolism. Our results provide a new understanding of the metabolic fate of common type I and type II pyrethroids in the malaria mosquito *An. funestus* that will aid in the development of new resistance-breaking compounds used in vector control applications.

4.2. Material and Methods

4.2.1. Mosquitoes

An. funestus FANG and FUMOZ-R mosquitoes were reared as recently described by Nolden et al. (2021). In brief: both strains were kept at 27.5 °C ± 0.5 °C, 65 % ± 5 % relative humidity and a photoperiod of 12/12 L:D with 1h dusk/dawn. Adults were kept in rearing cages (46 cm x 33 cm x 20 cm) and five days after hatching the first blood meal (bovine blood, obtained from Elocin Laboratory, Oberhausen, Germany) was provided according to standard protocols (Das et al., 2007).

4.2.2. Chemicals

Deltamethrin (CAS: 52918-63-5), permethrin (CAS: 52645-53-1; 61.3 % trans- and 30.5 % cis permethrin), β-nicotinamide adenine dinucleotide 2'-phosphate (NADPH) reduced tetrasodium salt hydrate (CAS: 2646-71-1 anhydrous, purity ≥93 %), 7-ethoxycoumarin (EC; CAS: 31005-02-4, >99 %), 7-methoxy-4-trifluoromethylcoumarin (MFC; CAS: 575-04-2, ≥99 %), 7-Ethoxy-4-trifluoromethylcoumarin (EFC; CAS: 115453-82-2, ≥98 %) 7-benzyloxy-4-trifluoromethylcoumarin (BFC; CAS: 220001-53-6, ≥ 99 %), 7- hydroxy-coumarin (HC; CAS: 93-35-6, 99 %) 7-hydroxy-4-trifluoromethylcoumarin (HFC; CAS: 575-03-1, 98) were purchased from Sigma Aldrich/Merck (Darmstadt, Germany). Cis-permethrin (CAS: 61949-76-6) and trans-permethrin (CAS: 61949-77-7) were purchased from Dr. Ehrenstorfer (LGC group, Teddington, UK). 7-benzyloxymethoxy-4-trifluoromethylcoumarin (BOMFC; CAS: 277309-33-8; purity 95 %) was synthesized by Enamine (Riga, Latvia). 4'OH permethrin (CAS: 67328-58-9 ≥ 97 %) was synthetized by Aragen (formerly GVK Bio, Hyderabad, India). 7-pentoxycoumarin and 4'OH-deltamethrin (CAS: 66855-89-8) were internally synthetized (Bayer AG, Leverkusen, Germany). All chemicals were of analytical grade unless otherwise stated.

4.2.3. Glazed tile bioassay

To generate dose-response curves of 4'OH-deltamethrin, 4'OH permethrin and cis- and trans-permethrin, *An. funestus* FANG and FUMOZ-R mosquitoes were exposed to a range of different concentrations in a glazed tile assay as recently described by Nolden et al. (2021). Insecticides were dissolved in acetone with a starting concentration of 100 mg/m² and diluted in 1:5 steps to 0.0064 mg/m². Using an Eppendorf pipette 1.125 µl of each concentration was applied onto a glazed tile (15 cm x 15 cm, ceramic, Vitra, Germany). After the evaporation of acetone and mosquito recovery from anaesthetation (1 h), female adults were exposed in triplicate (n = 10) for 30 min to each insecticide concentration and afterwards transferred back to an untreated paper card and kept in Petri dishes overnight. A 10% dextrose solution was provided overnight as a food source. Mortality was scored 24 h post-exposure. Acetone alone served as a control. Control mortality between 5 and 20% was corrected using Abbott's formula (Abbott, 1925), and bioassays exceeding 20% control mortality were considered invalid.

4.2.4. Heterologous expression of CYP6P9a and CYP6P9b

Heterologous baculovirus expression was conducted as previously described by (Nolden et al., 2022). In brief: sequence information of CYP6P9a/b from *An. funestus* and NADPH cytochrome P450 reductase (CPR) from *An. gambiae* (AgCPR) were obtained from GenBank (Table S1) and plasmids were created using GeneArt server (ThermoFisher). As a vector pFastBac1 and as restrictions sites BamHI and HindIII were chosen. Plasmids were transformed into MaxEfficiancyDH10 (Invitrogen, 10361012) competent cells according to manufacturer's instructions. The virus was transfected into Sf9 cells (Gibco, kept in Sf-900-SFM (1X) cell culture medium, containing 25 µg mL^{-1} gentamycin) and titre was determined employing Rapid Titer Kit (Clontech, 631406).

High five cells were kept in Express five medium (SFM (1X), Gibco, 10486-025) containing 18 mM Glutamax (100X, Gibco, 35050-061) and 10 µg mL^{-1} gentamycin (Gibco, 1670-037). Cells were incubated with 0.5 % fetal bovine serum (FBS; Sigma Aldrich, F2442), 0.2 mM delta-aminolevulinic acid (d-ALA; CAS: 5451-09-2, Sigma Aldrich), 0.2 mM Fe III citrate (CAS: 2338-05-8, Sigma Aldrich) and the respective amount of virus. After harvesting, cells were resuspended in buffer (0.1 M K_2HPO4, 1 mM DTT, 1mM EDTA, 200 mM saccharose, pH 7.6). FastPrep device (MP Biomedicals, Irvine, CA, USA) was used for shredding the cells followed

by a 10-minute centrifugation step at 4 °C and 700 x g (Eppendorf). The supernatant was centrifuged for one hour at 100,000 x g and 4 °C (Beckman, rotor: 45TI). The resulting microsomal pellet was resuspended in buffer (0.1 M K_2HPO4, 0.1 mM EDTA, 1 mM DTT, 5 % Glycerol, pH 7.6) and protein amount was determined according to Bradford (Bradford, 1976). Carbon monoxide (CO)-difference spectra were generated according to (Omura and Sato, 1964) in order to calculate K_{cat} values. Mock cells served as controls throughout the study as well as microsomal fractions without NADPH regeneration system.

4.2.5. Computational analysis, modelling and docking experiments

CYP6P9a (AFUN015792-RA) and CYP6P9b (AFUN015889-RA) transcripts show 92.7 % nucleotide identity and translated protein sequences are 94.3 % identical (Geneious alignment, Geneious 10.2.6; Fig S1a). Substrate recognition sites (SRS) were assigned to CYP6P9a and CYP6P9b based on CYP2A1 (*Rattus norvegicus*, GenBank NP_036824.1) according to Gotoh (Gotoh, 1992). To predict and analyse the potential metabolism of probe substrates and pyrethroids, 3D-homology models of CYP6P9a and CYP6P9b based on the crystal structure of human CYP3A4 (PDB: 1TQN) were created. 3D-structures of BOMFC, deltamethrin and permethrin were received from PubChem (https://pubchem.ncbi.nlm.nih.gov/) and transformed into PDB files using Chimera (USCF Chimera, Version 1.15). After performing dock-prep in Chimera, AutoDock Vina (Version 1.1.2) using Chimera software was performed, with a 20 $Å^3$ squared volume around the heme (Oleg and Olson, 2010). Five docking scenarios for each substrate were generated and analysed based on score (binding affinity kcal/mol) and putative sites of metabolic attack.

4.2.6. Site-directed mutagenesis of amino acid residue 310

In CYP6P9a isoleucine 310 is translated by the codon ATC at position 927-929 (transcript), in CYP6P9b valine is translated by GTG at position 927-929. We created two mutants: CYP6P9a I310V ($CYP6P9a^{I310V}$) and CYP6P9b V310I ($CYP6P9b^{V310I}$). Generated pFastBac vectors (as described above) containing either CYP6P9a or CYP6P9b were used for site-directed mutagenesis using a Q5- site-directed mutagenesis Kit following manufacturer's instructions (New England Biolabs, E0554). Specific primers were generated using NEBaseChanger (https://nebasechanger.neb.com/) (Table S1). Twenty-five ng of total plasmid DNA and each primer with a final concentration of 0.5 µM in 25 µL reactions were used. PCR conditions were

as follows: 98 °C for 30 sec, followed by 25 cycles of 98 °C for 10 sec, 66 °C for 30 sec and 72 °C for 3 min and 10 sec. Final extension step was at 72°C for 2 minutes. A kinase, ligase and Dpnl (KLD) treatment containing 1 µl PCR Product, 5 µl KLD Reaction buffer, 10X KLD Enzyme Mix and 3 µl Nuclease-free water was added and incubated at room temperature for 5 minutes. Afterwards 5 µl of KLD mix was added to 5-alpha-competent *E. coli* cells for transformation (New England Biolabs, C2987H) following manufacturer's instructions. Cells were diluted 10- and 40-times and incubated overnight on LB-Agar plates (MP biomedicals, 113002201-CF, capsules, concentration: 40g/L) containing carbenicillin (100 µg/ml, CAS: 4800-94-6). Mini- (3 ml) and Midi (25 ml) preps in LB medium (MP biomedicals, 113002011-CF, capsules, concentration: 25 g/L) containing 100 µg/ml carbenicillin were generated and plasmids were isolated using Qiafilter Plasmid Midi Kit following manufacturer's instructions (Qiagen, 12243, Hilden, Germany). DNA concentrations were photometrically determined using 260/280 ratio (NanoQuant Infinite 200, Tecan, Switzerland) and normalized to 100 ng/µl. To confirm successful mutagenesis, samples were sent for sequencing (TubeSeq Service, Eurofins). Sequencing primers can be found in Table S1. Plasmids containing substituted nucleotides were further processed as described above.

4.2.7. P450 activity assays with fluorinated coumarin probe substrates

P450 enzyme assays were conducted as previously described by Haas and Nauen (2021) with minor changes. Substrate competition kinetics were evaluated using eleven different BOMFC, BFC and EFC concentrations (stock 50 mM in DMSO) between 200 µM and 0.195 µM, diluted in 0.1 M potassium-phosphate buffer (pH 7.6) containing 0.01% zwittergent 3-10 (CAS 15163-36-7, Sigma-Aldrich), a range of pyrethroid concentrations (100, 10, 1 µM final concentration (fc)) and 1 mM NADPH at 20°C ± 1 °C. Enzymes were diluted to 0.16 mg/ml in buffer (0.1 M K_2HPO4, 0.1 mM EDTA, 1 mM DTT, 5 % glycerol pH 7.6), 0.05% bovine serum albumin (BSA), 0.01% zwittergent 3-10 – finally corresponding to 4 µg protein per 25 µl enzyme solution. Twenty-five µl enzyme solution and 25 µl substrate solution were incubated for 1 h in a black 384-well plate and the reaction stopped by adding 50 µl of red-ox mix (25% DMSO, 50 mM Tris–HCl buffer (pH 10), 5 mM glutathione oxidized, and 0.2 U glutathione reductase). Each reaction was replicated four times and the fluorescent product HFC was measured at 405 nm while excited at 510 nm. Substrate saturation kinetics were analyzed using GraphPad Prism

9.0 and were analyzed for competitive, non-competitive, and mixed-type inhibition (assuming Michaelis-Menten kinetics).

4.2.8. Inhibition assays with CYP6P9 variants

IC_{50} analysis was performed as previously described in Nolden et al. (2021) with minor modifications. Assay conditions were optimized for linearity in time and protein amount. Eleven concentrations of inhibitors and pyrethroids (pre-diluted in DMSO in 1:3.3 steps, final DMSO concentration (1 %), except for epoxiconazole (2 %)) to a final assay concentration ranging from 100 µM to 0.000596 µM in 0.1 M potassium-phosphate-buffer (pH 7.6). Microsomal fractions were diluted to a final amount of 4 µg of protein per 100 µL in buffer (0.1 M K_2HPO4, 0.1 mM EDTA, 1 mM DTT, 5 % glycerol pH 7.6) containing 0.01 % zwittergent and 0.05 % BSA. Enzymes were incubated with inhibitors and pyrethroids for 10 minutes at 20 °C ± 1°C. Afterwards 25 µL 20 µM BOMFC solution (10 µM final concentration, the approximate K_m for all variants) containing 0.125 mM (fc) NADPH was added. Each reaction was replicated four times, stopped after 30 minutes by adding stopping solution and evaluated as described above. Inhibition was analyzed using GraphPad Prism 9.0 four-parameter, non-linear regression model. Reactions containing no inhibitor served as controls.

4.2.9. UPLC-MS/MS analysis and pyrethroid metabolite quantification

Metabolism assays were conducted as previously described by Nolden et al. (2022) with minor changes. Deltamethrin and permethrin metabolism and quantification of the respective 4'OH-deltamethrin and 4'OH permethrin were assessed using UPLC-MS/MS analysis. Recombinantly expressed CYP6P9 variants and mutants were co-expressed with *An. gambiae* CPR (P450:CPR at MOI 1:0.5) and diluted to 0.8 mg protein ml^{-1} in buffer (0.1 M K2HPO4, 1 mM DTT, 0.1 mM EDTA, 5 % Glycerol, pH 7.6). Forty µl of recombinant proteins were incubated in 96-deepwell plates (Protein lobind, Eppendorf) in 100 µl reactions with 10 µM deltamethrin, permethrin or the respective 4'OH metabolite (solved in DMSO and further diluted to 100 µM in 0.1 M K_2HPO_4, 0.05 % bovine serum albumin (BSA), pH 7.6) and 50 µl of assay buffer containing NADPH-regeneration system (Promega, V9510). As control, wells without regeneration system and microsomal fractions from a control (mock) virus were included. The reactions were incubated at 450 rpm and 30 °C (Thermomixer, Eppendorf) and stopped with 400 µl ice-cold acetonitrile (100 %) after 90 minutes. Plates were stored at 4°C overnight, centrifuged (3220 x g, 4 °C, 30 minutes, Eppendorf 5810 R) and the resulting

supernatant was transferred into a 1000 mL collection plate (186002481, Waters, Eschborn, Germany).

UPLC-MS/MS chromatography was carried out using an Agilent 1290 Infinity II system with a Waters Acquity BEH C18 (50 x 2.1 mm, 1.7µm) column and eluted with methanol, 2mM ammonium acetate, and water, 2mM ammonium acetate with 1% acetic acid in gradient mode. After positive electrospray ionization, ion transitions were recorded on a Sciex API6500 Qtrap. Ion transition was as followed: for deltamethrin 523 > 281, for 4'OH-deltamethrin 539 > 281, for permethrin 183.051 > 152.200 and for 4'OH-permethrin 424.079 > 199.200. In positive ion mode the peak integrals were calibrated externally against a standard calibration curve. Samples were diluted prior to measurement if needed. Linear ranges were as followed: For deltamethrin: 0.5-500 ng/ml, for 4'OH deltamethrin: 0.3-100 ng/ml, for permethrin: 0.1-120 ng/ml (cis) and 0.05-26 ng/ml (trans) and for 4'OH-permethrin: 0.05-23 ng/ml (cis) and 0.1-27 ng/ml (trans). UPLC-TOF-MS was employed using an Acquity UPLC I-Class system coupled to a cyclic iMS mass spectrophotometer (Waters Corporation, MA, USA) as recently described (Haas et al., 2021). The mass spectrometer operated in positive ion mode for deltamethrin and permethrin and in negative ion mode for the respective 4'OH metabolites with a full scan resolution at 60,000 fwhm (full width at half maximum). Measurements and metabolite searches were conducted with MassLynx and MetaboLynx software (Waters Corporation, MA, USA).

4.3. Results

4.3.1. Inhibition potential of azole fungicides, pyrethroids and PBO towards CYP6P9a and CYP6P9b

The interactions of CYP6P9a and CYP6P9b with deltamethrin and permethrin and their primary metabolites 4'OH deltamethrin and 4'OH permethrin were compared by measuring their kinetic effects on the inhibition of the *O*-debenzylation of the fluorescent probe substrate BOMFC at three concentrations (100 µM, 10 µM and 1 µM) (Figure 1 and Table S2). The P450s showed a similar pattern of inhibition producing much weaker inhibition of BOMFC *O*-debenzylation with the parent deltamethrin and permethrin compounds compared with strong inhibition by 4'OH permethrin and 4'OH deltamethrin (Table 1). Inhibition by the 4'OH metabolites also produced an increase in K_m alongside significant decreases in reaction rate (V_{max}), indicating a mixed-type inhibition and no clear competitive inhibition (Table S2). For

example, the V_{max} of CYP6P9a BOMFC *O*-debenzylation decreased from 191 pmol product/min x mg protein^{-1} to 104 pmol product/min x mg protein^{-1} in the presence of 100 μM 4'OH deltamethrin, with a concomitant K_m increase from 8.64 μM to 74.8 μM suggesting BOMFC displacement (Table S2).

Several pyrethroids, azole fungicides, and PBO were tested against CYP6P9a and CYP6P9b to evaluate their potential to inhibit *O*-debenzylation of BOMFC (Table 1). Overall, similar patterns of inhibition were observed, with the strongest inhibitor being prochloraz with IC_{50} values of 235 nM and 59 nM for CYP6P9a and CYP6P9b, respectively (Table 1). The major differences were observed for ketoconazole, which showed ~7-fold stronger inhibition of CYP6P9b (IC_{50} 0.518 μM vs 3.71 μM), while uniconazole showed ~20-fold stronger inhibition of CYP6P9a (IC_{50} 0.365 μM vs 7.97 μM). All tested pyrethroids were weak inhibitors with IC_{50} values >100 μM. In contrast, the pyrethroid metabolites 4'OH deltamethrin and 4'OH permethrin were relatively strong inhibitors with respective IC_{50} values of 6.28 μM and 13.2 μM for CYP6P9a and 1.75 μM and 13.4 μM for CYP6P9b. PBO also exhibited rather low IC_{50} values of approx. 1 μM against both CYP6P9a and CYP6P9b, whereas 1-ABT was ineffective at 100 μM (Table 1).

Table 1. Biochemical analysis of CYP6P9 variant interaction with different compounds in fluorescence assays. Inhibition of O-debenzylation of 7-benzyloxymethoxy-4-(trifluoromethyl)-coumarin (BOMFC) by recombinantly expressed *An. funestus* CYP6P9a and CYP6P9b by pyrethroid insecticides, their metabolites and common P450 inhibitors. Date are mean values (n=4).

Compound	CYP6P9a IC_{50} [μM]	95 % CI*	CYP6P9b IC_{50} [μM]	95 % CI
Deltamethrin	> 100		> 100	
4'OH Deltamethrin	6.28	4.83 - 8.06	1.75	1.53 - 1.99
Permethrin	> 100		> 100	
4'OH Permethrin	13.2	9.67- 18.4	13.3	10.6 - 16.8
Cypermethrin	> 100		> 100	
Bifenthrin	> 100		> 100	
PBO	1.03	0.751- 1.39	1.09	0.751- 1.53
1-ABT	176	123 - 254	215	118 - 491
Triflumizole	1.29	1.03 - 1.63	0.723	0.444 - 1.16
Prochloraz	0.235	0.182 - 0.302	0.059	0.0396 - 0.0861
Uniconazole	0.365	0.267 - 0.497	7.97	4.86 - 13.9
Propiconazole	6.95	4.27 - 11.3	2.38	1.72 - 3.28
Ketoconazole	3.71	2.74 - 5.06	0.518	0.396 - 0.675
Triadimefon	18	11.8 - 28.4	19.2	10.5 - 40.6
Triadimenol	> 100		> 100	
Tebuconazole	9.09	8.17 - 10.1	2.11	1.86 - 2.4
Epoxiconazole	21.4	15.3 - 36	44.7	20.1 - 159

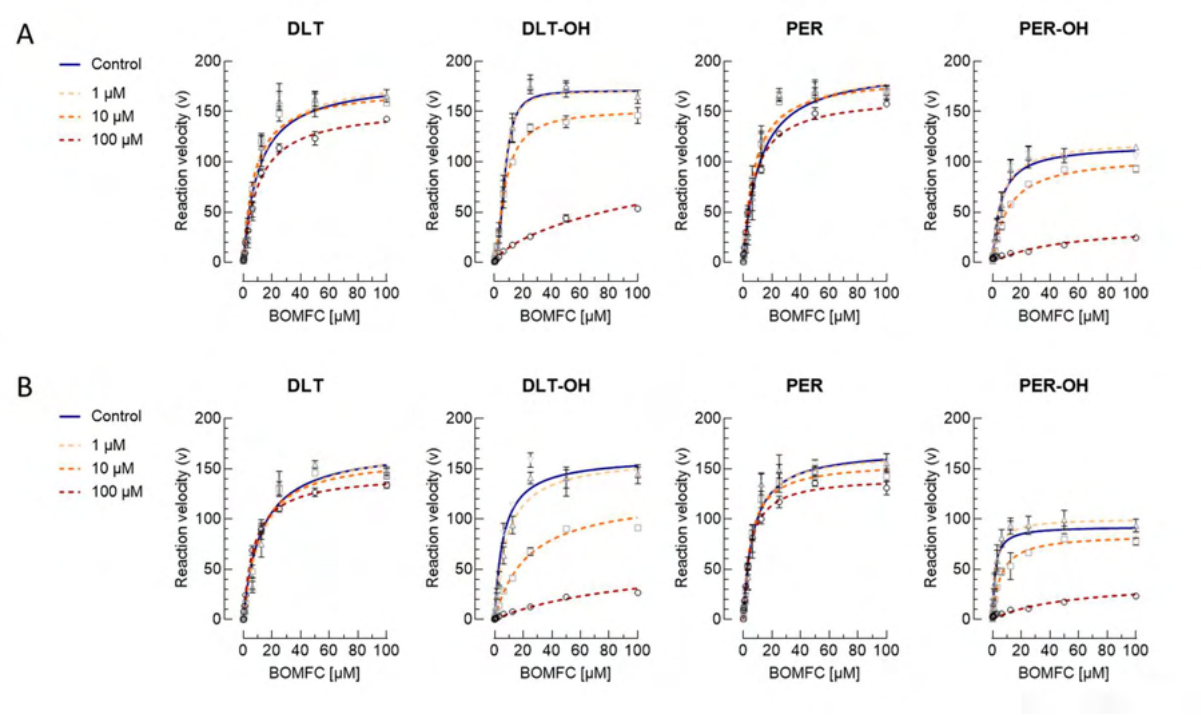

Figure 1. Effect of different pyrethroid substrates on the O-debenzylation of 7-benzyloxymethoxy-4-(trifluoromethyl)-coumarin (BOMFC) by recombinantly expressed *An. funestus* CYP6P9 variants. Michaelis–Menten kinetics of (A) CYP96P9a- and (B) CYP6P9b-mediated BOMFC metabolism using increasing concentrations of deltamethrin (DLT), 4´OH deltamethrin (DLT-OH), permethrin (PER) and 4´OH permethrin (PER-OH). Data are mean values ± SD (n=4). Reaction velocity is defined as pmol 7-hydroxy-4-trifluoromethylcoumarin (HFC) / min x mg protein. Details on Michaelis-Menten kinetic data analysis are given in the supporting information (Table S2).

4.3.2. Metabolism of permethrin and deltamethrin by CYP6P9a and CYP6P9b

To investigate pyrethroid metabolism by CYP6P9a and CYP6P9b substrate turnover was measured following incubation with recombinantly expressed P450s (Figure 2 and 3, Table S3). CYP6P9a produced similar levels of deltamethrin and permethrin depletion (~40%), whereas CYP6P9b produced slightly higher permethrin turnover (61.5%) compared with deltamethrin (40.4%) (Table S3). Compared with their respective parent compounds, both P450s produced significantly higher activity towards the 4'OH metabolites, with 65.3% and 67.3% depletion of 4´OH deltamethrin and 4'OH permethrin respectively for CYP6P9a and 68.9 % and 74.3% depletion with CYP6P9b (Table S3).

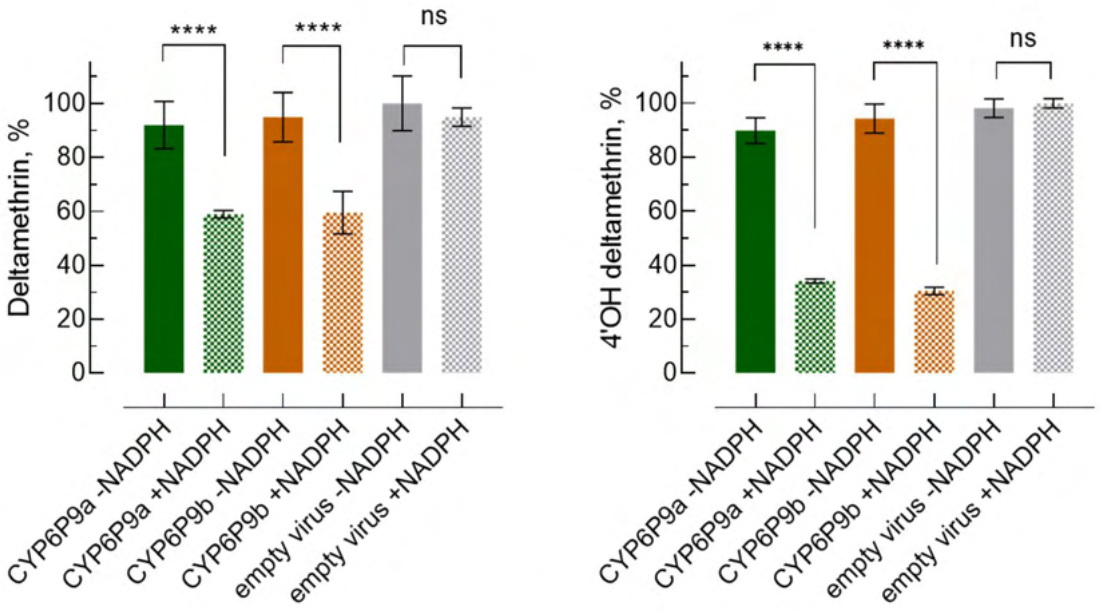

Figure 2. Pyrethroid substrate metabolism by *An. funestus* CYP6P9a and CYP6P9b. Depletion of (A) deltamethrin and (B) 4´OH deltamethrin by recombinantly expressed CYP6P9a and CYP6P9b ± NADPH measured by quantitative UPLC-MS/MS. Remaining parent compound was determined after 90min incubation at 30°C (starting concentration was 2 µM). Data were normalized to % parent compound and re mean values ± 95 % CI (n=3). Mock cells (empty virus) ± NADPH served as control. Original values are provided in Table S3.

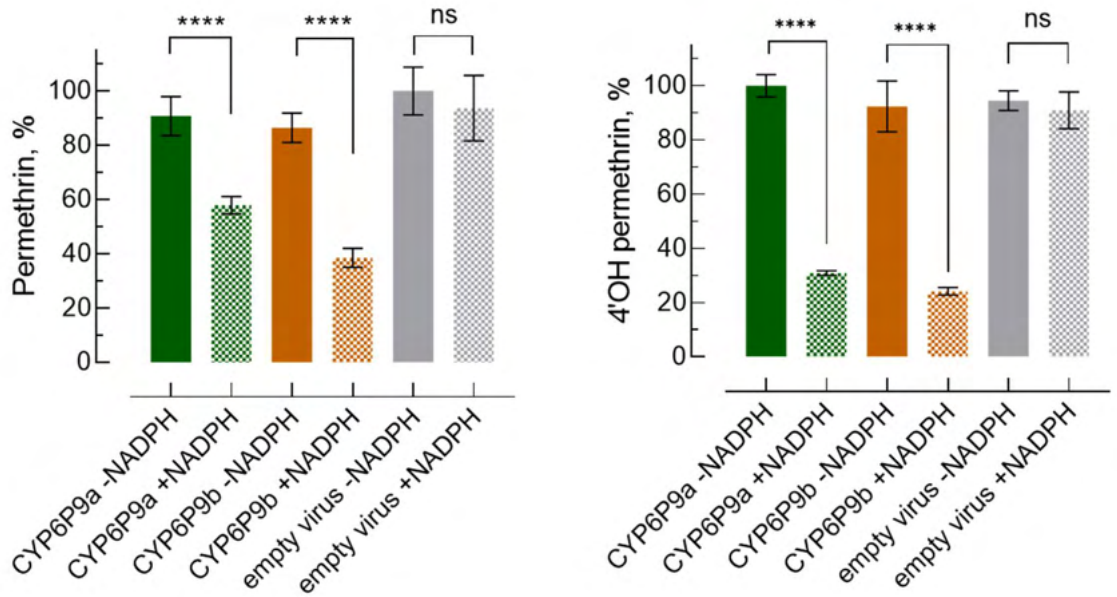

Figure 3. Pyrethroid substrate metabolism by *An. funestus* CYP6P9a and CYP6P9b. Depletion of (A) permethrin and (B) 4´OH permethrin by recombinantly expressed CYP6P9a and CYP6P9b ± NADPH measured by quantitative UPLC-MS/MS. Remaining parent compound was determined after 90min incubation at 30°C (starting concentration was 2.5µM). Data were normalized to % parent compound and are mean values ± 95 % CI (n=3). Mock cells (empty virus) ± NADPH served as control. Original values are provided in Table S3.

Additional investigation of deltamethrin and permethrin metabolism by CYP6P9a and CYP6P9b by MS/MS revealed further metabolism of 4'OH deltamethrin and 4'OH permethrin to cyano-(3-hydroxyphenyl) methyl deltamethrate and 3-hydroxyphenyl-methyl-permethrate respectively via ether cleavage of the phenoxybenzyl moiety, which was confirmed by MS fragment spectra showing the respective M-76 metabolites and supported by molecular docking studies exemplified by CYP6P9b homology models (Figure 4). Molecular docking of 4'OH metabolites into the active site of CYP6P9b revealed the aryl-ether of 4'OH permethrin coordinates closer to the heme iron centre than 4'OH deltamethrin with measured distances of 4.28 Å and 6.99 Å, respectively (Figure 4A, 4B). Compared with deltamethrin, permethrin metabolism produced double the number of peaks in ESI-TOF UPLC-MS spectra (Figure 4, Figure S2). These are indicative of *cis*- and *trans*-permethrin isomers with different retention times, which was confirmed when matched against diastereomerically pure *cis*- and *trans*-permethrin with the same retention times.

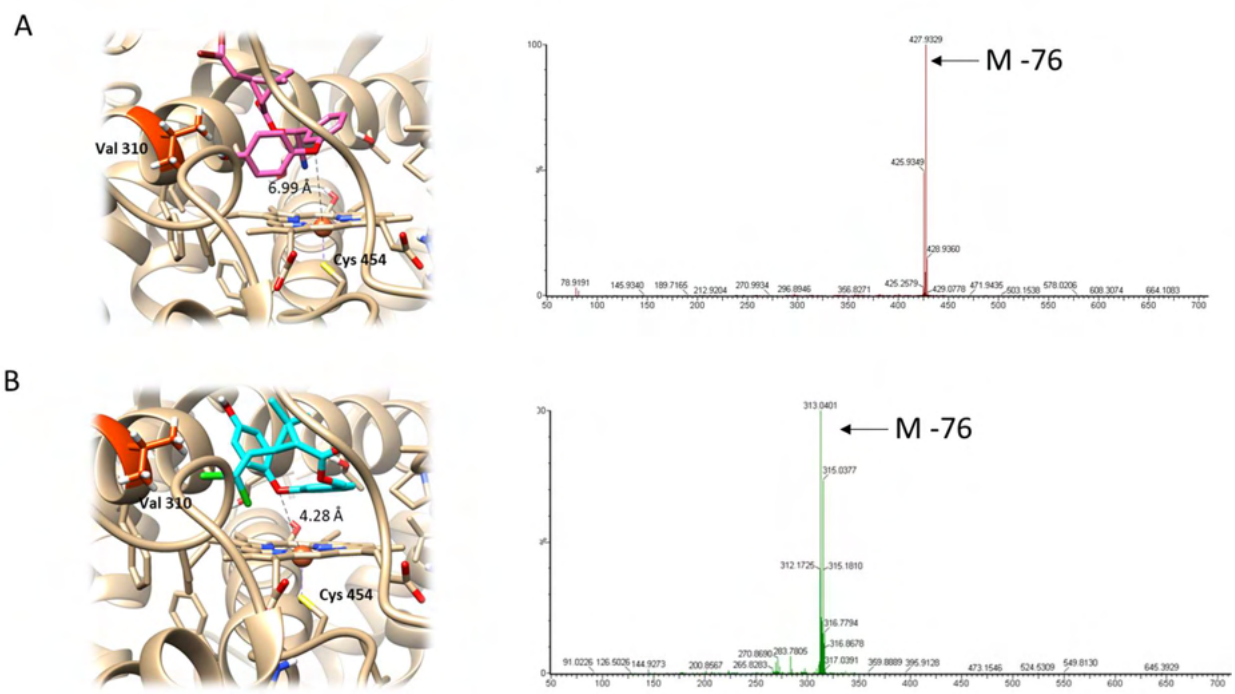

Figure 4. Molecular docking and analytical validation. Binding site model showing the predicted substrate-binding mode of (A) 4'OH deltamethrin and (B) 4'OH permethrin in *An. funestus* CYP6P9b and the respective MS fragment spectra of the corresponding metabolites cyano-(3-hydroxyphenyl) methyl deltamethrate and 3-hydroxyphenyl-methyl-permethrate, respectively, as determined by ESI-TOF UPLC-MS.

Based on the analytical results there were no obvious differences in metabolism between deltamethrin and permethrin, except for an additional M+32 metabolite of permethrin produced by both P450s, suggesting a second hydroxylation site. Overall, the MS analysis

supports the kinetics, which indicates very similar sequential oxidative substrate metabolism as outlined in Figure 5. Interestingly, the ether bond cleavage in permethrin/4'OH permethrin was only detected for CYP6P9b, whereas the deltamethrin ether bond was cleaved by both enzymes (Figure 5).

Table 2. Efficacy of hydroxylated pyrethroids against *An. funestus*. Log-dose mortality data of 4´OH-deltamethrin and 4´OH permethrin against female adults of *An. funestus* FANG in glazed-tile contact bioassays. Both metabolites were inactive against female adults of strain FUMOZ-R at the highest concentration tested (100 mg/m²). Respective graphs are given in the supporting information (Figure S3).

	An. funestus FANG				
	LC_{50}	95 % CI	Slope ± SE		n
4'OH deltamethrin	1.88	0.72-3.89	0.927	0.195	210
4'OH permethrin	34.7	15.8-91.7	0.953	0.242	210

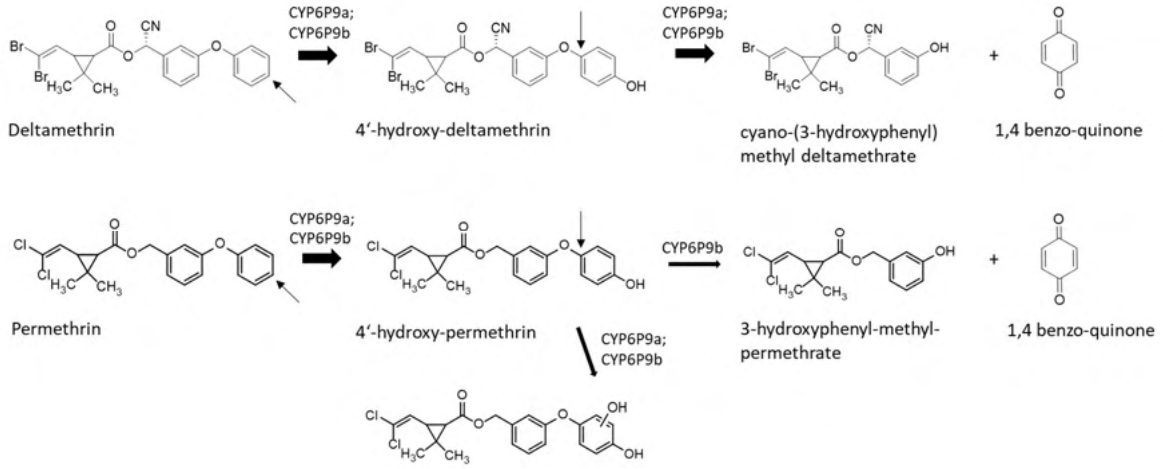

Figure 5. Oxidative metabolic fate of pyrethroids. Proposed scheme for the sequential metabolism of deltamethrin and permethrin, respectively, mediated by recombinantly expressed *An. funestus* CYP6P9a and CYP6P9b supported UPLC-MS analysis. Arrows indicate potential sites of oxidative attack.

4.3.3. Acute toxicity of 4´OH pyrethroid metabolites against *An. funestus*

The acute contact efficacy of the metabolites 4'OH deltamethrin and 4'OH permethrin was tested against *An. funestus* strains FANG and FUMOZ-R to assess their intrinsic toxicity (Table 2). None of the metabolites was active against female adults of FUMOZ-R at the highest concentration, 100 mg/m², tested (Figure S3). Interestingly, female adults of strain FANG showed an almost identical susceptibility to 4'OH deltamethrin (LC_{50}, 1.88 mg/m², CI95%: 0.72-3.89) and permethrin (LC_{50}, 0.543 mg/m², CI95%: 0.409–0.702 (Nolden et al., 2021)). Thus, suggesting that the detoxification of deltamethrin by hydroxylation only is not sufficient to render it ineffective in susceptible *An. funestus*, because intrinsically it remains almost as toxic as permethrin. Hydroxylated permethrin showed an LC_{50} of 34.7 mg/m² and is approx. 20-fold less active than 4´OH deltamethrin (Table 2). In a previous study deltamethrin showed a LC_{50} of 4.61 mg/m² and 0.0206 mg/m² LC_{50} towards FUMOZ-R and FANG mosquitoes, respectively (Nolden et al., 2021).

4.3.4. Degradation and biological efficacy of permethrin diastereomers

Significantly different rates of hydroxylation of *cis*- and *trans*-permethrin diastereomers by CYP6P9a and CYP6P9b were observed by MS/MS analysis (Figure 6A). Both enzymes preferentially depleted *trans*-permethrin over *cis*-permethrin, but CYP6P9b degraded *trans*-permethrin almost five-fold faster than CYP6P9a. To investigate toxicity differences towards susceptible FANG and pyrethroid resistant FUMOZ-R mosquitoes in relation to the low resistance ratio of permethrin (racemate) (RR 7.76; Nolden et al., 2021), diastereomerically pure *cis*- and *trans*-permethrin were evaluated in contact bioassays (Figure 6B). The resistance ratios of *cis*- and *trans*-permethrin were 10.4 and 6.55, respectively (Table S4). However, *cis*-permethrin (LC_{50} 0.154 mg/m²), had 9-times higher toxicity than *trans*-permethrin (LC_{50} 1.41 mg/m²) towards FANG mosquitoes and 6 times higher toxicity to FUMOZ-R, LC_{50} 1.6 and 9.24 mg/m², respectively (Table S4).

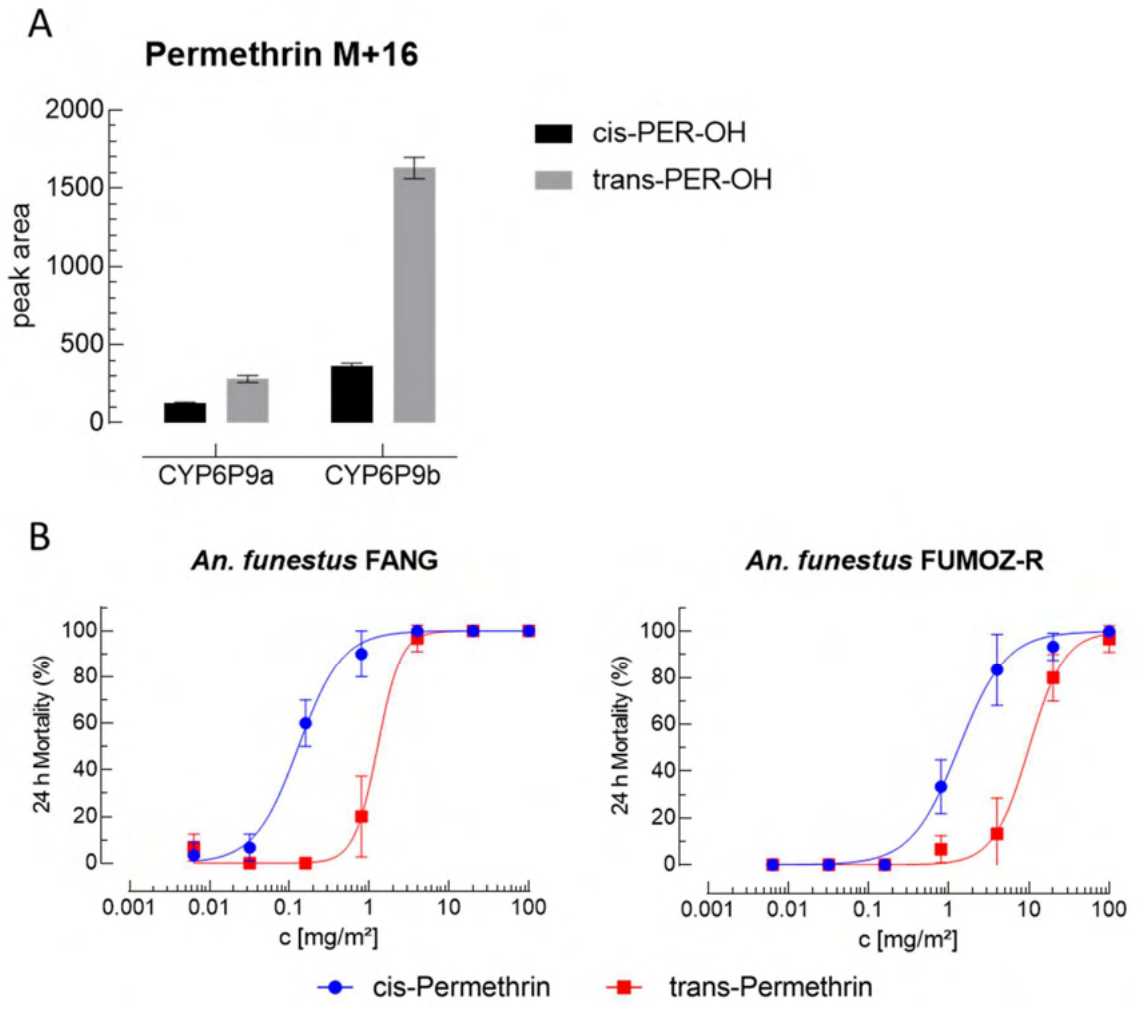

Figure 6. Degradation and biological efficacy of permethrin enantiomers. (A) Resolution of enantioselective metabolism of permethrin to cis/trans 4´hydroxy permethrin by recombinantly expressed CYP6P9a and CYP6P9b in the presence of NADPH (90min). (B) Efficacy of cis- and trans-permethrin towards female adults of *An. funestus strains* FANG and FUMOZ-R in glazed tile contact assays. Data are mean values ± 95% CI (n=3) and given supporting information (table S4).

4.3.5. Kinetics of CYP6P9 variants towards coumarin model substrates, type I and type II pyrethroids

The comparative metabolism of coumarin model substrates by CYP6P9a, CYP6P9b and their respective mutants CYP6P9a^{I310V} and CYP6P9b^{V310I} was investigated and generally followed Michaelis-Menten kinetics. Highest activity was measured with the benzylated coumarin BOMFC, with the four P450s producing similar rates of metabolism with V_{max} values in the range 167-196 pmol product/min x mg protein^{-1} (Figure 7, Table S5). The K_m values for CYP6P9b and CYP6P9b^{V310I} were similar (6.82 and 7.16 µM, respectively) whereas the K_m value for CYP6P9a^{I310V} (3.21 µM) was 4-fold lower than CYP6P9a (11.2 µM). The same trend was observed with BFC and EFC where CYP6P9a^{I310V} produced lower K_m values than the wildtype

CYP6P9a with minimal change in V_{max} (Table S5). CYP6P9b and CYP6P9b^{V310I} produced similar V_{max} values with BFC (33.8 and 40.8 µM) and higher than CYP6P9a and CYP6P9a^{I310V} (11.0 and 8.78 µM). Most notably, CYP6P9b^{V310I} with a V_{max} of 55.3 pmol product/min x mg protein^{-1} was 4-5-fold more active against EFC than CYP6P9b and CYP6P9a and CYP6P9a^{I310V} (Figure 7, Table S5).

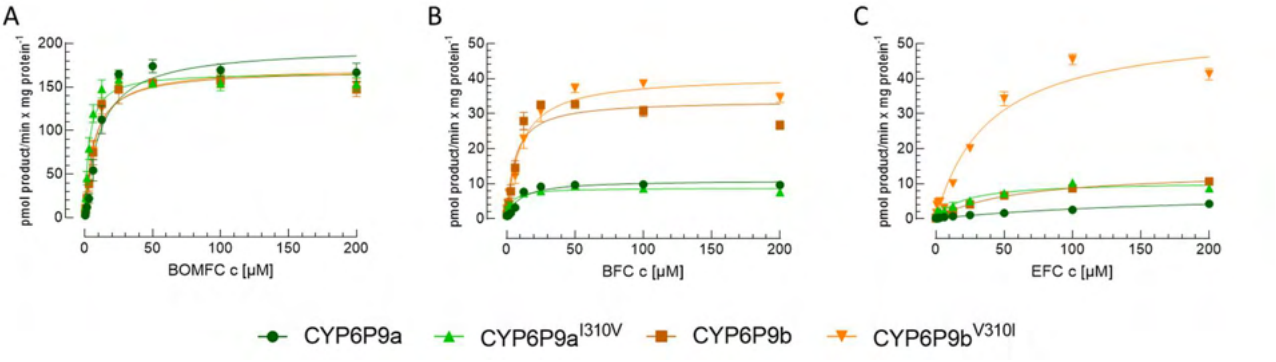

Figure 7. Saturation kinetics of selected coumarin substrates with different CYP6P9 variants. O-debenzylation of (A) 7-benzyloxymethoxy-4-trifluoromethylcoumarin (BOMFC) and (B) 7-benzyloxy-4-trifluoromethylcoumarin (BFC), as well as (C) the O-dealkylation of 7-ethoxy-4-trifluoromethylcoumarin (EFC) by recombinantly expressed CYP6P9a, CYP6P9b, CYP6P9a^{I310V} and CYP6P9b^{V310I}. Details on Michaelis-Menten kinetic data analysis are given in the supporting information (Table S5). Data are mean values ± SD (n=4).

Pyrethroid metabolism of the CYP6P9 variants was investigated by comparing the rates of production of the major 4'OH metabolites of deltamethrin and permethrin (Figure 8). The highest reaction rate for deltamethrin was observed by CYP6P9b^{V310I} with a V_{max} of 13.7 pmol product/min x mg protein^{-1}, which was slightly higher than wildtype CYP6P9b (10.6 pmol product/min x mg protein^{-1}) but the same as CYP6P9a (Table S6). CYP6P9a^{I310V} produced the lowest deltamethrin activity of 6.65 pmol product/min x mg protein^{-1}. The amino acid substitution at position 310 produces a small reduction (~ 2-fold) in K_m values for CYP6P9a^{I310V} (7.6 µM) and CYP6P9b^{V310I} (14.7 µM) relative to CYP6P9a (19.2 µM) and CYP6P9b (27 µM) respectively (Table S6), indicating slightly higher affinity towards deltamethrin.

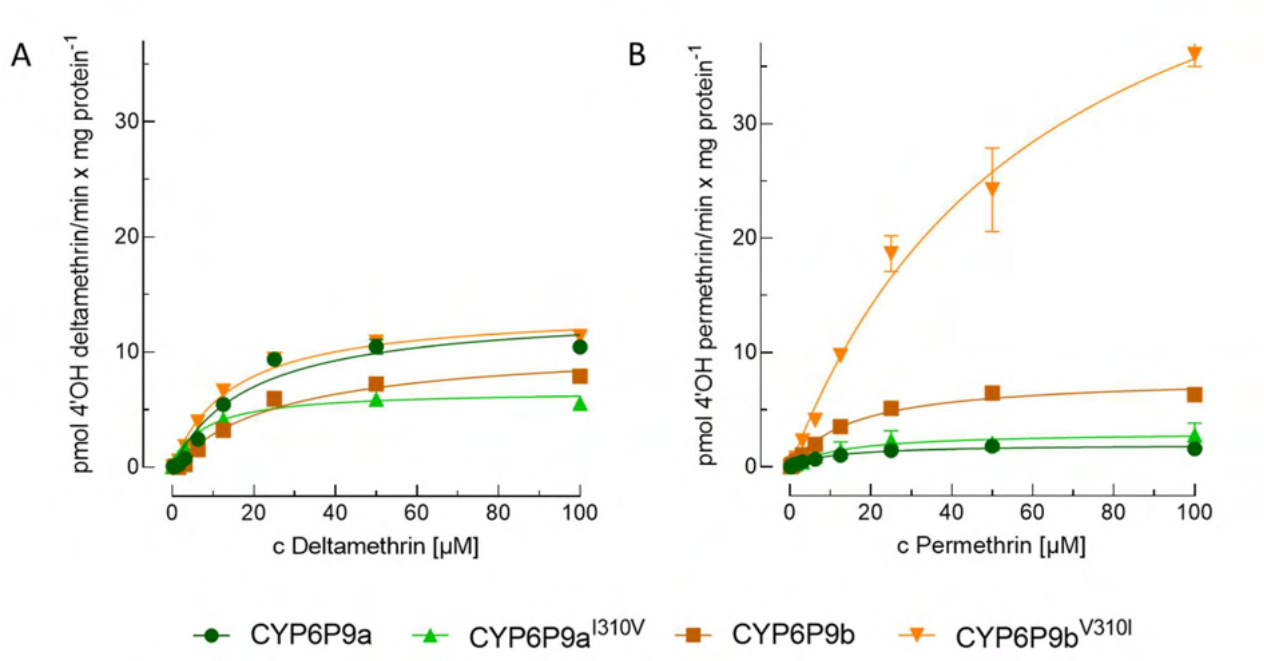

Figure 8. Saturation kinetics of pyrethroid substrates with different CYP6P9 variants. Hydroxylation of (A) deltamethrin and (B) permethrin by CYP6P9a, CYP6P9b, CYP6P9a^{I310V} and CYP6P9b^{V310I}. Details on Michaelis-Menten kinetic data analysis are given in the supporting information (Table S6). Data are mean values ± SD (n=3).

Compared with CYP6P9b (7.89 pmol product/min x mg protein^{-1}), CYP6P9a and CYP6P9a^{I310V} revealed relatively low activity towards permethrin with 1.97 and 3.07 pmol product/min x mg protein^{-1}, respectively (Table S6). Strikingly, the highest permethrin reaction rate was seen for CYP6P9b^{V310I} with 58 pmol product/min x mg protein^{-1}, a 7-fold increase compared with wildtype CYP6P9b (Figure 8, Table S6). Metabolism of permethrin by CYP6P9^{V310I} also produced a sigmoidal curve and a linear Hanes-Woolf fit suggests an allosteric interaction and positive cooperativity, contrasting with the hyperbolic behaviour of the other P450s towards deltamethrin and permethrin (Figure S4). Overall, the valine 310 to isoleucine substitution in CYP6P9b^{V310I} tended to enhance metabolic efficacy and produced higher affinity for all the inhibitors tested, whereas the reverse isoleucine to valine substitution at position 310 in CYP6P9a^{I310V} led to a weaker inhibition of all tested inhibitors (Table S7).

4.4. Discussion

Pyrethroid resistance in *An. funestus* is largely driven by the overexpression of duplicated P450s CYP6P9a and CYP6P9b, which have been shown to rapidly metabolise pyrethroids in functional assays employing prokaryotic and eukaryotic protein expression systems (Ibrahim

et al., 2015; Nolden et al., 2022; Riveron et al., 2013; Yunta et al., 2019). Previous studies mostly utilized parent depletion approaches (+NADPH vs -NADPH) to quantify the extent of pyrethroid metabolism by CYP6P9a and CYP6P9b (Ibrahim et al., 2016; Riveron et al., 2014, 2013), similar to P450 assays employed to predict pesticide clearance in mammalian toxicology (Scollon et al., 2009). We recently noticed a stochiometric inconsistency between deltamethrin depletion and 4´OH deltamethrin formation by functionally expressed CYP6P9 variants, and suggested the formation of additional, undetected metabolites (Nolden et al., 2022). Indeed, the present study revealed that the depletion of deltamethrin by recombinantly expressed CYP6P9a and CYP6P9b is principally based on sequential oxidative metabolism by, 1) hydroxylation of the 4´para position of the phenoxybenzyl ring, and 2) the formation of cyano-(3-hydroxyphenyl)-methyl-deltamethrate via ether cleavage of the phenoxybenzyl moiety. In addition, we confirmed sequential metabolism of the type I pyrethroid permethrin via the same route, but only for CYP6P9b. We failed to detect 3-hydroxyphenyl-methyl-permethrate in analytical assays with CYP6P9a, suggesting its lower catalytic capacity to oxidise 4´OH permethrin compared to CYP6P9b. This is supported by an overall higher permethrin depletion capacity of CYP6P9b compared to CYP6P9a, whereas no significant difference between both enzymes was detected for deltamethrin metabolism. Sequential P450-mediated metabolism of deltamethrin resulting in the formation of cyano-(3-hydroxyphenyl)-methyl-deltamethrate has so far only been described for *An. gambiae* CYP6M2 (Stevenson et al., 2011). Whereas CYP6P9b mediated ether cleavage of the phenoxybenzyl moiety of permethrin has been demonstrated for the first time in insects. A similar metabolic fate has so far only been observed in mammalian studies, e.g. with rat liver microsomes (Shono et al., 1979).

Interestingly, neither deltamethrin nor permethrin inhibited the *O*-debenzylation of BOMFC in a fluorescent probe assay we conducted with recombinantly expressed CYP6P9a and CYP6P9b, though we have detected low, but significant decrease of V_{max} values when both pyrethroids were tested at 100µM. Indeed, the inhibitory efficacy of other pyrethroids such as bifenthrin and cypermethrin was also too low to calculate IC_{50}-values. Such fluorescence (and luminescence) probe assays have been successfully used to predict interaction and/or P450-mediated metabolism of insecticides, e.g., for *Bemisia tabaci* CYP6CM1 and imidacloprid (Hamada et al., 2019), *Apis mellifera* CYP9Q2/3 and various insecticides (Haas et al., 2021; Haas and Nauen, 2021), several mosquito P450s including *An. gambiae* CYP6P3

(Yunta et al., 2019), and *An. funestus* CYP6P9a/b for various insecticides including pyrethroids (Ibrahim et al., 2016, 2015; Yunta et al., 2019). Our results with BOMFC and pyrethroids are in contrast to diethoxyfluorescein probe assays with CYP6P9a/b where various insecticides have been shown to inhibit its *O*-dealkylation in the lower micromolar range, including deltamethrin and permethrin (Ibrahim et al., 2016; Yunta et al., 2019). However, a few insecticides tested by Yunta et al. (2019) such as DDT turned out to be micromolar inhibitors of CYP6P9a and other mosquito P450s but were not metabolised by recombinantly expressed enzymes. Our fluorescent probe assays with deltamethrin, and permethrin revealed the opposite, i.e., no significant inhibition of CYP6P9a/b, but substantial depletion in analytical assays. The azole compounds and PBO used to validate the fluorescence probe assay have been described as strong *An. funestus* P450 inhibitors (Nolden et al., 2021), and showed strong inhibition of both CYP6P9a and CYP6P9b, not unexpected considering their *in vivo* potential as synergists in combination with pyrethroids (Horstmann and Sonneck, 2016; Williams et al., 2019). Further work is warranted to investigate the reasons for the discrepancy in pyrethroid inhibitory potential in fluorescent probe assays and metabolism.

Intriguingly, we observed a much stronger interaction in BOMFC fluorescent probe assays between CYP6P9a/b and the pyrethroid metabolites 4´OH-permethrin and 4´OH deltamethrin. The observed inhibition of the *O*-debenzylation of BOMFC by both hydroxy metabolites in fluorescent probe assays is linked to significantly higher CYP6P9a/b driven depletion rates in analytical assays when compared to the respective parent compound. To the best of our knowledge this is the first study investigating the oxidative metabolic fate of 4´para-hydroxylated pyrethroids by recombinantly expressed insect P450s. The MS fragment spectra of the resulting metabolites confirmed the formation of cyano-(3-hydroxyphenyl)-methyl deltamethrate and 3-hydroxyphenyl-methyl-permethrate and the sequential two-step reaction catalysed by either CYP6P9 variant. 4´OH-Deltamethrin is 100-fold less toxic than deltamethrin, but its intrinsic toxicity against *An. funestus* FANG remains high and is comparable to permethrin - thus clearly supporting the advantage of a two-step deltamethrin metabolisation mediated by upregulated CYP6P9 variants. Hydroxylated permethrin is much less toxic in bioassays and unlikely to confer phenotypic consequences by the lack of sequential metabolism mediated by CYP6P9a. A previous study suggested that high levels of pyrethroid-metabolising P450s in resistant *Brassicogethes aeneus* protect the pest by pyrethroid sequestration rather than facilitating 4´OH-deltamethrin formation, which has

indeed been shown to be intrinsically moderately toxic to pollen beetles overexpressing CYP6BQ23 (Zimmer et al., 2014; Zimmer and Nauen, 2011).

Next, we investigated if the significant differences in permethrin depletion we observed between CYP6P9a and CYP6P9b are linked to stereoselectivity issues as permethrin is a diastereomeric mixture of *trans*- and *cis*-permethrin. Indeed, we detected a preference of both CYP6P9 variants to hydroxylate more readily *trans*- over *cis*-permethrin, with CYP6P9b exhibiting a significantly higher metabolic capacity and preference to hydroxylate *trans*-permethrin compared with CYP6P9a. As we did not analyse the metabolism of the hydroxylated isomers separately, we can only speculate – based on the metabolic fate of racemic 4´OH permethrin – that CYP6P9b is the main permethrin metaboliser, because it was shown to catalyse the ether cleavage of the phenoxybenzyl moiety at detectable levels, whereas CYP6P9a did not. Interestingly, mammalian P450s involved in permethrin metabolism seem to be consistently more active on *cis*-permethrin (Hedges et al., 2019), whereas the preferred route of *trans*-permethrin detoxification is hydrolytic via ester cleavage by esterases (Casida et al., 1983; Scollon et al., 2009; Shono et al., 1979). We then assessed the acute toxicity of both permethrin isomers and found that *cis*-permethrin was significantly more toxic than *trans*-permethrin against female adults of both *An. funestus* FANG and FUMOZ. Based on this result it is tempting to speculate that the metabolism of *cis*-permethrin might be reduced in the presence of its diastereomer *trans*-permethrin, i.e., *in vivo* retaining higher levels of the intrinsically more toxic *cis* isomer, possibly explaining the rather low levels of permethrin resistance (compared to deltamethrin) we recently described in our selected *An. funestus* FUMOZ-R laboratory strain (Nolden et al., 2021). It would be interesting to further investigate if racemic mixtures of pyrethroids are advantageous over enantiomerically pure compounds to control mosquitoes expressing P450-based metabolic resistance such as *An. funestus*.

Finally, we have carried out site-directed mutagenesis to create two mutants CYP6P9a^{I310V} and CYP6P9b^{V310I} to compare their metabolic activity with CYP6P9a and CYP6P9b towards permethrin, deltamethrin and coumarins. V310 is part of the catalytic site and the only residue in SRS4 of CYP6P9b different from CYP6P9a (I310). Furthermore, this site has been described mutated (V310I) in CYP6P9b haplotypes of a pyrethroid resistant field population of *An. funestus* from Benin (Ibrahim et al., 2015). Interestingly, we observed a striking increase in permethrin but not deltamethrin turnover by CYP6P9b^{V310I} compared with wildtype

CYP6P9b, possibly explaining the high level of permethrin resistance observed in *An. funestus* strains from Benin showing this polymorphism. Ibrahim et al. (2015) described other key residues in CYP6P9b such as $Val^{109}Ile$, $Asp^{335}Glu$ and $Asn^{384}Ser$ as determinants of enhanced pyrethroid metabolism which has been confirmed by site-directed-mutagenesis as well. Here $CYP6P9b^{V310I}$ showed a similar increase in the *O*-dealkylation of 7-EC, but not for the *O*-debenzylation of BFC and BOMFC. Whereas the swapped residue only weakly affected the catalytic capacity of the CYP6P9a variants towards coumarin substrates and pyrethroids. Indeed, mutations in substrate recognition sites of several insect P450s have been shown to be determinants of selectivity. For example in *An. gambiae* CYP6Z1 and CYP6Z2 differences in SRS1, SRS2 and SRS4 have been demonstrated to determine the capacity of CYP6Z1 to metabolise DDT (Chiu et al., 2008). In another study with different CYP6ER1-variants of *Nilaparvata lugens,* a hemipteran rice pest, a serine residue in SRS4 determined elevated imidacloprid metabolism (Zimmer et al., 2018). In the cotton bollworm, *Helicoverpa armigera,* variants of the CYP6AE subfamily with a valine to isoleucine substitution in SRS4 showed increased esfenvalerate metabolism (Shi et al., 2020). Similar observations were described for substitutions in SRS4 of human CYP2A1 and CYP2A2 leading to higher hydroxylation rates and alterations in ethoxy-coumarin *O*-dealkylation (Hanioka et al., 1992; Hiroya et al., 1994).
Nonetheless, further molecular work is warranted to shed light on the determinants of pyrethroid metabolism and resistance by CYP6P9 variants, and whether SRS4 residue 310 of CYP6P9b can potentially serve as a molecular marker of enhanced levels of pyrethroid resistance in *An. funestus*.

Acknowledgements

We greatly acknowledge the help of Johannes Glaubitz, Udo König and Birgit Nebelsiek with the UPLC-MS/MS analysis and Sebastian Horstmann and Uwe Pluschkell for their helpful discussion and comments.

Declaration of competing interests

RN and MN are employed by Bayer AG, a manufacturer of pesticides. MN is also a PhD student affiliated with the Liverpool School of Tropical Medicine, funded by the Innovative Vector Control Consortium (IVCC) and Bayer AG.

4.5. References

Abbott, W.S., 1925. A Method of Computing the Effectiveness of an Insecticide. J. Econ. Entomol. 18, 265–267. https://doi.org/10.1093/jee/18.2.265a

Amenya, D.A., Naguran, R., Lo, T.-C.M., Ranson, H., Spillings, B.L., Wood, O.R., Brooke, B.D., Coetzee, M., Koekemoer, L.L., 2008. Over expression of a Cytochrome P450 (CYP6P9) in a Major African Malaria Vector,. Insect Mol. Biol. 17, 19–25.

Bhatt, S., Weiss, D.J., Cameron, E., Bisanzio, D., Mappin, B., Dalrymple, U., Battle, K.E., Moyes, C.L., Henry, A., Eckhoff, P.A., Wenger, E.A., Briët, O., Penny, M.A., Smith, T.A., Bennett, A., Yukich, J., Eisele, T.P., Griffin, J.T., Fergus, C.A., Lynch, M., Lindgren, F., Cohen, J.M., Murray, C.L.J., Smith, D.L., Hay, S.I., Cibulskis, R.E., Gething, P.W., 2015. The effect of malaria control on Plasmodium falciparum in Africa between 2000 and 2015. Nature 526, 207–211. https://doi.org/10.1038/nature15535

Brooke, B.D., Kloke, G., Hunt, R.H., Koekemoer, L.L., Tem, E.A., Taylor, M.E., Small, G., Hemingway, J., Coetzee, M., 2001. Bioassay and biochemical analyses of insecticide resistance in southern African Anopheles funestus (Diptera: Culicidae). Bull. Entomol. Res. 91, 265–272. https://doi.org/10.1079/ber2001108

Casida, J.E., Gammon, D.W., Glickman, A.H., Lawrence, L.J., 1983. Mechanism of Selective Action of Pyrethroid. Annu. Rev. Pharmacol. Toxicol. 413–438.

Chiu, T.L., Wen, Z., Rupasinghe, S.G., Schuler, M.A., 2008. Comparative molecular modeling of Anopheles gambiae CYP6Z1, a mosquito P450 capable of metabolizing DDT. Proc. Natl. Acad. Sci. U. S. A. 105, 8855–8860. https://doi.org/10.1073/pnas.0709249105

Das, S., Garver, L., Dimopoulos, G., 2007. Protocol for Mosquito Rearing (A. gambiae), Journal of Visualized Experiments. https://doi.org/10.3791/221

David, J., Ismail, H.M., Chandor-proust, A., Paine, M.J.I., 2013. Role of cytochrome P450s in insecticide resistance: impact on the control of mosquito-borne diseases and use of insecticides on Earth. Philos. Trans. R. Soc. B. http://dx.doi.org/10.1098/rstb.2012.0429

Feyereisen, R., 2019. Insect CYP Genes and P450 Enzymes, Reference Module in Life Sciences. https://doi.org/10.1016/b978-0-12-809633-8.04040-1

Gleave, K., Lissenden, N., Richardson, M., Ranson, H., 2018. Piperonyl butoxide (PBO) combined with pyrethroids in long-lasting insecticidal nets (LLINs) to prevent malaria in Africa. Cochrane Database Syst. Rev. https://doi.org/10.1002/14651858.CD012776

Gotoh, O., 1992. Substrate recognition sites in cytochrome P450 family 2 (CYP2) proteins inferred from comparative analyses of amino acid and coding nucleotide sequences. J. Biol. Chem. 267, 83–90. https://doi.org/10.1016/s0021-9258(18)48462-1

Haas, J., Glaubitz, J., Koenig, U., Nauen, R., 2021. A mechanism-based approach unveils metabolic routes potentially mediating chlorantraniliprole synergism in honey bees, Apis mellifera L., by azole fungicides . Pest Manag. Sci. https://doi.org/10.1002/ps.6706

Haas, J., Nauen, R., 2021. Pesticide risk assessment at the molecular level using honey bee cytochrome P450 enzymes : A complementary approach. Environ. Int. 147, 106372. https://doi.org/10.1016/j.envint.2020.106372

Hamada, A., Wahl, G.D., Nesterov, A., Nakao, T., Kawashima, M., Banba, S., 2019. Differential metabolism of imidacloprid and dinotefuran by Bemisia tabaci CYP6CM1 variants. Pestic. Biochem. Physiol. 159, 27–33. https://doi.org/10.1016/j.pestbp.2019.05.011

Hanioka, N., Gonzalez, F.J., Lindberg, N.A., Gao, L., Gelboin, H. V., Korzekwa, K.R., 1992. Site-Directed Mutagenesis of Cytochrome P450s CYP2A1 and CYP2A2: Influence of the Distal Helix on the Kinetics of Testosterone Hydroxylation. Biochemistry 31, 3364–3370. https://doi.org/10.1021/bi00128a009

Hedges, L., Brown, S., MacLeod, A.K., Vardy, A., Doyle, E., Song, G., Moreau, M., Yoon, M., Osimitz, T.G., Lake, B.G., 2019. Metabolism of deltamethrin and cis- and trans-permethrin by human expressed cytochrome P450 and carboxylesterase enzymes. Xenobiotica 49, 521–527. https://doi.org/10.1080/00498254.2018.1474283

Hiroya, K., Murakami, Y., Shimizu, T., Hatano, M., Ortiz De Montellano, P.R., 1994. Differential Roles of Glu318 and Thr319 in Cytochrome P450 1A2 Catalysis Supported by NADPH-Cytochrome P450 Reductase and tert-Butyl Hydroperoxide. Arch. Biochem. Biophys. https://doi.org/10.1006/abbi.1994.1184

Horstmann, S., Sonneck, R., 2016. Contact Bioassays with Phenoxybenzyl and Tetrafluorobenzyl Pyrethroids against Target-Site and Metabolic Resistant Mosquitoes. PLOS ONE 11, e0149738. https://doi.org/10.1371/journal.pone.0149738

Ibrahim, S.S., Amvongo-Adjia, N., Wondji, M.J., Irving, H., Riveron, J.M., Wondji, C.S., 2018. Pyrethroid resistance in the major malaria vector anopheles funestus is exacerbated by overexpression and overactivity of the P450 CYP6AA1 across Africa. Genes 9, 1–17. https://doi.org/10.3390/genes9030140

Ibrahim, S.S., Ndula, M., Riveron, J.M., Irving, H., Wondji, C.S., 2016. The P450 CYP6Z1 confers carbamate/pyrethroid cross-resistance in a major African malaria vector beside a novel carbamate-insensitive N485I acetylcholinesterase-1 mutation. Mol. Ecol. 25, 3436–3452. https://doi.org/10.1111/mec.13673

Ibrahim, S.S., Riveron, J.M., Bibby, J., Irving, H., Yunta, C., Paine, M.J.I., Wondji, C.S., 2015. Allelic Variation of Cytochrome P450s Drives Resistance to Bednet Insecticides in a Major Malaria Vector. PLoS Genet. 11, e1005618. https://doi.org/10.1371/journal.pgen.1005618

Irving, H., Wondji, C.S., 2017. Investigating knockdown resistance (kdr) mechanism against pyrethroids/DDT in the malaria vector Anopheles funestus across Africa. BMC Genet. 18, 76. https://doi.org/10.1186/s12863-017-0539-x

Martinez-Torres, D., Chandre, F., Williamson, M.S., Darriet, F., Berge, J.B., Devonshire, A.L., Guillet, P., Pasteur, N., Pauron, D., 1998. Molecular characterization of pyrethroid knockdown resistance (kdr) in the major malaria vector Anopheles gambiae s.s. Insect Mol. Biol. 7, 179–184.

Moyes, C.L., Lees, R.S., Yunta, C., Walker, K.J., Hemmings, K., Oladepo, F., Hancock, P.A., Weetman, D., Paine, M.J.I., Ismail, H.M., 2021. Assessing cross-resistance within the pyrethroids in terms of their interactions with key cytochrome P450 enzymes and resistance in vector populations. Parasit. Vectors 14, 115. https://doi.org/10.1186/s13071-021-04609-5

Nauen, R., Bass, C., Feyereisen, R., Vontas, J., 2022. The Role of Cytochrome P450s in Insect Toxicology and Resistance. Annu. Rev. Entomol. 67, 105–124. https://doi.org/10.1146/annurev-ento-070621-061328

Nolden, M., Brockmann, A., Ebbinghaus-kintscher, U., Brueggen, K., Horstmann, S., Paine, M.J.I., Nauen, R., 2021. Towards understanding transfl uthrin efficacy in a pyrethroid-resistant strain of the malaria vector Anopheles funestus with special reference to cytochrome P450-mediated detoxification. Curr. Res. Parasitol. Vector-Borne Dis. 1, 100041. https://doi.org/10.1016/j.crpvbd.2021.100041

Nolden, M., Paine, M.J.I., Nauen, R., 2022. Biochemical profiling of functionally expressed CYP6P9 variants of the malaria vector Anopheles funestus with special reference to cytochrome b5 and its role in pyrethroid and coumarin substrate metabolism. Pestic. Biochem. Physiol. 182. https://doi.org/10.1016/j.pestbp.2022.105051

Oleg, T., Olson, A.J., 2010. Software News and Update AutoDock Vina: Improving the Speed and Accuracy of Docking with a New Scoring Function, Efficient Optimization, and Multithreading. J. Comput. Chem. 31, 455–461. https://doi.org/DOI 10.1002/jcc.21334

Omura, T., Sato, R., 1964. The Carbon Monoxide-binding Pigment of Liver Microsomes. J. Biol. Chem. 239.

Paine, M.J.I., McLaughlin, L.A., Flanagan, J.U., Kemp, C.A., Sutcliffe, M.J., Roberts, G.C.K., Wolf, C.R., 2003. Residues glutamate 216 and aspartate 301 are key determinants of substrate specificity and product regioselectivity in cytochrome P450 2D6. J. Biol. Chem. 278, 4021–4027. https://doi.org/10.1074/jbc.M209519200

Protopopoff, N., Mosha, J.F., Lukole, E., Charlwood, J.D., Wright, A., Mwalimu, C.D., Manjurano, A., Mosha, F.W., Kisinza, W., Kleinschmidt, I., Rowland, M., 2018. Effectiveness of a long-lasting piperonyl butoxide-treated insecticidal net and indoor residual spray interventions, separately and together, against malaria transmitted by pyrethroid-resistant mosquitoes: a cluster, randomised controlled, two-by-two fact. The Lancet 391, 1577–1588. https://doi.org/10.1016/S0140-6736(18)30427-6

Ranson, H., N'Guessan, R., Lines, J., Moiroux, N., Nkuni, Z., Corbel, V., 2011. Pyrethroid resistance in African anopheline mosquitoes: What are the implications for malaria control? Trends Parasitol. 27, 91–98. https://doi.org/10.1016/j.pt.2010.08.004

Riveron, J.M., Ibrahim, S.S., Chanda, E., Mzilahowa, T., Cuamba, N., Irving, H., Barnes, K.G., Ndula, M., Wondji, C.S., 2014. The highly polymorphic CYP6M7 cytochrome P450 gene partners with the directionally selected CYP6P9a and CYP6P9b genes to expand the pyrethroid resistance front in the malaria vector Anopheles funestus in Africa. BMC Genomics 15, 817. https://doi.org/10.1186/1471-2164-15-817

Riveron, J.M., Irving, H., Ndula, M., Barnes, K.G., Ibrahim, S.S., Paine, M.J.I., Wondji, C.S., 2013. Directionally selected cytochrome P450 alleles are driving the spread of pyrethroid resistance in the major malaria vector Anopheles funestus. Proc. Natl. Acad. Sci. 110, 252–257. https://doi.org/10.1073/pnas.1216705110

Ruzo, L.O., Unai, T., Casida, J.E., 1978. Decamethrin Metabolism in Rats. J. Agric. Food Chem. 26, 918–925. https://doi.org/10.1021/jf60218a060

Scollon, E.J., Starr, J.M., Godin, S.J., DeVito, M.J., Hughes, M.F., 2009. In Vitro Metabolism of Pyrethroid Pesticides by Rat and Human Hepatic Microsomes and Cytochrome P450 Isoforms. Drug Metab. Dispos. 37, 221–228. https://doi.org/10.1124/dmd.108.022343

Shi, Y., O'Reilly, A.O., Sun, S., Qu, Q., Yang, Y., Wu, Y., 2020. Roles of the variable P450 substrate recognition sites SRS1 and SRS6 in esfenvalerate metabolism by CYP6AE subfamily enzymes in Helicoverpa armigera. Insect Biochem. Mol. Biol. 127, 103486. https://doi.org/10.1016/j.ibmb.2020.103486

Shono, T., Ohsawa, K., Casida, J.E., 1979. Metabolism of trans-and cis-Permethrin, trans-and cis-Cypermethrin, and Decamethrin by Microsomal Enzymes. J. Agric. Food Chem. 27, 316–325. https://doi.org/10.1021/jf60222a059

Soderlund, D.M., 2020. Neurotoxicology of pyrethroid insecticides, in: Neurotoxicity of Pesticides. Elsevier Inc., pp. 113–165. https://doi.org/10.1016/bs.ant.2019.11.002

Stevenson, B.J., Bibby, J., Pignatelli, P., Muangnoicharoen, S., O'Neill, P.M., Lian, L.Y., Müller, P., Nikou, D., Steven, A., Hemingway, J., Sutcliffe, M.J., Paine, M.J.I., 2011. Cytochrome P450 6M2 from the malaria vector Anopheles gambiae metabolizes pyrethroids: Sequential metabolism of deltamethrin revealed. Insect Biochem. Mol. Biol. 41, 492–502. https://doi.org/10.1016/j.ibmb.2011.02.003

WHO, 2021. World Malaria Report, World Malaria Report 2021.

WHO, 2020. World Malaria Report 2020, World Health Organization.

WHO, 2018. Global report on insecticide resistance in malaria vectors: 2010-2016.

Williams, J., Flood, L., Praulins, G., Ingham, V.A., Morgan, J., Lees, R.S., Ranson, H., 2019. Characterisation of Anopheles strains used for laboratory screening of new vector control products. Parasit. Vectors 12, 522. https://doi.org/10.1186/s13071-019-3774-3

Wondji, C.S., Hearn, J., Irving, H., Wondji, M.J., Weedall, G., 2022. RNAseq-based gene expression profiling of the Anopheles funestus pyrethroid-resistant strain FUMOZ highlights the predominant role of the duplicated CYP6P9a/b cytochrome P450s. G3 Genes Genomes Genet. 12. https://doi.org/10.1093/G3JOURNAL/JKAB352

Yunta, C., Hemmings, K., Stevenson, B., Koekemoer, L.L., Matambo, T., Pignatelli, P., Voice, M., Nász, S., Paine, M.J.I., 2019. Cross-resistance profiles of malaria mosquito P450s associated with pyrethroid resistance against WHO insecticides. Pestic. Biochem. Physiol. 161, 61–67. https://doi.org/10.1016/j.pestbp.2019.06.007

Zimmer, C.T., Bass, C., Williamson, M.S., Kaussmann, M., Wölfel, K., Gutbrod, O., Nauen, R., 2014. Molecular and functional characterization of CYP6BQ23, a cytochrome P450 conferring resistance to pyrethroids in European populations of pollen beetle, Meligethes aeneus. Insect Biochem. Mol. Biol. 45, 18–29. https://doi.org/10.1016/j.ibmb.2013.11.008

Zimmer, C.T., Garrood, W.T., Singh, K.S., Randall, E., Lueke, B., Gutbrod, O., Matthiesen, S., Kohler, M., Nauen, R., Davies, T.G.E., Bass, C., 2018. Neofunctionalization of Duplicated P450 Genes Drives the Evolution of Insecticide Resistance in the Brown Planthopper. Curr. Biol. 28, 268-274.e5. https://doi.org/10.1016/j.cub.2017.11.060

Zimmer, C.T., Nauen, R., 2011. Cytochrome P450 mediated pyrethroid resistance in European populations of Meligethes aeneus (Coleoptera: Nitidulidae). Pestic. Biochem. Physiol. 100, 264–272. https://doi.org/10.1016/j.pestbp.2011.04.011

4.6. Supplements (chapter 4)

Table S1: Primer sequences and GeneBank (Vector Base ID) numbers for target and reference genes used throughout the study

Construct	Forward 5' - 3'	Reverse 5' - 3'	Vector Base #	Gene Bank Acc #
pFastBac1-CYP6P9a	CCAGGCTTTCGTGTTCTTCCTCGC	GCAGCGAGTTCCCTCTGG		
pFastBac1-CYP6P9b	CCAGGCCTTCATCTTCTTCCTGGCTG	GCAGCGAGTTCCAGCTGG		
Sequencing primer	CTTACCCATCTCTCGTCCGC	TCAGTCCGACTTTGGTCTGC		
For recombinant expression only				
CYP6P9a			AFUN015792	KR866022.1
CYP6P9b			AFUN015889	KR866046.1
Ag CPR				AY183375.1

Table S2. Calculated V_{max} (pmol product/min x mg protein $^{-1}$) and K_m (µM) values of Michaelis-Menten kinetics of BOMFC O-debenzylation by *An. funestus* CYP6P9a and CYP6P9b with increasing concentrations of deltamethrin, permethrin and their respective 4'OH-metabolites (n=4).

CYP6P9a		c (inhibitor) in µM							
		100 µM	95 % CI*	10 µM	95 % CI	1 µM	95 % CI	0 µM	95 % CI
Deltamethrin	K_m	10.6	9.76-11.4	7.71	6.61-8.98	10.4	8.32-12.9	10.6	8.17-13.6
	V_{max}	155	151-158	174	167-181	186	175-198	183	170-197
Permethrin	K_m	7.84	7.12-8.62	7.51	6.53-8.62	9.65	7.9-11.8	11.2	8.98-13.9
	V_{max}	166	162-170	186	179-192	194	183-205	196	184-209
4'OH-deltamethrin	K_m	74.8	63.2-88.9	9.21	8.1-10.5	7.81	6.19-9.82	8.64	6.72-11.1
	V_{max}	104	97.2-113	165	159-170	188	177-200	191	178-204
4'OH-permethrin	K_m	51.2	31.7-83.4	10.8	9.84-11.9	5.98	5.07-7.06	5.63	4.66-6.8
	V_{max}	38.5	32.4-46	107	104-110	122	117-127	117	112-123

CYP6P9b		c (inhibitor) in µM							
		100 µM	95 % CI	10 µM	95 % CI	1 µM	95 % CI	0 µM	95 % CI
Deltamethrin	K_m	7.47	6.95-8.03	10.5	8.88-12.5	14.6	11.4-18.4	12.4	9.69-15.8
	V_{max}	145	142-147	163	156-171	176	165-189	173	162-184
Permethrin	K_m	4.99	4.61-5.41	5.26	4.63-5.98	6.19	5.09-7.5	6.82	5.56-8.35
	V_{max}	142	139-145	157	152-162	167	159-175	170	161-179
4'OH-deltamethrin	K_m	104	82.9-132	23	20.2-26.3	8.65	7.39-10.1	6.14	5.05-7.44
	V_{max}	63.1	56.7-71.2	125	120-130	163	156-170	162	154-170
4'OH-permethrin	K_m	52.4	35-79	5.58	4.65-6.67	2.11	1.71-2.58	1.81	1.5-2.16
	V_{max}	37.9	32.7-44.7	84.6	81.2-88.2	101	96.6-105	92.6	89.1-96.2

* 95 % confidence intervals

Table S3. Depletion of deltamethrin, permethrin, 4'OH deltamethrin and 4'OH permethrin (2µM each) after 90min incubation at 30°C with recombinantly expressed CYP6P9a and CYP6P9b. Data are mean values ± SD (n=4).

	% Insecticide depletion (± SD)			
	Deltamethrin	Permethrin	4'OH deltamethrin	4'OH permethrin
CYP6P9a	41.1 ± 0.857	42.1 ± 3.07	65.3 ± 0.738	67.3 ± 0.834
CYP6P9b	40.4 ± 4.97	61.5 ± 3.34	68.9 ± 1.3	74.3 ± 1.38

Table S4. Log dose-probit mortality data (24h) of cis- and trans-permethrin towards adults of *An. funestus strains* FANG and FUMOZ-R in glazed tile contact bioassays upon 30 min exposure. LC_{50}-values are expressed in mg/m². RR = resistance ratio.

Compound	*An. funestus* FANG				*An. funestus* FUMOZ-R				RR
	LC_{50}	95 % CI	Slope ± SE	n	LC_{50}	95 % CI	Slope ± SE	n	
cis-Permethrin	0.154	0.096-0.228	2.06 0.361	210	1.6	0.933-2.63	1.82 0.253	210	10.4
trans-Permethrin	1.41	1.04-1.92	3.8 0.72	210	9.24	6.24-13.8	1.84 0.255	210	6.55

Table S5. Michaelis-Menten kinetics of BOMFC and BFC O-debenzylation, and EFC O-dealkylation by recombinantly expressed CYP6P9 variants. Data are mean values ± 95 % confidence intervals (n=4). V_{max} is given in pmol product/min x mg protein $^{-1}$ and K_m in µM.

		CYP6P9a		**CYP6P9a^{I310V}**	
	V_{max}	196	184 - 209	167	163 - 171
	K_m	11.2	8.98 - 13.9	3.21	2.87 - 3.59
BOMFC		**CYP6P9b**		**CYP6P9b^{V310I}**	
	V_{max}	170	161 - 179	172	167 - 178
	K_m	6.82	5.56 - 8.35	7.16	6.35 - 8.07
		CYP6P9a		**CYP6P9a^{I310V}**	
	V_{max}	11	10.4 - 11.7	8.78	8.03 - 9.58
	K_m	9.18	7.37 - 11.4	3.53	2.28 - 5.32
BFC		**CYP6P9b**		**CYP6P9b^{V310I}**	
	V_{max}	33.8	31.5 - 36.1	40.8	38.7 - 43.1
	K_m	6.12	4.71 - 7.89	10.1	8.23 - 12.3
		CYP6P9a		**CYP6P9a^{I310V}**	
	V_{max}	8.04	6.76 - 9.95	10.6	9.38 - 12
	K_m	186	137 - 263	20.4	13.5 - 30.5
EFC		**CYP6P9b**		**CYP6P9b^{V310I}**	
	V_{max}	13.8	13.2 - 14.4	55.3	50.5 - 60.8
	K_m	57.8	52 - 64.3	39	30.4 - 50.1

Table S6. Michaelis-Menten kinetics of deltamethrin and permethrin hydroxylation by recombinantly expressed CYP6P9 variants. Data are mean values ± 95 % confidence intervals (n=4). V_{max} is given in pmol product/min x mg protein^{-1} and K_m in µM.

		CYP6P9a		CYP6P9a^{I310V}	
Deltamethrin	V_{max}	13.7	12.3 - 15.4	6.65	6.23 - 7.09
	K_m	19.2	14.3 - 26	7.6	6.09 - 9.46
	K_{cat}	1.15	1.03 - 1.29	0.47	0.44 - 0.502
		CYP6P9b		CYP6P9b^{V310I}	
	V_{max}	10.6	9.39 - 12.2	13.7	13 - 14.5
	K_m	27	19.7 - 37.5	14.7	12.5 - 17.3
	K_{cat}	1.61	1.43 - 1.85	21	20 - 37.6

		CYP6P9a		CYP6P9a^{I310V}	
Permethrin	V_{max}	1.97	1.84 - 2.11	3.07	2.51 - 3.83
	K_m	10.1	8.06 - 12.7	13.4	7.19 - 25.5
	K_{cat}	0.166	0.155 - 0.178	n.a.	-
		CYP6P9b		CYP6P9b^{V310I}	
	V_{max}	7.89	7.47 - 8.33	58	51.3 - 66.8
	K_m	15.7	13.4 - 18.3	62.5	49 - 81.2
	K_{cat}	1.2	1.14 - 1.27	n.a.	-

Table S7. Inhibition of the O-debenzylation of 7-benzyloxymethoxy-4-(trifluoromethyl)-coumarin (BOMFC) by recombinantly expressed *An. funes*tus mutant CYP6P9a^{I310V} and CYP6P9b^{V310I} by pyrethroid insecticides, their metabolites and common P450 inhibitors. Date are mean values (n=4).

mCYP6P9a	IC_{50}	95 % CI*
PBO	7.37	4.82 - 11.5
1-ABT		
Triflumizole	1.28	0.889 - 1.81
Prochloraz	0.24	0.156 - 0.353
Uniconazole	1.68	1.32 - 2.14
Propiconazole	5.73	4.12 - 7.95
Ketoconazole	2.36	1.22 - 4.56
Triadimefon	41.9	30.5 - 61.7
Triadimenol	> 100	
Tebuconazole	7.79	6.92 - 8.78
Deltamethrin	> 100	
Permethrin	> 100	
4'OH Permethrin	24.4	18.4 - 33.6
4'OH Deltamethrin	8.07	6.86 - 9.45
Cypermethrin	> 100	
Bifenthrin	> 100	
Epoxiconazole	37.9	26.4 - 82.4

mCYP6P9b	IC_{50}	95 % CI
PBO	0.835	0.613 - 1.13
1-ABT	151	120 - 190
Triflumizole	0.558	0.449 - 0.693
Prochloraz	0.061	0.0515 - 0.0733
Uniconazole	1.77	1.33 - 2.36
Propiconazole	3.31	2.63 - 4.14
Ketoconazole	0.425	0.354 - 0.509
Triadimefon	18.3	14.7 - 22.8
Triadimenol	> 100	
Tebuconazole	1.11	0.814 - 1.51
Deltamethrin	> 100	
Permethrin	> 100	
4'OH Permethrin	7.76	5.99 - 10.1
4'OH Deltamethrin	1.36	1.24 - 1.5
Cypermethrin	81.6	63.9 - 111
Bifenthrin	> 100	
Epoxiconazole	14.8	12.5 - 17.7

* 95 % confidence intervals

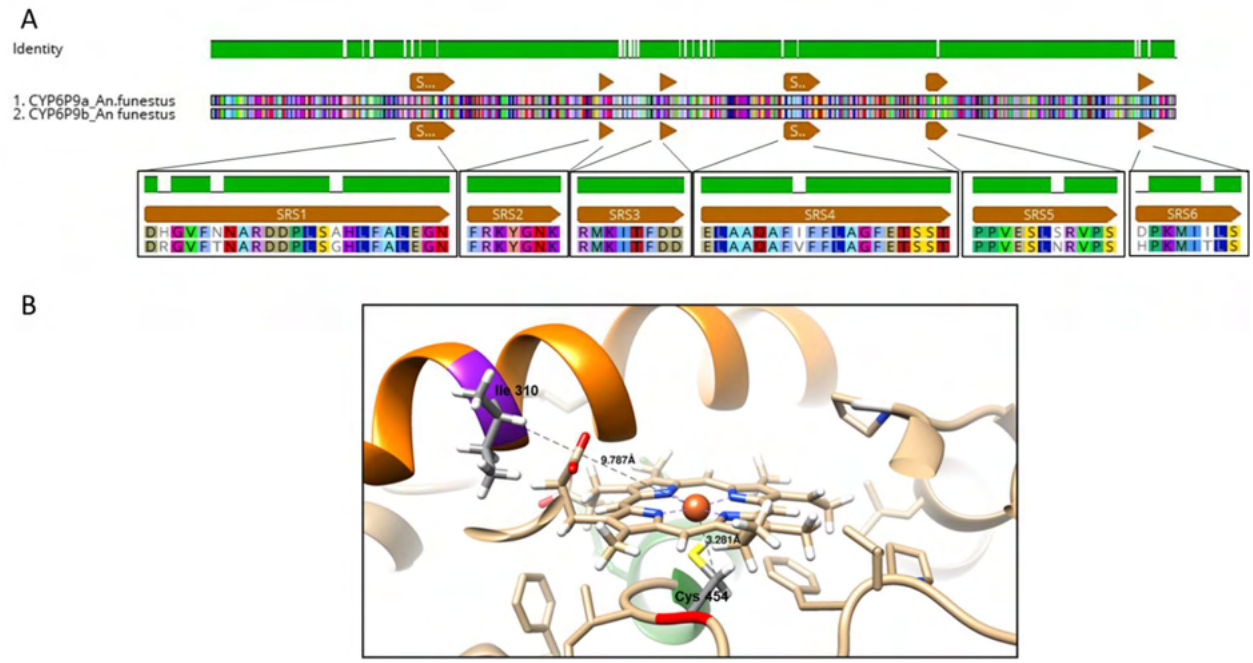

Figure S1. (A) Amino acid alignment of CYP6P9a and CYP6P9b revealed 94.3 % identity. Substrate recognition sites (SRS 1-6) are marked by brown arrows above and below the aligned sequences. The mutation site I/V310 in the I-helix is highlighted by a yellow arrow. (B) Predicted active site of CYP6P9a based on homology modelling employing human CYP3A4 (PDB ID: 1TQN). The I-helix is shown in orange and in purple the amino acid residue 310 (isoleucine) which differs between CYP6P9a (isoleucine) and CYP6P9b (valine). The heme-binding cysteine 454 is shown in red.

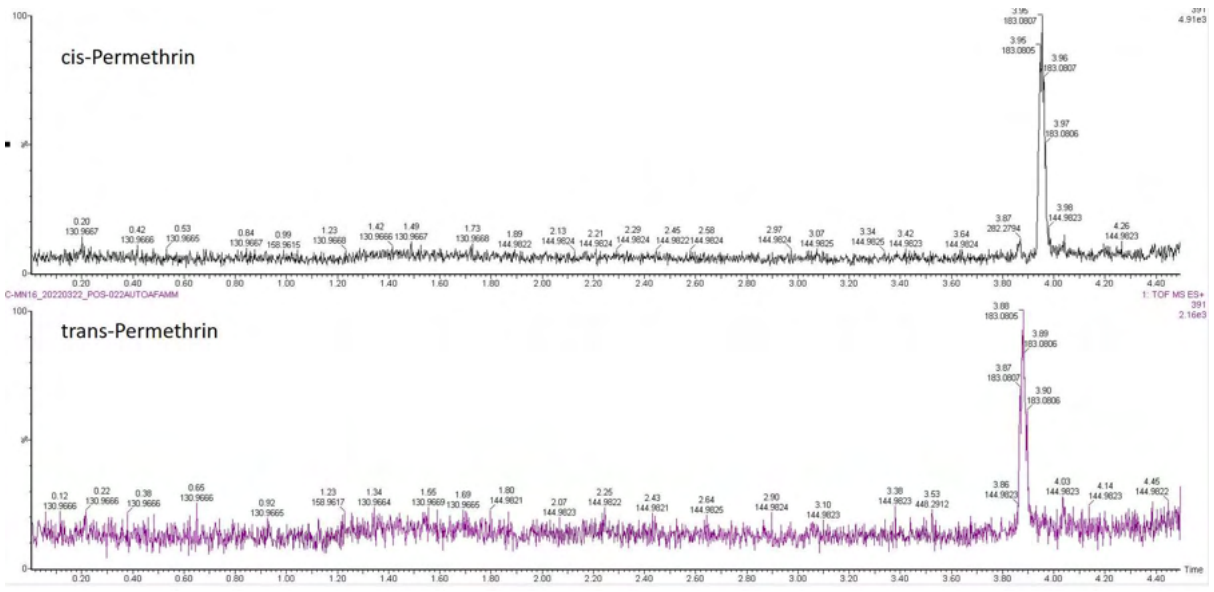

Figure S2. Total ion current chromatograms of the *cis*- and *trans*-permethrin isomers.

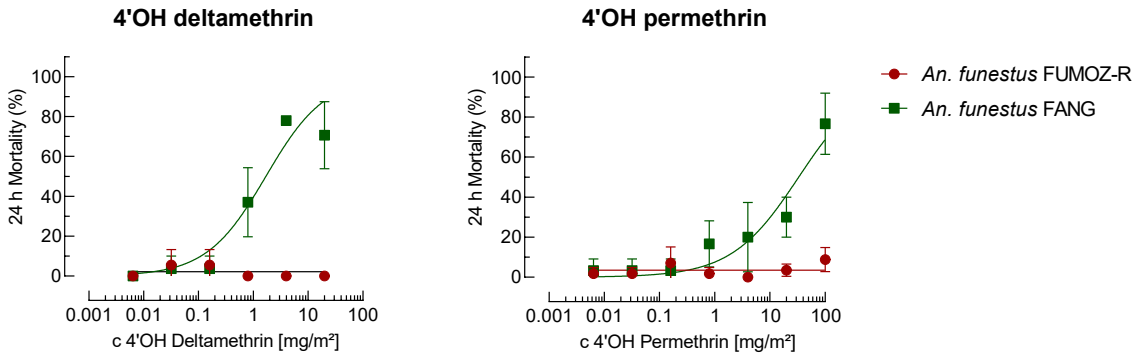

Figure S3. Dose response curves for (A) 4'OH deltamethrin and (b) 4'OH permethrin towards female adults of *An. funestus strains* FANG and FUMOZ-R in glazed tile bioassays (30min contact exposure; 24h bioassay).

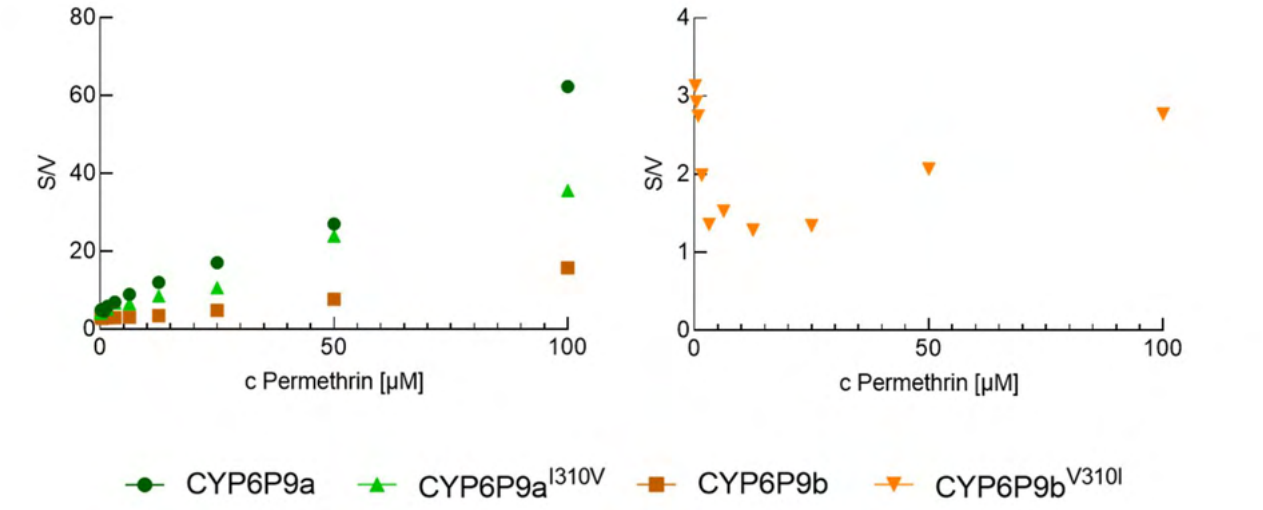

Figure S4. Hanes-Woolf linearization of Michaelis Menten kinetics of the hydroxylation of permethrin by CYP6P9 variants showing allosteric behaviour for CYP6P9b^{V310I}. Details on Michaelis-Menten kinetic based data analysis are given in the supporting information (table S3). Data are mean values ± SD (n=3).

5. Chapter 5. Resilience of transfluthrin to oxidative attack by duplicated CYP6P9 variants known to confer pyrethroid resistance in the major malaria mosquito *Anopheles funestus*

- Submitted manuscript in December 2022, to Pesticide Biochemistry and Physiology –

Melanie Nolden [a, b], Robert Velten [a], Mark J.I. Paine [b], Ralf Nauen [a], *

[a] Bayer AG, Crop Science Division, Alfred Nobel Str. 50, D-40789 Monheim am Rhein, Germany

[b] Department of Vector Biology, Liverpool School of Tropical Medicine, Pembroke Place, Liverpool L3 5QA, United Kingdom

* Corresponding author:

Email: ralf.nauen@bayer.com

Abstract

Resistance to common pyrethroids, such as deltamethrin and permethrin is widespread in the malaria mosquito *Anopheles funestus* and mainly conferred by upregulated cytochrome P450 monooxygenases (P450s). In the pyrethroid resistant laboratory strain *An. funestus* FUMOZ-R the duplicated genes *CYP6P9a* and *CYP6P9b* are highly upregulated and have been shown to metabolize various pyrethroids, including deltamethrin and permethrin. Here, we recombinantly expressed CYP6P9a and CYP6P9b from *An. funestus* using a baculovirus expression system and evaluated the interaction of the multifluorinated benzyl pyrethroid transfluthrin with these enzymes by different approaches. First, by Michaelis-Menten kinetics in a fluorescent probe assay with the model substrate 7-benzyloxymethoxy-4-trifluoromethylcoumarin (BOMFC), we showed the inhibition of BOMFC metabolism by increasing concentrations of transfluthrin. Second, we tested the metabolic capacity of recombinantly expressed CYP6P9 variants to degrade transfluthrin utilizing UPLC-MS/MS analysis and detected low depletion rates, explaining the virtual lack of resistance of strain FUMOZ-R to transfluthrin observed in previous studies. However, as both approaches suggested an interaction of CYP6P9 variants with transfluthrin, we analyzed the oxidative metabolic fate and detected significant, but low amounts of an M-2 transfluthrin metabolite, supporting the reduced capacity of CYP6P9 variants to degrade transfluthrin. Based on the detected metabolite we hypothesize oxidative attack of the *gem*-dimethyl substituted cyclopropyl moiety, resulting in the formation of an allyl cation upon ring opening. In conclusion, these findings support the resilience of transfluthrin to P450-mediated pyrethroid resistance, and thus, reinforces its employment as an important resistance-breaking pyrethroid in resistance management strategies to control the major malaria vector *An. funestus*.

Keywords: Cytochrome P450, transfluthrin, CYP6P9a, CYP6P9b, pyrethroids, *Anopheles*

5.1. Introduction

Malaria remains the most important vector-borne disease, especially in sub-Saharan Africa (SSA), transmitted by Anopheline mosquitoes of two species complexes, *Anopheles gambiae* s.l. and *Anopheles funestus* s.l. (Diptera: Culicidae). Out of an estimated 627,000 malaria deaths in 2020, >95 % were reported from the African continent (WHO, 2021). *An. funestus* is one of the major malaria vectors in SSA (Coetzee & Koekemoer, 2013; Sinka et al., 2010), and its control mainly relies on the application of insecticides, particularly as indoor residual spray (IRS) and long-lasting insecticidal nets (LLINs) (Sinka et al., 2016). Although insecticide driven interventions, particularly pyrethroid-treated LLINs, largely contributed to a massive decrease of reported malaria cases between 2000 and 2015 (Bhatt et al., 2015), an increased evolution of insecticide resistance has been observed (Hemingway et al., 2016; Ranson & Lissenden, 2016).

The insecticide portfolio to support vector control interventions is rather limited in terms of modes of action and chemical classes, so new high efficacy insecticides are urgently needed (Hoppé et al., 2016; Williams et al., 2019). Pyrethroids play a major role in Anopheline mosquito control, but high selection pressure resulted in increasing resistance levels jeopardizing the success of malaria control programs (Hemingway, 2018). Pyrethroids are fast acting insecticides targeting the insect neuronal voltage-gated sodium channels (VGSC) leading to rapid knock-down of the treated pests upon contact (Soderlund & Bloomquist, 1989). Based on the symptomology of poisoning they are broadly divided into type I (e.g. permethrin) and type II pyrethroids (e.g. deltamethrin), depending on the absence and presence of an α-cyano group, respectively (Soderlund, 2020). Transfluthrin (2,3,5,6-tetrafluorobenzyl(1R,3S)-3-(2,2-dichlorovinyl)-2,2-dimethylcyclopropane-carboxylate; syn. benfluthrin) is a volatile, enantiomerically pure type I pyrethroid, with a multifluorinated benzyl moiety instead of the more common 3-phenoxybenzyl moiety (Khambay, 2002). It exhibits good contact activity against adult mosquitoes (Horstmann & Sonneck, 2016), and has been shown to lack cross-resistance to 3-phenoxybenzyl substituted pyrethroids such as deltamethrin and cypermethrin in *An. funestus* strain FUMOZ-R (Nolden et al., 2021).

Pyrethroid insecticide resistance in pest insects, including vectors of human diseases, is predominantly conferred by target-site mutations in the VGSC, i.e., amino acid substitutions affecting pyrethroid binding (Rinkevich et al., 2013; Scott, 2019), and increased detoxification

driven by the constitutive overexpression and/or duplication of genes of metabolic enzymes, particularly cytochrome P450-monooxygenases (P450s) (Nauen et al., 2022; Vontas et al., 2020). In *An. funestus* resistance against different pyrethroid chemotypes has been shown to be conferred by upregulated P450s, but not target-site resistance (Irving & Wondji, 2017; Riveron et al., 2014; Wondji et al., 2009, 2022). Several *An. funestus* P450s were functionally expressed and shown to metabolize various pyrethroids, such as permethrin (type I) and deltamethrin (type II) (Ibrahim et al., 2018; Riveron et al., 2013, 2014, 2017; Wamba et al., 2021). Among those P450s recombinantly expressed, especially CYP6P9a and CYP6P9b are playing a key role in pyrethroid resistance in *An. funestus,* including the resistant laboratory reference strain FUMOZ-R originating from Mozambique (Nolden et al., 2022a; Williams et al., 2019; Wondji et al., 2022). Previous work revealed that common phenoxybenzyl-pyrethroids, such as deltamethrin are primarily hydroxylated at the 4'para position of the phenoxybenzyl-ring, as for example shown for CYP6M2 of *An. gambiae* (Stevenson et al., 2011). The same authors also demonstrated that 4'OH deltamethrin is further metabolised by the same enzyme resulting in the formation of cyano(3-hydroxyphenyl) methyl deltamethrate. Very recently, sequential metabolism of both deltamethrin and permethrin via hydroxylation followed by ether cleavage has been demonstrated in studies employing recombinantly expressed CYP6P9a and CYP6P9b of *An. funestus* (Nolden et al., 2022b).

We recently demonstrated that *An. funestus* strain FUMOZ-R lacks phenotypic cross-resistance to transfluthrin when compared to a susceptible reference strain, FANG. However, increased adult toxicity (synergism) has been observed in glazed tile bioassays in combination with P450 inhibitors such as piperonyl butoxide, principally suggesting oxidative metabolism of transfluthrin (Nolden et al., 2021). The objective of this study was to investigate the metabolic capacity of recombinantly expressed CYP6P9a and CYP6P9b to degrade transfluthrin by various approaches, including fluorescent probe competition assays and UPLC-MS/MS analysis to elucidate transfluthrin depletion rates and potential metabolites.

5.2. Material and Methods

5.2.1. Chemicals

Transfluthrin (CAS: 118712-89-3), β-Nicotinamide adenine dinucleotide 2'-phosphate (NADPH) reduced tetrasodium salt hydrate (CAS: 2646-71-1 anhydrous, purity ≥93 %) and 7-hydroxy-4-trifluoromethylcoumarin (HFC; CAS: 575-03-1, 98) were purchased from Sigma Aldrich/Merck (Darmstadt, Germany). Transfluthrin derivatives TF-0, TF-1, TF-3, and TF-5 were of analytical grade and obtained internally from Bayer (Leverkusen, Germany). NADPH regeneration system (V9510) was purchased from Promega (Madison, USA). 7-benzyloxymethoxy-4-trifluoromethylcoumarin (BOMFC; CAS: 277309-33-8; purity 95 %) was synthesized by Enamine Ltd. (Riga, Latvia). All other chemicals and solvents were of analytical grade and purchased from Sigma/Aldrich (Darmstadt, Germany) unless otherwise stated.

5.2.2. Heterologous expression of CYP6P9a and CYP6P9b

CYP6P9a (VectorBase ID: AFUN015792) and *CYP6P9b* (AFUN015889) were recombinantly co-expressed with NADPH cytochrome P450 reductase (CPR) from *An. gambiae* (GenBank: AY183375.1; Table S1) in High-5 insect cells as previously described (Nolden et al., 2022a). In brief: PFastBac1 vectors containing each gene of interest - codon optimized for expression in lepidopteran cell lines - were created employing the GeneArt server (ThermoFisher, Waltham, MA, USA). Plasmids were transformed using MaxEfficiancyDH10 (Invitrogen, Waltham, MA, USA) according to manufacturer instructions and isolated using large construct Kit (Qiagen, Hilden, Germany) following standard protocols. The recombinant baculovirus DNA was constructed and transfected into *Trichoplusia ni* High-5 cells using the Bac-to-Bac baculovirus expression system as described elsewhere (Manjon et al., 2018). CYP6P9a and CYP6P9b were co-expressed with *An. gambiae* CPR with a multiplicity of infection (MOI) of 1 (P450): 0.5 (CPR). High-5 cells were diluted to 1.5 x 10^6 cells/mL and incubated with 0.5 % fetal bovine serum (FBS), 0.2 mM *delta*-aminolevulinic acid (*d*-ALA), 0.2 mM iron (III) citrate and the respective amount of virus for 52 hours at 27 °C and 120 rpm. After harvesting, cells were resuspended in homogenization buffer (0.1 M K_2HPO_4, 1 mM DTT, 1 mM EDTA, 200 mM sucrose, pH 7.6). FastPrep device (MP Biomedicals, Irvine, CA, USA) was used for grinding the cells following a 10 min centrifugation step at 4 °C and 700 g. The resulting supernatant was centrifuged for one hour at 100,000 g and 4 °C. Afterwards the microsomal pellet was resuspended with a Dounce tissue grinder in buffer (0.1 M K_2HPO_4, 0.1 mM EDTA, 1 mM DTT,

5 % glycerol, pH 7.6). The amount of protein was measured using Bradford reagent (Bradford, 1976).

5.2.3. Fluorescent probe assays using BOMFC

Inhibition assays were conducted with minor changes as described previously (Nolden et al., 2022a). In brief: recombinantly expressed CYP6P9a and CYP6P9b were diluted in buffer (0.1 M K_2HPO_4, 0.1 mM EDTA, 1 mM DTT, 5 % glycerol pH 7.6), incl. 0.05% bovine serum albumin (BSA) and 0.01% zwittergent 3-10 to 0.16 mg/ml. BOMFC (stock solution 50 mM in DMSO) was diluted to eleven different concentration ranging from 200 µM to 0.0195 µM (final assay concentration (fc)) in assay buffer (0.1 M potassium-phosphate buffer (pH 7.6), containing 0.01% zwittergent 3-10 and different pyrethroid concentrations with and without 1 mM NADPH. Twenty-five µL of enzyme solution, corresponding to 4 µg total protein, were incubated with 25 µL of substrate solution in black 384-well plates (Fluotrac, Greiner bio-one, Belgium) for one hour at 20 ± 1 °C. Each reaction was replicated four times and the fluorescent product HFC was measured at 405 nm while excited at 510 nm. Substrate saturation kinetics (Michaelis-Menten plots) and enzyme inhibition were analyzed by non-linear regression using GraphPad Prism 9.0 (GraphPad Software, San Diego, Ca, USA). IC_{50} values were calculated to express the inhibition of BOMFC *O*-debenzylation by different pyrethroids.

5.2.4. UPLC-MS/MS analysis

Analysis of transfluthrin metabolism by CYP6P9a and CYP6P9b was conducted as described previously (Nolden et al., 2022b) with minor modifications. Forty µL of recombinantly expressed CYP6P9a and CYP6P9b, diluted to 0.8 mg protein ml^{-1} in buffer (0.1 M K_2HPO_4, 1 mM DTT, 0.1 mM EDTA, 5 % Glycerol, pH 7.6, containing 0.05 % BSA) were incubated with 10 µL of 10 µM (fc) transfluthrin (diluted in 0.1 M K_2HPO_4, 0.05 % bovine serum albumin (BSA), pH 7.6) and 50 µL assay buffer (0.1 M K_2HPO_4, pH 7.6) with and without NADPH regeneration system in 1 mL 96-deepwell plates (Protein-LoBind, Eppendorf). Microsomal fractions from High-5 cells infected with virus containing PFastbac1 vector with no inserted DNA served as control. Each reaction was replicated four times and incubated for 90 minutes at 30 °C and 450 rpm (Thermomixer, Eppendorf). The reactions were stopped with 400 µL ice-cold acetonitrile (100 %), incubated at 4 °C overnight, and centrifuged for 30 minutes at 3000 g and 4 °C. The resulting supernatant was analysed using an Agilent 1290 Infinity II UPLC system, equipped with a Waters Acquity BEH C18 column (2.1 x 50 mm, 1.7 µm). Chromatography

was carried out using 2 mM ammonium-acetate in methanol and 2 mM ammonium-acetate in water including 1 % acetic acid as the eluent in gradient mode. After positive electrospray ionization, ion transitions were recorded on a Sciex API6500 Qtrap. Transfluthrin was measured in positive ion mode (ion transition: transfluthrin 371 > 163). The linear range for transfluthrin quantification was 0.5 - 200 ng/mL.

5.2.5. Metabolite analysis

UPLC-TOF-MS was employed using an Acquity UPLC I-Class system coupled to a cyclic iMS mass spectrophotometer (Waters Corporation, MA, USA). A Zorbax Eclipse Plus C18 column (2.1 x 100 mm, 1.8 µm) (Agilent Technologies, CA, USA) was used with a column oven temperature of 60 °C. The mobile phase consisted of acetonitrile/0.25 % formic acid (eluent A) and water/0.25 % formic acid (eluent B) in gradient mode and a flow rate of 0.6 mL min^{-1} with eluent B starting at 90% for 4.5 min, decreasing to 5% for 2.5 min and increasing to 90% again for 1 min. The mass spectrometer operated in positive ion mode with a full scan resolution of 60 000 fwhm (full width at half maximum). Measurements and metabolite search were conducted with MassLynx and Metabolynx software (Waters Corporation, MA, USA).

5.2.6. Cheminformatic analysis

Minimum energy conformer alignments and three-dimensional ball-and-stick models of transfluthrin and deltamethrin in standard normalized orientation were generated using the software package Maestro (Schroedinger Release 2020-1: Maestro Schroedinger LLC, New York, NY, USA). Isosurfaces of the Fukui functions for attack by an electrophile as calculated from DFT (density functional theory) densities were done as described elsewhere (Beck, 2005).

5.3. Results

5.3.1. Fluorescent probe competition assays

Transfluthrin and its defluorinated benzyl derivative TF-0 showed IC_{50}-values for the inhibition of the *O*-debenzylation of BOMFC by recombinantly expressed CYP6P9a and CYP6P9b at similar micromolar concentrations (Table 1), therefore, principally suggesting interaction with the catalytic site of both P450s. Deltamethrin and the two other tested transfluthrin derivatives, TF-1 and TF-5 (Figure 1), exhibited IC_{50}-values of >100 µM, suggesting a weaker interaction with both enzymes (Table 1).

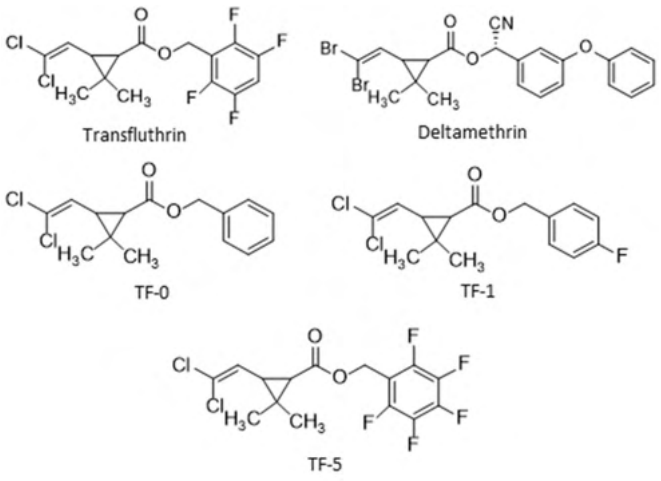

Figure 1. Chemical structures of deltamethrin, transfluthrin and its derivatives used in this study

Table 1. Interaction of pyrethroids with CYP6P9a and CYP6P9b. Inhibition of BOMFC O-debenzylation by recombinantly expressed CYP6P9a and CYP6P9b by transfluthrin, TF-5, TF-1 and TF-0. Data are mean values ± CI 95% (n=4). Deltamethrin data was taken from Nolden et al., 2022b.

Compound	CYP6P9a		CYP6P9b	
	IC_{50} (µM)	95 % CI*	IC_{50} (µM)	95 % CI*
Transfluthrin	66.3	50.3-92.6	69.9	49.6-105
TF-0	44.7	38.2-52.8	70.2	52-103
TF-5	> 100 µM		> 100 µM	
TF-1	> 100 µM		> 100 µM	
Deltamethrin	> 100 µM		> 100 µM	

* 95 % confidence intervals

Steady-state kinetic analyses of the *O*-debenzylation of BOMFC by recombinantly expressed CYP6P9a and CYP6P9b in the absence and presence of different concentrations of transfluthrin are shown in Figure 2. Further studies revealed a mixed type competitive/non-competitive inhibition (Table S2) based on kinetic characteristics of reversible P450 inhibition models (Fowler & Zhang, 2008). At the highest tested transfluthrin concentration of 100 µM the K_m-value for BOMFC significantly increased for both CYP6P9a and CYP6P9b, whereas the V_{max} values significantly decreased compared to co-incubations with 1 µM transfluthrin (Table S2).

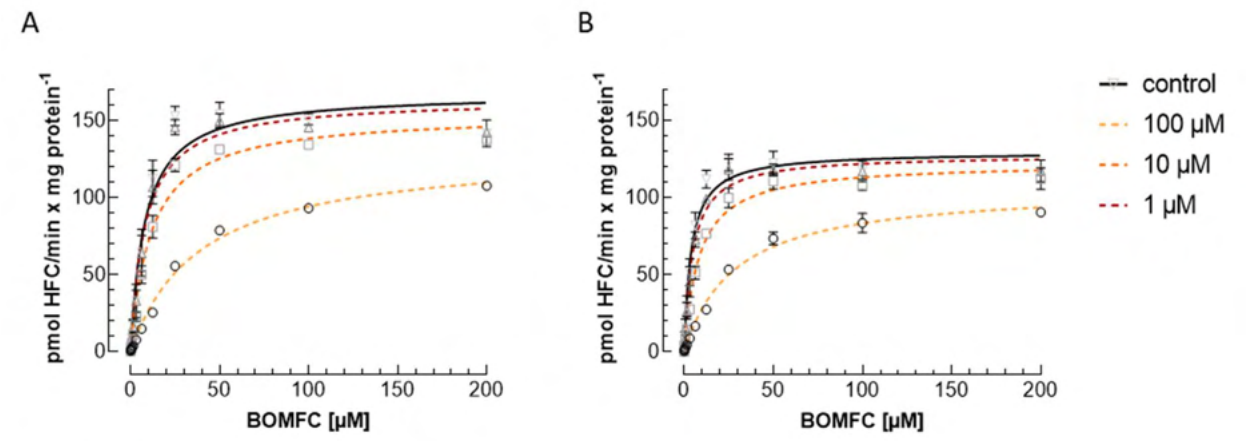

Figure 2. Effect of transfluthrin on the *O*-debenzylation of 7-benzyloxymethoxy-4-(trifluoromethyl)-coumarin (BOMFC) by recombinantly expressed *An. funestus* CYP6P9 variants. Michaelis–Menten kinetics of (A) CYP96P9a- and (B) CYP6P9b-mediated BOMFC metabolism at increasing concentrations of transfluthrin. Data are mean values ± SD (n=4). Reaction velocity is defined as pmol 7-hydroxy-4-trifluoromethylcoumarin (HFC) / min x mg protein. Details on Michaelis-Menten kinetic based data analysis are given in the Supporting Information, table S2.

5.3.2. Metabolism of transfluthrin by recombinantly expressed CYP6P9a and CYP6P9b

UPLC-MS/MS analysis revealed modest depletion of transfluthrin when incubated with recombinantly expressed CYP6P9 variants in the presence of NADPH in comparison to the control (empty virus, expressed in High-5 cells), and CYP6P9 variants in the absence of NADPH (Figure 3A). We observed no difference in the depletion of transfluthrin between microsomal membrane preparations expressing CYP6P9a or CYP6P9b (Table S3), confirming the results obtained in fluorescent probe competition assays (Table 1). Thus, suggesting that both enzymes exhibit the same capacity to interact with transfluthrin. Interestingly, we detected a significant depletion of transfluthrin between control-virus and microsomal membranes containing CYP6P9 variants but incubated in the absence of NADPH, most likely indicating sequestration. Metabolite identification employing UPLC-TOF-MS revealed the presence of DCCA, 3-(2,2-dichlorovinyl)-2,2-dimethylcyclo-propanecarboxylic acid (M-162; Figure S1), at very low levels in all samples, except those prepared from transfluthrin incubations without microsomal membranes, suggesting transfluthrin hydrolysis by microsomal preparations of High-5 cells irrespective of the expression of CYP6P9 variants and the presence or absence of NADPH. In addition, we identified a single M-2 metabolite (Figure 3B) specifically when recombinantly expressed CYP6P9a and CYP6P9b were incubated with transfluthrin in the

presence of NADPH, but not in the absence of the co-factor. We failed to detect an M+16 signal - indicative for a stable hydroxy metabolite - in any of the samples. The formation of the M-2 metabolite by both CYP6P9a and CYP6P9b likely explains the observed significant difference in oxidative transfluthrin metabolism in the presence and absence of NADPH shown in Figure 3A.

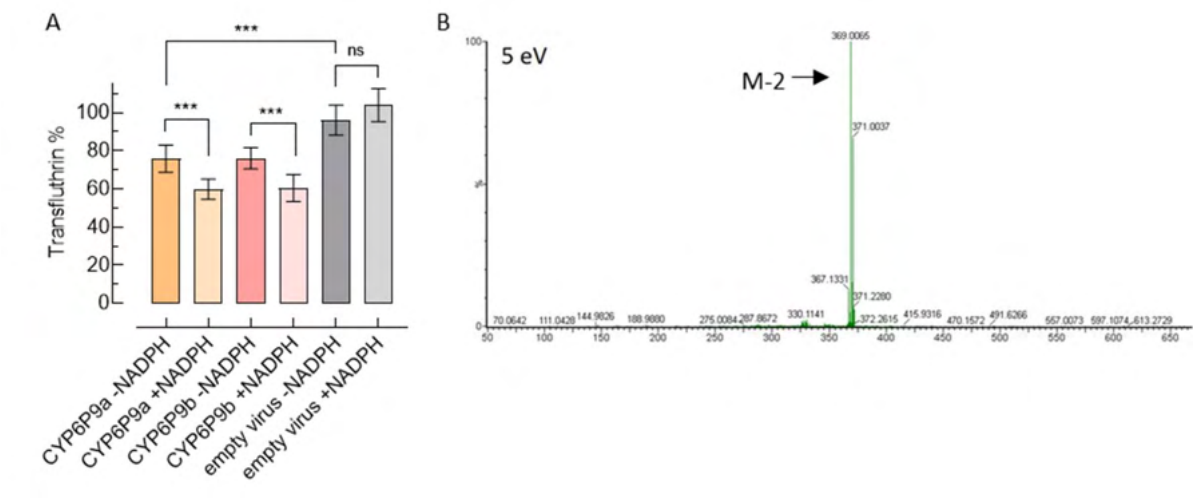

Figure 3. Transfluthrin metabolism by recombinantly expressed *An. funestus* CYP6P9 variants *in vitro*. (A) Transfluthrin remaining after 90 minutes incubation at 30°C with CYP6P9a and CYP6P9b, with and without NADPH. Empty virus served as control. Data are mean values ± CI 95% (n=6). (B) ESI-TOF high resolution MS/MS spectrum of the M-2 metabolite detected after incubation of transfluthrin with recombinantly expressed CYP6P9 variants in the presence of NADPH.

Based on these results, we suggest the hydroxylation of one of the methyl groups of the *gem*-dimethyl substituted cyclopropyl moiety, resulting in the formation of an intermediate allyl cation upon ring opening. Elimination of a proton results in the chemically stable M-2 metabolite proposed in Figure 4. A cheminformatic analysis of local reactivity descriptors by calculating the isosurfaces of the Fukui function (Beck, 2005) for an electrophilic attack of transfluthrin revealed the maximum of the Fukui function at the *gem*-dimethyl cyclopropyl moiety (Figure 5), providing *in-silico* support for the proposed oxidative metabolic fate of transfluthrin catalyzed by *An. funestus* CYP6P9a and CYP6P9b.

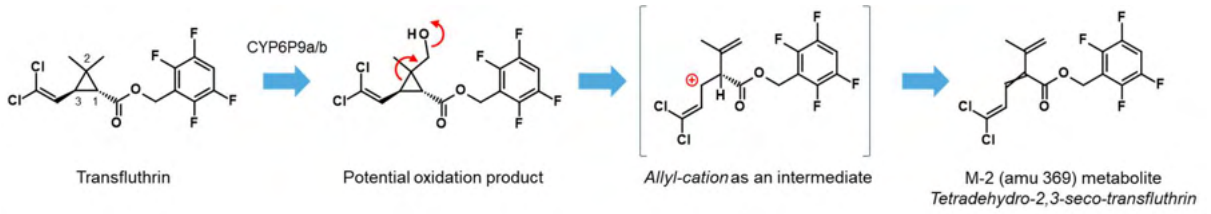

Figure 4. Oxidative metabolism of transfluthrin. (A) Proposed scheme for the oxidative metabolism of transfluthrin by *An. funestus* CYP6P9a and CYP6P9b based on a transfluthrin metabolite (M-2) detected by UPLC-MS/MS.

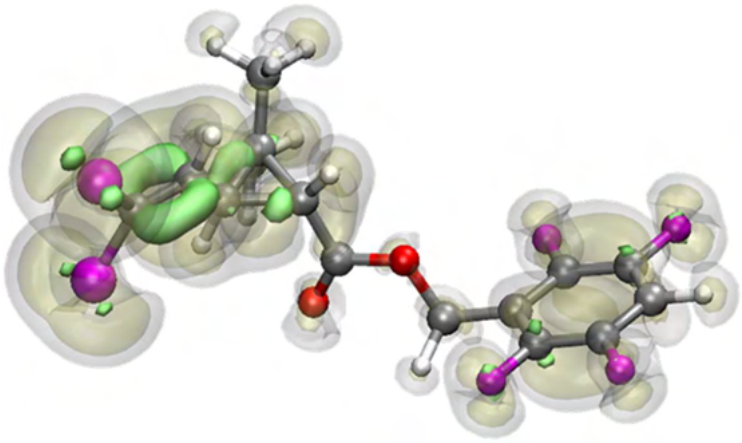

Figure 5. Cheminformatic modelling approaches. Isosurfaces of the Fukui functions for attack by an electrophile (green, solid; isolevel 0.05 au) as calculated from DFT densities for transfluthrin according to Beck et al. (2005).

5.4. Discussion

Transfluthrin is a multifluorinated benzyl pyrethroid which has been recently shown to virtually lack cross-resistance to common phenoxybenzyl pyrethroids such as deltamethrin and permethrin in *An. funestus* strain FUMOZ-R (Horstmann & Sonneck, 2016). When compared to the susceptible reference strain FANG, FUMOZ-R exhibited resistance ratios of >220-fold and 2.5-fold for deltamethrin and transfluthrin, respectively (Nolden et al., 2021). Previous studies demonstrated that the overexpression of duplicated P450s, *CYP6P9a* and *CYP6P9b*, confers high levels of pyrethroid resistance in *An. funestus* (Wondji et al., 2009, 2022), which has been confirmed for various pyrethroids by metabolism studies after functional expression of these enzymes (Nolden et al., 2022b; Riveron et al., 2013), whereas their metabolic capacity to interact with transfluthrin remains elusive.

Here we demonstrated by various approaches that recombinantly expressed CYP6P9a and CYP6P9b interact with transfluthrin and its non-fluorinated derivative TF-0. Transfluthrin (and TF-0) at mid-micromolar concentrations inhibited the *O*-debenzylation of the fluorescent probe substrate BOMFC by CYP6P9 variants. This provides a first line of evidence that transfluthrin binds to the active site of these enzymes and is possibly metabolized, as for example previously shown for hydroxylated phenoxybenzyl pyrethroids as products of the sequential metabolism of deltamethrin and permethrin, which themselves did not inhibit CYP6P9 variants (Nolden et al., 2022b). Interestingly, in another study, deltamethrin showed tight interaction with diethoxyfluorescein binding and its *O*-deethylation in fluorescent probe assays with *An. funestus* CYP6P9a and CYP6P9b (Ibrahim et al., 2015), whereas BOMFC (*O*-debenzylation) as a substrate failed to detect such an interaction with deltamethrin in the present and previous studies (Nolden et al., 2022b), suggesting that fluorescent substrates behave differently depending on the reaction type. Other P450s such as *An. gambiae* CYP6Z2 and *An. arabiensis* CYP6P4 have been demonstrated to tightly bind deltamethrin but lack the capacity to metabolize it (Ibrahim et al., 2016; Mclaughlin et al., 2008). Considering these results it is difficult to predict the metabolization of a pyrethroid insecticide solely based on inhibition data obtained in fluorescent probe assays with recombinantly expressed P450s. In contrast, similar fluorescent probe assays with P450s from other insect species such as whiteflies (CYP6CM1) and honeybees (e.g., CYP9Q3) have been predictive for the metabolism of a range of insecticidal chemotypes such as neonicotinoids, butenolides and diamides (Haas et al., 2021, 2022; Hamada et al., 2019). Future work is warranted to better understand the predictive power of such biochemical assays using recombinantly expressed P450s.

Next, we investigated the capacity of CYP6P9a and CYP6P9b to metabolize transfluthrin by employing UPLC-MS/MS and UPLC-TOF-MS analysis and detected two different metabolites, transfluthrin M-162 and transfluthrin M-2. Transfluthrin M-162 has been detected in all samples at rather low levels, except those lacking High-5 cell microsomal membranes, indicating an inherent capacity of High-5 cell microsomes to metabolize transfluthrin. The M-162 metabolite is known to represent DCCA (Yoshida, 2014), i.e., the acid moiety of transfluthrin resulting from its hydrolysis along with 2,3,5,6-tetrafluorobenzyl alcohol, representing the alcohol moiety of transfluthrin (Figure S1). Interestingly, High-5 cells originate from cabbage looper, *Trichoplusia ni*, which has been previously shown to partially

metabolize permethrin by microsomal hydrolysis, resulting in DCCA and 3-phenoxybenzylalcohol (Shono et al., 1979). DCCA is also a major metabolite in urinary excretions of rats administered transfluthrin (Yoshida, 2012). In a recent study with *Cunninghamella* spp., a fungi routinely used to model drug metabolism, it has been shown that the microsomal hydrolysis of transfluthrin is prevented by the addition of 1-aminobenzotriazole (Khan & Murphy, 2021), a well-described P450 inhibitor (de Montellano, 2018). Suggesting that most likely P450 activity in *Cunninghamella* spp. is mediating the hydrolysis of the ester bond of transfluthrin. However, if the detected DCCA levels in our study reflect microsomal hydrolysis of transfluthrin by High-5 cell P450s remains to be tested in future studies.

One of the major routes of oxidative pyrethroid metabolism is 4´hydroxylation of the phenoxybenzyl moiety (Khambay & Jewess, 2004). This route has been described for deltamethrin, permethrin, cypermethrin and other pyrethroids in mammalian and insect microsomal preparations (Anand et al., 2006; Scollon et al., 2009; Shono et al., 1979). Recombinantly expressed mosquito P450s such as *An. gambiae* CYP6M2 and *An. funestus* CYP6P9a/b have been shown to sequentially metabolize deltamethrin and permethrin by 4´hydroxylation and phenoxybenzyl ether cleavage (Nolden et al., 2022b; Stevenson et al., 2011). In the present study we failed to detect a hydroxylated M+16 transfluthrin metabolite, confirming the hypothesis that the *para*-position of the multifluorinated benzyl ring is protected from oxidative attack by P450s (Horstmann & Sonneck, 2016). Our study further supports this claim by fluorescent probe competition assays and the lack of interaction of CYP6P9 variants with the transfluthrin derivatives TF-1 and TF-5, which are fluorinated at the benzyl *para*-position. Instead, we detected a transfluthrin M-2 metabolite at low, but significant amounts after incubation of CYP6P9a and CYP6P9b with transfluthrin. This M-2 metabolite has not been detected in the absence of the cofactor NADPH, strongly supporting its P450-catalyzed formation. We hypothesize that this stable metabolite, tetradehydro-2,3-seco-transfluthrin (Figure 4), is formed by the oxidation of one of the methyl groups of the *gem*-dimethyl cyclopropyl moiety, followed by the elimination of a hydroxide ion, cationic cyclopropyl-methyl rearrangement and release of a proton (Suckling, 1988). Tetradehydro-2,3-seco-transfluthrin has been formally named by following IUPAC nomenclature and terminology (Favre & Powell, 2013). However, because we do not know the exact

hydroxylation site at the transfluthrin *gem*-dimethyl moiety, we could not provide the exact stereochemistry of the formed double-bond. Hydroxylation of one of the *gem*-dimethyl groups has also been described for deltamethrin upon incubation with recombinantly expressed *An. gambiae* CYP6M2 (Stevenson et al., 2011), but not *An. funestus* CYP6P9 variants (Nolden et al., 2022b). Previous work with other pyrethroids and insect microsomal preparations demonstrated that the proposed *gem*-dimethyl site for P450-mediated oxidative attack provides a valid hypothesis as a potential route for transfluthrin degradation (Shono et al., 1979).

In conclusion, we propose that the limited capacity of CYP6P9 variants to catalyse this reaction, as demonstrated here by a rather low depletion rate, likely explains the virtual lack of transfluthrin cross-resistance in *An. funestus* strain FUMOZ-R. Thus, qualifying transfluthrin as a valid option in resistance management strategies to control pyrethroid resistant populations of *An. funestus* under applied conditions

Declaration of Competing Interest

RN is employed by Bayer AG, a manufacturer of pesticides. MN is a PhD student affiliated with the LSTM and funded by the Innovative Vector Control Consortium (IVCC) and Bayer AG.

Acknowledgements

We are grateful to Johannes Glaubitz, Heidrun Thalheim, Birgit Nebelsiek and Udo König for the analytical support regarding the identification of transfluthrin metabolites.

5.5. References

Anand, S. S., Bruckner, J. V., Haines, W. T., Muralidhara, S., Fisher, J. W., & Padilla, S. (2006). Characterization of deltamethrin metabolism by rat plasma and liver microsomes. *Toxicology and Applied Pharmacology*, *212*(2), 156–166. https://doi.org/10.1016/j.taap.2005.07.021

Beck, M. E. (2005). Do Fukui Function Maxima Relate to Sites of Metabolism? A Critical Case Study. *Journal of Chemical Information and Modeling*, *45*(2), 273–282. https://doi.org/10.1021/ci049687n

Bhatt, S., Weiss, D. J., Cameron, E., Bisanzio, D., Mappin, B., Dalrymple, U., Battle, K. E., Moyes, C. L., Henry, A., Eckhoff, P. A., Wenger, E. A., Briet, O., Penny, M. A., Smith, T. A., Bennett, A., Yukich, J., Eisele, T. P., Griffin, J. T., Fergus, C. A., … Gething, P. W. (2015). The effect of malaria control on Plasmodium falciparum in Africa between 2000 and 2015. *Nature*, *526*, 207–211.

Bradford, M. M. (1976). A rapid and sensitive method for the quantitation of microgram quantities of protein utilizing the principle of protein-dye binding. *Analytical Biochemistry*, *72*(1), Art. 1. https://doi.org/10.1016/0003-2697(76)90527-3

Coetzee, M., & Koekemoer, L. L. (2013). Molecular Systematics and Insecticide Resistance in the Major African Malaria Vector Anopheles funestus. *Annual Review of Entomology*, *58*(1), Art. 1. https://doi.org/10.1146/annurev-ento-120811-153628

de Montellano, P. R. O. (2018). 1-Aminobenzotriazole: A Mechanism-Based Cytochrome P450 Inhibitor and Probe of Cytochrome P450 Biology. *Medicinal chemistry*, *8*(3), 038. https://doi.org/10.4172/2161-0444.1000495

Favre, H. A., & Powell, W. H. (2013). *Nomenclature of Organic Chemistry*. https://doi.org/10.1039/9781849733069

Fowler, S., & Zhang, H. (2008). In vitro evaluation of reversible and irreversible cytochrome P450 inhibition: Current status on methodologies and their utility for predicting drug-drug interactions. *The AAPS Journal*, *10*(2), Art. 2. https://doi.org/10.1208/s12248-008-9042-7

Haas, J., Glaubitz, J., Koenig, U., & Nauen, R. (2022). A mechanism-based approach unveils metabolic routes potentially mediating chlorantraniliprole synergism in honey bees, Apis mellifera L., by azole fungicides. *Pest Management Science*, *78*(3), Art. 3. https://doi.org/10.1002/ps.6706

Haas, J., Zaworra, M., Glaubitz, J., Hertlein, G., Kohler, M., Lagojda, A., Lueke, B., Maus, C., Almanza, M.-T., Davies, T. G. E., Bass, C., & Nauen, R. (2021). A toxicogenomics approach reveals characteristics supporting the honey bee (Apis mellifera L.) safety profile of the butenolide insecticide flupyradifurone. *Ecotoxicology and Environmental Safety*, *217*, 112247. https://doi.org/10.1016/j.ecoenv.2021.112247

Hamada, A., Wahl, G. D., Nesterov, A., Nakao, T., Kawashima, M., & Banba, S. (2019). Differential metabolism of imidacloprid and dinotefuran by Bemisia tabaci CYP6CM1

variants. *Pesticide Biochemistry and Physiology*, *159*, 27–33. https://doi.org/10.1016/j.pestbp.2019.05.011

Hemingway, J. (2018). Resistance: A problem without an easy solution. *Pesticide Biochemistry and Physiology*, *151*, 73–75. https://doi.org/10.1016/j.pestbp.2018.08.007

Hemingway, J., Ranson, H., Magill, A., Kolaczinski, J., Fornadel, C., Gimnig, J., Coetzee, M., Simard, F., Roch, D. K., Hinzoumbe, C. K., Pickett, J., Schellenberg, D., Gething, P., Hoppé, M., & Hamon, N. (2016). Averting a malaria disaster: Will insecticide resistance derail malaria control? *The Lancet*, *387*(10029), Art. 10029. https://doi.org/10.1016/S0140-6736(15)00417-1

Hoppé, M., Hueter, O. F., Bywater, A., Wege, P., & Maienfisch, P. (2016). Evaluation of Commercial Agrochemicals as New Tools for Malaria Vector Control. *Chimia*, *70*(10), 721–729. https://doi.org/10.2533/chimia.2016.721

Horstmann, S., & Sonneck, R. (2016). Contact Bioassays with Phenoxybenzyl and Tetrafluorobenzyl Pyrethroids against Target-Site and Metabolic Resistant Mosquitoes. *PLOS ONE*, *11*(3), Art. 3. https://doi.org/10.1371/journal.pone.0149738

Ibrahim, S. S., Amvongo-Adjia, N., Wondji, M. J., Irving, H., Riveron, J. M., & Wondji, C. S. (2018). Pyrethroid Resistance in the Major Malaria Vector Anopheles funestus is Exacerbated by Overexpression and Overactivity of the P450 CYP6AA1 Across Africa. *Genes*, *9*(3), Art. 3. https://doi.org/10.3390/genes9030140

Ibrahim, S. S., Riveron, J. M., Bibby, J., Irving, H., Yunta, C., Paine, M. J. I., & Wondji, C. S. (2015). Allelic Variation of Cytochrome P450s Drives Resistance to Bednet Insecticides in a Major Malaria Vector. *PLOS Genetics*, *11*(10), Art. 10. https://doi.org/10.1371/journal.pgen.1005618

Ibrahim, S. S., Riveron, J. M., Stott, R., Irving, H., & Wondji, C. S. (2016). The cytochrome P450 CYP6P4 is responsible for the high pyrethroid resistance in knockdown resistance-free Anopheles arabiensis. *Insect Biochemistry and Molecular Biology*, *68*, 23–32. https://doi.org/10.1016/j.ibmb.2015.10.015

Irving, H., & Wondji, C. S. (2017). Investigating knockdown resistance (kdr) mechanism against pyrethroids/DDT in the malaria vector Anopheles funestus across Africa. *BMC Genetics*, *18*(1), 76. https://doi.org/10.1186/s12863-017-0539-x

Khambay, B. P. S. (2002). Pyrethroid Insecticides. *Pesticide Outlook*, *13*(2), 49–54. https://doi.org/10.1039/B202996K

Khambay, B. P. S., & Jewess, P. J. (2004). *Pyrethroids* (Bd. 6, S. 1–29). Elsevier Pergamon, London. https://repository.rothamsted.ac.uk/item/895vq/pyrethroids

Khan, M. F., & Murphy, C. D. (2021). Cunninghamella spp. Produce mammalian-equivalent metabolites from fluorinated pyrethroid pesticides. *AMB Express*, *11*, 101. https://doi.org/10.1186/s13568-021-01262-0

Manjon, C., Troczka, B. J., Zaworra, M., Beadle, K., Randall, E., Hertlein, G., Singh, K. S., Zimmer, C. T., Homem, R. A., Lueke, B., Reid, R., Kor, L., Kohler, M., Benting, J., Williamson, M. S., Davies, T. G. E., Field, L. M., Bass, C., & Nauen, R. (2018). Unravelling the Molecular Determinants of Bee Sensitivity to Neonicotinoid Insecticides. *Current Biology*, *28*(7), Art. 7. https://doi.org/10.1016/j.cub.2018.02.045

Mclaughlin, L. A., Niazi, U., Bibby, J., David, J.-P., Vontas, J., Hemingway, J., Ranson, H., Sutcliffe, M. J., & Paine, M. J. I. (2008). Characterization of inhibitors and substrates of Anopheles gambiae CYP6Z2. *Insect Molecular Biology*, *17*(2), Art. 2. https://doi.org/10.1111/j.1365-2583.2007.00788.x

Nauen, R., Bass, C., Feyereisen, R., & Vontas, J. (2022). The Role of Cytochrome P450s in Insect Toxicology and Resistance. *Annual Review of Entomology*, *67*(1), Art. 1. https://doi.org/10.1146/annurev-ento-070621-061328

Nolden, M., Brockmann, A., Ebbinghaus-Kintscher, U., Brueggen, K.-U., Horstmann, S., Paine, M. J. I., & Nauen, R. (2021). Towards understanding transfluthrin efficacy in a pyrethroid-resistant strain of the malaria vector Anopheles funestus with special reference to cytochrome P450-mediated detoxification. *Current Research in Parasitology & Vector-Borne Diseases*, *1*, 100041. https://doi.org/10.1016/j.crpvbd.2021.100041

Nolden, M., Paine, M. J. I., & Nauen, R. (2022a). Biochemical profiling of functionally expressed CYP6P9 variants of the malaria vector Anopheles funestus with special reference to cytochrome b5 and its role in pyrethroid and coumarin substrate metabolism. *Pesticide Biochemistry and Physiology*, *182*, 105051. https://doi.org/10.1016/j.pestbp.2022.105051

Nolden, M., Paine, M. J. I., & Nauen, R. (2022b). Sequential phase I metabolism of pyrethroids by duplicated CYP6P9 variants results in the loss of the terminal benzene moiety and determines resistance in the malaria mosquito Anopheles funestus. *Insect Biochemistry and Molecular Biology*, *148*, 103813. https://doi.org/10.1016/j.ibmb.2022.103813

Ranson, H., & Lissenden, N. (2016). Insecticide Resistance in African Anopheles Mosquitoes: A Worsening Situation that Needs Urgent Action to Maintain Malaria Control. *Trends in Parasitology*, *32*(3), 187–196. https://doi.org/10.1016/j.pt.2015.11.010

Rinkevich, F. D., Du, Y., & Dong, K. (2013). Diversity and Convergence of Sodium Channel Mutations Involved in Resistance to Pyrethroids. *Pesticide Biochemistry and Physiology*, *106*(3), 93–100. https://doi.org/10.1016/j.pestbp.2013.02.007

Riveron, J. M., Ibrahim, S. S., Chanda, E., Mzilahowa, T., Cuamba, N., Irving, H., Barnes, K. G., Ndula, M., & Wondji, C. S. (2014). The highly polymorphic CYP6M7 cytochrome P450 gene partners with the directionally selected CYP6P9a and CYP6P9b genes to expand the pyrethroid resistance front in the malaria vector Anopheles funestus in Africa. *BMC Genomics*, *15*(1), Art. 1. https://doi.org/10.1186/1471-2164-15-817

Riveron, J. M., Ibrahim, S. S., Mulamba, C., Djouaka, R., Irving, H., Wondji, M. J., Ishak, I. H., & Wondji, C. S. (2017). Genome-Wide Transcription and Functional Analyses Reveal Heterogeneous Molecular Mechanisms Driving Pyrethroids Resistance in the Major Malaria

Vector Anopheles funestus Across Africa. *G3 (Bethesda, Md.)*, *7*(6), Art. 6. https://doi.org/10.1534/g3.117.040147

Riveron, J. M., Irving, H., Ndula, M., Barnes, K. G., Ibrahim, S. S., Paine, M. J. I., & Wondji, C. S. (2013). Directionally selected cytochrome P450 alleles are driving the spread of pyrethroid resistance in the major malaria vector Anopheles funestus. *Proceedings of the National Academy of Sciences*, *110*(1), Art. 1. https://doi.org/10.1073/pnas.1216705110

Scollon, E. J., Starr, J. M., Godin, S. J., DeVito, M. J., & Hughes, M. F. (2009). In Vitro Metabolism of Pyrethroid Pesticides by Rat and Human Hepatic Microsomes and Cytochrome P450 Isoforms. *Drug Metabolism and Disposition*, *37*(1), Art. 1. https://doi.org/10.1124/dmd.108.022343

Scott, J. G. (2019). Life and Death at the Voltage-Sensitive Sodium Channel: Evolution in Response to Insecticide Use. *Annual Review of Entomology*, *64*(1), 243–257. https://doi.org/10.1146/annurev-ento-011118-112420

Shono, T., Ohsawa, K., & Casida, J. E. (1979). Metabolism of trans- and cis-permethrin, trans- and cis-cypermethrin, and decamethrin by microsomal enzymes. *Journal of Agricultural and Food Chemistry*, *27*(2), Art. 2. https://doi.org/10.1021/jf60222a059

Sinka, M. E., Bangs, M. J., Manguin, S., Coetzee, M., Mbogo, C. M., Hemingway, J., Patil, A. P., Temperley, W. H., Gething, P. W., Kabaria, C. W., Okara, R. M., Van Boeckel, T., Godfray, H. C. J., Harbach, R. E., & Hay, S. I. (2010). The dominant Anopheles vectors of human malaria in Africa, Europe and the Middle East: Occurrence data, distribution maps and bionomic précis. *Parasites & Vectors*, *3*(1), 117. https://doi.org/10.1186/1756-3305-3-117

Sinka, M. E., Golding, N., Massey, N. C., Wiebe, A., Huang, Z., Hay, S. I., & Moyes, C. L. (2016). Modelling the relative abundance of the primary African vectors of malaria before and after the implementation of indoor, insecticide-based vector control. *Malaria Journal*, *15*(1), 142. https://doi.org/10.1186/s12936-016-1187-8

Soderlund, D. M. (2020). Neurotoxicology of pyrethroid insecticides. In *Advances in Neurotoxicology* (Bd. 4, S. 113–165). Elsevier. https://doi.org/10.1016/bs.ant.2019.11.002

Soderlund, D. M., & Bloomquist, J. R. (1989). Neurotoxic actions of pyrethroid insecticides. *Annual Review of Entomology*, *34*, 77–96. https://doi.org/10.1146/annurev.en.34.010189.000453

Stevenson, B. J., Bibby, J., Pignatelli, P., Muangnoicharoen, S., O'Neill, P. M., Lian, L.-Y., Müller, P., Nikou, D., Steven, A., Hemingway, J., Sutcliffe, M. J., & Paine, M. J. I. (2011). Cytochrome P450 6M2 from the malaria vector Anopheles gambiae metabolizes pyrethroids: Sequential metabolism of deltamethrin revealed. *Insect Biochemistry and Molecular Biology*, *41*(7), Art. 7. https://doi.org/10.1016/j.ibmb.2011.02.003

Suckling, C. J. (1988). The Cyclopropyl Group in Studies of Enzyme Mechanism and Inhibition. *Angewandte Chemie International Edition in English*, *27*(4), 537–552. https://doi.org/10.1002/anie.198805371

Vontas, J., Katsavou, E., & Mavridis, K. (2020). Cytochrome P450-based metabolic insecticide resistance in Anopheles and Aedes mosquito vectors: Muddying the waters. *Pesticide Biochemistry and Physiology*, *170*, 104666. https://doi.org/10.1016/j.pestbp.2020.104666

Wamba, A. N. R., Ibrahim, S. S., Kusimo, M. O., Muhammad, A., Mugenzi, L. M. J., Irving, H., Wondji, M. J., Hearn, J., Bigoga, J. D., & Wondji, C. S. (2021). The cytochrome P450 CYP325A is a major driver of pyrethroid resistance in the major malaria vector Anopheles funestus in Central Africa. *Insect Biochemistry and Molecular Biology*, *138*, 103647. https://doi.org/10.1016/j.ibmb.2021.103647

WHO. (2021). *World malaria report 2021*. https://www.who.int/teams/global-malaria-programme/reports/world-malaria-report-2021

Williams, J., Flood, L., Praulins, G., Ingham, V. A., Morgan, J., Lees, R. S., & Ranson, H. (2019). Characterisation of Anopheles strains used for laboratory screening of new vector control products. *Parasites & Vectors*, *12*(1), Art. 1. https://doi.org/10.1186/s13071-019-3774-3

Wondji, C. S., Hearn, J., Irving, H., Wondji, M. J., & Weedall, G. (2022). RNAseq-based gene expression profiling of the Anopheles funestus pyrethroid-resistant strain FUMOZ highlights the predominant role of the duplicated CYP6P9a/b cytochrome P450s. *G3 Genes|Genomes|Genetics*, *12*(1), Art. 1. https://doi.org/10.1093/g3journal/jkab352

Wondji, C. S., Irving, H., Morgan, J., Lobo, N. F., Collins, F. H., Hunt, R. H., Coetzee, M., Hemingway, J., & Ranson, H. (2009). Two duplicated P450 genes are associated with pyrethroid resistance in Anopheles funestus, a major malaria vector. *Genome Research*, *19*(3), Art. 3. https://doi.org/10.1101/gr.087916.108

Yoshida, T. (2012). Identification of urinary metabolites in rats administered the fluorine-containing pyrethroids metofluthrin, profluthrin, and transfluthrin. *Toxicological & Environmental Chemistry*, *94*(9), 1789–1804. https://doi.org/10.1080/02772248.2012.729838

Yoshida, T. (2014). Biomarkers for monitoring transfluthrin exposure: Urinary excretion kinetics of transfluthrin metabolites in rats. *Environmental Toxicology and Pharmacology*, *37*(1), 103–109. https://doi.org/10.1016/j.etap.2013.11.011

5.6. Supplements (chapter 5)

Table S1. GenBank (Vector Base ID) numbers for genes used for recombinant expression.

Gene name	Vector base ID	GenBank #
CYP6P9a	AFUN015792	KR866022.1
CYP6P9b	AFUN015889	KR866046.1
An. gambiae CPR		AY183375.1

Table S2. Michaelis–Menten kinetics of CYP96P9a- and CYP6P9b-mediated BOMFC metabolism at increasing concentrations of transfluthrin. Vmax and Km values are given in pmol product/min x mg protein -1 and µM, respectively. Data are mean values ± CI 95% (n=4). The inhibition type is based on kinetic characteristics of reversible inhibition models according to Fowler and Zhang (2008; AAPS J 10:410–424).

P450 variant		c (transfluthrin) in µM							
(inhibition type)		100 µM	95 % CI	10 µM	95 % CI	1 µM	95 % CI	0 µM	95 % CI
CYP6P9a	K_m	38.7	34.9-42.8	11.6	10.1-13.3	8.2	6.79-9.9	8.06	6.5-9.96
(mixed)	V_{max}	131	126-136	154	148-160	164	156-172	168	158-178
CYP6P9b	K_m	28.3	25.2-31.8	8.31	7.34-9.4	4.74	4.11-5.46	3.92	3.32-4.62
(mixed)	V_{max}	107	103-111	122	119-126	128	123-132	130	125-134

Table S3. Percentage depletion of transfluthrin by recombinantly expressed CYP6P9a and CYP6P9b, as well as mock cells (empty virus). Incubation for 90 min at 30 °C. Data are mean values ± CI 95% (n=6).

Variant	NADPH	Mean, %	CI 95%
CYP6P9a	-	24.2	17.1 - 31.3
	+	40.2	34.9 - 45.5
CYP6P9b	-	24.0	18.4 - 29.6
	+	39.5	32.5 - 46.6
Mock cells	-	3.90	-3.9 - 11.8
	+	-3.90	-12.6 - 4.8

Figure S1. Hydrolysis of transfluthrin in microsomal membrane preparations of High-5 cells. Transfluthrin hydrolysis resulted in a M-162 metabolite, 3-(2,2-dichlorovinyl)-2,2-dimethylcyclo-propanecarboxylic acid, which was detected via UPLC-TOF-MS analysis in all samples, except those prepared from transfluthrin incubations without microsomal membranes.

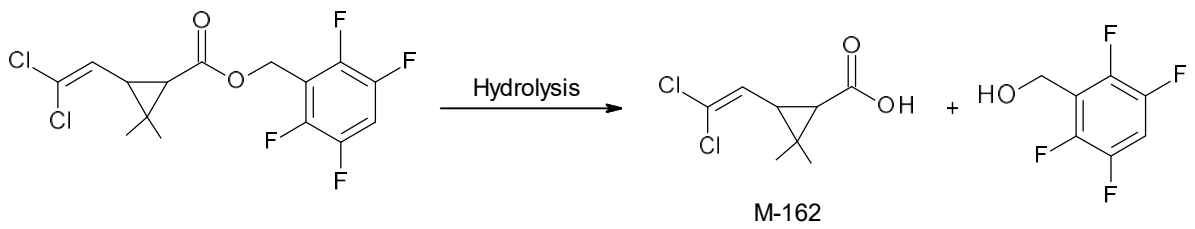

M-162

6. Chapter 6: General discussion

Anopheles funestus is amongst the deadliest animals on our planet as it transmits malaria, a disease responsible for 619 000 deaths each year (WHO, 2022a). Even though chemo-prophylaxes and drugs against malaria are available, bednets and IRS have contributed most towards the decline in malaria cases since 2000. Developed in the 1970s and 1980s, pyrethroids are still one of the major classes of insecticide used in agriculture and dominate vector control applications (WHO, 2022b).

This thesis focussed on the toxicity and the breakdown of the widely used pyrethroids permethrin (type I) and deltamethrin (type II) and the volatile, polyfluorinated pyrethroid transfluthrin by the P450 monooxygenases CYP6P9a and CYP6P9b (Riveron et al., 2013), two important P450s involved in metabolic pyrethroid resistance in the highly pyrethroid-resistant laboratory strain *An. funestus* FUMOZ-R (chapter 2). Transfluthrin is of evolving interest, as its volatility allows this molecule to be used in emanators, incorporated in chairs or eave ribbons (Masalu et al., 2020; Mwanga et al., 2019; Ogoma et al., 2012b) and can be used as additional vector control tools on top of bed nets and indoor residual sprays.

6.1. Baculovirus expression of CYP6P9a and CYP6P9b

An funestus FUMOZ-R is highly pyrethroid resistant (RR deltamethrin: 223, RR permethrin 7.76, RR cypermethrin 77.9). It exhibits much higher susceptibility (RR 2.51) towards the polyfluorinated pyrethroid transfluthrin than towards deltamethrin and permethrin and (chapter 2). *An. funestus* FUMOZ-R does not contain KDR mutations in the VGSC, thus the underlying resistance mechanism is predominantly P450-based, mainly due to the upregulation of CYP6P9a and CYP6P9b (Riveron et al., 2013) (chapter 2).

Using RT qPCR expression analysis, the upregulation of CYP6P9a and CYP6P9b in the pyrethroid resistant *An. funestus* FUMOZ-R strain was confirmed. Therefore, both enzymes were recombinantly expressed using for the first time in *Trichoplusia ni* cells (High Five) using baculorvirus-expression (chapter 4). The expression system was optimized, showing that CPRs from either *An. funestus* or *An. gambiae* could be used without no observable differences in metabolism (chapter 3). The involvement of cytochrome b5 was also investigated (chapter 3). Cytochrome b5 has also been described as a redox partner, however its role is not well defined (Schenkman and Jansson, 2003). Using the baculovirus system, the addition of CYB5

did not enhance deltamethrin metabolism, although it was effective in enhancing the metabolism of fluorescent model substrates. This differs with some *E. coli* expressed P450s such as CYP6M2 (Stevenson et al., 2011), suggesting that there may be membrane associated differences in CYB5 interactions depending on the expression systems that merits further investigation. This agrees with other studies that have evaluated CYB5 involvement in P450 redox systems and have found that its role depends on the system used, the specific P450 and the substrate.

As well as investigating the catalytic activities of CYP6P9a and CYP6P9b, we also investigated the microsomal activity of *An. funestus*. Microsomes extracted from human or rodent livers are commonly used to study drug metabolism. By contrast mosquito microsomes are not generally used for investigating insecticide metabolism as they are hard to purify in sufficient quantity. However, microsomes produced from *An. funestus* contained high levels of P450 activity that could be used to examine insecticide metabolism. Using *An. funestus* microsomes (chapter 2) and recombinantly expressed CYP6P9a and CYP6P9b we identified fluorescent coumarin model substrates BOMFC and BFC as good candidates to study P450 activity, which can be very helpful to conduct biochemical assays such as kinetic- or inhibition studies and which can be used as markers for CYP6P9a/b activity (chapter 4). BOMFC and BFC are good substrates for CYP6P9a/b and in a separate study it was found that they are also active against *Ae.aegypti* microsomes recombinantly expressed CYP9J24 and CYP9J28 (data not shown). This suggests they may have a broad spectrum of P450 activity, thus worth investigating further to assess suitability for diagnostic monitoring of P450 activity.

6.2. How are pyrethroids metabolised?

The metabolism of pyrethroids in insects and mosquitoes has been well studied using microsomal fractions or with certain recombinantly expressed P450s, such as CYP6M7 (Riveron et al., 2014a), CYP6P9a and CYP6P9b (Riveron et al., 2013) in *An. funestus,* CYP6M2 (Stevenson et al., 2011) or CYP6P3 (Müller et al., 2008) in *An. gambiae.* The main route of metabolism in pyrethroids is via the oxidative metabolism of the 4'para position of the phenoxybenzyl-ring (Kasai et al., 2014; Stevenson et al., 2011; Zimmer et al., 2014). Metabolism also occurs on the gem dimethyl site and to lesser extent the phenoxybenzyl-ether (Stevenson et al., 2011). Relatively few studies to date have examined the metabolites produced from pyrethroid metabolism by mosquito P450s. This thesis has shown that *An. funestus* CYP6P9a/b enzymes are capable of cleaving the phenoxybenzyl-ether of deltamethrin and permethrin, with approximately 20 % higher depletion rates than the respective parent compounds (chapter 4). Furthermore, we have shown that the 4'OH metabolite of deltamethrin and permethrin is still toxic towards susceptible *An. funestus* mosquitoes (4'OH deltamethrin: LC_{50}, 1.88 mg/m^2, CI95%: 0.72–3.89, 4'OH permethrin: LC_{50}, 34.7 mg/mg^2 CI95%: 15.8-91.7) (chapter 4). Moreover, we found that 4'OH metabolites inhibiting recombinant CYP6P9a and CYP6P9b in the range of some azole fungicides, which are known P450 inhibitors (chapter 4). Furthermore, the fluorescent BOMFC kinetic decreased to higher extent if 4'OH metabolites were used instead of the parent pyrethroids (chapter 4).

Further work is required to determine if ether-cleavage is a common degradation pathway. Overall, this information can help towards the design of new pyrethroid compounds that lack the ether bond and may be more resistant to oxidative P450 metabolism. This knowledge is helping to create chemistry which can resist oxidative metabolism by creating chemical compounds without ether bond.

While enhanced P450-mediated metabolism of pyrethroids is generally associated with upregulated gene expression, SNPs have also been associated with pyrethroid resistance. These include $Val^{109}Ile$, $Asp^{335}Glu$ and $Asn^{384}Ser$ in CYP6P9b (Ibrahim et al., 2015). We have produced the $Val^{310}Ile$ mutation in CYP6P9b and found that it causes a selective 7- fold increase in permethrin metabolism (chapter 4). This mutation is present in pyrethroid resistant mosquitoes collected in Benin (Ibrahim et al., 2015). Given that Olyset bednets that

contain permethrin were a first generation bednet that was widely distributed, it is feasible that this may exert a selective pressure for this particular mutation. It would be interesting to follow this up to determine if this is a diagnostic SNP for enhanced permethrin resistance. It also demonstrates that pyrethroid metabolising P450s are capable of evolving mutations that may fine tuning activity according to the pyrethroid molecule being used for control. This warrants further investigation and may have implications for vector control, emphasizing the need to reduce reliance on individual pyrethroids.

6.2.1. Effect of cis- and trans permethrin isomers towards metabolism/ Influence of isomerism towards metabolism

In the pyrethroid resistant *An. funestus* FUMOZ-R a low resistance ratio (7-fold) was observed towards permethrin (chapter 2). Permethrin is generally used as a racemate mixture of cis- and trans-enantiomers. It is known that the cis enantiomer is generally more toxic (Shono et al., 1979), which we confirmed against susceptible (9-fold) and pyrethroid resistant *An. funestus* (6-fold) (chapter 4). In analytical assays, CYP6P9b metabolised cis- and trans permethrin at a much higher rate (cis-permethrin 3-fold, trans-permethrin 5-fold) than CYP6P9a (chapter 4). Interestingly the trans-enantiomer was metabolised at a faster rate (~4-fold) than cis-permethrin by both enzymes. These results highlight both the selective toxicology of pyrethroid cis- and trans enantiomers and the stereoselective metabolism of P450s. Intuitively, vector control products that consist of pure cis permethrin enantiomer should be more effective than the racemate mixture, in particular in areas where *An. funestus* is found with upregulated CYP6P9b.

6.2.2. How the structural features protect transfluthrin

Transfluthrin lacks the phenoxybenzyl-ether present in many commonly used pyrethroids including permethrin, deltamethrin, alpha-cypermethrin contains a polyfluorinated benzene ring. This produces a steric constraint and reduces potential sites of P450 oxidation that has been shown to control pyrethroid resistant *An. funestus* mosquitoes (Horstmann and Sonneck, 2016). This thesis confirmed the resistant breaking potential of transfluthrin towards the highly pyrethroid resistant *An. funestus* FUMOZ-R strain (resistance ratio 2.51) (chapter 2). In analytical assays, recombinant CYP6P9a and CYP6P9b were shown capable of low levels of transfluthrin metabolism (20 % depletion). MS/MS analysis confirmed no

hydroxylation occurred on the phenoxybenzyl-moiety or on the 4'para-position that is the common site of P450 metabolism. Instead, a metabolite was produced that suggests a hydroxylation of the gem-dimethyl cyclopropyl moiety (chapter 5). Thus, while metabolism of transfluthrin is still feasible, it is restricted, therefore, the low resistance ratio for transfluthrin can be explained by the high fluorination at the benzene-ring and the lack of the phenoxybenzyl-moiety, which are the generally preferred sites of attack by CYP6P9a and CYP6P9b in pyrethroid molecules. Overall, this recommends the use of transfluthrin in vector control products to mitigate P450 driven pyrethroid resistance in *An. funestus* mosquitoes. Furthermore, this knowledge will help for the design and synthesis of pyrethroid based chemicals that can resist P450 mediated metabolism.

6.3. Azole fungicides as new synergists in vector control applications?

Synergists that can enhance the effectiveness of an insecticide are becoming increasingly important for extending the lifetime of a limited number of vector control reagents. However, the options available are limited and the only synergist on the market for use in agriculture and vector control is PBO, a general inhibitor of P450 enzymes that are associated with insecticide metabolism and detoxification (Hodgson and Levi, 1999). Currently, PBO is being successfully incorporated into bednets to overcome metabolic resistance and enhancing the efficacy of pyrethroid and bednet efficacy (Gleave et al., 2018; Protopopoff et al., 2018). However, there is recent evidence that mosquitoes are developing resistance towards PBO (Riveron et al., 2019; Zhou et al., 2022). Thus, there is a need to expand the pool of synergistic compounds to reduce the reliance of vector control on a single compound.

Azoles, which are mostly used as fungicides, are known to inhibit CYP51, a fungal 14-demethylase involved in ergosterol biosynthesis (Nakata et al., 1991; Ortiz De Montellano, 2018). They can synergize neonicotinoids and pyrethroids in toxicity bioassays with the honey bee *A. mellifera* (Iwasa et al., 2004; Pilling and Jepson, 1993) and can inhibit other P450s such as *A. mellifera* CYP9Q3 in vitro (Haas and Nauen, 2021). Given the potential for wider application, this thesis investigated the potential for azole compounds to be used as synergists for vector control. In vitro screen against microsomal and recombinant *An. funestus* demonstrated that several azole fungicides were stronger inhibitors than PBO. In particular, the imidazoles prochloraz and triflumizole were identified as extremely potent nanomolar inhibitors of *An. funestus* microsomal P450s (chapter 4). The synergistic potential of

triflumizole against 3-phenoxybenzyl pyrethroids was further confirmed in vivo (chapter 2). While this study has focused on *An. funestus*, to be effective for vector control, synergists need to work against a broad range of target insects and active ingredients. To date, the synergistic effect of triflumizole against pyrethroids has proven effective in contact bioassays towards pyrethroid resistant *Ae. aegypti* mosquitoes and in vitro inhibitions assays with pyrethroid resistant *Ae. aegypti* microsomes and recombinantly expressed *Ae. aegypti* CYP9J24 and CYP9J28 (data not shown), indicating that triflumizole may have broader application to other mosquitoes. Importantly, the testing of azole fungicides would need to be extended to semi-field and field settings to prove effectiveness under field conditions. If successful, this would help to increase the choices of synergists available to overcome P450 mediated insecticide-resistance in disease vectors and expand the lifetime of available insecticides in vector control and other markets.

Outlook and further research

This thesis has characterised the breakdown of the pyrethroids deltamethrin, permethrin and transfluthrin by CYP6P9a and CYP6P9b to provide mechanistic insight on the resistant breaking properties of transfluthrin towards pyrethroid resistant *An. funestus*. It would be worth investigating if the same toxicological profile of transfluthrin occurs under field settings or with field-collected *An. funestus*. We have shown that CYP6P9a and CYP6P9b are capable of cleaving the phenoxybenzylether in common pyrethroids. It would be interesting to investigate if the detected cleavage of the phenoxybenzylether of CYP6P9a and CYP6P9b is a general mechanism applying to other P450 enzymes from insects and mosquitoes. Therefore, we suggest analytical studies with other recombinantly expressed P450 candidates.

Furthermore, we have detected the $Val^{310}Ile$ mutation as a putative diagnostic marker for selective permethrin resistance, it would be interesting to confirm a direct association between the SNP and Olyset-bednet distribution in field environments. We have seen that residue changes within P450-enzymes can change the substrate profile, therefore for future work we are suggesting further changes with other residues to assess if similar effects are observed. Furthermore, we have demonstrated that azole compounds such as triflumizole and prochloraz are effective inhibitors of *An. funestus* P450 activity, with potential application as synergists to overcome metabolic resistance activity against pyrethroids and potentially other insecticides. It would be worth assessing the field feasibility of azole compounds, e.g., incorporated into a bednet together with a pyrethroid.

Taken together, these laboratory studies provide a strong platform for future research to further understand mechanisms of pyrethroid resistance in mosquitoes and other insects and the toxicological profile of transfluthrin in the field.

References

Adesanya, A.W., Cardenas, A., Lavine, M.D., Walsh, D.B., Lavine, L.C., Zhu, F., 2020. RNA interference of NADPH-cytochrome P450 reductase increases susceptibilities to multiple acaricides in Tetranychus urticae. Pestic Biochem Physiol 165, 104550. https://doi.org/10.1016/j.pestbp.2020.02.016

Adolfi, A., Poulton, B., Anthousi, A., Macilwee, S., Ranson, H., Lycett, G.J., 2019. Functional genetic validation of key genes conferring insecticide resistance in the major African malaria vector, Anopheles gambiae. Proc Natl Acad Sci U S A 116, 25764–25772. https://doi.org/10.1073/pnas.1914633116

Ahoua Alou, L.P., Koffi, A.A., Adja, M.A., Tia, E., Kouassi, P.K., Koné, M., Chandre, F., 2010. Distribution of ace-1Rand resistance to carbamates and organophosphates in Anopheles gambiae s.s. populations from Côte d'Ivoire. Malar J. https://doi.org/10.1186/1475-2875-9-167

Amezian, D., Nauen, R., Le Goff, G., 2021. Transcriptional regulation of xenobiotic detoxification genes in insects - An overview. Pestic Biochem Physiol. https://doi.org/10.1016/j.pestbp.2021.104822

Animut, A., Horstmann, S., 2022. Residual efficacy of Fludora Fusion against Anopheles arabiensis in simple huts in Ethiopia. PLoS One 17, e0263840. https://doi.org/10.1371/journal.pone.0263840

Antonio-Nkondjio, C., Awono-Ambene, P., Toto, J.-C., Meunier, J.-Y., Zebaze-Kemleu, S., Nyambam, R., Wondji, C.S., Tchuinkam, T., Fontenille, D., 2002. High Malaria Transmission Intensity in a Village Close to Yaounde, the Capital City of Cameroon. J Med Entomol. https://doi.org/10.1603/0022-2585-39.2.350

Awolola, T.S., Oduola, O.A., Strode, C., Koekemoer, L.L., Brooke, B., Ranson, H., 2009. Evidence of multiple pyrethroid resistance mechanisms in the malaria vector Anopheles gambiae sensu stricto from Nigeria. Trans R Soc Trop Med Hyg. https://doi.org/10.1016/j.trstmh.2008.08.021

Awolola, T.S., Oyewole, I.O., Koekemoer, L.L., Coetzee, M., 2005. Identification of three members of the Anopheles funestus (Diptera: Culicidae) group and their role in malaria transmission in two ecological zones in Nigeria. Trans R Soc Trop Med Hyg 99, 525–531. https://doi.org/10.1016/j.trstmh.2004.12.003

Balabanidou, V., Grigoraki, L., Vontas, J., 2018. Insect cuticle: a critical determinant of insecticide resistance. Curr Opin Insect Sci 27, 68–74. https://doi.org/10.1016/j.cois.2018.03.001

Balabanidou, V., Kampouraki, A., Maclean, M., Blomquist, G.J., Tittiger, C., Juárez, M.P., Mijailovsky, S.J., Chalepakis, G., Anthousi, A., Lynd, A., Antoine, S., Hemingway, J., Ranson, H., Lycett, G.J., Vontas, J., 2016. Cytochrome P450 associated with insecticide resistance catalyzes cuticular hydrocarbon production in Anopheles gambiae. Proc Natl Acad Sci U S A 113, 9268–9273. https://doi.org/10.1073/pnas.1608295113

Banks, S.D., Murray, N., Wilder-Smith, A., Logan, J.G., 2014. Insecticide-treated clothes for the control of vector-borne diseases: A review on effectiveness and safety. Med Vet Entomol 28, 14–25. https://doi.org/10.1111/mve.12068

Bayer, 2022. Bayer Vector Control Environmental Science [WWW Document]. Bayer. URL https://www.vectorcontrol.bayer.com/product-portfolio/products/fludora-comax

Bhatt, S., Weiss, D.J., Cameron, E., Bisanzio, D., Mappin, B., Dalrymple, U., Battle, K.E., Moyes, C.L., Henry, A., Eckhoff, P.A., Wenger, E.A., Briët, O., Penny, M.A., Smith, T.A., Bennett, A., Yukich, J., Eisele, T.P., Griffin, J.T., Fergus, C.A., Lynch, M., Lindgren, F., Cohen, J.M., Murray, C.L.J., Smith, D.L., Hay, S.I., Cibulskis, R.E., Gething, P.W., 2015. The effect of malaria control on Plasmodium falciparum in Africa between 2000 and 2015. Nature 526, 207–211. https://doi.org/10.1038/nature15535

Bibbs, C.S., Tsikolia, M., Bloomquist, J.R., Bernier, U.R., Xue, R. De, Kaufman, P.E., 2018. Vapor toxicity of five volatile pyrethroids against Aedes aegypti, Aedes albopictus, Culex quinquefasciatus, and Anopheles quadrimaculatus (Diptera: Culicidae). Pest Manag Sci 74, 2699–2706. https://doi.org/10.1002/ps.5088

Boaventura, D., Buer, B., Hamaekers, N., Maiwald, F., Nauen, R., 2021. Toxicological and molecular profiling of insecticide resistance in a Brazilian strain of fall armyworm resistant to Bt Cry1 proteins. Pest Manag Sci 77, 3713–3726. https://doi.org/10.1002/ps.6061

Boonsuepsakul, S., Luepromchai, E., Rongnoparut, P., 2008. Characterization of Anopheles minimus CYP6AA3 expressed in a recombinant baculovirus system. Arch Insect Biochem Physiol 69, 13–21. https://doi.org/10.1002/arch.20248

Bowman, L.R., Donegan, S., McCall, P.J., 2016. Is Dengue Vector Control Deficient in Effectiveness or Evidence?: Systematic Review and Meta-analysis. PLoS Negl Trop Dis 10, 1–24. https://doi.org/10.1371/journal.pntd.0004551

Bradley, J., Ogouyèmi-Hounto, A., Cornélie, S., Fassinou, J., De Tove, Y.S.S., Adéothy, A.A., Tokponnon, F.T., Makoutode, P., Adechoubou, A., Legba, T., Houansou, T., Kinde-Gazard, D., Akogbeto, M.C., Massougbodji, A., Knox, T.B., Donnelly, M., Kleinschmidt, I., 2017. Insecticide-treated nets provide protection against malaria to children in an area of insecticide resistance in Southern Benin. Malar J 16, 1–5. https://doi.org/10.1186/s12936-017-1873-1

Brengues, C., Hawkesy, N.J., Chandre, F., McCarroll, L., Duchon, S., Guillet, P., Manguin, S., Morgan, J.C., Hemingway, J., 2003. Pyrethroid and DDT crossresistance in Aedes aegypti is correlated with novel mutations in the voltaage-gated sodium channel. Med Vet Entomol 17, 87–94.

Brooke, B.D., Kloke, G., Hunt, R.H., Koekemoer, L.L., Tem, E.A., Taylor, M.E., Small, G., Hemingway, J., Coetzee, M., 2001. Bioassay and biochemical analyses of insecticide resistance in southern African Anopheles funestus (Diptera: Culicidae). Bull Entomol Res 91, 265–272. https://doi.org/10.1079/ber2001108

Casida, J.E., 1970. Mixed-Function Oxidase Involvement in the Biochemistry of Insecticide Synergists. J Agric Food Chem 18, 753–772. https://doi.org/10.1021/jf60171a013

Casida, J.E., Gammon, D.W., Glickman, A.H., Lawrence, L.J., 1983. Mechanism of Selective Action of Pyrethroid. Annual Review Pharmacology Toxicology 413–438.

Casida, J.E., Ruzo, L.O., 1980. Metabolic chemistry of pyrethroid insecticides. Pestic Sci 11, 257–269. https://doi.org/10.1002/ps.2780110219

Cataldo, N.P., Lea, C.S., Kelley, T., Richards, S.L., 2020. Assessment of Resistance to Organophosphates and Pyrethroids in Aedes aegypti (Diptera: Culicidae): Do Synergists Affect Mortality? J Med Entomol 1–5. https://doi.org/10.1093/jme/tjaa101

Chiu, T.L., Wen, Z., Rupasinghe, S.G., Schuler, M.A., 2008. Comparative molecular modeling of Anopheles gambiae CYP6Z1, a mosquito P450 capable of metabolizing DDT. Proc Natl Acad Sci U S A 105, 8855–8860. https://doi.org/10.1073/pnas.0709249105

Churcher, T.S., Lissenden, N., Griffin, J.T., Worrall, E., Ranson, H., 2016. The impact of pyrethroid resistance on the efficacy and effectiveness of bednets for malaria control in Africa. Elife. https://doi.org/10.7554/eLife.16090

Clark, A.G., Shamaan, N.A., 1984. Evidence that DDT-dehydrochlorinase from the house fly is a glutathione S-transferase. Pestic Biochem Physiol 22, 249–261. https://doi.org/10.1016/0048-3575(84)90018-X

Clarkson, C.S., Miles, A., Harding, N.J., O'Reilly, A.O., Weetman, D., Kwiatkowski, D., Donnelly, M.J., 2021. The genetic architecture of target-site resistance to pyrethroid insecticides in the African malaria vectors Anopheles gambiae and Anopheles coluzzii. Mol Ecol 30, 5303–5317. https://doi.org/10.1111/mec.15845

Coetzee, Maureen, Hunt, R.H., Wilkerson, R., Torre, A. Della, Coulibaly, M.B., Besansky, N.J., 2013. Anopheles coluzzii and anopheles amharicus, new members of the anopheles gambiae complex. Zootaxa. https://doi.org/10.11646/zootaxa.3619.3.2

Coetzee, M., Koekemoer, L.L., 2013. Molecular systematics and insecticide resistance in the major African malaria vector anopheles funestus. Annu Rev Entomol 58, 393–412. https://doi.org/10.1146/annurev-ento-120811-153628

Coetzee, M., Kruger, P., Hunt, R.H., Durrheim, D.N., Urbach, J., Hansford, C.F., 2013. Malaria in South Africa: 110 years of learning to control the disease. South African Medical Journal 103, 770–778. https://doi.org/10.7196/SAMJ.7446

Corbel, V., Chabi, J., Dabiré, R.K., Etang, J., Nwane, P., Pigeon, O., Akogbeto, M., Hougard, J.M., 2010. Field efficacy of a new mosaic long-lasting mosquito net (PermaNet® 3.0) against pyrethroid-resistant malaria vectors: A multi centre study in Western and Central Africa. Malar J. https://doi.org/10.1186/1475-2875-9-113

Dambach, P., Baernighausen, T., Traoré, I., Ouedraogo, S., Sié, A., Sauerborn, R., Becker, N., Louis, V.R., 2019. Reduction of malaria vector mosquitoes in a large-scale intervention trial in rural Burkina Faso using Bti based larval source management. Malar J 18, 311. https://doi.org/10.1186/s12936-019-2951-3

David, J.-P., Strode, C., Vontas, J., Nikou, D., Vaughan, A., Pignatelli, P.M., Louis, C., Hemingway, J., Ranson, H., 2005. The Anopheles gambiae detoxification chip: A highly specific microarray to study metabolic-based insecticide resistance in malaria vectors. Proceedings of the National Academy of Science 102.

Davies, T.G.E., Field, L.M., Usherwood, P.N.R., Williamson, M.S., 2007. DDT, pyrethrins, pyrethroids and insect sodium channels. IUBMB Life 59, 151–162. https://doi.org/10.1080/15216540701352042

Davies, T.G.E., O'Reilly, A.O., Field, L.M., Wallace, B.A., Williamson, M.S., 2008. Knockdown resistance to DDT and pyrethroids: From target-site mutations to molecular modelling. Pest Manag Sci. https://doi.org/10.1002/ps.1617

Dia, I., Moussa Wamdaogo Guelbeogo, Ayala, D., 2013. Advances and Perspectives in the Study of the Malaria Mosquito Anopheles funestus, in: Anopheles Mosquitoes - New Insights into Malaria Vectors. pp. 197–220.

Djouaka, R., Riveron, J.M., Yessoufou, A., Tchigossou, G., Akoton, R., Irving, H., Djegbe, I., Moutairou, K., Adeoti, R., Tamò, M., Manyong, V., Wondji, C.S., 2016. Multiple insecticide resistance in an infected population of the malaria vector Anopheles funestus in Benin. Parasit Vectors 9, 453. https://doi.org/10.1186/s13071-016-1723-y

Duangkaew, P., Pethuan, S., Kaewpa, D., Boonsuepsakul, S., Sarapusit, S., Rongnoparut, P., 2011. Characterization of mosquito CYP6P7 and CYP6AA3: Differences in substrate preference and kinetic properties. Arch Insect Biochem Physiol 76, 236–248. https://doi.org/10.1002/arch.20413

Elliott, M., Farnham, A.W., Janes, N.F., Needham, P.H., Pearson, B.C., 1967. 5-Benzyl-3-furylmethyl Chrysanthemate: a New Potent Insecticide. Nature 213, 493–494.

Enayati, A.A., Ranson, H., Hemingway, J., 2005. Insect glutathione transferases and insecticide resistance. Insect Mol Biol 14, 3–8. https://doi.org/10.1111/j.1365-2583.2004.00529.x

Feyereisen, R., 2019. Insect CYP Genes and P450 Enzymes, Reference Module in Life Sciences. https://doi.org/10.1016/b978-0-12-809633-8.04040-1

Feyereisen, R., 2015. Insect P450 inhibitors and insecticides: Challenges and opportunities. Pest Manag Sci 71, 793–800. https://doi.org/10.1002/ps.3895

Feyereisen, R., Vincent, D.R., 1984. Characterization of antibodies to house fly NADPH-cytochrome P-450 reductase. Insect Biochem 14, 163–168. https://doi.org/10.1016/0020-1790(84)90025-8

Finn, R.D., McLaughlin, L.A., Hughes, C., Song, C., Henderson, C.J., Wolf, R.R., 2011. Cytochrome b5 null mouse: a new model for studyinginherited skin disorders and the role of unsaturated fattyacids in normal homeostasis. Transgenic Res 20, 491–502. https://doi.org/10.1007/s11248-010-9426-1

Finn, R.D., McLaughlin, L.A., Ronseaux, S., Rosewell, I., Houston, J.B., Henderson, C.J., Wolf, C.R., 2008. Defining the in vivo role for cytochrome b5 in cytochrome P450 function through the conditional hepatic deletion of microsomal cytochrome b5. Journal of Biological Chemistry 283, 31385–31393. https://doi.org/10.1074/jbc.M803496200

Fiorenzano, J.M., Koehler, P.G., Xue, R. de, 2017. Attractive toxic sugar bait (ATSB) for control of mosquitoes and its impact on non-target organisms: A review. Int J Environ Res Public Health 14. https://doi.org/10.3390/ijerph14040398

Fongnikin, A., Houeto, N., Agbevo, A., Odjo, A., Syme, T., N'Guessan, R., Ngufor, C., 2020. Efficacy of Fludora® Fusion (a mixture of deltamethrin and clothianidin) for indoor residual spraying against pyrethroid-resistant malaria vectors: Laboratory and experimental hut evaluation. Parasit Vectors 13, 466. https://doi.org/10.1186/s13071-020-04341-6

Fouet, C., Ashu, A.F., Ambadiang, M.M., Tchapga, W.T., Wondji, C.S., Kamdem, C., 2020. Resistance of *Anopheles gambiae* to the new insecticide clothianidin associated with unrestricted use of agricultural neonicotinoids in Yaounde, Cameroon. bioRxiv 2020.08.06.239509. https://doi.org/10.1101/2020.08.06.239509

Fraser, K.J., Mwandigha, L., Traore, S.F., Traore, M.M., Doumbia, S., Junnila, A., Revay, E., Beier, J.C., Marshall, J.M., Ghani, A.C., Müller, G., 2021. Estimating the potential impact of Attractive Targeted Sugar Baits (ATSBs) as a new vector control tool for Plasmodium falciparum malaria. Malar J 20. https://doi.org/10.1186/s12936-021-03684-4

Gatton, M.L., Chitnis, N., Churcher, T., Donnelly, M.J., Ghani, A.C., Godfray, H.C.J., Gould, F., Hastings, I., Marshall, J., Ranson, H., Rowland, M., Shaman, J., Lindsay, S.W., 2013. The importance of mosquito behavioural adaptations to malaria control in Africa. Evolution (N Y). https://doi.org/10.1111/evo.12063

Gillies, M.T., Coetzee, M., 1987. A supplement to the Anophelinae of Africa South of the Sahara. South African Institute for Medical Research.

Gleave, K., Lissenden, N., Richardson, M., Ranson, H., 2018. Piperonyl butoxide (PBO) combined with pyrethroids in long-lasting insecticidal nets (LLINs) to prevent malaria in Africa. Cochrane Database of Systematic Reviews. https://doi.org/10.1002/14651858.CD012776

Glunt, K.D., Coetzee, M., Huijben, S., Koffi, A.A., Lynch, P.A., N'Guessan, R., Oumbouke, W.A., Sternberg, E.D., Thomas, M.B., 2017. Empirical and theoretical investigation into the potential impacts of insecticide resistance on the effectiveness of insecticide-treated bed nets. Evol Appl 11, 431–441. https://doi.org/10.1111/eva.12574

Goodyer, L., Schofield, S., 2018. Mosquito repellents for the traveller: Does picaridin provide longer protection than DEET? J Travel Med 25, S10–S15. https://doi.org/10.1093/jtm/tay005

Gotoh, O., 1992. Substrate recognition sites in cytochrome P450 family 2 (CYP2) proteins inferred from comparative analyses of amino acid and coding nucleotide sequences. Journal of Biological Chemistry 267, 83–90. https://doi.org/10.1016/s0021-9258(18)48462-1

Grant, G.G., Estrera, R.R., Pathak, N., Hall, C.D., Tsikolia, M., Linthicum, K.J., Bernier, U.R., Hall, A.C., 2020. Interactions of DEET and Novel Repellents With Mosquito Odorant Receptors. J Med Entomol 57, 1032–1040. https://doi.org/10.1093/jme/tjaa010

Grigoraki, L., Balabanidou, V., Meristoudis, C., Miridakis, A., Ranson, H., Swevers, L., Vontas, J., 2016. Functional and immunohistochemical characterization of CCEae3a, a carboxylesterase associated with temephos resistance in the major arbovirus vectors Aedes aegypti and Ae. albopictus. Insect Biochem Mol Biol. https://doi.org/10.1016/j.ibmb.2016.05.007

Gunning, R. V., Moores, G.D., Devonshire, A.L., 1998. Inhibition of Resistance-related Esterases by Piperonyl Butoxide in Helicoverpa armigera (Lepidoptera: Noctuidae) and Aphis gossypii (Hemiptera: Aphididae) 215–226.

Gutierrez, A., Grunau, A., Paine, M., Munro, A.W., Wolf, C.R., Roberts, G.C.K., Scrutton, N.S., 2003. Enzyme Mechanism – A Structural Perspective Electron transfer in human cytochrome P450 reductase Cytochrome P450 reductase (CPR) and its component domains 497–501.

Guzov, V.M., Houston, H.L., Murataliev, M.B., Walker, F.A., Feyereisen, R., 1996. Molecular cloning, overexpression in escherichia coli, structural and functional characterization of house fly cytochrome b5. Journal of Biological Chemistry 271, 26637–26645. https://doi.org/10.1074/jbc.271.43.26637

Haas, J., Glaubitz, J., Koenig, U., Nauen, R., 2021. A mechanism-based approach unveils metabolic routes potentially mediating chlorantraniliprole synergism in honey bees, Apis mellifera L., by azole fungicides . Pest Manag Sci. https://doi.org/10.1002/ps.6706

Haas, J., Nauen, R., 2021. Pesticide risk assessment at the molecular level using honey bee cytochrome P450 enzymes : A complementary approach. Environ Int 147, 106372. https://doi.org/10.1016/j.envint.2020.106372

Hancock, P.A., Hendriks, C.J.M., Tangena, J.-A., Gibson, H., Hemingway, J., Coleman, M., Gething, P.W., Cameron, E., Bhatt, S., Moyes, C.L., 2020. Mapping trends in insecticide resistance phenotypes in African malaria vectors. PLoS Biol 18, e3000633. https://doi.org/10.1371/journal.pbio.3000633

Hargreaves, K., Koekemoer, L.L., Brooke, B.D., Hunt, R.H., Mthembu, J., Coetzee, M., 2000. Anopheles funestus resistant to pyrethroid insecticides in South Africa. Med Vet Entomol 14, 181–189. https://doi.org/10.1046/j.1365-2915.2000.00234.x

Hawley, W.A., Phillips-Howard, P.A., Ter Kuile, F.O., Nahlen, B.L., Alaii, J.A., Gimnig, J.E., Kolczak, M.S., Terlouw, D.J., Kariuki, S.K., Shi, Y.P., Kachur, S.P., Hightower, A.W., Vulule, J.M., Ombok, M., Nahlen, B.L., Giminig, J.E., Kariuki, S.K., Kolczak, M.S., Hightower, A.W., 2003. Community-wide effects of permethrin-treated bed nets on child mortality and malaria morbidity in western Kenya. American Journal of Tropical Medicine and Hygiene 68, 121–127. https://doi.org/10.4269/ajtmh.2003.68.10

Heintze, T., Klein, K., Hofmann, U., Zanger, U.M., 2021. Differential effects on human cytochromes P450 by CRISPR/Cas9-induced genetic knockout of cytochrome P450 reductase and cytochrome b5 in HepaRG cells. Sci Rep 11, 1–14. https://doi.org/10.1038/s41598-020-79952-1

Hemingway, J., Ranson, H., 2000. Inseciticide Resistance in Insect Vectors of Human Diseases. Annu Rev Entomol 45, 371–391.

Hemingway, J., Ranson, H., Magill, A., Kolaczinski, J., Fornadel, C., Gimnig, J., Coetzee, M., Simard, F., Roch, D.K., Hinzoumbe, C.K., Pickett, J., Schellenberg, D., Gething, P., Hoppé, M., Hamon, N., 2016. Averting a malaria disaster: Will insecticide resistance derail malaria control? The Lancet 387, 1785–1788. https://doi.org/10.1016/S0140-6736(15)00417-1

Henderson, C.J., McLaughlin, L.A., Finn, R.D., Ronseaux, S., Kapelyukh, Y., Wolf, C.R., 2014. A role for cytochrome b5 in the in vivo disposition of anticancer and cytochrome P450 probe drugs in mice. Drug Metabolism and Disposition 42, 70–77. https://doi.org/10.1124/dmd.113.055277

Henderson, C.J., McLaughlin, L.A., Scheer, N., Stanley, L.A., Wolf, C.R., 2015. Cytochrome b5 is a major determinant of human cytochrome P450 CYP2D6 and CYP3A4 activity in vivo. Mol Pharmacol 87, 733–739. https://doi.org/10.1124/mol.114.097394

Hien, A.S., Soma, D.D., Maiga, S., Coulibaly, D., Diabaté, A., Belemvire, A., Diouf, M.B., Jacob, D., Koné, A., Dotson, E., Awolola, T.S., Oxborough, R.M., Dabiré, R.K., 2021. Evidence supporting deployment of next generation insecticide treated nets in Burkina Faso: bioassays with either chlorfenapyr or piperonyl butoxide increase mortality of pyrethroid-resistant Anopheles gambiae. Malar J 20, 1–12. https://doi.org/10.1186/s12936-021-03936-3

Hodgson, E., Levi, P.E., 1999. Interactions of Piperonyl Butoxide with Cytochrome P450. Piperonyl Butoxide. https://doi.org/10.1016/b978-012286975-4/50005-x

Horstmann, S., Sonneck, R., 2016. Contact Bioassays with Phenoxybenzyl and Tetrafluorobenzyl Pyrethroids against Target-Site and Metabolic Resistant Mosquitoes. PLoS One 11, e0149738. https://doi.org/10.1371/journal.pone.0149738

Ibrahim, S.S., Amvongo-Adjia, N., Wondji, M.J., Irving, H., Riveron, J.M., Wondji, C.S., 2018. Pyrethroid resistance in the major malaria vector anopheles funestus is exacerbated by overexpression and overactivity of the P450 CYP6AA1 across Africa. Genes (Basel) 9, 1–17. https://doi.org/10.3390/genes9030140

Ibrahim, S.S., Ndula, M., Riveron, J.M., Irving, H., Wondji, C.S., 2016. The P450 CYP6Z1 confers carbamate/pyrethroid cross-resistance in a major African malaria vector beside a novel carbamate-insensitive N485I acetylcholinesterase-1 mutation. Mol Ecol 25, 3436–3452. https://doi.org/10.1111/mec.13673

Ibrahim, S.S., Riveron, J.M., Bibby, J., Irving, H., Yunta, C., Paine, M.J.I., Wondji, C.S., 2015. Allelic Variation of Cytochrome P450s Drives Resistance to Bednet Insecticides in a Major Malaria Vector. PLoS Genet 11, e1005618. https://doi.org/10.1371/journal.pgen.1005618

Ingham, V.A., Wagstaff, S., Ranson, H., 2018. Transcriptomic meta-signatures identified in Anopheles gambiae populations reveal previously undetected insecticide resistance mechanisms. Nat Commun 9. https://doi.org/10.1038/s41467-018-07615-x

IRAC, 2021. Insecticide Resistance Training Basic Module: Crop Protection.

Irving, H., Wondji, C.S., 2017. Investigating knockdown resistance (kdr) mechanism against pyrethroids/DDT in the malaria vector Anopheles funestus across Africa. BMC Genet 18, 76. https://doi.org/10.1186/s12863-017-0539-x

Iwasa, T., Motoyama, N., Ambrose, J.T., Roe, R.M., 2004. Mechanism for the differential toxicity of neonicotinoid insecticides in the honey bee, Apis mellifera. Crop Protection 23, 371–378. https://doi.org/10.1016/j.cropro.2003.08.018

Jiao, L., Xue-yao, Z., Hai-hua, W., Wen, M., Wen-ya, Z., ZHU, K.-Y., En-bo, M., ZHANG Jian-zhen, 2020. Characteristics and roles of cytochrome b5 in cytochrome P450- mediated oxidative reactions in Locusta migratoria LIU. J Integr Agric 19, 1512–1521. https://doi.org/10.1016/S2095-3119(19)62827-3

Jones, C.M., Liyanapathirana, M., Agossa, F.R., Weetman, D., Ranson, H., Donnelly, M.J., Wilding, C.S., 2012. Footprints of positive selection associated with a mutation (N1575Y) in the voltage-gated sodium channel of Anopheles gambiae. Proc Natl Acad Sci U S A 109, 6614–6619. https://doi.org/10.1073/pnas.1201475109

Kaindoa, E.W., Mmbando, A.S., Shirima, R., Hape, E.E., Okumu, F.O., 2021. Insecticide - treated eave ribbons for malaria vector control in low - income communities. Malar J 1–12. https://doi.org/10.1186/s12936-021-03945-2

Karunaratne, P., De Silva, P., Weeraratne, T., Surendran, N., 2018. Insecticide resistance in mosquitoes: Development, mechanisms and monitoring. Ceylon Journal of Science 47, 299. https://doi.org/10.4038/cjs.v47i4.7547

Kasai, S., Komagata, O., Itokawa, K., Shono, T., Ng, L.C., Kobayashi, M., Tomita, T., 2014. Mechanisms of Pyrethroid Resistance in the Dengue Mosquito Vector, Aedes aegypti: Target Site

Insensitivity, Penetration, and Metabolism. PLoS Negl Trop Dis 8, e2948. https://doi.org/10.1371/journal.pntd.0002948

Katureebe, A., Zinszer, K., Arinaitwe, E., Rek, J., Kakande, E., Charland, K., Kigozi, R., Kilama, M., Nankabirwa, J., Yeka, A., Mawejje, H., Mpimbaza, A., Katamba, H., Donnelly, M.J., Rosenthal, P.J., Drakeley, C., Lindsay, S.W., Staedke, S.G., Smith, D.L., Greenhouse, B., Kamya, M.R., Dorsey, G., 2016. Measures of Malaria Burden after Long-Lasting Insecticidal Net Distribution and Indoor Residual Spraying at Three Sites in Uganda: A Prospective Observational Study. PLoS Med 13, 1–22. https://doi.org/10.1371/journal.pmed.1002167

Khambay, B.P.S., Jewess, P.J., 2010. Pyrethroids, in: Gilbert, L.I., Gill, S.S. (Eds.), Insect Control. Elsevier, pp. 1–29.

Killeen, G.F., Moore, S.J., 2012. Target product profiles for protecting against outdoor malaria transmission. Malar J 11, 1–6.

Kleinschmidt, I., Bradley, J., Knox, T.B., Mnzava, A.P., Kafy, H.T., Mbogo, C., Ismail, B.A., Bigoga, J.D., Adechoubou, A., Raghavendra, K., Cook, J., Malik, E.M., Nkuni, Z.J., Macdonald, M., Bayoh, N., Ochomo, E., Fondjo, E., Awono-Ambene, H.P., Etang, J., Akogbeto, M., Bhatt, R.M., Chourasia, M.K., Swain, D.K., Kinyari, T., Subramaniam, K., Massougbodji, A., Okê-Sopoh, M., Ogouyemi-Hounto, A., Kouambeng, C., Abdin, M.S., West, P., Elmardi, K., Cornelie, S., Corbel, V., Valecha, N., Mathenge, E., Kamau, L., Lines, J., Donnelly, M.J., 2018. Implications of insecticide resistance for malaria vector control with long-lasting insecticidal nets: a WHO-coordinated, prospective, international, observational cohort study. Lancet Infect Dis 18, 640–649. https://doi.org/10.1016/S1473-3099(18)30172-5

Kleinschmidt, I., Schwabe, C., Shiva, M., Segura, J.L., Sima, V., Mabunda, S.J.A., Coleman, M., 2009. Combining Indoor Residual Spraying and Insecticide-Treated Net Interventions. American Journal of Tropical Medicine and Hygiene 81, 519–524.

Kline, D.L., Urban, J., 2018. Potential for utilization of spatial repellents in mosquito control interventions. ACS Symposium Series 1289, 237–248. https://doi.org/10.1021/bk-2018-1289.ch013

Koener, J.F., Cariño, F.A., Feyereisen, R., 1993. The cDNA and deduced protein sequence of house fly NADPH-cytochrome P450 reductase. Insect Biochem Mol Biol 23, 439–447. https://doi.org/10.1016/0965-1748(93)90051-S

Kua, K.P., Lee, S.W.H., 2021. Randomized trials of housing interventions to prevent malaria and Aedes-transmitted diseases: A systematic review and meta-analysis. PLoS One 16, 1–23. https://doi.org/10.1371/journal.pone.0244284

Lees, R.S., Ismail, H.M., Logan, R.A.E., Malone, D., Davies, R., Anthousi, A., Adolfi, A., Lycett, G.J., Paine, M.J.I., 2020. New insecticide screening platforms indicate that Mitochondrial Complex I inhibitors are susceptible to cross-resistance by mosquito P450s that metabolise pyrethroids. Sci Rep 10, 1–10. https://doi.org/10.1038/s41598-020-73267-x

Lian, L.Y., Widdowson, P., McLaughlin, L.A., Paine, M.J.I., 2011. Biochemical comparison of Anopheles gambiae and human NADPH P450 reductases reveals different 2′-5′-ADP and FMN binding traits. PLoS One 6. https://doi.org/10.1371/journal.pone.0020574

Lindsay, S.W., Thomas, M.B., Kleinschmidt, I., 2021. Threats to the effectiveness of insecticide-treated bednets for malaria control: thinking beyond insecticide resistance. Lancet Glob Health 9, e1325–e1331. https://doi.org/10.1016/S2214-109X(21)00216-3

Liu, N., 2015. Insecticide resistance in mosquitoes: Impact, mechanisms, and research directions. Annu Rev Entomol 60, 537–559. https://doi.org/10.1146/annurev-ento-010814-020828

Lycett, G.J., McLaughlin, L.A., Ranson, H., Hemingway, J., Kafatos, F.C., Loukeris, T.G., Paine, M.J.I., 2006. Anopheles gambiae P450 reductase is highly expressed in oenocytes and in vivo knockdown increases permethrin susceptibility. Insect Mol Biol 15, 321–327. https://doi.org/10.1111/j.1365-2583.2006.00647.x

Masalu, J.P., Finda, M., Killeen, G.F., Ngowo, H.S., Pinda, P.G., Okumu, F.O., 2020. Creating mosquito-free outdoor spaces using transfluthrin-treated chairs and ribbons. Malar J 19, 109. https://doi.org/10.1186/s12936-020-03180-1

Matambo, T.S., Paine, M.J., Coetzee, M., Koekemoer, L.L., 2010. Sequence characterization of cytochrome P450 CYP6P9 in pyrethroid resistant and susceptible Anopheles funestus (Diptera: Culicidae). Genet Mol Res 9, 554–564. https://doi.org/10.4238/vol9-1gmr719

Matowo, J., Weetman, D., Pignatelli, P., Wright, A., Charlwood, J.D., Kaaya, R., Shirima, B., Moshi, O., Lukole, E., Mosha, J., Manjurano, A., Mosha, F., Rowland, M., Protopopoff, N., 2022. Expression of pyrethroid metabolizing P450 enzymes characterizes highly resistant Anopheles vector species targeted by successful deployment of PBO-treated bednets in Tanzania. PLoS One 17, e0249440. https://doi.org/10.1371/journal.pone.0249440

McCann, R.S., Kabaghe, A.N., Moraga, P., Gowelo, S., Mburu, M.M., Tizifa, T., Chipeta, M.G., Nkhono, W., di Pasquale, A., Maire, N., Manda-Taylor, L., Mzilahowa, T., van den Berg, H., Diggle, P.J., Terlouw, D.J., Takken, W., van Vugt, M., Phiri, K.S., 2021. The effect of community-driven larval source management and house improvement on malaria transmission when added to the standard malaria control strategies in Malawi: a cluster-randomized controlled trial. Malar J 20, 1–16. https://doi.org/10.1186/s12936-021-03769-0

McLaughlin, L.A., Niazi, U., Bibby, J., David, J.P., Vontas, J., Hemingway, J., Ranson, H., Sutcliffe, M.J., Paine, M.J.I., 2008. Characterization of inhibitors and substrates of Anopheles gambiae CYP6Z2. Insect Mol Biol 17, 125–135. https://doi.org/10.1111/j.1365-2583.2007.00788.x

Menze, B.D., Kouamo, M.F., Wondji, M.J., Tchapga, W., Tchoupo, M., Kusimo, M.O., Mouhamadou, C.S., Riveron, J.M., Wondji, C.S., 2020. An experimental hut evaluation of PBO-based and pyrethroid-only nets against the malaria vector anopheles funestus reveals a loss of bed nets efficacy associated with GSTe2 metabolic resistance. Genes (Basel) 11. https://doi.org/10.3390/genes11020143

Menze, B.D., Riveron, J.M., Ibrahim, S.S., Irving, H., Antonio-Nkondjio, C., Awono-Ambene, P.H., Wondji, C.S., 2016. Multiple insecticide resistance in the malaria vector Anopheles funestus from Northern Cameroon is mediated by metabolic resistance alongside potential target site insensitivity mutations. PLoS One 11, 1–14. https://doi.org/10.1371/journal.pone.0163261

Miyazaki, M., Ohyama, K., Dunlap, D.Y., Matsumura, F., 1996. Cloning and sequencing of the para-type sodium channel gene from susceptible and kdr-resistant German cockroaches (Blattella germanica) and house fly (Musca domestica). Molecular and General Genetics 252, 61–68. https://doi.org/10.1007/s004389670007

Montella, I.R., Schama, R., Valle, D., 2012. The classification of esterases: An important gene family involved in insecticide resistance - A review. Mem Inst Oswaldo Cruz 107, 437–449. https://doi.org/10.1590/S0074-02762012000400001

Moyes, C.L., Athinya, D.K., Seethaler, T., Battle, K.E., Sinka, M., Hadi, M.P., Hemingway, J., Coleman, M., Hancock, P.A., 2020. Evaluating insecticide resistance across African districts to aid malaria control decisions. Proceedings of the National Academy of Sciences 117, 202006781. https://doi.org/10.1073/pnas.2006781117

Moyes, C.L., Vontas, J., Martins, A.J., Ng, L.C., Koou, S.Y., Dusfour, I., Raghavendra, K., Pinto, J., Corbel, V., David, J.P., Weetman, D., 2017. Contemporary status of insecticide resistance in the major Aedes vectors of arboviruses infecting humans. PLoS Negl Trop Dis. https://doi.org/10.1371/journal.pntd.0005625

Müller, P., Warr, E., Stevenson, B.J., Pignatelli, P.M., Morgan, J.C., Steven, A., Yawson, A.E., Mitchell, S.N., Ranson, H., Hemingway, J., Paine, M.J.I., Donnelly, M.J., 2008. Field-caught permethrin-resistant Anopheles gambiae overexpress CYP6P3, a P450 that metabolises pyrethroids. PLoS Genet 4. https://doi.org/10.1371/journal.pgen.1000286

Murataliev, M.B., Feyereisen, R., 1999. Mechanism of cytochrome P450 reductase from the house fly: Evidence for an FMN semiquinone as electron donor. FEBS Lett. https://doi.org/10.1016/S0014-5793(99)00723-1

Murataliev, M.B., Feyereisen, R., Walker, F.A., 2004. Electron transfer by diflavin reductases. Biochim Biophys Acta Proteins Proteom 1698, 1–26. https://doi.org/10.1016/j.bbapap.2003.10.003

Murataliev, M.B., Guzov, V.M., Walker, F.A., Feyereisen, R., 2008. P450 reductase and cytochrome b5 interactions with cytochrome P450: Effects on house fly CYP6A1 catalysis. Insect Biochem Mol Biol 38, 1008–1015. https://doi.org/10.1016/j.ibmb.2008.08.007

Musiba, R.M., Tarimo, B.B., Monroe, A., Msaky, D., Ngowo, H., Mihayo, K., Limwagu, A., Chilla, G.T., Shubis, G.K., Ibrahim, A., Greer, G., Mcha, J.H., Haji, K.A., Abbas, F.B., Ali, A., Okumu, F.O., Kiware, S.S., 2022. Outdoor biting and pyrethroid resistance as potential drivers of persistent malaria transmission in Zanzibar. Malar J 21, 1–14. https://doi.org/10.1186/s12936-022-04200-y

Mwanga, E.P., Mmbando, A.S., Mrosso, P.C., Stica, C., Mapua, S.A., Finda, M.F., Kifungo, K., Kafwenji, A., Monroe, A.C., Ogoma, S.B., Ngowo, H.S., Okumu, F.O., 2019. Eave ribbons treated with transfluthrin can protect both users and non - users against malaria vectors. Malar J 1–14. https://doi.org/10.1186/s12936-019-2958-9

Nakata, A., Hashimoto, S., Ikura, K., Katsuura, K., 1991. Development of a New Fungicide, Triflumizole. J Pestic Sci 16, 301–313.

Nauen, R., 2007. Insecticide resistance in disease vectors of public health importance. Pest Manag Sci 63, 628–633. https://doi.org/10.1002/ps.1406

Nauen, R., Zimmer, C., Vontas, J., 2021. Heterologous expression of insect P450 enzymes that metabolize xenobiotics. Curr Opin Insect Sci 43, 78–84. https://doi.org/10.1016/j.cois.2020.10.011

Nelson, D.R., 1998. Metazoan cytochrome P450 evolution. Comparative Biochemistry and Physiology - C Pharmacology Toxicology and Endocrinology 121, 15–22. https://doi.org/10.1016/S0742-8413(98)10027-0

N'Guessan, R., Asidi, A., Boko, P., Odjo, A., Akogbeto, M., Pigeon, O., Rowland, M., 2010. An experimental hut evaluation of PermaNet®3.0, a deltamethrin-piperonyl butoxide combination net, against pyrethroid-resistant Anopheles gambiae and Culex quinquefasciatus mosquitoes in southern Benin. Trans R Soc Trop Med Hyg. https://doi.org/10.1016/j.trstmh.2010.08.008

Ngufor, C., Agbevo, A., Fagbohoun, J., Fongnikin, A., Rowland, M., 2020. Efficacy of Royal Guard, a new alpha-cypermethrin and pyriproxyfen treated mosquito net, against pyrethroid-resistant malaria vectors. Sci Rep 10, 1–15. https://doi.org/10.1038/s41598-020-69109-5

Nikou, D., Ranson, H., Hemingway, J., 2003. An adult-specific CYP6 P450 gene is overexpressed in a pyrethroid- resistant strain of the malaria vector, Anopheles gambiae. Gene. https://doi.org/10.1016/S0378-1119(03)00763-7

Nkya, T.E., Poupardin, R., Laporte, F., Akhouayri, I., Mosha, F., Magesa, S., Kisinza, W., David, J.P., 2014. Impact of agriculture on the selection of insecticide resistance in the malaria vector Anopheles gambiae: A multigenerational study in controlled conditions. Parasit Vectors. https://doi.org/10.1186/s13071-014-0480-z

Nouage, L., Elanga-Ndille, E., Binyang, A., Tchouakui, M., Atsatse, T., Ndo, C., Kekeunou, S., Wondji, C., 2020. Influence of GST- and P450-based metabolic resistance to pyrethroids on blood feeding in the major African malaria vector Anopheles funestus 1–17. https://doi.org/10.1101/2020.03.16.993535

Ochomo, E., Chahilu, M., Cook, J., Kinyari, T., Bayoh, N.M., West, P., Kamau, L., Osangale, A., Ombok, M., Njagi, K., Mathenge, E., Muthami, L., Subramaniam, K., Knox, T., Mnavaza, A., Donnelly, M.J., Kleinschmidt, I., Mbogo, C., 2017. Insecticide-treated nets and protection against Insecticide-Resistant malaria vectors in Western Kenya. Emerg Infect Dis 23, 758–764. https://doi.org/10.3201/eid2305.161315

Ogoma, S.B., Moore, S.J., Maia, M.F., 2012a. A systematic review of mosquito coils and passive emanators: Defining recommendations for spatial repellency testing methodologies. Parasit Vectors 5, 1. https://doi.org/10.1186/1756-3305-5-287

Ogoma, S.B., Ngonyani, H., Simfukwe, E.T., Mseka, A., Moore, J., Killeen, G.F., 2012b. Spatial repellency of transfluthrin-treated hessian strips against laboratory-reared Anopheles arabiensis mosquitoes in a semi-field tunnel cage. Parasit Vectors 5, 54. https://doi.org/10.1186/1756-3305-5-54

Ogoma, S.B., Ngonyani, H., Simfukwe, E.T., Mseka, A., Moore, J., Maia, M.F., Moore, S.J., Lorenz, L.M., 2014. The mode of action of spatial repellents and their impact on vectorial capacity of Anopheles gambiae sensu stricto. PLoS One 9, e110433. https://doi.org/10.1371/journal.pone.0110433

Ojuka, P., Boum, Y., Denoeud-Ndam, L., Nabasumba, C., Muller, Y., Okia, M., Mwanga-Amumpaire, J., De Beaudrap, P., Protopopoff, N., Etard, J.F., 2015. Early biting and insecticide resistance in the malaria vector Anopheles might compromise the effectiveness of vector control intervention in Southwestern Uganda. Malar J. https://doi.org/10.1186/s12936-015-0653-z

Oliva, C., Benedict, M., Collins, M., Baldet, T., Bellini, R., Bossin, H., Bouyer, J., Corbel, V., Facchinelli, L., Fouque, F., Geier, M., Michaelakis, A., Roiz, D., Simard, F., Tur, C., Gouagna, L.-C., 2021. Sterile Insect Technique (SIT) against Aedes Species Designing, Implementing and Evaluating Pilot Field Trials. Insects 12, 191.

O'Reilly, A.O., Khambay, B.P.S., Williamson, M.S., Field, L.M., Wallace, B.A., Davies, T.G.E., 2006. Modelling insecticide-binding sites in the voltage-gated sodium channel. Biochemical Journal 396, 255–263. https://doi.org/10.1042/BJ20051925

Ortiz De Montellano, P.R., 2018. 1-Aminobenzotriazole: A Mechanism-Based Cytochrome P450 Inhibitor and Probe of Cytochrome P450 Biology. Medical Chemistry 8. https://doi.org/10.4172/2161-0444.1000495

Ortiz De Montellano, P.R., 2005. Cytochrome P450 Structure, Mechanism, and Biochemistry, Third. ed. Kluwer Academic, New York, Boston, Dordrecht, London, Moscow.

Oyewole, I.O., Awolola, T.S., Ibidapo, C.A., Oduola, A.O., Okwa, O.O., Obansa, J.A., 2007. Behaviour and population dynamics of the major anopheline vectors in a malaria endemic area in southern Nigeria. J Vector Borne Dis 44, 56–64.

Paine, M.J.I., Brooke, B., 2016. Insecticide Resistance and Its Impact on Vector Control, in: Horowitz, A.R., Ishaaya, I. (Eds.), Advances in Insect Control and Resistance Management. Springer International Publishing Switzerland, pp. 286–312. https://doi.org/DOI 10.1007/978-3-319-31800-4_15 287

Paine, M.J.I., Scrutton, N.S., Munro, A.W., Gutierrez, A., Gordon C.K. Roberts, Wolf, C.R., 2005. Electron Transfer Partners of Cytochrome P450, in: Cytochrome P450 Structure, Mechanism and Biochemistry. pp. 115–148.

Pang, S.C., Chiang, L.P., Tan, C.H., Vythilingam, I., Lam-Phua, S.G., Ng, L.C., 2015. Low efficacy of delthamethrin-treated net against singapore aedes aegypti is associated with kdr-type resistance. Trop Biomed 32, 140–150.

Parker, J.E.A., Angarita-Jaimes, N., Abe, M., Towers, C.E., Towers, D., McCall, P.J., 2015. Infrared video tracking of Anopheles gambiae at insecticide-treated bed nets reveals rapid decisive impact after brief localised net contact. Sci Rep 5, 1–14. https://doi.org/10.1038/srep13392

Phillips, M.A., Burrows, J.N., Manyando, C., Van Huijsduijnen, R.H., Van Voorhis, W.C., Wells, T.N.C., 2017. Malaria. Nat Rev Dis Primers 3. https://doi.org/10.1038/nrdp.2017.50

Pilling, E.D., Jepson, P.C., 1993. Synergism between EBI fungicides and a pyrethroid insecticide in the honeybee (Apis mellifera). Pestic Sci 39, 293–297. https://doi.org/10.1002/ps.2780390407

Pluess, B., Tanser, F., Lengeler, C., Sharp, B., 2010. Indoor residual spraying for preventing malaria. Cochrane Database of Systematic Reviews 2010. https://doi.org/10.1002/14651858.CD006657.pub2

Porter, T.D., 2012. New insights into the role of cytochrome P450 reductase (POR) in microsomal redox biology. Acta Pharm Sin B 2, 102–106. https://doi.org/10.1016/j.apsb.2012.02.002

Poulos, T.L., 2003. Cytochrome P450 flexibility. Proc Natl Acad Sci U S A 100, 13121–13122. https://doi.org/10.1073/pnas.2336095100

Poulos, T.L., Finzel, B.C., Howard, A.J., 1987. High-resolution crystal structure of cytochrome P450cam. J Mol Biol 195, 687–700. https://doi.org/10.1016/0022-2836(87)90190-2

Poupardin, R., Srisukontarat, W., Yunta, C., Ranson, H., 2014. Identification of Carboxylesterase Genes Implicated in Temephos Resistance in the Dengue Vector Aedes aegypti. PLoS Negl Trop Dis 8. https://doi.org/10.1371/journal.pntd.0002743

Protopopoff, N., Mosha, J.F., Lukole, E., Charlwood, J.D., Wright, A., Mwalimu, C.D., Manjurano, A., Mosha, F.W., Kisinza, W., Kleinschmidt, I., Rowland, M., 2018. Effectiveness of a long-lasting piperonyl butoxide-treated insecticidal net and indoor residual spray interventions, separately and together, against malaria transmitted by pyrethroid-resistant mosquitoes: a cluster, randomised controlled, two-by-two fact. The Lancet 391, 1577–1588. https://doi.org/10.1016/S0140-6736(18)30427-6

Pryce, J., Medley, N., Choi, L., Pryce, J., Medley, N., Choi, L., 2022. Indoor residual spraying for preventing malaria in communities using insecticide-treated nets (Review). https://doi.org/10.1002/14651858.CD012688.pub3.www.cochranelibrary.com

Pryce, J., Richardson, M., Lengeler, C., 2018. Insecticide-treated nets for preventing malaria. Cochrane Database of Systematic Reviews. https://doi.org/10.1002/14651858.CD000363.pub3

Pulman, D.A., 2011. Deltamethrin: The cream of the crop. J Agric Food Chem 59, 2770–2772. https://doi.org/10.1021/jf102256s

Qualls, W.A., Müller, G.C., Revay, E.E., Allan, S.A., Arheart, K.L., Beier, J.C., Smith, M.L., Scott, J.M., Kravchenko, V.D., Hausmann, A., Yefremova, Z.A., Xue, R. de, 2014. Evaluation of attractive toxic sugar bait (ATSB)-Barrier for control of vector and nuisance mosquitoes and its effect on non-target organisms in sub-tropical environments in Florida. Acta Trop 131, 104–110. https://doi.org/10.1016/j.actatropica.2013.12.004

Ranson, H., Burhani, J., Lumjuan, N., Black IV, W.C., 2008. Insecticide resistance in dengue vectors. Tropika 307–316.

Ranson, H., Lissenden, N., 2016. Insecticide Resistance in African Anopheles Mosquitoes: A Worsening Situation that Needs Urgent Action to Maintain Malaria Control. Trends Parasitol. https://doi.org/10.1016/j.pt.2015.11.010

Ranson, H., N'Guessan, R., Lines, J., Moiroux, N., Nkuni, Z., Corbel, V., 2011. Pyrethroid resistance in African anopheline mosquitoes: What are the implications for malaria control? Trends Parasitol 27, 91–98. https://doi.org/10.1016/j.pt.2010.08.004

Riveron, J.M., Huijben, S., Tchapga, W., Tchouakui, M., Wondji, M.J., Tchoupo, M., Irving, H., Cuamba, N., Maquina, M., Paaijmans, K., Wondji, C.S., 2019. Escalation of Pyrethroid Resistance in the Malaria Vector Anopheles funestus Induces a Loss of Efficacy of Piperonyl Butoxide–Based Insecticide-Treated Nets in Mozambique. J Infect Dis 220, 467–475. https://doi.org/10.1093/infdis/jiz139

Riveron, J.M., Ibrahim, S.S., Chanda, E., Mzilahowa, T., Cuamba, N., Irving, H., Barnes, K.G., Ndula, M., Wondji, C.S., 2014a. The highly polymorphic CYP6M7 cytochrome P450 gene partners with the directionally selected CYP6P9a and CYP6P9b genes to expand the pyrethroid resistance front in the malaria vector Anopheles funestus in Africa. BMC Genomics 15, 817. https://doi.org/10.1186/1471-2164-15-817

Riveron, J.M., Ibrahim, S.S., Mulamba, C., Djouaka, R., Irving, H., Wondji, M.J., Ishak, I.H., Wondji, C.S., 2017. Genome-wide transcription and functional analyses reveal heterogeneous molecular mechanisms driving pyrethroids resistance in the major malaria vector Anopheles funestus across Africa. G3: Genes, Genomes, Genetics 7, 1819–1832. https://doi.org/10.1534/g3.117.040147

Riveron, J.M., Irving, H., Ndula, M., Barnes, K.G., Ibrahim, S.S., Paine, M.J.I., Wondji, C.S., 2013. Directionally selected cytochrome P450 alleles are driving the spread of pyrethroid resistance in the major malaria vector Anopheles funestus. Proceedings of the National Academy of Sciences 110, 252–257. https://doi.org/10.1073/pnas.1216705110

Riveron, J.M., Tchouakui, M., Mugenzi, L., Menze, B.D., Chiang, M.-C., Wondji, C.S., 2018. Insecticide Resistance in Malaria Vectors: An Update at a Global Scale, in: Manguin, S. (Ed.), Towards Malaria Elimination, A Leap Forward. Intechopen, pp. 149–175. https://doi.org/http://dx.doi.org/10.5772/intechopen.78375

Riveron, J.M., Yunta, C., Ibrahim, S.S., Djouaka, R., Irving, H., Menze, B.D., Ismail, H.M., Hemingway, J., Ranson, H., Albert, A., Wondji, C.S., 2014b. A single mutation in the GSTe2 gene allows tracking of metabolically based insecticide resistance in a major malaria vector. Genome Biol 15, 1–20. https://doi.org/10.1186/gb-2014-15-2-r27

Robert, V., 2020. Brief history of insecticide-treated bed nets in the fight against Malaria: A testimony on the crucial 1980's decade. Bulletin de la Societe de Pathologie Exotique 113, 88–103. https://doi.org/10.3166/BSPE-2020-0128

Ruiz-Castillo, P., Rist, C., Rabinovich, R., Chaccour, C., 2022. Insecticide-treated livestock: a potential One Health approach to malaria control in Africa. Trends Parasitol 38, 112–123. https://doi.org/10.1016/j.pt.2021.09.006

Russell, T.L., Govella, N.J., Azizi, S., Drakeley, C.J., Kachur, S.P., Killeen, G.F., 2011. Increased proportions of outdoor feeding among residual malaria vector populations following increased use of insecticide-treated nets in rural Tanzania. Malar J 10, 1–10. https://doi.org/10.1186/1475-2875-10-80

Saavedra-Rodriguez, K., Strode, C., Flores, A.E., Garcia-Luna, S., Reyes-Solis, G., Ranson, H., Hemingway, J., Black IV, W.C., 2014. Differential transcription profiles in Aedes aegypti detoxification genes after temephos selection. Insect Mol Biol 23, 199–215. https://doi.org/10.1111/imb.12073

Sanou, A., Nelli, L., Guelbéogo, W.M., Cissé, F., Tapsoba, M., Ouédraogo, P., Sagnon, N., Ranson, H., Matthiopoulos, J., Ferguson, H.M., 2021. Insecticide resistance and behavioural adaptation as a response to long-lasting insecticidal net deployment in malaria vectors in the Cascades region of Burkina Faso. Sci Rep 11, 1–14. https://doi.org/10.1038/s41598-021-96759-w

Schenkman, J.B., Jansson, I., 2003. The many roles of cytochrome b5. Pharmacol Ther 97, 139–152. https://doi.org/10.1016/S0163-7258(02)00327-3

Schenkman, J.B., Jansson, I., 1999. Interactions between cytochrome P450 and cytochrome b5. Drug Metab Rev 31, 351–364. https://doi.org/10.1081/DMR-100101923

Shen, A.L., O'Leary, K.A., Kasper, C.B., 2002. Association of multiple developmental defects and embryonic lethality with loss of microsomal NADPH-cytochrome P450 oxidoreductase. Journal of Biological Chemistry 277, 6536–6541. https://doi.org/10.1074/jbc.M111408200

Sherrard-Smith, E., Griffin, J.T., Winskill, P., Corbel, V., Pennetier, C., Djénontin, A., Moore, S., Richardson, J.H., Müller, P., Edi, C., Protopopoff, N., Oxborough, R., Agossa, F., N'Guessan, R., Rowland, M., Churcher, T.S., 2018. Systematic review of indoor residual spray efficacy and effectiveness against Plasmodium falciparum in Africa. Nat Commun 9. https://doi.org/10.1038/s41467-018-07357-w

Sherrard-Smith, E., Skarp, J.E., Beale, A.D., Fornadel, C., Norris, L.C., Moore, S.J., Mihreteab, S., Charlwood, J.D., Bhatt, S., Winskill, P., Griffin, J.T., Churcher, T.S., 2019. Mosquito feeding behavior and how it influences residual malaria transmission across Africa. Proceedings of the National Academy of Sciences 116, 15086–15095. https://doi.org/10.1073/pnas.1820646116

Shono, T., Ohsawa, K., Casida, J.E., 1979. Metabolism of trans-and cis-Permethrin, trans-and cis-Cypermethrin, and Decamethrin by Microsomal Enzymes. J Agric Food Chem 27, 316–325. https://doi.org/10.1021/jf60222a059

Silva, A.P.B., Santos, J.M.M., Martins, A.J., 2014. Mutations in the voltage-gated sodium channel gene of anophelines and their association with resistance to pyrethroids - A review. Parasit Vectors 7. https://doi.org/10.1186/1756-3305-7-450

Silva, J.J., Scott, J.G., 2020. Conservation of the voltage-sensitive sodium channel protein within the Insecta. Insect Mol Biol 29, 9–18. https://doi.org/10.1111/imb.12605

Silvério, F.O., de Alvarenga, E.S., Moreno, S.C., Picanço, M.C., 2009. Synthesis and insecticidal activity of new pyrethroids. Pest Manag Sci 65, 900–905. https://doi.org/10.1002/ps.1771

Simma, E.A., Dermauw, W., Balabanidou, V., Snoeck, S., Bryon, A., Clark, R.M., Yewhalaw, D., Vontas, J., Duchateau, L., Van Leeuwen, T., 2019. Genome-wide gene expression profiling reveals that cuticle alterations and P450 detoxification are associated with deltamethrin and DDT resistance in Anopheles arabiensis populations from Ethiopia. Pest Manag Sci 75, 1808–1818. https://doi.org/10.1002/ps.5374

Sinka, M.E., Bangs, M.J., Manguin, S., Coetzee, M., Mbogo, C.M., Hemingway, J., Patil, A.P., Temperley, W.H., Gething, P.W., Kabaria, C.W., Okara, R.M., Boeckel, T. Van, Godfray, H.C.J., Harbach, R.E., Hay, S.I., 2010a. The dominant Anopheles vectors of human malaria in Africa, Europe and the Middle East: occurrence data, distribution maps and bionomic précis. Parasit Vectors 3, 117.

Sinka, M.E., Golding, N., Massey, N.C., Wiebe, A., Huang, Z., Hay, S.I., Moyes, C.L., 2016. Modelling the relative abundance of the primary African vectors of malaria before and after the implementation of indoor, insecticide-based vector control. Malar J 15, 142. https://doi.org/10.1186/s12936-016-1187-8

Sinka, M.E., Pironon, S., Massey, N.C., Longbottom, J., Hemingway, J., Moyes, C.L., Willis, K.J., 2020. A new malaria vector in Africa: Predicting the expansion range of Anopheles stephensi and identifying the urban populations at risk. Proc Natl Acad Sci U S A 117, 24900–24908. https://doi.org/10.1073/pnas.2003976117

Sinka, M.E., Rubio-Palis, Y., Manguin, S., Patil, A.P., Temperley, W.H., Gething, P.W., Van Boeckel, T., Kabaria, C.W., Harbach, R.E., Hay, S.I., 2011. The dominant Anopheles vectors of human malaria in the Asia-Pacific region: occurrence data, distribution maps and bionomic précis. Parasit Vectors 4. https://doi.org/10.1186/1756-3305-4-210

Sinka, M.E., Rubio-Palis, Y., Manguin, S., Patil, A.P., Temperley, W.H., Gething, P.W., Van Boeckel, T., Kabaria, C.W., Harbach, R.E., Hay, S.I., 2010b. The dominant Anopheles vectors of human malaria in the Americas: Occurrence data, distribution maps and bionomic précis. Parasit Vectors 4, 1–26. https://doi.org/10.1186/1756-3305-4-210

Sochantha, T., van Bortel, W., Savonnaroth, S., Marcotty, T., Speybroeck, N., Coosemans, M., 2010. Personal protection by long-lasting insecticidal hammocks against the bites of forest malaria vectors. Tropical Medicine and International Health 15, 336–341. https://doi.org/10.1111/j.1365-3156.2009.02457.x

Soderlund, D.M., 2020. Neurotoxicology of pyrethroid insecticides, in: Neurotoxicity of Pesticides. Elsevier Inc., pp. 113–165. https://doi.org/10.1016/bs.ant.2019.11.002

Soderlund, D.M., Casida, J.E., 1977. Effects of pyrethroid structure on rates of hydrolysis and oxidation by mouse liver microsomal enzymes. Pestic Biochem Physiol 7, 391–401. https://doi.org/10.1016/0048-3575(77)90043-8

Soderlund, D.M., York, N., States, U., 2017. Targeting Voltage-Gated Sodium Channels for Insect Control : Past , Present , and Future.

Sparks, T.C., Lorsbach, B.A., 2017. Agrochemical Discovery - Building the Next Generation of Insect Control Agents 1–17.

Sparks, T.C., Nauen, R., 2015. IRAC: Mode of action classification and insecticide resistance management. Pestic Biochem Physiol 121, 122–128. https://doi.org/10.1016/j.pestbp.2014.11.014

Sparks, T.C., Wessels, F.J., Lorsbach, B.A., Nugent, B.M., Watson, G.B., 2019. The new age of insecticide discovery-the crop protection industry and the impact of natural products. Pestic Biochem Physiol 161, 12–22. https://doi.org/10.1016/j.pestbp.2019.09.002

Spencer, C.S., Yunta, C., de Lima, G.P.G., Hemmings, K., Lian, L.Y., Lycett, G., Paine, M.J.I., 2018. Characterisation of Anopheles gambiae heme oxygenase and metalloporphyrin feeding suggests a potential role in reproduction. Insect Biochem Mol Biol 98, 25–33. https://doi.org/10.1016/j.ibmb.2018.04.010

Spitzen, J., Ponzio, C., Koenraadt, C.J.M., Jamet, H.V.P., Takken, W., 2014. Absence of Close-Range Excitorepellent Effects in Malaria Mosquitoes Exposed to Deltamethrin-Treated Bed Nets 90, 1124–1132. https://doi.org/10.4269/ajtmh.13-0755

Srisawat, R., Komalamisra, N., Eshita, Y., Zheng, M., Ono, K., Itoh, T.Q., Matsumoto, A., Petmitr, S., Rongsriyam, Y., 2010. Point mutations in domain II of the voltage-gated sodium channel gene in deltamethrin-resistant aedes aegypti (diptera: culicidae). Appl Entomol Zool 45, 275–282. https://doi.org/10.1303/aez.2010.275

Stevenson, B.J., Bibby, J., Pignatelli, P., Muangnoicharoen, S., O'Neill, P.M., Lian, L.Y., Müller, P., Nikou, D., Steven, A., Hemingway, J., Sutcliffe, M.J., Paine, M.J.I., 2011. Cytochrome P450 6M2 from the malaria vector Anopheles gambiae metabolizes pyrethroids: Sequential metabolism of deltamethrin revealed. Insect Biochem Mol Biol 41, 492–502. https://doi.org/10.1016/j.ibmb.2011.02.003

Strode, C., Donegan, S., Garner, P., Enayati, A.A., Hemingway, J., 2014. The Impact of Pyrethroid Resistance on the Efficacy of Insecticide-Treated Bed Nets against African Anopheline

Mosquitoes: Systematic Review and Meta-Analysis. PLoS Med 11. https://doi.org/10.1371/journal.pmed.1001619

Suh, E., Grossman, M.K., Waite, J.L., Dennington, N.L., Sherrard-Smith, E., Churcher, T.S., Thomas, M.B., 2020. The influence of feeding behaviour and temperature on the capacity of mosquitoes to transmit malaria. Nat Ecol Evol 7, 940–951. https://doi.org/10.1038/s41559-020-1182-x

Sun, H., Mertz, R.W., Smith, L.B., Scott, J.G., 2021. Transcriptomic and proteomic analysis of pyrethroid resistance in the CKR strain of Aedes aegypti. PLoS Negl Trop Dis 15, e0009871. https://doi.org/10.1371/journal.pntd.0009871

Swai, J.K., Mmbando, A.S., Ngowo, H.S., Odufuwa, O.G., Finda, M.F., Mponzi, W., Nyoni, A.P., Kazimbaya, D., Limwagu, A.J., Njalambaha, R.M., Abbasi, S., Moore, S.J., Schellenberg, J., Lorenz, L.M., Okumu, F.O., 2019. Protecting migratory farmers in rural Tanzania using eave ribbons treated with the spatial mosquito repellent , transfluthrin. Malar J 1–13. https://doi.org/10.1186/s12936-019-3048-8

Tchigossou, G.M., Atoyebi, S.M., Akoton, R., Tossou, E., Innocent, D., Riveron, J., Irving, H., Yessoufou, A., Wondji, C., Djouaka, R., 2020. Investigation of DDT resistance mechanisms in Anopheles funestus populations from northern and southern Benin reveals a key role of the GSTe2 gene. Malar J 1–12. https://doi.org/10.1186/s12936-020-03503-2

Temu, E.A., Minjas, J.N., Tuno, N., Kawada, H., Takagi, M., 2007. Identification of four members of the Anopheles funestus (Diptera: Culicidae) group and their role in Plasmodium falciparum transmission in Bagamoyo coastal Tanzania. Acta Trop 102, 119–125. https://doi.org/10.1016/j.actatropica.2007.04.009

Thomsen, E.K., Koimbu, G., Pulford, J., Jamea-Maiasa, S., Ura, Y., Keven, J.B., Siba, P.M., Mueller, I., Hetzel, M.W., Reimer, L.J., 2017. Mosquito behavior change after distribution of bednets results in decreased protection against malaria exposure. Journal of Infectious Diseases 215, 790–797. https://doi.org/10.1093/infdis/jiw615

Toe, K.H., Mueller, P., Badolo, A., Traore, A., N'Falé, S., Dabire, R.K., Ranson, H., 2018. Do bednets including piperonyl butoxide offer additional protection against populations of Anopheles gambiae s.l. that are highly resistant to pyrethroids? An experimental hut evaluation in Burkina Faso.

Traore, M.M., Junnila, A., Traore, S.F., Doumbia, S., Revay, E.E., Kravchenko, V.D., Schlein, Y., Arheart, K.L., Gergely, P., Xue, R. de, Hausmann, A., Beck, R., Prozorov, A., Diarra, R.A., Kone, A.S., Majambere, S., Bradley, J., Vontas, J., Beier, J.C., Müller, G.C., 2020. Large-scale field trial of attractive toxic sugar baits (ATSB) for the control of malaria vector mosquitoes in Mali, West Africa. Malar J 19, 1–16. https://doi.org/10.1186/s12936-020-3132-0

Tungu, P.K., Michael, E., Sudi, W., Kisinza, W.W., Rowland, M., 2021. Efficacy of interceptor ® G2 , a long - lasting insecticide mixture net treated with chlorfenapyr and alpha - cypermethrin against Anopheles funestus : experimental hut trials in north - eastern Tanzania. Malar J 20. https://doi.org/10.1186/s12936-021-03716-z

Usherwood, P.N.R., Davies, T.G.E., Mellor, I.R., O'Reilly, A.O., Peng, F., Vais, H., Khambay, B.P.S., Field, L.M., Williamson, M.S., 2007. Mutations in DIIS5 and the DIIS4-S5 linker of Drosophila melanogaster sodium channel define binding domains for pyrethroids and DDT. FEBS Lett 581, 5485–5492. https://doi.org/10.1016/j.febslet.2007.10.057

Vais, H., Atkinson, S., Pluteanu, F., Goodson, S.J., Devonshire, A.L., Williamson, M.S., Usherwood, P.N.R., 2003. Mutations of the para sodium channel of Drosophila melanogaster identify putative binding sites for pyrethroids. Mol Pharmacol 64, 914–922. https://doi.org/10.1124/mol.64.4.914

Vais, H., Williamson, M.S., Devonshire, A.L., Usherwood, P.N.R., 2001. The molecular interactions of pyrethroid insecticides with insect and mammalian sodium channels. Pest Manag Sci 57, 877–888. https://doi.org/10.1002/ps.392

Vannini, L., Reed, T.W., Willis, J.H., 2014. Temporal and spatial expression of cuticular proteins of Anopheles gambiae implicated in insecticide resistance or differentiation of M/S incipient species. Parasit Vectors 7, 1–11. https://doi.org/10.1186/1756-3305-7-24

Vontas, J., Blass, C., Koutsos, A.C., David, J.P., Kafatos, F.C., Louis, C., Hemingway, J., Christophides, G.K., Ranson, H., 2005. Gene expression in insecticide resistant and susceptible Anopheles gambiae strains constitutively or after insecticide exposure. Insect Mol Biol. https://doi.org/10.1111/j.1365-2583.2005.00582.x

Vontas, J., Katsavou, E., Mavridis, K., 2020. Cytochrome P450-based metabolic insecticide resistance in Anopheles and Aedes mosquito vectors: Muddying the waters. Pestic Biochem Physiol 170, 104666. https://doi.org/10.1016/j.pestbp.2020.104666

Wang, M., Roberts, D.L., Paschke, R., Shea, T.M., Masters, B.S.S., Kim, J.J.P., 1997. Three-dimensional structure of NADPH-cytochrome P450 reductase: Prototype for FMN- and FAD-containing enzymes. Proc Natl Acad Sci U S A 94, 8411–8416. https://doi.org/10.1073/pnas.94.16.8411

Weedall, G.D., Mugenzi, L.M.J., Menze, B.D., Tchouakui, M., Ibrahim, S.S., Amvongo-Adjia, N., Irving, H., Wondji, M.J., Tchoupo, M., Djouaka, R., Riveron, J.M., Wondji, C.S., 2019. A cytochrome P450 allele confers pyrethroid resistance on a major African malaria vector, reducing insecticide-treated bednet efficacy. Sci Transl Med 11, eaat7386. https://doi.org/10.1126/scitranslmed.aat7386

WHO, 2022a. World Malaria Report 2022.

WHO, 2022b. Prequalified Vector Control Products.

WHO, 2022c. Determining discriminating concentrations of insecticides for monitoring resistance in mosquitoes: report of a multi-centre laboratory study and WHO expert consultations.

WHO, 2021. World Malaria Report, World Malaria Report 2021.

WHO, 2020. Vector-borne diseases [WWW Document]. Vector-borne diseases. URL https://www.who.int/news-room/fact-sheets/detail/vector-borne-diseases

WHO, 2018. Global report on insecticide resistance in malaria vectors: 2010-2016.

WHO, 2017. Conditions for deployment of mosquito nets treated with a pyrethroid and piperonyl butoxide. Global Malaria Programme, World Health Organization 2017, 1–4.

WHO, 2016. World Malaria Report 2016.

WHO, 2006. Pesticide and their Application for the control of vectors and pests of Public Health importance. World Health Organization 6. https://doi.org/10.1371/journal.pone.0170079

WHO, 2005. World Malaria Report. World Health Organization 316. https://doi.org/10.1007/SpringerReference_83401

Williams, P.A., Cosme, J., Sridhar, V., Johnson, E.F., McRee, D.E., 2000. Mammalian microsomal cytochrome P450 monooxygenase: Structural adaptations for membrane binding and functional diversity. Mol Cell 5, 121–131. https://doi.org/10.1016/S1097-2765(00)80408-6

Williamson, M.S., Martinez-Torres, D., Hick, C.A., Devonshire, A.L., 1996. Identification of mutations in the housefly para-type sodium channel gene associated with knockdown resistance (kdr) to pyrethroid insecticides. Molecular and General Genetics. https://doi.org/10.1007/BF02173204

Wondji, C.S., Hearn, J., Irving, H., Wondji, M.J., Weedall, G., 2022. RNAseq-based gene expression profiling of the Anopheles funestus pyrethroid-resistant strain FUMOZ highlights the predominant role of the duplicated CYP6P9a/b cytochrome P450s. G3: Genes, Genomes, Genetics 12. https://doi.org/10.1093/G3JOURNAL/JKAB352

Wood, O.R., Hanrahan, S., Coetzee, M., Koekemoer, L.L., Brooke, B.D., 2010. Cuticle thickening associated with pyrethroid resistance in the major malaria vector Anopheles funestus. Parasit Vectors 3, 67. https://doi.org/10.1186/1756-3305-3-67

Yahouédo, G.A., Chandre, F., Rossignol, M., Ginibre, C., Balabanidou, V., Mendez, N.G.A., Pigeon, O., Vontas, J., Cornelie, S., 2017. Contributions of cuticle permeability and enzyme detoxification to pyrethroid resistance in the major malaria vector Anopheles gambiae. Sci Rep 7, 1–10. https://doi.org/10.1038/s41598-017-11357-z

Yanola, J., Somboon, P., Walton, C., Nachaiwieng, W., Somwang, P., Prapanthadara, L. aied, 2011. High-throughput assays for detection of the F1534C mutation in the voltage-gated sodium channel gene in permethrin-resistant Aedes aegypti and the distribution of this mutation throughout Thailand. Tropical Medicine and International Health 16, 501–509. https://doi.org/10.1111/j.1365-3156.2011.02725.x

Yoshida, T., 2013. Analytical method for urinary metabolites of the fluorine-containing pyrethroids metofluthrin , profluthrin and transfluthrin by gas chromatography / mass spectrometry. Journal of Chromatography B 913–914, 77–83. https://doi.org/10.1016/j.jchromb.2012.11.025

Yoshida, T., 2012. Identification of urinary metabolites in rats administered the fluorine-containing pyrethroids metofluthrin , profluthrin , and transfluthrin 94, 1789–1804. https://doi.org/10.1080/02772248.2012.729838

Yunta, C., Grisales, N., Nász, S., Hemmings, K., Pignatelli, P., Voice, M., Ranson, H., Paine, M.J.I., 2016. Pyriproxyfen is metabolized by P450s associated with pyrethroid resistance in An. gambiae. Insect Biochem Mol Biol 78, 50–57. https://doi.org/10.1016/j.ibmb.2016.09.001

Yunta, C., Hemmings, K., Stevenson, B., Koekemoer, L.L., Matambo, T., Pignatelli, P., Voice, M., Nász, S., Paine, M.J.I., 2019. Cross-resistance profiles of malaria mosquito P450s associated with pyrethroid resistance against WHO insecticides. Pestic Biochem Physiol 161, 61–67. https://doi.org/10.1016/j.pestbp.2019.06.007

Zabalou, S., Riegler, M., Theodorakopoulou, M., Stauffer, C., Savakis, C., Bourtzis, K., 2004. Wolbachia-induced cytoplasmic incompatibility as a means for insect pest population control. Proc Natl Acad Sci U S A 101, 15042–15045. https://doi.org/10.1073/pnas.0403853101

Zhang, M., Scott, J.G., 1996. Cytochrome b5 is essential for cytochrome P450 6D1-mediated cypermethrin resistance in LPR house flies. Pestic Biochem Physiol 55, 150–156. https://doi.org/10.1006/pest.1996.0044

Zhang, M., Scott, J.G., 1994. Cytochrome b5 involvement in cytochrome P450 monooxygenase activities in house fly microsomes. Arch Insect Biochem Physiol 27, 205–216. https://doi.org/10.1002/arch.940270306

Zheng, X., Zhang, D., Li, Y., Yang, C., Wu, Y., Liang, X., Liang, Y., Pan, X., Hu, L., Sun, Q., Wang, X., Wei, Y., Zhu, J., Qian, W., Yan, Z., Parker, A.G., Gilles, J.R.L., Bourtzis, K., Bouyer, J., Tang, M., Zheng, B., Yu, J., Liu, J., Zhuang, J., Hu, Zhigang, Zhang, M., Gong, J.T., Hong, X.Y., Zhang, Z., Lin, L., Liu, Q., Hu, Zhiyong, Wu, Z., Baton, L.A., Hoffmann, A.A., Xi, Z., 2019. Incompatible and sterile insect techniques combined eliminate mosquitoes. Nature 572, 56–61. https://doi.org/10.1038/s41586-019-1407-9

Zhou, G., Li, Y., Jeang, B., Wang, X., Cummings, R.F., Zhong, D., Yan, G., 2022. Emerging Mosquito Resistance to Piperonyl Butoxide-Synergized Pyrethroid Insecticide and Its Mechanism. J Med Entomol 1–10. https://doi.org/https://doi.org/10.1093/jme/tjab231

Zhu, F., Sams, S., Moural, T., Haynes, K.F., Potter, M.F., Palli, S.R., 2012. RNA interference of NADPH-cytochrome P450 reductase results in reduced insecticide resistance in the bed bug, cimex lectularius. PLoS One 7. https://doi.org/10.1371/journal.pone.0031037

Zimmer, C.T., Bass, C., Williamson, M.S., Kaussmann, M., Wölfel, K., Gutbrod, O., Nauen, R., 2014. Molecular and functional characterization of CYP6BQ23, a cytochrome P450 conferring resistance to pyrethroids in European populations of pollen beetle, Meligethes aeneus. Insect Biochem Mol Biol 45, 18–29. https://doi.org/10.1016/j.ibmb.2013.11.008

7. Appendix

7.1. Publication chapter 2: Towards understanding transfluthrin efficacy in a pyrethroid-resistant strain of the malaria vector Anopheles funestus with special reference to cytochrome P450-mediated detoxification

Current Research in Parasitology & Vector-Borne Diseases 1 (2021) 100041

Contents lists available at ScienceDirect

Current Research in Parasitology & Vector-Borne Diseases

journal homepage: www.editorialmanager.com/crpvbd/default.aspx

Towards understanding transfluthrin efficacy in a pyrethroid-resistant strain of the malaria vector *Anopheles funestus* with special reference to cytochrome P450-mediated detoxification

Melanie Nolden [a,b], Andreas Brockmann [a,c], Ulrich Ebbinghaus-Kintscher [a], Kai-Uwe Brueggen [a], Sebastian Horstmann [a], Mark J.I. Paine [b], Ralf Nauen [a,*]

[a] Bayer AG, Crop Science Division, Alfred Nobel Str. 50, D-40789, Monheim am Rhein, Germany
[b] Department of Vector Biology, Liverpool School of Tropical Medicine, Pembroke Place, Liverpool, L3 5QA, United Kingdom
[c] Rheinische Friedrich-Wilhelms-Universität Bonn, D-53113, Bonn, Germany

ARTICLE INFO

Keywords:
Anopheles
Pyrethroid resistance
P450
Synergists
Azole fungicides
Sodium channel
Deltamethrin
FUMOZ-R
Malaria

ABSTRACT

Malaria vector control interventions rely heavily on the application of insecticides against anopheline mosquitoes, in particular the fast-acting pyrethroids that target insect voltage-gated sodium channels (VGSC). Frequent applications of pyrethroids have resulted in resistance development in the major malaria vectors including *Anopheles funestus*, where resistance is primarily metabolic and driven by the overexpression of microsomal cytochrome P450 monooxygenases (P450s). Here we examined the pattern of cross-resistance of the pyrethroid-resistant *An. funestus* strain FUMOZ-R towards transfluthrin and multi-halogenated benzyl derivatives, permethrin, cypermethrin and deltamethrin in comparison to the susceptible reference strain FANG. Transfluthrin and two multi-fluorinated derivatives exhibited micromolar potency - comparable to permethrin - to functionally expressed dipteran VGSC in a cell-based cation influx assay. The activity of transfluthrin and its derivatives on VGSC was strongly correlated with their contact efficacy against strain FUMOZ-R, although no such correlation was obtained for the other pyrethroids due to their rapid detoxification by the resistant strain. The low resistance levels for transfluthrin and derivatives in strain FUMOZ-R were only weakly synergized by known P450 inhibitors such as piperonyl butoxide (PBO), triflumizole and 1-aminobenzotriazole (1-ABT). In contrast, deltamethrin toxicity in FUMOZ-R was synergized > 100-fold by all three P450 inhibitors. The biochemical profiling of a range of fluorescent resorufin and coumarin compounds against FANG and FUMOZ-R microsomes identified 7-benzyloxymethoxy-4-trifluoromethylcoumarin (BOMFC) as a highly sensitive probe substrate for P450 activity. BOMFC was used to develop a fluorescence-based high-throughput screening assay to measure the P450 inhibitory action of potential synergists. Azole fungicides prochloraz and triflumizole were identified as extremely potent nanomolar inhibitors of microsomal P450s, strongly synergizing deltamethrin toxicity in *An. funestus*. Overall, the present study contributed to the understanding of transfluthrin efficacy at the molecular and organismal level and identified azole compounds with potential to synergize pyrethroid efficacy in malaria vectors.

1. Introduction

The annual infection of humans with malaria remains high with an estimated 219 million cases and 435,000 deaths worldwide in 2017 (WHO, 2018a), the majority (~80%) occurring in sub-Saharan Africa. In Africa malaria is primarily transmitted by sibling species from the Gambiae complex such as *Anopheles gambiae* and *An. arabiensis*, and *An. funestus* (Diptera: Culicidae) from the Funestus subgroup (Sinka et al., 2010; Wiebe et al., 2017). *Anopheles funestus* is one of the major malaria vectors in sub-Saharan-Africa (Temu et al., 2007; Sinka et al., 2010), but its predicted geographical occurrence differs from *An. gambiae* (Wiebe et al., 2017).

Vector control interventions targeting anopheline mosquitoes mainly rely on long-lasting insecticidal nets (LLINs) or indoor residual sprays (IRS) (Bhatt et al., 2015; Sinka et al., 2016), using longstanding chemical classes of insecticides addressing a few modes of action (Nauen, 2007; Hoppé et al., 2016). For over 50 years adult mosquito control has relied on four different chemical classes of insecticides, i.e. DDT,

* Corresponding author.
E-mail address: ralf.nauen@bayer.com (R. Nauen).

https://doi.org/10.1016/j.crpvbd.2021.100041
Received 24 May 2021; Received in revised form 23 June 2021; Accepted 13 July 2021

organophosphates, carbamates and pyrethroids, addressing two modes of action. This contrasts with a much larger arsenal of insecticides targeting a much wider range of modes of action that are available for the control of agricultural pest species (Hemingway et al., 2006; Nauen, 2006; Sparks and Nauen, 2015). It is only very recently that the neonicotinoid clothianidin was introduced, an agricultural pesticide with a new mode of action for vector control uses either alone or in combination with a pyrethroid (Fuseini et al., 2019; Fongnikin et al., 2020).

The success of pyrethroids as insecticides such as deltamethrin (Pulman, 2011) is mainly based on their broad activity against a diverse range of pests and their fast knock-down action (Soderlund, 2020) resulting from the modulation of voltage-gated sodium channels (VGSC) in the insects' central nervous system (Field et al., 2017; Scott, 2019). Pyrethroids are broadly divided into two classes designated as type-I and type-II pyrethroids (Soderlund, 2020), based on the respective absence and presence of an α-cyano substituent that increases VGSC potency that determines the evoked physiological responses (Casida et al., 1983; Laufer et al., 1984; Soderlund and Bloomquist, 1989). Pyrethroids as insecticide sprays for vector control were introduced in the early 1970's (permethrin) and remained the cornerstone for vector control through the introduction of pyrethroid treated bednets 20 years ago, an intervention amongst others contributing to a significant decline in clinical cases of malaria between 2000 and 2015 (Bhatt et al., 2015). However, the spatially expanded exposure of anopheline mosquitoes to pyrethroids in impregnated bednets (ITNs) and LLINs, resulted in an increasing selection of alleles conferring resistance (Coleman et al., 2017; WHO, 2018b; Moyes et al., 2020). Therefore, the efficacy of these control measures is increasingly compromised by the development and spread of pyrethroid resistance alleles in anopheline mosquitoes, including *An. funestus* (Hemingway et al., 2016; Coleman et al., 2017; Hemingway, 2019).

Two major mechanisms have been described to confer pyrethroid resistance in anopheline mosquitoes (Hemingway et al., 2004; Coleman et al., 2017); metabolic resistance, in particular detoxification mediated by elevated levels of microsomal cytochrome P450 monooxygenases (P450s) (Vontas et al., 2020) known to be involved in oxidative metabolism of xenobiotics (Feyereisen, 1999), and target-site mutations resulting in decreased affinity of pyrethroids to their site of binding in VGSC due to amino acid substitutions, also called knock-down resistance (kdr) (Davies et al., 2007; Scott, 2019; Smith et al., 2019). Other mechanisms such as changes in cuticular hydrocarbons - resulting in decreased penetration of pyrethroids - are factors shown to contribute to resistance (Balabanidou et al., 2018).

Pyrethroid resistance in *An. funestus* was first described in South Africa (Hargreaves et al., 2000) and shown to be synergized by piperonyl butoxide (PBO), an inhibitor of P450 enzymes (Brooke et al., 2001). Bednets co-impregnated with PBO and pyrethroids were only recently endorsed to mitigate the effects of P450 associated resistance (Gleave et al., 2018; Moyes et al., 2020). Interestingly, despite high levels of pyrethroid resistance in *An. funestus* VGSC mutations known to confer kdr have not yet been described (Irving and Wondji, 2017), whilst kdr has become essentially fixed in populations of *An. gambiae* (Coetzee and Koekemoer, 2013). Upregulated levels of P450s linked to pyrethroid resistance in *An. funestus* have been reported in many field studies in Africa (Cuamba et al., 2010; Morgan et al., 2010; Irving et al., 2012; Djouaka et al., 2016; Sangba et al., 2016; Tchigossou et al., 2018). The genetically duplicated and highly overexpressed P450 alleles CYP6P9a and CYP6P9b are key determinants of pyrethroid-resistance in *An. funestus* (Wondji et al., 2009; Riveron et al., 2013), that have been shown to compromise the efficacy of pyrethroid-treated bednets (Weedall et al., 2019). Many laboratory studies were conducted with the field-collected *An. funestus* colony FUMOZ, especially strain FUMOZ-R, a laboratory-selected reference strain expressing high levels of P450-mediated pyrethroid resistance and lacking kdr (Coetzee and Koekemoer, 2013). It was also shown that cuticle thickening in *An. funestus* (FUMOZ) could apparently affect pyrethroid penetration and thus contributing as an adjunct to the primary mechanism of resistance based on P450 overexpression (Wood et al., 2010).

Not all pyrethroids are similarly affected by P450-mediated resistance in *An. funestus* as recently demonstrated for the multi-halogenated benzyl pyrethroid transfluthrin (Horstmann and Sonneck, 2016). Transfluthrin (2,3,5,6-tetrafluorobenzyl(1R,3S)-3-(2,2-dichlorovinyl)-2,2-dimethylcyclo-propanecarboxylate; syn. benfluthrin) is an enantiomerically pure and volatile pyrethroid exhibiting spatial repellent activity against mosquitoes (Ogoma et al., 2012, 2014; Bibbs et al., 2018). It is under scrutiny as a complementary outdoor-protection tool to current vector control interventions (Kline and Urban, 2018; Masalu et al., 2020).

Here, we have examined the cross-resistance pattern of transfluthrin and halogenated benzyl derivatives against a susceptible strain (FANG) and the FUMOZ-R pyrethroid-resistant strain of *An. funestus*. We have also measured the interactions of pyrethroids with recombinantly expressed dipteran VGSC and explored the role of microsomal P450s in transfluthrin metabolism and resistance by synergist studies *in vivo* and *in vitro*. Overall, this has provided new insights on the efficacy and resistance-breaking properties of transfluthrin in pyrethroid-resistant *An. funestus* that will aid the development of new malaria control products.

2. Materials and methods

2.1. Mosquito strains

Anopheles funestus FUMOZ-R strain was obtained in 2011 from the National Institute for Communicable Diseases - Vector Control Reference Unit (VCRU) (Johannesburg, South Africa) and maintained at Bayer AG (Monheim, Germany) without insecticide selection pressure. It was originally collected in 2000 in South Mozambique and is highly resistant to pyrethroids (Brooke et al., 2001; Hunt et al., 2005), driven by the overexpression of cytochrome P450 monooxygenases (P450s) (Amenya et al., 2008). The insecticide susceptible *An. funestus* FANG strain was obtained in 2019 from the Liverpool Insecticide Testing Establishment (LITE) at the Liverpool School of Tropical Medicine (LSTM). The strain was originally received from the National Institute for Communicable Diseases (NICD) in South Africa and collected in Angola. Both strains were kept at 27.5 ± 0.5 °C, 65 ± 5% relative humidity and a photoperiod of 12/12 L:D with 1-h dusk/dawn. Adults were kept in rearing cages (46 cm × 33 cm × 20 cm) and five days after hatching the first blood meal (bovine blood, obtained from Elocin Laboratory, Oberhausen, Germany) was provided according to standard protocols (Das et al., 2007; Human Disease Vectors (HDV) group of the Insect Pest Control Laboratory, 2017).

2.2. Chemicals

Transfluthrin (CAS: 118712-89-3), deltamethrin (CAS: 52918-63-5), permethrin (CAS: 52645-53-1), 1-aminobenzotriazole (1-ABT) (CAS: 1614-12-6), triflumizole (CAS: 68694-11-1) and piperonyl butoxide (PBO) (CAS: 51-03-6) were obtained from Sigma-Aldrich/Merck (Darmstadt, Germany) of the highest purity available. Cypermethrin, and the transfluthrin derivatives TF-0, TF-1, TF-3 and TF-5 (Fig. 1) were of analytical grade and obtained internally from Bayer (Leverkusen, Germany). TF-5 is also known as fenfluthrin (Behrenz and Elbert, 1985). Transfluthrin is an enantiomerically pure compound (> 98% 1R-trans; < 1.0% 1S-trans). A similar enantiomeric purity is expected for the transfluthrin derivatives, which were synthesized starting from reactions of optically active 1R-trans-permethric acid chloride with the respective halogenated benzyl alcohol as described elsewhere (Naumann, 1990).

β-Nicotinamide adenine dinucleotide 2′-phosphate (NADPH) reduced tetrasodium salt hydrate (CAS: 2646-71-1 anhydrous, purity ≥ 93%), 7-ethoxycoumarin (EC; CAS: 31005-02-4, purity > 99%), 7-methoxy-4-trifluoromethylcoumarin (MFC; CAS: 575-04-2, purity ≥ 99%), 7-Ethoxy-4-trifluoromethylcoumarin (EFC; CAS: 115453-82-2, purity ≥ 98%) 7-benzyloxy-4-trifluoromethylcoumarin (BFC; CAS: 220001-53-6,

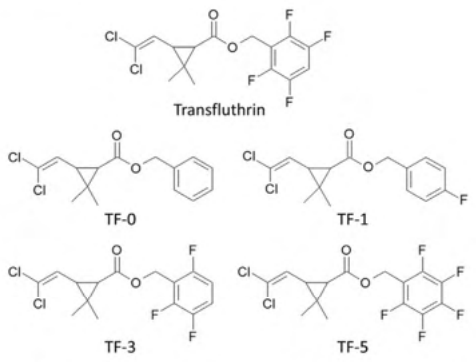

Fig. 1 Chemical structures of transfluthrin and its derivatives used in this study.

purity ≥ 99%), 7- hydroxy-coumarin (HC; CAS: 93-35-6, purity 99%) 7-hydroxy-4-trifluoromethylcoumarin (HFC; CAS: 575-03-1, purity 98%), 7-methoxyresorufin (MR; CAS: 5725-89-3, purity ≥ 98%), 7-ethoxyresorufin (ER; CAS: 5725-91-7, purity ≥ 95%), 7-benzoxyresorufin (BR; CAS: 87687-02-3), 7-n-pentoxyresorufin (PR; CAS: 87687-03-4) and resorufin sodium salt (CAS: 34994-50-8) were purchased from Sigma-Aldrich/Merck (Darmstadt, Germany). 7-Benzyloxymethoxy resorufin (BOMR; CAS: 87687-02-3; Vivid™ P2951) was purchased from Invitrogen, Thermo Fisher Scientific, Waltham, USA. 7-benzyloxymethoxy-4-trifluoromethylcoumarin (BOMFC; CAS: 277309-33-8; purity 95%) was synthesized by Enamine (Riga, Latvia). All chemicals were of analytical grade unless otherwise stated.

2.3. Glazed tile bioassay

To generate dose-response curves of pyrethroids, *An. funestus* FANG and FUMOZ-R mosquitoes were exposed to a range of different concentrations in a glazed tile assay as recently described by Horstmann and Sonneck (2016). Briefly: three to five days-old mosquitoes were anesthetized by placing them for 1 min at −20 °C and afterwards on a cooling plate at 2 °C. Ten females were placed in a Petri dish (diameter: 5 cm; height: 1 cm, including 12 ventilation holes) covered with a paper card. Insecticides were dissolved in acetone with a starting concentration of 2,000 ppm (equal to 100 mg/m^2) and diluted in 1:5 steps to 0.0256 ppm/0.00512 ppm (0.00128/0.000256 mg/m^2). Using an Eppendorf pipette 1,125 µl of each concentration was applied onto a glazed tile (15 cm × 15 cm, ceramic, Vitra, Germany). After the evaporation of acetone and mosquito recovery from anaesthetation (1 h), mosquitoes were exposed in two replicates ($n = 10$) for 30 min to each insecticide concentration and afterwards transferred back to the untreated paper card and kept in Petri dishes overnight. A 10% dextrose solution was provided overnight as a food source. Mortality was scored 24 h post-exposure. Acetone alone served as a control. Control mortality between 5 and 20% was corrected using Abbott's formula (Abbott, 1925), and bioassays exceeding 20% control mortality were considered invalid. All bioassays were replicated at least five times with two replicates ($n = 10$) unless otherwise stated.

2.4. Synergist bioassays

Final synergist concentrations of PBO, 1-ABT and triflumizole were chosen based on pre-assays assessing the toxicity of each P450 inhibitor by exposing adults of both strains for 30 min to a range of concentrations (10,000; 7,500; 5,000; 4,000; 2,000; 1,000; 500; and 250 ppm in acetone) in a glazed tile assay as described above. After 24 h, the mortality was evaluated. For the final bioassays the following concentrations were chosen: 2,000 ppm (100 mg/m^2) of triflumizole and PBO, and 5,000 ppm (250 mg/m^2) of 1-ABT for strain FUMOZ-R; 500 ppm (25 mg/m^2) of triflumizole and PBO, and 1,000 ppm (50 mg/m^2) of 1-ABT for strain FANG. Final synergist concentrations were applied onto glazed tiles as described above. Ten female adults were exposed for 30 min to each synergist and immediately afterwards transferred to pyrethroid treated glazed tiles as described above. As a control group, mosquitoes which were not exposed to the synergist and completely untreated mosquitoes were included. Mortality figures were corrected according to Abbott (1925), and tests exceeding 20% control mortality were considered invalid. All synergist bioassays were replicated at least twice.

2.5. UPLC-MS/MS analysis

As the synergists were applied *via* tarsal contact, ultra-performance liquid chromatography and mass spectrometry (UPLC/MS) was used to confirm their uptake by exemplarily analyzing exposed FUMOZ-R mosquito adults. PBO (2,000 ppm), triflumizole (2,000 ppm) and 1-ABT (5,000 ppm) were dissolved in acetone and applied onto a glazed tile as described above. After acetone evaporation (1 h) 10 female FUMOZ-R adults were exposed for 30 min to each synergist in replicates ($n = 2$). After exposure, mosquitoes were placed onto a cooling plate (2 °C) to separate legs and mosquito bodies. Legs and body fractions of ten mosquitoes were pooled ($n = 20$) in a 1.5 ml reaction tube, washed five times in 1,100 µl acetonitrile/water (80/20) and subsequently grinded using a micro-pestle in 1100 µl acetonitrile/water (80/20). The samples were centrifuged at 12,000× *g* for 10 min at room temperature (Centrifuge 5418R, Eppendorf, Hamburg, Germany) and the supernatant was transferred into a glass vial for subsequent UPLC-MS/MS analysis with slight modifications according to a previously published protocol (Manjon et al., 2018). Briefly, for the chromatography on an Agilent 1290 Infinity II, a Waters Acquity HSS T3 column (2.1 × 50 mm, 1.8 mm) with 0.025% formic acid in acetonitrile and 0.02% formic acid in water as the eluent in gradient mode was employed. After positive electrospray ionization, ion transitions were recorded on a Sciex API6500 Triple Quad. PBO, triflumizole and 1-ABT were measured in positive ion mode (ion transitions: PBO 356 > 177, triflumizole 346 > 278, 1-ABT 135 > 90.9). The peak integrals were calibrated externally against a standard calibration curve. The linear range for the quantification of PBO, triflumizole, and 1-ABT was 0.25–75 ng/ml, 0.25–100 ng/ml, and 0.5–1,000 ng/ml, respectively. Samples were diluted prior to measurement if needed. Recovery rates of mosquitoes exposed to the chosen synergist concentrations and acetone only were normally close to 100%.

2.6. Voltage-gated sodium channel measurements

The intrinsic potential of transfluthrin, its derivatives and common pyrethroids were measured in a HEK293 cell line expressing para-type voltage-gated sodium channels of *Musca domestica* (GenBank: AAB47604.1) using a Fluorescent Imaging Plate Reader, FLIPR Tetra (Molecular Devices, San Jose, CA, USA) fluorescence-based membrane potential assay (Molecular Devices, #R8034). Cells were plated at a density of 40,000 cells/well two days prior to the assay on black poly-D-lysine coated µClear 384-well plates (Greiner Bio-One, Essen, Germany), incubated overnight at 37 °C (5% CO_2) and subsequently stored 24 h at 26 °C. The FLIPR voltage membrane potential sensitive (MPs) dye assay was conducted with slight modifications according to Tay et al. (2019). Cell medium was removed, and cells were incubated for 1 h with 20 µl per well Tyrode buffer (Sigma T2397) containing 0.01% brilliant black (CAS: 2519-30-4) and 0.75 mg/ml MPs dye in the dark. Common pyrethroids and transfluthrin derivatives were pre-diluted in DMSO and further diluted to a final assay concentration of 50–0.0032 µM (deltamethrin: 50–0.0000256 µM; cypermethrin 10–0.00064 µM) in Tyrode buffer containing 0.03% Pluronic™ F-68 (Thermo Fisher Scientific,

Waltham, USA) (final DMSO concentration: 0.5%). Five µl of each concentration was added to each well and replicated four times and immediately measured every 5 s using the FLIPR high throughput cellular screening system at an emission wavelength of 565–625 nm while excited at 510–545 nm. Maximal response-over-baseline of each kinetic was subjected to further analysis using GraphPad Prism 8.4 (GraphPad Software, San Diego, USA). The assay was repeated three times on different days.

2.7. Isolation of microsomes and cytochrome P450 activity assays

Thirty to fifty adult mosquitoes (FUMOZ-R or FANG) were homogenized in an Eppendorf tube (2 ml) with a micro pestle in 500 µl homogenization-buffer (0.1 M K_2HPO_4, 1 mM DTT, 1 mM EDTA, 200 mM saccharose, pH 7.6) on ice and afterwards centrifuged at 5,000× *g* at 4 °C for 5 min. The supernatant was centrifuged again for 20 min at 15,000× *g* and 4 °C. The resulting supernatant was centrifuged for 1 h at 100,000× *g* and 4 °C (Beckman Coulter, Germany; Optima MAX-XP Benchtop Ultracentrifuge, rotor: MLA 130) and the microsomal pellet was resuspended in 250 µl 0.1 M buffer (0.1 M K_2HPO_4, 1 mM DTT, 0.1 mM EDTA, 5% glycerol, pH 7.6). The protein amount was determined according to Bradford (1976) and adjusted to 0.2 mg protein/ml.

The activity of microsomal monooxygenases was measured using a fluorescent probe assay with different model substrates at 20 ± 1 °C. Depending on the substrate, the final assay concentrations of fluorescence probes were 100 µM (PC), 50 µM (BFC, EC, EFC, MFC), 10 µM (BOMFC) and 4 µM (BOMR, BR, ER, MR, PR) adapted from Zimmer et al. (2014) and Manjon et al. (2018). Substrate stock solutions were prepared in DMSO at 100 mM (PC), 50 mM (BOMFC, BFC, EC, EFC, MFC), 2 mM (BOMR) and 1 mM (BR, ER, MR), and then diluted to the respective concentration with 0.1 M potassium-phosphate buffer (pH 7.6). Twenty-five µl of diluted substrate solution plus 25 µl of diluted enzymes were incubated for 1 h with and without 250 µM NADPH in a black 384-well plate (Greiner bio-one, F-bottom, PS). The reaction was replicated four times and stopped by adding 50 µl of red-ox mix (25% DMSO, 50 mM Tris–HCl buffer (pH 10), 5 mM glutathione oxidized, and 0.2 U glutathione reductase). Fluorescence was evaluated using a microplate reader (Tecan, Spark) at the respective excitation and emission wavelengths as described by Zaworra and Nauen (2019). As a positive control, rat liver microsomes (20 mg protein/ml; Sigma-Aldrich) were tested. The resulting reaction products, i.e. HC, HFC and resorufin were used to generate standard curves to calculate the amount of the respective product in pmol per mg/min (Ullrich and Weber, 1972; Manjon et al., 2018).

2.7.1. Michaelis-Menten kinetics of BOMFC O-dearylation by mosquito microsomes

Substrate concentration dependent microsomal monooxygenase kinetics was evaluated using eleven different BOMFC concentrations (stock 100 mM in DMSO) between 200 µM and 0.195 µM diluted in 0.1 M potassium-phosphate buffer (pH 7.6) containing 0.01% zwittergent 3-10 (CAS 15163-36-7, Sigma-Aldrich) and 1 mM NADPH at 20 ± 1 °C. Mosquito microsomal membranes were diluted in buffer (0.1 M K_2HPO_4, 0.1 mM EDTA, 1 mM DTT, 5% glycerol pH 7.6), (0.05% bovine serum albumin (BSA), 0.01% zwittergent 3-10) to 0.16 mg/ml corresponding to 4 µg protein per 25 µl enzyme solution. Twenty-five µl enzyme solution and 25 µl substrate solution were incubated for 1 h in a black 384-well plate and the reaction stopped as described above. Each reaction was replicated four times and the fluorescent product HFC was measured at 405 nm while excited at 510 nm. Substrate saturation kinetics were analyzed using GraphPad Prism 8.4 (Michaelis-Menten model).

2.7.2. Microsomal P450 inhibition kinetics

For the determination of IC50-values of different azole compounds and PBO on mosquito (FUMOZ-R) microsomal P450s the probe substrate BOMFC was used at a single concentration around the apparent Km value, i.e. 5 µM (Supplementary Fig. S1), following the general protocol recently described by Haas and Nauen (2021) with minor modifications. The chosen assay conditions were optimized for linearity with time and protein content of 7-hydroxy-4-(trifluoromethyl) coumarin (HC) fluorescent product formation. Microsomes of strain FUMOZ-R were incubated to eleven different concentrations of each inhibitor. Therefore, inhibitors were dissolved in 1:3.3 steps in DMSO at a final concentration of 0.5%, except for epoxiconazole (2%) and uniconazole (1%) to prevent precipitation at the highest concentration. Stock solutions were diluted with 0.1 M potassium-phosphate buffer (pH 7.6) containing 0.01% zwittergent 3-10 (final concentration range between 0.000596 µM and 1, 000 µM). Microsomal preparation was diluted in buffer (0.1 M K_2HPO_4, 0.1 mM EDTA, 1 mM DTT, 5% glycerol, pH 7.6) containing 0.01% zwittergent and 0.05% BSA to 0.16 mg/ml protein corresponding to 4 µg protein/well. Inhibitors and diluted microsomal preparations were applied to a 384-well microplate (384 wells, Greiner bio-one, F-bottom, PS) and incubated for 10 min at 20 ± 1 °C. Subsequently, 25 µl BOMFC/NADPH (final concentration 5 µM/125 µM) solution was added to each well and after 60 min the reaction was stopped as described above. Each reaction was repeated four times. Final assay evaluation was conducted in a microplate reader (Tecan Spark; Excitation: 405 nm; Emission: 510 nm) and reaction mix containing no inhibitor served as full enzyme activity control (100% activity). The controls lacking NADPH and BOMFC were subtracted from each data point. A standard curve was generated using HC to calculate the reaction velocity in pmol HC formed/min × mg protein^{-1}. Data were analysed and IC_{50}-values calculated using a four-parameter non-linear regression fitting routine in GraphPad Prism 8.4.

2.8. RNA extraction and cDNA preparation

RNA was extracted from ten adult female mosquitoes of each strain using TRIzol™ reaction kit following manufacturer's instructions. Afterwards RNA was purified using RNAeasy MINI Kit (Qiagen, Hilden, Germany) following manufacturer's instructions, including a DNAse-digest (RNase-free DNAse Set, 79254, Qiagen, Hilden, Germany) (modifications: Trizol incubation: 10 min, the column containing RNA sample was eluated twice to enhance RNA yields). The RNA concentrations were photometrically determined using 260/280 nm and 230/260 nm ratios (NanoQuant Infinite 200, Tecan, Switzerland). All samples were adjusted to 20 ng/µl.

Afterwards the RNA quality was checked using QIAxcel capillary electrophoresis technology following manufacturer instructions (QIAxcel Advanced, RNA Handbook, Qiagen, Hilden, Germany). RNA cartridge (QIAxcel RNA QC Kit v2.0, ID: 929104) and method CL-RNA were used. QX RNA Size Marker 200–6,000 nt (Qiagen ID: 929580) and QX RNA alignment marker (Qiagen ID: 929510) served as size marker and alignment marker, respectively. Once the RNA quality was confirmed, 0.3 µg of total RNA in 20 µl reaction volume was used for reverse transcription using IScript cDNA synthesis Kit (Bio-Rad, Hercules, USA) following manufacturer's instructions.

2.9. RT-qPCR

RT-qPCR measuring expression levels of CYP6P9a and CYP6P9b was done according to the method recently described by Boaventura et al. (2020) using SsoAdvanced Universal SYBR Green Supermix (Bio-Rad, Hercules, USA) with a total volume of 10 µl using CFX384™ Real-Time system (Bio-Rad, Hercules, USA). Samples were run in triplicate and a non-template control was included as the negative control. Two µl of cDNA with 5 ng/µl and each primer with 200 nM final concentrations were used. The PCR program was as follows: 95 °C for 30 s; 95 °C for 15 s; 55.5 °C for 15 s plate read; steps two and three were repeated 39 times followed by a melting curve from 65 °C to 95 °C in 0.5 °C steps for 5 s. Ribosomal protein S7 (RPS 7) and Actin 5c (Act) served as reference genes in this study. Primer efficiency for each target- and reference gene

was determined in advance with serial 1:5 cDNA dilution and revealed: CYP6P9a: 109.8%; CYP6P9b: 102.8%; Actin 5c: 105.9%; and RPS 7: 104.3%. Stability of the reference genes was checked with Bio-Rad CFX Maestro 1.0 v 4.0 software (Bio-Rad, Hercules, USA) (Vandesompele et al., 2002) and were used for normalization. In this study three to four biological replicates of each strain (FANG and FUMOZ-R) with three technical replicates were measured. Primers and GenBank accession numbers are given in the supplementary information (Supplementary Table S1).

2.10. Statistical analysis

Probit analysis of mosquito bioassay data was performed to calculate LC_{50} values and the 95% confidence intervals using SPSS version 25 (heterogeneity factor 0.5). EC_{50}-values for voltage-gated sodium channel binding of the different pyrethroids were calculated using GraphPad Prism 8.4 (Nonlinear regression, four parameters, variable slope, constraints: bottom: 0, top: 100). Pearson's correlations between mosquito bioassay data and EC_{50}-values were analyzed using GraphPad Prism 8.4. A one-way ANOVA was performed to analyze data for significant differences between data obtained for strains FANG and FUMOZ-R in the biochemical assays. Gene expression analysis was carried out employing Bio-Rad CFX Maestro 1.0 v. 4.0 software (Bio-Rad, Hercules, USA) followed by subsequent unpaired t-tests in qbase (Biogazelle) to compare for significant differences in gene expression levels.

3. Results

3.1. Efficacy of different pyrethroids in glazed tile bioassays

Full dose-response glazed tile bioassays produced a small difference in transfluthrin contact toxicity between *An. funestus* strains FANG and FUMOZ-R, resulting in a resistance ratio (RR) of 2.5 (Table 1). In contrast, FUMOZ-R exhibited high RRs of 223 and 78 against deltamethrin and cypermethrin, respectively. Permethrin and the transfluthrin derivatives TF-0 and TF-1 were the weakest pyrethroids against both strains, with highest LC_{50}-values, as opposed to transfluthrin and its multifluorinated benzyl derivatives TF-3 and TF-5 (Table 1). TF-5 (fenfluthrin) exhibited high contact activity similar to transfluthrin against both strains with a low RR for FUMOZ-R of 1.88, indicating a lack of cross-resistance with deltamethrin and cypermethrin. Based on LC_{50}-values the following efficacy ranking was obtained for the transfluthrin derivatives in glazed tile bioassays with strains FANG and FUMOZ-R: TF = TF-5 > TF-3 >> TF-0 = TF-1 and TF = TF-5 > TF-3 > TF-1 > TF-0, respectively. Those transfluthrin derivatives with a para-fluorinated benzyl ring, TF-1 and TF-5, showed the lowest RRs (< 2) in strain FUMOZ-R, followed by transfluthrin (2.51), TF-0 (3.77) and TF-3 (5.77).

3.2. Sensitivity of recombinantly expressed VGSC to pyrethroids

Pyrethroid activity to *M. domestica* VGSCs heterologously expressed in HEK293 cells was measured by sensing membrane potential changes using fluorescence imaging upon pyrethroid application (Fig. 2). The addition of deltamethrin to HEK293-VGSC cells increased the fluorescence signal in a concentration-dependent manner with an EC_{50}-value of 5.29 nM (95% CI: 4.43–6.30), suggesting high intrinsic VGSC activation (Supplementary Table S2). Cypermethrin and permethrin were significantly less effective and showed EC_{50}-values of 38.9 nM (95% CI: 34.2–44.3) and 721 nM (95% CI: 591–882), respectively (Fig. 2A; Supplementary Table S2). The most potent compound from the transfluthrin series was TF-5 exhibiting an EC_{50}-value similar to permethrin (736 nM (95% CI: 650–834)), followed by transfluthrin, TF-3, TF-1 and TF-0 (Fig. 2B; Supplementary Table S2). The EC_{50}-values of transfluthrin derivatives obtained *in vitro* were strongly correlated with their observed *in vivo* potential in glazed tile bioassays against adult mosquitoes of both strain FANG (Fig. 2C) and FUMOZ-R (Fig. 2D). Such a correlation was also observed for deltamethrin, cypermethrin and permethrin, but only in the pyrethroid susceptible strain FANG (Fig. 2C). In contrast no such correlation was obtained for the resistant strain FUMOZ-R (Fig. 2D). Interestingly transfluthrin and TF-5, despite being more than 100-fold less active on VGSC, exhibited a similar *in vivo* efficacy based on LC_{50}-values in glazed tile bioassays as deltamethrin against strain FANG (Fig. 2C), suggesting additional factors involved in acute contact toxicity than potency on VGSC.

3.3. Synergism of pyrethroid efficacy by different P450 inhibitors

Synergists were first tested for their solo contact toxicity in glazed tile assays to select concentrations not affecting adult survival. At the highest 1-ABT concentration tested (750 mg/m^2), mortality in both strains was < 10%. In contrast PBO and triflumizole were toxic against both strains, but at high concentrations. PBO and triflumizole were more active against the susceptible FANG strain with an LC_{50}-value of 325 mg/m^2 (95% CI: 199–707) and 136 mg/m^2 (95% CI: 40.5–188) respectively. Whereas both synergists were less toxic to the resistant strain FUMOZ-R as demonstrated by LC_{50}-values of > 1,000 mg/m^2 and 392 mg/m^2 (95% CI: 293–508) for PBO and triflumizole respectively. Sublethal concentrations of all synergists applied to glazed tiles were readily taken up after 30 min contact by FUMOZ-R adults as shown by UPLC/MS analysis of legs and body extracts, confirming their internalization (Fig. 3). All synergists were highly effective in strain FUMOZ-R in combination with deltamethrin (Fig. 4). This included both the azole compounds triflumizole and 1-ABT not previously tested for their synergistic potential in *An. funestus*. The synergistic ratios for deltamethrin in strain FUMOZ-R were > 100-fold, whereas permethrin, transfluthrin and derivatives were significantly lower (Fig. 4, Supplementary Table S3). There was minimal

Table 1
Log-dose probit-mortality data (24 h) for different pyrethroids against female adults of *Anopheles funestus* strains FANG and FUMOZ-R in glazed tile bioassays after contact exposure (30 min).

Compound	*An. funestus* FANG (susceptible)					*An. funestus* FUMOZ-R (resistant)					RR
	LC_{50} (mg/m^2)	95% CI	Slope ± SE		*n*	LC_{50} (mg/m^2)	95% CI	Slope ± SE		*n*	
Transfluthrin (TF)	0.023	0.0155–0.0324	1.47	0.168	420	0.0576	0.0191–0.112	1.6	0.218	360	2.51
TF-0	1.19	0.565–1.790	2.90	0.932	140	4.47	2.89–6.01	3.17	0.655	360	3.77
TF-1	1.42	1.02–1.85	2.97	0.453	560	1.41	1.15–1.83	4.79	0.772	350	0.99
TF-3	0.0494	0.0350–0.0664	1.96	0.256	420	0.285	0.225–0.354	3.32	0.495	360	5.77
TF-5	0.0237	0.0132–0.0394	2.03	0.243	420	0.0446	0.0299–0.0592	2.08	0.316	560	1.88
Permethrin	0.543	0.409–0.702	2.28	0.294	420	4.21	2.79–5.88	1.99	0.278	360	7.76
Cypermethrin	0.0968	0.0686–0.1260	2.74	0.479	420	7.54	5.24–10.40	1.86	0.204	540	77.9
Deltamethrin	0.0206	0.0153–0.0273	1.38	0.119	420	4.61	2.73–7.50	1.07	0.102	540	223

Note: Resistance ratio (RR) = LC_{50} FUMOZ-R divided by LC_{50} FANG.
Abbreviation: 95% CI, 95% confidence interval; SE, standard error.

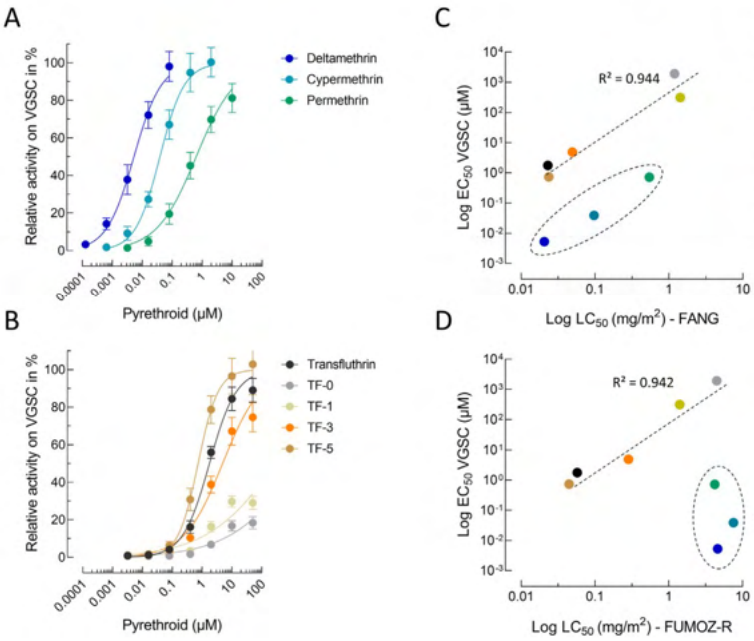

Fig. 2 Concentration response curves for common pyrethroids (**A**) and transfluthrin derivatives (**B**) measured on functionally expressed house fly voltage-gated sodium channels (VGSC) using a fluorescence-based membrane potential cation influx assay. Data are mean values ± standard deviation (SD) (n = 12). **C**, **D** Pearson's correlation analysis between *in vitro* VGSC EC_{50}-values and *in vivo* LC_{50}-values obtained from glazed tile bioassays against female adults of *Anopheles funestus* strains FANG (**C**) and FUMOZ-R (**D**). Data points circled with a dashed line represent deltamethrin, cypermethrin and permethrin.

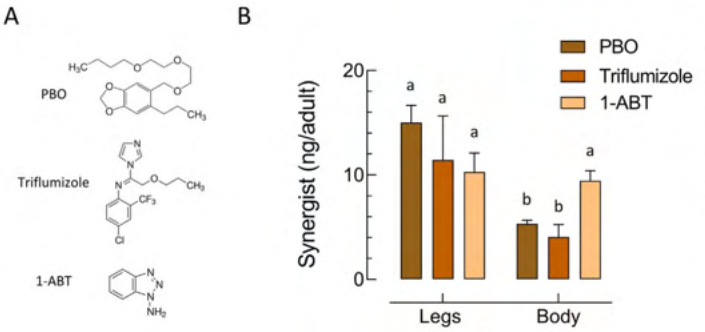

Fig. 3 Tarsal uptake of different synergists by adult females of *Anopheles funestus* strain FUMOZ-R by contact exposure for 30 min on glazed tiles. **A** Three different synergists were tested *in vivo*: piperonyl butoxide (PBO; 100 mg/m²), triflumizole (100 mg/m²) and 1-aminobenzotriazole (1-ABT; 250 mg/m²). **B** Amount of synergist internalized and detected in mosquito legs and bodies analyzed by UPLC/MS. Different letters denote a significant difference (One-way ANOVA, Tukey's *post-hoc* comparisons, $P < 0.05$). Data are mean values ± standard deviation (SD) (n = 20).

synergism of transfluthrin and derivative toxicity in the pyrethroid susceptible strain FANG, whereas moderate synergism was detected for the other pyrethroids - depending on the synergist applied (Supplementary Table S3). The synergistic ratios obtained for the transfluthrin derivatives tested against FUMOZ-R revealed weak or no synergism for TF-1 and TF-5 (Fig. 4), which are fluorinated at the para position of the benzyl ring (Fig. 1). A summary of all bioassay data including 64 calculated LC_{50}-values, resistance factors and synergistic ratios is provided in Supplementary Table S3.

3.4. Activity and inhibition of *An. funestus* microsomal cytochrome P450 monooxygenases

Microsomal membranes of *An. funestus* strain FUMOZ-R were isolated and tested for their capacity to metabolize a range of different coumarin and resorufin fluorescent probe substrates. The substrate profile obtained for FUMOZ-R microsomes revealed a clear preference for coumarins over resorufins. It is noteworthy that the O-debenzylation of bulkier substrates such as BFC, BOMFC and BOMR was the preferred reaction catalyzed by *An. funestus* microsomal P450s, followed by the O-dealkylation of smaller substrates such as EFC and MFC (Fig. 5). Those substrates showing the highest activity with FUMOZ-R microsomes were also tested with FANG microsomes. As expected, probe activity was consistently lower when compared to FUMOZ-R, consistent with higher P450 activity in the pyrethroid-resistant strain. The most active probe substrate was BOMFC. O-debenzylation by both FANG and FUMOZ-R microsomes followed Michaelis-Menten kinetics with apparent Km- and Vmax-values of 5.76 μM (95% CI: 3.31–9.67) and 21.5 pmol HFC/min/mg protein (95% CI: 18.9–24.4), and 4.41 μM (95% CI: 3.64–5.33) 114 pmol HFC/min/mg protein (95% CI: 109–119), respectively (Supplementary Fig. S1). The

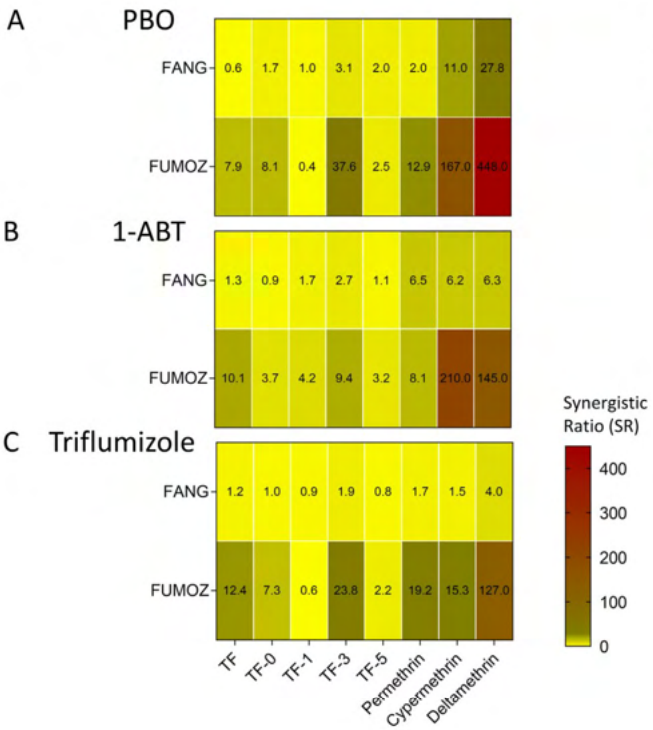

Fig. 4 Heat maps displaying the synergistic ratio obtained in glazed tile bioassays for different pyrethroid insecticides in *Anopheles funestus* strain FANG (susceptible) and FUMOZ-R (resistant) upon contact exposure to piperonyl butoxide (PBO) (**A**), 1-amino-benzotriazole (1-ABT) (**B**) and triflumizole (**C**), directly prior to insecticide application. Synergistic ratios (SR) were calculated by dividing the LC_{50} of the insecticide by the LC_{50} of the insecticide + synergist (see Supplementary Table S3 for details).

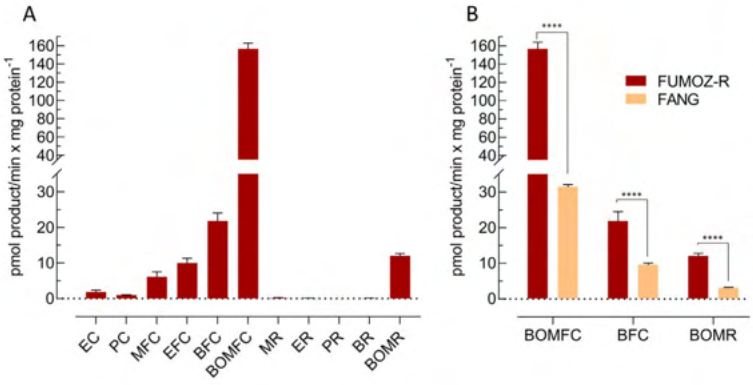

Fig. 5 Metabolism of different cytochrome P450 coumarin and resorufin model substrates by microsomal preparations of *Anopheles funestus*, strain FUMOZ-R (**A**) and strain FANG (**B**) in comparison to FUMOZ-R with those substrates displaying highest cytochrome P450 activity. Data are mean values ± standard deviation (SD) ($n = 4$). Significant differences are denoted by $^{****}P \leq 0.0001$. *Substrate abbreviations*: EC, 7-ethoxycoumarin; PC, 7-pentoxycoumarin; MFC, 7-methoxy-4-trifluoromethyl coumarin; EFC, 7-ethoxy-4-trifluoromethylcoumarin; BFC, 7-benzyloxy-4-trifluoromethylcoumarin; BOMFC, 7-benzyloxymethoxy-4-trifluoromethylcoumarin; MR, 7-methoxyresorufin; ER, 7-ethoxyresorufin; PR, 7-n-pentoxyresorufin; BR, 7-benzyloxyresorufin ether; BOMR, 7-benzyloxymethoxyresorufin.

significantly higher microsomal BOMFC probe activity of FUMOZ-R compared to FANG was correlated with the overexpression of the well-known P450 variants CYP6P9a and CYP6P9b, as shown by RT-qPCR (Fig. 6).

Using the highly active probe substrate BOMFC we developed a fluorescence-based high-throughput 384-well plate assay allowing us to assess compounds for their potential to inhibit P450 activity in microsomal preparations of *An. funestus* strain FUMOZ-R. PBO is a potent nanomolar P450 inhibitor that is commonly used in products to inhibit P450-based metabolism, whereas azole fungicides are known to act synergistic in combination with certain neonicotinoids and pyrethroids, particularly in honey bees (Iwasa et al., 2004). The azole fungicides prochloraz ($IC_{50} = 5.92$ nM), triflumizole ($IC_{50} = 46.8$ nM), uniconazole ($IC_{50} = 107$ nM) were stronger inhibitors than PBO ($IC_{50} = 260$ nM),

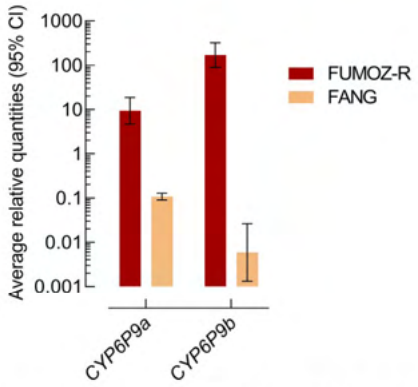

Fig. 6 Expression level (log-scale) of *CYP6P9a* and *CYP6P9b* in *Anopheles funestus* strains FUMOZ-R and FANG measured by qPCR. The expression level was normalized to *RPS7* and *Act* (5c) reference genes. Data are mean values ± 95% CI (n = 4 FUMOZ-R and n = 3 for FANG).

Table 2
Inhibition of cytochrome P450 activity in microsomal preparations of *Anopheles funestus* FUMOZ-R by different azole fungicides using BOMFC as a substrate. The calculated IC_{50}-values are based on the inhibition of total microsomal monooxygenase activity. Data are mean values (n = 4).

Compound	IC_{50} (μM)	95% CI
PBO	0.26	0.221–0.306
1-ABT	119	102–140
Triflumizole	0.0468	0.0416–0.0526
Prochloraz	0.00592	0.00527–0.00664
Uniconazole	0.107	0.0878–0.131
Propiconazole	0.35	0.313–0.39
Epoxiconazole	6.93	5.55–8.71
Triadimefon	1.09	0.967–1.23
Triadimenol	12.3	10.6–14.4
Tebuconazole	0.492	0.444–0.545
Ketoconazole	0.26	0.223–0.302

Abbreviation: 95% CI, 95% confidence interval.

whereas ketoconazole (IC_{50} = 260 nM) was similar (Table 2). Interestingly, 1-ABT, a widely known P450 inhibitor, showed a rather weak inhibitory potential (IC_{50} = 119 μM), although its synergistic potential *in vivo* in combination with pyrethroids such as deltamethrin against strain FUMOZ-R was comparable to triflumizole and PBO (Supplementary Table S3).

4. Discussion

Based on the lack of synergism with PBO, transfluthrin has been previously described to be less affected than phenoxybenzyl-substituted pyrethroids (e.g. deltamethrin) by P450-mediated metabolic resistance in the *An. funestus* laboratory strain FUMOZ-R (Horstmann and Sonneck, 2016), which has elevated levels of P450 activity driven by CYP6P9a and CYP6P9b (Hunt et al., 2005; Amenya et al., 2008; Coetzee and Koekemoer, 2013; Riveron et al., 2013). This study has confirmed that a very low level of cross-resistance exists between transfluthrin (RR = 2.57), and common pyrethroids such as deltamethrin (RR = 223) and cypermethrin (RR = 77.9) in FUMOZ-R compared to the susceptible strain FANG. The low resistance ratios also extended to other transfluthrin derivatives with varied levels of benzyl fluorination. The surprisingly low level of permethrin resistance in FUMOZ-R is comparable to a RR of 11.49 recently reported by Williams et al. (2019) in tarsal contact (glass plate) bioassays, but in comparison to the insecticide susceptible *An. gambiae* strain Kisumu.

Oxidation of the 4′-position on the phenoxybenzyl ring is one of the primary targets of P450 mediated metabolism of pyrethroids (Shono et al., 1979; Stevenson et al., 2011; Kasai et al., 2014; Zimmer et al., 2014), while other routes of metabolism include the gem dimethyl hydroxylation and an ester- or ether-cleavage (Casida et al., 1983; Weerasinghe et al., 2001; Stevenson et al., 2011). The most active compounds against the resistant FUMOZ-R strain were transfluthrin and TF-5 (fenfluthrin), followed by TF-3, where fluorination of the transfluthrin benzyl ring is expected to offer protection against P450 attack (Horstmann and Sonneck, 2016). However, this does not explain the low resistance ratio for the non-fluorinated TF-0 (RR = 3.77), where other factors may be contributing to reduced P450 metabolism. The most likely explanation is the lack of the 3-phenoxybenzyl moiety, which has been shown to be less susceptible to P450 metabolism in other pyrethroid-resistant insects such cotton bollworm (Tan and McCaffery, 2007) and does not correlate with pyrethroid resistance in house flies (Khan et al., 2017). Furthermore, P450 metabolism of transfluthrin in rats is *via* hydrolysis rather than benzyl ring hydroxylation (Yoshida, 2012, 2013). The RR for permethrin was also *c.*10 to 30-fold lower than for cypermethrin and deltamethrin, respectively. Taken together, this suggests a strong preference for the presence of a 3-phenoxybenzyl moiety and an alpha-cyano group in pyrethroid metabolism by *An. funestus* FUMOZ-R, possibly driven by the extensive use of deltamethrin-treated LLINs for malaria control in Africa that may have applied selective pressure on P450s with an active-site preference for deltamethrin and structurally related pyrethroids.

Pyrethroid resistance in *An. funestus* is strongly linked to the overexpression of CYP6P9a and CYP6P9b that can metabolize deltamethrin and permethrin (Riveron et al, 2013, 2014; Yunta et al., 2019). However, depending on the geographical origin of *An. funestus*, other P450s such as CYP6M7 were also shown to be highly overexpressed and involved in pyrethroid resistance (Riveron et al., 2014). Both CYP6P9a and CYP6P9b were highly expressed in the resistant FUMOZ-R strain relative to the susceptible FANG strain and the lack of cross-resistance with deltamethrin or cypermethrin suggests a limited role in transfluthrin metabolism; however, we did not test the expression level of CYP6M7. Transfluthrin has a 2,3,5,6-tetrafluorobenzyl substitution pattern that leaves the benzyl para-position (4′-position) free for P450 attack. In comparing the synergist ratios of the P450 inhibitors PBO, 1-ABT and triflumizole (Fig. 4) where a high ratio is indicative of P450 metabolism, it was striking that a single fluorination of the 4′-position in TF-1 was equally effective at blocking P450 metabolism as the fully fluorinated TF-5, as evidenced by very low synergist ratios. Whereas transfluthrin, TF-3 and TF-0 produced higher synergist ratios indicative of greater P450 metabolism possibly depending on the halogenation pattern, thus confirming to some extent previous mosquito studies on the importance of the 4′-position for oxidative attack (Horstmann and Sonneck, 2016).

The acute contact toxicity of permethrin against FANG was significantly lower compared to deltamethrin and cypermethrin. Interestingly, transfluthrin, TF-3 and TF-5 were also up-to 25-fold more active than permethrin in glazed tile bioassays against strain FANG, although their intrinsic activity on recombinantly expressed house fly VGSC *in vitro* was not different. Since we had no access to a mosquito VGSC, we employed a surrogate from *M. domestica*, a phylogenetically related dipteran species. Dipteran VGSC proteins show a high level of conservation (Silva and Scott, 2020) and a comparison of important amino acid residues described for pyrethroid binding and known to confer different levels of target-site resistance revealed 100% identity between *An. funestus* (GenBank KY499806.1) and *M. domestica* (GenBank X96668.1) VGSC (O'Reilly et al., 2006; Field et al., 2017). Therefore, the agonistic potency on house fly VGSC obtained here should be a good estimate of intrinsic pyrethroid potency in mosquitoes as well. This assumption is supported by earlier results showing a Kd of 4.7 nM for deltamethrin on *Drosophila* wildtype VGSC functionally expressed in *Xenopus* oocytes (Vais et al., 2003), a value strikingly similar to the EC_{50} of 5.3 nM we measured

(Supplementary Table S2), albeit in a different assay system. Electrophysiological recordings on expressed *Drosophila* para VGSC also revealed weaker activity of permethrin (Warmke et al., 1997), and another study with fenfluthrin (TF-5) on wildtype *Drosophila* VGSC reported a similar action to that for permethrin at low micromolar concentrations (Usherwood et al., 2007), correlating with our finding on house fly VGSC. The discrepancy in VGSC potency between deltamethrin and transfluthrin (and some of its derivatives) did not correlate with their almost identical contact toxicity in glazed tile bioassays and merits further research.

Fluorescent substrates are frequently used to measure P450 activity and could be applied to monitor changes in P450 activity associated with insecticide resistance. The biochemical profiling of resorufins and coumarins against P450-containing microsomes from *An. funestus* FUMOZ-R showed a strong preference for BOMFC, BFC and BOMR, all bulky substrates substituted with a benzyloxy-group. These were rapidly O-debenzylated to provide a robust and reliable fluorescence read-out through conversion to umbelliferone. A similar substrate preference has been described for CYP6BQ9 and CYP6BQ23 that are also associated with pyrethroid resistance in *Tribolium castaneum* and *Meligethes aeneus*, respectively (Zhu et al., 2010; Zimmer et al., 2014). Resorufin ether substrates have been used with mixed success, being suitable as substrate probes for *An. gambiae* CYP6M2, CYP6Z2 and CYP6P3, but unreactive against pyrethroid metabolising *Aedes aegypti* P450s. However, BOMR to the best of our knowledge was not included in previous studies with malaria vectors, though alternative resorufin substrates were described in combination with CYP6P9-variants (Ibrahim et al., 2015, 2016). In comparison with resorufin, the coumarin based substrates produced much stronger fluorescence signals (Fig. 5). BOMFC produced the highest fluorescence activity suggesting that this probe substrate could be applied to biochemically profile P450 activity in mosquito populations. This is supported by the fact that microsomal membrane preparations of strain FUMOZ-R were significantly more active with BOMFC than those of strain FANG. Considering the upregulation of CYP6P9a and CYP6P9b in strain FUMOZ-R tested here, it is likely that these P450s are contributing to BOMFC O-debenzylation and hydroxycoumarin formation, although we cannot exclude a potential role of other P450s.

We have used BOMFC to develop a biochemical microplate (384 wells) assay to screen the inhibitory potential of a range of azole compounds with *An. funestus* microsomal P450s. The assay is largely based on a recently described mechanistic bee pollinator risk assessment approach to assess pesticide synergism issues in honey bees (Haas and Nauen, 2021). Synergistic effects of azole fungicides in combination with pyrethroids and neonicotinoids, respectively, have been described in honey bees at the phenotypic level (Pilling and Jepson, 1993; Iwasa et al., 2004), but were only recently deciphered at the molecular level (Haas and Nauen, 2021). Here, we identified prochloraz and triflumizole as extremely potent nanomolar inhibitors of microsomal P450s of *An. funestus*, and at least for triflumizole we could confirm its synergistic potential in combination with 3-phenoxybenzyl pyrethroids against FUMOZ-R *in vivo*. Quite surprising was the rather low inhibitory potential of the triazole 1-ABT, a well-known pan-specific P450 inhibitor (Ortiz De Montellano, 2018). Despite its weak inhibition of FUMOZ-R microsomal P450s *in vitro* it was highly active in glazed tile bioassays, e.g. in combination with cypermethrin. However, future work is needed to further investigate the basis of the contrasting results. It would also be interesting to assess the efficacy of triflumizole and other azole compounds against functionally expressed *An. funestus* P450s such as CYP6P9a and CYP6P9b. McLaughlin et al. (2008) tested several drugs for their inhibitory action on the O-debenzylation of benzyloxy-resorufin by *An. gambiae* CYP6Z2, including clotrimazole and ketoconazole, but IC_{50} values were in the micromolar range and no *in vivo* synergist trials were conducted. Here we demonstrated that azole compounds such as triflumizole could serve as an alternative to PBO, known for its synergistic potential against pyrethroid-resistant mosquitoes. Our results would be a good starting point to foster additional studies on the potential of azoles as synergists to overcome P450-mediated pyrethroid resistance in anopheline mosquitoes.

5. Conclusions

The progress in malaria reduction since the turn of millennium has largely stagnated since 2015 with mosquito resistance to pyrethroids that are commonly used in vector control tools such as IRS and ITNs being a threat to the goal of eradicating malaria by 2040 (https://zeroby40.com/). For sustainable vector control interventions, it is therefore important to implement resistance management strategies that are based on the most active molecules available from chemical classes with the same mode of action. Such molecules may not necessarily break but could substantially delay resistance. The pyrethroids most often used in vector control possess the common structural motif of a phenoxybenzyl alcohol coupled with a cyclopropane ring with cross-resistance trends detectable across pyrethroid-resistant populations of *An. funestus*, *An. gambiae*, *An. arabiensis* and *An. coluzzii* (Moyes et al., 2021). It has been suggested that pyrethroid cross-resistance might be mitigated by employing structurally diverse pyrethroids such as bifenthrin (Moyes et al., 2021) and transfluthrin (Horstmann and Sonneck, 2016). Here, we provide further evidence that multifluorinated benzyl pyrethroids offer potential resistance breaking properties against P450-driven pyrethroid resistance in *An. funestus* that require further verification in resistant field populations. Since pyrethroid resistance in *An. funestus* field strains is largely driven by P450-mediated detoxification, we think that the findings presented here on transfluthrin and pyrethroid synergism are highly relevant for applied field conditions. Furthermore, we have expanded the vector control research toolbox by the introduction of a sensitive fluorescent probe substrate BOMFC for the biochemical monitoring of P450-mediated resistance, and the identification of azoles such as triflumizole as new compounds with potential to synergize pyrethroid toxicity in *An. funestus* FUMOZ-R.

Funding

The work was funded by the Innovative Vector Control Consortium (IVCC) and Bayer AG.

CRediT author statement

Melanie Nolden: Methodology, Investigation, Visualization, Formal analysis, Writing - Original draft preparation. Andreas Brockmann: Methodology, Investigation, Formal Analysis. Ulrich Ebbinghaus-Kintscher: Methodology, Writing - Reviewing and Editing. Kai-Uwe Brueggen: Funding acquisition. Sebastian Horstmann: Supervision, Funding acquisition, Writing - Reviewing and Editing. Mark Paine: Supervision, Writing - Reviewing and Editing. Ralf Nauen: Conceptualization, Supervision, Visualization, Writing - Reviewing and Editing.

Declaration of competing interests

The authors declare the following financial interests/personal relationships which may be considered as potential competing interests: Andreas Brockmann, Kai-Uwe Brüggen, Ralf Nauen, Sebastian Horstmann and Ulrich Ebbinghaus-Kintscher are employed by Bayer AG, a manufacturer of pesticides. Melanie Nolden is a PhD student affiliated with the LSTM and funded by the Innovative Vector Control Consortium (IVCC) and Bayer AG. Mark Paine declares that he has no known competing financial interests or personal relationships that could have appeared to influence the work reported in this paper.

Acknowledgements

We are grateful to Joerg Egger and Frederik Kaeding (Bayer Environmental Science) who reared and provided the mosquito strains.

Thanks to Bettina Lueke for the introduction and helpful advice on the biochemical work. We would also like to thank Johannes Glaubitz and Birgit Nebelsiek for analytical support.

Appendix A. Supplementary data

Supplementary data to this article can be found online at https://doi.org/10.1016/j.crpvbd.2021.100041.

References

Abbott, W.S., 1925. A method of computing the effectiveness of an insecticide. J. Econ. Entomol. 18, 265–267.

Amenya, D.A., Naguran, R., Lo, T.-C.M., Ranson, H., Spillings, B.L., Wood, O.R., et al., 2008. Over expression of a cytochrome P450 (CYP6P9) in a major African malaria vector. Insect Mol. Biol. 17, 19–25.

Balabanidou, V., Grigoraki, L., Vontas, J., 2018. Insect cuticle: a critical determinant of insecticide resistance. Curr. Opin. Insect Sci. 27, 68–74.

Behrenz, W., Elbert, A., 1985. Cyfluthrin and fenfluthrin, two new pyrethroidsfor the control of hygiene pests. Anzeiger für Schädlingskunde, Pflanzenschutz. Umweltschutz 58, 30–35.

Bhatt, S., Weiss, D.J., Cameron, E., Bisanzio, D., Mappin, B., Dalrymple, U., et al., 2015. The effect of malaria control on *Plasmodium falciparum* in Africa between 2000 and 2015. Nature 526, 207–211.

Bibbs, C.S., Tsikolia, M., Bloomquist, J.R., Bernier, U.R., De Xue, R., Kaufman, P.E., 2018. Vapor toxicity of five volatile pyrethroids against *Aedes aegypti*, *Aedes albopictus*, *Culex quinquefasciatus*, and *Anopheles quadrimaculatus* (Diptera: Culicidae). Pest Manag. Sci. 74, 2699–2706.

Boaventura, D., Ulrich, J., Lueke, B., Bolzan, A., Okuma, D., Gutbrod, O., et al., 2020. Molecular characterization of Cry1F resistance in fall armyworm, *Spodoptera frugiperda* from Brazil. Insect Biochem. Mol. Biol. 116, 103280.

Bradford, M.M., 1976. A rapid and sensitive method for the quantitation microgram quantities of protein utilizing the principle of protein-dye binding. Anal Biochem 72, 248–254.

Brooke, B.D., Kloke, G., Hunt, R.H., Koekemoer, L.L., Tem, E.A., Taylor, M.E., et al., 2001. Bioassay and biochemical analyses of insecticide resistance in southern African *Anopheles funestus* (Diptera: Culicidae). Bull. Entomol. Res. 91, 265–272.

Casida, J.E., Gammon, D.W., Glickman, A.H., Lawrence, L.J., 1983. Mechanism of selective action of pyrethroid. Annu. Rev. Pharmacol. Toxicol. 413–438.

Coetzee, M., Koekemoer, L.L., 2013. Molecular systematics and insecticide resistance in the major African malaria vector *Anopheles funestus*. Annu. Rev. Entomol. 58, 393–412.

Coleman, M., Hemingway, J., Gleave, K.A., Wiebe, A., Gething, P.W., Moyes, C.L., 2017. Developing global maps of insecticide resistance risk to improve vector control. Malar. J. 16, 86.

Cuamba, N., Morgan, J.C., Irving, H., Steven, A., Wondji, C.S., 2010. High level of pyrethroid resistance in an *Anopheles funestus* population of the Chokwe district in Mozambique. PloS One 5, e11010.

Das, S., Garver, L., Dimopoulos, G., 2007. Protocol for mosquito rearing (*A. gambiae*). JoVE 5, 221.

Davies, T.G.E., Field, L.M., Usherwood, P.N.R., Williamson, M.S., 2007. A comparative study of voltage-gated sodium channels in the Insecta: implications for pyrethroid resistance in Anophelinae and other Neopteran species. Insect Mol. Biol. 16, 361–375.

Djouaka, R., Riveron, J.M., Yessoufou, A., Tchigossou, G., Akoton, R., Irving, H., et al., 2016. Multiple insecticide resistance in an infected population of the malaria vector *Anopheles funestus* in Benin. Parasit. Vectors 9, 453.

Feyereisen, R., 1999. Insect P450 enzymes. Annu. Rev. Entomol. 44, 507–533.

Field, L.M., Emyr Davies, T.G., O'Reilly, A.O., Williamson, M.S., Wallace, B.A., 2017. Voltage-gated sodium channels as targets for pyrethroid insecticides. Eur. Biophys. J. 46, 675–679.

Fongnikin, A., Houeto, N., Agbevo, A., Odjo, A., Syme, T., N'Guessan, R., Ngufor, C., 2020. Efficacy of Fludora® Fusion (a mixture of deltamethrin and clothianidin) for indoor residual spraying against pyrethroid-resistant malaria vectors: laboratory and experimental hut evaluation. Parasit. Vectors 13, 466.

Fuseini, G., Phiri, W.P., von Fricken, M.E., Smith, J., Garcia, G.A., 2019. Evaluation of the residual effectiveness of FludoraTM fusion WP-SB, a combination of clothianidin and deltamethrin, for the control of pyrethroid-resistant malaria vectors on Bioko Island, Equatorial Guinea. Acta Trop. 196, 42–47.

Gleave, K., Lissenden, N., Richardson, M., Ranson, H., 2018. Piperonyl butoxide (PBO) combined with pyrethroids in long-lasting insecticidal nets (LLINs) to prevent malaria in Africa. Cochrane Database Syst. Rev. 11, CD012776. https://doi.org/10.1002/14651858.CD012776.pub2.

Haas, J., Nauen, R., 2021. Pesticide risk assessment at the molecular level using honey bee cytochrome P450 enzymes: a complementary approach. Environ. Int. 147, 106372.

Hargreaves, K., Koekemoer, L.L., Brooke, B.D., Hunt, R.H., Mthembu, J., Coetzee, M., 2000. *Anopheles funestus* resistant to pyrethroid insecticides in South Africa. Med. Vet. Entomol. 14, 181–189.

Hemingway, J., 2019. Malaria parasite tackled in mosquitoes. Nature 567, 185–186.

Hemingway, J., Beaty, B.J., Rowland, M., Scott, T.W., Sharp, B.L., 2006. The Innovative Vector Control Consortium: improved control of mosquito-borne diseases. Trends Parasitol. 22, 308–312.

Hemingway, J., Hawkes, N.J., McCarroll, L., Ranson, H., 2004. The molecular basis of insecticide resistance in mosquitoes. Insect Biochem. Mol. Biol. 34, 653–665.

Hemingway, J., Ranson, H., Magill, A., Kolaczinski, J., Fornadel, C., Gimnig, J., et al., 2016. Averting a malaria disaster: will insecticide resistance derail malaria control? Lancet 387, 1785–1788.

Hoppé, M., Hueter, O.F., Bywater, A., Wege, P., Maienfisch, P., 2016. Evaluation of commercial agrochemicals as new tools for malaria vector control. Chimia 70, 721–729.

Horstmann, S., Sonneck, R., 2016. Contact bioassays with phenoxybenzyl and tetrafluorobenzyl pyrethroids against target-site and metabolic resistant mosquitoes. PloS One 11, e0149738.

Human Disease Vectors (HDV) group of the Insect Pest Control Laboratory, 2017. Guidelines for standardised mass rearing of *Anopheles* mosquitoes.

Hunt, R.H., Brooke, B.D., Pillay, C., Koekemoer, L.L., Coetzee, M., 2005. Laboratory selection for and characteristics of pyrethroid resistance in the malaria vector *Anopheles funestus*. Med. Vet. Entomol. 19, 271–275.

Ibrahim, S.S., Ndula, M., Riveron, J.M., Irving, H., Wondji, C.S., 2016. The P450 CYP6Z1 confers carbamate/pyrethroid cross-resistance in a major African malaria vector beside a novel carbamate-insensitive N485I acetylcholinesterase-1 mutation. Mol. Ecol. 25, 3436–3452.

Ibrahim, S.S., Riveron, J.M., Bibby, J., Irving, H., Yunta, C., Paine, M.J.I., Wondji, C.S., 2015. Allelic variation of cytochrome P450s drives resistance to bednet insecticides in a major malaria vector. PLoS Genet. 11, e1005618.

Irving, H., Riveron, J.M., Ibrahim, S.S., Lobo, N.F., Wondji, C.S., 2012. Positional cloning of rp2 QTL associates the P450 genes CYP6Z1, CYP6Z3 and CYP6M7 with pyrethroid resistance in the malaria vector *Anopheles funestus*. Heredity 109, 383–392.

Irving, H., Wondji, C.S., 2017. Investigating knockdown resistance (kdr) mechanism against pyrethroids/DDT in the malaria vector *Anopheles funestus* across Africa. BMC Genet. 18, 76.

Iwasa, T., Motoyama, N., Ambrose, J.T., Roe, R.M., 2004. Mechanism for the differential toxicity of neonicotinoid insecticides in the honey bee, *Apis mellifera*. Crop Protect. 23, 371–378.

Kasai, S., Komagata, O., Itokawa, K., Shono, T., Ng, L.C., Kobayashi, M., Tomita, T., 2014. Mechanisms of pyrethroid resistance in the dengue mosquito vector, *Aedes aegypti*: target site insensitivity, penetration, and metabolism. PLoS Negl. Trop. Dis. 8, e2948.

Khan, H.A.A., Akram, W., Fatima, A., 2017. Resistance to pyrethroid insecticides in house flies, *Musca domestica* L. (Diptera: Muscidae) collected from urban areas in Punjab, Pakistan. Parasitol. Res. 116, 3381–3385.

Kline, D.L., Urban, J., 2018. Potential for utilization of spatial repellents in mosquito control interventions. ACS Symp. Ser. 1289, 237–248.

Laufer, J., Rochet, M., Pelhate, M., Elliotti, M., Janes, N.F., Sattelle, D.B., 1984. Pyrethroids insecticides: actions of deltamethrin and related compounds on insect axonal sodium channels. J. Insect Physiol. 30, 341–349.

Manjon, C., Troczka, B.J., Zaworra, M., Beadle, K., Randall, E., Hertlein, G., et al., 2018. Unravelling the molecular determinants of bee sensitivity to neonicotinoid insecticides. Curr. Biol. 28, 1137–1143.

Masalu, J.P., Finda, M., Killeen, G.F., Ngowo, H.S., Pinda, P.G., Okumu, F.O., 2020. Creating mosquito-free outdoor spaces using transfluthrin-treated chairs and ribbons. Malar. J. 19, 109.

McLaughlin, L.A., Niazi, U., Bibby, J., David, J.P., Vontas, J., Hemingway, J., et al., 2008. Characterization of inhibitors and substrates of *Anopheles gambiae* CYP6Z2. Insect Mol. Biol. 17, 125–135.

Morgan, J.C., Irving, H., Okedi, L.M., Steven, A., Wondji, C.S., 2010. Pyrethroid resistance in an *Anopheles funestus* population from Uganda. PloS One 5, e11872.

Moyes, C.L., Athinya, D.K., Seethaler, T., Battle, K.E., Sinka, M., Hadi, M.P., et al., 2020. Evaluating insecticide resistance across African districts to aid malaria control decisions. Proc. Natl. Acad. Sci. U.S.A. 117, 202006781.

Nauen, R., 2007. Insecticide resistance in disease vectors of public health importance. Pest Manag. Sci. 63, 628–633.

Moyes, C.L., Lees, R.S., Yunta, C., Walker, K.J., Hemmings, K., Oladepo, F., et al., 2021. Assessing cross-resistance within the pyrethroids in terms of their interactions with key cytochrome P450 enzymes and resistance in vector populations. Parasit. Vectors 14, 115.

Nauen, R., 2006. Insecticide mode of action: return of the ryanodine receptor. Pest Manag. Sci. 62, 690–692.

Naumann, K., 1990. Synthetic pyrethroid insecticides: formation of the pyrethroid-ester-linkage, chemistry and patents. In: Chemistry of Plant Protection, vol. 5. Springer-Verlag, Weinheim, pp. 129–173.

Ogoma, S.B., Ngonyani, H., Simfukwe, E.T., Mseka, A., Moore, J., Killeen, G.F., 2012. Spatial repellency of transfluthrin-treated hessian strips against laboratory-reared *Anopheles arabiensis* mosquitoes in a semi-field tunnel cage. Parasit. Vectors 5, 54.

Ogoma, S.B., Ngonyani, H., Simfukwe, E.T., Mseka, A., Moore, J., Maia, M.F., et al., 2014. The mode of action of spatial repellents and their impact on vectorial capacity of *Anopheles gambiae sensu stricto*. PloS One 9, e110433.

O'Reilly, A.O., Khambay, B.P.S., Williamson, M.S., Field, L.M., Wallace, B.A., Davies, T.G.E., 2006. Modelling insecticide-binding sites in the voltage-gated sodium channel. Biochem. J. 396, 255–263.

Ortiz De Montellano, P.R., 2018. 1-Aminobenzotriazole: a mechanism-based cytochrome P450 inhibitor and probe of cytochrome P450 biology. Med. Chem. 8, 038.

Pilling, E.D., Jepson, P.C., 1993. Synergism between EBI fungicides and a pyrethroid insecticide in the honey bee (*Apis mellifera*). Pestic. Sci. 39, 293–297.

Pulman, D.A., 2011. Deltamethrin: the cream of the crop. J. Agric. Food. Chem. 59, 2770–2772.

Riveron, J.M., Ibrahim, S.S., Chanda, E., Mzilahowa, T., Cuamba, N., Irving, H., et al., 2014. The highly polymorphic CYP6M7 cytochrome P450 gene partners with the directionally selected CYP6P9a and CYP6P9b genes to expand the pyrethroid

resistance front in the malaria vector *Anopheles funestus* in Africa. BMC Genomics 15, 817.
Riveron, J.M., Irving, H., Ndula, M., Barnes, K.G., Ibrahim, S.S., Paine, M.J.I., Wondji, C.S., 2013. Directionally selected cytochrome P450 alleles are driving the spread of pyrethroid resistance in the major malaria vector *Anopheles funestus*. Proc. Natl. Acad. Sci. U.S.A. 110, 252–257.
Sangba, M.L.O., Deketramete, T., Wango, S.P., Kazanji, M., Akogbeto, M., Ndiath, M.O., 2016. Insecticide resistance status of the *Anopheles funestus* population in Central African Republic: a challenge in the war. Parasit. Vectors 9, 230.
Scott, J.G., 2019. Life and death at the voltage-sensitive sodium channel: evolution in response to insecticide use. Annu. Rev. Entomol. 64, 243–257.
Shono, T., Ohsawa, K., Casida, J.E., 1979. Metabolism of trans-and cis-permethrin, trans- and cis-cypermethrin, and decamethrin by microsomal enzymes. J. Agric. Food. Chem. 27, 316–325.
Silva, J.J., Scott, J.G., 2020. Conservation of the voltage-sensitive sodium channel protein within the Insecta. Insect Mol. Biol. 29, 9–18.
Sinka, M.E., Bangs, M.J., Manguin, S., Coetzee, M., Mbogo, C.M., Hemingway, J., et al., 2010. The dominant *Anopheles* vectors of human malaria in Africa, Europe and the Middle East: occurrence data, distribution maps and bionomic précis. Parasit. Vectors 3, 117.
Sinka, M.E., Golding, N., Massey, N.C., Wiebe, A., Huang, Z., Hay, S.I., Moyes, C.L., 2016. Modelling the relative abundance of the primary African vectors of malaria before and after the implementation of indoor, insecticide-based vector control. Malar. J. 15, 142.
Smith, L.B., Sears, C., Sun, H., Mertz, R.W., Kasai, S., Scott, J.G., 2019. CYP-mediated resistance and cross-resistance to pyrethroids and organophosphates in *Aedes aegypti* in the presence and absence of kdr. Pestic. Biochem. Physiol. 160, 119–126.
Soderlund, D.M., 2020. Neurotoxicology of pyrethroid insecticides. In: Neurotoxicity of pesticides. Elsevier, Amsterdam, pp. 113–165.
Soderlund, D.M., Bloomquist, J.R., 1989. Neurotoxic actions of pyrethroid insecticides. Annu. Rev. Entomol. 34, 77–96.
Sparks, T.C., Nauen, R., 2015. IRAC: mode of action classification and insecticide resistance management. Pestic. Biochem. Physiol. 121, 122–128.
Stevenson, B.J., Bibby, J., Pignatelli, P., Muangnoicharoen, S., O'Neill, P.M., Lian, L.Y., et al., 2011. Cytochrome P450 6M2 from the malaria vector *Anopheles gambiae* metabolizes pyrethroids: sequential metabolism of deltamethrin revealed. Insect Biochem. Mol. Biol. 41, 492–502.
Tan, J., McCaffery, A.R., 2007. Efficacy of various pyrethroid structures against a highly metabolically resistant isogenic strain of *Helicoverpa armigera* (Lepidoptera: Noctuidae) from China. Pest Manag. Sci. 63, 960–968.
Tay, B., Stewart, T.A., Davis, F.M., Deuis, J.R., Vetter, I., 2019. Development of a high-throughput fluorescent no-wash sodium influx assay. PloS One 14, e0213751.
Tchigossou, G., Djouaka, R., Akoton, R., Riveron, J.M., Irving, H., Atoyebi, S., et al., 2018. Molecular basis of permethrin and DDT resistance in an *Anopheles funestus* population from Benin. Parasit. Vectors 11, 602.
Temu, E.A., Minjas, J.N., Tuno, N., Kawada, H., Takagi, M., 2007. Identification of four members of the *Anopheles funestus* (Diptera: Culicidae) group and their role in *Plasmodium falciparum* transmission in Bagamoyo coastal Tanzania. Acta Trop. 102, 119–125.
Ullrich, V., Weber, P., 1972. The O-dealkylation of 7-ethoxycoumarin by liver microsomes. Hoppe. Seylers. Z. Physiol. Chem. 353, 1171–1177.
Usherwood, P.N.R., Davies, T.G.E., Mellor, I.R., O'Reilly, A.O., Peng, F., Vais, H., et al., 2007. Mutations in DIIS5 and the DIIS4-S5 linker of *Drosophila melanogaster* sodium channel define binding domains for pyrethroids and DDT. FEBS Lett. 581, 5485–5492.
Vais, H., Atkinson, S., Pluteanu, F., Goodson, S.J., Devonshire, A.L., Williamson, M.S., Usherwood, P.N.R., 2003. Mutations of the para sodium channel of *Drosophila melanogaster* identify putative binding sites for pyrethroids. Mol. Pharmacol. 64, 914–922.
Vandesompele, J., De Preter, K., Pattyn, F., Poppe, B., Van Roy, N., De Paepe, A., Speleman, F., 2002. Accurate normalization of real-time quantitative RT-PCR data by geometric averaging of multiple internal control genes. Genome Biol. 3, 7.
Vontas, J., Katsavou, E., Mavridis, K., 2020. Cytochrome P450-based metabolic insecticide resistance in *Anopheles* and *Aedes* mosquito vectors: muddying the waters. Pestic. Biochem. Physiol. 170, 104666.
Warmke, J.W., Reenan, R.A.G., Wang, P., Qian, S., Arena, J.P., Wang, J., et al., 1997. Functional expression of *Drosophila* para sodium channels modulation by the membrane protein tipE and toxin pharmacology. J. Gen. Physiol. 110, 119–133.
Weedall, G.D., Mugenzi, L.M.J., Menze, B.D., Tchouakui, M., Ibrahim, S.S., Amvongo-Adjia, N., et al., 2019. A cytochrome P450 allele confers pyrethroid resistance on a major African malaria vector, reducing insecticide-treated bednet efficacy. Sci. Transl. Med. 11, eaat7386.
Weerasinghe, I.S., Kasai, S., Shono, T., 2001. Correlation of pyrethroid structure and resistance level in *Culex quinquefasciatus* Say from Saudi Arabia. J. Pestic. Sci. 26, 158–161.
WHO, 2018a. World malaria report 2018. World Health Organization, Geneva. https://www.who.int/publications/i/item/9789241565653.
WHO, 2018b. Global report on insecticide resistance in malaria vectors: 2010–2016. World Health Organization, Geneva. https://apps.who.int/iris/handle/10665/272533.
Wiebe, A., Longbottom, J., Gleave, K., Shearer, F.M., Sinka, M.E., Massey, N.C., et al., 2017. Geographical distributions of African malaria vector sibling species and evidence for insecticide resistance. Malar. J. 16, 85.
Williams, J., Flood, L., Praulins, G., Ingham, V.A., Morgan, J., Lees, R.S., Ranson, H., 2019. Characterisation of *Anopheles* strains used for laboratory screening of new vector control products. Parasit. Vectors 12, 522.
Wondji, C.S., Irving, H., Morgan, J., Lobo, N.F., Collins, F.H., Hunt, R.H., et al., 2009. Two duplicated P450 genes are associated with pyrethroid resistance in *Anopheles funestus*, a major malaria vector. Genome Res. 19, 452–459.
Yoshida, T., 2013. Analytical method for urinary metabolites of the fluorine-containing pyrethroids metofluthrin , profluthrin and transfluthrin by gas chromatography/mass spectrometry. J Chromatogr B 913–914, 77–83.
Wood, O.R., Hanrahan, S., Coetzee, M., Koekemoer, L.L., Brooke, B.D., 2010. Cuticle thickening associated with pyrethroid resistance in the major malaria vector *Anopheles funestus*. Parasit. Vectors 3, 67.
Yoshida, T., 2012. Identification of urinary metabolites in rats administered the fluorine-containing pyrethroids metofluthrin, profluthrin, and transfluthrin. Toxicol. Environ. Chem. 94, 1789–1804.
Yunta, C., Hemmings, K., Stevenson, B., Koekemoer, L.L., Matambo, T., Pignatelli, P., et al., 2019. Cross-resistance profiles of malaria mosquito P450s associated with pyrethroid resistance against WHO insecticides. Pestic. Biochem. Physiol. 161, 61–67.
Zaworra, M., Nauen, R., 2019. New approaches to old problems: removal of phospholipase A2 results in highly active microsomal membranes from the honey bee, *Apis mellifera*. Pestic. Biochem. Physiol. 161, 68–76.
Zhu, F., Parthasarathy, R., Bai, H., Woithe, K., Kaussmann, M., Nauen, R., et al., 2010. A brain-specific cytochrome P450 responsible for the majority of deltamethrin resistance in the QTC279 strain of *Tribolium castaneum*. Proc. Natl. Acad. Sci. U.S.A. 107, 8557–8562.
Zimmer, C.T., Bass, C., Williamson, M.S., Kaussmann, M., Wölfel, K., Gutbrod, O., Nauen, R., 2014. Molecular and functional characterization of CYP6BQ23, a cytochrome P450 conferring resistance to pyrethroids in European populations of pollen beetle, *Meligethes aeneus*. Insect Biochem. Mol. Biol. 45, 18–29.

7.2. Publication chapter 3: Biochemical profiling of functionally expressed CYP6P9 variants of the malaria vector Anopheles funestus with special reference to cytochrome b5 and its role in pyrethroid and coumarin substrate metabolism

Pesticide Biochemistry and Physiology 182 (2022) 105051

Contents lists available at ScienceDirect

Pesticide Biochemistry and Physiology

journal homepage: www.elsevier.com/locate/pest

Biochemical profiling of functionally expressed CYP6P9 variants of the malaria vector *Anopheles funestus* with special reference to cytochrome b_5 and its role in pyrethroid and coumarin substrate metabolism

Melanie Nolden [a,b], Mark J.I. Paine [b], Ralf Nauen [a,*]

[a] Bayer AG, Crop Science Division, Alfred Nobel Str. 50, D-40789 Monheim am Rhein, Germany
[b] Department of Vector Biology, Liverpool School of Tropical Medicine, Pembroke Place, Liverpool L3 5QA, United Kingdom

ARTICLE INFO

Keywords:
Cytochrome P450
Cytochrome b5
Anopheles funestus
CYP6P9
Resistance
Pyrethroid

ABSTRACT

Cytochrome P450 monooxygenases (P450s) are well studied enzymes catalyzing the oxidative metabolism of xenobiotics in insects including mosquitoes. Their duplication and upregulation in agricultural and public health pests such as anopheline mosquitoes often leads to an enhanced metabolism of insecticides which confers resistance. In the laboratory strain *Anopheles funestus* FUMOZ-R the duplicated P450s CYP6P9a and CYP6P9b are highly upregulated and proven to confer pyrethroid resistance. Microsomal P450 activity is regulated by NADPH cytochrome P450 oxidoreductase (CPR) required for electron transfer, whereas the modulatory role of cytochrome b_5 (CYB5) on insect P450 activity is less clear. In previous studies CYP6P9a and CYP6P9b were recombinantly expressed in tandem with *An. gambiae* CPR using *E. coli*-expression systems and CYB5 added to the reaction mix to enhance activity. However, the precise role of CYB5 on substrate turn-over when combined with CYP6P9a and CYP6P9b remains poorly investigated, thus one objective of our study was to address this knowledge gap. In contrast to the *CYP6P9* variants, the expression levels of both *CYB5* and *CPR* were not upregulated in the pyrethroid resistant FUMOZ-R strain when compared to the susceptible FANG strain, suggesting no immediate regulatory role of these genes in pyrethroid resistance in FUMOZ-R. Here, for the first time we recombinantly expressed *CYP6P9a* and *CYP6P9b* from *An. funestus* in a baculovirus expression system using High-5 insect cells. Co-expression of each enzyme with CPR from either *An. gambiae* or *An. funestus* did not reveal noteworthy differences in catalytic capacity. Whereas the co-expression of *An. funestus* CYB5 – tested at different multiplicity of infection (MOI) ratios – resulted in a significantly higher metabolization of coumarin substrates as measured by fluorescence assays. This was confirmed by Michaelis-Menten kinetics using the most active substrate, 7-benzyloxymethoxy-4-trifluoromethylcoumarin (BOMFC). We observed a similar increase in coumarin substrate turnover by adding human CYB5 to the reaction mix. Finally, we compared by UPLC-MS/MS analysis the depletion rate of deltamethrin and the formation of 4'OH-deltamethrin by recombinantly expressed CYP6P9a and CYP6P9b with and without CYB5 and detected no difference in the extent of deltamethrin metabolism. Our results suggest that co-expression (or addition) of CYB5 with CYP6P9 variants, recombinantly expressed in insect cells, can significantly enhance their metabolic capacity to oxidize coumarins, but not deltamethrin.

1. Introduction

Cytochrome P450 monooxygenases (P450s, encoded by *CYP* genes) are a diverse superfamily of membrane-bound heme-thiolate enzymes described across all kingdoms of life (Nelson, 2018), and involved in the oxidation of a vast range of endogenous and exogenous substrates (Coon, 2005; Esteves et al., 2021; Feyereisen, 2012; Schuler, 2011). P450s play a key role in the metabolism of xenobiotics (Lu et al., 2021; Nauen et al., 2022), including insecticides in many pests of agricultural and public health importance including mosquito vectors of human diseases (Feyereisen, 2012; Vontas et al., 2020). The control of *Anopheline* malaria vectors over the last decades has heavily relied on pyrethroids such as deltamethrin, cypermethrin and permethrin, incorporated in insecticide treated bed nets (ITN) and applied as indoor residual sprays (IRS) (WHO, 2018). This chemical class of insecticides acts on voltage-gated sodium channels in the central nervous system and

* Corresponding author.
E-mail address: ralf.nauen@bayer.com (R. Nauen).

https://doi.org/10.1016/j.pestbp.2022.105051
Received 22 December 2021; Received in revised form 24 January 2022; Accepted 24 January 2022
Available online 4 February 2022

induces a quick knock-down of pest insects upon contact exposure (Soderlund, 2020). Due to frequent applications and continuous selection pressure, mosquitoes have developed resistance to pyrethroids that is often linked to the upregulation of P450 isoforms, which facilitate pyrethroid metabolism in resistant phenotypes (Hemingway and Ranson, 2000). In *Anopheles funestus* s.s., one of the major malaria transmitting mosquitoes in Sub-Saharan-Africa (Coetzee and Koekemoer, 2013), a number of P450s have been associated with pyrethroid resistance, including CYP6P9a, CYP6P9b, CYP6M7, CYP6AA1, CYP9J11, CYP6Z1 and, very recently, CYP325A (Ibrahim et al., 2016a, 2018; Riveron et al., 2013, 2014, 2017; Wamba et al., 2021). Indeed, *CYP6P9a* and *CYP6P9b* are highly upregulated in *An. funestus* and have been functionally shown to play a key role in the oxidative metabolism of pyrethroids (Cuamba et al., 2010; Ibrahim et al., 2015; Riveron et al., 2013; Weedall et al., 2019). This upregulation was first demonstrated in one of the global laboratory reference strains, FUMOZ-R (Wondji et al., 2009), originally collected in 2000 in Mozambique (Brooke et al., 2001), and since then maintained in the laboratory under pyrethroid selection pressure (Hunt et al., 2005).

Functional validation of the importance of upregulated P450 isoforms in conferring insecticide resistance in both agricultural pests and mosquitoes is usually provided by their recombinant expression and subsequent analysis of insecticide depletion and metabolite formation in vitro, or alternatively, by the ectopic expression of candidate genes in model insects such as *Drosophila melanogaster* (Nauen et al., 2022). The most important systems employed for the functional expression of insect P450s are based on *Escherichia coli* and insect cell lines utilizing a baculovirus expression system (reviewed in (Nauen et al., 2021). Interestingly the majority of mosquito P450s involved in insecticide resistance, including *An. funestus* CYP6P9a and CYP6P9b, have been expressed using *E. coli* along with *Anopheles gambiae* cytochrome P450 reductase (CPR) (Table 1). CPR is an essential membrane-bound flavoprotein, located in close vicinity to P450s, and the principal redox-partner of microsomal P450s required for electron transfer utilizing NADPH as a co-factor (Gutierrez et al., 2003). In mammals, CPR has been shown to have many more essential functions, e.g., in steroid hormone synthesis, cholesterol homeostasis, heme catabolism and cholesterol biosynthesis (Porter, 2012). Its essential role is reflected by the fact that the germline deletion of CPR in mice was embryonic lethal (Shen et al., 2002). However, such studies are lacking in insects, but silencing of CPR by RNAi in *An. gambiae* showed enhanced sensitivity to permethrin (Lycett et al., 2006), while pest invertebrates resistant to insecticides resulted in increased insecticide sensitivity compared to susceptible individuals, indicating that lower expression of CPR negatively affected P450-mediated metabolism (Moural et al., 2020; Shi et al., 2015; Zhu et al., 2012).

The coupling of insect microsomal P450s and CPR in heterologous expression systems is essential for catalytic activity, whereas the role of another potential electron donor, cytochrome b_5 (CYB5), which is of particular importance in mammals (Schenkman and Jansson, 2003), remains nebulous in insects. Drug metabolism by several mammalian microsomal P450 isoforms was shown to be maximized by CYB5, either catalytically or allosterically, because its deletion resulted in a marked decrease in activity of several hepatic P450s (Finn et al., 2008; McLaughlin et al., 2010). CYB5 was also shown to significantly modulate the activity of some major human P450s such as CYP3A4 and CYP2D6 (Henderson et al., 2015). Therefore, CYB5 is considered to stimulate hepatic drug metabolism in combination with several P450 isoforms, rather than being an auxiliary player (Porter, 2012). However, despite its functional role, germline deletion of CYB5 in mice was not lethal, possibly indicating that other redox-proteins may substitute for its function (Finn et al., 2011). Its modulating role on insect P450 activity was first demonstrated using house fly microsomal preparations, where its inhibition resulted in decreased O-dealkylation of two coumarin substrates, while the metabolism of resorufins remained unaffected (Zhang and Scott, 1994). Another study confirmed its role as a modulator of house fly P450 activity by enhancing heptachlor epoxidation in a reconstituted system with CPR and CYP6A1 (Guzov et al., 1996). A more recent study revealed that CYB5 significantly increased the O-deethylation of 7-ethoxycoumarin by CYP6FD1 from *Locusta migratoria* (Liu et al., 2020). Although CYB5 was cloned and sequenced from two major anopheline mosquitoes, *An. gambiae* and *An. funestus*, many years ago (Matambo et al., 2010; Nikou et al., 2003), functional studies investigating its role in combination with CPR and pyrethroid-metabolizing P450s such as CYP6P9a and CYP6P9b are lacking.

To evaluate the role of CYB5 on the activity of recombinantly

Table 1
Selected examples of addition/co-expression of cytochrome *b*5 (CYB5) in heterologously expressed mosquito CYP genes.

Insect	*CYP*	Expression system	CPR* origin	CYB5 origin	CYB5 addition	Reference
Ae. aegypti	*CYP6Z8*	Yeast	*Ae. aegypti*	*Ae. aegypti*	Ratio 80 pmol:50 pmol (b5:P450) added to reaction mix	(Chandor-Proust et al., 2013)
Ae. aegypti	*CYP6CB1*	*E. coli*	*An. gambiae*	*An. gambiae*	Ratio 0.8:0.1 μM (b5:P450) added to reaction mix	(Stevenson et al., 2012)
Ae. aegypti	*CYP9J19*	*E. coli*	*An. gambiae*	*An. gambiae*	Ratio 0.8:0.1 μM (b5:P450) added to reaction mix	Ibid.
Ae. aegypti	*CYP9J24*	*E. coli*	*An. gambiae*	*An. gambiae*	Ratio 0.8:0.1 μM (b5:P450) added to reaction mix	Ibid.
Ae. aegypti	*CYP9J26*	*E. coli*	*An. gambiae*	*An. gambiae*	Ratio 0.8:0.1 μM (b5:P450) added to reaction mix	Ibid.
Ae. aegypti	*CYP9J28*	*E. coli*	*An. gambiae*	*An. gambiae*	Ratio 0.8:0.1 μM (b5:P450) added to reaction mix	Ibid.
Ae. aegypti	*CYP9J32*	*E. coli*	*An. gambiae*	*An. gambiae*	Ratio 0.8:0.1 μM (b5:P450) added to reaction mix	Ibid.
Ae. aegypti	*CYP9M6*	bac-to-bac, Sf9	*Ae. aegypti*	*Ae. aegypti*	Not indicated	(Kasai et al., 2014)
Ae. aegypti	*CYP6BB2*	bac-to-bac, Sf9	*Ae. aegypti*	*Ae. aegypti*	Not indicated	Ibid.
An. arabiensis	*CYP6P4*	*E. coli*	*An. gambiae*	*An. gambiae*	Not indicated	(Ibrahim et al., 2016b)
An. funestus	*CYP6P9a/b*	*E. coli*	*An. gambiae*	*An. gambiae*	Ratio 0.8 μM:45 pmol (b5:P450) added to reaction mix	(Riveron et al., 2014)
An. funestus	*CYP6M7*	*E. coli*	*An. gambiae*	*An. gambiae*	Ratio 0.8 μM:45 pmol (b5:P450) added to reaction mix	Ibid.
An. funestus	*CYP6Z1*	*E. coli*	*An. gambiae*	*An. gambiae*	Not indicated	(Ibrahim et al., 2016a)
An. funestus	*CYP6AA1*	*E. coli*	*An. gambiae*	*An. gambiae*	Not indicated	(Ibrahim et al., 2018)
An. funestus	*CYP9J11*	*E. coli*	*An. gambiae*	*An. gambiae*	Ratio 0.8 μM:45 pmol (b5:P450) added to reaction mix	(Riveron et al., 2017)
An. gambiae	*CYP6M2*	*E. coli*	*An. gambiae*	*An. gambiae*	Ratio 0.8 μM:0.1 μM (b5:P450) added to reaction mix	(Stevenson et al., 2011)
An. gambiae	*CYP6P3*	*E. coli*	*An. gambiae*	–	Without *CYB5*	(Müller et al., 2008)
An. gambiae	*CYP6Z2*	*E. coli*	*An. gambiae*	–	Without *CYB5*	(Mclaughlin et al., 2008)
An. gambiae	*CYP6Z1/2*	bac-to-bac, Sf9	*M. domestica*	*D. melanogaster*	co-expression, MOI 2:2:0.1	(Chiu et al., 2008)
An. gambiae	*CYP9J5*	*E. coli*	*An. gambiae*	*An. gambiae*	Ratio 10:1 (b5:P450) added to reaction mix	(Yunta et al., 2016) (2019)
An. gambiae	*CYP6P4*	*E. coli*	*An. gambiae*	*An. gambiae*	Ratio 10:1 (b5:P450) added to reaction mix	Ibid.
An. gambiae	*CYP6P2*	*E. coli*	*An. gambiae*	*An. gambiae*	Ratio 10:1 (b5:P450) added to reaction mix	Ibid.
An. gambiae	*CYP6P5*	*E. coli*	*An. gambiae*	*An. gambiae*	Ratio 10:1 (b5:P450) added to reaction mix	Ibid.
An. minimus	*CYP6AA3*	bac-to-bac, Sf9	*An. minimus*	–	Without *CYB5*	(Boonsuepsakul et al., 2008)
An. minimus	*CYP6P7*	bac-to-bac, Sf9	*An. minimus*	–	Without *CYB5*	(Duangkaew et al., 2011)

* CPR = cytochrome P450 reductase.

expressed insect P450s, it can either be co-expressed with the respective CPR and P450 of interest or added to the reaction mix, as done in most studies with heterologously expressed mosquito P450s utilizing an *E. coli* expression system (Table 1). *Aedes aegypti* CYP9M6 and CYP6BB2 were one of the few mosquito P450s heterologously expressed in Sf9 cells using the baculovirus system, but without CYB5 (Kasai et al., 2014). To the best of our knowledge only four *Anopheline* P450 isoforms, i.e. CYP6AA3 and CYP6P7 from *An. minimus* and CYP6Z1 and CYP6Z2 from *An. gambiae,* were yet expressed using a baculovirus expression system (Boonsuepsakul et al., 2008; Duangkaew et al., 2011). Whereas CYP6AA3 and CYP6P7 were co-expressed with *An. minimus* CPR (without CYB5), *An. gambiae* CYP6Z1 and CYP6Z2 were co-expressed with *M. domestica* CPR and *D. melanogaster* CYB5 (Chiu et al., 2008). None of the pyrethroid-metabolizing *An. funestus* P450s have yet been expressed in insect cells using a baculovirus expression system. Interestingly, most, if not all, of the functional insecticide metabolization assays with recombinantly expressed *An. funestus* P450s, particularly CYP6P9a and CYP6P9b, relied on the co-expression of CPR from *An. gambiae* and the addition of *An. gambiae* CYB5 (Table 1, and references cited there-in).

The role of CYB5 on substrate turn-over when combined with CYP6P9a and CYP6P9b has not been fully investigated, so the objective of our study was to address this knowledge gap. In this study, we expressed for the first time *An. funestus* CYP6P9a and CYP6P9b in High-5 cells utilizing a baculovirus expression system. We compared the impact of co-expressed *An. gambiae* CPR and *An. funestus* CPR in a fluorescent probe assay on CYP6P9-mediated substrate conversion. Furthermore, we either co-expressed or added *An. funestus* CYB5 to reaction mixes with recombinantly expressed CYP6P9a and CYP6P9b (and CPR) and tested different MOIs (multiplicity of infection rates). Finally, we conducted metabolism studies with and without co-expressed CYB5 to evaluate its impact on deltamethrin metabolism catalyzed by CYP6P9a and CYP6P9b.

2. Materials and methods

2.1. Chemicals

Deltamethrin (CAS: 52918–63-5), β-Nicotinamide adenine dinucleotide 2′-phosphate (NADPH) reduced tetrasodium salt hydrate (CAS: 2646-71-1 anhydrous, purity ≥93%), 7-ethoxycoumarin (EC; CAS: 31005–02-4, >99%), 7-methoxy-4-trifluoromethylcoumarin (MFC; CAS: 575–04-2, ≥99%), 7-Ethoxy-4-trifluoromethylcoumarin (EFC; CAS: 115453–82-2, ≥98%) 7-benzyloxy-4-trifluoromethylcoumarin (BFC; CAS: 220001–53-6, ≥ 99%), 7- hydroxy-coumarin (HC; CAS: 93–35-6, 99%) 7-hydroxy-4-trifluoromethylcoumarin (HFC; CAS: 575–03-1, 98) were purchased from Sigma Aldrich/Merck (Darmstadt, Germany). 7-benzyloxymethoxy-4-trifluoromethylcoumarin (BOMFC; CAS: 277309–33-8; purity 95%) was synthesized by Enamine Ltd. (Riga, Latvia). 7-pentoxycoumarin and 4′OH-deltamethrin (CAS: 66855–89-8) were internally synthetized (Leverkusen, Germany). Human CYB5 was purchased from Sigma (St. Louis, MO, USA; product no. C1427). All other chemicals and solvents were of analytical grade unless otherwise stated.

2.2. Insects

Anopheles funestus strains FANG and FUMOZ-R are known reference strains susceptible and resistant to pyrethroids (Amenya et al., 2008), respectively. Both strains were kept at 27.5 ± 0.5 °C, 65 ± 5% relative humidity and a photoperiod of 12/12 L:D with one-hour dusk/dawn period, under laboratory conditions as described elsewhere (Nolden et al., 2021). The LC_{50}-values for deltamethrin against adults of strain FANG and FUMOZ-R maintained in our laboratory were 0.021 (CL95%: 0.015–0.027) and 4.61 (CL95%: 2.73–7.50) mg/m^2 in glazed tile bioassays, respectively, resulting in a resistance ratio of >200-fold (Nolden et al., 2021).

2.3. mRNA extraction and RT-qPCR

RNA was extracted from ten 3–5 days old adult females of strain FANG and FUMOZ-R TRIzol™ reaction kit following manufacturer's instructions. Afterwards RNA was purified using RNAeasy MINI Kit (Qiagen, Hilden, Germany) following manufacturer's instructions, including a DNAse-digest (RNase-free DNAse Set, 79,254, Qiagen, Hilden, Germany) (modifications: Trizol incubation: 10 min, the column containing RNA sample was eluated twice to enhance RNA yields). RNA quantity was determined photometrically by measuring 260/280 nm and 230/260 nm ratios (NanoQuant Infinite 200, Tecan, Switzerland). All samples were adjusted to 20 ng/μL and RNA quality was checked using QIAxcel capillary electrophoresis as recently described (Nolden et al., 2021). For cDNA synthesis 0.3 μg of total RNA in 20 μL reaction volume was used employing IScript cDNA synthesis Kit (Bio-Rad, Hercules, USA).

Expression levels of the potential P450 redox partners CYB5 and CPR were measured by RT-qPCR following the method described earlier (Boaventura et al., 2020) using SsoAdvanced Universal SYBR Green Supermix (Bio-Rad, Hercules, USA) with a total volume of 10 μL using Real-Time CFX384™system (Bio-Rad, Hercules, USA). Samples were run in triplicate and a non-template control was included as negative control. Two μL of cDNA with 5 ng/μL of each primer with 200 nM final concentrations were used following the PCR program recently described (Nolden et al., 2021). Two reference genes were employed for normalization, *ribosomal protein S7* (*RPS 7*) and *actin 5c* (*Act*). Primer efficiencies were as follows: CYB5 99.5% and CPR 100%. The experiment was replicated (biological replicates) at least three times. Primer sequences and GenBank accession numbers of all relevant genes are given in Table S1.

2.4. Recombinant expression of CYP genes and its redox partners in insect cells

Gene sequences of *An. funestus CYP6P9a*, *CYP6P9b*, CPR (*AfCPR*), *CYB5*, and *An. gambiae* CPR (*AgCPR*) were retrieved from GenBank (Table S1). The respective expression plasmids were created using GeneArt server (Thermo Fisher), and PFastBac1 with BamHI and *Hin*dIII restriction sites was chosen. The sequences were codon optimized for final expression in High-Five cells (*Trichoplusia ni*). A PFastBac1 vector containing no insert served as a control. For the recombinant expression of P450 genes and their respective redox partners we followed the baculovirus expression protocol previously published (Manjon et al., 2018). In brief: MaxEfficiencyDH10 (Invitrogen, Waltham, MA, USA) competent *E. coli* cells containing a baculovirus shuttle vector (bacmid) were transformed according to manufacturer's instructions. The final bacmid was extracted using Large construct Kit (Qiagen, Hilden, Germany) following standard protocols. Subsequently Sf9 cells (Gibco™, kept in Sf-900-SFM (1×) cell culture medium, containing 25 μg/mL gentamycin) were virus transfected and the virus titer was determined according to Rapid Titer Kit (Takara Bio, San Jose, CA, USA).

High five cells were kept at 27 °C and 120 rpm in Express five medium (SFM (1×), Gibco™, Thermo Fisher, Waltham, MA, USA) containing 18 mM GlutaMAX (100×, Gibco™) and 10 μg mL^{-1} gentamycin (Gibco™). Preliminary experiments revealed highest CYP6P9a and CYP6P9b activity with a multiplicity of infection (MOI) of 1:0.5 for CYP6P9a/b:CPR (Fig. S2). To obtain the best working MOI for CYB5 co-expression we tested the following MOIs (CYP6P9a/b:CPR:CYB5): 1:0.5:0.1; 1:0.5:0.2; 1:0.5:0.5. Cells were diluted to a concentration of 1.5 × 10^6 cells mL^{-1} and incubated with 0.5% fetal bovine serum (FBS; Sigma Aldrich), 0.2 mM delta-aminolevulinic acid (d-ALA; Sigma Aldrich), 0.2 mM Fe III citrate (Sigma Aldrich) and the respective amount of virus for 52 h at 27 °C and 120 rpm. After harvesting, cells were resuspended in homogenization buffer (0.1 M K_2HPO_4, 1 mM DTT,

1 mM EDTA, 200 mM saccharose, pH 7.6). FastPrep device (MP Biomedicals, Irvine, CA, USA) was used for grinding the cells following a 10 min centrifugation step at 4 °C and 700 *g*. The resulting supernatant was centrifuged for one hour at 100,000 g and 4 °C. The resulting microsomal pellet was resuspended with a Dounce tissue grinder in buffer (0.1 M K_2HPO_4, 0.1 mM EDTA, 1 mM DTT, 5% Glycerol, pH 7.6) and protein amount was determined according to Bradford (Bradford, 1976). The functional expression of P450s was validated by their capacity to metabolize coumarin substrates and deltamethrin, and their concentrations were calculated based on CO difference spectra as described elsewhere (Omura and Sato, 1964).

2.5. Fluorescent probe bioassays

The enzymatic activity and substrate profile of each functionally expressed CYP6P9 isoform co-expressed with CPR (± CYB5) at different MOIs was measured in 384-well plates with six different coumarin substrates using the same fluorescent probe assay as recently described (Haas and Nauen, 2021; Nolden et al., 2021). *An. funestus* CYB5 was either co-expressed with the different CYP6P9 variants, or commercial human CYB5 was added to the reaction mix at a concentration of 0.8 μM. This concentration was based on other studies utilizing *An. gambiae* CYB5 (Table 1). Each assay was replicated four times. Michaelis Menten kinetics of BOMFC O-debenzylation by CYP6P9a and CYP6P9b with and without *An. funestus* CYB5 in order to check the impact of CYB5 on substrate conversion followed the same protocol as mentioned above. All incubations were done under conditions linear with respect to time and protein concentration.

2.6. UPLC-MS/MS measurement of deltamethrin metabolism

UPLC-MS/MS analysis was carried out with slight modifications as previously described (Manjon et al., 2018). Briefly, for the chromatography on an Agilent 1290 Infinity II, a Waters Acquity HSS T3 column (2.1 × 50 mm, 1.8 mm) with 2 mM ammonium-acetate in methanol and 2 mM ammonium-acetate in water as the eluent in gradient mode was employed. After positive electrospray ionization, ion transitions were recorded on a Sciex API6500 Triple Quad. Deltamethrin and 4'OH deltamethrin were measured in positive ion mode (ion transitions: deltamethrin 523.000 > 281.000, 4'OH deltamethrin 539.000 > 281.000). The peak integrals were calibrated externally against a standard calibration curve. The linear ranges for the quantification of deltamethrin and 4'OH deltamethrin were 0.5–100 ng/mL and 0.1–200 ng/mL, respectively. Samples were diluted prior to measurement if needed. The experiment was replicated thrice.

2.7. Data analysis

Gene expression analysis was done by employing Bio-Rad CFX Maestro 1.0 v 4.0 software (Bio-Rad, 2017, Hercules, USA) followed by subsequent unpaired *t*-tests in qbase (Biogazelle, Zwijnaarde, Belgium) to compare for significant differences in gene expression levels. Michaelis Menten kinetics were analyzed by nonlinear regression using Graph Pad Prism 9.0 (GraphPad Software Inc., CA, USA). CYB5 sequence alignments were conducted using the Geneious Alignment tool in Geneious software v. 10.2.3 (Biomatters Ltd., New Zealand).

3. Results

3.1. Expression levels of CPR and CYB5

As described previously LC_{50}-values for deltamethrin against adults of *An. funestus* strain FANG and FUMOZ-R maintained in our laboratory were 0.021 (CL95%: 0.015–0.027) and 4.61 (CL95%: 2.73–7.50) mg/m^2 in glazed tile bioassays, respectively, resulting in a resistance ratio of >200-fold (Nolden et al., 2021). Deltamethrin resistance in strain FUMOZ-R is correlated with the upregulation of *CYP6P9a* and *CYP6P9b* in comparison to strain FANG (Fig. 1a). In contrast to the *CYP6P9* variants, the expression levels of both *CYB5* and *CPR* as measured by RT-qPCR were not upregulated in female adults of the pyrethroid resistant FUMOZ-R strain when compared to the susceptible FANG strain, suggesting no immediate regulatory role of these P450 redox partners in pyrethroid resistance in FUMOZ-R (Fig. 1b).

3.2. Functional expression and coumarin substrate profiling of An. funestus CYP6P9 variants in concert with CPR and CYB5 in insect cells

The heterologous baculovirus-mediated expression of CYP6P9a and CYP6P9b in High-5 cells co-infected with *An. gambiae* CPR (AgCPR) at different multiplicity of infection (MOI) ratios, revealed highest fluorescent probe substrate metabolization capacity in the presence of NADPH at a P450:CPR ratio of 1:0.5 across six different alkylated and benzylated coumarins (Table S2). No basal metabolizing activity against any of the six coumarin probe substrates was detected when microsomal membranes resulting from mock virus infections were incubated with NADPH (data not shown), suggesting that the observed substrate profile is based on the expression of the respective *An. funestus* CYP6P9 variant. This confirmed functional expression in High-5 cells despite weak CO difference spectra (Fig. S2). The O-debenzylation of 7-benzyloxymethoxy-4-(trifluoromethyl)-coumarin (BOMFC) resulting in 7-hydroxy-4-(trifluoromethyl)coumarin (HC) revealed the highest enzyme activity with both P450s at all tested P450:CPR MOIs (Fig. 3A-C), followed by the O-debenzylation of 7-benzyloxy-4-trifluoromethylcoumarin (BFC). Less preferred substrates were the alkylated coumarin derivatives tested such 7-methoxy-4-trifluoromethylcoumarin (MFC). However, we observed a slight, but significant difference between CYP6P9a and CYP6P9b in their ability to metabolize BFC and EFC, with CYP6P9b showing higher activity. The overall results and trends in coumarin substrate preference did not change when both CYP6P9 isoforms were co-expressed with *An. funestus* CPR (AfCPR) instead of AgCPR at a MOI of 1:0.5 (Fig. 2A and Fig. S3D). Based on these results we decided to conduct all other experiments with recombinantly expressed CYP6P9a and CYP6P9b in concert with AfCPR.

Next, we tested the impact of the co-expression of *An. funestus* CYB5 (AfCYB5) on coumarin substrate metabolism at different MOIs in combination with CYP6P9 variants and AfCPR. The highest enzyme activity was obtained from microsomal preparations of High-5 cells infected at a MOI of 1:0.5:0.1 (P450:CPR:CYB5) (Fig. 2B). Increasing the level of co-expressed AfCYB5 resulted in a significantly lower enzyme activity with all tested coumarin substrates (Fig. 2B). The overall coumarin substrate profile of both CYP6P9 variants did not change when co-expressed with AfCYB5. However, at a MOI of 1:0.5:0.1 (P450:CPR:CYB5) the activity of both CYP6P9 isoforms was significantly higher with the preferred probe substrates BOMFC, BFC, and EFC when compared to CYP6P9 expressions without AfCYB5. Finally, we checked if the addition of a mammalian CYB5, commercial human CYB5, results in a similar increase in activity. We demonstrated that human CYB5 added to the reaction mix at 0.8 μM increased the activity of CYP6P9a and CYP6P9b co-expressed with AfCPR (MOI 1:0.5) without changing the substrate profile (Fig. 2C), confirming its ability to substitute *An. funestus* or *An. gambiae* CYB5. The metabolic activity of both CYP6P9 variants towards preferred coumarin substrates is not influenced by the choice of the CPR source (AgCPR vs. AfCPR), but the addition of CYB5 increased their activity up to ~6-fold depending on the coumarin substrate (e.g., BFC, Table S2).

3.3. Michaelis Menten kinetics of the O-debenzylation of BOMFC by CYP6P9 variants

Based on the probe substrate activity profiling presented above we have chosen the coumarin substrate BOMFC for a more detailed steady-state kinetic analysis with recombinantly expressed CYP6P9a and

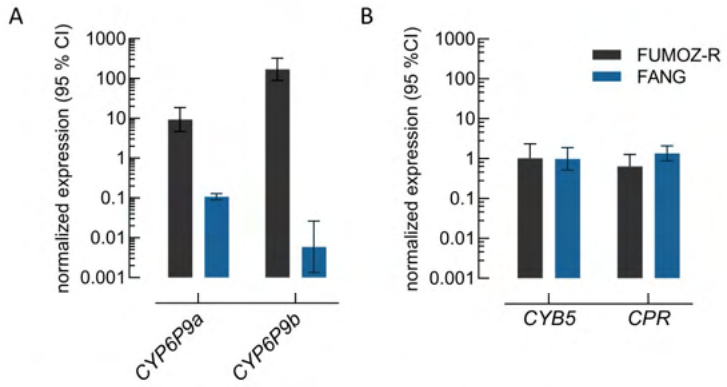

Fig. 1. RT-qPCR analysis of gene expression in female adults. Expression level of (A) *CYP6P9a* and *CYP6P9b*, and (B) cytochrome *b*5 (CYB5) and cytochrome P450-reductase (CPR) of *An. funestus* strains FUMOZ-R and FANG measured by RT-qPCR. The expression levels were normalized to *RPS7* and *Act* (5c) reference genes. Data are mean values ±95% CI (n = 4). The expression data shown in (A) were taken from Nolden et al. (2021).

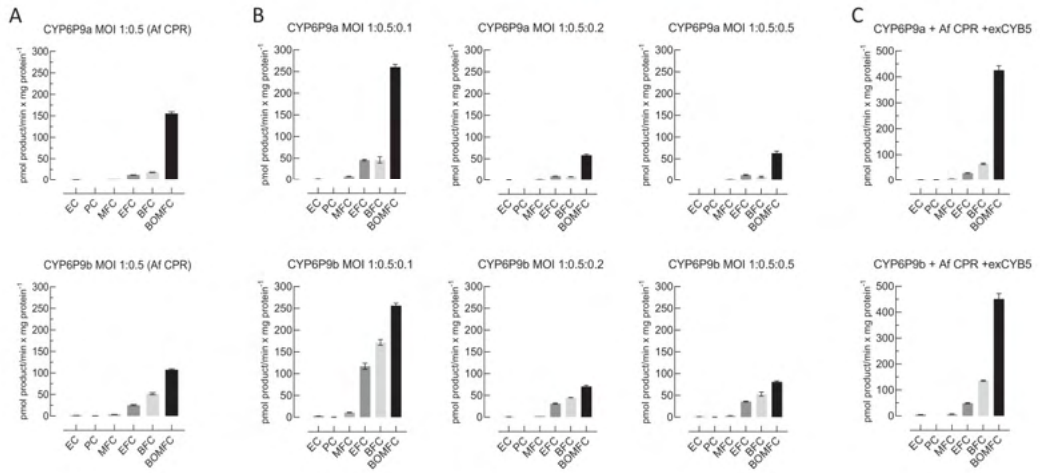

Fig. 2. Coumarin substrate profiling of recombinantly expressed CYP6P9a and CYP6P9b co-expressed with *An. funestus* CPR with and without CYB5. (A) Coumarin substrate metabolism by recombinantly expressed CYP6P9a and CYP6P9b co-expressed with *An. funestus* cytochrome P450-reductase (Af CPR) at MOI 1:0.5, (B) co-expressed with *An. funestus* CYB5 at different MOI ratios stated as P450:CPR:CYB5, and (C) supplemented with exogenous 0.8 μM human CYB5 (exCYB5) while expressed at MOI 1:0.5 (P450:CPR). Data are mean values ± SD (n = 4). Abbreviations: BFC, 7-benzyloxy-4-trifluoromethyl coumarin; MFC, 7-methoxy-4-trifluoromethyl coumarin; EFC, 7-ethoxy-4-rifluoromethyl coumarin; BOMFC, 7-benzyloxymethoxy-4-trifluoromethyl coumarin; PC, 7-n-pentoxy coumarin; EC, 7-ethoxy coumarin.

CYP6P9b with and without the co-expression of *An. funestus* CYB5. The rate of the O-debenzylation of BOMFC by recombinantly expressed CYP6P9a and CYP6P9b was time dependent and followed Michaelis-Menten kinetics in response to BOMFC concentration (Fig. 3), resulting in a K_m-value of 4.07 μM (CI95%: 3.44–4.80) and 2.13 μM (CI95%: 1.62–2.79), and a catalytic activity K_{cat} of 1.59 ± 0.034 min^{-1} and 1.10 ± 0.034 min^{-1}, respectively. The co-expression of CYB5 did not significantly change the K_m-value obtained for BOMFC; CYP6P9a: 4.89 μM (CI95%: 4.10–5.83), and CYP6P9b: 3.25 μM (CI95%: 2.61–4.05). Whereas K_{cat} increased significantly at 2.83 ± 0.067 min^{-1} and 2.29 ± 0.064 min^{-1} in the presence of CYB5 for CYP6P9a and CYP6P9b, respectively. Thus, suggesting a supportive role of CYB5 in CYP6P9 driven BOMFC metabolism, and overall, a slightly lower catalytic capacity of CYP6P9a compared to CYP6P9b.

3.4. Deltamethrin metabolism by CYP6P9 variants with and without CYB5

UPLC-MS/MS analysis of microsomal preparations of High-5 cells expressing CYP6P9a and CYP6P9b, respectively, in concert with *An. funestus* CPR at a MOI of 1:0.5 revealed a time-dependent depletion of deltamethrin in the presence of NADPH (Fig. 4A and B). The co-

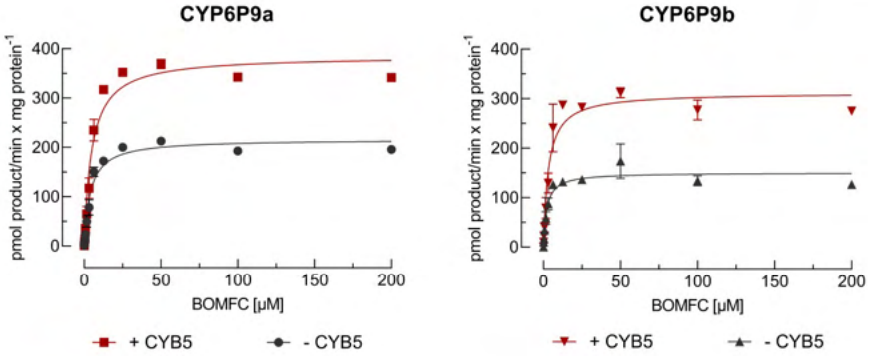

Fig. 3. Steady-state enzyme kinetics of product formation. Michaelis-Menten kinetics of BOMFC O-debenzylation leading to 7-hydroxy-4-(trifluoromethyl)coumarin (HC) by recombinantly expressed CYP6P9a and CYP6P9b (co-expressed with AfCPR, MOI 1:0.5) with and without co-expression of cytochrome *b*5 (CYB5; MOI 1:0.5:0.1). Data are mean values ± SD (n = 4). K_m- and V_{max}-values (and 95% confidence intervals) were calculated by nonlinear regression analysis using GraphPad Prism 9.0.

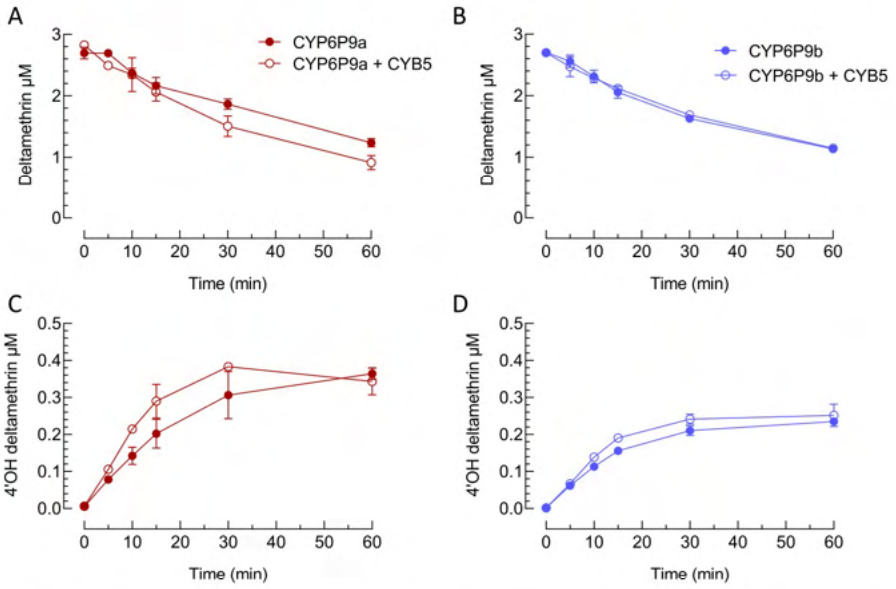

Fig. 4. Kinetics of deltamethrin metabolism by baculovirus-expressed *An. funestus* CYP6P9 variants. Deltamethrin depletion and formation of the respective 4'OH metabolite in the presence of NADPH by recombinantly expressed *An. funestus* CYP6P9a (A,C) and CYP6P9b (B,D) co-expressed with (open circles) and without (closed circles) *An. funestus* cytochrome *b*5 (CYB5). Data are mean values ± SD (*n* = 3).

expression of *An. funestus* CYB5 did not change the metabolic efficiency of both enzymes. Furthermore, we confirmed the formation of 4'OH deltamethrin by both enzymes (Fig. 4C and D), suggesting that the deltamethrin depletion is largely based on its metabolism rather than sequestration. The co-expression of CYB5 had no impact on the extent of hydroxylated deltamethrin formation. However, we noticed a stochiometric inconsistency between deltamethrin depletion and 4OH deltamethrin formation, possibly suggesting the presence of other undetected metabolites.

4. Discussion

Metabolic resistance towards pyrethroids in Anopheline mosquitoes such as *An. funestus* is largely driven by upregulated P450s of which a number have been recombinantly expressed, most of them in bacterial expression systems using competent *E. coli* cells (Nauen et al., 2021;

Vontas et al., 2020). Among upregulated P450s mediating pyrethroid resistance in *An. funestus*, CYP6P9a and CYP6P9b, were most prominent and shown to metabolize different pyrethroids when functionally expressed in *E. coli* (Riveron et al., 2013; Weedall et al., 2019). Here we successfully expressed both P450 genes in combination with either AfCPR or AgCPR at different MOI ratios in High-5 cells employing a baculovirus expression system. Microsomal insect cell preparations revealed highest CYP6P9a/b activities with the fluorescent probe substrate BOMFC at a MOI ratio of 1:0.5 (P450:CPR), resembling findings with other insect P450s utilizing similar expression conditions (Bass et al., 2013; Manjon et al., 2018; Zimmer et al., 2018). Many functional studies conducted with recombinantly expressed *An. funestus* P450s showed that their co-expression with *An. gambiae* CPR as a surrogate for the homologous *An. funestus* CPR worked well (Table 1). Our study demonstrated and confirmed that the overall enzymatic activity of the duplicated CYP6P9 isoforms did not differ if co-expressed with either *An. gambiae* CPR or *An. funestus* CPR. Indeed, CPR incompatibilities as observed for *Tetranychus urticae* CYP392A11 and CYP392A16 ectopically expressed in phylogenetically distant *D. melanogaster*, are rather unlikely in closely related species (Riga et al., 2020).

The baculovirus system recruiting High-5 cells for P450 expression is thought to offer some advantages over *E. coli* such as insect-specific posttranslational modifications of the expressed P450s, though meaningful comparative studies with insect P450s are lacking. Comparative studies utilizing prokaryotic and eukaryotic expression systems were especially conducted with human P450 isoforms (Hiratsuka, 2012), and revealed for example significantly different catalytic efficiencies in benzo[*a*]pyrene detoxification by functionally expressed human CYP1A1, possibly linked to differences in lipid membrane composition (Stiborová et al., 2017). Although optimized *E. coli* expression systems often resulted in higher P450 yields as demonstrated for human CYP3A4 and CYP17A1 (Schroer et al., 2010), it was shown that they have limitations in contrast to insect and mammalian cells (Kumondai et al., 2020). On the other hand, *E. coli* preparations do not express basal P450 activity as they lack endogenous P450s possibly interfering with those P450s recombinantly expressed (Nauen et al., 2021), which facilitates the screening of compounds for metabolic liabilities including insecticides (Lees et al., 2020; Yunta et al., 2019). Future studies with insect P450s are necessary to shed light on possible differences in P450 catalytic efficiency towards various substrates between prokaryotic and eukaryotic expression systems.

We recently confirmed high expression levels of the duplicated *CYP6P9* genes in the laboratory reference strain FUMOZ-R (Nolden et al., 2021), whereas *CPR*, the principal redox partner of microsomal P450s, is not overexpressed when compared to the susceptible strain FANG. Another potential redox partner, *CYB5*, often added or co-expressed along with mosquito P450s such as CYP6P9a and CYP6P9b (Table 1), is also not overexpressed in strain FUMOZ-R compared to FANG. In contrast to our findings, Nikou et al. (2003) found a 2.3-fold upregulation of *CYB5* expression in the pyrethroid resistant *An. gambiae* RSP strain in comparison to the susceptible Kisumu strain. This was also demonstrated in a cypermethrin resistant strain of *Plutella xylostella* showing elevated *CPR* and *CYB5* expression levels (Chen and Zhang, 2015). It would be interesting to evaluate *CPR* and *CYB5* expression levels in pyrethroid resistant field-collected populations of *An. funestus* to rule out possible effects related to the fact that FUMOZ-R has been kept without selection pressure under laboratory conditions for many years. However, our qPCR data do not suggest an obvious role of CYB5 in the amplification of CYP6P9-mediated pyrethroid resistance in *An. funestus* strain FUMOZ-R. This is supported by experimental data showing no difference in deltamethrin depletion measured by UPLC-MS/MS when recombinantly expressed CYP6P9a and CYP6P9b were co-expressed with and without *An. funestus* CYB5. Interestingly, pyrethroid-mimetic activity-based probes were far less active in labelling P450s in CYB5 deficient mouse microsomes, indicating potential species and/or enzyme differences in CYB5 effects (Ismail et al., 2013).

In contrast we were able to demonstrate that *An. funestus* CYB5 co-expressed at a MOI ratio of 1:0.5:0.1 (P450:CPR:CYB5) significantly increased the catalytic capacity of both CYP6P9a and CYP6P9b to O-debenzylate BOMFC and BFC, the preferred coumarin substrates as recently shown with microsomal preparations of female adults of FUMOZ-R (Nolden et al., 2021). Thus, suggesting that at least for some of the coumarin substrates CYB5 possibly improved the electron transfer through CPR, but didn't change the coumarin substrate profile. However, the coumarin profiling results obtained in this study also indicated that both CYP6P9 isoforms contributed greatly to the microsomal P450 activity of the pyrethroid resistant FUMOZ-R recently described (Nolden et al., 2021), and that CYB5 is not necessary to resemble in vivo microsomal activity. Other tested MOI ratios using higher amounts of CYB5 resulted in lower enzyme activity, possibly linked to lower overall expression yields of the respective CYP genes as for example shown for human CYP1A2, CYP2C9 and CYP3A4 in other heterologous expression systems (Kumondai et al., 2020). Studies with recombinantly expressed human CYP2B4 revealed that depending on the P450:CYB5 ratio its catalytic efficiency was impaired, because CPR and CYB5 are competing for the same binding site at the enzyme (Zhang et al., 2008). These findings are in line with our results of different MOI ratios tested: A ratio of 1:0.5:0.1 (CYP:CPR:CYB5) revealed highest coumarin substrate activity, whereas a ratio of 1:0.5:0.2 drastically reduced P450 activity.

CYP6M2 from *An. gambiae* was shown to better metabolize deltamethrin and permethrin if 0.8 μM *An. gambiae* CYB5 was supplemented to the reaction (Stevenson et al., 2011), whereas in our study with *An. funestus* CYP6P9 variants the co-expression of CYB5 did not enhance deltamethrin metabolism, suggesting a minor, if any role for CYB5 in facilitating deltamethrin metabolism. Future studies with CYP6P9a/b are necessary to clarify if this is also true for other pyrethroids than deltamethrin. High-5 cell microsomal membranes are highly likely to contain endogenous CYB5 possibly sufficient to support P450 mediated deltamethrin hydroxylation as an additional redox partner. Knock-out of the endogenous *CYB5* in High-5 cells by genome editing would help to address this point. Such an endogenous CYB5 supply is absent in *E. coli* expression systems, possibly explaining why supplementation with exogenous *An. gambiae* CYB5 may have a larger impact, e.g., on recombinantly expressed CYP6M2 (Stevenson et al., 2011).

Quite a few studies demonstrated elevated microsomal levels of CYB5 linked to a resistant phenotype in insects. In a multiple resistant house fly strain microsomal P450 and CYB5 levels were found upregulated in some tissues (Zhang et al., 1998). Similar results were obtained with microsomal fractions of a carbamate and pyrethroid resistant *Blattella germanica* strain (Valles and Yu, 1996). In the cypermethrin resistant house fly LPR strain CYP6D1 and CYB5 were found to be upregulated, and inhibition of CYB5 with a specific antibody prevented the formation of 4'OH-cypermethrin (Liu and Scott, 1996; Zhang and Scott, 1996). In a previous study the same authors reported that specific CYB5 inhibition in house fly microsomes did not affect methoxyresorufin-*O*-demethylase and ethoxyresorufin-O-deethylase activity, but ethoxycoumarin-O-deethylase activity. Another study demonstrated an enhanced metabolism of heptachlor and aldrin if CYP6A2 from *D. melanogaster* was supplemented with CYB5 (Dunkov et al., 1997). This was also observed with recombinantly expressed house fly CYP6A1 and it was shown that even apo-CYB5 (devoid of heme) enhanced the metabolic activity against heptachlor and steroid-substrates, and it was concluded that CYB5 mainly enhanced metabolism by CYP6A1 in two ways, by delivering the second electron to CYP6A1 and by allosteric interactions (Murataliev et al., 2008). Similar interactions were also described between a number of recombinantly expressed human P450s and apo-CYB5 (Yamazaki et al., 2002). For recombinantly expressed CYP6FD1 from L. *migratoria* it was shown that silencing of the respective CYB5 gene, did not alter metabolism towards deltamethrin, chlorpyrifos, imidacloprid and carbaryl, but the co-expression of recombinant CYP6FD1 with CYB5 enhanced the metabolism of 7-ethoxycoumarin (Liu et al., 2020).

The examples above and our data obtained with CYP6P9 variants suggest that the involvement of CYB5 in xenobiotic P450-mediated metabolism depends on P450 and substrate-specificity, as reviewed earlier (Schenkman and Jansson, 2003). Our results suggest that co-expression (or addition) of CYB5 with CYP6P9 variants, recombinantly expressed in insect cells, can significantly enhance their metabolic capacity to degrade coumarins, but not deltamethrin.

Declaration of Competing Interest

RN is employed by Bayer AG, a manufacturer of pesticides. MN is a PhD student affiliated with the LSTM and funded by the Innovative Vector Control Consortium (IVCC) and Bayer AG.

Data availability

Data will be made available on request.

Acknowledgements

We greatly acknowledge the help of Johannes Glaubitz and Birgit Nebelsiek with the UPLC-MS/MS analysis. We are thankful to Sebastian Horstmann and Uwe Pluschkell for their support and useful discussions.

Appendix A. Supplementary data

Supplementary data to this article can be found online at https://doi.org/10.1016/j.pestbp.2022.105051.

References

Amenya, D.A., Naguran, R., Lo, T.-C.M., Ranson, H., Spillings, B.L., Wood, O.R., Brooke, B.D., Coetzee, M., Koekemoer, L.L., 2008. Over expression of a cytochrome P450 (CYP6P9) in a major African malaria vector, *Anopheles Funestus*, resistant to pyrethroids. Insect Mol. Biol. 17, 19–25. https://doi.org/10.1111/j.1365-2583.2008.00776.x.

Bass, C., Zimmer, C.T., Riveron, J.M., Wilding, C.S., Wondji, C.S., Kaussmann, M., Field, L.M., Williamson, M.S., Nauen, R., 2013. Gene amplification and microsatellite polymorphism underlie a recent insect host shift. Proc. Natl. Acad. Sci. 110, 19460–19465. https://doi.org/10.1073/pnas.1314122110.

Boaventura, D., Martin, M., Pozzebon, A., Mota-Sanchez, D., Nauen, R., 2020. Monitoring of target-site mutations conferring insecticide resistance in *Spodoptera frugiperda*. Insects 11, 545. https://doi.org/10.3390/insects11080545.

Boonsuepsakul, S., Luepromchai, E., Rongnoparut, P., 2008. Characterization of *Anopheles minimus* CYP6AA3 expressed in a recombinant baculovirus system. Arch. Insect Biochem. Physiol. 69, 13–21. https://doi.org/10.1002/arch.20248.

Bradford, M.M., 1976. A rapid and sensitive method for the quantitation of microgram quantities of protein utilizing the principle of protein-dye binding. Anal. Biochem. 72, 248–254. https://doi.org/10.1016/0003-2697(76)90527-3.

Brooke, B.D., Kloke, G., Hunt, R.H., Koekemoer, L.L., Tem, E.A., Taylor, M.E., Small, G., Hemingway, J., Coetzee, M., 2001. Bioassay and biochemical analyses of insecticide resistance in southern African *Anopheles funestus* (Diptera: Culicidae). Bull. Entomol. Res. 91, 265–272. https://doi.org/10.1079/ber2001108.

Chandor-Proust, A., Bibby, J., Régent-Kloeckner, M., Roux, J., Guittard-Crilat, E., Poupardin, R., Riaz, M.A., Paine, M., Dauphin-Villemant, C., Reynaud, S., David, J.-P., 2013. The central role of mosquito cytochrome P450 CYP6Zs in insecticide detoxification revealed by functional expression and structural modelling. Biochem. J. 455, 75–85. https://doi.org/10.1042/BJ20130577.

Chen, X., Zhang, Y., 2015. Identification and characterization of NADPH-dependent cytochrome P450 reductase gene and cytochrome b5 gene from *Plutella xylostella*: possible involvement in resistance to beta-cypermethrin. Gene 558, 208–214. https://doi.org/10.1016/j.gene.2014.12.053.

Chiu, T.-L., Wen, Z., Rupasinghe, S.G., Schuler, M.A., 2008. Comparative molecular modeling of *Anopheles gambiae* CYP6Z1, a mosquito P450 capable of metabolizing DDT. Proc. Natl. Acad. Sci. 105, 8855–8860. https://doi.org/10.1073/pnas.0709249105.

Coetzee, M., Koekemoer, L.L., 2013. Molecular systematics and insecticide resistance in the major African malaria vector *Anopheles funestus*. Annu. Rev. Entomol. 58, 393–412. https://doi.org/10.1146/annurev-ento-120811-153628.

Coon, M.J., 2005. CYTOCHROME P450: nature's most versatile biological catalyst. Annu. Rev. Pharmacol. Toxicol. 45, 1–25. https://doi.org/10.1146/annurev.pharmtox.45.120403.100030.

Cuamba, N., Morgan, J.C., Irving, H., Steven, A., Wondji, C.S., 2010. High level of Pyrethroid resistance in an *Anopheles funestus* population of the Chokwe District in Mozambique. PLoS One 5, e11010. https://doi.org/10.1371/journal.pone.0011010.

Duangkaew, P., Pethuan, S., Kaewpa, D., Boonsuepsakul, S., Sarapusit, S., Rongnoparut, P., 2011. Characterization of mosquito CYP6P7 and CYP6AA3: differences in substrate preference and kinetic properties. Arch. Insect Biochem. Physiol. 76, 236–248. https://doi.org/10.1002/arch.20413.

Dunkov, B.C., Guzov, V.M., Mocelin, G., Shotkoski, F., Brun, A., Amichot, M., Ffrench-Constant, R.H., Feyereisen, R., 1997. The *Drosophila* cytochrome P450 gene Cyp6a2: structure, localization, heterologous expression, and induction by phenobarbital. DNA Cell Biol. 16, 1345–1356. https://doi.org/10.1089/dna.1997.16.1345.

Esteves, F., Rueff, J., Kranendonk, M., 2021. The central role of cytochrome P450 in xenobiotic metabolism—a brief review on a fascinating enzyme family. J. Xenobiotics 11, 94–114. https://doi.org/10.3390/jox11030007.

Feyereisen, R., 2012. 8 - insect CYP genes and P450 enzymes. In: Gilbert, L.I. (Ed.), Insect Molecular Biology and Biochemistry. Academic Press, San Diego, pp. 236–316. https://doi.org/10.1016/B978-0-12-384747-8.10008-X.

Finn, R.D., McLaughlin, L.A., Ronseaux, S., Rosewell, I., Houston, J.B., Henderson, C.J., Wolf, C.R., 2008. Defining the in vivo role for cytochrome b5 in cytochrome P450 function through the conditional hepatic deletion of microsomal cytochrome b5. J. Biol. Chem. 283, 31385–31393. https://doi.org/10.1074/jbc.M803496200.

Finn, R.D., McLaughlin, L.A., Hughes, C., Song, C., Henderson, C.J., Roland Wolf, C., 2011. Cytochrome b5 null mouse: a new model for studying inherited skin disorders and the role of unsaturated fatty acids in normal homeostasis. Transgenic Res. 20, 491–502. https://doi.org/10.1007/s11248-010-9426-1.

Gutierrez, A., Grunau, A., Paine, M., Munro, A.W., Wolf, C.R., Roberts, G.C.K., Scrutton, N.S., 2003. Electron transfer in human cytochrome P450 reductase. Biochem. Soc. Trans. 31, 497–501. https://doi.org/10.1042/bst0310497.

Guzov, V.M., Houston, H.L., Murataliev, M.B., Walker, F.A., Feyereisen, R., 1996. Molecular cloning, overexpression in *Escherichia coli*, structural and functional characterization of house Fly cytochrome b5. J. Biol. Chem. 271, 26637–26645. https://doi.org/10.1074/jbc.271.43.26637.

Haas, J., Nauen, R., 2021. Pesticide risk assessment at the molecular level using honey bee cytochrome P450 enzymes: a complementary approach. Environ. Int. 147, 106372 https://doi.org/10.1016/j.envint.2020.106372.

Hemingway, J., Ranson, H., 2000. Insecticide resistance in insect vectors of human diseases. Annu. Rev. Entomol. 45, 371–391.

Henderson, C.J., McLaughlin, L.A., Scheer, N., Stanley, L.A., Wolf, C.R., 2015. Cytochrome b5 is a major determinant of human cytochrome P450 CYP2D6 and CYP3A4 activity in vivo. Mol. Pharmacol. 87, 733–739. https://doi.org/10.1124/mol.114.097394.

Hiratsuka, M., 2012. *In vitro* assessment of the allelic variants of cytochrome P450. Drug Metab. Pharmacokinet. 27, 68–84. https://doi.org/10.2133/dmpk.DMPK-11-RV-090.

Hunt, R.H., Brooke, B.D., Pillay, C., Koekemoer, L.L., Coetzee, M., 2005. Laboratory selection for and characteristics of pyrethroid resistance in the malaria vector *Anopheles funestus*. Med. Vet. Entomol. 19, 271–275. https://doi.org/10.1111/j.1365-2915.2005.00574.x.

Ibrahim, S.S., Riveron, J.M., Bibby, J., Irving, H., Yunta, C., Paine, M.J.I., Wondji, C.S., 2015. Allelic variation of cytochrome P450s drives resistance to Bednet insecticides in a major malaria vector. PLoS Genet. 11, e1005618 https://doi.org/10.1371/journal.pgen.1005618.

Ibrahim, S.S., Ndula, M., Riveron, J.M., Irving, H., Wondji, C.S., 2016a. The P450 CYP6Z1 confers carbamate/pyrethroid cross-resistance in a major African malaria vector beside a novel carbamate-insensitive N485I acetylcholinesterase-1 mutation. Mol. Ecol. 25, 3436–3452. https://doi.org/10.1111/mec.13673.

Ibrahim, S.S., Riveron, J.M., Stott, R., Irving, H., Wondji, C.S., 2016b. The cytochrome P450 CYP6P4 is responsible for the high pyrethroid resistance in knockdown resistance-free *Anopheles arabiensis*. Insect Biochem. Mol. Biol. 68, 23–32. https://doi.org/10.1016/j.ibmb.2015.10.015.

Ibrahim, S.S., Amvongo-Adjia, N., Wondji, M.J., Irving, H., Riveron, J.M., Wondji, C.S., 2018. Pyrethroid resistance in the major malaria vector *Anopheles funestus* is exacerbated by overexpression and overactivity of the P450 CYP6AA1 across Africa. Genes 9, 1–17. https://doi.org/10.3390/genes9030140.

Ismail, H.M., O'Neill, P.M., Hong, D.W., Finn, R.D., Henderson, C.J., Wright, A.T., Cravatt, B.F., Hemingway, J., Paine, M.J.I., 2013. Pyrethroid activity-based probes for profiling cytochrome P450 activities associated with insecticide interactions. Proc. Natl. Acad. Sci. 110, 19766–19771. https://doi.org/10.1073/pnas.1320185110.

Kasai, S., Komagata, O., Itokawa, K., Shono, T., Ng, L.C., Kobayashi, M., Tomita, T., 2014. Mechanisms of Pyrethroid resistance in the dengue mosquito vector, Aedes aegypti: target site insensitivity, penetration, and metabolism. PLoS Negl. Trop. Dis. 8, e2948 https://doi.org/10.1371/journal.pntd.0002948.

Kumondai, M., Hishinuma, E., Gutiérrez Rico, E.M., Ito, A., Nakanishi, Y., Saigusa, D., Hirasawa, N., Hiratsuka, M., 2020. Heterologous expression of high-activity cytochrome P450 in mammalian cells. Sci. Rep. 10, 14193. https://doi.org/10.1038/s41598-020-71035-5.

Lees, R.S., Ismail, H.M., Logan, R.A.E., Malone, D., Davies, R., Anthousi, A., Adolfi, A., Lycett, G.J., Paine, M.J.I., 2020. New insecticide screening platforms indicate that mitochondrial complex I inhibitors are susceptible to cross-resistance by mosquito P450s that metabolise pyrethroids. Sci. Rep. 10, 16232. https://doi.org/10.1038/s41598-020-73267-x.

Liu, N., Scott, J.G., 1996. Genetic analysis of factors controlling high-level expression of cytochrome P450, CYP6D1, cytochrome b5, P450 reductase, and monooxygenase activities in LPR house flies, *Musca domestica*. Biochem. Genet. 34, 133–148. https://doi.org/10.1007/BF02396246.

Liu, J., Zhang, X., Wu, H., Ma, W., Zhu, W., Zhu, K.-Y., Ma, E., Zhang, J., 2020. Characteristics and roles of cytochrome b5 in cytochrome P450-mediated oxidative reactions in *Locusta migratoria*. J. Integr. Agric. 19, 1512–1521. https://doi.org/10.1016/S2095-3119(19)62827-3.

Lu, K., Song, Y., Zeng, R., 2021. The role of cytochrome P450-mediated detoxification in insect adaptation to xenobiotics. Curr. Opin. Insect Sci. 43, 103–107. https://doi.org/10.1016/j.cois.2020.11.004.

Lycett, G.J., McLaughlin, L.A., Ranson, H., Hemingway, J., Kafatos, F.C., Loukeris, T.G., Paine, M.J.I., 2006. *Anopheles gambiae* P450 reductase is highly expressed in oenocytes and in vivo knockdown increases permethrin susceptibility. Insect Mol. Biol. 15, 321–327. https://doi.org/10.1111/j.1365-2583.2006.00647.x.

Manjon, C., Troczka, B.J., Zaworra, M., Beadle, K., Randall, E., Hertlein, G., Singh, K.S., Zimmer, C.T., Homem, R.A., Lueke, B., Reid, R., Kor, L., Kohler, M., Benting, J., Williamson, M.S., Davies, T.G.E., Field, L.M., Bass, C., Nauen, R., 2018. Unravelling the molecular determinants of bee sensitivity to Neonicotinoid insecticides. Curr. Biol. 28, 1137–1143.e5. https://doi.org/10.1016/j.cub.2018.02.045.

Matambo, T.S., Paine, M.J.I., Coetzee, M., Koekemoer, L.L., 2010. Sequence characterization of cytochrome P450 CYP6P9 in pyrethroid resistant and susceptible *Anopheles funestus* (Diptera: Culicidae). Genet. Mol. Res. 9, 554–564. https://doi.org/10.4238/vol9-1gmr719.

Mclaughlin, L.A., Niazi, U., Bibby, J., David, J.-P., Vontas, J., Hemingway, J., Ranson, H., Sutcliffe, M.J., Paine, M.J.I., 2008. Characterization of inhibitors and substrates of *Anopheles gambiae* CYP6Z2. Insect Mol. Biol. 17, 125–135. https://doi.org/10.1111/j.1365-2583.2007.00788.x.

McLaughlin, L.A., Ronseaux, S., Finn, R.D., Henderson, C.J., Roland Wolf, C., 2010. Deletion of microsomal cytochrome b_5 profoundly affects hepatic and Extrahepatic drug metabolism. Mol. Pharmacol. 78, 269–278. https://doi.org/10.1124/mol.110.064246.

Moural, T.W., Ban, L., Hernandez, J.A., Wu, M., Zhao, C., Palli, S.R., Alyokhin, A., Zhu, F., 2020. Silencing NADPH-Cytochrome P450 Reductase Affects Imidacloprid Susceptibility, Fecundity, and Embryonic Development in *Leptinotarsa decemlineata*. https://doi.org/10.1101/2020.09.29.318634.

Müller, P., Warr, E., Stevenson, B.J., Pignatelli, P.M., Morgan, J.C., Steven, A., Yawson, A.E., Mitchell, S.N., Ranson, H., Hemingway, J., Paine, M.J.I., Donnelly, M. J., 2008. Field-caught Permethrin-resistant *Anopheles gambiae* overexpress CYP6P3, a P450 that Metabolises Pyrethroids. PLoS Genet. 4, e1000286 https://doi.org/10.1371/journal.pgen.1000286.

Murataliev, M.B., Guzov, V.M., Walker, F.A., Feyereisen, R., 2008. P450 reductase and cytochrome b5 interactions with cytochrome P450: effects on house fly CYP6A1 catalysis. Insect Biochem. Mol. Biol. 38, 1008–1015. https://doi.org/10.1016/j.ibmb.2008.08.007.

Nauen, R., Zimmer, C.T., Vontas, J., 2021. Heterologous expression of insect P450 enzymes that metabolize xenobiotics. Curr. Opin. Insect Sci. 43, 78–84. https://doi.org/10.1016/j.cois.2020.10.011.

Nauen, R., Bass, C., Feyereisen, R., Vontas, J., 2022. The role of cytochrome P450s in insect toxicology and resistance. Annu. Rev. Entomol. 67, null. https://doi.org/10.1146/annurev-ento-070621-061328.

Nikou, D., Ranson, H., Hemingway, J., 2003. An adult-specific CYP6 P450 gene is overexpressed in a pyrethroid-resistant strain of the malaria vector, *Anopheles gambiae*. Gene 318, 91–102. https://doi.org/10.1016/S0378-1119(03)00763-7.

Nolden, M., Brockmann, A., Ebbinghaus-Kintscher, U., Brueggen, K.-U., Horstmann, S., Paine, M.J.I., Nauen, R., 2021. Towards understanding transfluthrin efficacy in a pyrethroid-resistant strain of the malaria vector *Anopheles funestus* with special reference to cytochrome P450-mediated detoxification. Curr. Res. Parasitol. Vect.-Borne Dis. 1, 100041 https://doi.org/10.1016/j.crpvbd.2021.100041.

Omura, T., Sato, R., 1964. The carbon monoxide-binding pigment of liver Microsomes: I. Evidence for its hemoprotein nature. J. Biol. Chem. 239, 2370–2378. https://doi.org/10.1016/S0021-9258(20)82244-3.

Porter, T.D., 2012. New insights into the role of cytochrome P450 reductase (POR) in microsomal redox biology. Acta Pharm. Sin. B Drug Metab. Transp. 2, 102–106. https://doi.org/10.1016/j.apsb.2012.02.002.

Riga, M., Ilias, A., Vontas, J., Douris, V., 2020. Co-expression of a homologous cytochrome P450 reductase is required for in vivo validation of the *Tetranychus urticae* CYP392A16-based Abamectin resistance in Drosophila. Insects 11, 829. https://doi.org/10.3390/insects11120829.

Riveron, J.M., Irving, H., Ndula, M., Barnes, K.G., Ibrahim, S.S., Paine, M.J.I., Wondji, C. S., 2013. Directionally selected cytochrome P450 alleles are driving the spread of pyrethroid resistance in the major malaria vector *Anopheles funestus*. Proc. Natl. Acad. Sci. 110, 252–257. https://doi.org/10.1073/pnas.1216705110.

Riveron, J.M., Ibrahim, S.S., Chanda, E., Mzilahowa, T., Cuamba, N., Irving, H., Barnes, K.G., Ndula, M., Wondji, C.S., 2014. The highly polymorphic CYP6M7 cytochrome P450 gene partners with the directionally selected CYP6P9a and CYP6P9b genes to expand the pyrethroid resistance front in the malaria vector *Anopheles funestus* in Africa. BMC Genomics 15, 817. https://doi.org/10.1186/1471-2164-15-817.

Riveron, J.M., Ibrahim, S.S., Mulamba, C., Djouaka, R., Irving, H., Wondji, M.J., Ishak, I. H., Wondji, C.S., 2017. Genome-wide transcription and functional analyses reveal heterogeneous molecular mechanisms driving pyrethroids resistance in the major malaria vector *Anopheles funestus* across Africa. G3 Genes Genomes Genet. 7, 1819–1832. https://doi.org/10.1534/g3.117.040147.

Schenkman, J.B., Jansson, I., 2003. The many roles of cytochrome b5. Pharmacol. Ther. 97, 139–152. https://doi.org/10.1016/S0163-7258(02)00327-3.

Schroer, K., Kittelmann, M., Lütz, S., 2010. Recombinant human cytochrome P450 monooxygenases for drug metabolite synthesis. Biotechnol. Bioeng. 106, 699–706. https://doi.org/10.1002/bit.22775.

Schuler, M.A., 2011. P450s in plant–insect interactions. Biochim. Biophys. Acta BBA 1814, 36–45. https://doi.org/10.1016/j.bbapap.2010.09.012.

Shen, A.L., O'Leary, K.A., Kasper, C.B., 2002. Association of Multiple Developmental Defects and Embryonic Lethality with loss of microsomal NADPH-cytochrome P450 Oxidoreductase. J. Biol. Chem. 277, 6536–6541. https://doi.org/10.1074/jbc.M111408200.

Shi, L., Zhang, J., Shen, G., Xu, Z., Wei, P., Zhang, Y., Xu, Q., He, L., 2015. Silencing NADPH-cytochrome P450 reductase results in reduced acaricide resistance in *Tetranychus cinnabarinus* (Boisduval). Sci. Rep. 5, 15581. https://doi.org/10.1038/srep15581.

Soderlund, D.M., 2020. Neurotoxicology of pyrethroid insecticides. In: Advances in Neurotoxicology. Elsevier, pp. 113–165. https://doi.org/10.1016/bs.ant.2019.11.002.

Stevenson, B.J., Bibby, J., Pignatelli, P., Muangnoicharoen, S., O'Neill, P.M., Lian, L.-Y., Müller, P., Nikou, D., Steven, A., Hemingway, J., Sutcliffe, M.J., Paine, M.J.I., 2011. Cytochrome P450 6M2 from the malaria vector *Anopheles gambiae* metabolizes pyrethroids: sequential metabolism of deltamethrin revealed. Insect Biochem. Mol. Biol. Spec. Issue 41, 492–502. https://doi.org/10.1016/j.ibmb.2011.02.003.

Stevenson, B.J., Pignatelli, P., Nikou, D., Paine, M.J.I., 2012. Pinpointing P450s associated with Pyrethroid metabolism in the dengue vector, *Aedes aegypti*: developing new tools to combat insecticide resistance. PLoS Negl. Trop. Dis. 6, e1595 https://doi.org/10.1371/journal.pntd.0001595.

Stiborová, M., Indra, R., Moserová, M., Bořek-Dohalská, L., Hodek, P., Frei, E., Kopka, K., Schmeiser, H.H., Arlt, V.M., 2017. Comparison of human cytochrome P450 1A1-catalysed oxidation of benzo[a]pyrene in prokaryotic and eukaryotic expression systems. Monatshefte Für Chem. 148, 1959–1969. https://doi.org/10.1007/s00706-017-2002-0.

Valles, S.M., Yu, S.J., 1996. Detection and biochemical characterization of insecticide resistance in the German cockroach (Dictyoptera: Blattellidae). J. Econ. Entomol. 89, 21–26. https://doi.org/10.1093/jee/89.1.21.

Vontas, J., Katsavou, E., Mavridis, K., 2020. Cytochrome P450-based metabolic insecticide resistance in Anopheles and Aedes mosquito vectors: muddying the waters. Pestic. Biochem. Physiol. 170, 104666 https://doi.org/10.1016/j.pestbp.2020.104666.

Wamba, A.N.R., Ibrahim, S.S., Kusimo, M.O., Muhammad, A., Mugenzi, L.M.J., Irving, H., Wondji, M.J., Hearn, J., Bigoga, J.D., Wondji, C.S., 2021. The cytochrome P450 CYP325A is a major driver of pyrethroid resistance in the major malaria vector *Anopheles funestus* in Central Africa. Insect Biochem. Mol. Biol. 138, 103647 https://doi.org/10.1016/j.ibmb.2021.103647.

Weedall, G.D., Mugenzi, L.M.J., Menze, B.D., Tchouakui, M., Ibrahim, S.S., Amvongo-Adjia, N., Irving, H., Wondji, M.J., Tchoupo, M., Djouaka, R., Riveron, J.M., Wondji, C.S., 2019. A cytochrome P450 allele confers pyrethroid resistance on a major African malaria vector, reducing insecticide-treated bednet efficacy. Sci. Transl. Med. 11 https://doi.org/10.1126/scitranslmed.aat7386 eaat7386.

WHO, 2018. Global Report on Insecticide Resistance in Malaria Vectors, pp. 2010–2016.

Wondji, C.S., Irving, H., Morgan, J., Lobo, N.F., Collins, F.H., Hunt, R.H., Coetzee, M., Hemingway, J., Ranson, H., 2009. Two duplicated P450 genes are associated with pyrethroid resistance in *Anopheles funestus*, a major malaria vector. Genome Res. 19, 452–459. https://doi.org/10.1101/gr.087916.108.

Yamazaki, H., Nakamura, M., Komatsu, T., Ohyama, K., Hatanaka, N., Asahi, S., Shimada, N., Guengerich, F.P., Shimada, T., Nakajima, M., Yokoi, T., 2002. Roles of NADPH-P450 Reductase and Apo- and Holo-cytochrome b5 on xenobiotic oxidations catalyzed by 12 recombinant human cytochrome P450s expressed in membranes of *Escherichia coli*. Protein Expr. Purif. 24, 329–337. https://doi.org/10.1006/prep.2001.1578.

Yunta, C., Grisales, N., Nász, S., Hemmings, K., Pignatelli, P., Voice, M., Ranson, H., Paine, M.J.I., 2016. Pyriproxyfen is metabolized by P450s associated with pyrethroid resistance in *An. gambiae*. Insect Biochem. Mol. Biol. 78, 50–57. https://doi.org/10.1016/j.ibmb.2016.09.001.

Yunta, C., Hemmings, K., Stevenson, B., Koekemoer, L.L., Matambo, T., Pignatelli, P., Voice, M., Nász, S., Paine, M.J.I., 2019. Cross-resistance profiles of malaria mosquito P450s associated with pyrethroid resistance against WHO insecticides. Pestic. Biochem. Physiol. 61–67. https://doi.org/10.1016/j.pestbp.2019.06.007. Special issue: 2018 INSTAR Summit 161.

Zhang, M., Scott, J.G., 1994. Cytochrome b5 involvement in cytochrome P450 monooxygenase activities in house fly microsomes. Arch. Insect Biochem. Physiol. 27, 205–216. https://doi.org/10.1002/arch.940270306.

Zhang, M., Scott, J.G., 1996. Cytochrome b5Is essential for cytochrome P450 6D1-mediated cypermethrin resistance in LPR house flies. Pestic. Biochem. Physiol. 55, 150–156. https://doi.org/10.1006/pest.1996.0044.

Zhang, L., Kasai, S., Shono, T., 1998. In vitro metabolism of pyriproxyfen by microsomes from susceptible and resistant housefly larvae. Arch. Insect Biochem. Physiol. 37, 215–224. https://doi.org/10.1002/(SICI)1520-6327(1998)37:3<215::AID-ARCH4>3.0.CO;2-R.

Zhang, H., Hamdane, D., Im, S.-C., Waskell, L., 2008. Cytochrome b5 inhibits electron transfer from NADPH-cytochrome P450 reductase to ferric cytochrome P450 2B4. J. Biol. Chem. 283, 5217–5225. https://doi.org/10.1074/jbc.M709094200.

Zhu, F., Sams, S., Moural, T., Haynes, K.F., Potter, M.F., Palli, S.R., 2012. RNA interference of NADPH-cytochrome P450 Reductase results in reduced insecticide resistance in the bed bug, *Cimex lectularius*. PLoS One 7, e31037. https://doi.org/10.1371/journal.pone.0031037.

Zimmer, C.T., Garrood, W.T., Singh, K.S., Randall, E., Lueke, B., Gutbrod, O., Matthiesen, S., Kohler, M., Nauen, R., Davies, T.G.E., Bass, C., 2018. Neofunctionalization of duplicated P450 genes drives the evolution of insecticide resistance in the Brown Planthopper. Curr. Biol. 28, 268–274.e5. https://doi.org/10.1016/j.cub.2017.11.060.

7.3. Publication chapter 4: Sequential phase I metabolism of pyrethroids by dubliacted CYP6P9 variants results in the loss of the terminal benzene moiety and determines resistance in the malaria mosquito *Anopheles funestus*

Insect Biochemistry and Molecular Biology 148 (2022) 103813

Contents lists available at ScienceDirect

Insect Biochemistry and Molecular Biology

journal homepage: www.elsevier.com/locate/ibmb

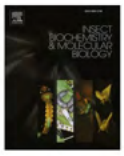

Sequential phase I metabolism of pyrethroids by duplicated CYP6P9 variants results in the loss of the terminal benzene moiety and determines resistance in the malaria mosquito *Anopheles funestus*

Melanie Nolden [a,b], Mark J.I. Paine [b,**], Ralf Nauen [a,*]

[a] Bayer AG, Crop Science Division, Alfred Nobel Str. 50, D-40789, Monheim am Rhein, Germany
[b] Department of Vector Biology, Liverpool School of Tropical Medicine, Pembroke Place, Liverpool, L3 5QA, United Kingdom

ARTICLE INFO

Keywords:
Cytochrome P450
Vector control
Pyrethroid
Insecticide
Resistance
Anopheles

ABSTRACT

Pyrethroid resistance in *Anopheles funestus* is threatening the eradication of malaria. One of the major drivers of pyrethroid resistance in *An. funestus* are cytochrome P450 monooxygenases CYP6P9a and CYP6P9b, which are found upregulated in resistant *An. funestus* populations from Sub-Saharan Africa and are known to metabolise pyrethroids. Here, we have functionally expressed CYP6P9a and CYP6P9b variants and investigated their interactions with azole-fungicides and pyrethroids. Some azole fungicides such as prochloraz inhibited CYP6P9a and CYP6P9b at nanomolar concentrations, whereas pyrethroids were weak inhibitors (>100 μM). Amino acid sequence comparisons suggested that a valine to isoleucine substitution at position 310 in the active site cavity of CYP6P9a and CYP6P9b, respectively, might affect substrate binding and metabolism. We therefore swapped the residues by site directed mutagenesis to produce CYP6P9a^{I310V} and CYP6P9b^{V310I}. CYP6P9b^{V310I} produced stronger metabolic activity towards coumarin substrates and pyrethroids, particularly permethrin. The V310I mutation was previously also detected in a pyrethroid resistant field population of *An. funestus* in Benin. Additionally, we found the first metabolite of permethrin and deltamethrin after hydroxylation, 4′OH permethrin and 4′OH deltamethrin, were also suitable substrates for CYP6P9-variants, and were depleted by both enzymes to a higher extent than as their respective parent compounds (approximately 20% more active). Further, we found that both metabolites were toxic against *An. funestus* FANG (pyrethroid susceptible) but not towards FUMOZ-R (pyrethroid resistant) mosquitoes, the latter suggesting detoxification by overexpressed CYP6P9a and CYP6P9b. We confirmed by mass-spectrometric analysis that CYP6P9a and CYP6P9b are capable of cleaving phenoxybenzyl-ethers in type I pyrethroid permethrin and type II pyrethroid deltamethrin and that both enzymes preferentially metabolise trans-permethrin. This provides new insight into the metabolism of pyrethroids and a greater understanding of the molecular mechanisms of pyrethroid resistance in *An. funestus*.

1. Introduction

In 2020 Malaria caused 627 000 deaths globally, with the large majority (602 000 deaths) occurring in Africa (WHO, 2021). The use of interventions such as insecticide treated bednets (ITN) and indoor residual sprays (IRS) to control indoor biting mosquitoes was estimated to have been responsible for ~80% of the reduction in Malaria cases from 2000 to 2019 (Bhatt et al., 2015; WHO, 2020). Until recently pyrethroids were the only insecticidal class used in ITN thus driving the rapid spread of pyrethroid resistance in *Anopheles* populations across the African continent (WHO, 2018). Pyrethroid resistance is mainly conferred by an altered target, the voltage gated sodium channel (VGSC), and/or upregulated P450 enzymes, which are responsible for phase I xenobiotic metabolism and clearance (David et al., 2013; Martinez-Torres et al., 1998; Nauen et al., 2022; Ranson et al., 2011).

Pyrethroids are synthetic insecticides derived from the natural compound pyrethrin. They are designated as type I and type II pyrethroids based on the respective absence or presence of an *alpha*-cyano group, which enhances the toxicity of the insecticide (Soderlund, 2020). Permethrin and deltamethrin, type I and II pyrethroids respectively, are amongst the most widely used insecticides for vector control applications. Structurally similar, they share a phenoxybenzyl moiety and a

* Corresponding author.
** Corresponding author.
E-mail addresses: Mark.Paine@lstmed.ac.uk (M.J.I. Paine), ralf.nauen@bayer.com (R. Nauen).

https://doi.org/10.1016/j.ibmb.2022.103813
Received 8 June 2022; Received in revised form 17 July 2022; Accepted 17 July 2022
Available online 21 July 2022

cyclopropane ring. It is widely accepted that the 4'para position of the phenoxybenzyl structure is the preferred site of oxidation by insect P450s (Ruzo et al., 1978; Stevenson et al., 2011; Nolden et al., 2022; Zimmer et al., 2014), along with other routes of metabolism including hydroxylation of the gem-dimethyl site or ester-cleavage (Casida et al., 1983; Shono et al., 1979). Furthermore, analysis of deltamethrin metabolism by *Anopheles gambiae* CYP6M2 has revealed that sequential breakdown of the 4′-hydroxy deltamethrin primary metabolite can occur (Stevenson et al., 2011) as well as ether-cleavage of the diphenyl moiety., To date CYP6M2 is the only insect P450 enzyme in which this has been shown (Feyereisen, 2019). Permethrin is composed of four different isomers (R-cis, S-cis, R-trans and S-trans) although their individual interactions with P450 enzymes are not clear. Structurally different pyrethroids, such as etofenprox (non-ester-pyrethroid), bifenthrin or transfluthrin are also used as insecticides, where fluorination of P450 sites of oxidation can limit metabolism and reduce cross-resistance (Moyes et al., 2021; Zimmer and Nauen, 2011).

Anopheles funestus s.s. is a major vector for the transmission of malaria in Africa. Unlike *An. gambiae* and many other Anopheline malaria vectors, knock down resistance (*kdr*) mutations to the voltage gated sodium channel are uncommon (Irving and Wondji, 2017). Instead, pyrethroid resistance is driven primarily by metabolic mechanisms that are predominantly associated with the upregulation of P450 enzymes (Amenya et al., 2008; Ibrahim et al., 2016, 2018; Riveron et al., 2013, 2014). These include CYP6P9a and CYP6P9b, which are the result of a gene duplication event and often highly expressed in pyrethroid resistant field populations of *An. funestus* as well as the laboratory reference strain FUMOZ-R (Nolden et al., 2021; Wondji et al., 2022). Since inhibition of P450 activity can revert metabolic resistant mosquitoes to a susceptible phenotype (Brooke et al., 2001), the inclusion of piperonyl butoxide (PBO), a strong P450 inhibitor, is being used in the latest generation of pyrethroid treated bednets to combat pyrethroid resistance (Gleave et al., 2018; Protopopoff et al., 2018). We have recently shown that BOMFC is a highly active fluorescent probe substrate for recombinant CYP6P9a and CYP6P9b (Nolden et al., 2022), and demonstrated that azole fungicides are also efficient inhibitors of P450 activity in microsomal preparations of *An. funestus*, recommending further characterization of their interactions with individual P450s associated with pyrethroid resistance (Nolden et al., 2021).

CYP6P9a and CYP6P9b can metabolise pyrethroids (Riveron et al., 2013, 2014; Yunta et al., 2019), although detailed biochemical characterisation of their interactions with pyrethroid substrates and products of metabolism are lacking. The two P450s are highly similar sharing 94% amino acid sequence identity (Fig. S1a). While this suggests a similar substrate profile, even single amino acid changes can have a profound effect on substrate binding, altering substrate specificity and metabolism (Paine et al., 2003). We were therefore interested in comparing the interactions of CYP6P9a and CYP6P9b with pyrethroid insecticides and azole inhibitors and to identify amino acid residues in the active sites of the enzymes that might differentiate substrate binding and metabolism. As a starting point we focussed on I-helix amino acid residue 310, which is close (~10 Å) to the reactive heme iron centre and different between CYP6P9a and CYP6P9b. It is present as an isoleucine residue in CYP6P9a and valine in CYP6P9b (Fig. S1b).

In this study, we have compared the enzymatic activity of the recombinantly expressed gene duplicates, *CYP6P9a* and *CYP6P9b* against various substrates. We have also used mass-spectrometry to identify the products of deltamethrin, racemic permethrin (and its *cis*- and *trans*-diastereomers) metabolism by CYP6P9a and CYP6P9b and the mechanism of substrate breakdown. We have carried out site-directed mutagenesis to create two mutants CYP6P9a^{I310V} and CYP6P9b^{V310I} to compare their metabolic activity with CYP6P9a and CYP6P9b towards permethrin, deltamethrin and fluorescent probe substrates to examine the role of amino acid 310 in CYP6P9a/b substrate metabolism. Our results provide a new understanding of the metabolic fate of common type I and type II pyrethroids in the malaria mosquito *An. funestus* that will aid in the development of new resistance-breaking compounds used in vector control applications.

2. Materials and methods

2.1. Mosquitoes

An. funestus FANG and FUMOZ-R mosquitoes were reared as recently described by Nolden et al. (2021). In brief: both strains were kept at 27.5 °C ± 0.5 °C, 65% ± 5% relative humidity and a photoperiod of 12/12 L:D with 1h dusk/dawn. Adults were kept in rearing cages (46 cm × 33 cm x 20 cm) and five days after hatching the first blood meal (bovine blood, obtained from Elocin Laboratory, Oberhausen, Germany) was provided according to standard protocols (Das et al., 2007).

2.2. Chemicals

Deltamethrin (CAS: 52918-63-5), permethrin (CAS: 52645-53-1; 61.3% trans- and 30.5% cis permethrin), β-nicotinamide adenine dinucleotide 2′-phosphate (NADPH) reduced tetrasodium salt hydrate (CAS: 2646-71-1 anhydrous, purity ≥93%), 7-ethoxycoumarin (EC; CAS: 31005-02-4, >99%), 7-methoxy-4-trifluoromethylcoumarin (MFC; CAS: 575-04-2, ≥99%), 7-Ethoxy-4-trifluoromethylcoumarin (EFC; CAS: 115453-82-2, ≥98%) 7-benzyloxy-4-trifluoromethylcoumarin (BFC; CAS: 220001-53-6, ≥99%), 7- hydroxy-coumarin (HC; CAS: 93-35-6, 99%) 7-hydroxy-4-trifluoromethylcoumarin (HFC; CAS: 575-03-1, 98) were purchased from Sigma Aldrich/Merck (Darmstadt, Germany). Cis-permethrin (CAS: 61949-76-6) and trans-permethrin (CAS: 61949-77-7) were purchased from Dr. Ehrenstorfer (LGC group, Teddington, UK). 7-benzyloxymethoxy-4-trifluoromethylcoumarin (BOMFC; CAS: 277309-33-8; purity 95%) was synthesized by Enamine (Riga, Latvia). 4′OH permethrin (CAS: 67328-58-9 ≥ 97%) was synthetized by Aragen (formerly GVK Bio, Hyderabad, India). 7-pentoxycoumarin and 4′OH-deltamethrin (CAS: 66855-89-8) were internally synthetized (Bayer AG, Leverkusen, Germany). All chemicals were of analytical grade unless otherwise stated.

2.3. Glazed tile bioassay

To generate dose-response curves of 4′OH-deltamethrin, 4′OH permethrin and cis- and trans-permethrin, *An. funestus* FANG and FUMOZ-R mosquitoes were exposed to a range of different concentrations in a glazed tile assay as recently described by Nolden et al. (2021). Insecticides were dissolved in acetone with a starting concentration of 100 mg/m^2 and diluted in 1:5 steps to 0.0064 mg/m^2. Using an Eppendorf pipette 1.125 µl of each concentration was applied onto a glazed tile (15 cm × 15 cm, ceramic, Vitra, Germany). After the evaporation of acetone and mosquito recovery from anaesthetation (1 h), female adults were exposed in triplicate (n = 10) for 30 min to each insecticide concentration and afterwards transferred back to an untreated paper card and kept in Petri dishes overnight. A 10% dextrose solution was provided overnight as a food source. Mortality was scored 24 h post-exposure. Acetone alone served as a control. Control mortality between 5 and 20% was corrected using Abbott's formula (Abbott, 1925), and bioassays exceeding 20% control mortality were considered invalid.

2.4. Heterologous expression of CYP6P9a and CYP6P9b

Heterologous baculovirus expression was conducted as previously described by (Nolden et al., 2022). In brief: sequence information of CYP6P9a/b from *An. funestus* and NADPH cytochrome P450 reductase (CPR) from *An. gambiae* (AgCPR) were obtained from GenBank (Table S1) and plasmids were created using GeneArt server (ThermoFisher). As a vector pFastBac1 and as restrictions sites BamHI and HindIII were chosen. Plasmids were transformed into MaxEfficiancyDH10

(Invitrogen, 10361012) competent cells according to manufacturer's instructions. The virus was transfected into Sf9 cells (Gibco, kept in Sf-900-SFM (1X) cell culture medium, containing 25 μg/mL gentamycin) and titre was determined employing Rapid Titer Kit (Clontech, 631406).

High five cells were kept in Express five medium (SFM (1X), Gibco, 10486–025) containing 18 mM Glutamax (100X, Gibco, 35050–061) and 10 μg/mL gentamycin (Gibco, 1670–037). Cells were incubated with 0.5% fetal bovine serum (FBS; Sigma Aldrich, F2442), 0.2 mM delta-aminolevulinic acid (d-ALA; CAS: 5451-09-2, Sigma Aldrich), 0.2 mM Fe III citrate (CAS: 2338-05-8, Sigma Aldrich) and the respective amount of virus. After harvesting, cells were resuspended in buffer (0.1 M K_2HPO4, 1 mM DTT, 1 mM EDTA, 200 mM saccharose, pH 7.6). FastPrep device (MP Biomedicals, Irvine, CA, USA) was used for shredding the cells followed by a 10-min centrifugation step at 4 °C and 700×*g* (Eppendorf). The supernatant was centrifuged for 1 h at 100 000×*g* and 4 °C (Beckman, rotor: 45TI). The resulting microsomal pellet was resuspended in buffer (0.1 M K_2HPO4, 0.1 mM EDTA, 1 mM DTT, 5% Glycerol, pH 7.6) and protein amount was determined.

Carbon monoxide (CO)-difference spectra were generated according to (Omura and Sato, 1964) in order to calculate K_{cat} values. Mock cells served as controls throughout the study as well as microsomal fractions without NADPH regeneration system.

2.5. Computational analysis, modelling and docking experiments

CYP6P9a (AFUN015792-RA) and CYP6P9b (AFUN015889-RA) transcripts show 92.7% nucleotide identity and translated protein sequences are 94.3% identical (Geneious alignment, Geneious 10.2.6; Fig. S1a). Substrate recognition sites (SRS) were assigned to CYP6P9a and CYP6P9b based on CYP2A1 (*Rattus norvegicus*, GenBank NP_036824.1) according to Gotoh (1992). To predict and analyse the potential metabolism of probe substrates and pyrethroids, 3D-homology models of CYP6P9a and CYP6P9b based on the crystal structure of human CYP3A4 (PDB: 1TQN) were created. 3D-structures of BOMFC, deltamethrin and permethrin were received from PubChem (https://pubchem.ncbi.nlm.nih.gov/) and transformed into PDB files using Chimera (USCF Chimera, Version 1.15). After performing dock-prep in Chimera, AutoDock Vina (Version 1.1.2) using Chimera software was performed, with a 20 $Å^3$ squared volume around the heme (Oleg and Olson, 2010). Five docking scenarios for each substrate were generated and analysed based on score (binding affinity kcal/mol) and putative sites of metabolic attack.

2.6. Site-directed mutagenesis of amino acid residue 310

In CYP6P9a isoleucine 310 is translated by the codon ATC at position 927–929 (transcript), in CYP6P9b valine is translated by GTG at position 927–929. We created two mutants: CYP6P9a I310V ($CYP6P9a^{I310V}$) and CYP6P9b V310I ($CYP6P9b^{V310I}$). Generated pFastBac vectors (as described above) containing either CYP6P9a or CYP6P9b were used for site-directed mutagenesis using a Q5-site-directed mutagenesis Kit following manufacturer's instructions (New England Biolabs, E0554). Specific primers were generated using NEBaseChanger (https://nebasechanger.neb.com/) (Table S1). Twenty-five ng of total plasmid DNA and each primer with a final concentration of 0.5 μM in 25 μl reactions were used. PCR conditions were as follows: 98 °C for 30 s, followed by 25 cycles of 98 °C for 10 s, 66 °C for 30 s and 72 °C for 3 min and 10 s. Final extension step was at 72 °C for 2 min. A kinase, ligase and DpnI (KLD) treatment containing 1 μl PCR Product, 5 μl KLD Reaction buffer, 10X KLD Enzyme Mix and 3 μl Nuclease-free water was added and incubated at room temperature for 5 min. Afterwards 5 μl of KLD mix was added to 5-alpha-competent *E. coli* cells for transformation (New England Biolabs, C2987H) following manufacturer's instructions. Cells were diluted 10- and 40-times and incubated overnight on LB-Agar plates (MP biomedicals, 113002201-CF, capsules, concentration: 40 g/L) containing carbenicillin (100 μg/ml, CAS: 4800-94-6). Mini- (3 ml) and Midi (25 ml) preps in LB medium (MP biomedicals, 113002011-CF, capsules, concentration: 25 g/L) containing 100 μg/ml carbenicillin were generated and plasmids were isolated using Qiafilter Plasmid Midi Kit following manufacturer's instructions (Qiagen, 12243, Hilden, Germany). DNA concentrations were photometrically determined using 260/280 ratio (NanoQuant Infinite 200, Tecan, Switzerland) and normalized to 100 ng/μl. To confirm successful mutagenesis, samples were sent for sequencing (TubeSeq Service, Eurofins). Sequencing primers can be found in Table S1. Plasmids containing substituted nucleotides were further processed as described above.

2.7. P450 activity assays with fluorinated coumarin probe substrates

P450 enzyme assays were conducted as previously described by Haas and Nauen (2021) with minor changes. Substrate competition kinetics were evaluated using eleven different BOMFC, BFC and EFC concentrations (stock 50 mM in DMSO) between 200 μM and 0.195 μM, diluted in 0.1 M potassium-phosphate buffer (pH 7.6) containing 0.01% zwittergent 3–10 (CAS 15163-36-7, Sigma-Aldrich), a range of pyrethroid concentrations (100, 10, 1 μM final concentration (fc)) and 1 mM NADPH at 20 °C ± 1 °C. Enzymes were diluted to 0.16 mg/ml in buffer (0.1 M K_2HPO4, 0.1 mM EDTA, 1 mM DTT, 5% glycerol pH 7.6), 0.05% bovine serum albumin (BSA), 0.01% zwittergent 3–10 – finally corresponding to 4 μg protein per 25 μl enzyme solution. Twenty-five μl enzyme solution and 25 μl substrate solution were incubated for 1 h in a black 384-well plate and the reaction stopped by adding 50 μl of red-ox mix (25% DMSO, 50 mM Tris–HCl buffer (pH 10), 5 mM glutathione oxidized, and 0.2 U glutathione reductase). Each reaction was replicated four times and the fluorescent product HFC was measured at 405 nm while excited at 510 nm. Substrate saturation kinetics were analysed using GraphPad Prism 9.0 and were analysed for competitive, non-competitive, and mixed-type inhibition (assuming Michaelis-Menten kinetics).

2.8. Inhibition assays with CYP6P9 variants

IC_{50} analysis was performed as previously described in Nolden et al. (2021) with minor modifications. Assay conditions were optimized for linearity in time and protein amount. Eleven concentrations of inhibitors and pyrethroids (pre-diluted in DMSO in 1:3.3 steps, final DMSO concentration (1%), except for epoxiconazole (2%)) to a final assay concentration ranging from 100 μM to 0.000596 μM in 0.1 M potassium-phosphate-buffer (pH 7.6). Microsomal fractions were diluted to a final amount of 4 μg of protein per 100 μl in buffer (0.1 M K_2HPO4, 0.1 mM EDTA, 1 mM DTT, 5% glycerol pH 7.6) containing 0.01% zwittergent and 0.05% BSA. Enzymes were incubated with inhibitors and pyrethroids for 10 min at 20 °C ± 1 °C. Afterwards 25 μl 20 μM BOMFC solution (10 μM final concentration, the approximate K_m for all variants) containing 0.125 mM (fc) NADPH was added. Each reaction was replicated four times, stopped after 30 min by adding stopping solution and evaluated as described above. Inhibition was analysed using GraphPad Prism 9.0 four-parameter, non-linear regression model. Reactions containing no inhibitor served as controls.

2.9. UPLC-MS/MS analysis and pyrethroid metabolite quantification

Metabolism assays were conducted as previously described by Nolden et al. (2022) with minor changes. Deltamethrin and permethrin metabolism and quantification of the respective 4′OH-deltamethrin and 4′OH permethrin were assessed using UPLC-MS/MS analysis. Recombinantly expressed CYP6P9 variants and mutants were co-expressed with *An. gambiae* CPR (P450:CPR at MOI 1:0.5) and diluted to 0.8 mg protein ml^{-1} in buffer (0.1 M K2HPO4, 1 mM DTT, 0.1 mM EDTA, 5% Glycerol, pH 7.6). Forty μl of recombinant proteins were incubated in 96-deepwell plates (Protein lobind, Eppendorf) in 100 μl reactions with

10 μM deltamethrin, permethrin or the respective 4′OH metabolite (solved in DMSO and further diluted to 100 μM in 0.1 M K_2HPO_4, 0.05% bovine serum albumin (BSA), pH 7.6) and 50 μl of assay buffer containing NADPH-regeneration system (Promega, V9510). As control, wells without regeneration system and microsomal fractions from a control (mock) virus were included. The reactions were incubated at 450 rpm and 30 °C (Thermomixer, Eppendorf) and stopped with 400 μl ice-cold acetonitrile (100%) after 90 min. Plates were stored at 4 °C overnight, centrifuged (3220×*g*, 4 °C, 30 min, Eppendorf 5810 R) and the resulting supernatant was transferred into a 1000 ml collection plate (186002481, Waters, Eschborn, Germany).

UPLC-MS/MS chromatography was carried out using an Agilent 1290 Infinity II system with a Waters Acquity BEH C18 (50 × 2.1 mm, 1.7 μm) column and eluted with methanol, 2 mM ammonium acetate, and water, 2 mM ammonium acetate with 1% acetic acid in gradient mode. After positive electrospray ionization, ion transitions were recorded on a Sciex API6500 Qtrap. Ion transition was as followed: for deltamethrin 523 > 281, for 4′OH-deltamethrin 539 > 281, for permethrin 183.051 > 152.200 and for 4′OH-permethrin 424.079 > 199.200. In positive ion mode the peak integrals were calibrated externally against a standard calibration curve. Samples were diluted prior to measurement if needed. Linear ranges were as followed: For deltamethrin: 0.5–500 ng/ml, for 4′OH deltamethrin: 0.3–100 ng/ml, for permethrin: 0.1–120 ng/ml (cis) and 0.05–26 ng/ml (trans) and for 4′OH-permethrin: 0.05–23 ng/ml (cis) and 0.1–27 ng/ml (trans). UPLC-TOF-MS was employed using an Acquity UPLC I-Class system coupled to a cyclic iMS mass spectrophotometer (Waters Corporation, MA, USA) as recently described (Haas et al., 2021). The mass spectrometer operated in positive ion mode for deltamethrin and permethrin and in negative ion mode for the respective 4′OH metabolites with a full scan resolution at 60 000 fwhm (full width at half maximum). Measurements and metabolite searches were conducted with MassLynx and MetaboLynx software (Waters Corporation, MA, USA).

3. Results

3.1. Inhibition potential of azole fungicides, pyrethroids and PBO towards CYP6P9a and CYP6P9b

The interactions of CYP6P9a and CYP6P9b with deltamethrin and permethrin and their primary metabolites 4′OH deltamethrin and 4′OH permethrin were compared by measuring their kinetic effects on the inhibition of the *O*-debenzylation of the fluorescent probe substrate BOMFC at three concentrations (100 μM, 10 μM and 1 μM) (Fig. 1 and Table S2). The P450s showed a similar pattern of inhibition producing much weaker inhibition of BOMFC *O*-debenzylation with the parent deltamethrin and permethrin compounds compared with strong inhibition by 4′OH permethrin and 4′OH deltamethrin (Table 1). Inhibition by the 4′OH metabolites also produced an increase in K_m alongside significant decreases in reaction rate (V_{max}), indicating a mixed-type inhibition and no clear competitive inhibition (Table S2). For example, the V_{max} of CYP6P9a BOMFC *O*-debenzylation decreased from 191 pmol product/min x mg protein^{-1} to 104 pmol product/min x mg protein^{-1} in the presence of 100 μM 4′OH deltamethrin, with a concomitant K_m increase from 8.64 μM to 74.8 μM suggesting BOMFC displacement (Table S2).

Several pyrethroids, azole fungicides, and PBO were tested against CYP6P9a and CYP6P9b to evaluate their potential to inhibit *O*-debenzylation of BOMFC (Table 1). Overall, similar patterns of inhibition were observed, with the strongest inhibitor being prochloraz with IC_{50} values

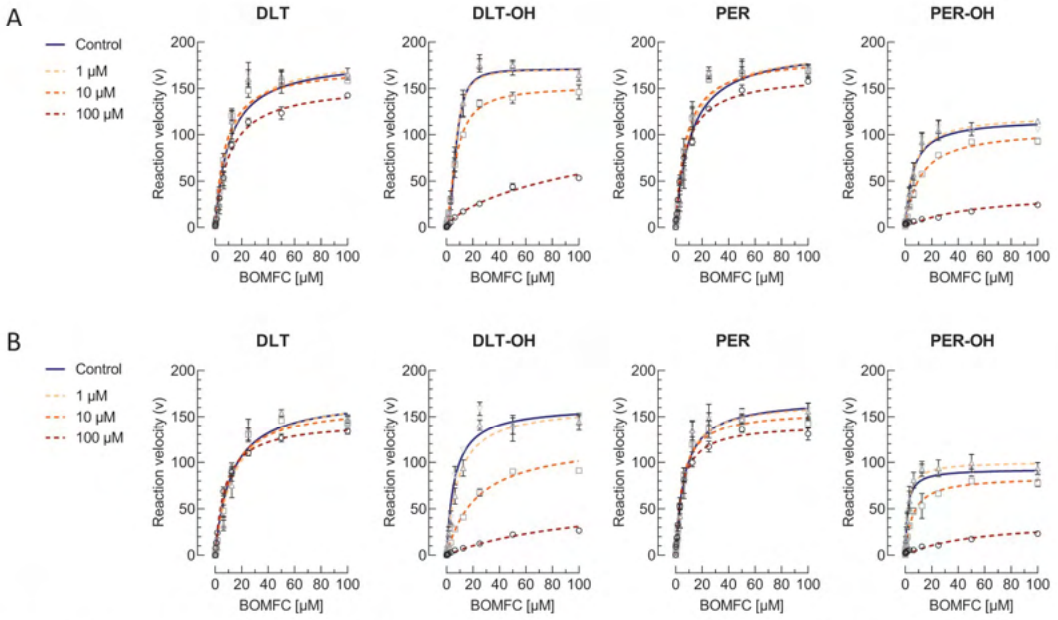

Fig. 1. Effect of different pyrethroid substrates on the O-debenzylation of 7-benzyloxymethoxy-4-(trifluoromethyl)-coumarin (BOMFC) by recombinantly expressed *An. funestus* CYP6P9 variants. Michaelis–Menten kinetics of (A) CYP96P9a- and (B) CYP6P9b-mediated BOMFC metabolism using increasing concentrations of deltamethrin (DLT), 4′OH deltamethrin (DLT-OH), permethrin (PER) and 4′OH permethrin (PER-OH). Data are mean values ± SD (n = 4). Reaction velocity is defined as pmol 7-hydroxy-4-trifluoromethylcoumarin (HFC)/min x mg protein. Details on Michaelis-Menten kinetic data analysis are given in the supporting information (Table S2).

Table 1
Biochemical analysis of CYP6P9 variant interaction with different compounds in fluorescence assays. Inhibition of O-debenzylation of 7-benzyloxymethoxy-4-(trifluoromethyl)-coumarin (BOMFC) by recombinantly expressed *An. funestus* CYP6P9a and CYP6P9b by pyrethroid insecticides, their metabolites and common P450 inhibitors. Date are mean values ± 95% CI (n = 4).

Compound	CYP6P9a		CYP6P9b	
	IC_{50} [μM]	95% CI	IC_{50} [μM]	95% CI
Deltamethrin	>100		>100	
4′OH Deltamethrin	6.28	4.83–8.06	1.75	1.53–1.99
Permethrin	>100		>100	
4′OH Permethrin	13.2	9.67–18.4	13.3	10.6–16.8
Cypermethrin	>100		>100	
Bifenthrin	>100		>100	
PBO	1.03	0.751–1.39	1.09	0.751–1.53
1-ABT	176	123–254	215	118–491
Triflumizole	1.29	1.03–1.63	0.723	0.444–1.16
Prochloraz	0.235	0.182–0.302	0.059	0.0396–0.0861
Uniconazole	0.365	0.267–0.497	7.97	4.86–13.9
Propiconazole	6.95	4.27–11.3	2.38	1.72–3.28
Ketoconazole	3.71	2.74–5.06	0.518	0.396–0.675
Triadimefon	18	11.8–28.4	19.2	10.5–40.6
Triadimenol	>100		>100	
Tebuconazole	9.09	8.17–10.1	2.11	1.86–2.4
Epoxiconazole	21.4	15.3–36	44.7	20.1–159

of 235 nM and 59 nM for CYP6P9a and CYP6P9b, respectively (Table 1). The major differences were observed for ketoconazole, which showed ~7-fold stronger inhibition of CYP6P9b (IC_{50} 0.518 μM vs 3.71 μM), while uniconazole showed ~20-fold stronger inhibition of CYP6P9a (IC_{50} 0.365 μM vs 7.97 μM). All tested pyrethroids were weak inhibitors with IC_{50} values > 100 μM. In contrast, the pyrethroid metabolites 4′OH deltamethrin and 4′OH permethrin were relatively strong inhibitors with respective IC_{50} values of 6.28 μM and 13.2 μM for CYP6P9a and 1.75 μM and 13.4 μM for CYP6P9b. PBO also exhibited rather low IC_{50} values of approx. 1 μM against both CYP6P9a and CYP6P9b, whereas 1-ABT was ineffective at 100 μM (Table 1).

3.2. Metabolism of permethrin and deltamethrin by CYP6P9a and CYP6P9b

To investigate pyrethroid metabolism by CYP6P9a and CYP6P9b substrate turnover was measured following incubation with recombinantly expressed P450s (Figs. 2 and 3, Table S3). CYP6P9a produced similar levels of deltamethrin and permethrin depletion (~40%), whereas CYP6P9b produced slightly higher permethrin turnover (61.5%) compared with deltamethrin (40.4%) (Table S3). Compared with their respective parent compounds, both P450s produced significantly higher activity towards the 4′OH metabolites, with 65.3% and 67.3% depletion of 4′OH deltamethrin and 4′OH permethrin respectively for CYP6P9a and 68.9% and 74.3% depletion with CYP6P9b (Table S3).

Additional investigation of deltamethrin and permethrin metabolism by CYP6P9a and CYP6P9b by MS/MS revealed further metabolism of 4′OH deltamethrin and 4′OH permethrin to cyano-(3-hydroxyphenyl) methyl deltamethrate and 3-hydroxyphenyl-methyl-permethrate respectively via ether cleavage of the phenoxybenzyl moiety, which was confirmed by MS fragment spectra showing the respective M-76 metabolites and supported by molecular docking studies exemplified by CYP6P9b homology models (Fig. 4). Molecular docking of 4′OH metabolites into the active site of CYP6P9b revealed the aryl-ether of 4′OH permethrin coordinates closer to the heme iron centre than 4′OH deltamethrin with measured distances of 4.28 Å and 6.99 Å, respectively (Fig. 4A and B). Compared with deltamethrin, permethrin metabolism produced double the number of peaks in ESI-TOF UPLC-MS spectra (Fig. 4, Fig. S2). These are indicative of *cis*- and *trans*-permethrin isomers with different retention times, which was confirmed when matched against diastereomerically pure *cis*- and *trans*-permethrin with the same retention times.

Based on the analytical results there were no obvious differences in metabolism between deltamethrin and permethrin, except for an additional M+32 metabolite of permethrin produced by both P450s, suggesting a second hydroxylation site. Overall, the MS analysis supports the kinetics, which indicates very similar sequential oxidative substrate metabolism as outlined in Fig. 5. Interestingly, the ether bond cleavage in permethrin/4′OH permethrin was only detected for CYP6P9b, whereas the deltamethrin ether bond was cleaved by both enzymes (Fig. 5).

3.3. Acute toxicity of 4′OH pyrethroid metabolites against An. funestus

The acute contact efficacy of the metabolites 4′OH deltamethrin and 4′OH permethrin was tested against *An. funestus* strains FANG and FUMOZ-R to assess their intrinsic toxicity (Table 2). None of the metabolites was active against female adults of FUMOZ-R at the highest concentration, 100 mg/m^2, tested (Fig. S3). Interestingly, female adults of strain FANG showed an almost identical susceptibility to 4′OH deltamethrin (LC_{50}, 1.88 mg/m^2, CI95%: 0.72–3.89) and permethrin (LC_{50}, 0.543 mg/m^2, CI95%: 0.409–0.702 (Nolden et al., 2021)). Thus, suggesting that the detoxification of deltamethrin by hydroxylation only is not sufficient to render it ineffective in susceptible *An. funestus*, because intrinsically it remains almost as toxic as permethrin. Hydroxylated

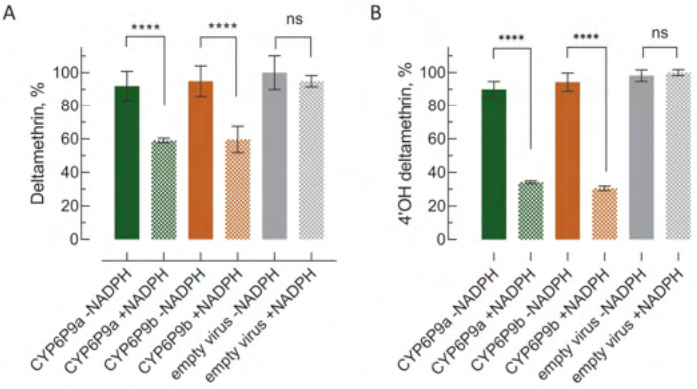

Fig. 2. Pyrethroid substrate metabolism by *An. funestus CYP6P9a and CYP6P9b.* Depletion of (A) deltamethrin and (B) 4′OH deltamethrin by recombinantly expressed CYP6P9a and CYP6P9b ± NADPH measured by quantitative UPLC-MS/MS. Remaining parent compound was determined after 90min incubation at 30 °C (starting concentration was 2 μM). Data were normalized to % parent compound and are mean values ± 95% CI (n = 3). Mock cells (empty virus) ± NADPH served as control. Original values are provided in Table S3.

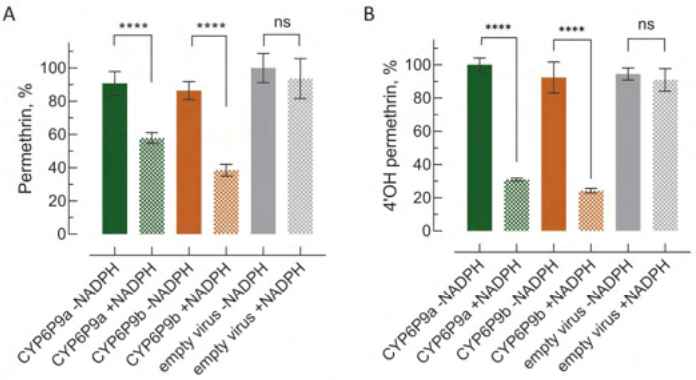

Fig. 3. Pyrethroid substrate metabolism by *An. funestus CYP6P9a and CYP6P9b.* Depletion of (A) permethrin and (B) 4′OH permethrin by recombinantly expressed CYP6P9a and CYP6P9b ± NADPH measured by quantitative UPLC-MS/MS. Remaining parent compound was determined after 90min incubation at 30 °C (starting concentration was 2.5 μM). Data were normalized to % parent compound and are mean values ± 95% CI (n = 3). Mock cells (empty virus) ± NADPH served as control. Original values are provided in Table S3.

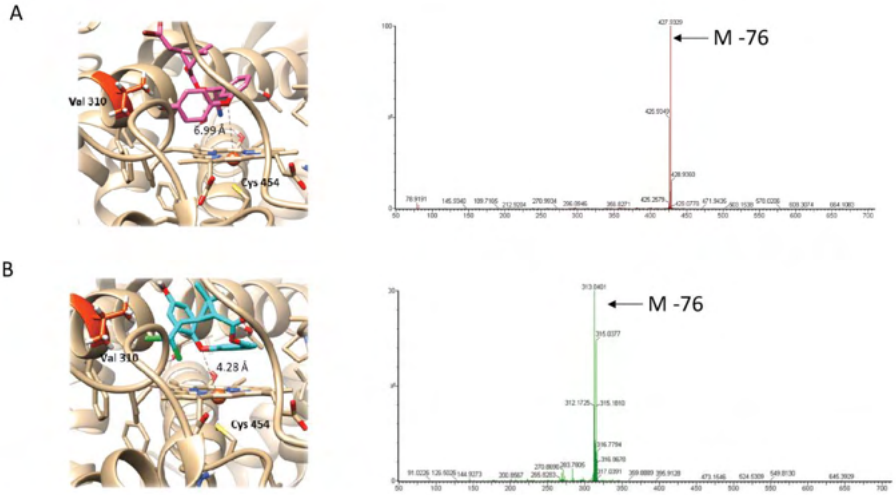

Fig. 4. Molecular docking and analytical validation. Binding site model showing the predicted substrate-binding mode of (A) 4′OH deltamethrin and (B) 4′OH permethrin in *An. funestus* CYP6P9b and the respective MS fragment spectra of the corresponding metabolites cyano-(3-hydroxyphenyl) methyl deltamethrate and 3-hydroxyphenyl-methyl-permethrate, respectively, as determined by ESI-TOF UPLC-MS.

permethrin showed an LC_{50} of 34.7 mg/m^2 and is approx. 20-fold less active than 4′OH deltamethrin (Table 2). In a previous study deltamethrin showed an LC_{50} of 4.61 mg/m^2 and 0.0206 mg/m^2 towards FUMOZ-R and FANG mosquitoes, respectively (Nolden et al., 2021).

3.4. Degradation and biological efficacy of permethrin diastereomers

Significantly different rates of hydroxylation of *cis*- and *trans*-permethrin diastereomers by CYP6P9a and CYP6P9b were observed by MS/MS analysis (Fig. 6A). Both enzymes preferentially depleted *trans*-permethrin over *cis*-permethrin, but CYP6P9b degraded *trans*-permethrin almost five-fold faster than CYP6P9a. To investigate toxicity differences towards susceptible FANG and pyrethroid resistant FUMOZ-R mosquitoes in relation to the low resistance ratio of permethrin (racemate) (RR 7.76; Nolden et al., 2021), diastereomerically pure *cis*- and *trans*-permethrin were evaluated in contact bioassays (Fig. 6B). The resistance ratios of *cis*- and *trans*-permethrin were 10.4 and 6.55, respectively (Table S4). However, *cis*-permethrin (LC_{50} 0.154 mg/m^2), had 9-times higher toxicity than *trans*-permethrin (LC_{50} 1.41 mg/m^2) towards FANG mosquitoes and 6 times higher toxicity to FUMOZ-R, LC_{50} 1.6 and 9.24 mg/m^2, respectively (Table S4).

3.5. Kinetics of CYP6P9 variants towards coumarin model substrates, type I and type II pyrethroids

The comparative metabolism of coumarin model substrates by CYP6P9a, CYP6P9b and their respective mutants CYP6P9a^{I310V} and CYP6P9b^{V310I} was investigated and generally followed Michaelis-Menten kinetics. Highest activity was measured with the benzylated coumarin BOMFC, with the four P450s producing similar rates of metabolism with V_{max} values in the range 167–196 pmol product/min x mg protein^{-1} (Fig. 7, Table S5). The K_m values for CYP6P9b and CYP6P9b^{V310I} were similar (6.82 and 7.16 μM, respectively) whereas the K_m value for CYP6P9a^{I310V} (3.21 μM) was 4-fold lower than CYP6P9a

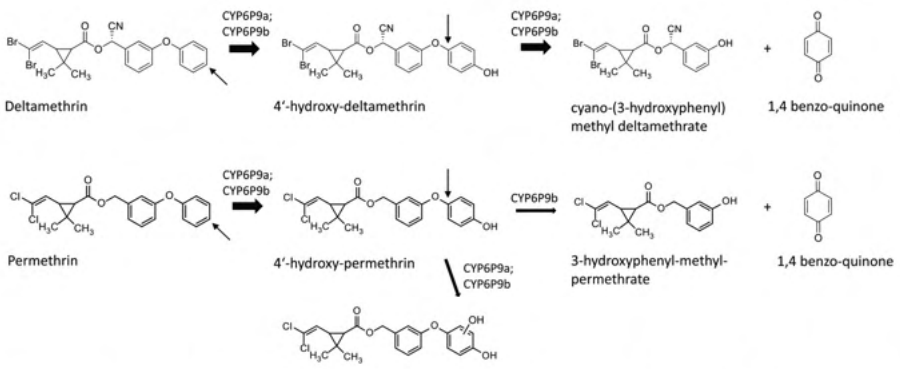

Fig. 5. Oxidative metabolic fate of pyrethroids. Proposed scheme for the sequential metabolism of deltamethrin and permethrin, respectively, mediated by recombinantly expressed *An. funestus* CYP6P9a and CYP6P9b supported by UPLC-MS analysis. Arrows indicate potential sites of oxidative attack.

Table 2
Efficacy of hydroxylated pyrethroids against *An. funestus*. Log-dose mortality data of 4'OH-deltamethrin and 4'OH permethrin against female adults of *An. funestus* FANG in glazed-tile contact bioassays. Both metabolites were inactive against female adults of strain FUMOZ-R at the highest concentration tested (100 mg/m^2). Respective graphs are given in the supporting information (Fig. S3).

	An. funestus FANG				
	LC_{50}	95% CI	Slope ± SE		n
4'OH deltamethrin	1.88	0.72–3.89	0.927	0.195	210
4'OH permethrin	34.7	15.8–91.7	0.953	0.242	210

(11.2 μM). The same trend was observed with BFC and EFC where CYP6P9a^{I310V} produced lower K_m values than the wildtype CYP6P9a with minimal change in V_{max} (Table S5). CYP6P9b and CYP6P9b^{V310I} produced similar V_{max} values with BFC (33.8 and 40.8 μM) and higher than CYP6P9a and CYP6P9a^{I310V} (11.0 and 8.78 μM). Most notably, CYP6P9b^{V310I} with a V_{max} of 55.3 pmol product/min x mg protein^{-1} was 4-5-fold more active against EFC than CYP6P9b and CYP6P9a and CYP6P9a^{I310V} (Fig. 7, Table S5).

Pyrethroid metabolism of the CYP6P9 variants was investigated by comparing the rates of production of the major 4'OH metabolites of deltamethrin and permethrin (Fig. 8). The highest reaction rate for deltamethrin was observed by CYP6P9b^{V310I} with a V_{max} of 13.7 pmol product/min x mg protein^{-1}, which was slightly higher than wildtype CYP6P9b (10.6 pmol product/min x mg protein^{-1}) but the same as CYP6P9a (Table S6). CYP6P9a^{I310V} produced the lowest deltamethrin activity of 6.65 pmol product/min x mg protein^{-1}. The amino acid substitution at position 310 produces a small reduction (~2-fold) in K_m values for CYP6P9a^{I310V} (7.6 μM) and CYP6P9b^{V310I} (14.7 μM) relative to CYP6P9a (19.2 μM) and CYP6P9b (27 μM) respectively (Table S6), indicating slightly higher affinity towards deltamethrin.

Compared with CYP6P9b (7.89 pmol product/min x mg protein^{-1}), CYP6P9a and CYP6P9a^{I310V} revealed relatively low activity towards permethrin with 1.97 and 3.07 pmol product/min x mg protein^{-1}, respectively (Table S6). Strikingly, the highest permethrin reaction rate was seen for CYP6P9b^{V310I} with 58 pmol product/min x mg protein^{-1}, a 7-fold increase compared with wildtype CYP6P9b (Fig. 8, Table S6). Metabolism of permethrin by CYP6P9^{V310I} also produced a sigmoidal curve and a linear Hanes-Woolf fit suggests an allosteric interaction and positive cooperativity, contrasting with the hyperbolic behaviour of the other P450s towards deltamethrin and permethrin (Fig. S4). Overall, the valine 310 to isoleucine substitution in CYP6P9b^{V310I} tended to enhance metabolic efficacy and produced higher affinity for all the inhibitors tested, whereas the reverse isoleucine to valine substitution at position 310 in CYP6P9a^{I310V} led to a weaker inhibition of all tested inhibitors (Table S7).

4. Discussion

Pyrethroid resistance in *An. funestus* is largely driven by the overexpression of duplicated P450s CYP6P9a and CYP6P9b, which have been shown to rapidly metabolise pyrethroids in functional assays employing prokaryotic and eukaryotic protein expression systems (Ibrahim et al., 2015; Nolden et al., 2022; Riveron et al., 2013; Yunta

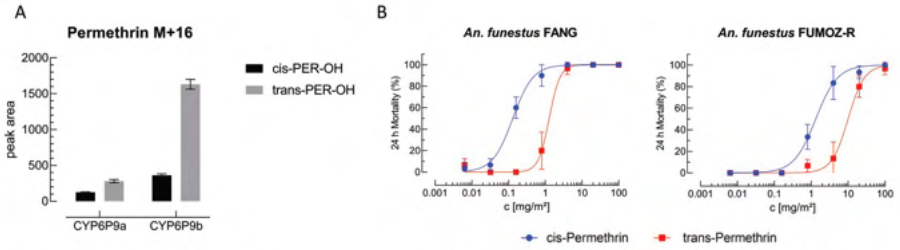

Fig. 6. Degradation and biological efficacy of permethrin enantiomers. (A) Resolution of enantioselective metabolism of permethrin to *cis/trans* 4'hydroxy permethrin by recombinantly expressed CYP6P9a and CYP6P9b in the presence of NADPH (90min). (B) Efficacy of *cis*- and *trans*-permethrin towards female adults of *An. funestus strains* FANG and FUMOZ-R in glazed tile contact assays. Data are mean values ± 95% CI (n = 3) and given in the supporting information (table S4).

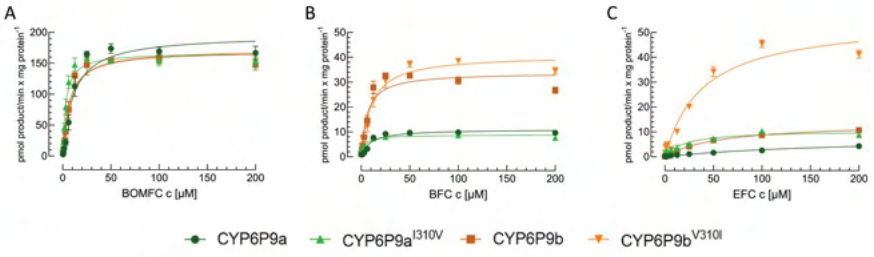

Fig. 7. Saturation kinetics of selected coumarin substrates with different *An. funestus* CYP6P9 variants. O-debenzylation of (A) 7-benzyloxymethoxy-4-trifluoromethylcoumarin (BOMFC) and (B) 7-benzyloxy-4-trifluoromethylcoumarin (BFC), as well as (C) the O-dealkylation of 7-ethoxy-4-trifluoromethylcoumarin (EFC) by recombinantly expressed CYP6P9a, CYP6P9b, CYP6P9aI310V and CYP6P9bV310I. Details on Michaelis-Menten kinetic data analysis are given in the supporting information (Table S5). Data are mean values ± SD (n = 4).

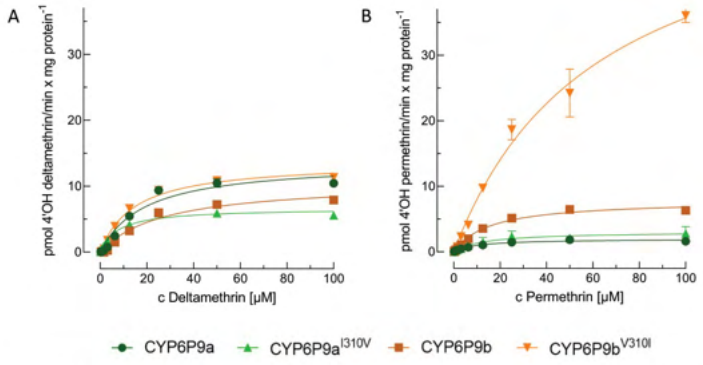

Fig. 8. Saturation kinetics of pyrethroid substrates with different *An. funestus* CYP6P9 variants. Hydroxylation of (A) deltamethrin and (B) permethrin by CYP6P9a, CYP6P9b, CYP6P9aI310V and CYP6P9bV310I. Details on Michaelis-Menten kinetic data analysis are given in the supporting information (Table S6). Data are mean values ± SD (n = 3).

et al., 2019). Previous studies mostly utilized parent depletion approaches (+NADPH vs -NADPH) to quantify the extent of pyrethroid metabolism by CYP6P9a and CYP6P9b (Ibrahim et al., 2016; Riveron et al., 2013, 2014), similar to P450 assays employed to predict pesticide clearance in mammalian toxicology (Scollon et al., 2009). We recently noticed a stochiometric inconsistency between deltamethrin depletion and 4′OH deltamethrin formation by functionally expressed CYP6P9 variants, and suggested the formation of additional, undetected metabolites (Nolden et al., 2022). Indeed, the present study revealed that the depletion of deltamethrin by recombinantly expressed CYP6P9a and CYP6P9b is principally based on sequential oxidative metabolism by, 1) hydroxylation of the 4′para position of the phenoxybenzyl ring, and 2) the formation of cyano-(3-hydroxyphenyl)-methyl-deltamethrate via ether cleavage of the phenoxybenzyl moiety. In addition, we confirmed sequential metabolism of the type I pyrethroid permethrin via the same route, but only for CYP6P9b. We failed to detect 3-hydroxyphenyl-methyl-permethrate in analytical assays with CYP6P9a, suggesting its lower catalytic capacity to oxidise 4′OH permethrin compared to CYP6P9b. This is supported by an overall higher permethrin depletion capacity of CYP6P9b compared to CYP6P9a, whereas no significant difference between both enzymes was detected for deltamethrin metabolism. Sequential P450-mediated metabolism of deltamethrin resulting in the formation of cyano-(3-hydroxyphenyl)-methyl-deltamethrate has so far only been described for *An. gambiae* CYP6M2 (Stevenson et al., 2011). Whereas CYP6P9b mediated ether cleavage of the phenoxybenzyl moiety of permethrin has been demonstrated for the first time in insects. A similar metabolic fate has so far only been observed in mammalian studies, e.g. with rat liver microsomes (Shono et al., 1979).

Interestingly, neither deltamethrin nor permethrin inhibited the *O*-debenzylation of BOMFC in a fluorescent probe assay we conducted with recombinantly expressed CYP6P9a and CYP6P9b, though we have detected low, but significant decrease of V_{max} values when both pyrethroids were tested at 100 µM. Indeed, the inhibitory efficacy of other pyrethroids such as bifenthrin and cypermethrin was also too low to calculate IC_{50}-values. Such fluorescence (and luminescence) probe assays have been successfully used to predict interaction and/or P450-mediated metabolism of insecticides, e.g., for *Bemisia tabaci* CYP6CM1 and imidacloprid (Hamada et al., 2019), *Apis mellifera* CYP9Q2/3 and various insecticides (Haas et al., 2021; Haas and Nauen, 2021), several mosquito P450s including *An. gambiae* CYP6P3 (Yunta et al., 2019), and *An. funestus* CYP6P9a/b for various insecticides including pyrethroids (Ibrahim et al., 2015, 2016; Yunta et al., 2019). Our results with BOMFC and pyrethroids are in contrast to diethoxyfluorescein probe assays with CYP6P9a/b where various insecticides have been shown to inhibit its *O*-dealkylation in the lower micromolar range, including deltamethrin and permethrin (Ibrahim et al., 2016; Yunta et al., 2019). However, a few insecticides tested by Yunta et al. (2019) such as DDT turned out to be micromolar inhibitors of CYP6P9a and other mosquito P450s but were not metabolised by recombinantly expressed enzymes. Our fluorescent probe assays with deltamethrin, and permethrin revealed the opposite, i.e., no significant inhibition of CYP6P9a/b, but substantial depletion in analytical assays. The azole compounds and PBO used to

validate the fluorescence probe assay have been described as strong *An. funestus* P450 inhibitors (Nolden et al., 2021), and showed strong inhibition of both CYP6P9a and CYP6P9b, not unexpected considering their *in vivo* potential as synergists in combination with pyrethroids (Horstmann and Sonneck, 2016; Williams et al., 2019). Further work is warranted to investigate the reasons for the discrepancy in pyrethroid inhibitory potential in fluorescent probe assays and metabolism.

Intriguingly, we observed a much stronger interaction in BOMFC fluorescent probe assays between CYP6P9a/b and the pyrethroid metabolites 4′OH-permethrin and 4′OH deltamethrin. The observed inhibition of the *O*-debenzylation of BOMFC by both hydroxy metabolites in fluorescent probe assays is linked to significantly higher CYP6P9a/b driven depletion rates in analytical assays when compared to the respective parent compound. To the best of our knowledge this is the first study investigating the oxidative metabolic fate of 4′para-hydroxylated pyrethroids by recombinantly expressed insect P450s. The MS fragment spectra of the resulting metabolites confirmed the formation of cyano-(3-hydroxyphenyl)-methyl deltamethrate and 3-hydroxyphenyl-methyl-permethrate and the sequential two-step reaction catalysed by either CYP6P9 variant. 4′OH-Deltamethrin is 100-fold less toxic than deltamethrin, but its intrinsic toxicity against *An. funestus* FANG remains high and is comparable to permethrin - thus clearly supporting the advantage of a two-step deltamethrin metabolisation mediated by upregulated CYP6P9 variants. Hydroxylated permethrin is much less toxic in bioassays and unlikely to confer phenotypic consequences by the lack of sequential metabolism mediated by CYP6P9a. A previous study suggested that high levels of pyrethroid-metabolising P450s in resistant *Brassicogethes aeneus* protect the pest by pyrethroid sequestration rather than facilitating 4′OH-deltamethrin formation, which has indeed been shown to be intrinsically moderately toxic to pollen beetles over-expressing CYP6BQ23 (Zimmer et al., 2014; Zimmer and Nauen, 2011).

Next, we investigated if the significant differences in permethrin depletion we observed between CYP6P9a and CYP6P9b are linked to stereoselectivity issues as permethrin is a diastereomeric mixture of *cis*- and *trans*-permethrin. Indeed, we detected a preference of both CYP6P9 variants to hydroxylate more readily *trans*-over *cis*-permethrin, with CYP6P9b exhibiting a significantly higher metabolic capacity and preference to hydroxylate *trans*-permethrin compared with CYP6P9a. As we did not analyse the metabolism of the hydroxylated isomers separately, we can only speculate – based on the metabolic fate of racemic 4′OH permethrin – that CYP6P9b is the main permethrin metaboliser, because it was shown to catalyse the ether cleavage of the phenoxybenzyl moiety at detectable levels, whereas CYP6P9a did not. Interestingly, mammalian P450s involved in permethrin metabolism seem to be consistently more active on *cis*-permethrin (Hedges et al., 2019), whereas the preferred route of *trans*-permethrin detoxification is hydrolytic via ester cleavage by esterases (Casida et al., 1983; Scollon et al., 2009; Shono et al., 1979). We then assessed the acute toxicity of both permethrin isomers and found that *cis*-permethrin was significantly more toxic than *trans*-permethrin against female adults of both *An. funestus* FANG and FUMOZ. Based on this result it is tempting to speculate that the metabolism of *cis*-permethrin might be reduced in the presence of its diastereomer *trans*-permethrin, i.e., *in vivo* retaining higher levels of the intrinsically more toxic *cis* isomer, possibly explaining the rather low levels of permethrin resistance (compared to deltamethrin) we recently described in our selected *An. funestus* FUMOZ-R laboratory strain (Nolden et al., 2021). It would be interesting to further investigate if racemic mixtures of pyrethroids are advantageous over enantiomerically pure compounds to control mosquitoes expressing P450-based metabolic resistance such as *An. funestus*.

Finally, we have carried out site-directed mutagenesis to create two mutants CYP6P9a^{I310V} and CYP6P9b^{V310I} to compare their metabolic activity with CYP6P9a and CYP6P9b towards permethrin, deltamethrin and coumarins. V310 is part of the catalytic site and the only residue in SRS4 of CYP6P9b different from CYP6P9a (I310). Furthermore, this site has been described mutated (V310I) in CYP6P9b haplotypes of a pyrethroid resistant field population of *An. funestus* from Benin (Ibrahim et al., 2015). Interestingly, we observed a striking increase in permethrin but not deltamethrin turnover by CYP6P9b^{V310I} compared with wildtype CYP6P9b, possibly explaining the high level of permethrin resistance observed in *An. funestus* strains from Benin showing this polymorphism. Ibrahim et al. (2015) described other key residues in CYP6P9b such as Val^{109}Ile, Asp^{335}Glu and Asn^{384}Ser as determinants of enhanced pyrethroid metabolism which has been confirmed by site-directed-mutagenesis as well. Here CYP6P9b^{V310I} showed a similar increase in the *O*-dealkylation of 7-EC, but not for the *O*-debenzylation of BFC and BOMFC. Whereas the swapped residue only weakly affected the catalytic capacity of the CYP6P9a variants towards coumarin substrates and pyrethroids. Indeed, mutations in substrate recognition sites of several insect P450s have been shown to be determinants of selectivity. For example in *An. gambiae* CYP6Z1 and CYP6Z2 differences in SRS1, SRS2 and SRS4 have been demonstrated to determine the capacity of CYP6Z1 to metabolise DDT (Chiu et al., 2008). In another study with different CYP6ER1-variants of *Nilaparvata lugens*, a hemipteran rice pest, a serine residue in SRS4 determined elevated imidacloprid metabolism (Zimmer et al., 2018). In the cotton bollworm, *Helicoverpa armigera*, variants of the CYP6AE subfamily with a valine to isoleucine substitution in SRS4 showed increased esfenvalerate metabolism (Shi et al., 2020). Similar observations were described for substitutions in SRS4 of human CYP2A1 and CYP2A2 leading to higher hydroxylation rates and alterations in ethoxy-coumarin *O*-dealkylation (Hanioka et al., 1992; Hiroya et al., 1994).

Nonetheless, further molecular work is warranted to shed light on the determinants of pyrethroid metabolism and resistance by CYP6P9 variants, and whether SRS4 residue 310 of CYP6P9b can potentially serve as a molecular marker of enhanced levels of pyrethroid resistance in *An. funestus*.

Declaration of competing interest

RN and MN are employed by Bayer AG (Germany), a manufacturer of pesticides. MN is also a PhD student affiliated with the Liverpool School of Tropical Medicine (UK), funded by the Innovative Vector Control Consortium (IVCC) and Bayer AG.

Acknowledgements

We greatly acknowledge the help of Johannes Glaubitz, Udo König and Birgit Nebelsiek with the UPLC-MS/MS analysis and Sebastian Horstmann and Uwe Pluschkell for their helpful discussion and comments.

Appendix A. Supplementary data

Supplementary data to this article can be found online at https://doi.org/10.1016/j.ibmb.2022.103813.

References

Abbott, W.S., 1925. A method of computing the effectiveness of an insecticide. J. Econ. Entomol. 18, 265–267. https://doi.org/10.1093/jee/18.2.265a.

Amenya, D.A., Naguran, R., Lo, T.-C.M., Ranson, H., Spillings, B.L., Wood, O.R., Brooke, B.D., Coetzee, M., Koekemoer, L.L., 2008. Over expression of a cytochrome P450 (CYP6P9) in a major african malaria vector. Insect Mol. Biol. 17, 19–25.

Bhatt, S., Weiss, D.J., Cameron, E., Bisanzio, D., Mappin, B., Dalrymple, U., Battle, K.E., Moyes, C.L., Henry, A., Eckhoff, P.A., Wenger, E.A., Briët, O., Penny, M.A., Smith, T. A., Bennett, A., Yukich, J., Eisele, T.P., Griffin, J.T., Fergus, C.A., Lynch, M., Lindgren, F., Cohen, J.M., Murray, C.L.J., Smith, D.L., Hay, S.I., Cibulskis, R.E., Gething, P.W., 2015. The effect of malaria control on Plasmodium falciparum in Africa between 2000 and 2015. Nature 526, 207–211. https://doi.org/10.1038/nature15535.

Brooke, B.D., Kloke, G., Hunt, R.H., Koekemoer, L.L., Tem, E.A., Taylor, M.E., Small, G., Hemingway, J., Coetzee, M., 2001. Bioassay and biochemical analyses of insecticide resistance in southern African Anopheles funestus (Diptera: Culicidae). Bull. Entomol. Res. 91, 265–272. https://doi.org/10.1079/ber2001108.

Casida, J.E., Gammon, D.W., Glickman, A.H., Lawrence, L.J., 1983. Mechanism of selective action of pyrethroid. Annu. Rev. Pharmacol. Toxicol. 413–438.
Chiu, T.L., Wen, Z., Rupasinghe, S.G., Schuler, M.A., 2008. Comparative molecular modeling of Anopheles gambiae CYP6Z1, a mosquito P450 capable of metabolizing DDT. Proc. Natl. Acad. Sci. U.S.A. 105, 8855–8860. https://doi.org/10.1073/pnas.0709249105.
Das, S., Garver, L., Dimopoulos, G., 2007. Protocol for mosquito rearing (A. gambiae). JoVE. https://doi.org/10.3791/221.
David, J., Ismail, H.M., Chandor-proust, A., Paine, M.J.I., 2013. Role of cytochrome P450s in insecticide resistance: impact on the control of mosquito-borne diseases and use of insecticides on Earth. Philos. Trans. R. Soc. B. https://doi.org/10.1098/rstb.2012.0429.
Feyereisen, R., 2019. Insect CYP Genes and P450 Enzymes, Reference Module in Life Sciences. https://doi.org/10.1016/b978-0-12-809633-8.04040-1.
Gleave, K., Lissenden, N., Richardson, M., Ranson, H., 2018. Piperonyl butoxide (PBO) combined with pyrethroids in long-lasting insecticidal nets (LLINs) to prevent malaria in Africa. Cochrane Database Syst. Rev. https://doi.org/10.1002/14651858.CD012776.
Gotoh, O., 1992. Substrate recognition sites in cytochrome P450 family 2 (CYP2) proteins inferred from comparative analyses of amino acid and coding nucleotide sequences. J. Biol. Chem. 267, 83–90. https://doi.org/10.1016/s0021-9258(18)48462-1.
Haas, J., Glaubitz, J., Koenig, U., Nauen, R., 2021. A mechanism-based approach unveils metabolic routes potentially mediating chlorantraniliprole synergism in honey bees, Apis mellifera L., by azole fungicides. Pest Manag. Sci. https://doi.org/10.1002/ps.6706.
Haas, J., Nauen, R., 2021. Pesticide risk assessment at the molecular level using honey bee cytochrome P450 enzymes : a complementary approach. Environ. Int. 147, 106372 https://doi.org/10.1016/j.envint.2020.106372.
Hamada, A., Wahl, G.D., Nesterov, A., Nakao, T., Kawashima, M., Banba, S., 2019. Differential metabolism of imidacloprid and dinotefuran by Bemisia tabaci CYP6CM1 variants. Pestic. Biochem. Physiol. 159, 27–33. https://doi.org/10.1016/j.pestbp.2019.05.011.
Hanioka, N., Gonzalez, F.J., Lindberg, N.A., Gao, L., Gelboin, H.V., Korzekwa, K.R., 1992. Site-directed mutagenesis of cytochrome P450s CYP2A1 and CYP2A2: influence of the distal helix on the kinetics of testosterone hydroxylation. Biochem. 31, 3364–3370. https://doi.org/10.1021/bi00128a009.
Hedges, L., Brown, S., MacLeod, A.K., Vardy, A., Doyle, E., Song, G., Moreau, M., Yoon, M., Osimitz, T.G., Lake, B.G., 2019. Metabolism of deltamethrin and cis- and trans-permethrin by human expressed cytochrome P450 and carboxylesterase enzymes. Xenobiotica 49, 521–527. https://doi.org/10.1080/00498254.2018.1474283.
Hiroya, K., Murakami, Y., Shimizu, T., Hatano, M., Ortiz De Montellano, P.R., 1994. Differential roles of Glu318 and Thr319 in cytochrome P450 1A2 catalysis supported by NADPH-cytochrome P450 reductase and tert-butyl hydroperoxide. Arch. Biochem. Biophys. https://doi.org/10.1006/abbi.1994.1184.
Horstmann, S., Sonneck, R., 2016. Contact bioassays with phenoxybenzyl and tetrafluorobenzyl pyrethroids against target-site and metabolic resistant mosquitoes. PLoS One 11, e0149738. https://doi.org/10.1371/journal.pone.0149738.
Ibrahim, S.S., Amvongo-Adjia, N., Wondji, M.J., Irving, H., Riveron, J.M., Wondji, C.S., 2018. Pyrethroid resistance in the major malaria vector anopheles funestus is exacerbated by overexpression and overactivity of the P450 CYP6AA1 across Africa. Genes 9, 1–17. https://doi.org/10.3390/genes9030140.
Ibrahim, S.S., Ndula, M., Riveron, J.M., Irving, H., Wondji, C.S., 2016. The P450 CYP6Z1 confers carbamate/pyrethroid cross-resistance in a major African malaria vector beside a novel carbamate-insensitive N485I acetylcholinesterase-1 mutation. Mol. Ecol. 25, 3436–3452. https://doi.org/10.1111/mec.13673.
Ibrahim, S.S., Riveron, J.M., Bibby, J., Irving, H., Yunta, C., Paine, M.J.I., Wondji, C.S., 2015. Allelic variation of cytochrome P450s drives resistance to bednet insecticides in a major malaria vector. PLoS Genet. 11, e1005618 https://doi.org/10.1371/journal.pgen.1005618.
Irving, H., Wondji, C.S., 2017. Investigating knockdown resistance (kdr) mechanism against pyrethroids/DDT in the malaria vector Anopheles funestus across Africa. BMC Genet. 18, 76. https://doi.org/10.1186/s12863-017-0539-x.
Martinez-Torres, D., Chandre, F., Williamson, M.S., Darriet, F., Berge, J.B., Devonshire, A.L., Guillet, P., Pasteur, N., Pauron, D., 1998. Molecular characterization of pyrethroid knockdown resistance (kdr) in the major malaria vector Anopheles gambiae s.s. Insect Mol. Biol. 7, 179–184.
Moyes, C.L., Lees, R.S., Yunta, C., Walker, K.J., Hemmings, K., Oladepo, F., Hancock, P. A., Weetman, D., Paine, M.J.I., Ismail, H.M., 2021. Assessing cross-resistance within the pyrethroids in terms of their interactions with key cytochrome P450 enzymes and resistance in vector populations. Parasites Vectors 14, 115. https://doi.org/10.1186/s13071-021-04609-5.
Nauen, R., Bass, C., Feyereisen, R., Vontas, J., 2022. The role of cytochrome P450s in insect toxicology and resistance. Annu. Rev. Entomol. 67, 105–124. https://doi.org/10.1146/annurev-ento-070621-061328.
Nolden, M., Brockmann, A., Ebbinghaus-kintscher, U., Brueggen, K., Horstmann, S., Paine, M.J.I., Nauen, R., 2021. Towards understanding transfl uthrin efficacy in a pyrethroid-resistant strain of the malaria vector Anopheles funestus with special reference to cytochrome P450-mediated detoxification. Curr. Res. Parasitol. Vector-Borne Dis. 1, 100041 https://doi.org/10.1016/j.crpvbd.2021.100041.
Nolden, M., Paine, M.J.I., Nauen, R., 2022. Biochemical profiling of functionally expressed CYP6P9 variants of the malaria vector Anopheles funestus with special reference to cytochrome b5 and its role in pyrethroid and coumarin substrate metabolism. Pestic. Biochem. Physiol. 182 https://doi.org/10.1016/j.pestbp.2022.105051.
Oleg, T., Olson, A.J., 2010. Software news and update AutoDock Vina: improving the speed and accuracy of docking with a new scoring function, efficient optimization, and multithreading. J. Comput. Chem. 31, 455–461. https://doi.org/10.1002/jcc.21334.
Omura, T., Sato, R., 1964. The carbon monoxide-binding pigment of liver microsomes. J. Biol. Chem. 239.
Paine, M.J.I., McLaughlin, L.A., Flanagan, J.U., Kemp, C.A., Sutcliffe, M.J., Roberts, G.C. K., Wolf, C.R., 2003. Residues glutamate 216 and aspartate 301 are key determinants of substrate specificity and product regioselectivity in cytochrome P450 2D6. J. Biol. Chem. 278, 4021–4027. https://doi.org/10.1074/jbc.M209519200.
Protopopoff, N., Mosha, J.F., Lukole, E., Charlwood, J.D., Wright, A., Mwalimu, C.D., Manjurano, A., Mosha, F.W., Kisinza, W., Kleinschmidt, I., Rowland, M., 2018. Effectiveness of a long-lasting piperonyl butoxide-treated insecticidal net and indoor residual spray interventions, separately and together, against malaria transmitted by pyrethroid-resistant mosquitoes: a cluster, randomised controlled, two-by-two fact. Lancet 391, 1577–1588. https://doi.org/10.1016/S0140-6736(18)30427-6.
Ranson, H., N'Guessan, R., Lines, J., Moiroux, N., Nkuni, Z., Corbel, V., 2011. Pyrethroid resistance in African anopheline mosquitoes: what are the implications for malaria control? Trends Parasitol. 27, 91–98. https://doi.org/10.1016/j.pt.2010.08.004.
Riveron, J.M., Ibrahim, S.S., Chanda, E., Mzilahowa, T., Cuamba, N., Irving, H., Barnes, K.G., Ndula, M., Wondji, C.S., 2014. The highly polymorphic CYP6M7 cytochrome P450 gene partners with the directionally selected CYP6P9a and CYP6P9b genes to expand the pyrethroid resistance front in the malaria vector Anopheles funestus in Africa. BMC Genom. 15, 817. https://doi.org/10.1186/1471-2164-15-817.
Riveron, J.M., Irving, H., Ndula, M., Barnes, K.G., Ibrahim, S.S., Paine, M.J.I., Wondji, C. S., 2013. Directionally selected cytochrome P450 alleles are driving the spread of pyrethroid resistance in the major malaria vector Anopheles funestus. Proc. Natl. Acad. Sci. USA 110, 252–257. https://doi.org/10.1073/pnas.1216705110.
Ruzo, L.O., Unai, T., Casida, J.E., 1978. Decamethrin metabolism in rats. J. Agric. Food Chem. 26, 918–925. https://doi.org/10.1021/jf60218a060.
Scollon, E.J., Starr, J.M., Godin, S.J., DeVito, M.J., Hughes, M.F., 2009. In vitro metabolism of pyrethroid pesticides by rat and human hepatic microsomes and cytochrome P450 isoforms. Drug Metab. Dispos. 37, 221–228. https://doi.org/10.1124/dmd.108.022343.
Shi, Y., O'Reilly, A.O., Sun, S., Qu, Q., Yang, Y., Wu, Y., 2020. Roles of the variable P450 substrate recognition sites SRS1 and SRS6 in esfenvalerate metabolism by CYP6AE subfamily enzymes in Helicoverpa armigera. Insect Biochem. Mol. Biol. 127, 103486 https://doi.org/10.1016/j.ibmb.2020.103486.
Shono, T., Ohsawa, K., Casida, J.E., 1979. Metabolism of trans-and cis-Permethrin, trans- and cis-Cypermethrin, and Decamethrin by Microsomal Enzymes. J. Agric. Food Chem. 27, 316–325. https://doi.org/10.1021/jf60222a059.
Soderlund, D.M., 2020. Neurotoxicology of pyrethroid insecticides. In: Neurotoxicity of Pesticides. Elsevier Inc., pp. 113–165. https://doi.org/10.1016/bs.ant.2019.11.002
Stevenson, B.J., Bibby, J., Pignatelli, P., Muangnoicharoen, S., O'Neill, P.M., Lian, L.Y., Müller, P., Nikou, D., Steven, A., Hemingway, J., Sutcliffe, M.J., Paine, M.J.I., 2011. Cytochrome P450 6M2 from the malaria vector Anopheles gambiae metabolizes pyrethroids: sequential metabolism of deltamethrin revealed. Insect Biochem. Mol. Biol. 41, 492–502. https://doi.org/10.1016/j.ibmb.2011.02.003.
WHO, 2021. World Malaria Report. World Malaria Report 2021.
WHO, 2020. World Malaria Report 2020. World Health Organization.
WHO, 2018. Global Report on Insecticide Resistance in Malaria Vectors: 2010-2016.
Williams, J., Flood, L., Praulins, G., Ingham, V.A., Morgan, J., Lees, R.S., Ranson, H., 2019. Characterisation of Anopheles strains used for laboratory screening of new vector control products. Parasites Vectors 12, 522. https://doi.org/10.1186/s13071-019-3774-3.
Wondji, C.S., Hearn, J., Irving, H., Wondji, M.J., Weedall, G., 2022. RNAseq-based gene expression profiling of the Anopheles funestus pyrethroid-resistant strain FUMOZ highlights the predominant role of the duplicated CYP6P9a/b cytochrome P450s. G3 Genes Genomes Genet. 12 https://doi.org/10.1093/G3JOURNAL/JKAB352.
Yunta, C., Hemmings, K., Stevenson, B., Koekemoer, L.L., Matambo, T., Pignatelli, P., Voice, M., Nász, S., Paine, M.J.I., 2019. Cross-resistance profiles of malaria mosquito P450s associated with pyrethroid resistance against WHO insecticides. Pestic. Biochem. Physiol. 161, 61–67. https://doi.org/10.1016/j.pestbp.2019.06.007.
Zimmer, C.T., Bass, C., Williamson, M.S., Kaussmann, M., Wölfel, K., Gutbrod, O., Nauen, R., 2014. Molecular and functional characterization of CYP6BQ23, a cytochrome P450 conferring resistance to pyrethroids in European populations of pollen beetle, Meligethes aeneus. Insect Biochem. Mol. Biol. 45, 18–29. https://doi.org/10.1016/j.ibmb.2013.11.008.
Zimmer, C.T., Garrood, W.T., Singh, K.S., Randall, E., Lueke, B., Gutbrod, O., Matthiesen, S., Kohler, M., Nauen, R., Davies, T.G.E., Bass, C., 2018. Neofunctionalization of duplicated P450 genes drives the evolution of insecticide resistance in the Brown planthopper. Curr. Biol. 28, 268–274. https://doi.org/10.1016/j.cub.2017.11.060 e5.
Zimmer, C.T., Nauen, R., 2011. Cytochrome P450 mediated pyrethroid resistance in European populations of Meligethes aeneus (Coleoptera: nitidulidae). Pestic. Biochem. Physiol. 100, 264–272. https://doi.org/10.1016/j.pestbp.2011.04.011.